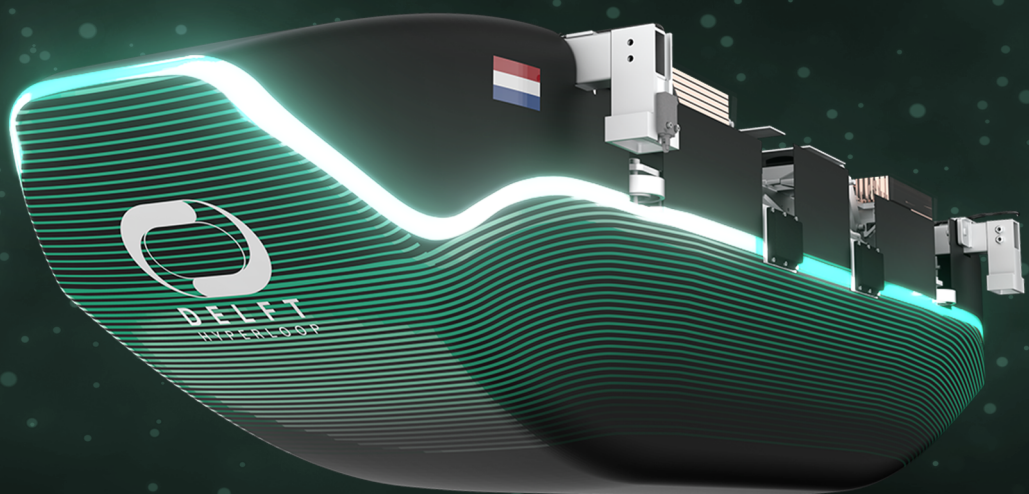




# FINAL DEMONSTRATION DOCUMENTATION

2022 EUROPEAN HYPERLOOP WEEK



EUROPEAN HYPERLOOP WEEK

DELFT HYPERLOOP

---

## Final Demonstration Documentation

---

10 May 2023



# Contents

<b>1 EXAMPLES</b>	<b>5</b>
1.1 EXAMPLE: equations . . . . .	5
1.2 EXAMPLE: figures . . . . .	5
1.3 EXAMPLE: other tables . . . . .	5
1.4 EXAMPLE: requirements . . . . .	5
1.5 EXAMPLE: trade-offs . . . . .	6
<b>2 Introduction</b>	<b>7</b>
2.1 Delft Hyperloop . . . . .	7
2.2 Outline Final Demonstration Document . . . . .	7
2.3 List of Team Members and Advisors . . . . .	7
<b>3 System Overview</b>	<b>8</b>
3.1 The Full-Scale Hyperloop System . . . . .	8
3.2 Design Objective . . . . .	8
3.3 Top Level Specifications . . . . .	8
3.4 Top Level Performance . . . . .	8
3.5 Propulsion . . . . .	8
3.6 Levitation . . . . .	8
3.7 Sense and Control . . . . .	8
3.8 Mechanical . . . . .	8
<b>4 Propulsion</b>	<b>9</b>
4.1 Introduction . . . . .	9
4.2 Introduction . . . . .	9
4.3 LRM . . . . .	9
4.4 Cooling System Design . . . . .	9
4.5 Motor Control System . . . . .	9
4.6 Integration with other Systems . . . . .	9
4.7 Production . . . . .	9
4.8 Design Adaptations for a Full-Scale Hyperloop System . . . . .	9
<b>5 Levitation</b>	<b>10</b>
5.1 Introduction . . . . .	10
5.2 Full-Scale Levitation Method . . . . .	10
5.3 Hybrid Electromagnetic Suspension . . . . .	10
5.4 Electromagnetic Suspension . . . . .	10
5.5 Safety Wheels . . . . .	10
5.6 Control System . . . . .	10
5.7 Integration with other Systems . . . . .	10
5.8 Vehicle Dynamics . . . . .	10
5.9 Production . . . . .	10
5.10 Design Adaptations for a Full-Scale Hyperloop System . . . . .	10
<b>6 Power</b>	<b>11</b>
6.1 Introduction . . . . .	11
6.1.1 Introduction to subsystems . . . . .	11
6.1.2 Intent of power . . . . .	12
6.1.3 Symbols and abbreviations . . . . .	12
6.1.4 Requirements and specifications . . . . .	13
6.2 High Voltage Battery . . . . .	14
6.2.1 Requirements . . . . .	14
6.2.2 Topology . . . . .	15
6.2.3 Cell Choice . . . . .	15
6.2.4 Battery Pack . . . . .	16
6.2.5 Battery Enclosure . . . . .	17
6.2.6 Powertrain Floor . . . . .	19

6.2.7	Cables and Connectors . . . . .	22
6.2.8	Heat analysis . . . . .	22
6.3	<b>Low Voltage Battery</b> . . . . .	23
6.3.1	Topology . . . . .	24
6.3.2	Cell Choice . . . . .	24
6.3.3	Enclosure . . . . .	25
6.3.4	Cables and connectors . . . . .	25
6.4	<b>Power Control System</b> . . . . .	26
6.4.1	Powertrain Controller . . . . .	27
6.4.2	PTC Finite State Machine . . . . .	29
6.4.3	Hardware Design . . . . .	34
6.4.4	High Voltage Battery Management System . . . . .	35
6.4.5	Low Voltage Battery Management system . . . . .	37
6.5	<b>Power Distribution</b> . . . . .	37
6.5.1	Low Voltage Power Distribution Board A . . . . .	37
6.5.2	Low Voltage Power Distribution Boards B1 and B2 . . . . .	42
6.5.3	High Voltage Power Distribution Board . . . . .	43
6.5.4	Pre Charge Circuit . . . . .	46
6.6	<b>On-Board Charger</b> . . . . .	47
6.6.1	Design features . . . . .	48
6.6.2	Charging Modes . . . . .	50
6.7	<b>Regenerative Braking</b> . . . . .	51
6.7.1	Features . . . . .	51
6.7.2	Architecture . . . . .	51
6.7.3	Hardware Design . . . . .	52
6.8	<b>Production</b> . . . . .	53
6.8.1	Enclosures . . . . .	53
6.8.2	Electronics . . . . .	53
6.8.3	Batteries . . . . .	53
6.9	<b>Design Adaptations for a Full-Scale Hyperloop System</b> . . . . .	54
<b>7</b>	<b>Sense and Control</b> . . . . .	<b>55</b>
7.1	<b>Introduction</b> . . . . .	55
7.1.1	Introduction to subsystems . . . . .	55
7.1.2	Intent of Sense & Control . . . . .	56
7.1.3	Symbols and abbreviations . . . . .	56
7.1.4	Requirements and specifications . . . . .	56
7.2	<b>Sensing</b> . . . . .	58
7.2.1	Overview . . . . .	58
7.2.2	Vacuum Box Thermal sensing system . . . . .	59
7.2.3	Battery Sensors . . . . .	60
7.2.4	Safety Sensors . . . . .	61
7.2.5	Emergency brake Sensors . . . . .	62
7.2.6	Levitation Sensors . . . . .	63
7.2.7	Localization sensors . . . . .	64
7.3	<b>Localization</b> . . . . .	65
7.3.1	Introduction . . . . .	65
7.3.2	Optical Localization . . . . .	66
7.3.3	Inductive Localization . . . . .	74
7.3.4	Inertial Measurement Unit . . . . .	75
7.3.5	Integrated system . . . . .	76
7.4	<b>Internal Control System</b> . . . . .	77
7.4.1	Main Controller . . . . .	78
7.4.2	Braking PCB . . . . .	82
7.4.3	Thermal Controller PCB . . . . .	83
7.4.4	Industrial/Automotive Ethernet Bus . . . . .	83
7.5	<b>Pod Software</b> . . . . .	86
7.5.1	Requirements . . . . .	86

7.5.2	Finite State Machine . . . . .	86
7.5.3	Software architecture . . . . .	90
7.5.4	Core controller . . . . .	90
7.5.5	Continuous integration/Continuous Deployment Pipeline . . . . .	90
7.5.6	Firmware updates . . . . .	91
7.6	<b>Communication &amp; Ground Station</b> . . . . .	92
7.6.1	Requirements . . . . .	92
7.6.2	External communication . . . . .	92
7.6.3	Ground Station . . . . .	93
7.6.4	Over-the-air updates . . . . .	96
7.7	<b>Physical Layout</b> . . . . .	97
7.7.1	Placement of subsystems . . . . .	97
7.7.2	Cable management . . . . .	99
7.8	<b>Thermal management</b> . . . . .	104
7.8.1	Requirements & Nomenclature . . . . .	105
7.8.2	Expected system characteristics . . . . .	106
7.8.3	Trade-off for Helios II . . . . .	109
7.8.4	Cooling Design . . . . .	110
7.8.5	Thermal Model . . . . .	111
7.8.6	Final dimensioning . . . . .	114
7.8.7	CFD . . . . .	116
7.9	<b>Production</b> . . . . .	119
7.9.1	Printed circuit boards . . . . .	119
7.9.2	Sensors and localization . . . . .	119
7.9.3	Track Markers . . . . .	119
7.9.4	Thermal management . . . . .	119
7.10	<b>Design Adaptations for a Full-Scale Hyperloop System</b> . . . . .	120
7.10.1	Control . . . . .	120
7.10.2	Sensing . . . . .	120
7.10.3	Communication . . . . .	120
7.10.4	Thermal Management . . . . .	120
<b>8</b>	<b>Mechanical</b>	<b>122</b>
8.1	<b>Introduction</b> . . . . .	122
8.2	<b>Chassis</b> . . . . .	122
8.3	<b>Track</b> . . . . .	122
8.4	<b>Brakes</b> . . . . .	122
8.5	<b>Vacuum Box</b> . . . . .	122
8.6	<b>Aeroshell</b> . . . . .	122
8.7	<b>Production</b> . . . . .	122
8.8	<b>Design Adaptations for a Full-Scale Hyperloop System</b> . . . . .	122
<b>9</b>	<b>Demonstration</b>	<b>123</b>
9.1	<b>Procedures</b> . . . . .	123
9.2	<b>Infrastructure</b> . . . . .	123
<b>10</b>	<b>Safety</b>	<b>124</b>
10.1	<b>Hazardous Energy Storage</b> . . . . .	124
10.2	<b>Hazardous Materials</b> . . . . .	124
10.3	<b>Safety Features of the Pod</b> . . . . .	124
10.4	<b>Subsystem-Specific Safety Features</b> . . . . .	124
<b>11</b>	<b>Testing</b>	<b>125</b>
11.1	<b>Testing Overview</b> . . . . .	125
11.2	<b>Test Setups</b> . . . . .	125
<b>12</b>	<b>Conclusion</b>	<b>126</b>
<b>A</b>	<b>Propulsion</b>	<b>130</b>

<b>B</b>	<b>Levitation</b>	<b>130</b>
<b>C</b>	<b>Sense and Control</b>	<b>130</b>
C.0.1	Vacuum feedthrough connectors . . . . .	241
<b>D</b>	<b>Mechanical</b>	<b>254</b>
<b>E</b>	<b>Power</b>	<b>254</b>

# 1 EXAMPLES

## 1.1 EXAMPLE: equations

Make sure to always reference to formulas in-text. Also, do not forget to cite formulas if they are clearly coming from an external source.

$$H = 2 \cdot \frac{N}{L} \cdot I \quad (1.1)$$

## 1.2 EXAMPLE: figures

Note that for figures the caption is below the figure.



**Figure 1.1:** EXAMPLE FIGURE

## 1.3 EXAMPLE: other tables

Note that for tables the caption is above the table.

**Table 1.1:** EXAMPLE PARAMETER TABLE

Parameter	Name	Value	Unit
$W_c$	Width coil	64	mm
$W_{bb}$	Width bobbin	32.5	mm
$W_{cb}$	Width coil wires	15.76	mm
$L_{bb}$	Length bobbin	215	mm
$L_c$	Length coil	246.5	mm
$H_c$	Height coil	43.8	mm
$D_w$	Diameter wire	0.8425	mm
$C_c$	Circumference coil average	0.56	m
$N_L$	Number of turns	1000	-
$R_L$	Resistance	16.67	$\Omega$
$m_{L,c}$	Weight of the coil	2.76	kg

## 1.4 EXAMPLE: requirements

Note that for requirements the caption is above the table

**Table 1.2: EXAMPLE REQUIREMENTS LIST**

<b>ID</b>	<b>Requirement</b>
LE.GE.T.1	The subsystem shall not weight more than 100 [kg].
LE.GE.T.2	The subsystem should be vacuum compatible at 10 mbar.

## 1.5 EXAMPLE: trade-offs

Note that for trade-off tables the caption is above the table.

**Table 1.3: EXAMPLE TRADE-OFF TABLE**

<b>Criteria</b>	<b>SC EDS</b>	<b>RPM EDS</b>	<b>8C EDS</b>	<b>IDT</b>	<b>EMS</b>	<b>HEMS</b>	<b>SC ME</b>
<b>Is as light as possible</b>	-	+	++	++	-	0	-
<b>Can be manufactured and assembled within X months.</b>	-	0	--	0	+	0	--
<b>Is developed using technology fully developed by the team</b>	0	+	++	++	0	0	0
<b>Is a unique idea, not seen before</b>	++	+	++	++	-	0	+
<b>Is scalable, into a full-size Hyperloop system</b>	-	--	--	+	-	0	--
<b>Is easy to keep the pod stable at the desired height</b>	+	++	++	++	--	0	+
<b>Requires little energy consumption from the batteries</b>	-	--	++	++	--	0	+
<b>The cost should be as low as possible</b>	--	+	--	--	+	0	--
<b>Introduces as few safety hazards as possible</b>	--	0	-	+	-	0	-
<b>Is lane switch compatible</b>	0	0	-	0	0	0	++
<b>Is reliable (low chance of failure &amp; low severity of failure)</b>	--	-	++	+	0	0	--
<b>Can be integrated with propulsion and/or lateral levitation system</b>	--	++	0	-	0	0	+
<b>Wide range of operating speeds</b>	--	+	--	++	0	0	++

## **2 Introduction**

### **2.1 Delft Hyperloop**

### **2.2 Outline Final Demonstration Document**

### **2.3 List of Team Members and Advisors**

### **3 System Overview**

**3.1 The Full-Scale Hyperloop System**

**3.2 Design Objective**

**3.3 Top Level Specifications**

**3.4 Top Level Performance**

**3.5 Propulsion**

**3.6 Levitation**

**3.7 Sense and Control**

**3.8 Mechanical**

## **4 Propulsion**

**4.1 Introduction**

**4.2 Introduction**

**4.3 LRM**

**4.4 Cooling System Design**

**4.5 Motor Control System**

**4.6 Integration with other Systems**

**4.7 Production**

**4.8 Design Adaptations for a Full-Scale Hyperloop System**

## **5 Levitation**

**5.1 Introduction**

**5.2 Full-Scale Levitation Method**

**5.3 Hybrid Electromagnetic Suspension**

**5.4 Electromagnetic Suspension**

**5.5 Safety Wheels**

**5.6 Control System**

**5.7 Integration with other Systems**

**5.8 Vehicle Dynamics**

**5.9 Production**

**5.10 Design Adaptations for a Full-Scale Hyperloop System**

## 6 Power

### 6.1 Introduction

#### 6.1.1 Introduction to subsystems

Helios II is designed to minimize its trackside infrastructure to make the design as scalable as possible. This means that all electrical subsystems are located on the pod, including the levitation and propulsion systems, which require high amounts of power to operate. To meet this power demand, a power system is designed, consisting of a high and a low-voltage battery. These batteries both consist of lithium-ion battery cells. To safely operate these batteries, a power control system is designed, consisting of a powertrain system controller, two battery management systems, and multiple safety electronics. Moreover, to distribute the high and low-voltage power to all subsystems as required, a power distribution subsystem is designed, consisting of multiple power distribution boards. Lastly, to ensure effective charging and efficient usage of power, an onboard charger, as well as a regenerative braking system, are designed. An overview of all different subsystems, with a short explanation, is given below. The goal of this chapter is to explain the design and functionality of all of these subsystems, as well as their corresponding safety and integration features. A render of the full power system is shown in figure 6.1.

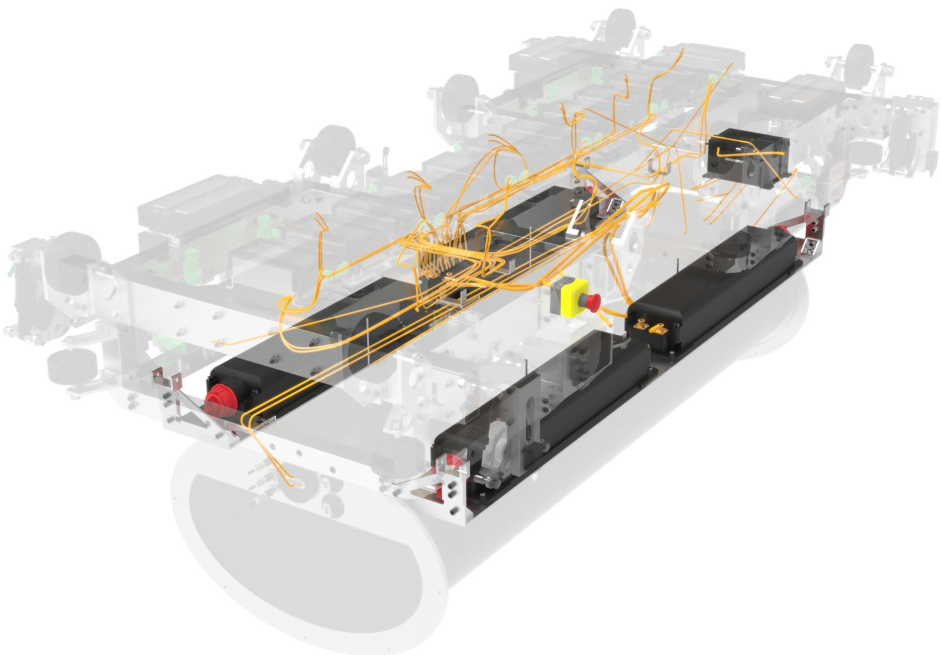


**Figure 6.1:** Render of the full power system and its most prominent components.

- **High-voltage battery**

The high-voltage (HV) battery is responsible for powering both the levitation and propulsion coils. This battery consists of a 6-parallel-112-series (6P112S) configuration of lithium-ion cells, allowing it to continuously supply up to 150 A at 400 V. These cells are split over 4 packs, each with its own enclosure.

- **High-voltage enclosures**

Four enclosures are made to protect the high-voltage battery cells from impacts and keep them in place. These enclosures are made of PLA plastic and use a sliding mechanism to easily remove them from the pod when necessary.

- **Low-voltage battery**

A low-voltage (LV) battery is responsible for powering all low-voltage electronics on the pod. This battery has a 4P7S configuration of lithium-ion cells, allowing it to continuously supply up to 40 A at 24 V.

- **Powertrain System Controller**

The powertrain system controller (PTSC) serves as the central hub for all operations of the power system. It analyzes all measured data and makes decisions accordingly. Additionally, it facilitates communication between the power system and the rest of the pod.

- **Battery management systems**

Both the high and low-voltage battery are equipped with their dedicated battery management system (BMS), which is responsible for guaranteeing operational performance and safety at all times. It does this by monitoring the cell voltage, pack voltage, pack current, temperature and state of charge of the batteries. All of this data is communicated to the PTC.

- **Safety electronics**

For an extra layer of safety on top of the battery management systems, more safety electronics are installed, including fuses, an insulation monitoring device, manual disconnect buttons a pre-charge circuit and an emergency button .

- **Power distribution units**

To distribute the high and low-voltage power to all subsystems at the desired voltage and current levels, one high-voltage and three low-voltage power distribution boards (PDB's) are designed.

- **On-board charger**

The on board charger (OBC) converts alternating current (AC) from the grid to direct current (DC) power that can be used to directly charge the high-voltage battery. This charger can be used for either normal-speed or fast-speed charging.

- **Regenerative braking circuit**

The regenerative braking circuit (RBC) allows the power that is generated by the propulsion system during braking, to flow back into the low-voltage battery. This allows the low-voltage battery to be charged during a run and therefore makes the pod more energy efficient.

### **6.1.2 Intent of power**

As the design towards a full-scale hyperloop advances, more and more subsystems, requiring both high and low-voltage power, are added to the design. The intent of the power subsystem is to meet these power requirements, while optimizing for weight and volume reduction. Moreover, as one of the goals of the hyperloop system is transport of people or cargo, safety is a high priority at all times. Therefore, multiple layers of safety have been implemented, both mechanically and electrically, which all have to be extremely reliable.

Having a fully charged battery before the start of every run as quickly as possible is a significant challenge for the design of a full-scale hyperloop. This can be done by either replacing the batteries after every run, or by fast charging them. In line with these options, the high-voltage batteries have been made to be as modular as possible by being placed on the sides of the pod and split over multiple enclosures. On top of that, the on-board charger allows for convenient and fast charging of the high-voltage battery. Lastly a regenerative braking circuit allows for charging the high-voltage batteries during braking, and therefore expanding the lifetime of the batteries.

### **6.1.3 Symbols and abbreviations**

In this chapter various symbols and abbreviations are used for clarity and readability. Table 6.1 below gives an explanation of all symbols that are used. All requirements have a specific ID, which is of the form PO.XX.YZ, where XX determines the subsystem, Y indicates the sort of requirement, and Z is the number of the requirement. Table 6.2 below gives an overview of the meaning of all these abbreviations.

**Table 6.1:** Power subsystem list of symbols

Property	Symbol	Unit
Current	$I$	A
Voltage	$U$	V
Energy	$E$	Ah, kWh
Power	$P$	W
Weight	$m$	g
Capacitance	$C$	F
Resistance	$R$	$\Omega$
Frequency	$f$	Hz
Minimum output current	$I_{OUT(min)}$	A
Duty cycle	$D$	%
Oscillator frequency	$f_{OSC}$	Hz
Output voltage	$V_{OUT}$	V
Coil current	$I_L$	A
Equivalent series resistance	$ESR$	$\Omega$
Timing resistor resistance	$R_t$	$\Omega$
Timing capacitor capacitance	$C_t$	F
Ripple voltage	$\Delta V$	V
Time constant	$\tau$	s

**Table 6.2:** Abbreviations used for the ID's

Category	Abbreviation
General	GE
(HV) Enclosure	EN
Power Distribution	PD
On Board Charger	CH
High Voltage	HV
Low Voltage	LV
Technical	T
Monitoring	M
Safety	S
Planning	P

#### 6.1.4 Requirements and specifications

A list of general requirements that are essential for an optimal and safe operation of the power subsystem as well as the full pod are given in table 6.3 below. These requirements shall all be met during the European Hyperloop Week 2023.

**Table 6.3:** Power system Requirements

ID	Power Requirement
PO.GE.T.1	The power system shall not weigh more than 50 kg.
PO.GE.T.2	All parts of the system that are outside the vacuum box shall be fully operational in a near-vacuum (10 mbar).
PO.GE.T.3	The low-voltage battery shall be able to give sufficient power to all low-voltage electronics on the pod for at least 7 runs.
PO.GE.T.4	The high-voltage battery shall be able to give sufficient power to all high-voltage electronics on the pod for at least 7 runs.
PO.GE.T.5	Power distribution circuits ensure that all high and low-voltage power is distributed to all subsystems at the right voltage and amperage.
PO.GE.T.6	An onboard charger is installed allowing the high-voltage batteries to be directly charged from the power grid.
PO.GE.T.7	A regenerative braking circuit is installed that allows the low-voltage battery to charge during normal braking.
PO.GE.S.1	All subsystems which use power shall be grounded to the chassis
PO.GE.S.2	The minimal distance between two conductors shall be at least twice the arcing distance of the maximum voltage in a near vacuum.
PO.GE.S.3	The batteries must survive all impacts, collisions and vibrations that are possible to happen during any operation.
PO.GE.S.4	Safety electronics shall be installed to guarantee safe operation of all battery packs at all time during operation.
PO.GE.S.5	A high-voltage battery management system is installed that monitors the voltage, amperage, state of charge and temperature of the high-voltage battery.
PO.GE.S.6	A low-voltage battery management system is installed that monitors the voltage, amperage, state of charge and temperature of the low-voltage battery.
PO.GE.S.7	All high-voltage wiring will have an orange color
PO.GE.P.1	All high-voltage battery modules shall be fully welded and tested before the 13th of March 2023

The most important top-level specifications of the power subsystem can be seen in Table 6.4.

**Table 6.4:** Power system main specifications

Specification	Value
Total mass	48 kg
Total number of cells	700
Total power usage	23.2 W
Total peak power output	99.8 kW
Nominal High-Voltage Output	400 V
Nominal Low-Voltage Outputs	5, 12, 24 V

## 6.2 High Voltage Battery

To provide the power for the lateral and vertical levitation subsystems, as well as the propulsion system, a high-voltage battery is installed on the pod. The HV battery is custom-made to provide sufficient power to these systems while optimizing for weight and volume. The aim of this chapter is to elaborate on the HV battery topology, cell choice, specifications, enclosure design, electrical components, and wiring. The corresponding electronics for control and safety, together with those of the low voltage system, will be explained in section 6.4. A visual representation of the high-voltage system can be found in figure 6.2.

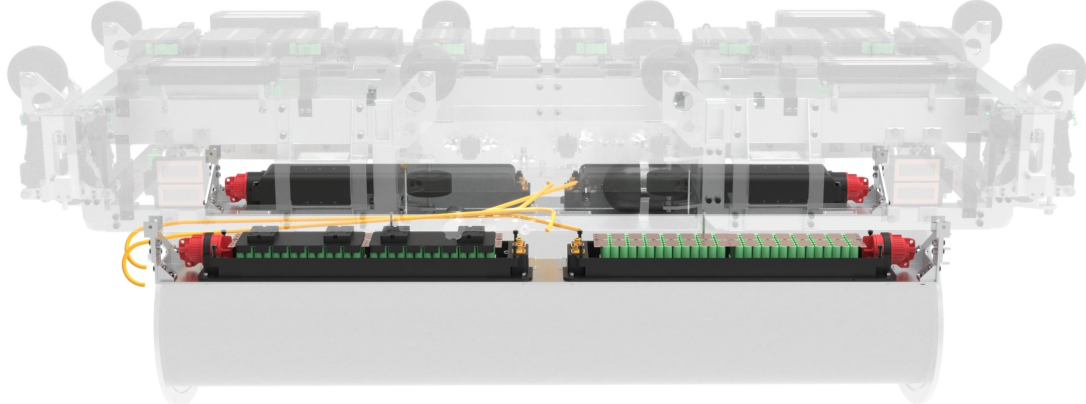


**Figure 6.2:** High Voltage battery packs. In green are the Li-ion cells, topped by copper plates. Every pack is contained in a black enclosure with a red manual power switch.

### 6.2.1 Requirements

The most prominent requirements for the high-voltage batteries are listed in the table 6.5. They include both an EHW regulatory requirement (PO.HV.T.1) and DH07 performance requirements (PO.HV.T.2, PO.HV.T.3, PO.HV.T.4). The list of EHW requirements includes the mandatory safety, technical, and display and monitoring requirements. The performance requirements contain sufficient capacity and power delivery.

**Table 6.5:** High voltage requirements

ID	Requirement
PO.HV.T.1	The high-voltage system shall fulfill all EHW safety requirements.
PO.HV.T.2	The high-voltage system shall be able to deliver sufficient energy to complete 7 runs without recharging.
PO.HV.T.3	The power distribution system shall provide all elements of the pod with the required power and voltage for their correct functioning during all stages of idle and active pod operation.
PO.HV.T.4	The high-voltage system shall be able to deliver the required power for the course of 7 consecutive runs before needing internal cooling.
PO.HV.T.4	The high-voltage system shall be able to operate in a near vacuum environment of 10 mbar.

### 6.2.2 Topology

An overview of all subsystems that have to be powered by the HV battery, with their nominal and maximum power requirements during acceleration can be found in 6.6.

**Table 6.6:** Power requirements that the high-voltage system should provide for

subsystem	Motor Qty.	Drive	Nom. voltage	Nom. current	Max. current	Capacity <sup>1</sup>
Propulsion	1		400 V	60 A	100 A	0.25 Ah
Vertical levitation	4		400 V	11.2A	22.4A	0.54 Ah
Lateral levitation	1		400 V	11.2A	22.4A	0.13 Ah

Summing all Max. current values, it can be concluded that the battery pack should be able to provide maximum current of 212A and nominal current of 126A at 400 V. Moreover, to perform the 2 intended runs at the at the EHW, i.e. the acceleration and the cruise run, a capacity of 2.54 Ah, or 1.0 kWh is required. The system should be able to perform these runs at least 7 times without having to charge, which results in a minimum required capacity of 5.1 kWh.

To fulfill these demands, the designed battery consists of a 112S6P (112 in series and 6 in parallel) configuration split over 4 packs, all in their own enclosure. Each pack has a 66S3P cell configuration. By placing 2 of these packs in series and 2 in parallel, the full desired high-voltage battery system is formed. More information on a single pack is given in section 6.2.4. The specifications of the full high-voltage system are shown in table 6.7.

**Table 6.7:** High voltage battery specifications

Parameter	Value
Number of cells	672
Configuration	112S6P
Number of modules	16
Peak power	98.7 kW
Nom. power	60 kW
Nom. Capacity	6.3 kWh
Nom. voltage	403.2 V
Max. voltage	470 V
Nom. continuous discharge current	150 A
Max. continuous discharge current	210 A
Total HV system mass	40 kg
Dimensions	4x (760x 160 x 100) mm <sup>3</sup>

### 6.2.3 Cell Choice

Nine different options for the power supply of the on-pod electronics are displayed in the powertrain trade-off table 6.8. The first seven are the options of the chemical substructure of the batteries, and the last two options are the concepts for an off-track power supply.

<sup>1</sup>This is the estimated required capacity for performing 2 runs, as intended during the EHW

**Table 6.8:** Powertrain trade off

	NiCd	NiMH	NaS	Lead Acid	Li-ion	Li-ion polymer	Reusable Alkaline	Physical Contact	Contactless Transfer
<b>Energy Density</b>	-	+	++	--	++	++	+	-	-
<b>Internal Resistance</b>	o	-	++	++	o	-	--	++	o
<b>Cycle life</b>	++	-	++	--	+	o	--	-	++
<b>Cell voltage</b>	o	o	+	+	++	++	o	++	++
<b>Load Current -peak</b>	++	+	++	+	o	o	-	++	++
<b>-best result</b>	+	-	+	-	+	+	-	++	+
<b>Operating Temperature</b>	+	+	--	+	+	o	o	+	+
<b>Costs</b>	+	o	-	+	o	o	+	--	--
<b>Safety</b>	+	+	--	-	o	o	o	--	-
<b>Vacuum compatibility</b>	+	+	--	o	+	--	+	++	++

Although both off-track power supplies were ascribed a proper score on a number of aspects, their extreme high costs in combination with its additional safety hazards made these options non-preferable. This is because the main focus of DH07 is to develop scalable and robust hyperloop technology, ruling out these two options. The battery technology that is most commonly used in Electronic Vehicles (EV's) is Lithium-ion [1]. This is because of their high specific energy, advanced manufacturing technology and high cycle life [2][3]. Lithium-ion batteries have a much higher energy density than other types of batteries, such as lead- or nickel based batteries [4]. Another advantage of lithium-ion batteries is that they have almost no memory effect, which means that it does not lose its maximum energy capacity after multiple charge-discharge cycles [5]. In addition, the commercially available 18650 lithium-ion battery cells show no vacuum leak, size expansion or performance reduction when vacuum pressure tested [6][7]. They have a more robust safety design as they use a solid electrolyte, whereas lithium-polymer batteries use a liquid or gel electrolyte, which can be less stable and more prone to leakage. Overall, lithium-ion show more advantageous potential in EV batteries than other chemical compounds [8]. The single cells that have been chosen in the design are 18650 lithium-ion cells. These type of cells have been chosen for their characteristics described above, i.e. energy density, cycle life, cell voltage and availability. Moreover, cylinder cells warm up less [3], have a current-cut device inside the cell, provide better structural integrity to the battery cell compared to pouches/prismatic cell, which tends to deform and swell easily when overcharged or placed in a vacuum [9]. Lastly, the 18650 cell size is relatively safe in comparison with other sizes because they heat up less [10]. Specifically, the 'Sony/Murata 18650 VTC5A' was chosen because of its high discharge current capabilities. Sony's 18650 series are also preferred in satellite battery choice, because of its high-voltage per cell, energy density, low cost, weight, and excellent heat transfer for thermal management [11]. This high-performance cell used in this design has a capacity of 2600mAh and a safe continuous discharge rate of 25A, allowing for a lightweight design with minimal cells needed to meet the high amperage demands. An overview of the specifications of this cell can be found in table 6.3b.

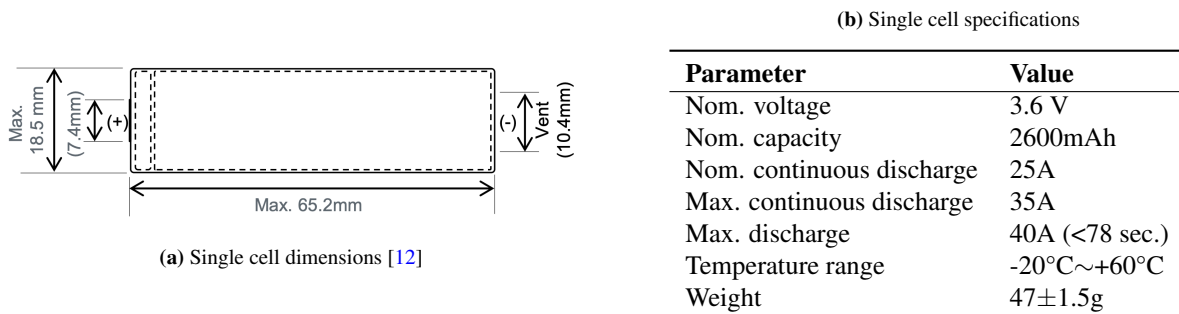


**Figure 6.3:** Specifications of the chosen Sony/Murata 18650 VTC5A cell

#### 6.2.4 Battery Pack

The design choice for the battery packs mainly focuses on incorporating accessibility and modularity. The 40 kg HV battery mass is divided in 4 separate battery packs that can be easily detached from the pod providing greater flexibility and ease of maintenance. A render of one such battery pack is given in figure 6.4 below.

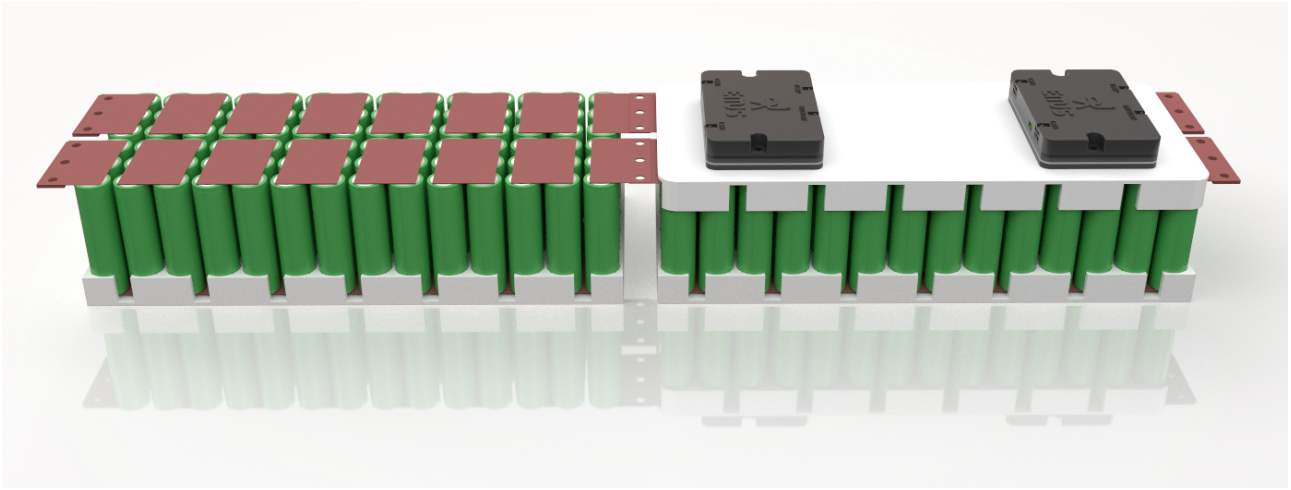


**Figure 6.4:** Render of one high-voltage battery pack without its enclosure

Each *pack* houses 168 battery cells in a 66S3P configuration and has a weight that falls below the maximum 10kg weight a single agent is allowed to lift during the EHW. The design includes modularity by consisting of 4 separate *modules* with a 14S3P configuration, which can be replaced in case of battery failure. Within each module, the batteries are welded to a copper strip to conduct the current from cell to cell. Copper, which has significantly higher conductive properties than nickel, is preferred for welding 18650 cells together due to its increased efficiency and reduced heat production [13]. To ensure that the gauge on the copper strip is large enough to carry the required power, the thickness of the strip is maximized. Laser welding can guarantee a mechanical connection between strip and cell for thicker strips than other welding methods. The bottleneck for the thickness of the copper strip is the wall-thickness of the 18650 battery. The strip can't be thicker than this wall-thickness or else the laser penetrates the the battery and cause internal damage to the cell. The wall-thickness of 18650 batteries is  $300\mu\text{m}$  [14].

Every module is attached to a Centralized Cell Group Module that measures its voltage, current, temperature and state of charge. In every pack, 4 of these modules are placed in series using copper bus bars to achieve the required voltage, as can be seen in figure 6.4. The modules are connected with each other with bolts and nuts to maintain modularity. In summary; 1 module has a 14S3P configuration, there are 4 modules in one battery pack, and every battery pack is confined by a battery enclosure. 4 battery packs are used to achieve the required voltage and amperage, 2 packs in series for the voltage, and a copy of that setup in parallel to reach to amperage.

To prevent individual battery cells from moving, vibrating, or undertaking other motions, they are secured in module holders designed by DH07. Any movement can negatively affect the mechanical connection between the batteries and the copper plates, and cells could collide with each other, causing damage to the batteries. The module holders prevent the battery module from experiencing unwanted movements, thus ensuring the integrity and longevity of the battery system. Its custom design allows for easy removal when necessary, preserving the ease of maintenance. It serves as a dedicated location for the placement of the BMS of each module while also providing protection to the copper strips. The notches on the side of the module holder are meant for the BMS cables to reach each battery cell accordingly.

### 6.2.5 Battery Enclosure

As stated above, the high-voltage battery is split over 4 different packs, where each pack is contained inside its own battery enclosure. The scope of these enclosures, apart from holding the pack together, is to protect the single battery cells from impacts and potential fractures, as well as providing protection against the elements when operating *en plain air*. On top of that, the enclosure is meant to make each battery pack electrically insulated. This way, it can safely separate the agents, bystanders and anything else around from the batteries themselves. This is done by choosing materials that offer high current insulation.

At the same time, the intent is to keep the modules as accessible and modular as possible. To accomplish this, the 4 modules share the same exact design, one that allows for replacing and swapping without constraints. This feature makes manufacturing less complicated and allows for complete freedom in module displacement on the pod.

One major decision in the design of the battery enclosure is whether the enclosure has to be pressurized or not. Partially due to their cylindrical structure, the batteries have been tested to be able to withstand a pressure of 10 mbar. Therefore, a non pressurized enclosure has been chosen. This allows the enclosure to be lighter and more accessible, as well as permitting more design freedom.

The enclosure consists of a top and a bottom part, which are connected using bolts. By removing the bolts, the top part can easily be taken off and the pack is made accessible. The battery pack is placed inside the lower part of the enclosure using a battery holder made with PLA, as shown in picture 6.5. This holder keeps the cells in place and electrically insulates them from their environment. The holder is glued to the bottom part of the enclosure.

The properties of the material used to print the enclosures are carefully selected, together with the manufacturing company, to be able to come out with a material that could give the best performances in regard to its structural, thermal and electrical insulation features. The material selected for the enclosure is then *Nylon 6*. Polyamides, or nylons, are considered industry-best when prioritizing structural toughness and thermal capabilities (i.e. the ability to withstand high temperatures), among others.

The choice of 3D-printing the enclosures is driven by the will for even simpler and faster manufacturing, and it allows for a more custom fitting design. A wall thickness of 5 mm is chosen, given as minimum thickness requirement by the manufacturer.

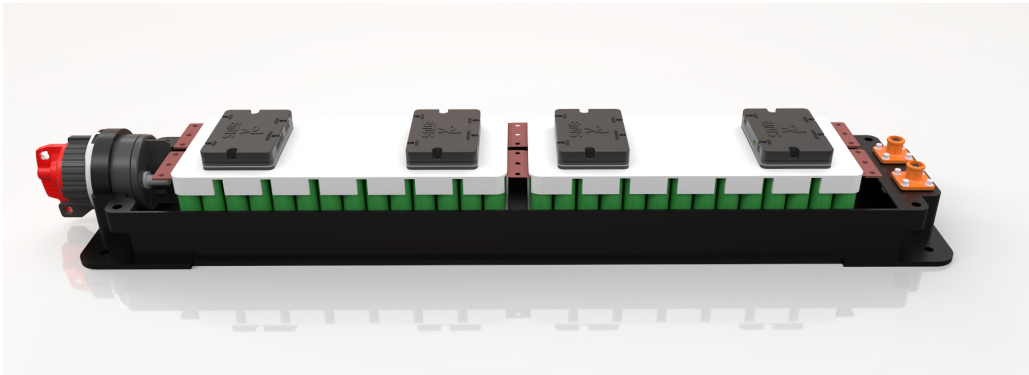


**Figure 6.5:** HV Battery in its lower enclosure

The rigidity of the enclosure is then investigated. This is taken care by simulating its structural behaviour via FEA software Simcenter 3D. The model in picture 6.6 is used. Material properties for nylon were used to carry out the simulations.

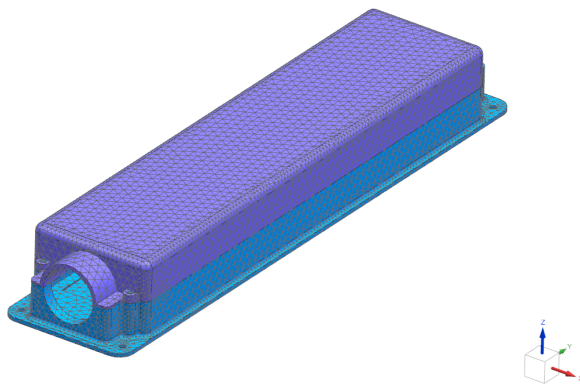


**Figure 6.6:** FEM model of the battery enclosure

Two load cases are studied:

- In load case 1 (6.7) the enclosure is tested for being transported while lifted, holding the weight of the batteries times a safety factor of 2.2.
- In load case 2 (6.8) the enclosure has to withstand an uneven emergency breaking situation, in which the brakes touch the track on one side of the pod first.

Given the symmetry of the design, the load cases apply to both sides of the powertrain floor.

batterypack.enclosure\_fem1\_sim1 : Solution 1 Result  
Subcase - Statics 1, Static Step 1  
Displacement - Nodal, Magnitude  
Min : 0.000, Max : 0.798, Units = mm  
Deformation : Displacement - Nodal Magnitude

batterypack.enclosure\_fem1\_sim1 : Solution 1 Result  
Subcase - Statics 1, Static Step 1  
Stress - Elemental, Von-Mises  
Min : 0.000, Max : 3.347, Units = MPa  
Deformation : Displacement - Nodal Magnitude

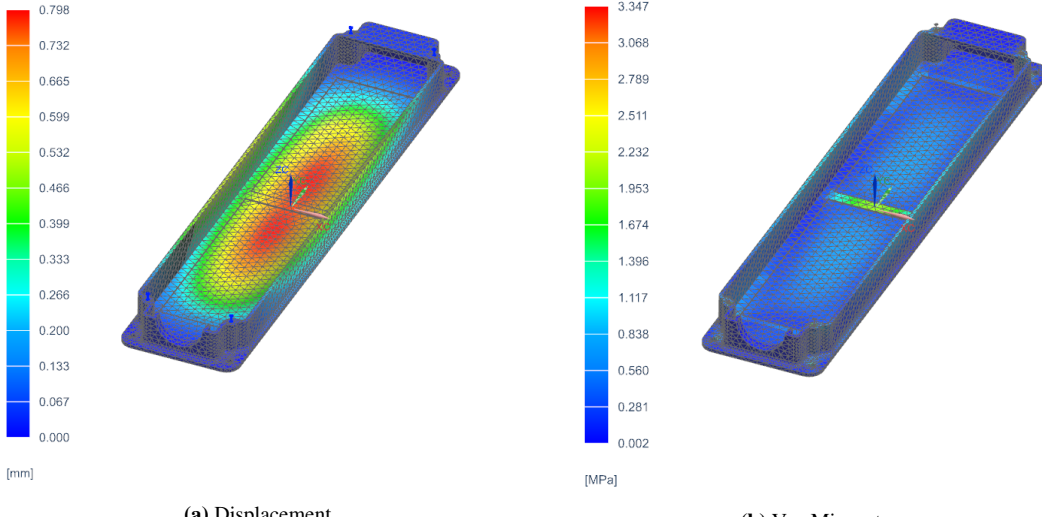


**Figure 6.7: Load case 1**

batterypack.enclosure\_fem1\_sim1 : Solution 1 Result  
Subcase - Statics 1, Static Step 1  
Displacement - Nodal, Magnitude  
Min : 0.000, Max : 0.127, Units = mm  
Deformation : Displacement - Nodal Magnitude

batterypack.enclosure\_fem1\_sim1 : Solution 1 Result  
Subcase - Statics 1, Static Step 1  
Stress - Elemental, Von-Mises  
Min : 0.000, Max : 1.462, Units = MPa  
Deformation : Displacement - Nodal Magnitude

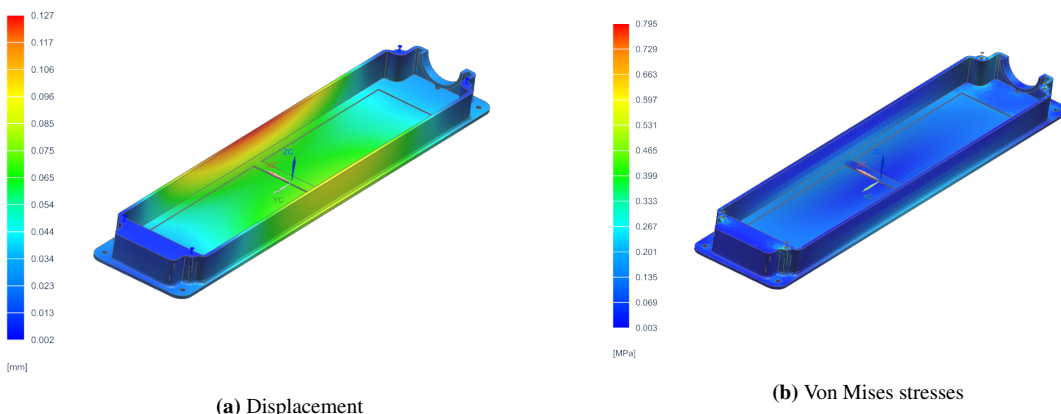


**Figure 6.8: Load case 2**

The results show a maximum deflection under 2mm for both load cases, which is in line with the safety requirements. The same thing goes for the stress concentrations, which fall far below the yield strength values of the materials.

### 6.2.6 Powertrain Floor

The placement of the battery packs is taken care by means of dedicated structures placed underneath the sides of the chassis and above the vacuum box. These structures, which constitute the *Powertrain Floor*, are designed to hold the battery packs in place while allowing the battery system to remain easily accessible at all times, especially with the pod on the track.

Each side of the assembly comprises two 4mm aluminum *chassis brackets*, two 5 mm aluminum *plate brackets*, two 6mm aluminum pull-push rods and an aluminum honeycomb sandwich plate. The structure is held together via M8 bolts and aluminum corner pieces that are bought off-the-shelf. By means of aluminum *sliding rails*, the plate allows the enclosures to be removed by sliding them off sideways (see model in figure 6.9). Each enclosure is then attached to the plate via two M8 steel bolts on the outer side and held onto it by the sliding rails on the inner side. Movement on any axis is prevented.

The choice of creating a completely new structure below the chassis was dictated by the presence of the track's lateral levitation I-beams, which would prevent accessibility to the batteries from the sides during track operations, if these were placed inside the chassis. The structural integrity of the floors is verified using Simcenter 3D.

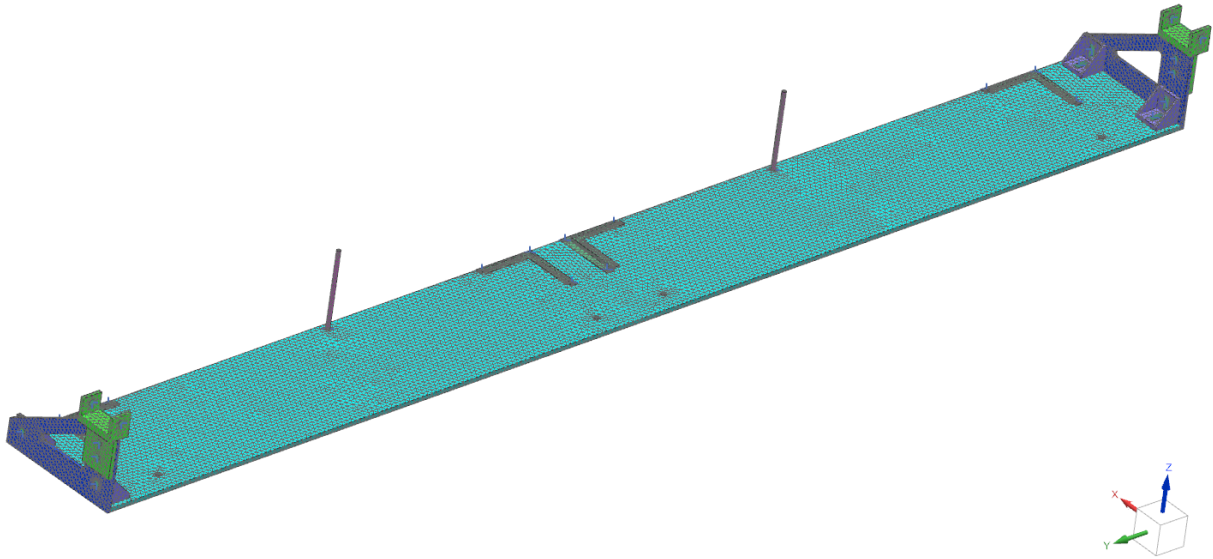


**Figure 6.9:** FEM model of the *Powertrain Floor* assembly

Four load cases are hereby analysed:

- Load case 1: (figure 6.10) the assembly is tested for holding 2 battery packs. This, with a safety factor of 2.2, gives a force of 550N acting on the top surface of the floor.

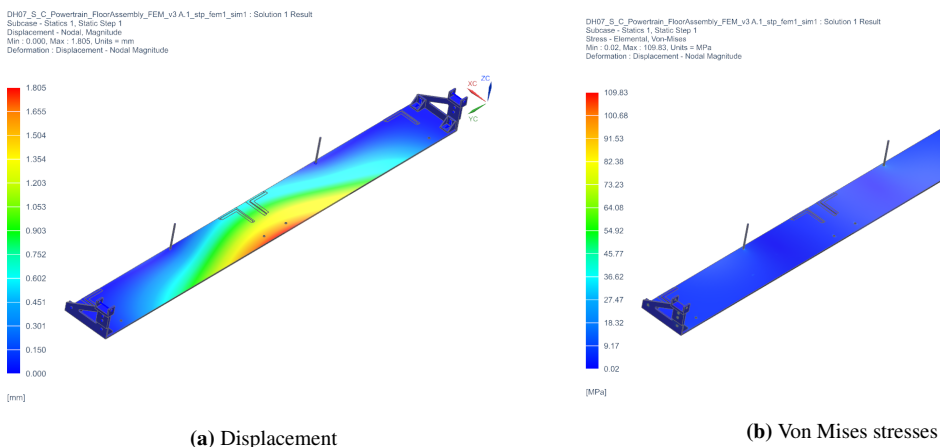


**Figure 6.10:** Load case 1

- Load case 2: (figure 6.11) the structure is tested against an uneven emergency breaking situation. This creates a sideways force on the plate through a reaction moment on the brackets. A safety factor of 2.2 was applied to this load case.

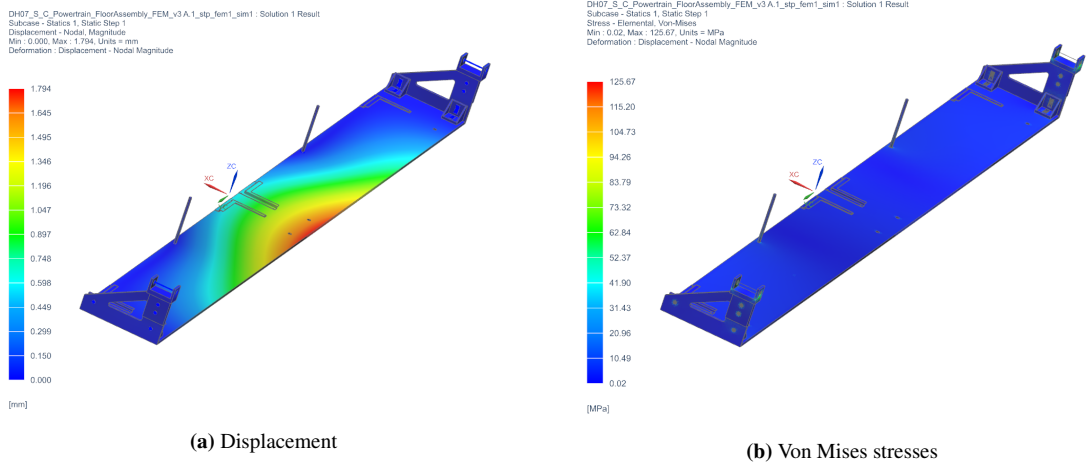


**Figure 6.11:** Load case 2 - uneven emergency braking

- Load case 3: (figure 6.12) the floor has to withstand a situation in which the pod is attracted to the upper part of the track by the vertical levitation magnets. This is most critical for the sliding rails.

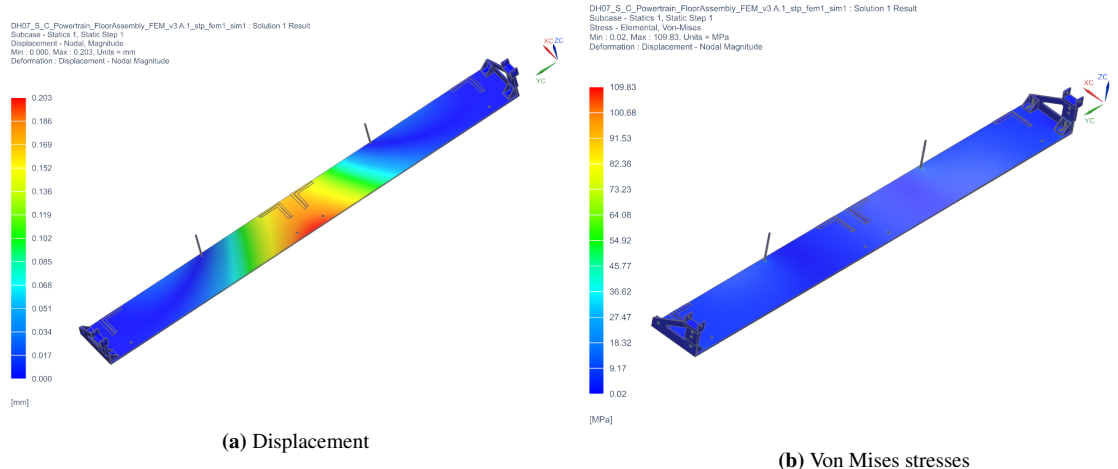


**Figure 6.12:** Load case 3 - vertical levitation pod uplift

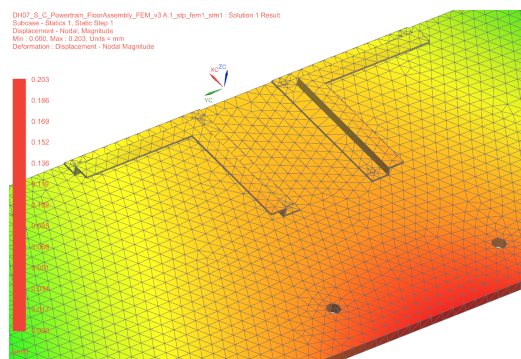


**Figure 6.13:** Detail of the inner sliding rails

- Load case 4: (figure 6.14) the floor has to tolerate a drop test, in which the pod is dropped to the track after vertical levitation is turned off or not working. A safety factor of 2.2 has been applied to the load case.

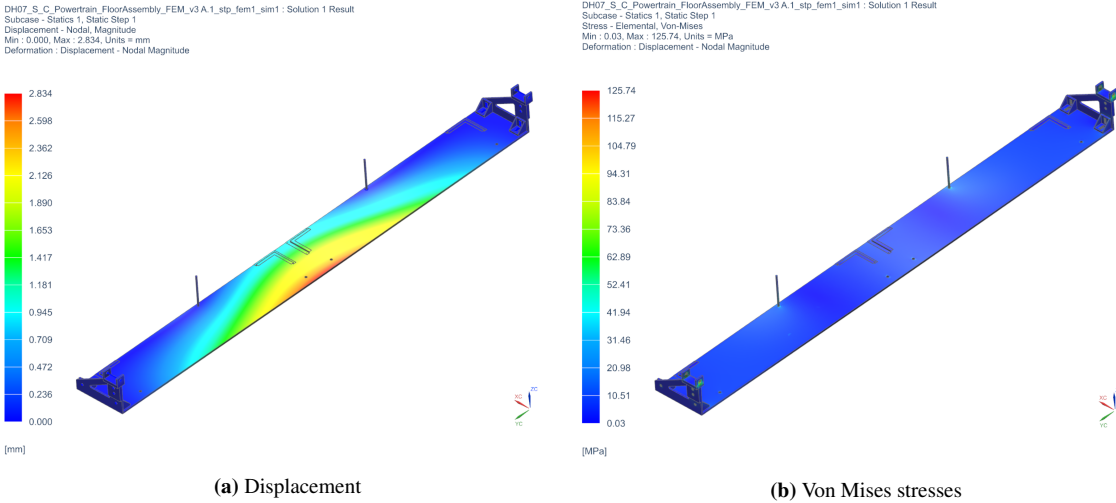


**Figure 6.14:** Load case 4 - drop test

The results show that both maximum stress and displacement are within the safety range of below 4 mm for displacement and below yield strength for the stresses. This entails that the structure is indeed structurally rigid.

To ensure complete safety and meet requirements (DM 4.4.5), each pack is provided with its own MID switch, to be able to singularly be turned on and off.

### 6.2.7 Cables and Connectors

Because of the high-voltage and current that is delivered by the high-voltage battery, it is essential that the corresponding wires and connectors are selected with care. The biggest considerations for picking these connectors are heat and arcing. Since the batteries are located in a near vacuum, connectors become prone to arcing. To calculate the maximum arcing distance in a near vacuum environment the Paschen curve was used, denoted by the following equation:

$$V_B = \frac{Bpd}{\ln(Apd) - \ln[\ln(1 + \frac{1}{\gamma_{se}})]} \quad (6.1)$$

Here  $V_B$  is the breakdown voltage,  $p$  is the pressure in Pascal,  $d$  is the gap distance,  $\gamma_{se}$  is the secondary-electron-emission coefficient (0.01 [15]),  $A$  ( $112.50 \text{ kPa cm}^{-1}$ ) and  $B$  ( $2737.50 \text{ V/(kPa cm)}$ ) are gas dependent coefficients found experimentally [16]. The maximum arcing distance in an environment of 10 mbar at 400 Volts is found to be 2.813 mm,. A safety factor of 2 is added to ensure completely safe operation, which results in a minimum distance of 5.625 mm between any two conductors.

The power that is supplied by the two parallel pack groups is combined and fed into the vacuum box on the side of the levitation department. All connectors and cables in between the packs and the vacuum box are manufactured by Phoenix Contact: "Connector - ES-FT-BPC 16-25 OG"-series and the "Connector - ES-BPC-C 16-25 OG" are both rated for 1500V nominal voltage and 120A nominal current, which far exceeds the maximum expected value of 400V and 63A per pack. The high-voltage cables leaving a single pack have a cross-section of  $50\text{mm}^2$  (7.98mm diameter), this wire gauge size is more than sufficient for the power demands [17]. All high-voltage cables and connectors are orange colored.

The battery cells are interconnected using copper strips, which connect 6 cells at a time; three in parallel and two sets in series. The copper strips are laser welded onto the cells to ensure a safe and secure connection. To prevent overheating, the copper strips are designed to be 0.3mm thick and 52mm wide, to provide adequate current flow while staying within the maximum arcing distance. This design was found to be sufficient after testing showed that the copper strips did not heat up while the desired range of current 25A was flowing through a 0.3mm thick and 17mm wide copper strip, where 25A and 17mm are both a third of what the true copper strip .

### 6.2.8 Heat analysis

Given the hazardous nature of lithium-ion cells, it is commendable to prevent high temperatures (above 60 degrees) in order not to create a harmful environment for both bystanders and the pod. For this, heat tests have been carried out to dislodge any heat event possibility. These tests, conducted by (fast) charging and discharging the cells at maximum

discharge of 30A, showed that the cells do not actually heat up more than 9°C when discharged for at least 60 seconds. Internal resistance  $IR$  of the cells is also taken from these tests to be *0.007 ohms*, which is substantially lower than the data provided by the manufacturer.

Moreover, in order to get a better overview of the heating behavior of the cells, a heat FEA was carried out (see figure 6.15). This showed that, in the conditions the cells are going to operate, risks of overheating are kept to a minimum as the temperature never reached 40°C. Furthermore, this is also avoided by the battery Management System signaling an error message and cutting power off from the system at 55°C.

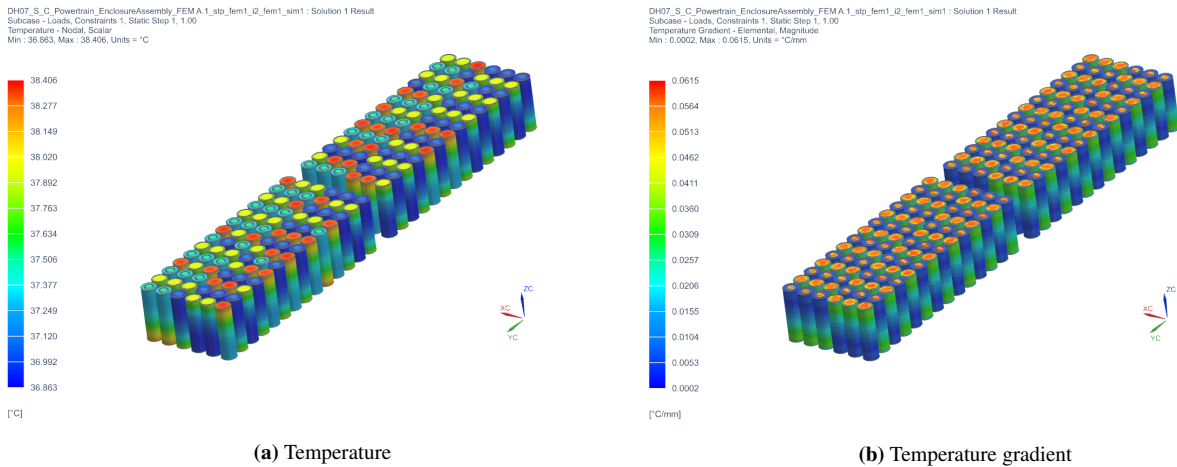


**Figure 6.15:** Heat analysis

### 6.3 Low Voltage Battery

All subsystem on the pod, including the sensors, brakes, propulsion and levitation motor drives, PCBs, BMS and localization system, requires low-voltage power to operate. To provide this power, a low-voltage battery is designed. The aim of this chapter is to elaborate on the design of the low-voltage battery. More information on its control, safety and power distribution can be found in chapters 6.4 and 6.5 respectively. The requirements for the low-voltage system are displayed in table 6.9. PO.LV.T.2 states that the LV-system should be able to last 2 hours, significantly longer than the HV-system is designed to last (PO.HV.T.2). The reason of this augmented safety factor is because the low-voltage battery needs to provide energy to certain systems even in between runs, e.g. battery management systems.

**Table 6.9:** Low voltage requirements

ID	Requirement
PO.LV.T.1	The low-voltage system shall be able to provide the peak power of 1095W for when all systems are on simultaneously.
PO.LV.T.2	The low-voltage system shall be able to deliver sufficient power to complete 10 runs, i.e. run 2 hours, without recharging.
PO.LV.T.3	The low-voltage system shall provide all elements of the pod with the required power and voltage for their correct functioning during all stages of idle and active pod operation.
PO.LV.T.4	The low-voltage system shall be able to operate in a near vacuum environment of 10 mbar.

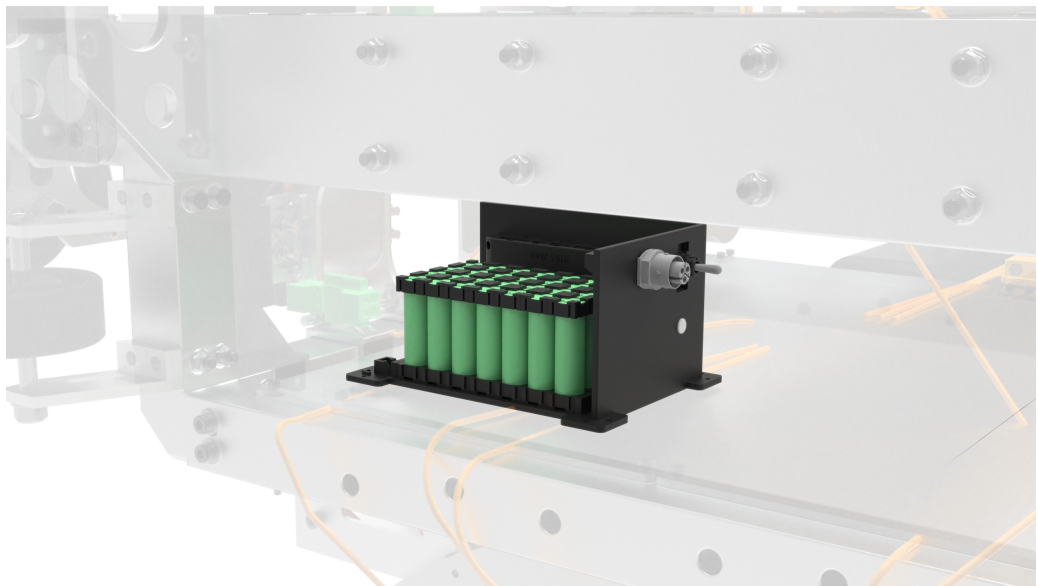


**Figure 6.16:** Render of the low-voltage battery inside the pod with the enclosure left out partly

### 6.3.1 Topology

The low-voltage battery pack consists of a 7S4P configuration of lithium-ion cells. This configuration is chosen by analyzing the power demands of all low-voltage subsystems to find the maximum discharge, as well as the necessary capacity to perform a run. An overview of all subsystems that require low-voltage power is given in 6.13. By analyzing these requirements, a peak power demand of 840 W is found. When booting 120W of power is used for 300 seconds of preparation time. When the entire system is on 430W of power is required. System checking will take 60 seconds, the bidirectional cruise is the longer lasting run of the two intended runs, and will take about 30 seconds. Preparing, checking, and completing one run will therefore require a total energy of 20.7Wh. To complete 10 runs, and applying a safety factor of 1.44 a total required energy of 298Wh is obtained. The 7S4P cell configuration fulfills the power demand as well as the capacity demand. By putting 7 cells in series a nominal voltage of 25.2 V is achieved, which is sufficient to power all low-voltage systems. More information on the cells is given in 6.3.2. The complete specifications of the LV battery pack are shown in 6.10 below.

**Table 6.10:** Low voltage pack specifications

Specification	Value	Unit
Configuration	7S4P	-
Number of cells	28	-
Nom. Power	1.024	kW
Max. Power	1.536	kW
Nom. Voltage	25.2	V
Nom. capacity	322	Wh
Mass	1.372	kg
Dimensions	80x142x69	mm <sup>3</sup>

### 6.3.2 Cell Choice

The cell chosen for the low-voltage battery is the NCR18650BD Panasonic 18650 battery. This cell has been carefully selected for its relatively high capacity and its adequate discharge rate. Moreover, a lithium-ion 18650 cell has been selected for numerous reasons, like vacuum compatibility and energy density, all of which are listed in section 6.2.3 on the high-voltage cell choice. The specifications of the low-voltage battery cell are given in table 6.11 below.

**Table 6.11:** Low voltage cell specifications

Specification	Value	
Nom. voltage	3.6	V
Min. capacity	3100	mAh
Nom. capacity	3180	mAh
Max. continuous discharge	10	A
Max. discharge	15	A
Temperature range	-20~+60	°C
Height	65.30	mm
Diameter	18.50	mm
Weight	49.5±1.5	g

### 6.3.3 Enclosure

The enclosure of the low-voltage battery pack protects it from external loads and holds the pack in place. Moreover, the enclosure electrically insulates the battery from its environment. To do this, ABS plastic material is used.

A FEM analysis of the heat generated by the battery is shown in 6.17 below. The results of this analysis show that the temperature does not reach above 42°C, which is safely under the cutout temperature for the cells.

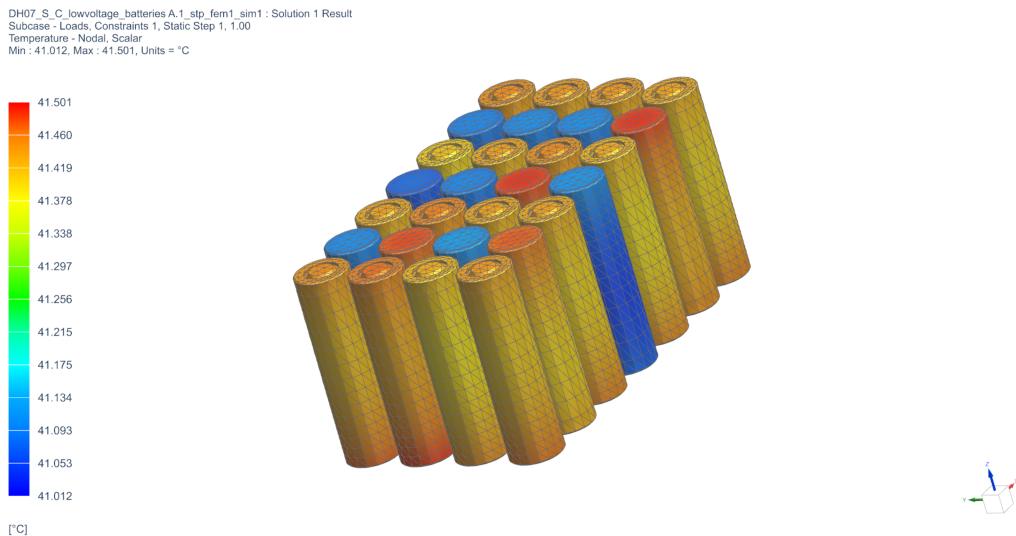


**Figure 6.17:** Heat analysis of the low voltage battery pack - absolute temperature

### 6.3.4 Cables and connectors

The battery cells are interconnected by copper strips. These are laser welded onto the batteries to guarantee a rigid connection. The copper strips are 0.3mm thick and 7mm wide. Each of the 4 cells in parallel are connected to its successor in series. The 4 cells in parallel are connected with an additional strip. The electrical power leaves the LV-enclosure by a panel feed-through - QPD W 4PE6,0 12-20 M25 1,0 BK, by Phoenix Contact. This power outlet is rated for 690V and 40A, far exceeding the power demands of the low-voltage system. The low-voltage cables are connected to the power distribution board by a PCB terminal block. Here, no soldering is needed to maintain a modular design. The data feed-through used is a circular push pull connector by LEMA.

## 6.4 Power Control System

As lithium-ion batteries are very flammable, it is essential that their operation is performed correctly and safely. To do this, a power control system is implemented. This control system consists of a powertrain controller (PTC) two battery management systems (BMS) an insulation monitoring device (IMD) and contactors. As a last layer of safety, an emergency switch is also installed.

The powertrain controller is the main entity within this power system, and has control over all other subsystems within it. It interprets all measured data and makes the appropriate decisions based on it. Additionally, it communicates with the rest of the systems located on the pod. More information on the controller is given in 6.4.1.

To control the system in a structured way, the PTC makes use of a finite state machine (FSM) software architecture. This ensures that the system is always in exactly one predefined state. On the finite state machine is elaborated in section 6.4.2. There are two battery management systems on the pod, one for low-voltage and one for high-voltage. These BMS's are responsible for monitoring the batteries by continuously measuring their voltage, current, state of charge and temperature. These are explained in 6.4.4 and 6.4.5.

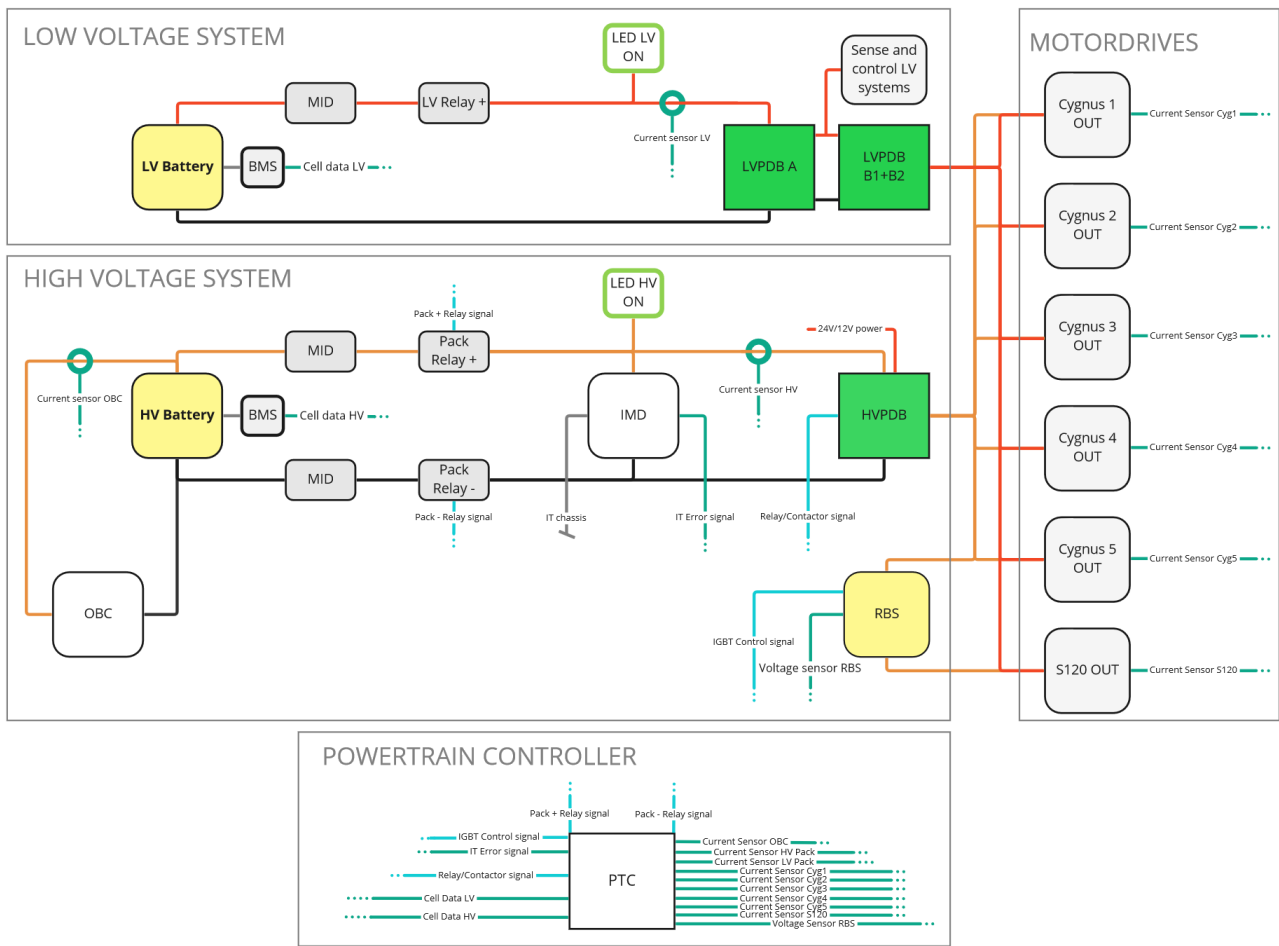


**Figure 6.18:** Schematic of the full power system and its most prominent components.

**Table 6.12: SAFETY ELECTRONICS**

Component	Manufacturer	Model	Qty
Powertrain Controller	Delft Hyperloop		1
HV BMS - Control Unit	EMUS	G1 BMS Control Unit	1
HV BMS - Monitoring Unit	EMUS	G1 Centralized CAN Cell Group Module	16
HV BMS - Current sensor	EMUS	G1 Loop Style Dual Range Current Sensor	2
HV BMS - Temp. sensors	EMUS	ETS04-45	48
LV BMS	EMUS	BMS Mini 3	1
Insulation Monitoring Device	Bender	IR155-3203	1
HV Contactors	Gigavac	GV200 CAC-1	4
Emergency switch	Schneider Electric	Harmony XAP Emergency Stop Switch	1

#### 6.4.1 Powertrain Controller

The Powertrain System Controller (PTC) is a critical component of the powertrain system that enables seamless communication and efficient operation between various subsystems. It is responsible for monitoring and controlling critical parameters, such as temperature, voltage, and current, across the entire powertrain system. It monitors the health and behavior of high-voltage and low-voltage battery cells, and reports faults and power limitations. Additionally, the PTC runs a finite state machine for the high-voltage system and manages the high-voltage interlock loop, setting alerts and acting on unexpected interruptions. It also calculates the power available at any time and manages the charge and fast charging capabilities of the pod charging system. The PTC uses an ARM based micro-controller with extended system checking capabilities that provide fault coverage on the hardware logic associated with the execution of powertrain FSM states and processes. Its fail-safe mode ensures a safe system shutdown in events of errors or pod malfunction, which is crucial for a complete system analysis. The following section includes the technical details of the PTC, its functionality, and the critical role it plays in ensuring safe and reliable operation of the powertrain system. The PTC is located centrally on the pod within the ladder frame as can be seen in Figure 6.19 below.

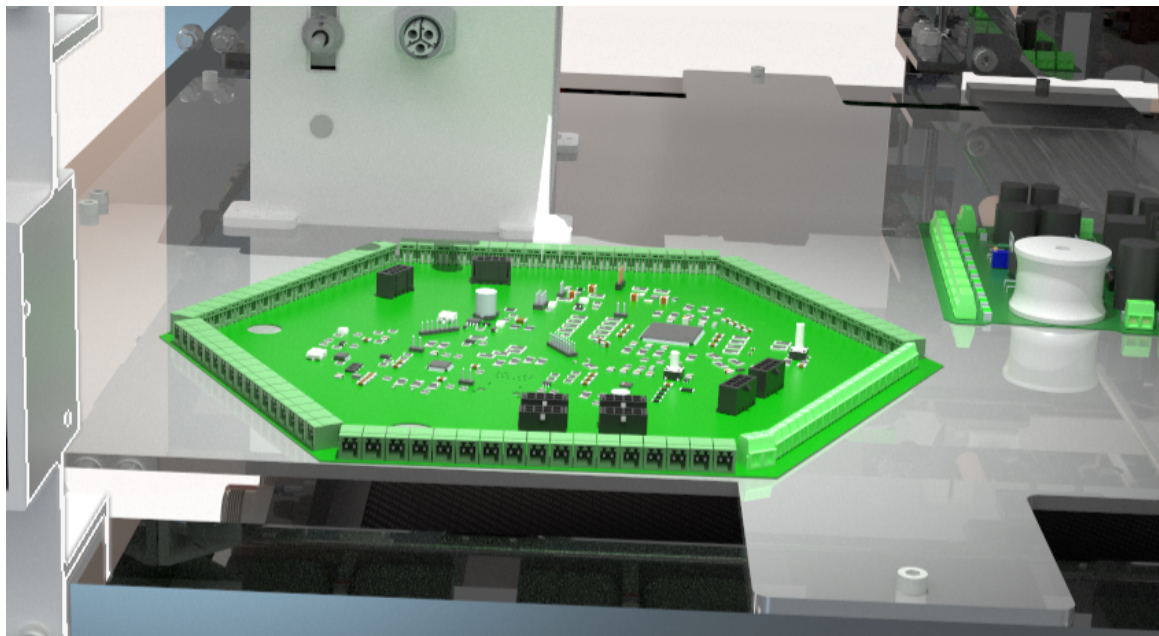


**Figure 6.19:** Render of the powertrain controller (without wires)

#### Features

The PTC exchanges data between the previously mentioned subsystems in the powertrain. This process must run reliably since all subsystems depend heavily on one another. The PTC uses a 32-bit M7 micro-controller, which has extended system checking capabilities. With this, the PTC has fault coverage on the hardware logic associated with the execution of the powertrain states and processes, this includes detecting temperature sensor faults or battery cell failures. Systems

checks are run during the SYSTEM CHECKING state of the finite state machine (see 6.4.2) at start up when the LV battery is turned on and continuously run after the HV battery is turned on. The PTC has control over the powertrain relays which are toggled based on the FSM state and data received by sense and control subsystems.

All data gets logged in the sense and control processor to later examine in events of faults or for further system optimizations. Powertrain temperature data is analyzed in real-time by the PTC in order to quickly step in and take action in events of sudden abnormal rises or drops in values. The controller has current and voltage monitoring capabilities across the entire powertrain system. It must ensure that the subsystems do not exceed their specified current draw during a certain FSM state or event and that the voltages do not fall short or exceed the specified safely operational values and remain within the set thresholds. In events of error or pod malfunction, the PTC takes precautionary measures to ensure a safe system disable or in extreme situations a complete HV and LV shutdown. Before the system is disabled or cut from a supply, it operates in a fail-safe mode until it completes the currently running process and makes sure that the data logging process is completed after the last running process. This is crucial to enable full fault analysis and system optimization. The controller can initiate a fail-safe mode where the pod is slowed down or brought to a standstill to prevent further damage or injury. This mode of operation is designed to ensure that the system can still operate safely in the event of a subsystem failure.

The PTC monitors the voltage levels to prevent over- or undervoltage of the levitation and propulsion systems and calculates the available number of runs it can successfully complete with the current battery capacity and health data. This analysis is influenced by the current draw over a certain period which can be used to generate a prediction of how many runs can be completed or whether the pod will complete the current run. This analysis is sent to ground control which will decide to proceed with the run or verify the error and subsequently let the PTC plan a controlled pod standstill event.

The controller communicates with the powertrain subsystems, such as levitation and propulsion. It additionally communicates with the sense and control processor which sends subsystem and peripheral error events which are handled accordingly by the PTC. Ground control can send instructions to manipulate the pod behaviour which can be in the manner of event manipulation or individual instructions. During events of external subsystem failures, the sense and control processor will signal the faulty subsystem location and send a specific error type which in turn sends the PTC into a corresponding FSM state or triggers the PTC to execute a certain instruction to either disable the supply to that subsystem, plan a pod standstill, disable the HV battery or plan a complete HV and LV shutdown.

A highly efficient control algorithm is implemented which is based on an event-driven FSM. This is used in order to make the code better-suited for fast debugging and troubleshooting. It is implemented by both of the major controllers on the pod (PTC and MCU 7.5.2).

The PTC monitors the state of all powertrain relays and high power fuses during the SYSTEM CHECKING state, this is done to ensure all safety features can be deployed during operation and are not faulty.

The High Voltage Interlock Loop (HVIL) is interrupted when the pod is being maintained unexpectedly or when the aerodynamic shell is removed exposing the powertrain system. Additionally, since the pod chassis is a floating ground, the systems are working in an IT (interrupt terra) system.

An insulation monitoring devie (IMD) is used for ground fault detection. The IMD sends error signals to the controller during an event of ground fault. When these are detected the controller initiates a complete shutdown sequence to prevent further damage to the system.

## Architecture

In the powertrain system, a single centralised controller monitors all incoming and outgoing data to the subsystems, including current monitoring, acceleration and deceleration control, energy management and error analysis. An overview of all components that are in contact with the high voltage controller is given in 6.20 below.

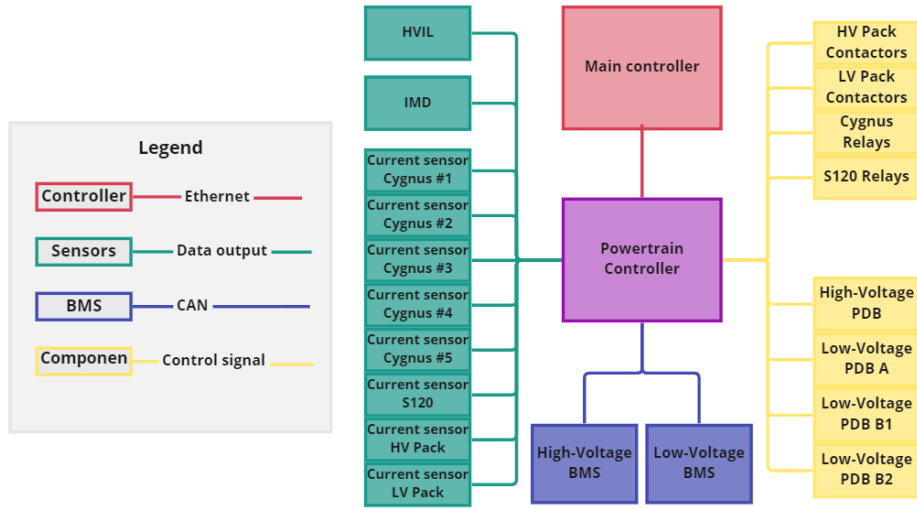


**Figure 6.20:** Overview of the powertrain controller architecture

One of the advantages of using a centralised system is that it optimizes the power system as a whole, taking into account factors such as energy management as previously mentioned and event-based safety features which are only triggered when crossing above or below a threshold set for a particular event. The controller can provide adjusted acceleration and deceleration profiles for the actuators to minimize energy consumption while providing a smooth operation for a scalable concept.

This system operates based on the feedback mechanisms in the sense and control subsystems which monitor data based on sensor feed-backs. The sensors detect the position, speed, and other critical parameters of the pod, these sensors send their data to the centralized controller, which uses it to make decisions about the operation of the system.

Overall, the powertrain centralized control architecture is designed to provide reliable and safe operation of the pod, while maximizing performance and efficiency. The architecture is complex and requires careful design and integration with all subsystems, but it provides a high degree of control and flexibility in managing the operation of the pod.

#### 6.4.2 PTC Finite State Machine

The powertrain system makes use of a finite state machine to design and implement the control system it is meant to perform. The system is always in exactly one state, and it transitions from one state to another based on inputs and rules that govern the system's behavior.

The finite state machine of the powertrain system includes states which are run during all phases leading up to the start of a run. These states ensure a reliable system checking before getting ready to perform careful sensor readings, calculations and mapping of the analysed or obtained data. This is done so that in turn the pod is capable of performing runs reliably and eliminating any possible chance of error or an escalation of certain discovered errors, by taking precautionary measures and simultaneously providing a real-time data analysis to ground control on all obtained and analysed data readings. Once the pod health is checked and prompted to be in a qualified state to perform a run, the PTC will proceed to go through the states to start performing a run. The pod will start the routines necessary to start levitating, accelerating to the specified velocity and cruising at the target velocity in a reliable and safe manner. After the target position is reached, the PTC will signal the subsystems to start decelerating and coming to a controlled standstill. In an event of a subsystem failure, the PTC will take action to enter a fail-safe mode and bring the pod to a standstill as fast as it can happen safely. The PTC FSM is designed to react to sensor readings based on the state it is in. For example, during the ACCELERATING state, the propulsion subsystem is allowed to draw a current set at a high value for the upper threshold limit and this would not trigger an error if the propulsion coils would draw a current slightly under this limit. However, if this same current draw value would be sensed during the CRUISING event, a propulsion error will be triggered for over-current protection. This is done to enable versatility with a high focus on scalability. An overview of the entire finite state machine is shown in 6.21. As can be seen in the picture, there is a strict separation between states where the pod is safe and unsafe to approach. Whenever the HV power line is live, the pod goes into the unsafe state which means that no person is allowed to touch or come near the pod. This is to ensure safety of bystanders and engineers. Below figure 6.21, the purpose and functionality of every state is further elaborated.

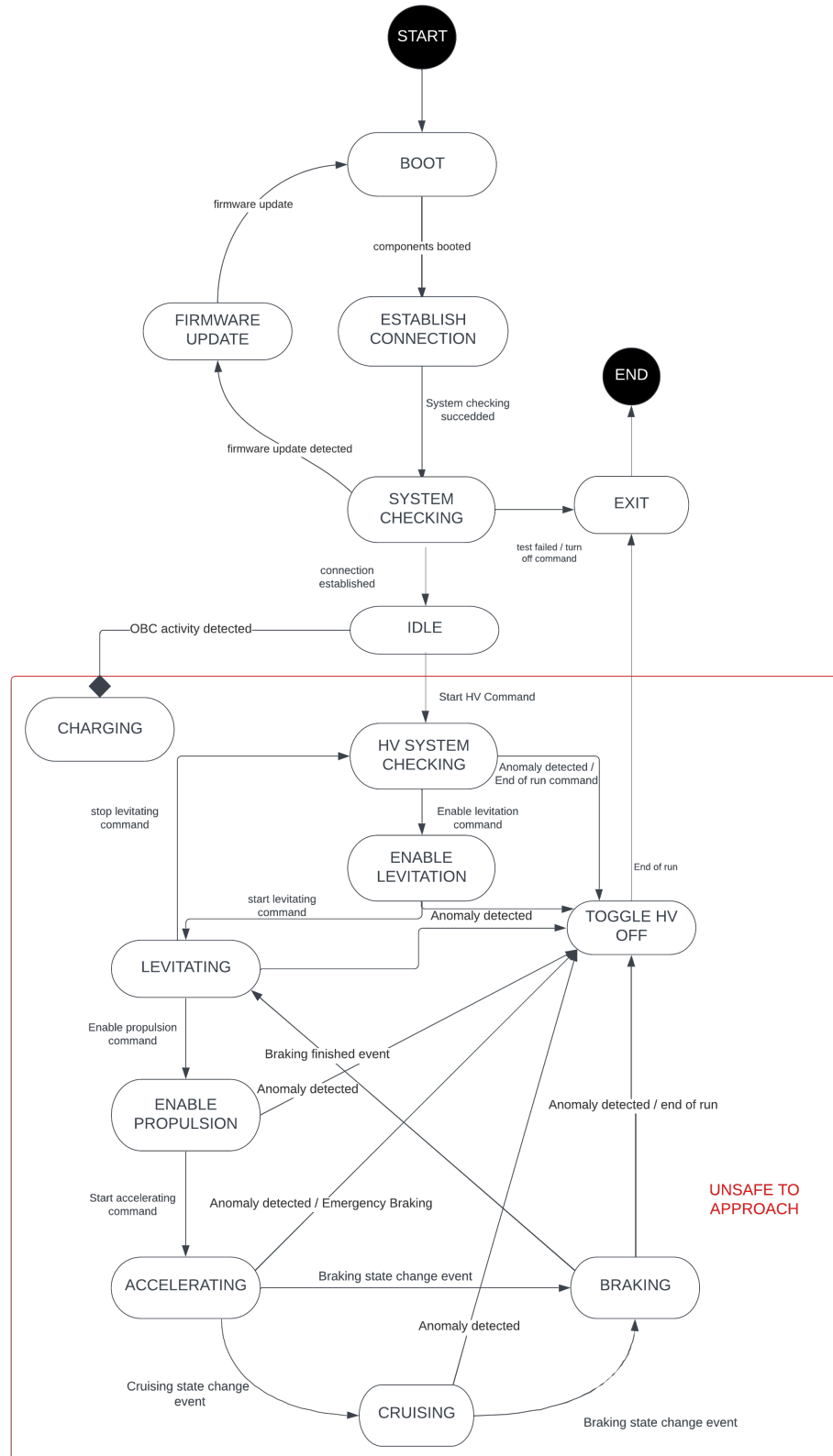


**Figure 6.21:** The Finite State Machine of the Powertrain with all the states and transitions

BOOT

During boot state, the LV battery is switched on and most low-voltage devices, including the PTC, start to receive power.

The systems are initialized and are prepared for operation. One of the processes ran during this state is the POST (power-on self-test), hardware and software initialization, system configuration and calibration. Once these processes are successful, the PTC proceeds to do system checks and establish connection to the sense and control processor. If the BOOT state fails, SYSTEM CHECKING will send the PTC to the EXIT state and maintenance will be required on the pod.

### ESTABLISH CONNECTION

During this state, the PTC will attempt to establish connection with the sense and control processor through Ethernet. There will be three attempts in total to connect, if all of the attempts fail, the PTC will enter the SYSTEM CHECKING state and display an LED sequence for connection failed. On the aerodynamic shell of the pod an LED PCB is mounted which consists of eight LEDs in total. Two of them are uncontrollable and light up as soon as the HV battery and LV battery are switched on. The two non-RGB LEDs for HV and LV are independent of each other and are purely dependent of the battery packs. The six other RGB lamps are software controlled to display error sequences when connection with ground control is failed. Since it cannot be seen what the pod is experiencing, a visual indication of the specific reasoning behind the connection fault is necessary for safety. It could be possible that multiple critical errors are present, which can be displayed by this LED board and seen from a distance. This is particularly useful in order to approach the pod prepared and with an expectation of where the error is located, purely to take high precautionary measures. Three of the RGB LEDs are used by the power system and the other three by sense and control.

Once connection is successfully established, the PTC will send the acknowledgements or warnings created during the BOOT state. These statements and additional data are extensively sent to the MCU in the SYSTEM CHECKING state and will be further explained. Once the connection between PTC and MCU is successful, and during the SYSTEM CHECKING state, the PTC detected activity from the OBC, the FSM will proceed to the IDLE state and from there to the CHARGING state.

### SYSTEM CHECKING

The PTC enters this state after the low-voltage battery is switched on and ESTABLISH CONNECTION is successful or fails. During this state, the controller pulls down the HV PDB (6.5.3) relay control pins and consequently opens all relays on the HV PDB. This is done to reset the pin states and make sure that none of the relays are closed after a sudden power disconnection or any type of unplanned event taking place while HV is powering the subsystems. Note that during the PTC SYSTEM CHECKING state, none of the subsystems are receiving HV power and the main HV battery contactors are open by default since the relays are of normally open type. The control pins for the two HV battery contactors are also pulled down and resetted to open the relays, if an unforeseen shutdown or power disconnect took place before the current SYSTEM CHECKING.

During the SYSTEM CHECKING state, the OBC (On-Board Charger 6.6) current draw will be monitored to check whether the pod is being charged or not. After this check, an interrupt service routine is set to be triggered if the current draw exceeds a set threshold. This ISR can be triggered and is active during all of the states in the FSM. When the ISR is triggered, the PTC FSM will proceed to transition directly to CHARGING state. However if the PTC senses that the OBC is actively charging the HV battery when the SYSTEM CHECKING state initiates, it will proceed to the IDLE state. This process will be further explained in the IDLE and CHARGING states.

In this state, the HVIL is checked for the first time and an ISR will be active so that it can be triggered during all the coming states. The same will happen for the IMD. If any of these are already triggered in SYSTEM CHECKING, the pod will transmit a HVIL error and a ground fault error to ground station. If communication is not yet established between ground station or if it fails after three attempts. The error LEDs will display a unique sequence of colors indicating the specific errors. The LED error indicators will be explained in detail in the 6.4.3 section below.

Additionally, in this state, the LV battery current draw is monitored and a low-value maximum threshold is set, if the battery is supplying a larger current than the maximum limit for longer than the set amount of time, a LV over-current error is triggered and the pod will plan a shutdown. Further the levitation and propulsion driver currents are read to make sure they are operating as intended. If either is sending abnormal readings, a propulsion or levitation error is triggered for over-current and the powertrain plans an emergency shutdown, since in this state the contactors are all set to open and these errors are triggered in this state only if the powertrain powerlines, control lines or the contactors contain a fault.

Most importantly, during this state, the high- and low-voltage battery management systems send all the necessary data regarding the battery health, charge level, temperatures and cell voltages. Both BMS's send the module voltages, DOD (depth of discharge) values, a derived SOC (state of charge) value by performing coulomb counting internally and send the constantly monitored temperature of the pack cells. All the previously mentioned parameters are utilized to calculate return data to send events and acknowledgements to the ground station and sense and control processor. After analyzing the voltage, the PTC returns a one of the following acknowledgements or warnings, "OVER VOLTAGE", "UNDER VOLTAGE" and "OPTIMAL VOLTAGE". The same is done for the battery currents and the the following are returned, "OVER-CURRENT", "SHORT-CIRCUIT" and "OPTIMAL CURRENT". The HVIL state is acknowledged by returning, "HVIL SAFE" and "HVIL TRIGGERED". The following are returned regarding the OBC behaviour, "OBC ACTIVE" or "OBC INACTIVE". There are driver acknowledgements aswell, which include, "DRIVER OPTIMAL", "DRIVER UNKNOWN" and "DRIVER ERROR". As previously mentioned, the IMD state is also returned, "IMD SAFE" and "IMD TRIGGERED". The current state of charge is returned and a result of coulomb counting in the BMS, which is derived from the depth of discharge to see where the BMS has to restart coulomb counting to pick up the charge level from the previous session and check how much the charge has reduced since the previous shutdown sequence. Finally, the temperature readings are analyzed and the following return statements are generated, "TEMP HIGH", "TEMP ERROR" or "TEMP OPTIMAL".

### CHARGING

During this state, the PTC will continue to perform the tasks in the SYSTEM CHECKING state and additionally perform the ones for the CHARGING state. In this state, the PTC continuously monitors the OBC current draw to optimize the charging sequence during FAST-, NOMINAL- and SLOW-CHARGING. Firstly when the PTC realises that the pod is being charged, it opens the main HV battery contactors, cutting off the power to HV PDB. This overrides even if the contactors were already open. Next, the LED board will start blinking with the most left LED in the red color and building up to green, which indicates a fully charged HV battery. The most right LED indicates the charge level of the LV battery which is also able to be charged at the same time. The PTC monitors the SOC of the entire battery in real-time and triggers when the target charge is reached. This target can be calibrated and adjusted at any time. The charging states are processed and based on the SOC, the PTC switches from slow charging to nominal charging or fast charging and vise versa, the thresholds for transition events are calibrated in the PTC code. Also, the PTC can signal to cut and supply power to the modules individually, for when a module is charged quicker or slower than the other modules.

### IDLE

During IDLE the PTC does continuous system checks and awaits instruction from the ground control to prepare for a run or take a certain safety action. If all goes well in the SYSTEM CHECKING state, in this state, the PTC constantly pings the ground control with the following acknowledgements, "Powertrain ready", "HVIL safe", "Levitation optimal" and "Propulsion optimal". A real-time value for the SOC is pinged, along with the HV battery voltage, individual module voltage, cell temperatures, powertrain relay data (this includes the state of the relay which is open or closed, and the address of the specific relay in the entire powertrain system). The PTC also sends the number of runs that can be completed, which is calculated based on the received battery data. Also, a live representation of charge cycles performed on the batteries up to this point is sent. LV and HV power consumption in real-time is continuously sent to ground control for sanity checks by ground control engineers. The overall efficiency and the individual efficiency of subsystems are also sent to ground control and used for fault analysis and system optimization.

In this state, ground control sends the "Start HV" command and this sends the PTC to the HV SYSTEM CHECKING state. This state sends the pod to the UNSAFE TO APPROACH mode. After the IDLE, all of the processes performed by the PTC will continue so that the ground station has all of the powertrain statistics of the pod in real-time.

### HV SYSTEM CHECKING

As soon as ground control signals the PTC to arm the HV battery to supply the powertrain, the PTC closes the HV battery contactors and makes sure that by doing so, everything remains below the maximum thresholds to return the acknowledgement, "HV ready". After that, the HV data is sent in real-time to ground control and the drivers are ready to receive power. If in this state a threshold is exceeded, an HV system error is triggered and the FSM proceeds to toggle

the HV off. During this state the pre-charge relays for all drivers are closed to charge up the input capacitors and get them ready for the run.

#### ENABLE LEVITATION

The ground control signals the PTC that the cygnus drivers for vertical and lateral levitation must be enabled. The high current relays for the levitation drivers are shut, and the pre-charge relays are afterwards opened for all of the drivers. Levitation is now able to draw their currents that have a set maximum threshold limit in the PTC which is being monitored and checked for potential errors.

#### LEVITATING

The pod is now fully levitating and has no physical contact with the track. The PTC carefully monitors the powertrain to make sure that the power draw is within expectations. The drivers are allowed to draw their maximum current for a period of 1 seconds without triggering a levitation over-current error.

#### ENABLE PROPULSION

Ground control signals the PTC to close the high current relays for propulsion and afterwards open the pre-charge relays. The regenerative braking system provides a line voltage value and the PTC monitors this to prevent over voltage that trigger an operation error in the levitation drivers. The regenerative braking system contains a line voltage feedback sensor to provide an indication on when the insulated-gate bipolar transistor (IGBT) gate needs to get activated to protect the high voltage line and send the current to the braking shunt resistor. During this state, the voltage sensor is read carefully to make sure that the pod is operating as intended.

#### ACCELERATING

In this state, the pod is accelerating to reach a set velocity, after which it maintains the velocity until the end of the run. During ACCELERATING, both levitation and propulsion will draw their known maximum currents. This is authorised by the PTC since it is expected and planned to happen. Therefor the current error thresholds are set higher than the ones set during the ENABLE LEVITATION and ENABLE PROPULSION states. The actuators propelling the pod, will create an upward force that needs to be countered by the levitation actuators, therefore the power consumption of the pod will be maximum during this state. This is held into account in the PTC and ground control is continuously monitoring the powertrain system data in real time to ensure all subsystems behave as intended.

#### CRUISING

After reaching the set velocity, the drivers maintain it until the end of the track is reached. The levitation drivers modulate the current draw of the coils in the vertical and lateral system to make the integration with the propulsion system run flawlessly. During this state the levitation drivers, draw a minimal amount of current and the maximum threshold for over-current is reduced to trigger at a lower value. Propulsion, similarly, draws a reduced amount of current and the same applies for the thresholds set for their drivers.

Any anomaly detected by the system, will trigger the previously mentioned safety features such as levitation errors, propulsion errors, HV battery errors, etc. These errors will send the FSM to TOGGLE HV OFF, and automatically trigger the emergency brakes, since the emergency brakes are controlled by an AND gate with the HV battery influencing the behaviour of the input of this logic circuit. This circuit is explained in the 6.4.3 section bellow.

#### BRAKING

The regenerative braking circuit is monitored closely during this state, since the propulsion system is not drawing current anymore, but supplying current back into the system. If the voltage exceeds the set maximum threshold, the braking shunt resistor will be dissipating the energy pumped into the system. In this state, the emergency brakes are deployed by signaling the ANG gate circuit from the PTC. If an error occurs in the powertrain system before the PTC can signal the brakes to deploy, the brakes will still function when HV is cut off to the system, thanks to this AND gate circuit. While braking, the system checks whether the pod is decelerating and if the power consumption is approaching zero. If the pod is behaving different to what is expected, the FSM will immediately proceed to the TOGGLE HV OFF state. This ensures the emergency brakes will be deployed by force. Otherwise, the HV remains on until the pod comes to standstill and afterwards, the FSM transitions to TOGGLE HV OFF.

TOGGLE HV OFF

After bringing the pod to a controlled standstill, the brakes remain deployed while the HV line of the powertrain is still live. In this state, the PTC signals the HV PDB high current relays open and in turn also opens both HV battery contactors. Now the powertrain is no longer under high voltage and the FSM proceeds to finish logging all the data it processed during the run and sending it to the sense and control processor and ground control. After the last logging process, the FSM proceeds to the EXIT state.

EXIT

After a run, the pod is ready to run a shutdown sequence and have the LV battery supply cut from the system. The necessary data is stored in the sense and control processor memory card and power can be turned off without data being lost or interrupting the system.

#### 6.4.3 Hardware Design

##### MCU

The selection of the appropriate microcontroller unit (MCU) is a critical step in designing a controller board with high-performance capabilities. The chosen MCU for this application is the STM32H743ZIT6 chip from ST microelectronics, which is a highly advanced and versatile device that offers a broad range of features and functions. To ensure optimal performance of this MCU, two external oscillator crystals have been added to the PCB design. These crystals provide a stable clock signal to the MCU, with frequencies of 32 kHz and 25 MHz, respectively, in accordance with industry-standard best practices.

Furthermore, the phase-locked loop (PLL) in the MCU is used to achieve a high clock speed of 480 MHz, enabling the device to process data at high speeds. The MCU requires a power supply of 3.3 V, which is not directly provided by the LV PDB (6.5.1). To step down the input voltage from the 5V board input to the required 3.3 V, a voltage regulator is implemented to create a stable and consistent power supply. Additionally, a current-limited switch (PS1) is included as an extra protection layer so that the MCU is not damaged due to overvoltage or overcurrent conditions.

To stabilize the voltage and current inputs to the MCU, a decoupling capacitor is added for each of the supply voltage pins. This helps to ensure that the MCU receives a stable and noise-free power supply, which is essential for its proper functioning. Moreover, a separate voltage source is provided for the Analog-to-Digital Converter (ADC) reference, which further enhances the accuracy of the data acquisition process.

##### Ethernet

The Ethernet interface is an essential component in the powertrain control system, providing high-speed communication capabilities. In this design, the Ethernet interface from the MCU is utilized to communicate with both the ground control and the sense and control processor. To achieve this, the signals from both sources are combined externally using an Ethernet switch.

The Ethernet subcircuit is equipped with an Ethernet PHY transceiver (LAN8720A), which is a critical component that enables the communication between the MCU and the Ethernet network. A 25 MHz crystal oscillator is also integrated, which provides quick clock synchronization for reliable data transmission. Additionally, a Local Area Network (LAN) transformer is included in the design, which is compliant with IEE standards for Ethernet signals. This transformer, which

is integrated in the Ethernet connector, provides electrical isolation by decoupling DC common mode signals, which is essential for ensuring the integrity of the Ethernet signals and preventing damage to the connected devices.

### **LED board**

The LED board is meant to display errors and warnings present on the pod when the communication between pod and ground control fails. These RGB LEDs light up in different color sequences and indicate the errors present on the pod. In total there are eight LEDs connected to this LED board, of which two are uncontrollable lamps that indicate the presence of LV and HV power on the pod. Six of the LEDs are controllable and RGB, these are used by powertrain and sense and control to display their data separately. The three top LEDs indicate powertrain errors, and the bottom ones, sense and control errors. These LEDs are placed on the pod as an extra layer of safety in case data cannot be received from a distance by ground control. Additionally, precautions will be taken when approaching the pod in an event of communication loss based on the error provided by the LEDs. This helps to avoid certain areas on the pod when approaching the pod, knowing where the source of the fault is thanks to the light sequences.

### **Lateral levitation signal separation board**

The lateral levitation operate by exciting the coils with a positive or negative alternation analogue signal. This signal is generated internally, however it contains both alternations since it is constantly increasing and reducing the field strength. On the sides of the pod, these coils are mounted to guide the pods between lateral beams. One alternation goes to one side and the other alternation to the other side. As a result, two half bridge rectifiers are used on each cygnus output to split the power in two individual alternations.

#### **6.4.4 High Voltage Battery Management System**

A battery management system is vital for ensuring the safe use of any battery system, especially those using lithium-ion cells. The designed battery management system uses products from the EMUS Centralized G1 BMS system catalogue. These products are used to monitor and control the following entities at all times:

- State of charge (SOC): The SOC represents the battery charge in a percentage of its capacity.
- Pack voltage: The voltage of every battery pack is measured
- Pack Current: The current flow out of every battery pack is measured
- Cell Voltage: The voltage across all battery cells is measured
- Cell-Temperature: The temperature of 35 % of all cells is directly measured via thermistors

When any of these values exceeds a safe threshold, for example when the battery overheats or when excessive current is drawn, the BMS instantly disconnects the battery to prevent hazards from happening.

### **Architecture**

The BMS is constructed in a distributed architecture, with 16 Centralized CAN Cell Group Modules (CCGM) and 1 Control Unit. This means that the control unit can communicate to all while only having a direct cable connection to the first CCGM. An overview of this architecture is shown in 6.22 below.

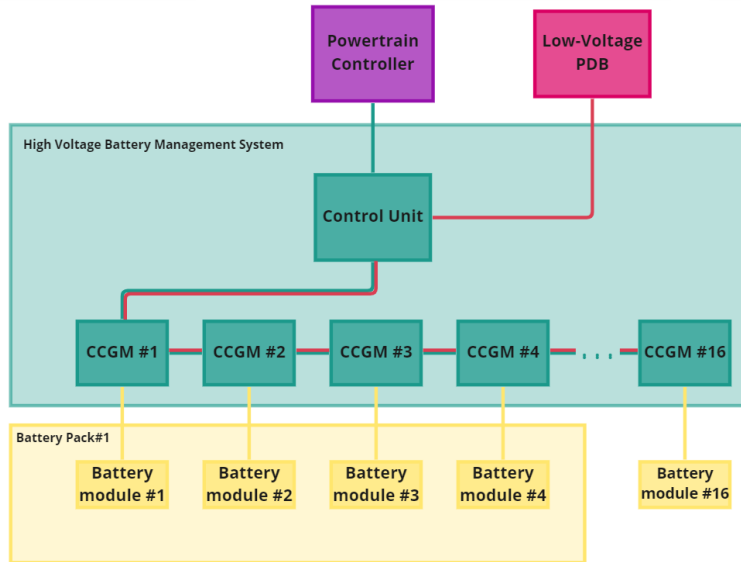


**Figure 6.22:** 4 CCGM's located on top of a battery pack

The Control Unit functions as the main hub of the BMS. It obtains all measured data and uses this to make decisions for the whole BMS. It also logs all this data to the powertrain controller. This communication, as well as all internal communication within the BMS is done via CAN Protocol. To illustrate this, direct CAN communication is shown in 6.22 with a green line. Power within the BMS is distributed likewise, so that every red line in 6.22 implies a power connection. Every Centralized Cell Group Module is used to measure a 14S3P configuration of cells. We define this to be one *battery module*. One battery pack is made up of 4 of these modules. Therefore, there are 4 CCGM's within each pack. These CCGM's are located in the top part of the enclosure, as can be seen in 6.23.

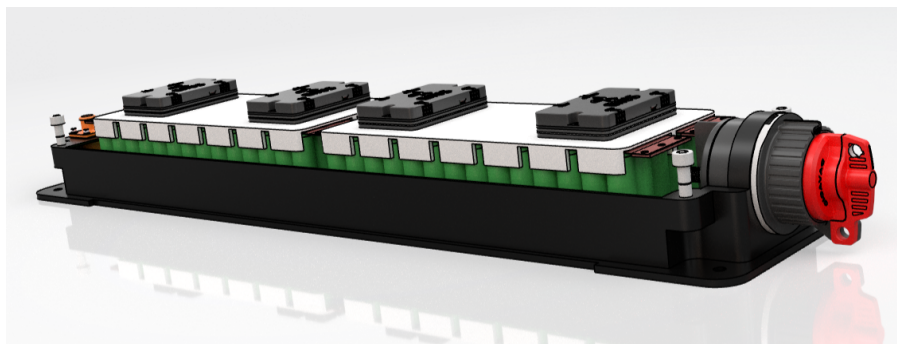


**Figure 6.23:** Four CCGM's located on top of a battery pack

Every CCGM is equipped with its own voltage sensors to measure the voltage of the cells in its module and uses this to calculate the corresponding state of charge. Moreover, for every CCGM a temperature extension board from EMUS is attached, which allows for measuring the temperature of 15 different cells, instead of 5, which is what a CCGM would be able to measure without a temperature board. This way, the temperature of 35% of all cells is measured.

A G1 Loop Style Dual Range Current Sensor from EMUS is used to measure the current of the entire high-voltage battery, which it directly communicates to the control unit.

### Balance Charging

To ensure that all battery cells remain at the same level during charging, every CCGM uses a passive balance circuit. This means that it actively measures the state of charge (SOC) of every cell, and drains a small current from the cells that have the highest SOC until they are at the same level as all other cells. This way all cells remain at the same state of charge, ensuring that the battery performs safely and optimally.

Passive balance charging is not as energy efficient as active balance charging, where the energy from cells with a high

SOC is directed into cells with a lower SOC. However, to keep the system robust and to ensure safety of such a critical and hazardous system, it is decided to use passive balance charging within the design.

#### 6.4.5 Low Voltage Battery Management system

The low-voltage battery is monitored by a BMS Mini 3 from EMUS. Just like the high-voltage BMS, it continuously measures the state of charge, pack voltage, cell voltage, current flow and temperature of the low-voltage battery pack. Also similar to the high-voltage BMS, it balance charges the cells using a passive balance charging circuit. The low-voltage BMS communicates all of its measured data to the powertrain controller via CAN protocol. A render of the LV BMS located within the low-voltage battery is shown in 6.24 below.

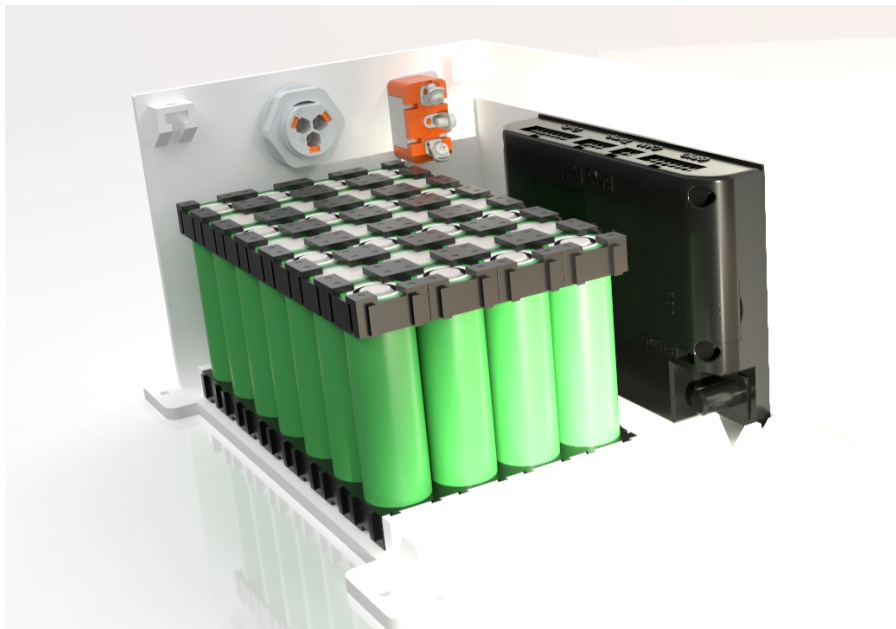


**Figure 6.24:** Render of the low-voltage BMS inside the low-voltage battery pack

### 6.5 Power Distribution

As there are numerous subsystems that require power, multiple power distribution boards (PDB's) are implemented to safely and effectively distribute this power from the battery packs. Power distribution to all high-voltage systems is done via a single high-voltage power distribution board (HV PDB), which is located within the vacuum box. This PDB is further explained in 6.5.3.

Power to all low-voltage systems is supplied using three different low-voltage power distribution boards (LV PDB's), called Low-voltage PDB A, B1 and B2.

LV PDB A is responsible for distributing its power to all components outside of the vacuum box as well as to the two other PDB's. More information on this PDB can be found in 6.5.1.

LV PDB's B1 and B2 are located within both sides of the vacuum box and are responsible for the further distribution of all power. They are further explained in section 6.5.2.

This section aims to explain the design and functionality of all of these power distribution boards.

#### 6.5.1 Low Voltage Power Distribution Board A

Low-Voltage Power Distribution Board A can be seen as the main low-voltage PDB. It is located centrally on the pod, directly onto the ladder frame. (See figure 6.25).

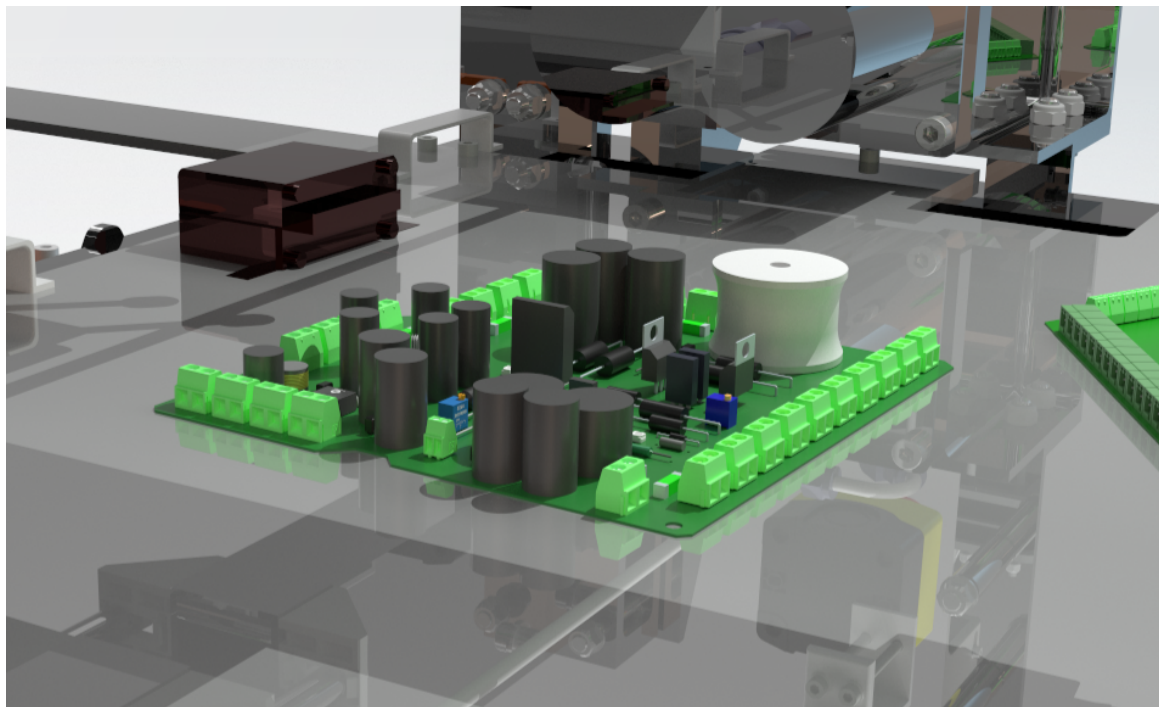


**Figure 6.25:** Render of low-voltage power distribution board A (without wires)

The PDB is responsible for supplying power to all low-voltage electronics outside of the vacuum box, as well as to the other two low-voltage PDB's. An overview of all electronics that directly gain power from LV PDB A is given in table 6.13 below.

**Table 6.13:** Overview of all low-voltage that directly gain power from low-voltage PDB A

Component	Amount	Voltage [V]	Nom Power [W]	Max. Power [W]
Main Controller	1	5	0.5	0.5
Localization Master	1	24	0.24	0.48
Optical localization	1	12	3	4
Brake pressure sensor	2	12	0.06	0.06
Brake valves (NO)	2	24	16	16
Brake valve (NC)	1	24	9	120
Ubiquity nanostation	1	24	4	8
Powertrain Controller	1	5	0.5	0.5
HV BMS Control Unit	1	12	1.3	1.3
HV BMS CCGM	16	12	1.3	1.3
Current sensor	3	12	0.1	0.1
LV PDB B1	1	12, 24	225	484
LV PDB B2	1	12, 24	136.5	170.5

This power has to be supplied at the appropriate voltage. Therefore, the PDB converts the 24 volt output from the low-voltage battery to three output voltages; 5V, 12V and 24V. To do this, the PDB makes use of power converters and regulators which are located directly on the PDB. A functional diagram of PDB A is shown in figure 6.26 below. The rest of this subsection will elaborate on the hardware design and operation of the PDB, including its voltage stabilization and current limiting functionalities.

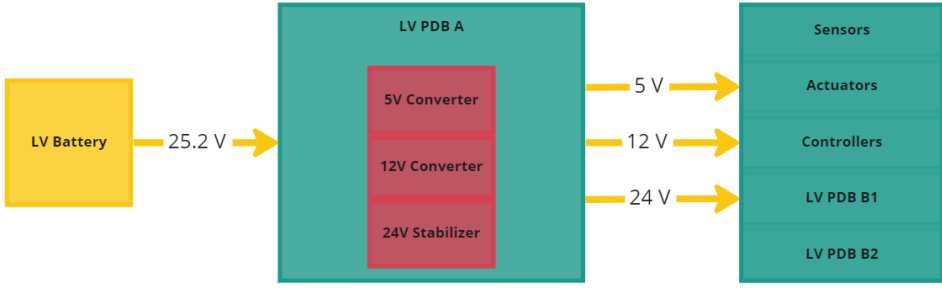


**Figure 6.26:** LV PDB functional diagram

The 25.2V to 12V and 5V DC-DC converters are custom adjustable buck converter devices that convert a 25.2V DC input voltage from the battery pack to a 12V and 5V DC output voltage. This accordingly powers the controllers, actuators, and sensors which require different voltage levels.

The input voltage range of the converter is 7V to 40V DC. The output voltages can be adjusted by a trimmer for fine-tuning.

The converter can output a maximum current of 14A and 5A for 12V and 5V respectively. Additionally, the 12V converter has an adjustable current output of 40mA to 14A, the device is therefore passively protected against over-current and short circuits. The 12V DC-DC converter steps the voltage down at a switching frequency of 45kHz while the 5V DC-DC converter has a fixed IC switching frequency of 150kHz.

### Hardware design

The 12V converter unit is designed based on the Pulse Width Modulation (PWM) controller TL494 from Texas Instruments [18]. The output of this IC is fed into a current amplifier, which plays the role of a driver circuit. This driver is designed for proper control of power transistors which are P-channel FETs. Since there are two FETs placed in parallel to increase the power delivery, the PWM IC would have trouble controlling the gate, however, the driver on the complementary part handles the control very well. The output capacitors are chosen to be high enough to keep a stable and noise-free output. This value is obtained through the following formula, which is based on the desired voltage ripple formula.

$$C_{OUT(min)} = \frac{I_{OUT(min)} \cdot D}{f_{OSC} \cdot \Delta V_{OUT}} \quad (6.2)$$

The equivalent series resistance (ESR) of the output capacitor adds more voltage ripple, which is given by the following formula.

$$\Delta V_{OUT} = ESR \cdot \left( \frac{I_{OUT(max)}}{1-D} - \frac{\Delta I_L}{2} \right) \quad (6.3)$$

The output capacitors are large enough to store energy for sudden current draw surges that tend to happen frequently in the motor driver circuits. It is ensured that the ESR is kept low by parallel connections and a 1nF bypass capacitor which primarily filters out the high-frequency noise and transients, preventing them from affecting the performance of the circuit. In addition to providing stability and filtering out noise, the output capacitors improve the overall efficiency of the power converter. By reducing the voltage ripple, the capacitor helps to minimize the amount of energy lost as heat.

A bleed resistor is used at the output to discharge the capacitors when the power converter is disconnected from power. This resistor heats up during operation and has a power rating of 5W. With a value of 680Ω, it discharges the capacitors quickly enough while drawing a low idle current.

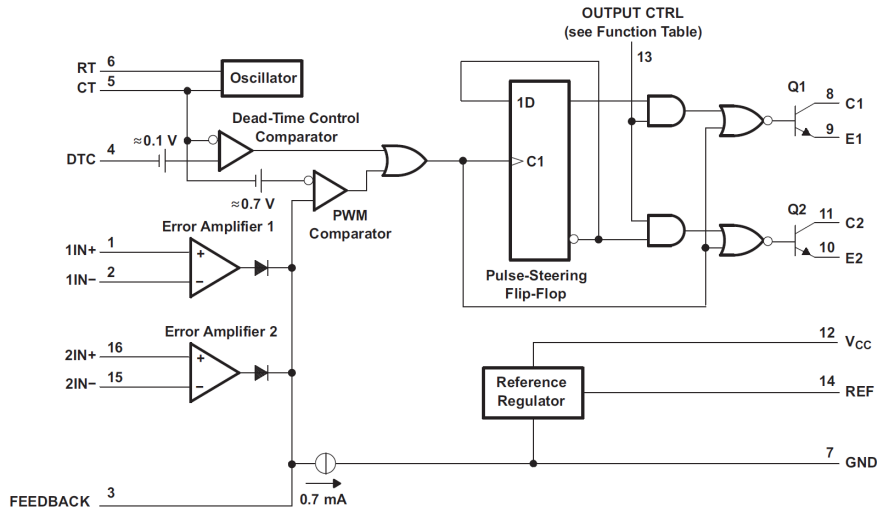


Figure 6.27: TL494 internal circuit

### Principle of operation

In the following section, a detailed flow of operation will be explained on how the converter performs the power conversion. The PWM controller generates control pulses for the power FETs and the drivers that control them, during the high state of the control pulse, the FETs are open and the power is delivered through the open channel and the choke to the storage capacitor. The choke is a  $82\mu\text{H}$  14.4A power inductor. Knowing that there are two P-FETs in parallel, the control signal is removed from pins 8 and 11 (seen in figure 6.27) and instead, pins 9 and 10 are used. The internal transistors Q1 and Q2 emitters are connected to GND, which means that the FETs will open when the output level of the PWM IC is low and close when its high. Knowing that the choke is an inductive load, which is characterized by the accumulation of energy and returned due to self inductance, when the FET closes the energy accumulated in the choke through Schottky diode will keep supplying the load, the diode will block the current in this event because the voltage from the choke has reverse polarity. The Schottky diode is a fast recovering 30A forward current, 200A reverse current and  $500\mu\text{A}$  reverse leakage current unit. The previously mentioned process of the diode blocking and conducting as a result of the FETs state will take place approximately 45000 times per second.

Figure 6.28 shows how the input power is fed into the components of the circuit to get a stable 12V output.

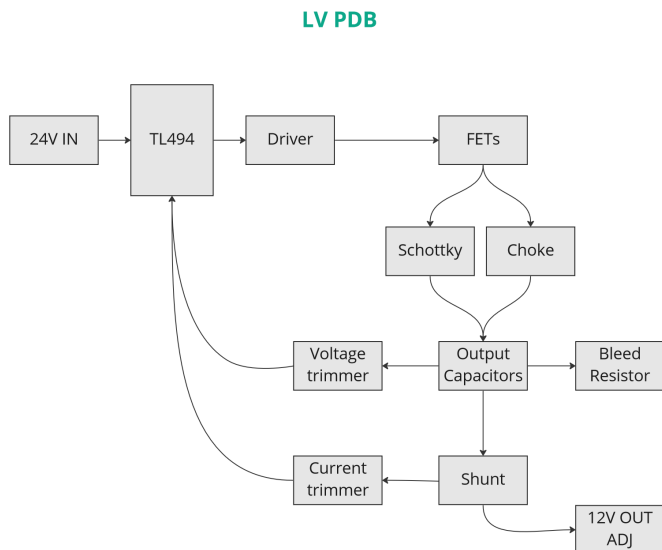
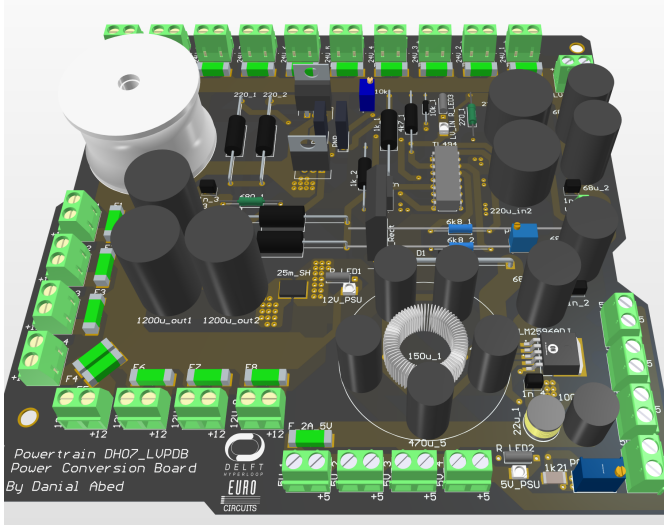
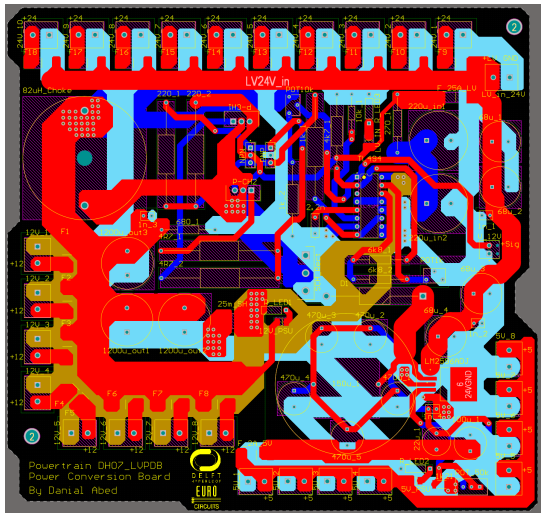


Figure 6.28: LVPDB A Functional diagram



(a) LV PDB top view



(b) LV PDB Traces

## Voltage stabilization

The PWM IC needs an external voltage to compare to the internal reference voltage, the external voltage represents the output voltage of the power converter and this is obtained by measuring the voltage drop over a shunt resistor by creating a voltage divider. This is done so that the output is always at 12V and 5V for both power converters.

The PWM IC constantly monitors the voltage on the output capacitors. The non-inverting input to first error amplifier (pin 1) receives the output voltage of the stabilizer, next this is compared to the reference voltage located on pin 2. If the output voltage decreases, the voltage on pin 1 will follow, if it is less than the reference voltage, which is set at 2V, the PWM IC will increase the pulse duration, as a result the FETs will be open for a longer time and more energy will be supplied into the choke. If the output voltage is larger than the reference voltage, then the opposite will happen, the IC will reduce the pulse duration. By using a trimmer as a voltage divider, the voltage can be forcibly adjusted and consequently an adjustable output voltage can be obtained for the DC/DC converter. The minimum voltage is 2V which is determined by the voltage divider on pin 2 and 14.

## Current limiting

In this power converter, there is the option to set a maximum current limit to set a variable over-current protection feature. This is achieved by a current limiting circuit that has a feedback to the TL494 IC.

The current limiting system operates similarly to the voltage stabilization. A current shunt is used to measure a voltage drop that will be compared to a reference. The larger the current, the larger the voltage drop will be over the shunt. For the current limiting function, the second error amplifier is used (pins 15 and 16). The voltage drop across the shunt is fed into the non-inverting input of the error amplifier. The current shunt is a very low value resistor, a  $25m\Omega$  2W resistor is used. By placing a trimmer as a voltage divider on pin 15, an adjustable current limiting function can be added to the DC/DC converter.

The converter has built-in protection for over voltage, over current, and short circuit. It will automatically shut down if it detects an over voltage, over current, or short circuit condition. This helps to protect the converter and the devices that are powered by it. This data will be continuously monitored by the PTC to report a fault to the sense and control processor in all cases.

## PWM IC frequency

The oscillator frequency  $f_{osc}$  is equal to the output frequency only for single-ended applications. For push-pull applications, the output frequency is one-half the oscillator frequency. The 12V DC/DC converter is based on the single-ended circuit topology where one output signal is referenced to a common ground. This signal controls the driver circuit which consequently drive the FETs. The following formula calculates the oscillator frequency  $f_{osc}$  that is dictated by the timing

capacitor  $C_T$  on pin 5 and timing resistor  $R_T$  on pin 6.

$$f_{osc} = \frac{1}{R_t \cdot C_T} = 45.454\text{kHz} \quad (6.4)$$

The high efficiency is accomplished by using relatively high frequency control pulses, low gate capacitance and internal resistance FETs, low ESR capacitors, low ripple and noise-free output power by using large enough chokes and capacitors. This not only keeps the output free of parasitic noise, it also increases the reliability of the power during surges and high demand events.

### **TL494 internal circuit function**

The TL494 internal 5V reference regulator output functionality will be explained for the custom regulator application. While providing a stable reference, it functions as a preregulator and establishes a stable supply from which the output control logic, pulse steering flip flop, oscillator, dead-time control comparator, and PWM comparator are powered.

The previously mentioned pulse steering flip-flop is a type of flip-flop circuit that is designed to latch data based on a pulse shaping technique. In such a pulse steering flip-flop, the data input is combined with a clock signal through a logic gate or a network of logic gates. The resulting signal is then used to drive the input of a flip-flop.

The primary advantage of pulse steering flip-flops is that they can be designed to operate with very short pulse duration, making it a useful technique to implement in high speed switching ICs such as the used PWM ICs. The pulse steering technique also helps to reduce power consumption and minimize the risk of glitches, which can occur when the input signals change rapidly.

Short circuit protection is provided to protect the internal reference and preregulator. A load current of 10mA is available for supplementary bias circuits. The reference is internally programmed to a startup accuracy of  $\pm 5\%$  and maintains a stable output of less than 25mV variation over an input voltage range of 7V to 40V.

**Output voltage ripple** Despite designing for a minimal voltage ripple, some is inevitable. The magnitude of these ripples is calculated in 6.5 and 6.6 below.

$$\Delta V_{12V} = \frac{(1 - D) \cdot V_{out}}{8LCf^2} = \frac{(1 - 0.5) \cdot 12}{8 \cdot 82 \cdot 10^{-6}H \cdot 3600 \cdot 10^{-6}F \cdot 45454^2} = 1.22\text{mV} \quad (6.5)$$

$$\Delta V_{5V} = \frac{(1 - D) \cdot V_{out}}{8LCf^2} = \frac{(1 - 0.5) \cdot 12}{8 \cdot 150 \cdot 10^{-6}H \cdot 2350 \cdot 10^{-6}F \cdot 150000^2} = 0.0394\text{mV} \quad (6.6)$$

The converter produces less than 1.2mVpp of ripple and noise for the 12V converter and less than 0.04mVpp for the 5V converter. Ripple and noise can cause interference with electronic devices and affect their performance. By choosing the inductor and output capacitor values carefully, the output is filtered of all unwanted behaviour.

### **6.5.2 Low Voltage Power Distribution Boards B1 and B2**

Low-voltage power distribution boards B1 and B2 are placed within both halves of the vacuum box, where they further distribute power to all subsystems located there. The reason for having PDB's within the vacuum box is to reduce the amount of low-voltage cables that have to go in through both sides of the vacuum box, as these connectors are very expensive. By distributing the low-voltage power from within the vacuum box, only two cables (power in and power out) are necessary on both sides. The reason that there are two separate PDB's is to minimize the wires running through the middle of the vacuum box. These are inaccessible, and need a lot of slack for when both sides of the box are to be opened at the same time. By having two separate PDB's, there are no low-voltage wires that have to run through the vacuum box, keeping all wiring manageable.

## LVPDB B1

One side of the vacuum box houses all motor drives of the levitation system. This is the side that the LV PDB B1 distributes power to. Moreover, it also distributes power to the thermal controller and the fans that the thermal system uses, these fans are PWM controlled, and the LVPDB B1 contains the switching circuit which is controlled by a PWM signal from the thermal management processor. The circuit switches an NMOS device gate to supply the fans with 24V PWM power. A full overview of all components that are powered by LV PDB B1 is given in 6.14 below.

**Table 6.14:** Overview of low-voltage systems that are powered by LV PDB B1

Component	Amount	Voltage [V]	Nom Power [W]	Max. Power [W]
Prodrive Arcas	1	24	20	35
Prodrive Cygnus	5	24	36	72
Thermal Controller	1	12	0.5	0.5
Fans in Vacuum Box	8	12	1.5	3.25

## LVPDB B2

On the other side of the vacuum box, the motor drive of propulsion is located. This is where LV PDB B2 distributes power to. Just like PDB B1, the board does also distribute power to the fans of the thermal management system and also has a PWM-NMOS-gate-controlled circuit for PWM power to the fans. An overview of all components that are powered via LV PDB B2 is given in 6.15 below.

**Table 6.15:** Overview of low-voltage systems that are powered by LV PDB B2

Component	Amount	Voltage [V]	Nom Power [W]	Max. Power [W]
Siemens S120	1	24	36	36
Siemens 200SP	1	24	43	43
Siemens SMC30	1	24	5	10
Siemens CU320	1	24	24	24
Siemens I/O module	4	24	3.5	3.5
Thermal Controller	2	12	0.5	0.5
Fans in Vacuum Box	16	12	1.5	3.25

### 6.5.3 High Voltage Power Distribution Board

The high-voltage power distribution board (HV PDB) is responsible for distributing the power coming from the HV battery pack to the motor drives from levitation and propulsion. An overview of these motor drives is given in 6.16 below.

**Table 6.16:** Overview of all high-voltage systems with their power requirements

Subsystem	Driver	Amount	Current draw	Voltage operating range
Levitation	Cygnus	5	$30A_{max}$	390V - 430V
Propulsion	S120	1	$120A_{max}$	390V - 470V

Since all of these motor drives are placed within the vacuum box, this is also where the high voltage PDB is located. To minimize the amount of cables running through the vacuum box, the HV PDB is located on the side where all levitation motor drives are housed. This subsection aims to explain the design and functionality of the PDB. A render of the high-voltage power distribution board is given in 6.30 below.

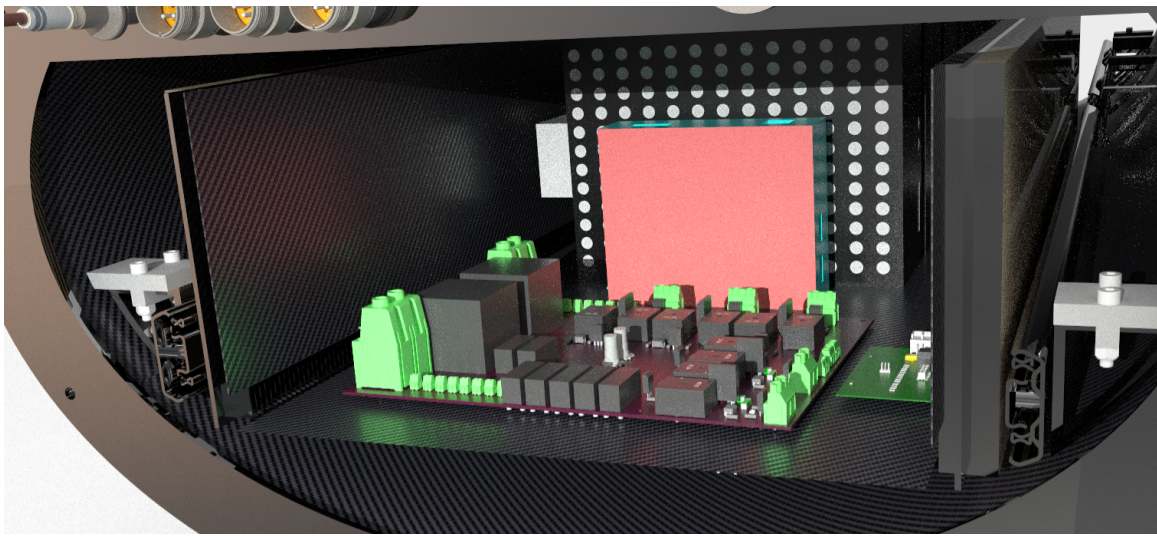
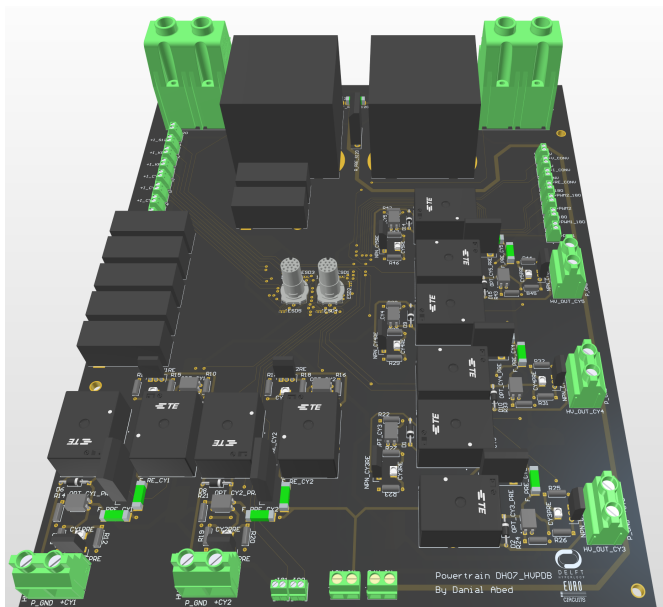
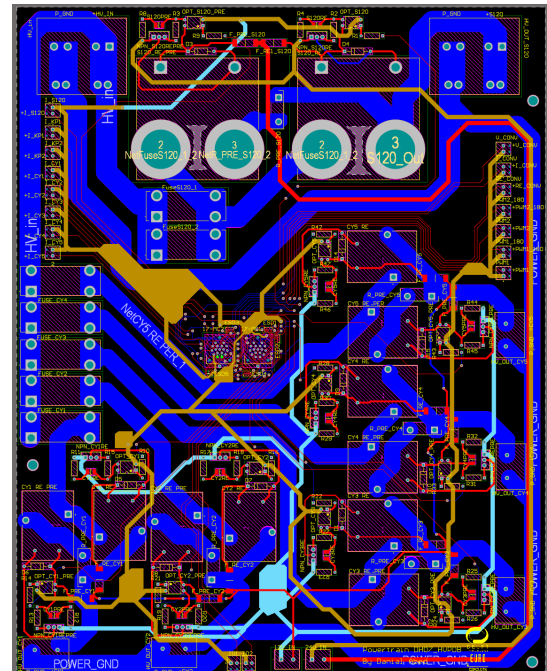


**Figure 6.30:** Render of the high-voltage power distribution board inside the vacuum box

The board is equipped with the pre-charge system (6.5.4), fuses, and current monitoring inputs are read by the PTC help to protect and regulate the flow of electricity and prevent overloading of the system. The distribution board provides a centralized location for connecting the high-voltage levitation and propulsion devices, allowing for a streamlined and organized approach to managing the electrical system. This helps reduce the risk of high voltage accidents in multiple areas of the powertrain, and allows for quick and easy maintenance and troubleshooting. Overall, the power distribution board plays a critical role in ensuring the safe and efficient operation of the power train system.



(a) HV PDB top view



(b) HV PDB Traces

The distribution board has integrated pre-chargers for each motor drive. This enables the switching of drives on or off independent of each other. This is particularly chosen for the ease in troubleshooting and testing of the motor drivers individually. It also enables the switching of the motor drives in any desired starting sequence during tests and system compatibility checks with subsystems. All relays are controlled via the centralized processing unit of the power system, the powertrain system controller (PTC).

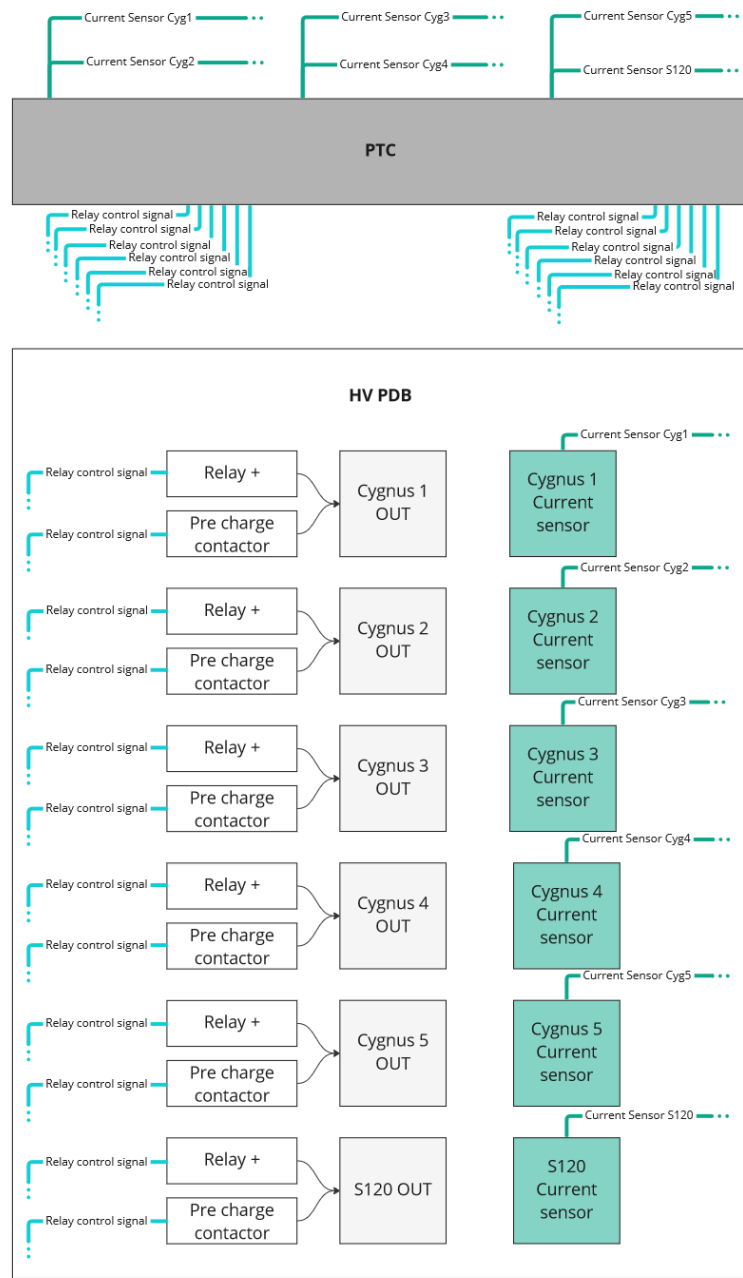


**Figure 6.32:** HV PDB Signals diagram

## Features

The HV PDB is compatible with systems running on up to 800V with peak currents of 150A. The PCB traces are thickened by applying solder on the exposed trace areas, Afterwards these exposed lines are insulated with solder mask. This protects the environment from leakage and contains the HV power safely. The board consists of five 30A outputs and one 150A output. The high current output is used by the propulsion driver and the lower current outputs by the levitation drivers.

The PDB relays are controlled by a 12V and 24V signal which are supplied by LVPDB B1 inside the vacuum box. A control signal received by the PTC will trigger the optocoupler input and let current flow to the transistor base. This will let a small signal be amplified the the supply voltage which will close the relays and let current flow in the HV rails. This board has fuse protection on all individual output rails. These are fast triggering fuses that disconnect the lines during surges of more than one second. This protection is in effect both on the pre-charge line as well as the high current line. It is compatible with a regenerative braking system for the propulsion subsystem which is explained in subsection 6.7. The board is operational between -40 °C and 85 °C and has the protection class IP20 and IK02. This implies that the PCB is

protected against 0.2 joules of impact and solid objects over 12mm, e.g. fingers.

**Table 6.17:** Overview of all components located on the high-voltage PDB

Component	Model	Amount	Subsystem
Relay	Omron G9KA	2	Propulsion
Relay	TE T9GV1L14	10	Levitation
Optocoupler	Wurth WL-OCPT	12	Levitation & Propulsion
Transistor	Onsemi 2N4401TF	12	Levitation & Propulsion
Fuse	Littelfuse 0607050	5	Levitation
Fuse	Littelfuse 0607063	2	Propulsion
Connector	Phoenix contact 1856126	2	Propulsion
Connector	Phoenix contact 1714971	5	Levitation
Connector	Phoenix contact 17-MC2	2	Powertrain

The relays provide a reliable method of controlling the outputs of the distribution board by switching them on or off. Since a relatively high current runs through the devices, a larger relay is used for the propulsion distribution path compared to the smaller relays for the levitation drivers.

These relays are controlled by the PTC with a switching circuit isolating the microcontroller unit with the relay input. An optocoupler galvanically isolates the low current input signal from the PTC by separating the controller and LV grounds. The optically isolated signal activates the gate of an NPN and enables power to flow to the relay coils to close the circuit. A flyback diode is crucial since the large relay coils generate large current spikes when the relays are opening.

High current connectors are used by Phoenix Contact, which can handle continuous currents up to 192A. This helps prevent overloading the system and makes sure that the entire PDB will operate in the high demanding conditions.

#### 6.5.4 Pre Charge Circuit

A pre-charge circuit (PCC) is used because the motor drives contain large input capacitors. This is why the HV battery contactors cannot close directly on the HV rail, the capacitors in the drive inverters would draw large amount of current. This would cause arcing, potential failure of the battery contactors and damages to the batteries from the excessive current draws. That is why a pre-charge sequence is constructed, which allows the capacitors to charge at a slower rate. This pre-charge sequence is described below. A schematic of the pre-charge circuit is given in figure 6.33.

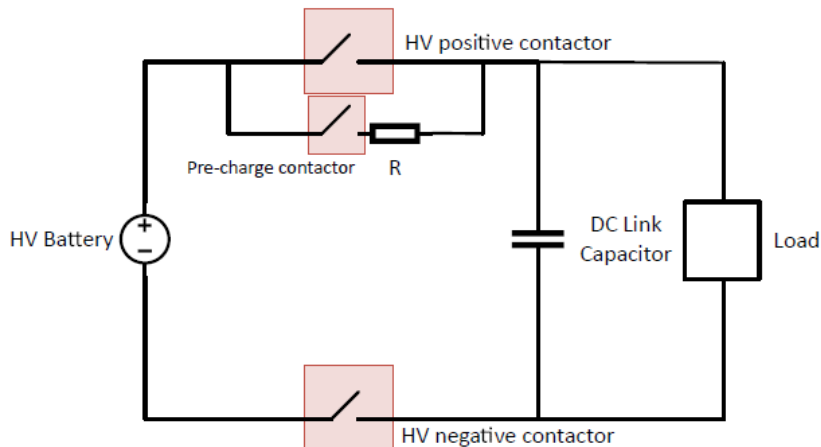


**Figure 6.33:** Pre-charger schematic

#### Pre-Charge sequence

The ground control sends a request to connect HV to the drivers. The PTC switches to the state to prepare for a run by signaling the pre-charge relays to close. The cygnus capacitors will charge up in less than a second. Once the capacitor

has reached the maximum voltage, the high current relays will close and the pre charge relay will open which connects the drives to the HV rail, allowing them to draw the necessary current for the start of a run. The capacitance measured is 0.73 mF. Each drive has its own pre-charge circuit with individually controlled relays. Durin the pre-charge sequence, the drivers receive current that is limited by a resistor, in order to charge their capacitors up in a controlled manner. After the capacitors are fully charged, the inverters can safely be connected to a non-current-limited source, so they can draw high currents for the levitation and acceleration stages.

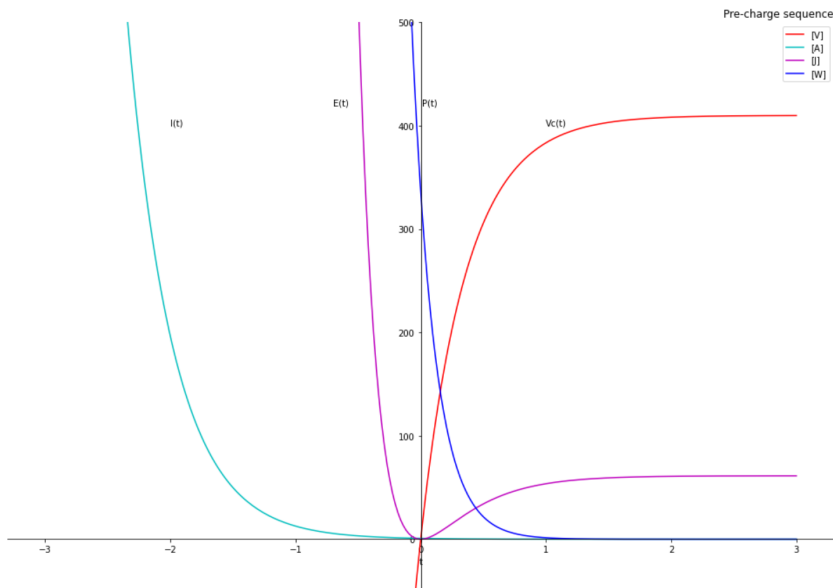


**Figure 6.34:** Pre-charger behaviour

The pre-charger-integrated PDB contains current limiting resistors of  $500\Omega$  which will limit the current to a maximum of 0.82A. The time it takes to charge the capacitors is calculated in 6.7.

$$\tau = RC = 0.365s \quad (6.7)$$

With equation 6.7. , the pre-charge time can be calculated as  $T = 5\tau = 1.83s$ . The magnitude of the instantaneous power drawn by the pre charge resistors is calculated in 6.8.

$$P = \frac{V^2}{R} = 336W \quad (6.8)$$

This peak power dissipation only lasts for a very short time, namely, less than 2s. The nominal power rating of the resistor is chosen at 100W, as it can stand 5 times the max load ( $P_{max,t<5s} = 5P_{nom}$ ) for up to 5 seconds, which is 500W and thus more than the demanded  $P_{max} = 336W$ .

## 6.6 On-Board Charger

Being able to charge the system in an efficient and convenient manner is an important milestone towards a fully scalable and operational hyperloop. To address this requirement, an on-board charger(OBC) is installed to facilitate charging of the high-voltage and low-voltage battery packs directly from the power grid. The on-board charger does this by converting the Alternating Current (AC) from the power grid to Direct Current (DC) power which can be used for charging purposes. The aim of this chapter is to explain the design of the on-board charger, together with its functionality and safety features.

The first phase is to send the AC grid current through a full wave rectifier existing of silicon controlled rectifiers (SCRs) and HV diode bridges. This is a T-type Vienna rectifier which implements power factor correction (PFC). During the next phase the PFC will be done with the help of MOSFETs, gate drivers, HV diodes and gate protection ICs. The power factor is defined as the ratio of the active power used by a load to the apparent power supplied to a circuit. During the next phase DC signal is inverted and the primary side is magnetically coupled to the secondary side. The secondary winding voltage is set to have an RMS equivalent to the module voltage of 58.8V. Before getting fed to the modules, the signal is filtered to remove any noise and feed a constant and regulated DC signal that is fed to the HV battery pack.

## Features

The OBC has the ability to supply the modules with 40A of current with each output being 60V to match the module voltage. The charger is designed to minimize energy losses and maximize charging efficiency. The charger utilizes a switch-mode power supply technique to reduce energy loss and uses buck-boost converters to stabilize the output voltage and current.

The charger is designed with safety features to prevent overheating, overcharging, and other potentially hazardous conditions. The PTC monitors the battery pack temperature, voltage, and current throughout the charging process and is capable of stopping charging or reducing the charging rate if necessary to prevent damage to the battery pack or the charger.

The OBC is designed to operate reliably under high demanding conditions and over a long period of time. It is able to withstand vibrations, shocks, and temperature variations that may occur during pod operation. The charger can also function properly in different charging environments and with different power sources.

Lastly, the charger is compatible with the specific battery pack and charging infrastructure of the pod. It is able to communicate with the PTC and other components of the powertrain system to ensure proper operation and avoid potential compatibility issues.

## Architecture

The OBC architecture is a modular AD-DC design. This architecture uses an AC-DC converter to convert AC power from the charging infrastructure to DC power, which is then used to charge the battery pack. The AC-DC converter is a multi-stage converter, which is superior to a single-stage due to better voltage regulation, higher efficiency and lower ripple (further explained in subsection 6.6.1). This architecture is used in order to charge the pod from a standard AC outlet.

This architecture uses multiple small, modular chargers that are connected in parallel to charge the battery pack. Each charger module designed for a specific voltage and current rating, and can be easily replaced or upgraded as needed. This architecture is used in the pod with a main focus on high flexibility and scalability, and also improves reliability by allowing redundancy in the charging system.

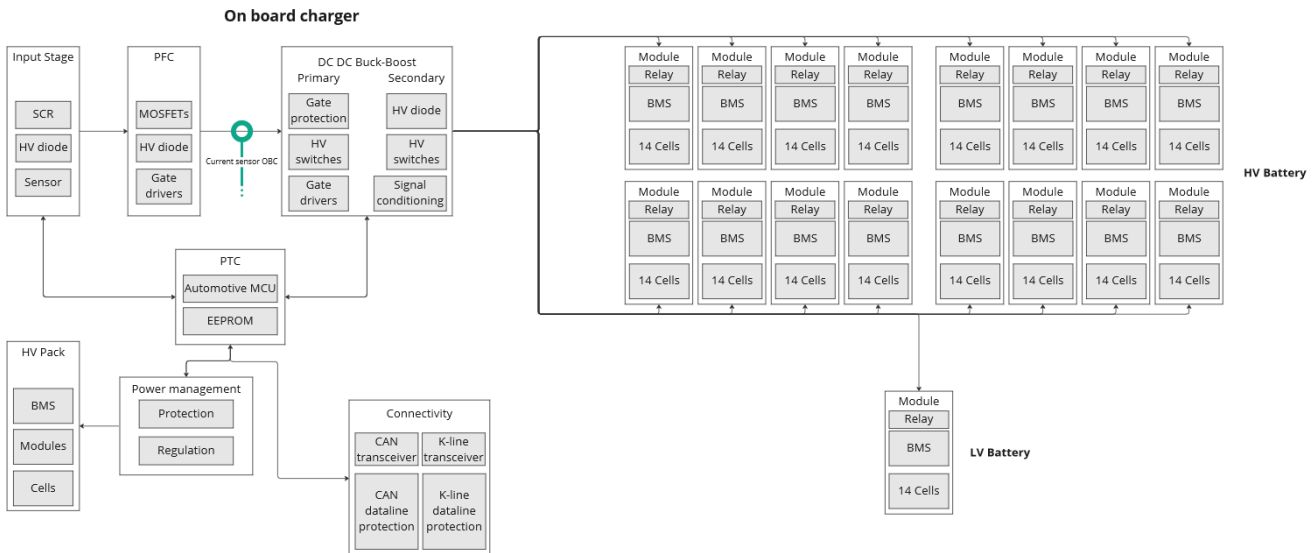


Figure 6.35: OBC functional diagram

### 6.6.1 Design features

The first stage of the converter consists of a rectifier, which converts the input AC voltage into a pulsating DC voltage. The output of the rectifier is then fed into a DC-DC converter, which smooths out the pulsations in the DC voltage and regulates the voltage to a fixed level. This second stage implemented using the buck-boost converter topology. A third stage is integrated in the buck-boost converter to provide additional features, such as power factor correction to improve

the efficiency of the converter and reduce harmonic distortion in the input current.

As explained earlier, the OBC contains charger modules which can charge each battery module individually or simultaneously. This is done by relay connections to each battery module. When a module is at the maximum desired charge level, the relay can be opened and there will be no energy loss due to passive balance charging done by the BMS. The remaining battery modules can charge up at their own pace and not influence the energy loss in other modules because of their internal chemistry and impedance. This also reduces the risk of overcharging, as another layer of protection on top of the one provided by the BMS.

The charger can be divided into 16 identical modules, each capable of charging one battery module. These charging modules supply a maximum of 60V each and are capable of supplying 40A of current. This allows for faster charging times and multiple charging modes. As can be seen in figure 6.36

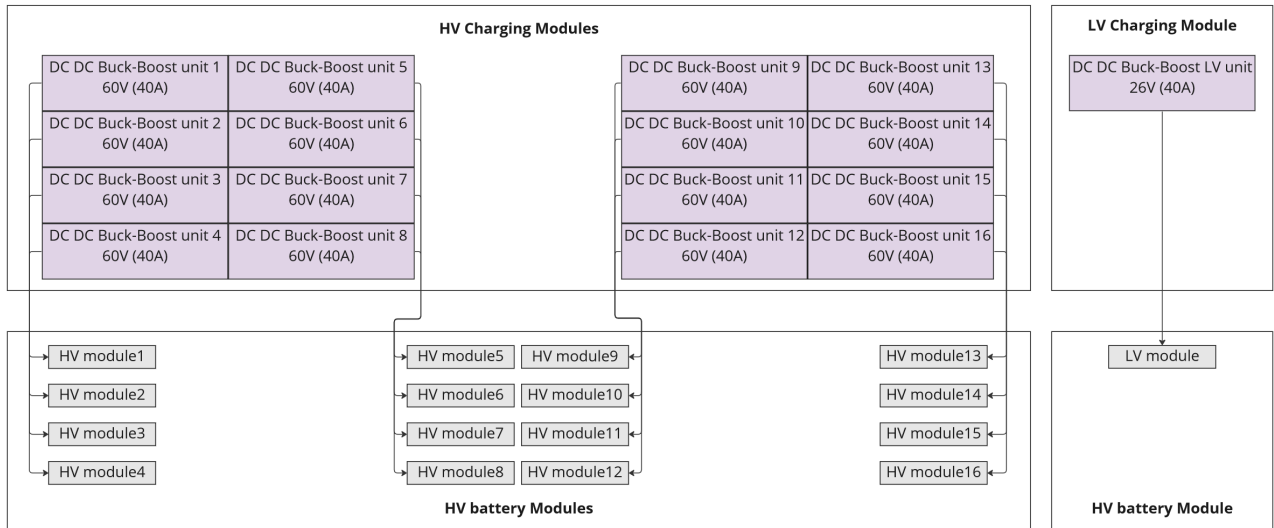


**Figure 6.36:** OBC charging modules diagram

The OBC communicates to the PTC via the CAN communication interface. This allows the PTC to monitor the buck-boost state, PFC process, input/output current of the OBC and charger temperature. At the same time the OBC receives data from the PTC to toggle the charger module relays with the specific battery module address. It also instructs the charger to initiate the charging modes based on the data it receives from the BMS. The PTC also monitors both the BMS and OBC to react in an event of a malfunction or a fault. The safety measures are especially increased in this subsystem to prevent accidents and major damages to the pod and the internal subsystems. The charger has multiple safety features, such as overvoltage protection, overcurrent, short circuit, and overheating protection. It has a temperature management system to monitor the temperature of the OBC internally and adjust the charging current accordingly. This current adjustment is also based on the received battery module temperature. It prevents the battery pack from overheating and prolongs the lifespan of both the OBC and the battery modules.

Batteries are sensitive to voltage fluctuations, this could in some cases lead to major accidents. Therefore, the charger has a voltage regulation system to maintain the voltage within the desired range during charging. This ensures that the battery module is charged optimally and prevents overcharging or undercharging. The PTC runs diagnostic and monitoring tools to allow for easy troubleshooting and maintenance of the OBC. This includes the LED indicators and the graphical user interface on ground control for displaying charging status and fault codes.

The charger has high voltage isolation to ensure that the low voltage charging module is separated from the high voltage battery modules and charging modules. This ensures that the low voltage system is not affected by the high voltage system and reduces the risk of interference. The LV battery can be charged at the same time as the HV modules thanks to this isolation. Additionally, the system is galvanically isolated from the grid to not influence the grid safety features due to false triggers caused by input-output voltage imbalances that may be seen as an error by the fast acting residual current devices protecting the grid.

In addition to the features mentioned, there is a cooling system integrated in the OBC. The cooling system is used to dissipate the heat generated by the power stage and the fast switching MOS and IGBT devices in the conversion stage. It includes a set of fans and heat sinks that are mounted on the power stage and converter units. The fans help to circulate air over the heat sinks, which transfer the heat to the surrounding environment. The temperature sensed, will be sent to the ground control to monitor the data in real time.

The ground control user interface provides the user with information about the charging process and allows them to control various charging parameters. It includes a set of indicators and buttons that are used to display information such as charger module temperature, battery module temperature, charging status, charging rate, and battery status. The user interface also allows the user to adjust the charging parameters such as charging rate and charging mode.

### **6.6.2 Charging Modes**

The charger supports multiple charging modes, such as fast charging, nominal charging, and slow charging. These charging modes are fully dependant on the battery SOC which is being monitored continuously by the PTC. The controller changes the charge mode when the SOC value enters a range that is calibrated for one of the specified modes. However, there are more charging modes featured in the OBC for added safety and versatility to make the charger as scalable as possible.

#### **Fast Charging Mode**

In this mode, the on-board charger delivers a high current to the battery modules to rapidly charge them. This mode is useful when the battery needs to be charged quickly, such as during a brief stop or when a high level of charge is needed in a short amount of time. However, this mode generates more heat than other modes and may reduce the overall lifespan of the battery.

#### **Nominal Charging Mode**

The on-board charger delivers a moderate current to the battery modules to slowly charge them. This mode is suitable for routine charging, as it provides a balance between charging time and battery lifespan. Nominal charging mode is the most commonly used charging mode.

#### **Trickle Charging Mode**

In this mode, the on-board charger delivers a low current to the battery modules to maintain their charge level over an extended period. This mode is useful when the pod is being stored for an extended period, as it helps to prevent the battery from discharging completely.

#### **Module Isolation Charging Mode**

In this mode, the on-board charger isolates one or more modules from the rest of the battery pack and charges them separately. This mode is useful when one or more modules have lower capacity or need to be charged separately due to a fault or defect.

#### **Discharge Recovery Mode**

In this mode, the on-board charger charges the battery modules after a deep discharge has occurred. This mode is useful in situations where the battery has been completely drained and needs to be recharged to a safe level. In this mode, the sensors from the BMS, battery modules and OBC are put on high alert and the PTC sets the safety thresholds at very tight minimum and maximum limits. This is done so that the PTC can take safety measures immediately when a limit is exceeded or when a minimum limit is triggered. Doing this, the PTC ensures full safety and reliability when charging an unpredictable, discharged battery.

The charging modes of the on-board charger provide flexibility in charging the battery modules to ensure efficient and safe operation of the pod. Different charging modes can be selected based on the specific charging requirements, battery health, and operating conditions.

## 6.7 Regenerative Braking

Regenerative braking is a crucial technology in modern powertrain system that recovers energy from the pod's kinetic energy and converts it back into electrical energy. This energy can then be stored in the pod's HV battery and used to power the actuators. Regenerative braking not only increases the pod's energy efficiency but also reduces the emergency brake wear and improves overall pod performance.

The regenerative braking system (RBS) consists of various components, including the actuators, propulsion inverters, HV battery, and the PTC. To ensure the safe and efficient operation of the system, several requirements are met, and various features are incorporated. In this subsection, some of the critical requirements and features of a regenerative braking system will be discussed, that have been considered during the design phase.

### 6.7.1 Features

The regenerative braking system is designed with safety as the top priority. It has fail-safe mechanisms to ensure that it will not cause any harm to the pod (and in the future to the passengers). The system also has features to prevent over-charging or over-discharging of the HV battery.

It is designed to recover as much energy as possible during braking. It is able to convert the kinetic energy of the pod into electrical energy with high efficiency. The system is also able to efficiently store this energy in the battery.

The system is designed to be compatible with other powertrain systems such as the PTC and the HV PDB. It must also be able to work seamlessly with the vehicle's existing braking system.

### Safety Features

The RBS contains a fuse placed in series with the braking resistor, this is done to protect the insulated-gate bipolar transistor(IGBT) and the braking resistor when an excessive amount of current is flowing in the energy dissipating path. When the PTC senses that the positive DC bus is above a safe limit, the dissipating path is activated to remove the large amount energy by turning it into heat. This is done because the batteries will not be able to receive energy above their safe limit. The fuse plays an important role in keeping the batteries safe during these events when large energies return into the system.

After every boot sequence, when the HV system is toggled on, the PTC runs a system check on the status of this fuse. It closes the IGBT and checks if indeed a voltage drop can be read across the resistor or not. If the voltage drop is present, the fuse is intact and the pod is allowed to perform a run. Otherwise, the HV rail is toggled off and the pod must undergo maintenance for this specific subsystem.

If the braking resistor series fuse would fail, the current can no longer run through the dissipating circuit, and it will go towards the HV battery. An excessively high current will trigger the HV PDB fuse which is fast acting. The system is designed in a way to cut off the current so that the HV battery is protected in all cases.

### 6.7.2 Architecture

A chopper based regenerative braking system with a braking resistor works by detecting when the pod is in a braking mode and then activating the brake chopper. The brake chopper connects the braking resistor across the DC bus of the inverter, causing the excess energy generated by the actuator during braking to be dissipated as heat in the resistor. This slows down the pod and recovers some of the energy that would otherwise be lost as heat. The PTC monitors the actuator velocity, current, and voltage, and adjusts the amount of braking torque applied to the motor to ensure that the pod slows down smoothly and safely.

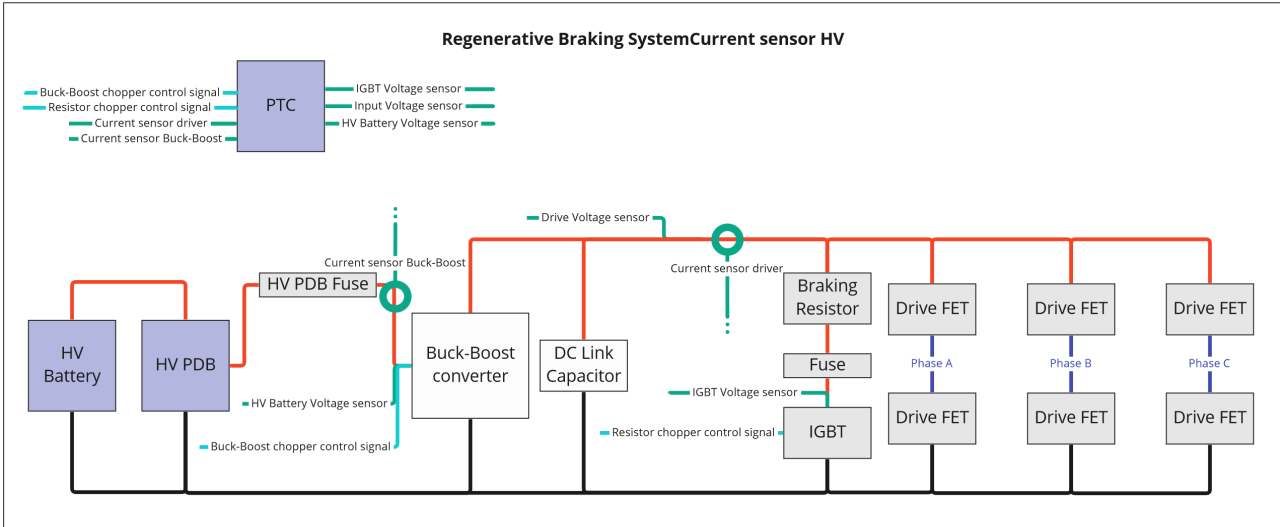


**Figure 6.37:** Regenerative Braking System diagram

### 6.7.3 Hardware Design

The propulsion inverter converts the DC voltage from the battery into AC voltage to drive the motor. In a regenerative braking system, the inverter also acts as a rectifier to convert the AC voltage generated by the motor during braking back into DC voltage for storage in the battery. As long as the voltage is within the battery's safe limits, the energy returned into the system will be stored back into the HV battery. When the PTC senses over-voltage, the brake chopper is activated.

The brake chopper is a switch that connects the braking resistor across the DC bus of the inverter during regenerative braking. It allows the excess energy generated by the actuator during braking to be dissipated as heat in the braking resistor. The braking resistor has a high power rating and is used to dissipate the excess energy generated by the actuator during braking. The PTC monitors and controls the regenerative braking system by directly controlling the brake chopper. It does this based on the actuator's power consumption data. It determines when to activate the brake chopper during regenerative braking. It also controls the amount of braking torque applied to the motor.

#### DC link capacitor

The DC link capacitor plays a crucial role in smoothing out the voltage and current ripple caused by the chopper circuit. When the actuator operates as a generator during braking, the energy generated needs to be stored in a device, and the DC link capacitor is used for this purpose. The capacitor stores the excess energy and makes it available to the inverter when it needs to supply power to the actuator. The DC link capacitor is rated for the high voltage and high current levels of the system.

#### Buck-Boost function

The chopper circuit is a type of DC-to-DC converter that is used to control the flow of energy between the motor and the battery during regenerative braking.

At this time, the actuator is used as a generator; however, since the voltage generated by the motor is in most cases higher than the battery voltage, the chopper circuit is used to step down the voltage and control the flow of current into the battery. It consists of a high-power switching device, a diode for freewheeling (flyback), and an inductor to smooth out the current waveform. The switching device is controlled by the PTC, which adjusts the duty cycle of the chopper to regulate the voltage and current flowing into the battery. Since the levitation drivers signal an over-voltage for line voltages above 430V, stepping the voltage down enables the powertrain to fully make use of the regenerative function present.

## 6.8 Production

This section aims to explain all production methods used for the power subsystem, both by Delft Hyperloop and externally.

### 6.8.1 Enclosures

The enclosures of both the high and low-voltage battery are fully designed by Delft Hyperloop.

The low-voltage enclosure is produced by Delft Hyperloop using 3d-printing techniques using PLA plastic.

High voltage enclosure is manufactured with the help of a large 3d printer which was made available by CEAD B.V. For its material also nylon plastic is used.

### 6.8.2 Electronics

The Battery management systems, for both the high and low-voltage battery, are bought off the shelf from EMUS and assembled by Delft Hyperloop.

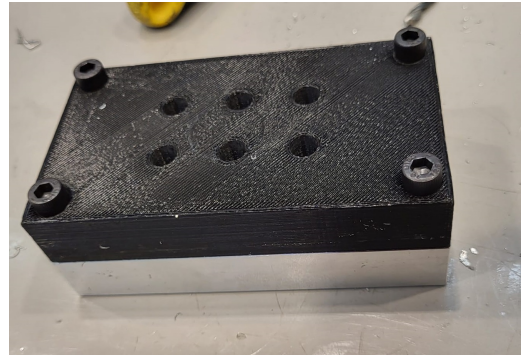
All printed circuit boards and corresponding electronic circuits are fully designed by Delft Hyperloop. This includes the high and low-voltage power distribution boards, the powertrain controller, the regenerative braking circuit and the on board charger. All used boards are manufactured at Eurocircuits, after which all electronic components are soldered on by Delft Hyperloop engineers.

### 6.8.3 Batteries

The copper strips that form the connections between the high-voltage batteries are completely manufactured by Delft Hyperloop. This is done by cutting a 0.3 mm thick copper plate into smaller pieces. These pieces are put into a mold, consisting of a plastic top and aluminium bottom, which are screwed together. A small aluminium rod is placed in the top part and then the required indentations are made by punching the rod. Afterwards, the holes are made in these indentations using a ponsing machine from the TU Delft Dream Hall. When the shape of the plates is finished, they are sanded and cleaned using iso-propanol, after which they are ready to be welded onto the batteries. A picture of the mold can be seen in figure 6.38a and 6.38b below.



(a) Bottom piece



(b) Full mold

**Figure 6.38:** Bottom and full mold for copper strip production

The welding of all batteries has been done by Delft Hyperloop engineers. This is done using a laser welder, which was provided by the Reactor Institute of the Technical University of Delft. To ensure that there is minimal harm to the batteries, the batteries are welded using a large amount of relatively small pulses which have an intensity of 800 Watts and take 1 ms. After welding all batteries are inspected under a microscope to ensure that there is no significant damage to leakage. To check that all welds are strong enough, stress tests will be performed on each module.

Moreover, all holders inside the enclosures that keep the batteries in place are designed and manufactured by Delft Hyperloop using 3D printing techniques.

## 6.9 Design Adaptations for a Full-Scale Hyperloop System

Although the powertrain system of Helios II aims for direct full-scale implementation, this section elaborates on design adaptations that could benefit the performance of a full-scale hyperloop powertrain system.

Providing the required power for both on-pod propulsion and levitation will be a significant challenge in a full-scale hyperloop system. One expected requirement for the power supply is that the voltage across the inverter inputs present in the pod will need to be at least 1500 V and presumably higher [19]. This comes, for example, from the fact that the electrical frequency of the propulsion subsystem grows linear with speed, therefore it is inevitable that the back-EMF and impedance become too high for the voltage available.

One conceptual approach that's encouraging is the usage of an external power supply during the acceleration phase of the pod, as this phase has a high power consumption. The internal power supply is then used during the cruising and regenerative braking phase. With this, the kinetic energy induced by the external power supply can now be used to recharge the battery modules on-pod. In case regenerative braking generates too much power, a DC supercapacitor can be used for temporary power storage for later discharge to the power grid to minimize energy losses.

Additionally, the recharging time of the on-pod batteries needs to be minimized in order to facilitate high-capacity transport. Since the required energy capacity cannot be recharged within minutes, a different approach is needed. The high-voltage battery modularity incorporated in Helios II promotes the concept of autonomously interchanging an empty battery module with a charged one at a station. This minimizes the battery charging time at a station.

Safety is the most essential value within Delft Hyperloop while designing. The safety of the powertrain system can be increased when the motor drives of both the propulsion system and the levitation system have the maximum and minimum operational thresholds. This reduces the risks of overvoltage and individual subsystem errors, especially during regenerative braking.

Another essential adaptation that is necessary for the safe and optimal operation of the full-scale hyperloop is a battery thermal management system. These can heat up easily and become very hazardous because of the flammable nature of lithium. As the transport of people and/or cargo is the end goal of a hyperloop system, these safety hazards have to be eliminated as much as possible. These safety hazards can be minimized by using an active battery thermal management system, which controls the thermal energy in the powertrain subsystem in two ways. Firstly, this thermal system should actively reduce the thermal energy in the powertrain subsystem with working fluid cooling. Moreover, the active battery thermal management system should utilize power management, which optimizes the powertrain system so that minimal power loss is generated and the largest part of power is used in the HV subsystems. The powertrain controller of Delft Hyperloop VII already utilized this technique, but in a full-scale implementation, it should be optimized to perform on a larger scale.

## 7 Sense and Control

### 7.1 Introduction

#### 7.1.1 Introduction to subsystems

The sense & control system is a critical subsystem of Helios II. It enables the pod to sense and interpret its environment, make decisions based on the collected data, and execute those decisions. The system is split up into 5 subsystems, namely sensors, localization, control, communication and thermal management. All of these are briefly explained below. The goal of this chapter is to explain the design and functionality of these subsystems, as well as their corresponding safety and integration features. Figure 7.1 presents a rendering of the complete sense and control system.

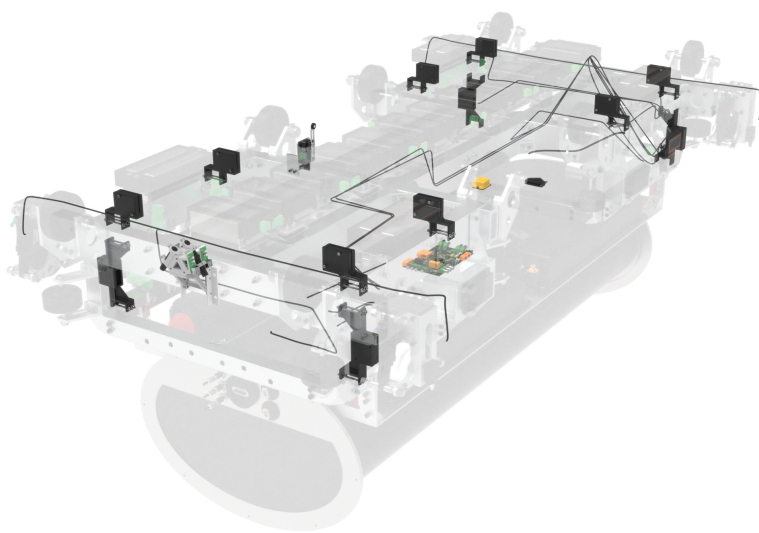


**Figure 7.1:** Sense & Control subsystem

#### Sensors

A network of different sensors is installed to gather all necessary data to operate the system. This data includes ambient temperature and pressure, vacuum box pressure, the pressure inside the brake valves, acceleration and the offset distance to the track.

#### Localization

To be able to optimally control the propulsion motor, it must know very accurately where the pod is located along the track. Therefore, a localization system is implemented. Though this is technically part of sensors, it is described in a separate section because it's such an extensive system which is custom made by Delft Hyperloop. It is split into three different subsystems: an optical sensor, an offset sensor, and an inductive sensor. These signals are combined with a PCB and fed to the propulsion system to ensure optimal operation.

#### Control

The top-level control of the pod done within the main controller. This controller communicates with all other control boards, as well as the ground station.

#### Communication

To be able to monitor and control the pod remotely, and to log all data, a ground control station is installed. This station communicates wirelessly with the main PCB on the pod.

#### Thermal management

A lot of heat is generated by the motor drives that are within the vacuum box. This heat can barely be dissipated outside of the box by convection, as it is located in a near vacuum environment. Therefore, a thermal management system is implemented to ensure that the motor drives can perform within their operating temperature range.

### 7.1.2 Intent of Sense & Control

With the goal of designing a full-scale hyperloop system the mechanical, levitation and propulsion systems become more advanced and extensive. The intent of the sense & control system is to provide these subsystems with the corresponding sensing, control, communication and thermal management capabilities to ensure safe and optimal operation. Therefore, the sense & control system has to advance rapidly, while remaining tailored to their respective demands. This involves gathering increasingly precise and varied data, ensuring more efficient and robust communication, establishing the required top-level control and designing a vacuum-proof thermal management system.

### 7.1.3 Symbols and abbreviations

In this chapter various symbols and abbreviations are used for clarity and readability. A table 7.1 below gives an explanation of all symbols that are used. All requirements have a specific ID, which is of the form PO.XX.Y.Z, where XX determines the subsystem, Y indicates the sort of requirement, and Z is the number of the requirement. Table 7.2 below gives an overview of the meaning of all these abbreviations.

**Table 7.1:** Propulsion subsystem list of symbols

Property	Symbol	Unit
Current	I	A
Voltage	U	V
Energy	E	Ah, kWh
Power	W	W
Mass	M	kg
Distance	S	m
Capacitance	C	F
Resistance	R	ohm
Frequency	F	Hz
Temperature	T	°C

**Table 7.2:** Abbreviations used for the ID's

Category	Abbreviation
General	GE
Sensing	SE
Internal Control System	IC
Localization	LO
Pod software	SW
Ground Control Communication	GC
Technical	T
Monitoring	M
Safety	S

### 7.1.4 Requirements and specifications

A list of fundamental requirements that are essential for optimal performance of both the sense & control subsystem as well as the full pod are given in table 7.3 below. All of these requirements shall be met during the European Hyperloop Week 2023.

**Table 7.3:** Sense & Control requirements

ID	Sense & Control Requirement
SC.GE.T.1	The system shall not weight more than 30 kg.
SC.GE.T.2	All components that are outside the vacuum box should fully operate in a near-vacuum(10 mbar).
SC.GE.T.3	All subsystems shall be grounded to the chassis
SC.GE.T.4	The ground control station shall have a clear interface to control the pod externally
SC.GE.T.5	The system shall be able to measure the position of the pod along the track with a minimal precision of 3.1 mm at all times
SC.GE.M.1	The system shall be able to log all relevant data to the ground station and have a latency under 100ms and it should transmit at least 2Hz
SC.GE.S.1	When the system detects any hazardous abnormalities, it should initiate the corresponding safety procedures
SC.GE.S.2	The system should be able to deploy the emergency brakes within 100 ms

An overview of the top level specifications of the sense & control system is given in Table 7.4 below.

**Table 7.4:** Sense & Control system main specifications

Specification	Value
Total mass	34.1 kg
Total mass without thermal system	9.2 kg
Total number of sensors <sup>2</sup>	39
Total peak power usage	66 W

---

<sup>2</sup>Excluding sensors from the power system

## 7.2 Sensing

In order for the various subsystems to function correctly and safely, the state of the pod must be monitored at all times. Various data regarding the pod's orientation, offset from the track, subsystem temperatures, battery charges, and precise location must be collected and monitored. The hyperloop system is designed to operate at high speeds, therefore, the sensing system must be able to provide accurate and real-time information about the state of the system. This is why the pod is equipped with a sensing network, consisting of many different sensors that monitor different aspects of the system and its elements. All sensors will be located on the pod in order to mitigate communicative issues. Additionally, positioning the sensing subsystem solely on the pod has the added benefit of limiting latency compared to locating the sensing system both on- and off-board the pod. This subsection outlines all the different types of sensors on the system, their specifications, and their primary function.

Additionally, to effectively integrate the sensing subsystem with other systems on the pod. the systems must meet some requirements that are outlined in table 7.5.

**Table 7.5:** Sensing subsystem requirements

ID	Sense & Control Requirement
SC.SE.T.1	The system shall be able to measure the vertical offset to the track with 0.01 mm accuracy
SC.SE.T.2	The system shall be able to measure the lateral offset to the track with 0.01 mm accuracy
SC.SE.T.3	The system shall be able to measure the ambient temperature and pressure
SC.SE.T.4	The system shall be able to measure the temperature and pressure within the vacuum box
SC.SE.T.5	The system shall be able to measure the pressure in the braking valves
SC.SES.6	Thy system shall be able to detect any hazardous abnormalities

### 7.2.1 Overview

The efficient and safe operation of the system relies heavily on the use of sensors. These sensors are essential for monitoring various aspects of the system, detecting any potential issues, and ensuring that the system operates as intended. A comprehensive schematic overview of all the sensors used in the hyperloop system is depicted in Figure 7.2. The sensors are categorized into six subcategories based on their placement and function: thermal, battery, safety, brakes, localization, and levitation sensors.

Thermal sensors are responsible for monitoring and regulating the temperature of the system components. These sensors ensure that no components reach critical temperatures causing them to overheat and impacting the performance of the pod. Battery sensors are critical for the system's efficient operation. These sensors monitor the state of the battery, including the voltage and current, to ensure that it is functioning optimally and providing the necessary power to all systems. Safety sensors are another crucial component. These sensors detect potential hazards or unsafe conditions such as the pod falling from the track or reaching the end of the track allowing the system to take appropriate action to prevent calamities from happening. Brake sensors are responsible for monitoring the braking system's performance, ensuring that it is functioning optimally, and alerting the system's control system if there are any issues with the brakes. Localization sensors play a crucial role in determining the hyperloop's position along the track. This Localization system relies on a combination of laser sensors and inductive sensors and will be elaborated on further in section 7.3. Finally, levitation sensors are essential for maintaining the hyperloop's offset from the track. The sensors used for measuring this offset are laser triangulation sensors. The categorization of sensors into specific subcategories helps to understand their specific function and placement within the hyperloop system. Overall, the sensors used in the hyperloop system are critical for its safe and efficient operation.

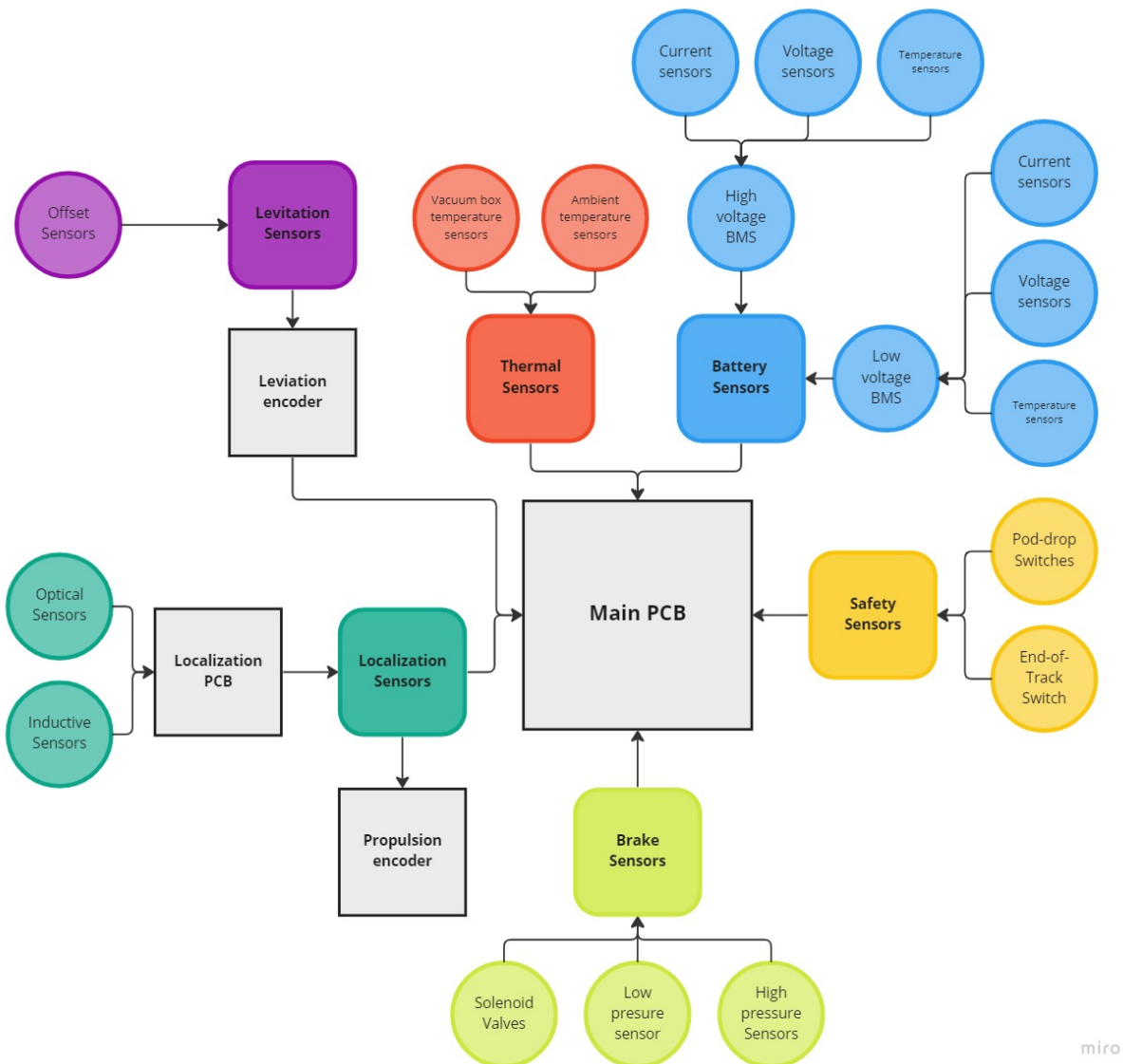


**Figure 7.2:** Sensor Overview

### 7.2.2 Vacuum Box Thermal sensing system

In total, the inside of the vacuum box is equipped with 16 thermal sensors. Together, 15 temperature sensors give an accurate reading of the temperature of all components inside the vacuum box. These components include the motor drives for propulsion and levitation, the high- and low-voltage power distribution boards and the inlet and outlet of the heat batteries. All these systems must operate at a temperature ranging from 0 °C to 40 °C at all times. Additionally, the PCB is equipped with one more ambient temperature sensor to monitor the temperature the pod is operating in. Table 7.6 gives an overview of the temperature sensors used on the pod.

**Table 7.6:** Thermal Sensors

Sensor type	Manufacturer	Model	Qty.	Range	Accuracy
Vacuum box temperature	Tru Components	MJSTS-103-3950-1-600-3D	15	-30 to 105 °C	1%
Ambient temperature	Nova Sensors	NPA-700B-015A	1	-50 to 150 °C	2.5 °C
Ambient pressure	Nova Sensors	NPA-700B-015A	1	0.025 to 1.03	0.015 bar

### Vacuum Box Sensors

The goal of the vacuum box is to maintain a normal pressure of 1 bar so that the motor drives can properly function. The pressure in this box is monitored to verify that there are no leaks, which ensures a safe operation. Moreover, the motor drives and other components generate a lot of heat inside the vacuum box. The intent of the thermal management system is to ensure that the temperature inside of the vacuum box never reaches any dangerous or critical values. To verify that the temperature remains within the desired operating range, a collection of 15 temperature sensors is installed inside the vacuum box. These sensors are assigned to designated heat-generating subsystems.

The sensors used are thermocouples, meaning that their resistance changes respectively to temperature differences. This change in resistance can be measured using a voltage divider circuit which, for every thermocouple, is printed on a designated PCB. The variable resistance brings about a change in voltage which is measured using a microcontroller. Lastly, the voltage reading can be mapped to the thermocouple resistance, resulting in a temperature reading for each sensor. 7.3 shows a 3d-render of the temperature controller placed next to the high voltage power distribution board.

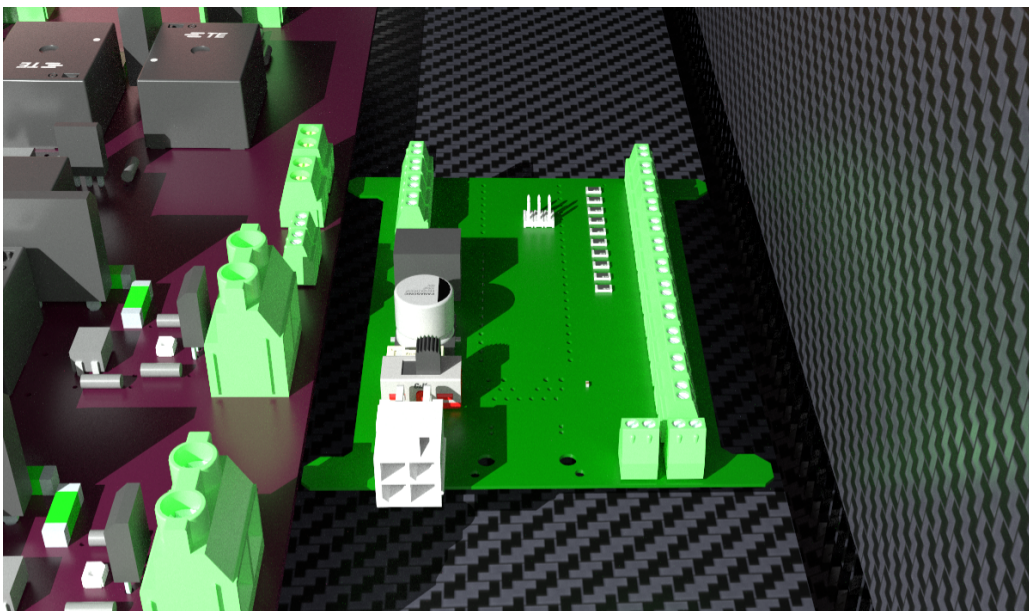


**Figure 7.3:** 3D render of the Temperature controller

In order to address the potential for noise and reliability problems with analog signals generated by multiple thermocouples, they are converted into digital signals. This is particularly important as the signal must travel a significant distance from the vacuum box to the main PCB. To accomplish this, an Ethernet protocol is used due to its ability to transmit large data packets with low latency, which is ideal for handling the signals from a large number of thermocouples. Once the individual signals are combined into a single Ethernet signal, they are transmitted to the main PCB located outside of the vacuum box.

### Ambient Sensor

The pod must know what conditions it is operating in because unusually high and low temperatures or operating in a vacuum might lead to anomalies or even unexpected failures. While unlikely, possible failures must be discovered and their root cause must be traceable. Therefore, the ambient pressure and temperature must be monitored at all times. For this reason, the pod is equipped with Nova Sensor's NPA-700B-015A ambient sensor. This sensor is mounted on the main PCB and its data is continuously logged.

#### 7.2.3 Battery Sensors

The pod is also equipped with two battery management systems (BMS). A BMS is an essential component in any device or system that uses a rechargeable battery. The BMS is responsible for monitoring, protecting and controlling the charging and discharging of the battery, ensuring that the battery is used safely and efficiently. This is particularly important in applications where the battery is critical for the proper functioning of the device or system, such as in electric vehicles like the hyperloop.

The BMS monitors the battery's voltage, temperature, and current in real-time, and uses this information to protect the battery from overcharging, over-discharging, and overheating. Additionally, it ensures that charging and discharging are done at the optimal rate and that the battery is not overworked. This helps to prolong the life of the battery and ensure that it can operate safely. For these reasons, the pod is equipped with a BMS for both the low voltage (LV) and the high voltage (HV) systems. Table 7.7 gives an overview of the these BMS' that are used on the pod. The Battery management system is further elaborated on in Section 6.

**Table 7.7:** Battery Sensors

Sensor type	Manufacturer	Model	Qty.	Measurement
HV BMS	EMUS	G1 Centralized BMS	1	Cell voltage
				Current draw
				Cell temperature
LV BMS	EMUS	BMS Mini 3	1	Cell voltage
				Current draw
				Cell temperature

#### 7.2.4 Safety Sensors

To guarantee safety, even when electrical systems fail, mechanical safety switches are installed. All of them are directly hooked up to a circuit that will initiate the emergency brakes and disable all power on the pod. There are three kinds of safety sensors: the pod-drop switches, the end-of-track switch, and the emergency switch. The pod-drop switches detect when the pod falls off the track and onto the safety track. Furthermore, as the name suggests, the end-of-track switch will activate the emergency brakes when the pod closes in on the end of the track. More specifically, the end-of-track switches will be placed 4 meters before the end of the track. Lastly, the emergency switch allows all power to be manually cut off from the system in case of emergency.

**Table 7.8:** Safety sensor overview

Sensor type	Manufacturer	Model	Qty.	Measurement
Pod-drop switch	Panasonic	MEM1G12ZD	4	Pod detachment
End-of-track switch	Panasonic	MEM1G51ZD	1	End of track limit

#### Pod-drop switches

As stated earlier, the pod-drop switches monitor whether the pod has fallen from the track during a run. There are 4 vertical pod-drop switches on every corner of the pod. When the pod drops, a button gets pressed which opens a circuit meaning that the emergency braking system gets activated. Figure 7.4 shows the placement of the pod-drop switch on the chassis.

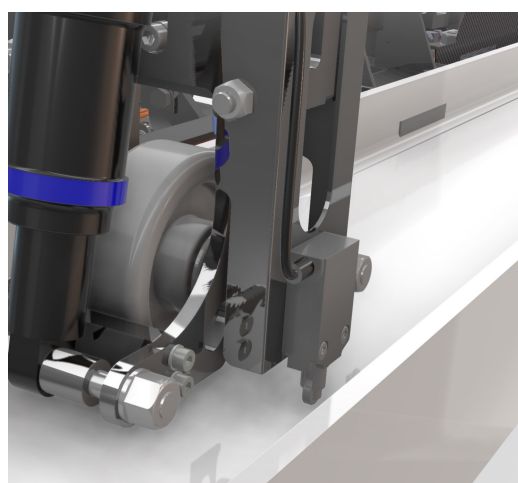


**Figure 7.4:** Pod-drop switch

### End of track switch

The end-of-track switch is an extra safety measure to prevent the pod from hitting the end of the track. If the pod reaches a position that is too close to the end, this switch will mechanically flip because of a bump mounted on the track. This will open an electrical circuit activating the emergency braking system. Figure 7.5 shows the placement of the end-of-track switch on the chassis.

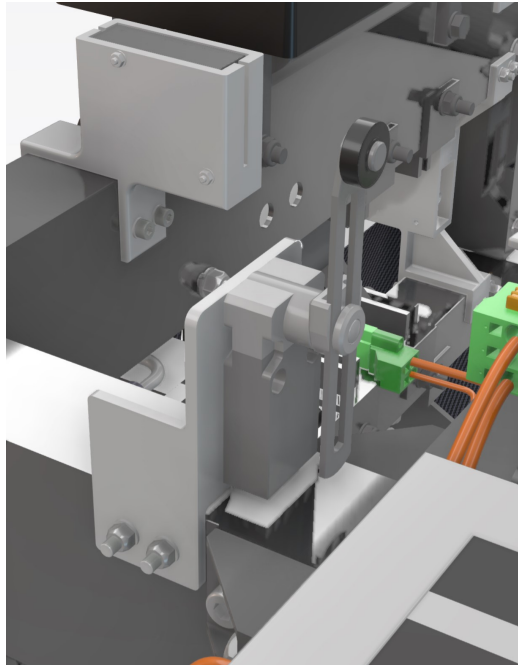


**Figure 7.5:** End-of-track switch

### Emergency switch

The emergency switch directly cuts off power from the low-voltage battery towards all other subsystems on the pod. This is why it has been placed close to the low-voltage battery. It has to be easily reachable from the sides, and therefore its sticking out of the aeroshell, above the lateral beams of the track. A render of the placement of the emergency switch is given in 7.6 below



**Figure 7.6:** Placement renders of emergency switch, both with and without the track

#### 7.2.5 Emergency brake Sensors

An emergency braking system is an essential safety component of any transportation system, and this is particularly true for the high hyperloop system. Knowing the pressure of the pneumatics at all times is crucial as it helps to ensure that the braking system is working at optimal levels and that the pod is able to stop in a safe and controlled manner.

Therefore, it is important to have a monitoring system in place that can measure the pressure of the pneumatics at all times, as this allows for the detection of any issues or malfunctions and ensures that the pressure of the pneumatics is within safe levels. As stated in section 8, the breaking system consists of a high and a low-pressure system. The maximum operating

pressure for the low-pressure system is 55 Pa and the maximum pressure for the high-pressure system is 250 Pa. An overview of the sensors used to measure these respective pressure levels is given in 7.9.

**Table 7.9:** Brake sensor overview

Sensor type	Manufacturer	Model	Qty.	Range	Accuracy
High pressure sensor	SICK	PFT-SRB100AG1SSAAMSSZ	1	0 - 100 bar	$\pm 0.25$ bar
Low pressure sensor	SICK	PFT-SRB250AG1SSAAMSSZ	1	0 - 250 bar	$\pm 0.625$ bar

### Brake pressure sensors

Two pressure sensors have been installed in the braking subsystem, one for the first part of the circuit and the other for the final part. The first pressure sensor is located before the first solenoid valve that arms the brakes. This sensor is responsible for measuring the pressure on the first part of the circuit, where the pressure should be at its highest. The second pressure sensor is located on the final part of the circuit, where a lower pressure is expected. This sensor is responsible for measuring the pressure at the final stage of the braking process, ensuring that the correct pressure is being maintained throughout the entire braking process.

To ensure the accuracy and reliability of the pressure sensors, two different sensors have been selected, these being the PFT-SRB100 and the PFT-SRB250, from SICK. These sensors have been specifically chosen for their ability to measure pressure up to 250 bar and 60 bar, respectively. The range of these sensors is larger than actually required, to account for any inaccuracies and to ensure that all required pressures can be measured accurately.

### 7.2.6 Levitation Sensors

To enable the pod to levitate fully, the offset to the track, both laterally and vertically, is measured. Measuring this offset is done with extreme accuracy, at very high precision and at a high frequency. The measured data is fed directly into the levitation subsystem, which it uses to control its magnets.

The track offset is measured using four laser triangulation sensors laterally and four sensors vertically. Details of the sensors used can be found in table 7.10.

**Table 7.10:** Levitation sensor overview

Sensor type	Manufacturer	Model	Qty.	Measurement range	Accuracy
Vertical offset sensor	Althen Sensors	FDRF603-25/25	4	25 - 50 mm	$\pm 0.0025$ mm
Lateral offset sensor	Althen Sensors	FDRF603-25/25	4	25- 55 mm	$\pm 0.0025$ mm

### Offset sensors

The sensors used for both the lateral and the vertical levitation are single-point triangulation sensors from Althen Sensors. They operate at a frequency of 9400 Hz, which allows the magnets to adapt to track inconsistencies on time. As a result, the pod will never touch the track and the air gap can be kept constant. Furthermore, the sensors have an operating range of 25 mm, which is sufficient for the operating range of the levitation system.

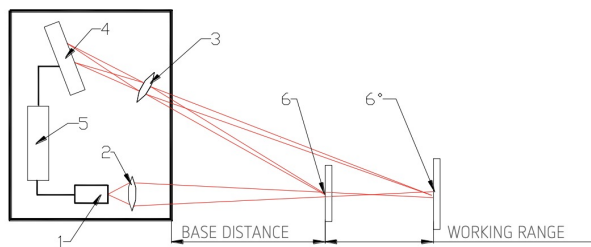


**Figure 7.7:** Working principle of the offset sensors

An overview of the working principles of the offset sensors is given in figure 7.7. A laser is projected upon a surface. This laser gets reflected by the surface and is refracted by a lens. Based on the distance between the two refracted lasers the distance can be computed very accurately.

### 7.2.7 Localization sensors

It is of great importance to know the precise location of the pod at all times. From a scalability perspective, the location of the pods must constantly be known. However, the propulsion system of the pod also heavily relies on the exact location of the pod. Therefore, to have maximum redundancy, there are three different systems that directly measure the location of the pod. These are further explained in section 7.3. However, a brief overview of them is given in table 7.11. Moreover, an inertial measurement unit that measures the acceleration is used to validate the custom localization sensors.

**Table 7.11:** Localization sensor overview

Sensor type	Manufacturer	Model	Qty.	Measurement	Measurement range	Accuracy
Optical sensor	Delft Hyperloop	-	1	Localization strip	-	1.0 mm
Offset sensor	Althen Sensors	FDRF603-25/25	2	Localization strip	25 mm	1.0 mm
Inductive sensor	Bäumer sensors	-	1	Propulsion Stator	-	20 mm
IMU	XSens	MTi-300	1	Acceleration Rate of turn	$\pm 20 \text{ g}$ $1000 \text{ deg s}^{-1}$	$15 \mu\text{g}$ $0.2 {}^\circ\text{s}^{-1}$

## 7.3 Localization

### 7.3.1 Introduction

For proper control of the propulsion system, it is essential to know the pod's position along the track. The switching of the coils has to be timed to the alignment of the teeth on the mover and the stator of the LSFPM. Additionally, positional information is important for general control of the pod, including knowledge of where to start and stop.

The localization consists of two separate systems working together, both using different measurement principles for increased reliability: a different optically-based localization systems and an inductive localization system. When speaking of *the* localization system denotes the fusion of the two systems, wherein their measurements serve to validate each other. The signals from the different systems are combined in the *localization master* also referred to as the *main localization PCB*.

### Requirements

**Table 7.12:** Localization Requirements

ID	Requirement
SC.LOC.T.1	The localization subsystem should be vacuum compatible at 10 mbar.
SC.LOC.T.2	The localization subsystem shall be able to determine position within a 25th of the stator pitch. (Which is equivalent to a resolution of 3.1 mm.)
SC.LOC.T.3	The localization subsystem shall be able to determine the position at the desired precision at our current maximum speed of 10 m/s and scale to the full-scale target speed of 278 m/s.
SC.LOC.T.4	The localization subsystem should work without physical contact between the track and pod.
SC.LOC.S.1	The localization subsystem should not be sensitive to measurement noise.
SC.LOC.S.2	The localization subsystem should be redundant, so that if one sensor fails the system can continue to operate.

### Trade-off

Here we provide an overview of design options that were seriously considered for the localization system. Options like GPS are not present, since it was clear early on that the desired precision of 3.1 mm is not achievable with GPS. Options like sonar were also discarded since, obviously, no air is present in a vacuum tube.

The *Optical* system is in essence a linear encoder, which means that the position is determined based on codes measured on a marker. The optical part refers to the way these would be read out by means of a laser system. In the case of the optical system the markers will have to be separately attached to the track. An advantage of optical systems are that they are generally suited to fast applications, thanks to the quick response times of photodiodes ( $\sim 10$  ns range).

The *Inductive* system is in essence a metal detector also based on the linear encoder principle. The inductive sensor can sense metal extrusions on the track and count these to determine its whereabouts. However, in certain implementations, no extra markers need to be installed. Since the LSFPM stator can be sensed directly, adding no extra complexity to the infrastructure.

The *LiDAR* system entails using LiDARs mounted in the track to sense the pods position. It makes use of time-of-flight (ToF) measurements, determining distance by the time it takes light to travel. By far the biggest drawback of this system is its cost if it is to be used along the entire track. Additionally, in a turn many systems would be needed to be able to constantly know the whereabouts of the pod, since the laser can only measure in a straight line.

The *Offset* system is essentially using a laser distance sensor to measure (slanted) indentations along the track. Again making it an encoder system, however with the extra option of knowing its phase within a encoder step if the indentations are slanted (as opposed to the optical system knowing its somewhere within in a single increment). Producing precisely slanted marker increments would significantly increase costs, which makes simple rectangular increments more attractive from a full-scale perspective.

The *Hall effect* system is what Delft Hyperloop VI used. Determining the phase and position of the pod by measuring the magnetic field emanating from permanent magnets on the pod with hall effect sensors mounted along the track. This shares the advantage of directly measuring the motor with the inductive system. However, it requires extensive track infrastructure, leading to high infrastructure cost.

The measurement resolution and measurement frequency requirements are linked to a certain extent. At a given speed a higher measurement frequency will translate to more samples per meter. However, fundamental limits in measurement resolution exist, thus the measurement resolution criterion is defined considering a hypothetically infinite measurement frequency.

The phase calibration requirement refers to the extent in which it is necessary to re-calibrate the localization system to the correct phase. In other words, how easily the system can acquire a constant error in its location estimate.

**Table 7.13:** Localization sensors trade-off

Criteria	Optical	Inductive	LiDAR	Offset	Hall effect
<b>Measurement resolution</b>	+	+	+	+	0
<b>Measurement frequency</b>	++	-	-	+	0
<b>Phase calibration</b>	-	0	0	-	0
<b>Full-scale cost</b>	+	++	--	+	0
<b>Measurement range</b>	+	-	++	+	0

In the end the choice was made for the optical localization system, for its high potential measurement frequency, which is a very desirable trait in full-scale, full speed operation. This is enabled by the quick response times of optoelectronic components, typically in the nanosecond range.

Additionally the inductive system is also employed, because of its full-scale potential in terms of low infrastructure cost. Its main disadvantage in term of measurement frequency currently compensated for by the optical system. It provides a valuable and relatively cheap option to check the optical localization measurements against.

### 7.3.2 Optical Localization

Firstly the top level concept of the optical localization is explained, before going into detail about the technical challenges and implementation. The localization system will be mounted on the pod, this is done to ensure low signal latency to the propulsion system which is also pod-borne. Furthermore, it has advantages in terms of cost for full-scale infrastructure, since no expensive electronics will have to be mounted along the track.

The optical localization system, as the name implies, uses light to determine its position. The way it does this is by measuring markers placed on the track. The markers are made up filled segments and holes, 3.1 mm in width, which act as the optical contrast. These markers can be classified in the two following categories: The linear markers and the encoding markers. The linear markers are simply alternating between reflecting and non-reflecting, these can be counted to determine the distance travelled along the track. The encoding markers serve as a binary code, on which any arbitrary information can be encoded. To interpret these bits the linear markers are used as a clock signal. In our application the encoder strip will mainly be used for positional calibration and to announce special events such as a gap between markers (for example, due to spacing left for thermal expansion). However, in a full-scale implementation they could be used to encode more types of information, such as announcing a lane switch location (since precise switching of the localization and propulsion systems might be necessary) or encoding track identifiers in a complex infrastructural network with many stations, this will be elaborated further in the following section.

In essence the system consists of the following parts:

- A marker strip on the track, which alternating stripes which encode position and other, programmable, indicators.
- A (modulated) laser which illuminates the lines.
- A photodiode, with readout circuit, which measures the reflection.

- A lock-in amplifier which ensures good signal fidelity, making it possible to distinguish the laser light from the ambient light.
- A logic unit, to interpret the linear signal and convert it to a position, as well as interpreting the information on the encoder strip.

The optical localization sensor is mounted at the front and back of the pod, aligned with the markers on the track, this can be seen in Figure 7.8. The mount consists of three separate laser-photodiode systems arranged in an "A"-shape, each connected to their own lock-in amplifier, as shown in the system diagram in Figure 7.12. The distance between the top of the sensor and the marker strips is 40 mm. The exact distance is somewhat arbitrary, as the sensor can work at longer ranges, however mounting it closer to the track reduces the absolute laser dot displacement caused by vibrations of the pod. 40 mm was deemed sufficient to make these effects negligible, while providing advantages in physical layout design as opposed to shorter ranges, where components could clash.

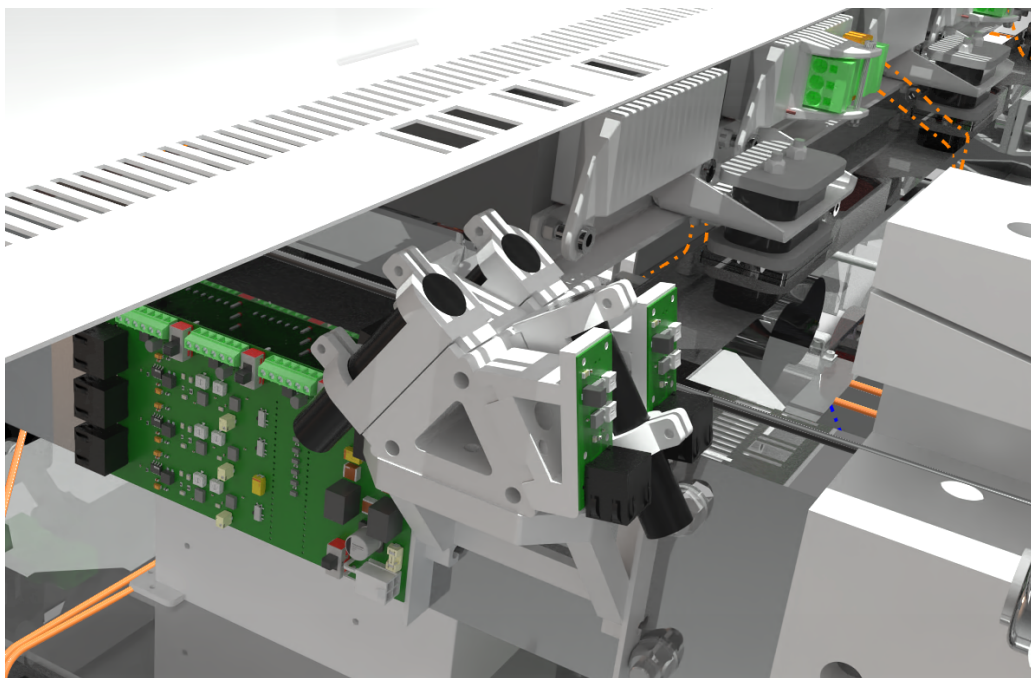


**Figure 7.8:** The optical localization sensor mounted at the ends of the pod. In the middle the laser-photodiode modules are visible in their "A"-shaped arrangements. To the bottom left is the processing board containing most of the signal processing. Above it both the linear and encoder markings can be seen.

The angled design was chosen for various reasons. Firstly, an angled design allows for precisely adjusting the reflection of the laser into the photodiode, maximizing the signal, as opposed to a parallel setup. However, a parallel setup brings the advantage of being insensitive to vertical displacement, whereas the laser reflection in an angular setup will move. This disadvantage is nullified however by the tight operating range of the levitation subsystem. Additionally, tests have shown that the reflection is sufficiently diffuse to allow for up to 5 mm of reflection displacement, which translates to roughly  $\pm 10$  mm tolerance in the vertical direction.

### Marker Concept

The marker strip consists of two parts, as previously mentioned. The *linear strip*, whose increments are counted to determine the position of the pod and the *encoder strip*, on which arbitrary binary information can be encoded. An important feature of the encoder strip is to feature as calibration for the linear strip, since this is an incremental encoder it has no idea of its absolute position nor if mistakes have been made in the count. The encoder strip solves this by having calibration marks, which periodically communicate the exact phase and position of the pod along the track, to allow the localization system to realign itself. This calibration can be split up into two categories: relative and absolute calibration. In normal operation the system could incorrectly count a stripe, thus causing a misalignment in the localization of 3.1 mm, which could build up over time. It would be advantageous to periodically communicate to the system that exactly another  $x$  stripes have passed, so that it can realign to the correct value. This is the function of the relative calibration. Absolute calibration communicates the exact position along the entire track, which is useful in many cases. For instance on startup,

when the pod does not know its whereabouts. Additionally when a incidental event, like a power outage occurs, these absolute markings allow the pod to relocate and resume operations. Without the absolute calibration this would not be possible, since there would be no way to know when to start accelerating/decelerating to, for instance, not miss a station, or worse, crash into the end of the track. The reason for having both relative and absolute calibration is simply efficiency of encoding. Assume you want to calibrate every 437 mm, like in our design, for reasons discussed later. For a 1 km long track this would take 2290 unique absolute calibration marks or 1 repeated relative mark. This matters because a trade-off exists between between information size and readout time, longer messages take more track length to encode. For minimal readout time it is advantageous to keep them as short as possible, thus the length of the binary packets will be scaled to the information requirement of a track.

Calibration is not the only function of the encoder. Another important function is the announcement of gaps in the localization strip. Since the strip is mounted in segments along the track, as is the stator, they have to be manually aligned. For a small track precise alignment is possible, but it is costly in a full-scale implementation. In anticipation of this challenge the system is designed to handle rough alignment in separate strips. This is achieved by using the encoder to precisely signal when a marker strip ends; allowing for a different interpretation of the signal while passing over the gap. While normally the gap would have to be tuned to 3.1 mm, the current design allows for arbitrarily large gaps. Another important fact in understanding this is that the markers are always precisely aligned to the stator, thus any gaps between localization markers are identical to gaps between stator elements, meaning they can be neglected. Another way of putting this is that their position is always correct in stator-space.

There is more useful information for a full-scale implementation. For instance, in a network of many separate tracks it is useful to know not only the distance travelled along the track, but also the specific track that the pod is travelling along. Such a network would definitely have an external traffic controller, which optimizes the traffic flow and deals with emergencies, for whom this information is extremely useful. Of course one could argue that the track number could be inferred by the chosen settings of lane-switches, however such a system would have no simple way of confirming if said lane switch was properly executed.

The exact location of the lane switches themselves is also useful data to encode on the track, since it is likely that such an electromagnetic lane switch will require an exception in the pod guidance and might depend on precise timing of motor operation. Embedding this information into the track guarantees proper timing for such control.

Another useful marking would be alignment markings for possible vacuum doors at hyperloop stations. Achieving a vacuum seal will most likely require precise alignment, for this markings on the encoder could be used. In essence these could the same as absolute position markings, but with a clear specialized purpose, for which further protocols could be taken into account.

The functioning of the calibration marks is critical, if they are read out incorrectly the alignment will be completely off. Error correction bits are used to ensure proper readout of these markings. A (15, 11, 3)-Hamming code is used, which can detect and repair an error in one bit. Additionally an extra parity bit is added to be able to detect a possible second error. Leading to chunks of 16 bits of which 11 are data bits. An 11-bit code allows for 2048 different values per chunk. These chunks of data are combined into packets. The first chunk is always the starting chunk and the last the stop chunk, this enables the system to know where the message starts and stops, allowing for an arbitrary (and variable) amount of data chunks in between. The amount of chunks can be dimensioned to the data complexity needs. This system is displayed graphically in Figure 7.9.

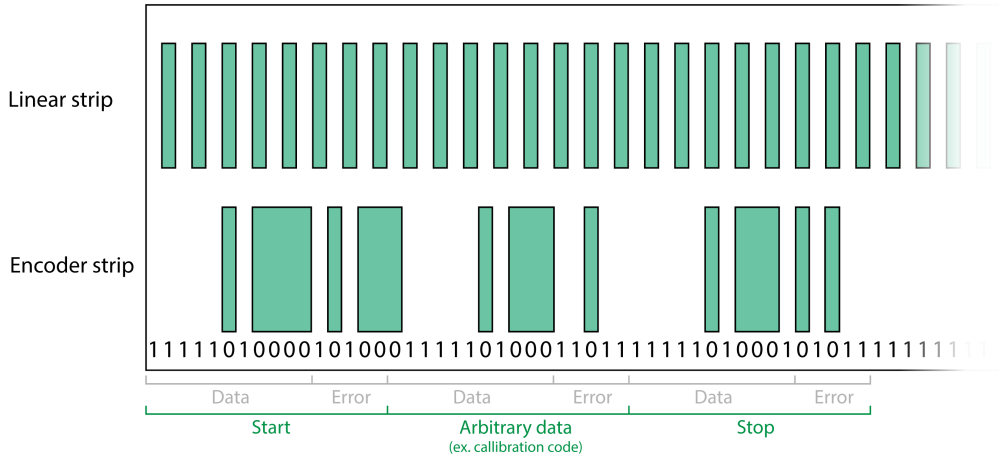


**Figure 7.9:** A schematic depiction of the optical localization markers. The top strip is referred to as the *linear strip*, the bottom strip as the *encoder strip*. It is shown how the encoder strip can be used to encode arbitrary binary information. The holes in the sheet represent zeros, the parts with material represent ones.

To estimate the data requirements let us consider a hypothetical track. Hyperloop tracks will most likely run between large population centers. To simplify, only national capitals were chosen as population centers which is a worst case scenario, since many population centers may lie between them. Within Europe Paris-Madrid is the largest inter-capital distance. The track would be approximately 1400 km long (estimated by loosely following the roads), incorporating a safety factor of approximately 1.5 this is rounded up to 2000 km. In an optimistic case absolute calibration would be necessary every 10 m, the same order of magnitude as the pod length, leading to  $2 \cdot 10^5$  unique absolute calibration marks. Additionally relative calibration could be placed every 0.5 m to ensure proper calibration. This would only require a single unique code, repeated  $4 \cdot 10^6$  times. Adding almost negligible 10 unique codes for start-stop chunks, lane switch, door alignment and gap announcement leaves only the track identifier; A high estimate would be a network of  $10^5$  unique tracks. This leads to a total unique code requirement of  $3 \cdot 10^5$ , which is easily covered in packets containing two 11-bit data chunks, which, combined, have  $4 \cdot 10^6$  unique values, more than an order of magnitude higher than the minimum requirement. Showing the data requirements are easily met using this encoder system. Even if the limits were reached an arbitrary amount of data chunks could be added without adapting the system, allowing us the increase the data complexity when necessary.

In the application on the demonstration track, the scope of data is very limited because of the relatively short track length and simple infrastructure. Here we provide an overview of the types of information encoded on the track for the EHW demonstration.

**Table 7.14:** Information encoded on the marker strips.

Parameter	Name	Values
Absolute position calibration	Signifying absolute position along track, for instance start and end.	0-99
Gap announcement	Signifying upcoming gap between markers.	500-501
Phase calibration	Correcting measurements of linear strip	1000-1005
Start and stop bytes	Signifying beginning and end of packets	2000-2001

## Marker Engineering

The markers are most important for the propulsion system. To ensure alignment with the LFSPM stator the markers are directly mounted to the stator. Since the stator will expand about 2 mm for a temperature increase of 20°C, the thermal expansion coefficients of the marker and the stator should be (approximately) matched to prevent misalignment or even mechanical failure of the marker. Additionally, the marker material should be non-magnetic to not interfere with the LF-SMP operation. For these reasons, austenitic stainless steel was chosen. It is rigid, essentially non-magnetic and closely matched in thermal expansion with regular steel. Other materials with matched thermal expansion coefficients do exist, but they do not possess other desired properties. For example, concrete is relatively closely matched, but hard to manufacture with the desired precision and very dense. Additionally, some foams occupy this class, but those are structurally

unsuitable for obvious reasons.

Another important aspect of the marker design is the contrast for the optical localization. Multiple contrast options are available, such as black and white paint, which would provide a light-dark contrast by the difference in reflectivity. Typically white paint will have a reflectivity of 0.8 – 0.9, meaning that 80 – 90% of incoming light is reflected. Black paint typically has a reflectivity around 0.2. Meaning white paint reflects 4 times more light, making it seem 4 times brighter to the sensor. However powder coating metal at the desired precision of 0.5 mm is quite challenging, making this option rather costly to manufacture.

An alternative can be found in using holes in the metal sheet as contrast, since, quite obviously, a hole doesn't reflect any light. Thus making it a perfect dark-contrast for the optical sensor. The light-contrast is simply the exposed stainless steel, which has a reflectivity between 0.5 – 0.6 at the laser wavelength of 670 nm. Stainless steel is non-corrosive, ensuring the reflectivity does not degrade over time. Aluminum has a higher reflectivity, between 0.8 – 0.9, however the aluminum would have to be coated to prevent the oxidation from reducing the reflectivity. Additionally, aluminium has a thermal expansion coefficient approximately twice as high as steel, making it unsuitable as a marker material.

## Sensing System

The lasers used in the optical localization system are the Global Laser Beta TX series 1060-42-000. This is a 670 nm laser, which can be modulated at frequencies up to 50 MHz. It features an elliptical beam of 5.0 x 2.0 mm, which is crucially smaller than the 3.1 mm marker width. The included lens can be used to focus it to a smaller spot size, but this is not strictly necessary.

The photodiode used to detect this signal is the Osram SFH 203 P. This photodiode sports a short typical switching time of 5 ns. The maximum response frequency is typically taken as the knee frequency for a digital pulse with a particular rise time. As a rough rule of thumb this frequency is equal to[20]:

$$f_{\text{knee}} = \frac{0.35}{t_{\text{response}}} \quad (7.1)$$

This yields a knee frequency of 70 MHz, which is more than sufficient for our modulation frequency at 1 MHz. These values can be worse in practice, due to additional parasitic capacitances and resistances in the circuit. Special care is taken in the PCB design to minimize these, this is elaborated on in the PCB design section. The photodiode is operated in reverse bias to increase its sensitivity and reduce noise. It is read out via a transimpedance amplifier[20] (current-to-voltage converter), since the photodiode's response to an increase in light intensity is stronger in its current than in its voltage, as can be seen in Figure 7.10. Converting the current to a voltage allows for using the current as the measured quantity, taking advantage of its steeper slope.

Additionally an optical band-pass filter is used to only let light in the 670 nm range reach the diode. Assuming a band gap of 40 nm, this should filter out approximately 90% of ambient light. This places the operating point of the photodiode at lower light intensity, allowing for a larger relative signal from the laser light. A drawback to using optical filters is that, depending on the type of filter used, the filters also absorb light in the pass-region, up to 50% for traditional coated filters.

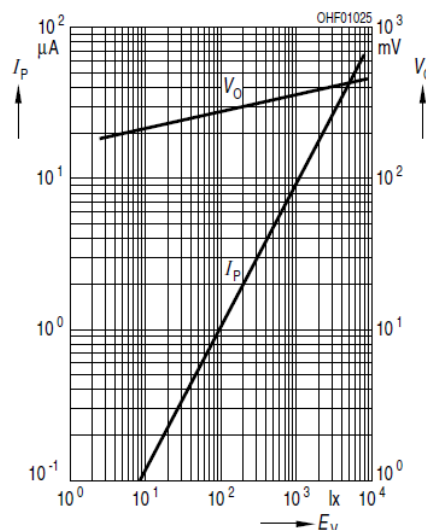


**Figure 7.10:** The voltage and current response to light intensity for the SFH 203 P.

After absorption the photodiode signal will still contain a lot of noise, since the amount of laser light reflected is small compared to the ambient light. However, by using a custom lock-in amplifier the modulated laser signal can be detected from background. The lock-in amplifier uses the fact that the modulation frequency is known to filter very specifically for that frequency. In a lock-in amplifier the measured signal is mixed (multiplied by) a reference signal of the same frequency as the signal of interest. For simplicity we will assume that our signal of interest  $v_{sig}(t)$  only has a single frequency  $\omega_s$ , this assumption is allowed since the modulation frequency can be chosen. This operation can be portrayed the following way:

$$v(t) = v_{sig}(t)v_{ref}(t) \quad (7.2)$$

This corresponds to the following convolution in the Fourier domain.

$$V(\omega) = V_{sig}(\omega_{sig}) * V_{ref}(\omega_{ref}) \quad (7.3)$$

Since  $V_{sig}$  and  $V_{ref}$  have only a single frequency they can be modeled as sinusoids with arbitrary phases  $\phi_{sig}$  and  $\phi_{ref}$  and amplitudes  $A_{sig}$  and  $A_{ref}$ . In the Fourier domain a sine wave transforms in the following way:

$$A_s \sin(\omega_s t + \phi_s) \longleftrightarrow j A_s \pi(e^{j\phi_s} \delta(\omega - \omega_s) - e^{-j\phi_s} \delta(\omega + \omega_s)) \quad (7.4)$$

Performing the convolution shown in equation 7.3 with the sinusoid assumption yields:

$$\begin{aligned} V(\omega) = A_{sig} A_{ref} \pi &((e^{j(\phi_{sig}-\phi_{ref})} \delta(\omega - (\omega_{sig} - \omega_{ref})) + e^{-j(\phi_{sig}-\phi_{ref})} \delta(\omega + (\omega_{sig} - \omega_{ref}))) \\ &-(e^{j(\phi_{sig}+\phi_{ref})} \delta(\omega - (\omega_{sig} + \omega_{ref})) + e^{-j(\phi_{sig}+\phi_{ref})} \delta(\omega + (\omega_{sig} + \omega_{ref})))) \end{aligned} \quad (7.5)$$

Returning to the time domain the following formula is obtained:

$$\begin{aligned} v_{sig}(t)v_{ref}(t) = A_{sig} A_{ref} &(\cos((\omega_{sig} - \omega_{ref})t + (\phi_{sig} - \phi_{ref})) \\ &- \cos((\omega_{sig} + \omega_{ref})t + (\phi_{sig} + \phi_{ref}))) \end{aligned} \quad (7.6)$$

The frequency of the reference signal is chosen to be equal to the signal frequency. Thus for this case the formula reduces to the following form.

$$v_{sig}(t)v_{ref}(t) = A_{sig} A_{ref} (\cos(\phi_{sig} - \phi_{ref}) - \cos(2\omega_{sig}t + (\phi_{sig} + \phi_{ref}))) \quad (7.7)$$

Which, upon applying a low pass filter simplifies to the concise and comprehensive form:

$$v_{sig}(t)v_{ref}(t) = A_{sig} A_{ref} \cos(\phi_{sig} - \phi_{ref}) \quad (7.8)$$

Thus if the phases  $\phi_{sig}$  and  $\phi_{ref}$  are equal, we simply get a DC signal proportional to the amplitude of our signal. This phase dependence can be circumvented by running 2 separate mixers in quadrature, meaning with a  $90^\circ$  phase difference. This way the signal is always picked up by at least one of the mixers. Technically speaking the phasor of the signal is obtained by this method, allowing us to find both its amplitude and phase. However, this is not especially useful since only the amplitude matters. In our design the need for two quadrature mixing circuits is circumvented by having the reference signal be phase-tunable to any arbitrary phase. Thus on startup the ideal phase is determined by performing a sweep in the interval  $[0, \pi]$  and optimizing for the highest signal amplitude.

The lock-in process can be visually understood by considering the multiplication of two signals as shown in Figure 7.11. In the top image the two signals are matched in frequency, resulting in an average value above 0, in the bottom image the frequencies are mismatched, resulting in an average of 0.

The way in which all these systems come together to form the sensor can be visualized in the schematic overview of the sensor system in Figure 7.12.

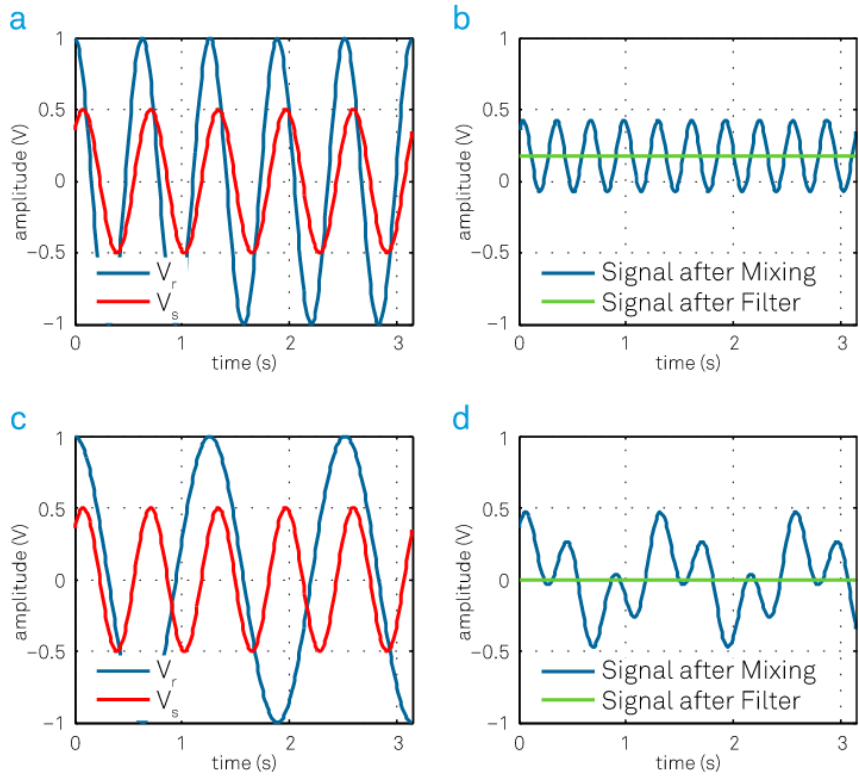


**Figure 7.11:** An example of how a lock in amplifier can select for a specific frequency. In images a and b the reference wave is in frequency with the signal, which means they interfere constructively in the mixer circuit. Which, after integrating, results in a non-zero signal. Whereas the out-of-sync signals in c result in an average signal amplitude of 0. Image taken from: [21].

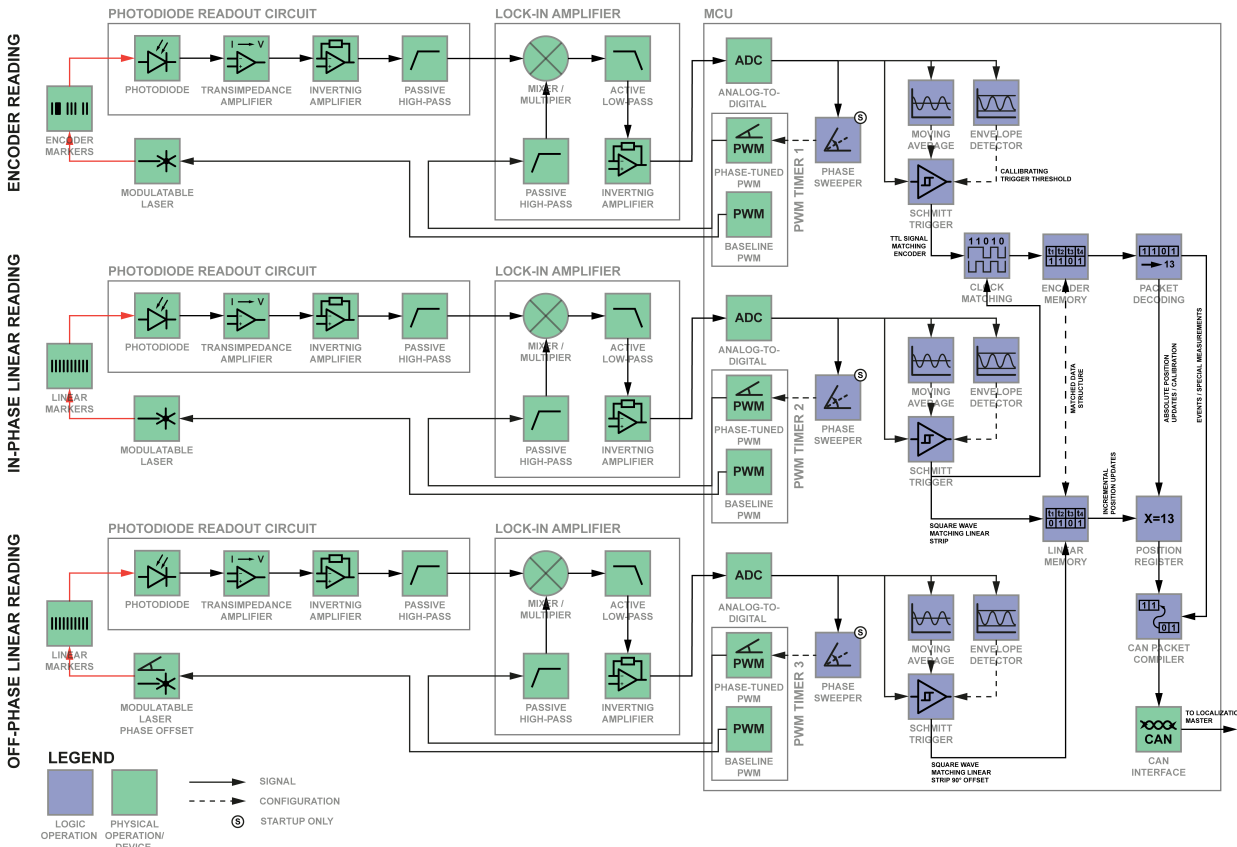


**Figure 7.12:** System diagram for an optical localization sensor.

Signals are first measured on separate photodiode PCBs, on which the *Photodiode Readout Circuit* (PRC) is positioned. The signals from the three PRCs are sent to the *optical sensor master* (OSM) on which they are fed to their respective lock-in amplifiers, each modulated at a unique frequency, as to not interfere with each other. After lock-in amplification the signals are digitized. At this stage the digitized signals are binary in nature, meaning either a reflection or no reflection is measured. However, they still contain noise, which would ideally be removed. An automatically tuned Schmitt trigger is used for this purpose. A naive trigger determines if a signal is high or low, by ascertaining if it is above or below a certain threshold. A Schmitt trigger does essentially the same thing, but it introduces hysteresis to the threshold. In simple terms that implies that the threshold moves down if the current value is high and vice versa. The effect of this is that the signal has to change significantly to pass the threshold, suppressing noise. This is illustrated in Figure 7.13.

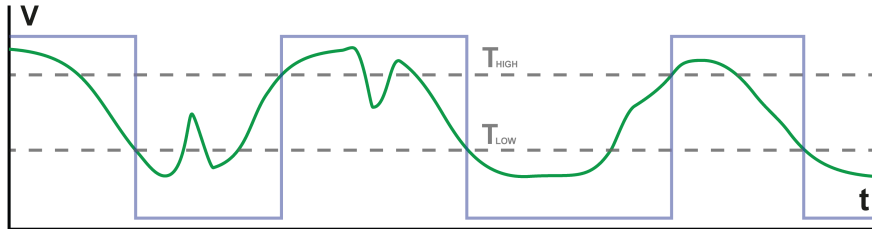


**Figure 7.13:** A schematic demonstration of the operating principle of a Schmitt trigger. The output of the trigger is switched when the threshold is passed, the threshold moves up and down to increase resistance to noise.

In the optical system the threshold values are automatically tuned to the signal statistics, to prevent varying environmental conditions from changing the signal enough that the old thresholds no longer suffice. Changes in environment are slow compared to the measurement speed. Thus statistics can be calculated using long time averages. Since these statistics are preferably computed over multiple periods, the minimum integration time varies with speed. The formula relating velocity  $v$  to integration time  $T_{\text{int}}$  is given in Equation 7.9; with  $N$  being the amount of periods to integrate over and  $d_{\text{marker}}$  the marker width. For example, at standstill the integration time approaches infinity, thus the statistics should not be tweaked. Whereas at 10 m/s the minimum integration time will be in the order of 6 ms, assuming  $N = 10$ .

$$T_{\text{int}} = 2N \frac{d_{\text{marker}}}{|v|} \quad (7.9)$$

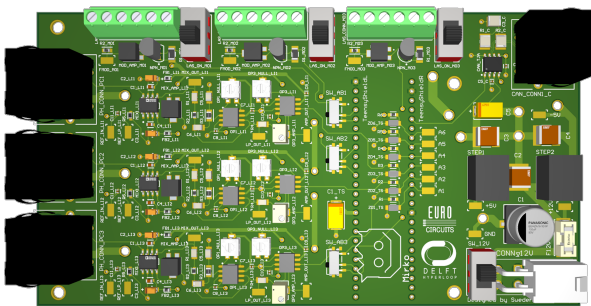
The statistics used for tweaking the threshold values are the complete signal average and both the signal-high and signal-low averages. The thresholds are then placed at positions  $v_{\text{thresh, high}}$  and  $v_{\text{thresh, low}}$ , which are computed in the following way:

$$\begin{aligned} v_{\text{thresh, high}} &= v_{\text{avg}} + a(v_{\text{avg, high}} - v_{\text{avg}}) \\ v_{\text{thresh, low}} &= v_{\text{avg}} + b(v_{\text{avg, low}} - v_{\text{avg}}) \end{aligned} \quad (7.10)$$

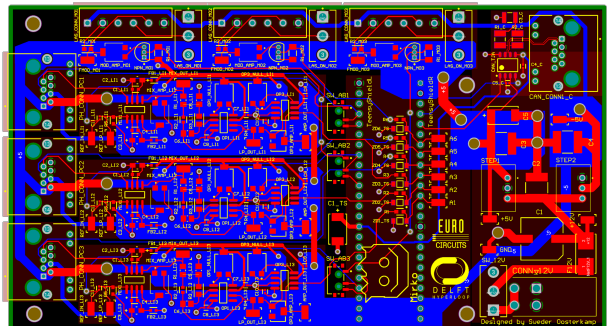
The values of  $a$  and  $b$  can be tuned manually to strike the optimal balance between noise suppression and detection reliability. Based on early tests a good value for  $a$  and  $b$  is 0.8.

## PCB Design

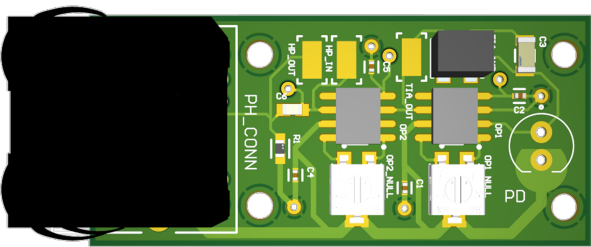
The physical PCB layout for the different localization system PCBs can be seen in Figure 7.14. A 4 layer stackup was chosen in the SIG/POW-GND-GND-SIG/POW configuration. This stackup allows for excellent coupling between signals and ground, because a ground plane is always adjacent. This reduces crosstalk between traces by keeping the electromagnetic fields confined to a small volume [22], essential for reliable analog signal processing. Additionally, digital and analog signals are spatially kept separate to reduce crosstalk from high frequency digital signals to the sensitive analog signals [22].



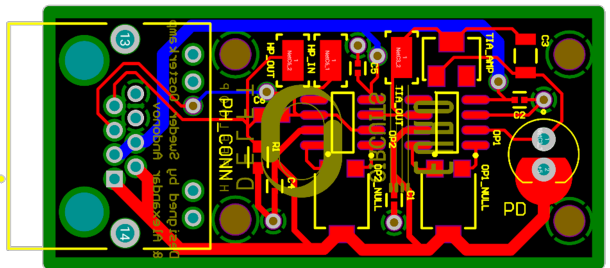
(a) 3D render of the Optical Sensor Master



(b) PCB tracing of the Optical Sensor Master



(c) 3D render of the Optical Sensor Photodiode Readout Circuit



(d) PCB tracing of the Optical Sensor Photodiode Readout Circuit

**Figure 7.14:** Various renders of the optical localization system PCBs.

The reason for creating the PRCs is simple: Mounting the photodiodes on the OSM creates a bulky, difficult spatial design, which is hard to integrate with the laser modules. The photodiode signal is immediately amplified on the PRC board, since this reduces the *relative* amplitude of EMI noise obtained during signal transmission to the OSM, ensuring higher signal quality.

### 7.3.3 Inductive Localization

Inductive localization uses magnetic induction to detect metal nearby the sensor, it is effectively a metal detector. It achieves this by using a solenoid to induce eddy currents in the metal, which generate an opposing magnetic field. This field can be detected by the induction coil itself.

Inductive localization has the great advantage of being able to use the LSFPMS stator as a reference, since it is made of conductive metal by design. This reduces infrastructure cost by removing the need for separate markers on the track, which are necessary for, for instance, optical localization. Additionally, the system has the advantage of always being perfectly aligned. By virtue of this, the reference is also always perfectly aligned to the stator, since it is the stator itself. In our application the inductive system exists in conjunction with the optical system, which technically reduces the infrastructure cost advantage. However, it should be stressed that both are present as a proof of concept, showing the capabilities of both, to make more informed choices for a full-scale implementation.

### Sensor Design

Inductive localization uses magnetic induction to detect metal nearby the sensor. It achieves this by using a solenoid to induce eddy currents in the metal, which generate an opposing magnetic field. This field reaches the solenoid changing its effective inductance. This means the inductance will change when the coil is over a tooth of the stator, thus inductance provides our contrast, this is further illustrated in Figure 7.15. The inductance is measured by placing it in a (parallel) RLC resonator circuit. The resonance frequency of which is given by:

$$\omega_0 = \frac{1}{\sqrt{LC}} \quad (7.11)$$

Since  $L$  increases in the presence of metal, the resonance frequency will drop. This can be read out by driving the circuit with a voltage at a set frequency. If the resonance frequency changes the signal will be attenuated more. This change in signal amplitude can consequently be measured.

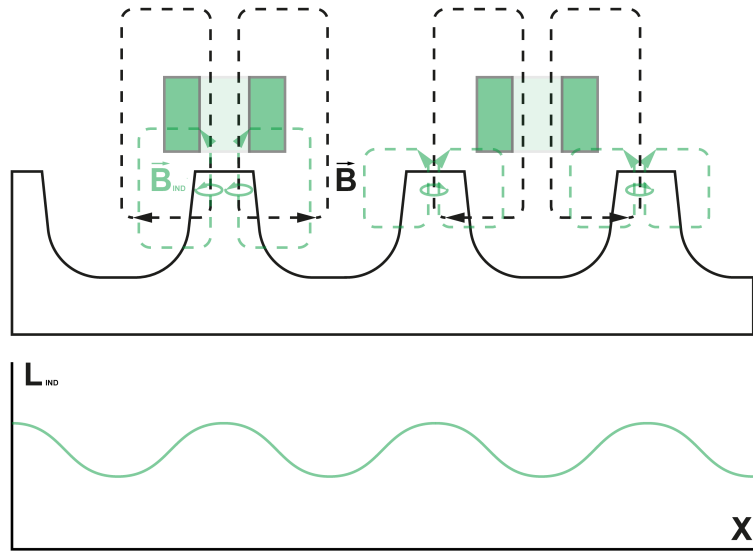


**Figure 7.15:** The measurement principle of the inductive system. The effective inductance changes along the length of the track, by the varying mutual inductance between the coil and the eddy currents induced in the stator metal.

There are important considerations for the coil design, since it is the sensing instrument. Importantly the range of the coil is not strongly influenced by the total flux generated, but rather by its diameter [23]. As a rule of thumb, the sensor's range should be assumed to be half of its diameter. The low impact of the total flux implies that the inductive sensor can operate effectively at low current, which allows for thin coil wires/traces. For this reason, the coil can be directly printed on the PCB. Additionally, this has the benefit of having lower parasitic capacitance, which increases signal fidelity by raising the self-resonance frequency of the coil, away from the operating frequency.

Coil shape also influences the sensor operation. For our application, a rectangular coil is preferred, since these are more sensitive to movements in the sensor plane, i.e. sideways movement. Whereas circular coils are more sensitive to vertical movements[23].

Another important consideration is placement. Since the inductive sensors use magnetic fields for sensing, thus they are very sensitive to EMI. Firstly the sensors will need to be magnetically shielded by placing them as far as possible from strong magnetic sources. Additionally, metal may be used to block the fields. Another consideration is the remaining magnetization of the stator by the LFSPM. To circumvent this influencing the inductive position sensor the sensor should always be mounted in front of the LFSPM motor. Since the pod can move bidirectionally, this implies a sensor array should be mounted on both sides.

A sensor that matches the imposed requirements is the Baumer IR30.D24S-N60.UA1Z.7BO; an inductive distance sensor with 24 mm range and a 30 mm diameter and a minimum measurement frequency of 500 Hz. Which suits the frequency specifications for a coarser positional measurement. The inductive is mostly used as a means to confirm measurements made by the higher resolution optical system.

### 7.3.4 Inertial Measurement Unit

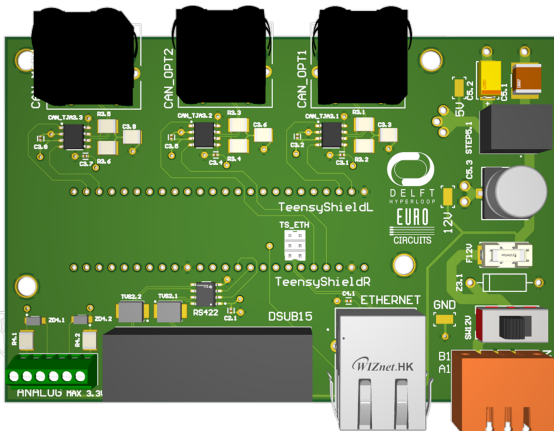
The Inertial Measurement Unit (XSens MTi-300) contains vibration-rejecting gyroscopes for accurate inertial data, together with an accelerometer and magnetometer. The output frequency expected reaches up to 2 kHz and the latency is less than 2 ms. Since there is no separate unit for velocity estimation, the acceleration data from the IMU is compared to accelerations and velocities measured by the other localization systems. The reason the IMU is not used to get positional data is that the integration of acceleration to position has an unbounded error, due to any error in acceleration measurement being integrated over time twice, which causes values to quickly deviate from reality. All of the computation is done on the Localization Master and acts as an auxiliary parameter to the localization modules for redundancy and safety. The connection between the IMU and the localization master is established through the UART protocol. The Localization Master can also signal to the unit to be restarted for rebooting purposes. The IMU is mounted to the pod's chassis and complements the other localization sensors.

### 7.3.5 Integrated system

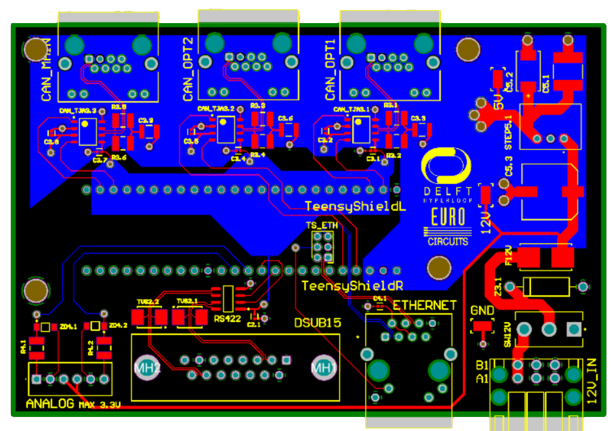
The signals originating from the different localization systems are consolidated at the *localization master board*. Here the signals are combined to get a more reliable estimation of the position. The position signal will be relayed to the propulsion SMC30 encoder interface via Synchronous Serial Interface (SSI). In this protocol 16 bit packets are sent containing the absolute position along the track at a baud rate of 1 MHz, translating to 62.5 ksamples/s. Additionally the location is relayed to the ground station and the main controller via Ethernet. Here measurements performed at different timesteps are bundled and sent together to optimally use the Ethernet bandwidth. This can be done since the information here is less time-critical than that used for the propulsion control loop.

The localization master board is controlled by a Teensy 4.1 microcontroller, which is based on the i.MX RT1062 MCU by NXP. Which sports a Cortex-M7 architecture clocked at 600 MHz.

The board layout can be seen in Figure 7.16. In this image the Teensy mount is left empty.



(a) 3D render of the Localization Master Board



(b) PCB traces of the Localization Master Board

**Figure 7.16:** The renders of the the first iteration of the localization master.

One of the key features of the combined localization system is redundancy in measurement and sensing principle. The different localization information streams are integrated via a Kalman filter, a data fusion algorithm that takes multiple measurements, including the noise that comes with them, and produces an estimations of unknown parameters, that are more accurate than the ones given, by producing a joint probability distribution over the variables, and when combining the measurements of the optical, inductive and inertial sensing systems, provides an accurate estimation of the distance. This ensures a highly reliable positional signal, taking into account three different measurement systems and pattern in their past measurements. The advantage of this is that if any of the systems produces anomalous data for any reason, the system recognizes the anomaly and is able to neglect it. Reasons for data anomalies could be as simple as dirt on the track or other imperfections in the measurement. Since the localization system is critical for the propulsion to work it is paramount that its output is reliable, since small deviations will result in significantly lower motor efficiency and large deviations will result in accidental, uncontrolled, braking.

## 7.4 Internal Control System

This section illustrates the design of the controller PCBs, responsible for the internal logic and computation of the pod, and how they interface with the other major subsystems. It also highlights specific design choices made that allow our electronics architecture to be robust and scalable in terms of data transmission, memory management and the ability to adopt new modules for future improvements and iterations. The main goal of the system is to be able to accommodate the increased amount of sensor data, different types of data and distribution of subsystem logic and computation that a future hyperloop pod and infrastructure entail.

The "Main Controller" is the central computational unit, responsible for the core functionalities and the Finite State Machines of the system. To ensure data bandwidths never congest the data pipeline, the MCU only receives events from the other subsystems and sensor data, that is filtered for modules that may encumber it, because of size of packets or frequency of transmission. Therefore, the computation for each logical domain is done on-site at the respective unit, ensuring a more modular and scalable design. This also allows for a higher plug-and-play and testing capabilities. The Main Controller acts as a central hub for decision making, connection with the Ground Station and persistent memory, while also being decoupled from the other computational modules as much as possible, in order to maintain a fast and reliable internal communication.

The braking system is housed on a separate PCB. This integrated circuit is relatively rudimentary and doesn't require a computational module for any of its functionality and, as a result, is not as sensitive to EMI and data transmission issues as other subsystems. Despite that, it is a critical component of the embedded system architecture. Recognising that and separating the modules from the other systems allows for a greater adaptability to revisions and scales to bigger systems. Different types of redundancy can be implemented by adding additional modules with the same or similar functionality and different braking mechanisms can be adopted and tested with less friction than if it was integrated with another logical domain like the MCU. Alongside the commands from the Main Controller, signals, related to emergencies, trigger the breaking system automatically, ensuring minimal latency,

The separation of the internal pod logic systems in a centralized vehicle controller and separate modules based on functionality and types of computations needed supports both a Domain and a Zonal architecture, but leans towards the zone-based design, because of the Ethernet-centered core communication. Each PCB on the pod aggregates functions in a singular domain, i.e. localization, power distribution, braking, state transition. This lessens the load on the centralized bus, since only events and filtered data is transmitted between systems and the bulk of the computational work is done within each subsystem. The domain architecture also groups the set of sensors and Electronic Core Units (ECUs), based on function, but relies on a CAN (Centralized Area Network) bus to prioritize to introduce hierarchy in the communication, with other protocols usually being used for smaller, and non-critical systems. This design is becoming outdated in modern vehicles, because of the high bandwidth of sensor data and the high-frequency processing that is required for all of the systems from autonomous driving, data logging, infotainment, etc. The centralized CAN bus can carry a maximum of 1 Mbps (5 Mbps for CAN-FD), unlike the industrial Ethernet that can transmit more than a hundred fold that. The cable management also becomes cumbersome with this architecture as it increases weight and cost significantly. The Ethernet-based zonal design resolves a lot of these issues by aggregating the data and computation of modules based on location and then utilizes the bandwidth capacity of the protocol to transmit them around the vehicle. It is also a better fit for the topology and the potential amount of data collection in a full-scale system, since the aforementioned issues would only be exacerbated. The specific design choices supporting the scalable architecture with the industrial Ethernet bus are explained in the last section of the chapter.

## Requirements

**Table 7.15:** Internal Control System Requirements

ID	Requirement
SC.IC.T.1	The MCU on the Main Controller should be mainly responsible for changing state and persistent memory.
SC.IC.T.2	The design of the circuits and the distribution of computations should optimize for modularity and robustness, meaning each PCB is responsible for one functional domain and exchanges primarily synthesized data and events for change of state.
SC.IC.T.3	The data bus should be able to handle the bandwidth and integrity requirements of all the messages and signals. It should also be appropriate for a full-scale real-time system with more subsystems, sensors and general data transmission.
SC.IC.T.4	The overall architecture of the system should have plug-and-play capability, so that if any of the subsystem has to be extended or enhanced with scaling of the pod it can be reintegrated with minimal change of any of the other ones or the communication means.
SC.IC.T.5	All of the PCBs need to be designed with industrial grade components and should facilitate signal integrity and high-frequency communication of various signals through their layout, layer stack, tracing, and thermal and EMI/EMC compliance.
SC.IC.M.1	There should be persistent memory in the Main Controller that can log events and data in a standardized format.
SC.IC.M.2	There should be warning LEDs that display information about the state and health of the pod and can be seen from outside through the aeroshell.
SC.IC.M.2	The subsystems should use events and filtered data for the control of the pod, but should actively monitor as much sensor data as possible for diagnostics.
SC.IC.S.1	The braking system circuit should be able to automatically activate the brakes in case of emergency, like losing connection to the Powertrain system controller (PTSC) or the Main Controller. It should also activate independently if the temperature in the Vacuum Box is too high.
SC.IC.S.2	The signals activating the brakes should hold priority in case of emergency and should have minimal latency in addition to the decoupling from the other systems.

### 7.4.1 Main Controller

The Main Controller PCB is the logic center of the pod. Data from all of the sensors and the power system is streamlined through the Ethernet bus in order to be interpreted by the MCU, which extrapolates the current state of the machine and computes the next state the pod should enter, based on the “events” and the Finite State Machine schematic, described in the Software section. The board contains the MCU and components that support its functionality. It only needs interfaces for the different protocols and subsystems to feed it the events and data from sensors with minimum latency and EMI issues. The layer stack, materials, components, layout and circuit design optimize for reliable transmission of signals from and to the MCU. The separation of the main PCB from any other subsystem relates to the modular design philosophy, but also makes it easier to decouple and shield sensitive signals. The specifications and reasoning for the different components, interfaces and PCB design choices is provided below.

#### Main Controller Unit (MCU)

The STM32H742ZIT6 is used as the MCU of the pod. It features the 32-bit ARM Cortex-M7 architecture, operating at 480MHz. The unit supports Mbed OS, the real-time operating system and it also provides an abstract API which simplifies development. The L1 cache, 2 Mbytes of Flash memory and 1MB of RAM will provide sufficient storage for the data computed by the MCU. The MCU requires 3.3V of power supply, provided through the low-voltage buck converter from

the LV PDU. It supports two CAN, four UART/USART and four I2C transmission lines, along with an Ethernet interface. To boost performance levels for the STM32 microcontroller, a stable clock signal is provided through the two external oscillator crystals, X1 and X2, with frequencies of 32 kHz and 8 MHz, respectively. Moreover, its internal phase-locked loop is used to attain the highest possible performance, described in its datasheet. The capacitors and resistors connected to the microcontroller have been placed as close as possible to it, in order to remove noise and retain the signal integrity. The vias underneath and next to it also act as a sink for the heat it will produce.

## SD Card

An SD Card is used as a non-volatile storage of data for logging and testing purposes. While data is continuously communicated to the Ground Station through wireless telemetry, the on-board memory provides data retention in case connection is lost or we want to use on-site memory to test and track the activity of the MCU. The interface with the controller unit is done through a three-state octal bus transceiver (SN74LVCH245APW). This integrated circuit is designed so as to establish proper data transmission between the chip and the SD card.

## Watchdog Timer

For additional protection from system failures a watchdog timer (STWD100NYWY3F) is used in order to reset the MCU in case of different types of hardware errors (non-responding peripherals, bus contention, etc.) or software errors (bad code jump, code stuck in loop, etc.). The input, WDI, is used to clear the internal watchdog timer periodically within the specified timeout period, twd - factory set to 102 ms. The system sends a signal - the heartbeat, to the timer every 50 ms, restarting it. If this signal doesn't reach the timer, the watchdog sends its inverted WDO signal and the MCU is reset, preventing further damage to the operations of the system.

## Ambient Pressure Sensor

The mounted pressure sensor (NPA-700B-015A) is placed to ensure the integrity of the main PCB and provide information on the pressure inside of the pod. The sensor has a rated pressure of 15 psi (approx. 1 bar) with an accuracy (total error band) of  $\pm 1.5$  percent of the full scale output. The operating pressure is 15 psi and the max pressure is rated as 60 psi. Bit rates up to 400 kHz are supported, compatible with the Standard-mode (Sm) - 100 kbit/s, and Fast-mode (Fm) - 400 kbit/s, standards, through the industry standard I2C protocol. The sensor also provides digital temperature reading, ranging from  $-50^{\circ}\text{C}$  to  $+150^{\circ}\text{C}$ , for an additional safety metric. The operating range of a vacuum-compatible pod should be from 0 to 1.1 bar, so anything outside of these values would be considered a danger to the correct functionality of our system and will trigger an emergency state.

## Braking Pressure Sensors

To ensure the correct functioning of the mechanical braking system, the low and high pressure sections are monitored. Both sensors output analog current between 4 mA and 20 mA, linearly dependent on the measured pressure and their respective output ranges. The current is converted to analog voltage in the range between 0.6 and 3.3V using a 165 Ohm resistors. Furthermore, a low-pass filter with a cut-out frequency of 96.5 Hz is implemented, filtering out high-frequency noise, in order to avoid the pressure measurements to deviate from the actual values due to, for example, a sudden change of pressure on the tanks. This can occur when the brakes are engaged or are being rearmed. The low pressure sensor's range is between 0 and 100 bar, while the high pressure one can measure between 0 and 250 bar.

## Safety Warnings LEDs

Warning LEDs that automatically trigger based on the error message, emergency, or signal related to the state or health of the pod have to be present on the pod to ensure the safety of people standing close to the pod and during testing and working with the system. Three of the nine LEDs visible on the aeroshell. The color coding and purpose of the different information they display is described in the external communication chapter.

## Ethernet Interface

This section outlines the signals and data transmission of the Main Controller on the Ethernet bus that connects it with the Powertrain controller, the Router, The Localization Master, The Levitation Motor Controller, The Propulsion Open Controller, and the Thermal Controllers. The tables below provide an overview of the data, events, and messages the Main Controller receives and sends from and to the other subsystems. The general overview does not include all of the events,

errors, messages that can be sent or received. They can always be extended, based on future needs of the system.

**Table 7.16:** Inputs to the MCU.

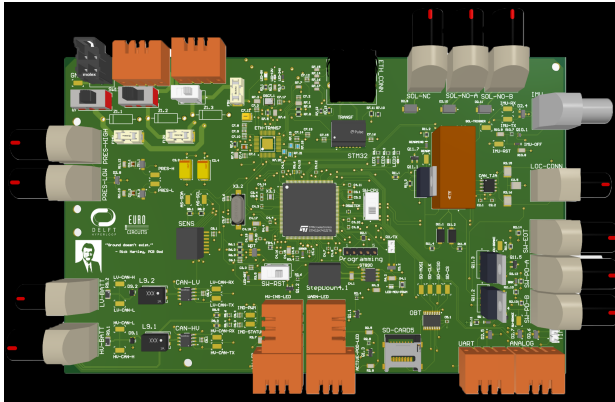
System	Data	Event/Message
Localization Master	vector integers (timestamps along with the position - calibrated to an absolute position along the track)	localization system error messages - no signal detected from sensors, clearly incorrect values, no agreement between the different localization systems, specific localization system fails, start and done calibrating thresholds, message indicating that the position is either relative or absolute.
Powertrain Controller	BMS data - battery health, SOC, capacity available, runs available, power consumption of subsystems, real-time data HV and LV batteries	Error messages and acknowledgements as described in the Power Controller subsection.
Thermal Controller	temperature readings in vacuum box (16 sensors), fan speeds recording RPM (12 fans), pressure sensor data	specific fan not working, temperature critical range for the 16 individual sensors, pressure sensor failure, acknowledgements of sensors and fans working properly
Levitation Motor Controller	Lateral and vertical airgap data (8 sensors), bus voltage of each cygnus, target airgap, current output	Error bus voltage too low, error bus voltage too high
Propulsion Open Controller	Run data (efficiency, velocity, speed), current usage	State change ok, State change failed, various error messages
Ground Station	Commands that will override the current behaviour of the pod or configure the next run (messages represented by ethernet packets that will be decoded)	Pre-defined commands (such as start levitating, start driving, reset battery cells) and configurations such as the run profile for the propulsion subsystem. All commands will be present on the ground station main control scene.

**Table 7.17:** Outputs from the MCU.

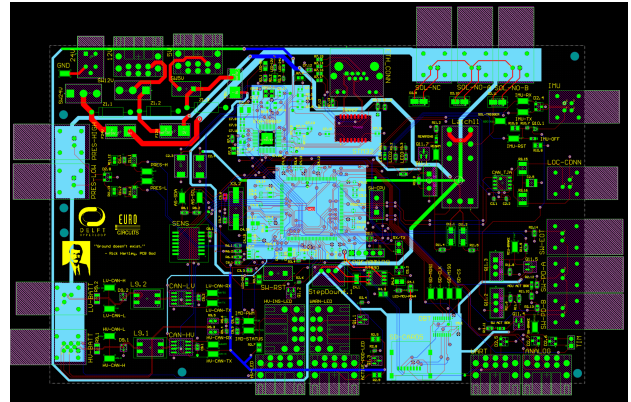
System	Data	Event/Message
Localization Master	-	initialization event
Powertrain Controller	propulsion positioning, system health (verification by main controller of other subsystems - verification or error event from each)	start HV instruction, HV on/off, error events (propulsion/loc errors, levitation position error - lateral, vertical), enable levitation events, levitating event, enable propulsion, accelerating event (levi and prop peak power consumption, cruising event (to determine if it's effectively cruising), start braking event
Thermal Controller	-	initialization event, stop event
Levitation Motor Controller	Arcas busstate machine state (pre-operational, safe operational, operational), axiscontrol state (disabled, ready to switch on, switched on, operation enabled)	Set Levi-state (launch from top, launch from bottom, stay at nominal airgap, search for zero-current, controlled landing)
Propulsion Open Controller	Run trajectory, SMC30 machine state, (pre-operational, safe operational, operational)	Set propulsion state (accelerating, cruising, braking)
Ground Station	messages that contain the data from all the sensing or control subsystems on the pod, including data and error messages	packets with all sensors data and a list of warnings and errors that the different sensors and subsystems reported

### Main Controller PCB Specifications

The stackup of the PCB board was chosen prioritizing signal integrity, and frequency and power needs. The board was configured to fit on its designated position on the pod and have room for all of the subcomponents on it. The 6-layer composition of Signal - Ground - Power - Signal - Ground - Signal is more than sufficient for proper functionality of the subsystems on the Main Controller PCB. At least two signal layers are needed, in order to route the different signals coming to and going out of the microcontroller. The additional signal layer allows for a more efficient layout and better signal separation, ensuring their integrity. Furthermore, this allows us to completely isolate the routing of analog and slower digital signals. The ground and power planes in the middle are placed to provide shielding and decoupling of the signals on these signal layers. Furthermore, a power and ground plane, when placed next to each other, will result in an interplane capacitance. Digital and analog signals are as far away as possible on the board, in order to avoid EMI problems with their respective return paths. This configuration supports boards in industry with much higher clock and signal frequencies. The materials for the build of the board are also optimised for high-frequency and sensitivity of signals. In figure 7.17 the topview and traces of the main controller are shown. It is important to note that the braking circuit and the main controller are currently integrated onto one board in these images, while in the final design these will be separated over two distinct boards.



(a) Topview of the Main Controller PCB



(b) PCB tracing of the Main Controller

**Figure 7.17:** Renders of the provisional design of the Main Controller PCB

#### 7.4.2 Braking PCB

The braking system is separated from the main PCB for the purpose of modularity, increased plug-and-play capability for critical systems for continuous integration, and adherence to the Zonal architecture for future scalability. Only the Main Controller sends commands to the Braking System directly.

The braking system circuit is designed for robustness and simplicity. The system itself and its components are described in section 8.4 of the Mechanical chapter. It needs to be purely mechanical, as to not be reliant on the other subsystems of the pod, in case of emergency. Also there has to be minimal latency between an emergency signal or a “manual” signal from the program running on the MCU to ensure safety. The circuit itself consists of a main latch and main MOSFETs - defining the three types of signals coming in. The central latch has three coils for operation - SET, RESET and the power voltage with a constant supply of 12V. The bridge is between 24V and ground and is connected to the signals, connected to the solenoid valves. When 24V are transmitted the brakes recharge and when it goes to 0V the brakes engage. On the SET side of the latch, the ACT-REARM-BR signal from the MCU resets the latch to its 24V position to refill the brakes. The signal first goes through a MOSFET that is off for 0V and on for anything above. On the RESET side of the latch we have two types of signals - the emergency sensor signals and the ACT-BRAKE-SOL from the MCU. Both types are normally 0V and go through N-channel Enhancement MOSFETs respectively to get to the latch. The emergency signals come from the pod drop sensors and the End-of-track switch. They should automatically engage the brakes without the input from the MCU or any other subsystem. The ACT-BRAKE-SOL comes from the MCU and is used to “manually” engage the brakes from the executed program on the main PCB.

To ensure maximal level of safety, there are signals that bypass the central Ethernet bus and the Main Controller’s commands, and activate the brakes automatically. These analog signals form a multi-input AND logic gate and ensure that the system will trigger with minimal latency without the need of commands from the Main Controller in case of emergency. Signals that bypass the need for commands from the Main Controller for are disconnection from the MCU or the Powertrain controller, the pod-drop sensors, the end-of-track sensor and the emergency switch. Together these signals form an Automatic Emergency Braking (AEB).

#### Braking System PCB Specifications

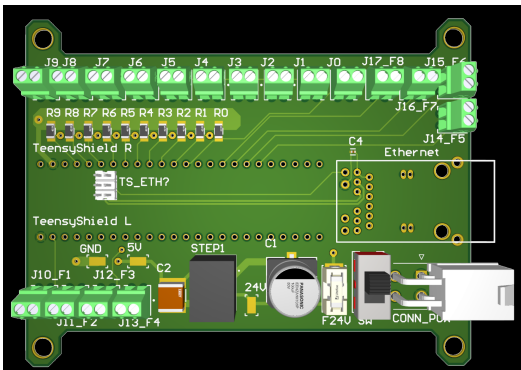
This Braking System PCB is designed with focus on robustness and signal integrity. It features a Signal - Power - Ground - Signal layer stack with the correlating interfaces with the Main Controller, the Automatic Emergency Braking and the brakes themselves. It doesn’t require more layers, because the signals do not transmit sensitive data, but rather digital serial signals that signal the change of states in the circuit. The two signal layers decouple signals and ensure reliable and fast transmission. The PCB has three power supplies - 5V, 12V, and 24V, because taking a singular 24V supply and splitting it into smaller ones will result in loss of efficiency. To ensure the proper power propagation and thermal resistance several design choices, regarding the power needs, have been made. Firstly, the PCB includes a solid power supply ground plane to provide electromagnetic shielding. Furthermore, the traces are as short and wide as possible to reduce resistive losses and electromagnetic noise emissions. Also, the traces that carry the sensitive signals for the command of the circuit are routed away from the power distribution ones.

### 7.4.3 Thermal Controller PCB

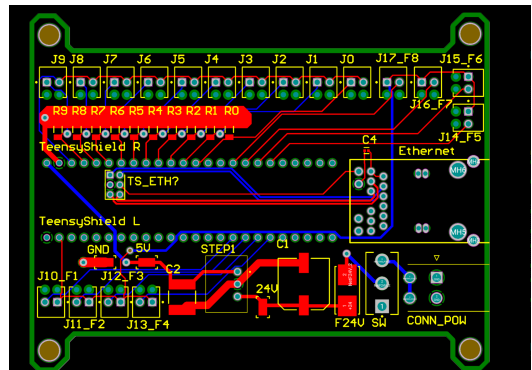
As stated earlier it is of critical importance that the temperature of the motor drives for propulsion and levitation, the high- and low-voltage power distribution boards and the inlet and outlet of the heat batteries is monitored and remain below 40 °C. The principle of the thermal management system is further explained in Section 7.8. One of the main components of this system are fans that create airflow inside the vacuum box. These fans require feedback control.

The fans are managed by the thermal controller. As stated in Section 7.2 this controller senses the temperature of all components in the vacuum box. According to these temperatures, the Thermal controller sends a signal to each of the fans to increase or decrease their rotation speed, thus adjusting the temperature inside the vacuum box.

The Thermal control uses two physical PCBs, one of which is located in the right side of the vacuum box and one that is located on the left. Each of these PCBs is used to control 6 fans. The thermal controller and its traces are shown in figure 7.18.



(a) 3D render of the Temperature PCB



(b) PCB tracing of the Temperature PCB

**Figure 7.18:** Top view and traces of the Temperature Controller.

### Thermal Management Interface

The fans used in the vacuum box require a PWM signal to operate. The Thermal controller sends this PWM signal. However, the fans work on a Voltage of 24 V and the thermal controller can only output a 5 V signal. Therefore, the PWM signal must be amplified using a switching board. Two switchboard convert the 5 V PWM signal to a 24 V signal for both of the Thermal Control PCB's. Furthermore, the correct functioning of the fans must be monitored so that malfunctions can be detected and resolved. This is also done using the Thermal Controller which sends the temperature data and fans operation data to the main PCB which is located outside of the vacuum box.

### 7.4.4 Industrial/Automotive Ethernet Bus

With the increase of bandwidth requirements for sensors and systems in the modern vehicle and industrial automation industry, the amount of computation and bus transmission rates become a bottleneck for the E/E architecture, especially the standard centralized bus for cars - CAN (Controlled Area Network). The bandwidth of 1 Mbit/s (5 Mbit/s and 20 Mbit/s for the enhanced CAN-FD and CAN-XL) is insufficient for the systems of modern vehicles, which are transitioning to a more computationally intensive and software-oriented design. The usual solution for that is increasing the number of wires/buses that make up the abstract main bus. Coupled with the domain driven architecture that usually accompanies the CAN-central system organization, cable management becomes a severe issue. The layout and sheer number of different cables needed introduce layout and weight issues. The network topology of a full-scale system would only exacerbate these problems. The automotive Ethernet bus supports various other protocols and features system interoperability, compatibility, and strong resource sharing capability, when needed. In addition, low latency, safe persistency, safe data transmission, and high security in network play a pivotal role in contemporary vehicles and will be pivotal for future ones. Moreover, it's better suited for external communication such as the connection with Ground station and over-the-air updates.

Industrial Ethernet bus provides a backbone for the system that can support large bandwidths, zonal architecture, high frequency transmission, more universal means of communication between systems, while also mitigating the weight and

cabling issues and inefficiencies. However, Ethernet is non-deterministic and also does not have predictable latency and guaranteed bandwidth. The standard protocol provides Quality of Service, error correction and identification of transmission problems, but it's crucial for the system of the pod to have real-time time sync and timeliness to the signals on the bus. To standardize timely communication between industrial networks, Profinet's IRT (Isochronous Real-Time) defines a set of standards for how time-dependent data is transmitted over Ethernet networks, by enabling time synchronization and scheduling. Profinet skips the TCP/IP packing and unpacking for real-time processes. Therefore, every data packet takes the same time every time and determinism is achieved. Through bandwidth reservation two channels, - the Real-Time and the TCP/IP, used for different types of data, are parallelized and a higher level of determinism is achieved. Each transmission cycle has an IRT reserved period, where time-sensitive, deterministic signals bypass the slow, asynchronous standard protocol. Through built-in processes like fast forwarding, dynamic frame packaging and fragmentation of frames, it achieves cycle times in the range of microseconds.

The communication is established through Phoenix Contact's FL SWITCH 1108N. It supports the Profinet industrial protocol and can transmit at a maximum rate of 1000 Mbit/s. It has 8 RJ45 ports and industrial grade life conditions, in terms of temperature, pressure and humidity. Three of these switches are used on board - 2 on each side of the vacuum box - for the levitation and propulsion systems respectively, and one central node on the outside. The ones inside both connect to the temperature sensor hub and each to the levitation and propulsion control modules respectively. The main gateway switch is on the outside and connects the Main Controller, the Localization master, the Powertrain controller, and the Ground Station router to the systems in the vacuum box. The data connections displayed for the Ethernet bus, formed through the switches, are for overview purposes. In reality, the connection between any two switches is established through one cable. Also, some subsystems and sensors are grouped for simplicity and many of the powertrain subsystems are omitted, because they are explained thoroughly in the Power section.

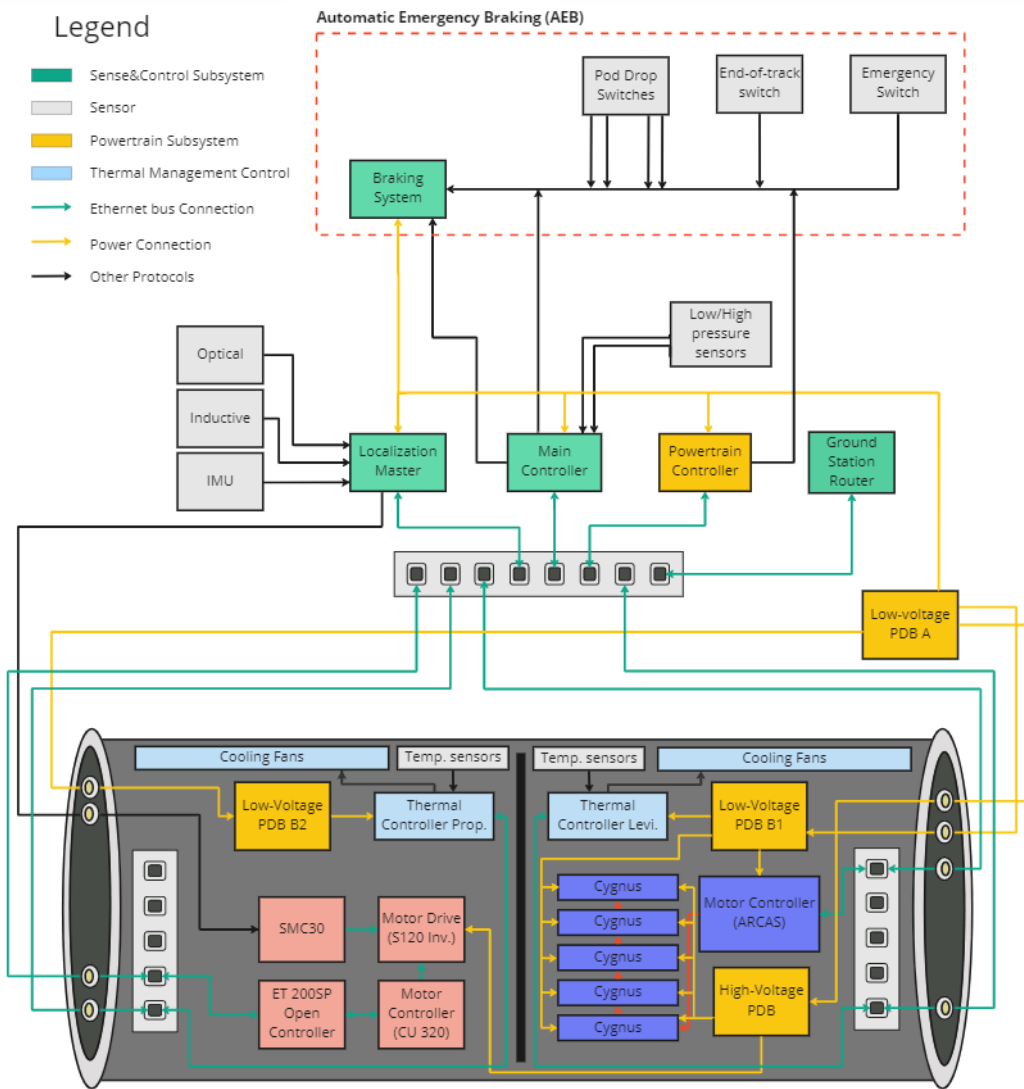


**Figure 7.19:** System diagram with switches and PCB connections

## 7.5 Pod Software

This section provides an overview of the software architecture and design of the Hyperloop pod's subsystems, with a focus on the pod controller. The section outlines the functional and non-functional requirements that the software must fulfill and delves into the use of a Hierarchical Event-Driven Finite State Machine (HEDFSM) [24] to control the pod's behavior. The software architecture that will be employed to meet these requirements is also discussed, which is based on the internal communication constraints Section 7.4.4. Additionally, the implementation of a continuous integration and continuous deployment (CI/CD) pipeline is covered, ensuring safe redeployment of the software, and the process for updating the firmware on the pod over the air (OTA) is also explained.

As hardware systems become more complex, the trend has been to move from centralized communication systems to local area networks [25] that perform computations locally and transmit only relevant data. This shift has led to a decrease in demand for memory-constrained software for embedded systems, while the need for low latency remains critical. This transition towards decentralized processing systems necessitates using a gateway for communication with a Ground Station for security reasons, which can become later multiple instances of the main PCB to handle load-balancing of different parts of the pod to minimize the number of cables throughout the pod. The new system architecture, which can be compared to a 'microservice-based' architecture, offers advantages such as increased scalability, flexibility, and communication reliability while maintaining the low latency required for real-time applications. The design choice to use a decentralized 'microservice-based' architecture is emphasized.

### 7.5.1 Requirements

The requirements for the pod software are outlined in detail, ensuring the smooth and safe operation of the Hyperloop system. This section provides a detailed understanding of the functional and non-functional requirements that the software must satisfy. Table Table 7.18 summarizes the specific needs and expectations for the software that will be utilized on the pod side in the Hyperloop system.

**Table 7.18:** Requirements for pod Software

ID	Requirement
SC.SW.T.1	The pod software shall provide a highly available and fault-tolerant system to ensure consistent, error-free performance. The system shall detect and mitigate software and hardware failures in real time.
SC.SW.T.2	The pod software shall include autonomous decision-making capabilities to minimize the need for human intervention.
SC.SW.T.3	The pod software shall provide comprehensive data logging and telemetry capabilities for debugging and performance analysis. The system shall log all sensor data and store it for future analysis, including analysis of system performance and optimization.
SC.SW.T.4	The pod software shall support firmware updates through a secure, over-the-air (OTA) mechanism. The OTA mechanism shall ensure that the firmware is up to date and that the system is secure from unauthorized access.
SC.SW.T.5	The pod software shall allow software updates without requiring a physical connection to ensure safe and easy deployments of an improved system. The software shall provide a mechanism for verifying the authenticity and integrity of software updates before installation.

### 7.5.2 Finite State Machine

The usage of the Hierarchical Event-Driven Finite State Machine was needed to control the various behaviors of the pod. It is an extension of the classical Finite State Machines (FSM) that are widely used to control embedded systems. The extensions came from the need to react fast to sensor data and commands (which represent events in the system), hence the 'event-driven'. Furthermore, since there are multiple independent systems in the pod, each with its own specifics and its own Finite State Machine, the high-level abstraction is the usage of the Hierarchical Finite-State Machine that encapsulates all different control behaviors of the different subsystems, while maintaining the semantics of the main FSM. Any subsystem finite state machine can be easily showcased by extending the main Finite State Machine since the states have been created in such a way that every subsystem is dependent only on the main state of the machine, and not on other subsystem states. This way, each subsystem is exposed only to the pod controller Finite State Machine, removing

inter-dependencies between subsystems, hence making the system scalable horizontally (the workload can be distributed between multiple 'machines' rather than making the current 'machine' handle more load). For simplicity, this chapter will explain only the high-level pod FSM Figure 7.20, with emphasis on the main states and the conditions that lead to transitions between them.

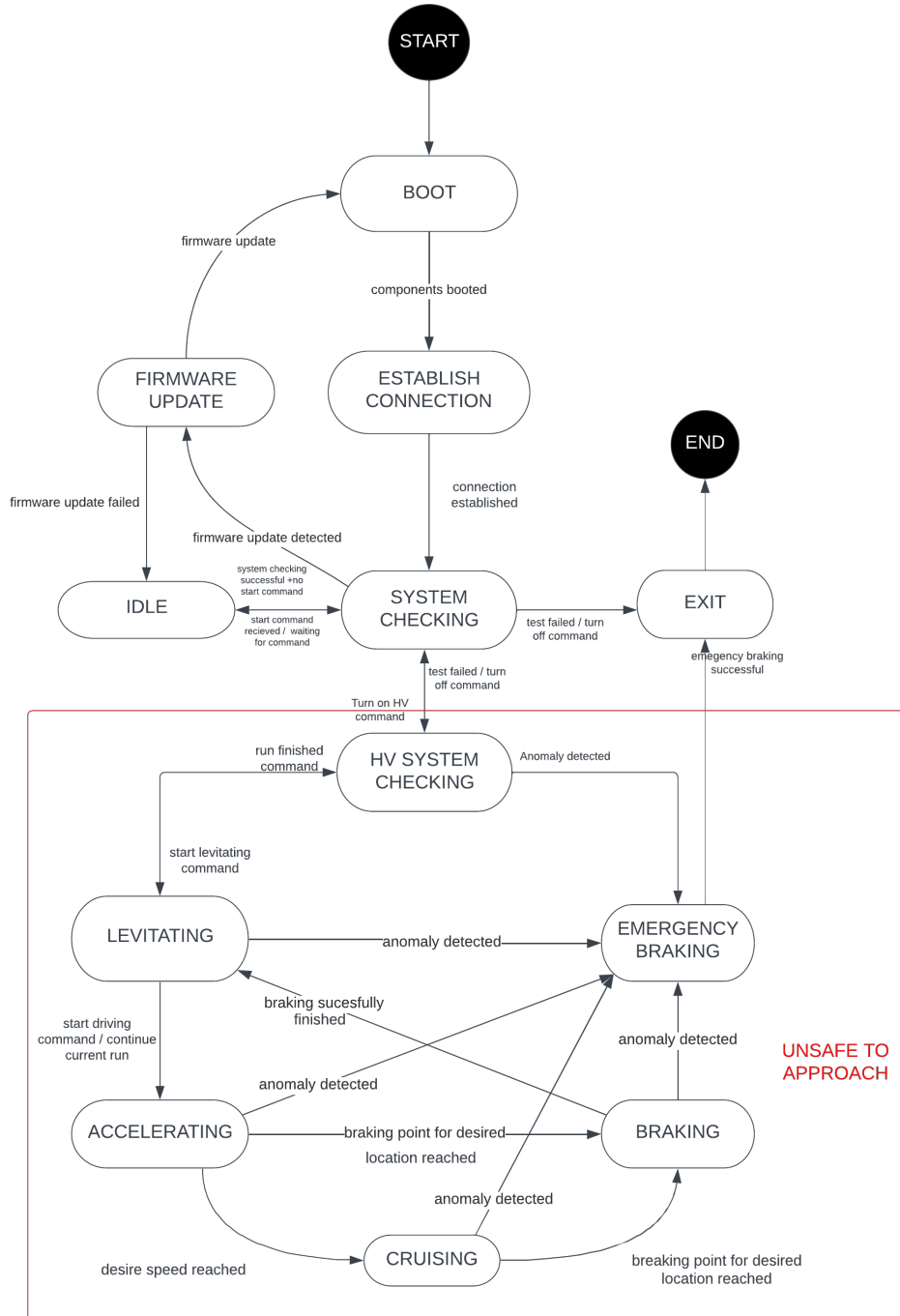


**Figure 7.20:** The Core Finite State Machine of the pod with all the states and transition between states

The pod FSM is used to control the behavior of the pod. It manages the various states that the pod can be in and the transition between these states are triggered by events based on readings from sensor data or user input. This approach allows for a clear and organized way of controlling the behavior of the pod, making it easy to identify and troubleshoot any issues that may arise. Additionally, every state/event combination mentioned throughout the chapter will contain a mapping to the LEDs Section 7.4.1 that will showcase the error message or confirmation of a successful action.

## BOOT

The pod enters this state the moment it is turned on. In this state, all electrical components are initialized. Depending on the output of the initialization, this part will generate 2 possible events: *BootingFailedEvent* which would lead to the pod shutting off, and *BootingCompleteEvent* which would trigger a transition into **Establish Connection state**.

## Establish connection

The pod enters this state after it has successfully booted. In this state, a connection bridge is set between the pod and the Ground Station Section 7.6.2. Depending on the result of the operation, two possible events are being generated: *ConnectionEstablishmentFailedEvent* in case no connection was established in 3 minutes, which would lead to the pod being turned off, and *ConnectionEstablishedEvent* in case the connection is successful, which leads to the pod transitioning to the **System check state**.

## System checking

Upon successful establishment of a connection with the Ground Station, the pod enters the **System checking state**. In this state, various safety protocols are implemented to ensure the integrity of sensor data and to verify that the pod is in the desired configuration for a run. Out of the checks, the most important one is checking the bounds of sensor values and checking the state of the low-voltage powered subsystems such as powertrain, levitation, and propulsion. If any of these tests fail, the pod will automatically initiate a shutdown sequence and log the associated error. These checks are performed at the initialization of the pod, prior to initiating a run, and post-run to ensure that the pod is in a safe state. Additionally, this state includes a query to the Ground Station to check if the current version of the firmware is up-to-date. If a new version of the firmware is available, the *FirmwareUpdateDetectedEvent* will be triggered, initiating a transition to the **Firmware Update state**. If the state is entered as a result of a *RunFinishedEvent*, the pod will transition to the **Exit state**, otherwise, if all checks pass, it will transition to the **Idle state**.

## Firmware update

The pod enters this state when a *FirmwareUpdateEvent* is detected during the **System Checking state**. In this state, the pod downloads the code image from the specified location and performs a firmware update Section 7.5.6 if the CI/CD pipeline Section 7.5.5 has passed. This action can result in two possible events: a *FirmwareUpdateFailedEvent*, which will move the pod to the **Idle state** with a flag set that will trigger a warning when attempting to run the pod, or a *FirmwareUpdateSuccessfulEvent*, which will restart the pod with the new firmware.

## Idle

The pod enters this state when the **System checking** is complete and the pod is waiting for a command from the Ground Station. When a command is received, such as a *TurnONHVCommand*, the pod will transition back to the **System checking state** again, and then, if everything is working properly, to the *HV System Checking state*. This is also the only state in which configurations of different components can be set up, such as run configuration for propulsion subsystem Section 4.5.

## HV System Checking

The HV System Checking state is initiated when the pod receives the *TurnONHVCommand*. Before executing the command, confirmation is sent to ensure that no one is in the proximity of the pod. In this state, a command is sent to the powertrain to power on the High Voltage system. If the state is entered as a result of a *RunFinishedEvent*, the pod will transition to the **System Checking state** while turning off the High Voltage system. On the other hand, if the pod received a *StartLevitatingCommand*, it will transition to the **Levitating state** if all safety checks pass.

## Levitating

The HV System Checking state is initiated when the pod receives the *TurnONHVCommand*. Before executing the command, confirmation is sent to ensure that no one is in the proximity of the pod. In this state, a command is sent to the powertrain to power on the High Voltage system. If the state is entered as a result of a *RunFinishedEvent*, the pod will transition to the **System Checking** state while turning off the High Voltage system. On the other hand, when the pod receives *StartLevitatingCommand*, if all safety checks pass, it will transition to the **Levitating state**.

### Accelerating

The pod enters this state when the *StartAcceleratingCommand* is received while the pod is already levitating. In this state, the run configuration is sent to the Propulsion subsystem Section 4.5, along with a signal to start the run. If all pre-driving checks pass (such as the configuration being a valid one and that the propulsion subsystem is ready to accelerate), the pod will begin accelerating until the maximum desired acceleration is reached, represented by *MaximumAccelerationReachedEvent*. When this event occurs, there will be a transition to the **Cruising state**. If an anomaly is detected, represented by *AnomalyDetectedEvent*, the pod will transition to the **Emergency Brake state**.

### Cruising

The pod enters this state when the *MaximumAccelerationReachedEvent* is received while the pod is in the **Accelerating state**. In this state, the pod continues to respond to safety checks from levitation and propulsion subsystems. If an anomaly is detected, represented by *AnomalyDetectedEvent*, the pod will transition to the **Emergency Braking state**. Otherwise, the pod will wait until *BrakingPointReachedEvent* is received, at which point a transition to the **Brake state** will occur.

### Braking

The pod enters this state when the *BrakingPointReachedEvent* is received while the pod is in the **Cruising state**. In this state, the Regenerative Braking circuit Section 6.7 is activated. If an anomaly is detected, such as a *BrakingFailedEvent*, the pod will transition to the **Emergency braking state**. If a successful braking event is detected, represented by *BrakingSuccessfulEvent*, the pod will transition back to the **Levitating state** and wait for the next command.

### Emergency braking

The pod enters this state when an *AnomalyDetectedEvent* is received. This event can be triggered by a variety of child events, including *SensorsErrorEvent* (when a sensor output a value out of the nominal operational range), *LevitationErrorEvent* (when Levitation subsystems send an error code), *PropulsionErrorEvent* (when the Propulsion subsystems send an error code), *PowerTrainErrorEvent* (when PowerTrain subsystem send an error code), and *ConnectionLossEvent* (in case the connection with the Ground Station is lost for more than 0.5 seconds). In this state, the Emergency Brakes will be deployed and the pod will come to a stop while decoupling the High-Voltage Batteries. In the case of an *LVErrorEvent* everything listed previously will happen and in addition to that the low-voltage system will be turned off due to safety reasons. It is not turned off otherwise because there is still the need to communicate with the pod and to make debugging possible without approaching the pod.

### Exit

The pod enters the exit state after finishing or aborting a run, in which it is shutting down and preparing for removal from the track. This state is triggered by a *RunAbortCommand* or a command to shut down the pod. These types of commands will be executed on a pod only when it has to be taken out of the track for maintenance purposes or for recharging the batteries. In the *Exit state*, the pod will go through several steps to ensure that it is safe for removal from the track, such as shutting down all subsystems and systems and securing the pod for transport. In this state, the pod will no longer respond to commands and will be in a dormant state until it is reactivated for the next run. Additionally, the pod will send a message to the Ground Station to notify that the pod is exiting the service and it will be no longer operational until the next activation.

### 7.5.3 Software architecture

The design of the pod's software architecture is tightly integrated with its hardware subsystems and is made up of seven major components, which are the Core Controller, Localization, High-Voltage Controller, Levitation, Propulsion, and Braking subsystems. These subsystems communicate with each other either via the Main PCB for non-safety-critical functions or directly for safety-critical functions like braking where low latency is necessary.

In order to ensure the system is efficient and reliable, communication between subsystems is kept to a minimum, with only the essential data required for logging and event triggers being sent between them. This is in accordance with industry standards, where the local computation of necessary information is prioritized, and only the relevant data or compressed versions of the data are sent to prevent system overload or reaching operational limits.

The Core Controller is responsible for coordinating and managing the other subsystems and acts as the central hub of the system. The Localization subsystem enables the pod to navigate and determine its position accurately. The High-Voltage Controller regulates and manages the power supply to the other subsystems, while Levitation provides the necessary lift and suspension for the pod to move. Propulsion controls the pod's speed and direction, and the Emergency Braking subsystem is responsible for stopping the pod in case of any emergency.

Overall, the software architecture of the pod is designed to be robust and efficient, with a focus on maintaining a high level of safety and reliability. The subsystems are engineered to work together seamlessly, while still maintaining a degree of independence to ensure optimal performance.

### 7.5.4 Core controller

The Core controller is one of several controllers that serve different functions, such as High Voltage, Localization, Levitation, and Propulsion. The Core Controller code is written in C++ and it runs on the Main PCB Section 7.4.1. The choice of C++ was due to its low latency requirements and its better semantics compared to languages like C, which are typically used in similar applications [26] [27]. The Core controller runs on top of Mbed-OS, an open-source Real-Time Operating System tailored for ARM microcontrollers Section 7.4.1, chosen for its high performance and efficiency in meeting the pod's requirements.

The Core controller acts as a gateway of communication between the pod and the Ground Station, by propagating the needed information to each of the subsystems, while also playing the role of a data aggregation subsystem that will pack all the data from the pod and send it to the Ground Station as a compressed message to limit the used bandwidth of the system Section 7.6.2.

In order to build a reliable and robust Core controller, the future has to be taken into account and realize which components to scale for (for example, a higher number of sensors). Taking this into account we have decided that the most probable scale direction is having multiple decentralized controllers that control parts of the pod and big chunks of data will have to be processed. Taking this into account, the Active Object design pattern [28], which allows for the encapsulation of an object's behavior behind a message-passing interface, enabling the concurrent execution of multiple objects in a single thread.

In the architecture of this embedded system, the Active Object design pattern is used to manage concurrency, ensuring that the system could handle multiple tasks simultaneously without the need for complex and error-prone multi-threading.

### 7.5.5 Continuous integration/Continuous Deployment Pipeline

A Continuous Integration/Continuous Deployment (CI/CD) pipeline is a software development methodology that involves continuous integration, testing, and deployment of software updates. It is a process that automates the build, testing, and deployment of software updates in a controlled and efficient manner. This approach allows developers to rapidly iterate on software updates while ensuring that the changes are thoroughly tested before deployment to production systems.

For embedded systems, which are typically characterized by limited resources and real-time constraints, the pipeline must be tailored to these specific needs. To ensure that updates are thoroughly tested before deployment, the pipeline includes automated tests that check all known common behaviors of the system. These tests include unit tests, integration tests, and functional tests.

The pipeline is triggered every time a code push is done in the Github repository. If a merge request is approved to the *main* branch, a deployment is scheduled for the next time the pod is turned on.

In addition to the automated test suite, the pipeline can also include hardware in the loop testing (HIL) [29], which involves testing the software update's ability to communicate with the existing hardware. HIL testing involves connecting the system under test to a physical or virtual hardware system that mimics the target system's behavior. By doing so, the pipeline can ensure that the updated software will work correctly with the existing hardware, reducing the risk of incompatibilities or errors.

#### 7.5.6 Firmware updates

Firmware updates are a critical aspect of maintaining the functionality and security of embedded systems, and Ethernet-based firmware updates are an efficient and remote method for delivering software updates. This allows embedded systems to be updated quickly and easily without the need for manual intervention.

The process of updating firmware via Ethernet typically involves three main steps: obtaining the new firmware, transferring it to the embedded system, and installing it. To obtain the new firmware, the pod queries the Ground Station if there is an updated version of the software that should be uploaded on the pod. The firmware is then transferred to the embedded system using Ethernet communication. Once the firmware is transferred, it is installed on the embedded system, and the system is rebooted to allow the new firmware to take over and start running [30]. Any MCU-based device on the pod can have its firmware updated using this method, which ensures easy bug-solving methods that do not involve high costs for moving the faulty devices to a safe location where an update would be possible [31].

It's important to note that before deploying firmware updates, it's essential to thoroughly test them to ensure that they don't introduce new bugs or cause compatibility issues with other components of the system. The CI/CD pipeline Section 7.5.5 is an automated process that tests and integrates updates before deployment, reducing the risk of errors and ensuring that the update is thoroughly tested before being deployed to production systems. This approach allows developers to rapidly iterate on software updates while ensuring that the changes are thoroughly tested before deployment to production systems.

## 7.6 Communication & Ground Station

The Pod relies heavily on effective communication between its various subsystems and systems in order to operate safely and efficiently. To achieve this, the system utilizes communication protocols to facilitate the transmission of information between components. Throughout this chapter, the main focus is the communication protocols with the Ground Station.

In addition to communication protocols, the system also utilizes a graphical user interface (GUI) to provide real-time monitoring and control of the system. The GUI allows operators to view the status of the Pod and its subsystems, as well as to input commands and make adjustments as needed. The design and functionality of the GUI will be discussed in more detail in this chapter.

The Pod software shall also include the capability for over-the-air (OTA) updates to ensure that the system remains up-to-date with the latest software and security patches. This will allow for easy maintenance and troubleshooting of the system, as well as the ability to quickly implement new features and improvements as they become available. The OTA updates shall be secure and shall not compromise the safety and integrity of the system. The system shall also have a rollback feature that allows it to revert to the previous version of the software in case of a failure in the update process.

### 7.6.1 Requirements

**Table 7.19:** Requirements Pod Communication & Ground Station

ID	Requirement
SC.GC.T.1	The communication and ground station shall have a communication latency of less than 100ms for sending commands to the Pod and receiving data from the Pod.
SC.GC.T.2	The communication and ground station shall have a communication frequency of at least 2Hz between the Pod and the ground station.
SC.GC.T.3	The communication and ground station shall have a robust and reliable communication protocol to ensure the safe and efficient operation of the Hyperloop system.
SC.GC.T.4	The communication and ground station shall have the ability to handle a large amount of data and be scalable to accommodate a growing number of Pods in the system.
SC.GC.T.5	The communication and ground station shall have a user-friendly graphical interface for monitoring and controlling the Pod.
SC.GC.T.6	The system should allow for over-the-air updates.

### 7.6.2 External communication

The external communication is realized between the Pod and the Ground Station. The link between the Pod and the Ground Station is bi-directional and made through a pairing with a Ubiquity NanoStation M5, running on the 5 GHz frequency band. The information that needs to be transmitted through this link is serialized into a Nanopb message and sent. For sending the message there was implemented the MQTT (MQ Telemetry Transport) connection protocol, over TCP/IP (Transmission Control Protocol/Internet Protocol) to fit our system requirements: reliability and minimal end-to-end latency. Being a bi-directional connection, both the Pod and the Ground Station can send data. Pod will send mostly sensor data and decisions taken logs. The Ground Station will be able to update the state of the Pod by sending several commands that will map to Pod actions Section 7.5.2

Apart from the data, we send heartbeats between the Ground Station and the pod to monitor the connection status. If the Pod has not received any acknowledgment in the predefined amount of time (a period that depends on the current state of the pod, e.g. location or speed - for now it was decided for 0.5 seconds but might vary depending on testing results), it will either try to reconnect if it's in a safe state or it will emergency break in case it is in an unsafe state Figure 7.20

We have decided to use the Ubiquity Nanostation M5 because it offers reliability and low-latency transmission for the desired data, offering us a high theoretical frequency for our data transmission [32].

**Table 7.20:** TCP vs UDP

TCP	UDP
Connection-oriented protocol	Connectionless protocol
Messages move from one computer to another	Do not require connections for packets to be sent from program to program
Rearranges packets in a specific order	Has no fixed order
Slow transmission speed	Faster transmission speed due to no error recovery
Performs error checking and error recovery	Performs light error checking, but discards broken packets
Acknowledgement segments	No acknowledgement segments
Reliable transmission delivery	No delivery guarantee
Extensive error checking	Single error checking are used for checksums

Based on a thorough assessment that prioritized reliability as the paramount factor, the verdict was reached that TCP was the optimal selection despite the existence of alternatives such as Quick, a hybrid protocol that combines aspects of UDP and a connection-oriented approach, which may have appeared more promising at first glance. However, Quick's relative novelty and lack of established stability, coupled with its tendency to exhibit unexpected behaviors, ultimately disqualified it from consideration.

The foremost objective of establishing a dependable protocol necessitates the optimization of end-to-end latency, a goal that can be accomplished through the transmission of smaller packets. With this objective in mind, a comparative analysis was conducted between MQTT and HTTP protocols.

**Table 7.21:** MQTT vs HTTP

	MQTT Bytes	HTTP Bytes
Establish connection	5572	2261
Disconnect	376 (optional)	0
For each message published	388	3285
Sum for 1 message	6336	5546
Sum for 10 messages	9829	55460
Sum for 100 messages	44748	554600

In accordance with the system's specifications, our objective is to minimize throughput while maintaining a consistent level of transmitted data. Following an evaluation of relevant data presented in the table, MQTT emerged as the ideal protocol for meeting these requirements.

To further maximize throughput, it is critical to select the most efficient serialization protocol. Additionally, given the need for high-frequency operation and the presence of C++ code on the PCB, minimizing latency is also of utmost importance. In light of these considerations, we have opted to use the embedded version of Protobufs, a reliable and efficient serialization protocol that can process data quickly while occupying minimal memory [33].

### 7.6.3 Ground Station

The Ground Station is an essential component of the pod transport system, and it is a desktop application developed using C++ with Qt. It serves as a control panel that provides the operator with real-time data and control functionalities, such as starting and aborting runs. The system gathers data from various sensors to give a complete overview of each subsystem and redundant component. The interface is user-friendly and intuitive, with detailed guides to help the operator understand all the functionalities available. In the event of an emergency, the system can also control the pod and provide useful insights into how the components perform over time and under different conditions.

The development of the Ground Station focused on building a modular application that could accommodate multiple commands and an increased amount of data display. The application has two main parts: *the main control scene* and *the data visualization scene*.

**The main control scene** serves as a summary of all the pod's data and allows the operator to perform any command, configure subsystems, and start a run. The scene also provides an explanation of all warnings and errors, and the operator can send an emergency break command if they believe the pod is not responding appropriately to the data or if there is any external information that the sensors cannot detect or infer. It is composed of the different elements illustrated in Figure 7.21

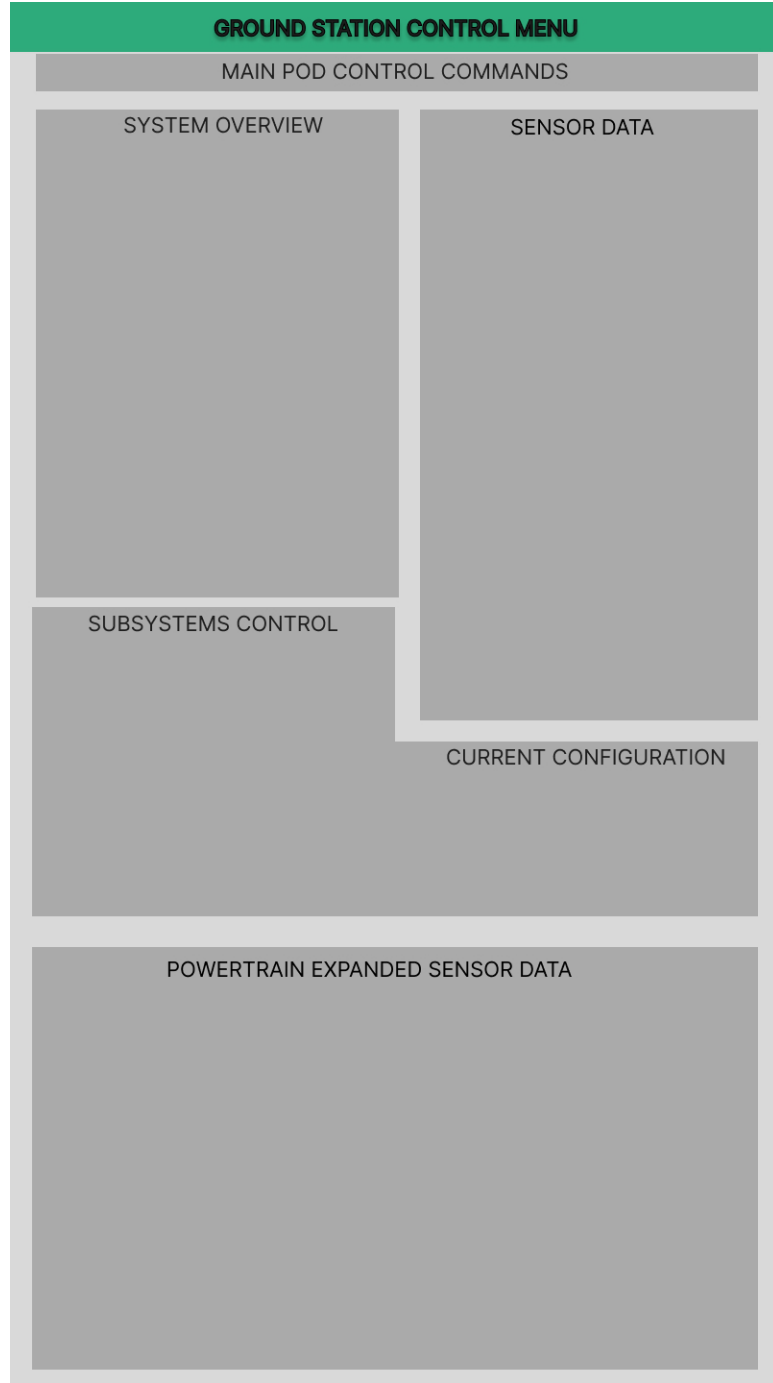


**Figure 7.21:** Wireframe of the main control scene

**The Ground Station control menu** plays a critical role in monitoring and controlling the pod. The Ground Station Control Menu offers quick access to all the functionalities available in the application, providing the operator with an intuitive way to navigate through the interface.

**The Main POD control commands** section offers essential high-level commands, such as start levitating, start driving, and emergency break, to ensure the safe operation of the pod. The emergency brake button is easily accessible and has a

key shortcut to trigger it quickly, while the other critical commands require additional confirmation to avoid unintended behavior.

**The System overview** provides a summary of important information related to the pod, such as the status of every subsystem, the current location on the track, the direction of movement, the speed, and the acceleration. Sensor data displays data from various sensors, including temperature, pressure, and position, among others. The Subsystem control section enables the operator to configure the subsystems, such as setting up the run configurations, adjusting battery settings, and other related parameters.

**The Current Configuration** section provides a summary of all settings that can be changed and applied to the current run. This section displays crucial information such as the current levitation air gap, propulsion run profile, and the type of run. This information is essential for monitoring and adjusting the pod's performance during a run.

**The Powertrain expanded sensor data** section displays detailed information such as voltage and temperature for the monitored packs without averaging or applying min/max thresholds for monitoring. This section allows the operator to analyze the data from the powertrain sensors and make informed decisions based on the information obtained.

**The Data Visualization Scene** is a powerful tool for analyzing sensor data over time and identifying patterns that can inform operators' decisions. In addition to the Ground Station Control Menu and Main Pod Control Commands, which are consistent across all scenes, this scene includes the Data Comparison Selection and Sensor Data Graphs Figure 7.22.

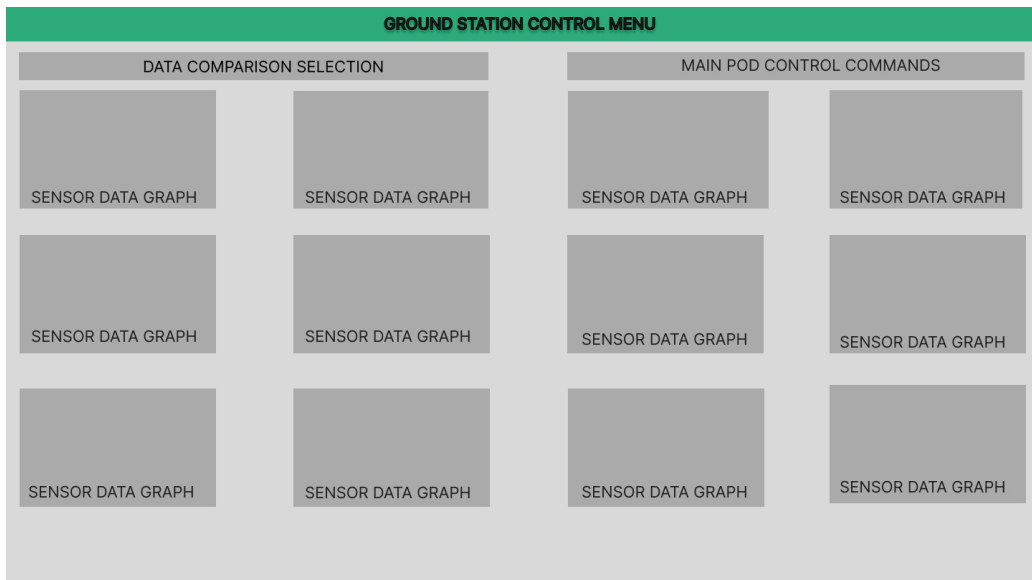


**Figure 7.22:** Wireframe of the data visualization scene

**The Data Comparison Selection** is a key feature of this scene, allowing operators to compare current sensor data to data from previous runs. This can be done by selecting a specific run at a certain timestamp or an average of runs from a particular day. This reference data is displayed on the graph as an additional line, providing valuable context for the current data. This feature can help operators detect anomalies or potential safety risks and take action accordingly. In the future, machine learning algorithms could be applied to this comparison data to automatically detect patterns and potential failures.

**The Sensor Data Graphs** section is where the sensor data is displayed. The graphs can include multiple values over time from various sensors and subsystems of the pod. Typically, each graph displays one line representing the current sensor values, with the option to add a reference line from a previous run for comparison. However, in some cases, such as with powertrain systems where multiple battery cells are monitored, two lines are displayed to show the minimum and maximum values for both the current and reference data. These graphs provide a visual representation of the sensor data and allow operators to quickly identify any trends or abnormalities.

#### **7.6.4 Over-the-air updates**

Over-the-air (OTA) updates have gained popularity as a means of updating software on devices without requiring physical access. In the automotive industry, OTA updates are particularly useful for vehicles with numerous subsystems that are challenging to access. With the advent of Ethernet-enabled microcontrollers, it is now possible to perform OTA updates for all subsystems in a vehicle, including the Core Controller, Localization, High-Voltage Controller, and Braking.

Ethernet enables rapid and convenient delivery of firmware updates to all subsystems in a vehicle. This provides an efficient way to ensure that all components remain up-to-date with the latest features and security updates. The firmware updates can be thoroughly tested before deployment by implementing a Continuous Integration/Continuous Deployment (CI/CD) pipeline Section 7.5.5, ensuring their reliability and bug-free performance.

It is critical that all subsystems in a vehicle support OTA updates to guarantee that every component is up-to-date and functioning correctly. The implementation of OTA updates via Ethernet is a valuable addition to the hyperloop system, offering a dependable and efficient way to keep vehicles updated and safe.

Any OTA update is a transactional operation that follows several steps. First, a pull request to the main branch in Github is accepted, and the code is compiled into binaries by the Ground Station and stored locally. When the Pod detects that the latest software on the Ground Station is newer than the current version, it requests the new software. The image of the software is then sent to the component that requested the update, and the component does a Firmware Update Section 7.5.6. If any of the operations fail, the entire process is canceled, and any updates that were made are reversed.

## 7.7 Physical Layout

The aim in this section is to explain the reasoning behind the placement of all subsystems, as well as the way they are attached to the chassis. One of the main reasons behind all placements is to keep all required cables as simple as possible, while splitting high and low voltage cables from each other and from communication cables. Section 7.7.2 goes further into detail into cable management.

### 7.7.1 Placement of subsystems

Since the sense & control system is integrated with nearly every subsystem on the pod, placement of the subsystems is crucial for smooth and well-organized operation. A render of the whole sense & control subsystem, with its wires and electronics, is given in figure 7.23 below. I WANT THIS RENDER WITH THE HOLE POD BUT IDK HOW

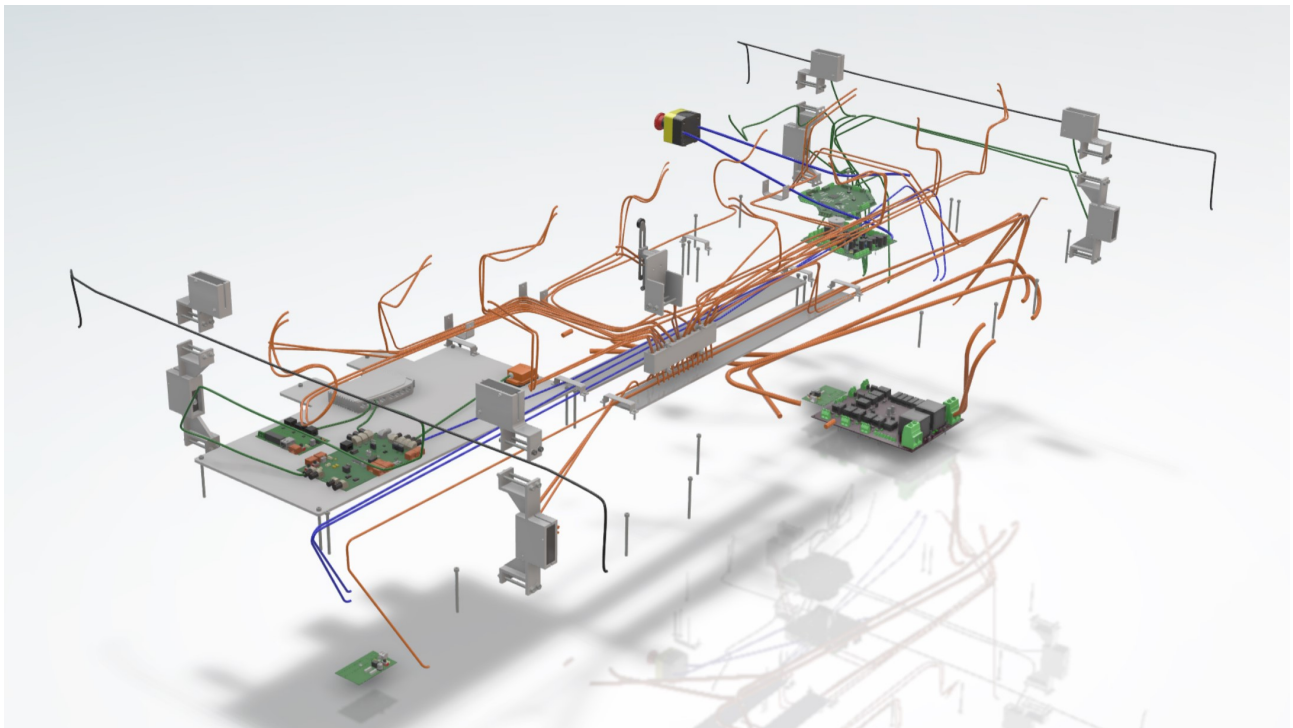


**Figure 7.23:** Render of the full sense & control subsystem

An overview of all sense & control components, together with their placement, is given in table 7.22 below. Here *propulsion side* refers to the front of the pod, which is where all the propulsion motor drive is located within the vacuum box. In the same manner the *levitation side* is the back of the pod where all levitation motor drives are located inside the vacuum box.

**Table 7.22:** Overview of placement of all sense & control subsystems.

Component	Quantity	Placement
<i>On top of the ladder frame</i>		
End of track switch	1	Centrally on the chassis
Localization inductive sensor	2	Centrally on the front and back
Localization optical sensors	6	Centrally on the front and back
Vertical offset sensor	4	Next to the vertical levitation coils
Fall off switch	4	Next to the levitation coils
Emergency Switch	1	Near the low voltage battery above the brake pad
<i>Inside the ladder frame</i>		
Main PCB	1	Near the propulsion side
Braking PCB	1	Next to the main PCB
Localization PCB	1	Near the propulsion side
IMU	1	Centrally on the pod near the PCB
High Voltage Controller	1	Near the levitation side
Horizontal offset sensor	4	Next to the lateral levitation coils
<i>Inside the vacuum box</i>		
Vacuum box temperature	15	On every heat source
Vacuum box pressure	1	Attached to the side of the vacuum box

For more clarity, a brief elaboration on the placement and reasoning for some of these components is given below.

### Main PCB

The main PCB is located on the front of the pod, inside the ladder frame. This position has been chosen for multiple reasons. First of all, this is one of the most accessible positions on the pod as soon as the aeroshell is taken off. Moreover, placing the PCB on the ladderframe makes sure its located at a centralized location, close to both the propulsion side of the vacuum box as well as all subsystems located on top of the pod, like the pod-drop switches. Lastly, and most importantly, the PCB is placed sufficiently far away from any high-voltage wiring and systems, to ensure it is shielded as much as possible from electromagnetic interference.

### Localization PCB

The localization PCB is placed next to the main PCB, for many of the same reasons as were given for the placement of the main PCB. Moreover, the placement is optimized to be as close as possible to the ET 200SP propulsion controller, to optimize for latency and cable length.

A render of the placement of both the main controller and the localization master board can be seen in 7.24 below. For clarity, all wiring has been hidden.

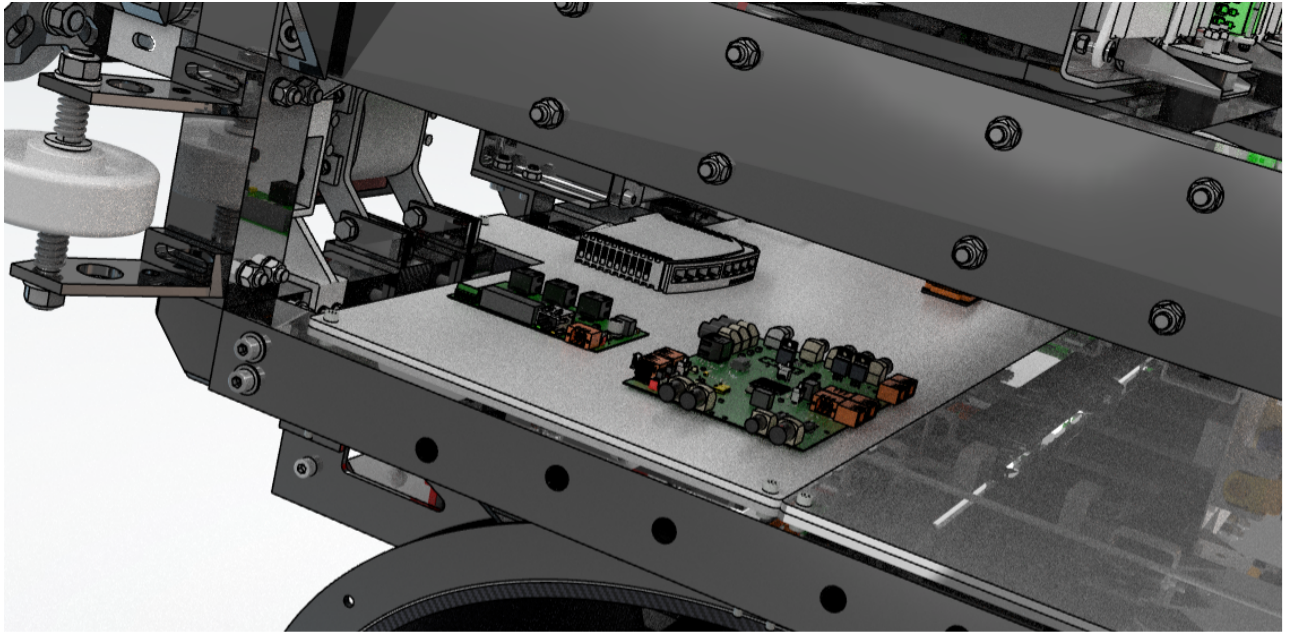
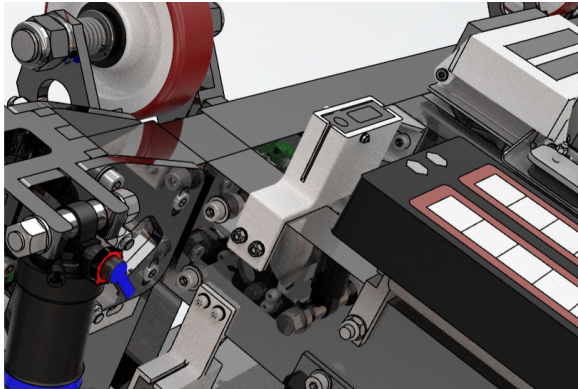


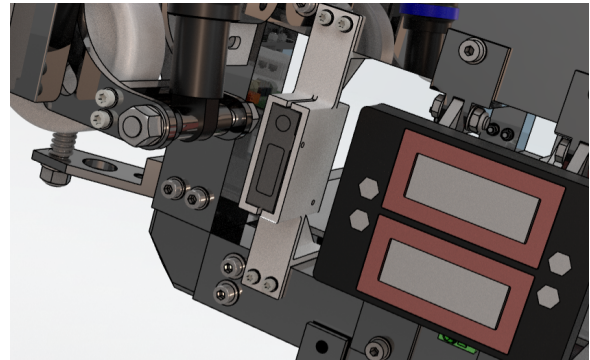
**Figure 7.24:** Render of both the main controller (right) and the localization master board(left) on the pod.

### Offset sensors

The sensors, both for lateral and vertical offset, are mounted as close to the levitation coils as deemed possible. This ensures that the difference between the detection of bumps in the track and the actual offset above the levitation coils is minimized. A render of both offset sensor placements is shown in 7.25 below.



(a) Vertical offset sensor



(b) Lateral offset sensor

**Figure 7.25:** Placement of both lateral and vertical offset sensors

### Thermal

Thermocouples will be located at the air vent of every key electrical component in the vacuum box. This is to ensure optimal operating temperature. Specifically, the Cygnus and Siemens motor drives will be equipped with thermocouples at each air vent as these drives must not exceed a temperature of  $> 40^{\circ}\text{C}$ . Additionally thermocouples are placed at the opening and end of the heat fins to measure the total heat transfer and efficiency of the cooling system.

### 7.7.2 Cable management

Since the sense & control system is integrated with almost any component on the pod via cables, good cable management is very important to keep an organized overview of the system. For uniformity, all cables and their organization have been deemed a part of sense & control. Therefore, this subsection gives an overview of all cables on the pod, including the cables that connect the power, levitation and propulsion systems. All of these cables have been split up into three categories, high voltage, low voltage and communication. This section gives an overview of all these cables, together with an argumentation behind their specific choices. Moreover, it shows a layout of all cables which minimizes the EMI

between cables of different voltage levels.

### Power cables overview

The power cables can be split up into 2 categories, high and low voltage. An overview of all these cables is given in table 7.23 below. For clarity, any connection to the vacuum box is omitted. Instead, any cable that runs through the sides of the vacuum box is indicated using an L or a P, where L means levitation side and P means propulsion side. Also the voltage, and amperage for all high-voltage wiring is included.

**Table 7.23:** Overview of all power wiring.

Between components		Type	Qty.	Voltage	Amperes
LV Battery	-	Emergency switch	1	25.2	
Emergency switch	-	LV PDB	1	25.2	
LV PDB A	-	main PCB	1	5, 12, 24	
LV PDB A	P	LV PDB B2	1	12,24	
LV PDB B2	-	Propulsion system	8	24	
LV PDB B2	-	Thermal controller	1	12	
LV PDB A	L	LV PDB B1	1	12,24	
LV PDB B1	-	Levitation system	6	24	
LV PDB B1	-	Thermal controller	1	12	
LV PDB A	L	Arcas Drive	1	24	
LV PDB A	-	Main Localization PCB	1	12	
LV PDB A	-	High Voltage Controller	1	24	
LV PDB A	-	Ethernet Switch	1	24	
LV PDB A	-	Braking Circuit	1	12, 24	
Main Localization PCB	-	Localization Sensors	3	12	
HV Battery Pack	-	HV PDB	1	470	150
HV PDB	-	S120 Motor Drive	1	400	100
Propulsion S120 Inverter	P	Distribution Blocks	4	400	56
Distribution Blocks	-	Propulsion Coils	12	400	14
HV PDB	-	Cygnus drives	5	400	15
Cygnus drives	L	Vertical Levitation Coils	8	400	8
Cygnus drive	L	Lateral Levitation Coils	8	400	5

### Communication cables overview

An overview of all wiring used for communication is given in table 7.24. Again, any cable running through the sides of the vacuum box is indicated using an L or a P.

**Table 7.24:** Overview of all communication wiring.

Between components			Wire/protocol Type	Qty.
Main Ethernet Switch	-	Main Controller	Ethernet	1
Main Ethernet Switch	L/P	Ethernet Switches P/L-side	Ethernet	2
Main Ethernet Switch	-	Localization Master	Ethernet	1
Main Ethernet Switch	-	High Voltage Controller	Ethernet	1
Main Controller	-	Brake Pressure sensors	Analog	2
Main Controller	-	Braking Circuit	0/1 signal	1
Localization Master	-	Inductive localization sensors	CAN	2
Localization Master	-	Optical Localization	CAN	1
Localization Master	-	Offset Localization	CAN	1
Localization Master	-	IMU	UART	1
Localization Master	-	Braking Circuit	0/1 signal	1
High Voltage Controller	-	HV BMS Control Unit	CAN	1
High Voltage Controller	-	LV BMS	CAN	1
High Voltage Controller	L	HV Power Distribution Board	Digital	1
High Voltage Controller	-	LV Power Distribution Board	Digital	1
High Voltage Controller	-	Braking Circuit	0/1 signal	1
Ethernet Switch P-Side	-	SMC 30	Ethernet	1
Ethernet Switch P-Side	-	200 SP	Ethernet	1
200SP Controller	-	CU320	Ethernet	1
CU320	-	S120 Inverter	Ethernet	1
SMC20	-	S120 Inverter	Ethernet	1
Ethernet Switch P-Side	-	Thermal Controller P-Side	Ethernet	1
Thermal Controller P-Side	-	Temperature Sensors	Analog	8
Thermal Controller P-Side	-	Pressure Sensor	Analog	1
Ethernet Switch L-Side	-	Arcas Controller	Ethernet	1
FDRF Offset Sensors	L	Arcas Controller	Analog	8
Arcas Controller	-	Cygnus drives	Ethercat	4
Ethernet Switch L-Side	-	Thermal Controller L-Side	Ethernet	1
Thermal Controller L-Side	-	Temperature Sensors	Analog	8
Thermal Controller L-Side	-	Pressure Sensor	Analog	1
Fall-Off Sensors	-	Braking Circuit	0/1 Signal	4
End Of Track Switch	-	Braking Circuit	0/1 Signal	1

### Cable layout

Power cables can have a detrimental effect on the integrity of sent data if they are placed closely to the data cables, because of the EMI they cause. To ensure optimal performance, all data and power cables are separated as much as possible. For extra safety and performance, high and low-voltage cable are separated as well. Moreover, this division of cables gives a clear overview of the layout of the pod. An overview of the placement of all cables can be found in the pictures below. All communication cables are marked blue, all low-voltage cables are marked yellow and all high-voltage cables are marked red. Moreover, sensors are marked purple and any cable going up or down between the two pictures is marked with a star.

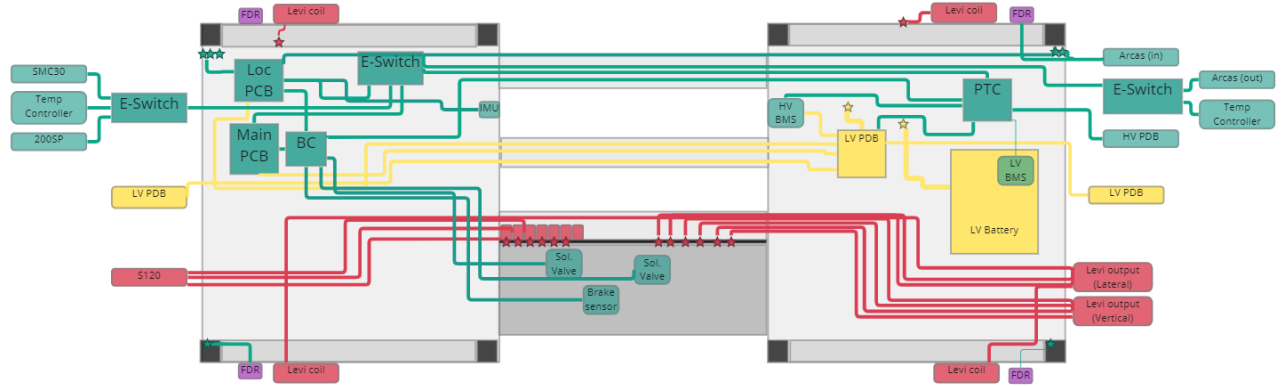


**Figure 7.26:** Top view of all cables located on the lower part of the ladder frame

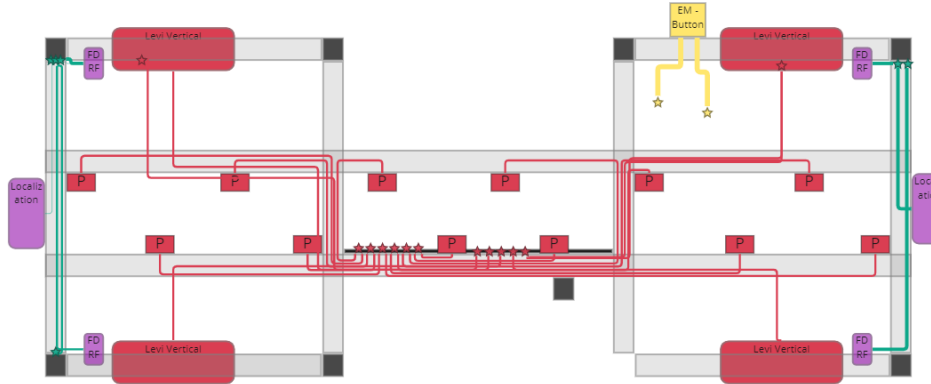


**Figure 7.27:** Bottom view of all cables located on the upper part of the ladder frame

As power flow can cause serious electromagnetic fields, it is essential to split up high voltage, low voltage and communication cables as much as possible to ensure that the interference between them is minimized.

This is done in multiple ways. First of all, as can be seen in picture 7.26, the inside of the ladder frame is roughly split up into three areas, one for high voltage (bottom) one for low voltage (middle) and one for communication (top). These correspond to the three plates that connect the two sides of the pod in its center. Moreover, this split of cables also agrees with the connector configurations on both sides of the vacuum box, which is further explained in 8.5.

As, crossing of some cables is inevitable, a wiring bridge is installed between the braking communication wires and the high voltage cables from propulsion to shield them for EMI.

Moreover, as a lot of sensors and high power systems are located on top of the pod, the top beams of the ladder frame are split into high voltage and communication beams. Both the front and back beam are used for communication wires, while all other beams are used for high power wires. In accordance with this, the vertical beams in the outer corners of the ladder frame are solely used for communication wires, while the backplate of the braking system is used for all high power wires. An overview of these cables can be seen in 7.27.

### Cable trays

To form an extra layer of safety for all cables, and to prevent anything and anyone to get stuck behind protruding cables, cable trays are installed. Three types of cable trays are used: those placed atop of the plates on the bottom of the ladder frame, those located on the backplate of the brakes and those hanging underneath the top beams of the ladder frame. The trays on the bottom are placed on both sides of each of the central plates, as shown in 7.28 below.

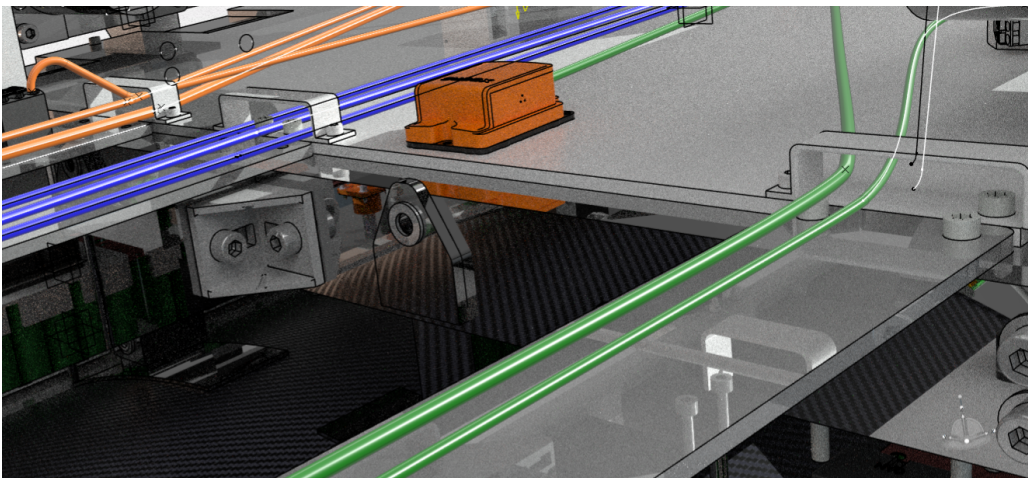


**Figure 7.28:** Render of wires running through cable trays on the ladder frame

A three 3d-printed cable holders are installed on the backplate of the brakes, where all propulsion power cables go upwards from the distribution blocks. For convenience, the front of this holder can be taken off and put back on using a sliding mechanism. The purpose of this holder is to maintain a clear overview of what cable is part of which E-module. Each holder bundles all the respective cables for one phase output of the propulsion motor. Moreover, it provides stability to all these cables as well as an extra layer of protection. A render of the cables going up through the cable holder is shown in 7.29 below.

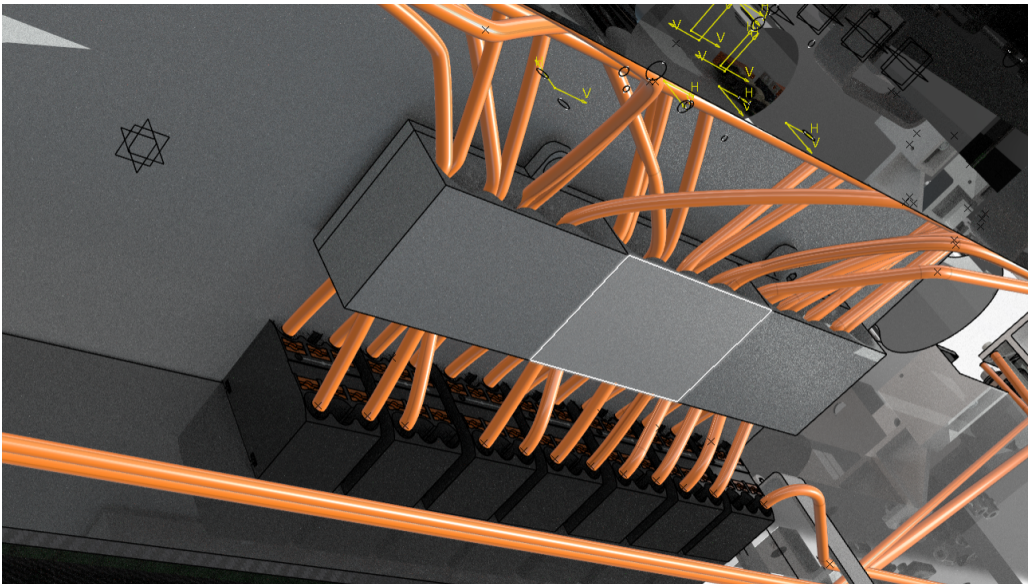


**Figure 7.29:** Render of wires running through cable trays on the ladder frame

Lastly, the trays hanging underneath the top of the ladderframe are located on both sides of every crossing that contains wires. An example of wires running through such a tray can be seen in 7.30 below.

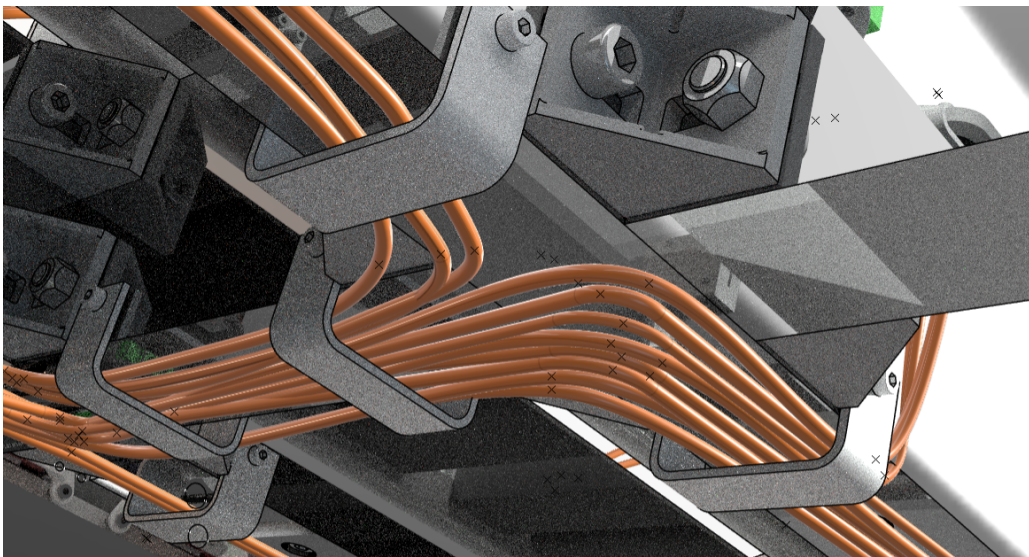


**Figure 7.30:** Render of wires running through cable trays underneath the ladder frame

## 7.8 Thermal management

One of the most critical challenges for a hyperloop is managing the heat generated by the system. Thermal management is essential to ensure the safety, reliability, and efficiency of the hyperloop system. The pod can experience heating as a result of various phenomena, such as heat produced by the levitation and propulsion coils by the current. This can cause temperatures to rise to extremely high levels and can lead to material degradation, structural damage, and even endanger the passengers. In addition, the power electronics, motor drives, and other components of the system also generate heat, which needs to be dissipated effectively to prevent them from overheating and malfunctioning. Another large but rather ignored source of heat in a full scale hyperloop is the heat generation of passengers.

A well-defined overview of critical heat-producing components is necessary for designing an optimal cooling system. Understanding the heat generation, dissipation, and transport mechanisms in the system is crucial to ensure its efficient and reliable operation. This allows for the identification of hot spots and the optimization of cooling strategies to remove heat from these regions effectively. The overview should also consider the heat transfer mechanisms and the thermal properties of the materials involved in the system, such as thermal conductivity and heat capacity. An optimal cooling system design involves selecting the appropriate cooling method, such as natural or forced convection, liquid cooling, or phase-change cooling. The design should also consider the placement of the cooling components, such as heat sinks, fans, or pumps, to ensure efficient heat removal and minimize the impact on the overall system performance.

The thermal overview will feature a distinction between critical components and non-critical components from a thermal perspective is based on the heat generation of each system as well as the maximum allowable temperature.

The heat estimations show that the main critical components are the motor drives for propulsion and levitation alongside the motor controllers, and power distribution boards. This is due to the high heat production and the low maximum temperature.

The cooling system in the Delft Hyperloop VII pod is based on transferring heat generated by components on the pod to a phase change material-based heat battery. This heat battery uses the latent heat storage of a PCM to capture all heat.

The heat battery is located in the vacuum box to capture all heat produced from the motor drives and power distribution boards. It is designed to operate as a temporary heat storage during a Hyperloop run and is discharged after the completion of a run.

**Table 7.25:** Thermal component heat overview as described in Section 7.8.2

Name	Qty	Total heat	Unit
Siemens motor drive	1	800	W
Prodrive Cygnus	5	2500	W
LFSPM E-core	12	177.2	W
Vertical HEMS U-core	4	633.6	W
Lateral EMS U-core	4	262.4	W
High voltage batteries	672	2688	W
Low voltage batteries	28	112	W

### 7.8.1 Requirements & Nomenclature

In order to achieve its cooling functionality, the thermal management system must comply with a set of requirements. An overview of the most important requirements regarding this system are presented in Table 7.28. The following abbreviations are used for the ID's: GE = General, GS = General Safety. The requirements for a specific subsystem can be found underneath its respective subsection.

**Table 7.26:** Abbreviations used

Category	Abbreviation
General	GE
General safety	GS
European Hyperloop week	EHW
Linear Flux Switching Permanent Magnet Motor	LFSPM
Hybrid Electro Magnetic Suspension	HEMS
Electro Magnetic Suspension	EMS
Vacuum Box	VB
High Voltage	HV
Low voltage	LV
Phase Change Material	PCM
Safety	SF
Finite Element Method	FEM
Computational Fluid Dynamics	CFD

**Table 7.27:** Nomenclature

Symbol	Unit	Definition
$W$	Watt	Power
$Q$	J	Heat
$I$	A	Current
$R_{coil}$	$\Omega$	Electrical resistance
$R_{1,2,3}$	$K/W$	Thermal resistance
$\Delta T$	K	Temperature difference
$\Delta t$	s	Time difference
$c_p$	$Jkg^{-1}K^{-1}$	Specific heat capacity
$h_c$	$Wm^{-2}K^{-1}$	Heat transfer coefficient
$k$	$Wm^{-1}K^{-1}$	Thermal conductivity
$\eta$	-	Thermal efficiency
$\epsilon$	-	Emissivity
Nu	-	Nusselt number
Re	-	Reynold's number

**Table 7.28:** Requirements Thermal System

ID	Requirement
SC.TH.GE.1	The chosen cooling system shall be able to absorb more than all the heat generated by the critical components for at least 20 seconds.
SC.TH.GE.2	The thermal management system shall prevent all critical subsystems from overheating
SC.TH.GE.3	The chosen thermal management system shall fit onto the dimensions of the vacuum-box.
SC.TH.GE.4	The mass of the system must be <20 kg.
SC.TH.GE.5	The costs must be < €2000.
SC.TH.GS.1	The thermal management system shall not contain any CRM (carcinogenic, mutagenic and reprotoxic) chemicals.

### 7.8.2 Expected system characteristics

The objective of this section is to specify the influence of a thermal management system on the pod and to highlight which subsystems are critical from a thermal point of view when operating in a vacuum environment. This is done by determining the maximum allowable temperature of each subsystem and whether this is ever reached during a run. From here the most important subsystems that require cooling can be evaluated. Each subsystem is subjected to different loads and differ in their forms of heat generation, the analysis is given below. The heat generation is based on the heat that will be generated during a run at the EHW.

**LFSPM** The LFSPM motor consists of twelve E-core modules with a coil winding around it. To determine the heat generation through this coil, one can use the Joule's first law:

$$Q_{heat} = I_{RMS}(t)^2 R_{total} t \quad (7.12)$$

It is important to consider the most extreme scenarios of heat production to find the maximum reached temperature. Propulsion has three main scenarios in which heat are produced: bidirectional forward run, bidirectional backward run and a top speed run. The bidirectional runs are happen over a longer time period, however require lower currents. On the other hand, a top speed run will take place in a shorter time span but requires a higher current. Equation 7.12 shows that heat generated by coils scales linearly with time while the current has a quadratic scaling relation. Because a top speed run employs a higher current, this will be a leading scenario regarding heat generation.

The maximum allowable temperature for an E-core module is determined by the temperature at which the components lose their electrical and/or structural performance. The bulk of an E-core module consists of two materials, the copper coils and the Coolmag 32 epoxy. Copper as a conductor gains more electrical resistance when the temperature is increased. The temperature coefficient of copper is  $0.393\%K^{-1}$  [34]. For the propulsion modules, a 10% resistance increase is considered maximally allowable. This means the maximum allowable temperature increase is equal to  $\Delta T = \frac{10\%}{0.393\%K^{-1}} = 25.4K$ . The Coolmag 32 epoxy can withstand temperatures of up to  $125^{\circ}C$  for 25 minutes according to the technical datasheet. That means that the coil resistance is the defining factor when it comes to determining maximum allowable temperature, which for a propulsion E-core module is  $\Delta T_{max} = 20K$ .

Considering a total resistance of  $1.6\Omega$ , as determined in section ?? and a total run time of 9.14 seconds ??, the following graph can be plotted: Figure 7.31.

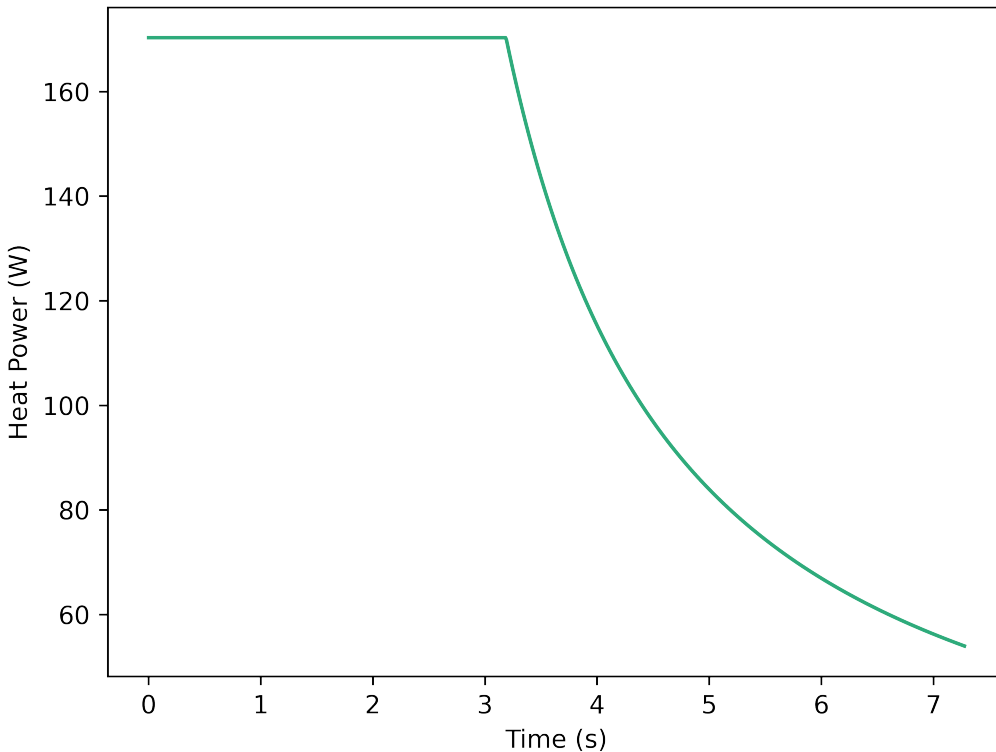


**Figure 7.31:** Heat produced by one LFSPM motor coil during a top speed run, heat production is depicted on the vertical axis in Watt and time depicted on the horizontal axis in seconds

The total heat dissipated during a full speed run equals 10.8 kJ. If this heat is fully absorbed by the copper, the temperature increase is calculated in Equation 7.13, with  $m_{copper} = 1.6 \text{ kg}$  from section 4 and  $c_{p,copper} = 385 \frac{\text{J}}{\text{kgK}}$ .

$$\begin{aligned}
 Q_{LFSPM} &= m_{copper,LFSPM} * c_{p,copper} \Delta T \\
 \Delta T &= \frac{Q_{copper,LFSPM}}{m_{copper,LFSPM} * c_{p,copper}} \\
 &= 17.53 \text{ K}
 \end{aligned} \tag{7.13}$$

This is below the maximum allowable temperature increase of  $\Delta T_{max} = 20 \text{ K}$  and thus this system is not characterised as 'critical'. In reality the total temperature increase would be lower than 17.27 K due to the heat absorption of the Coolmag and convection with air, which gives an additional safety factor.

**Vertical HEMS U-core** The vertical HEMS U-core coils follow the same equation (Equation 7.12). The vertical HEMS coils have a resistance of  $9.9 \Omega$  from measurements of the produced coils. The current going through the coil is given in section 5. The maximum current that one Cygnus requires can alternate between -5.6 and +5.6 Ampères as described in section 5 .

The levitation modules are expected to run for 30 seconds during a run as described in section 5 . Total heat produced during a run is defined as the heat produced during launch with heat produced during normal operation. For Normal operation it is assumed that the coils will receive the rated output of the Cygnus, which is 5.6 A, and for lift-off the power required is 682 W for 1 second. The total heat produced as described in ?? is then equal to 23.2 kJ.

For the HEMS coils the maximum allowable temperature increase for the vertical HEMS modules is defined as the temperature at which the permanent magnets will experience demagnetization, which for the levitation subsystem happens at  $\Delta T_{max} = 60^\circ\text{C}$ . The mass of the HEMS coils is 1.51 kg from Section 5.3 . The temperature distribution over time of one HEMS module is seen as a lumped thermal capacitance model. Relevant data regarding heat capacity of all materials are given in Section 5.3. From this the total temperature increase can be calculated which is equal to  $\Delta T = 3.8 \text{ K}$ . If one starts with initial conditions of  $T_1 = 20^\circ\text{C}$ , the temperature after a run becomes:  $T_2 = 23.8^\circ\text{C}$ .

This shows that the temperature increase of the HEMS coils is also below the maximum value of  $60^\circ\text{C}$ , thus making it not critical.

**Lateral EMS U-core** The lateral EMS coils are powered in the same way as the vertical HEMS coils. Therefore heat production can be calculated in a similar manner. However, the resistance of the lateral coils is lower than that of the vertical, with  $R = 4.1 \Omega$ . Therefore filling in Equation 7.12 with this resistance gives a power of heating of 128.6 W of one lateral module and 514.3 W the whole system. Over a period of thirty seconds, this gives a heat production of 3.858 kJ for one lateral coil and 15.429 kJ for all four EMS units.

The maximum allowable temperature increase for the lateral modules is in line with that of the LFSPM and HEMS coils and is  $\Delta T_{max} = 20K$ . The mass of one coil is equal to  $m_{copper,EMS} = 0.57 \text{ kg}$ , from Section 5.4.

$$\begin{aligned} Q_{copper,EMS} &= m_{copper,EMS} c_{p,copper} \Delta T \\ \Delta T &= \frac{Q_{copper,EMS}}{m_{copper,EMS} c_{p,copper}} \\ &= 17.6K \end{aligned} \quad (7.14)$$

The EMS coils also fall within the tolerable temperature range of  $\Delta T = 20K$  and hence is not defined as critical.

**HV and LV batteries** The batteries used for Helios II are of the 18650 type. As discussed in Section 6.2.8, the temperature increase by a single battery cell when discharged at 75 A for 60 seconds is equal to 5 °C. This is the most extreme scenario as a single cell will not have a discharge rate above 25 A during testing and demonstration see Figure 6.3b. The specific heat capacity of this battery is  $1044 \text{ Jkg}^{-1}\text{K}^{-1}$  [35] and the weight is 47 grams. The maximum power of heating by one battery cell then equals 4 W. The high voltage battery system contains 672 cells (Table 6.7) and the low voltage systems contains 28 (Table 6.10). Thus, the HV battery will produce 2688 W of heat power if it is discharged at an extreme current of 75A, and the low voltage system will produce 112 W of heat.

$$\dot{Q}_{battery} = \frac{c_{p,battery} * m_{battery} * \Delta T}{\Delta t} \quad (7.15)$$

The maximum allowable temperature for an 18650 type battery is 80 °C. Comparing that to the 5 °C temperature increase from the tests, this sits well below the threshold and thus the batteries are not considered critical.

**Motor drives** All the levitation and propulsion subsystems need to be driven by the motor drives. For the LFSPM motor, the Siemens 6SL3120-1TE28-5AA3 motor module, see the Propulsion Appendix. This motor module has a rated power loss of 800 W and has an operating temperature range of 0 - 40 °C. At normal operation the motor drive has a cooling air requirement of  $0.044 \text{ m}^3/\text{h}$ . The power loss of 800 W is power which is the difference between the electrical power input and output and comes in the form of heat. The total heat generated by this motor module is dependent on this power loss, as well as the total time for which the motor module is at nominal operation. This time is 20 s, which is twice the time of a bidirectional run. Due to the large heat power and the low maximum operating temperature of 40 °C, the Siemens 6SL3120-1TE28-5AA3 motor module is a critical component in Helios IIthat will require cooling.

The levitation vertical HEMS and lateral EMS modules are driven by the Prodrive Cygnus motor drive, of which 5 in total are employed. This motor drive has a power loss of 500 W, see the Levitation Appendix and may also be operated within an operating temperature range of 0 - 40 °C. Due to the large heat production of these motor drives and its limited operating temperature range, the Cygnus motor drive is also critical component in Helios IIwhich will require cooling.

To obtain the final heat design load on which will a thermal management system will be designed, the critical subsystems are tabulated in Table 7.29 with a safety factor of 2. The end result is a total heat design load of 6600which is to be cooled in 20 s.

**Table 7.29:** Heat design load

Name	Qty	Total power loss	Unit
Siemens motor drive	1	800	W
Prodrive Cygnus	5	2500	W
Safety factor		2	-
<b>Total</b>		6600	W

### 7.8.3 Trade-off for Helios II

Taking into account the design requirements as defined in Table 7.28, such as the mass requirement of less than 20 kg, costs requirement of less than €2000 and dimensional constraints of the vacuum box as well as the critical components defined in Table 7.29, the decision was made to limit the use of heavy, large and expensive cooling loops. This meant that cooling cycles containing large heavy pumps, compressors, and heat exchangers are phased out. The goal was to make a light and compact thermal management system that satisfies the design heat load. The decision was made to accomplish this by designing a heat storage system using phase changing materials. This section dives further into the material considerations for this heat storage system. When determining the appropriate PCM for a heat battery, one can formulate the following criteria on which each material is to be evaluated:

- Safety
- Corrosivity
- Reusability
- Melting temperatures
- Latent heat of fusion
- Density
- Thermal conductivity
- Costs

**Salt hydrates:** A salt hydrate can be seen as an alloy of inorganic salt and water. Salt hydrates come in many different types, with a wide variety of transition points and heat capacities. Salt hydrates however generally have an incongruent transition point. At this transition point, three phases are in equilibrium: two solid phases and a saturated liquid phase with salt. Due to incomplete solubility the hydrate that is in a solid phase will settle to the bottom of the heat battery. This makes it unavailable for recombination with water when it is heated up once again. With each phase change the material would slowly deteriorate in its heat storage performance. Thus, due to the incongruent transition point of salt hydrates they can not undergo reversible melting and freezing [36].

**Organic PCM:** Organic PCMs can be classified into two categories: paraffins and non-paraffin PCMs.

Paraffin waxes come in the form of hydrocarbons of type  $C_nH_{2n+2}$ . All types with  $n \leq 5$  are in gaseous state at room temperature, types between  $C_5$  and  $C_{15}$  are typically in liquid state at room temperature and for values above  $C_{15}$ , the paraffin becomes a wax [36]. Paraffin have rather high enthalpies of fusion while being low in density. Paraffin waxes have very low thermal conductivities, thus making a temperature gradient within the material nearly unavoidable without additional measures. Compared to other PCMs paraffin waxes are easy to work with, safe, non-corrosive, reusable and predictable. However their moderate flammability and low thermal conductivity limit their usage in industries.

Non-paraffin PCMs are plentiful and show a large variety of properties. When working with organic PCMs, one must be careful with subjecting it to high temperatures as this can lead to decomposition of the material - releasing toxic fumes. Additionally these organic PCMs tend to be more flammable than paraffin waxes. For those safety reasons, non-paraffin PCMs are not recommended.

**Metallic alloys:** As a phase changing material, low melting point metallic alloys could be used. These metallics perform well when volume is a major constraint, as they possess a high enthalpy of fusion per unit volume. Metallic alloys are also excellent in thermal conduction, in contrast to organic PCMs. Also contrary to organic PCMs, metallic alloys perform significantly worse on mass. Also melting points of metals are not as abundant as for PCM types and generally range much higher.

**Ice:** Ice is a good medium of heat storage due to its high latent heat of fusion. Its safety and availability is good for application, but its melting temperature is too low to be feasible for usage in Helios II. Additionally, the corrosivity of water makes it an inadequate material choice.

From this analysis the paraffin wax is chosen due to its low corrosivity on metals, high latent heat of fusion and high safety. The advantage of using paraffin wax is its high latent heat of fusion and low volumetric and mass density. This allows for a compact and light weight design while being able to store and release large amounts of energy. The biggest challenge when working with this material however is its low thermal conductivity. The goal is to store 6600W in a period of 20 s.

**Table 7.30:** PCM trade-off

Criteria	Ice	Salt hydrate	Paraffin wax	Organic non-paraffin	Metallic alloys
<b>Safety</b>	0	-	-	--	--
<b>Corrosivity</b>	0	-	++	++	+
<b>Reusability</b>	0	--	+	+	-
<b>Melting temperatures</b>	0	++	++	++	--
<b>Latent heat of fusion</b>	0	-	-	-	-
<b>Density</b>	0	+	++	++	--
<b>Thermal conductivity</b>	0	-	--	-	++
<b>Costs</b>	0	-	-	-	--

#### 7.8.4 Cooling Design

The main challenge that needs to be overcome when designing a thermal storage system based on paraffin wax is its low conductivity, paraffin waxes typically have a thermal conductivity around 0.2 W/mK [37]. To improve heat transfer through conductivity one can optimize on three variables as described in Equation 7.16: maximalization of the area ( $A$ ) or maximizing the temperature gradient ( $\frac{dT}{dx}$ ). The latter is achieved by either creating a very large temperature difference between the heat source and the PCM, or by minimizing the distance that the generated heat must travel.

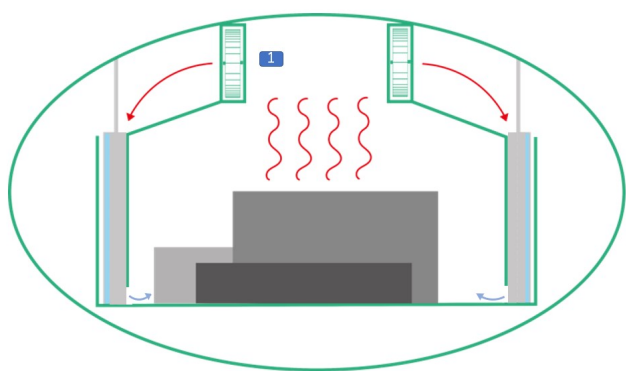
Optimization of heat transfer is not a novel problem and has seen many solutions in a wide array of industries, one particular industry in which this is often applied is the process industry. Where large batches of chemical reactions require very specific thermal and pressure conditions to take place. This is often achieved in heat exchangers, of which there are plentiful. Commonly used in the heat exchangers in the process industry are: Double pipe heat exchangers, shell-and-tube heat exchangers, gasketed and welded plate heat exchangers, air-cooled heat exchangers and many more [38]. Unfortunately many of these heat exchangers are designed for large scale chemical industrial purposes and thus do not fare well when scaled down to Hyperloop relevant sizes. This is often due to size constraints: tubes in shell-and-tube heat exchangers most commonly have a diameter of 20 - 25 mm, with a standard shell diameter of 610 mm [39]. With these dimensions, one can only scale down such a system so much until it loses its effectiveness, not to mention increasing complexity of production.

The heat exchanger that will be used in the heat battery of Helios II is a double sided aluminium heat sink. One side is saturated with PCM, while the other side allows for convective heat transfer with the environment. Heat sinks maximize the available area through which heat transfer can take place and also optimizes the temperature gradient ( $\frac{dT}{dx}$ ) by minimizing the length ( $dx$ ) through which conduction takes place. Heat sinks additionally have the benefit of being highly producable, easy to maintain and being relatively cheap.

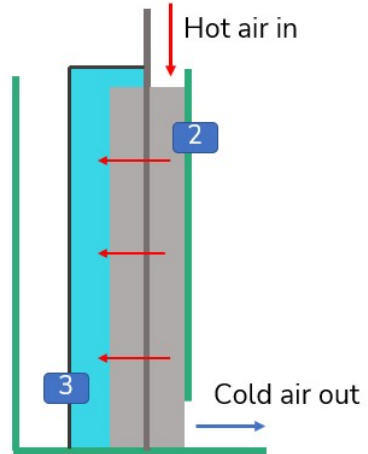
The design of the heat battery can be subdivided in three stages. First the heat needs to be captured from the main heat generating components. Secondly the heat will need to be conducted towards the PCM. Finally the heat needs to be stored in the PCM. The aim is to achieve this while maintaining a high thermal efficiency Equation 7.19.

Firstly the heat generated from the components must be captured and transmitted to a heat transfer medium. This is done through placing cooling fans in the vacuum box that allow for convective heat transfer from the motor drives to air. This hot air is then directed to a set of heat fins which collects the heat.

The back of the first heat fin is glued to a second set of heat fins which is connected to the PCM. Heat travels from heat fin (1) to heat fin (2) through conductive heat transfer. Heat fin (2) then passes the heat on to the PCM through a combination of conductive and convective heat transfer.



(a) Schematic overview of the operating principle of the heat battery with heat sink depicted in grey and the PCM is indicated in blue.



(b) Schematic overview of the heat battery. Hot air blown from the fans is absorbed by the PCM, cooled air is blown away at the bottom.

**Figure 7.32:** 1: Heat generated from the motor drives is blown away using fans. 2: Hot air is guided through a grid of aluminium heat fins, heat is transferred through convection. 3: Heat moves through the heat sink and is absorbed into the PCM, allowing it to change phase.

The three modes of heat transfer are: conduction, convection and radiation, with corresponding equations: Equation 7.16, Equation 7.17 and Equation 7.18. For the PCM battery, only conduction and convection are relevant. Radiation is negligibly low, which one can determine by filling in Equation 7.18 with an emissivity  $\epsilon$  of 1.0 (assume black body), Stefan-Boltzmann coefficient  $\sigma$  of  $5.67 \times 10^{-8}$ ,  $T_2$  of  $40^\circ\text{C}$  (maximum allowable temperature of motor drives) and  $T_1$  of  $20^\circ\text{C}$  (standard reference temperature). If this formula is solved for the area, a total area of  $19.9 \text{ m}^2$  is needed to obtain steady state heat transfer. Compared to the available area in the vacuum box of  $3.1 \text{ m}^2$ , this is already too high without taking into account the negative effect of view factors and transient behaviour of heat transfer.

$$\dot{Q}_{conduction} = kA \frac{dT}{dx} \quad (7.16)$$

$$\dot{Q}_{convection} = h_c A \Delta T \quad (7.17)$$

$$\dot{Q}_{radiation} = \epsilon \sigma A (T_2^4 - T_1^4) \quad (7.18)$$

$$\eta = \frac{\dot{Q}_{in}}{\dot{Q}_{out}} \quad (7.19)$$

### 7.8.5 Thermal Model

To analyse thermal systems, many thermal boundaries can be described as a thermal resistance, which is analogous to an electrical resistance. Using the electrical analogy, the different forms of conduction, convection and heat storage would form a thermal circuit with thermal resistances and a capacitor in series. Temperatures in the system will become voltages, and heat will become current in this analogy. Our heat source will be simulated as a current source since the heat in our system is constant.

The thermal circuit is shown in Figure 7.33, this heat diagram consists of three thermal resistances and a thermal capacitance. The first thermal resistance represents the resistance of hot air to heat fin through convection and is described in Equation 7.20. The second thermal resistance represents the conduction of heat through the heat sink base and is described in Equation 7.21. The third resistance is the conduction of heat from heat sink to PCM and is described by Equation 7.22. Lastly the heat is collected in the PCM and is modeled as a capacitor which is described in Equation 7.23.

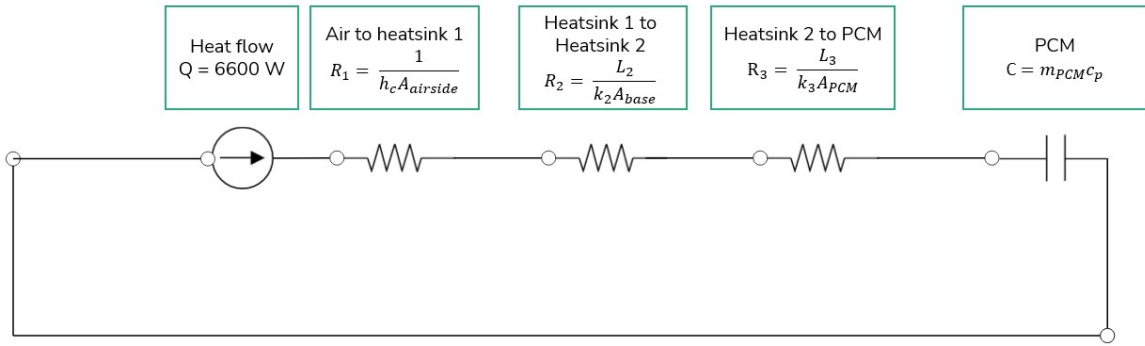


**Figure 7.33:** Thermal circuit using the electrical analogy, the system is modeled as a circuit with the thermal boundaries as thermal resistances and the PCM as a thermal capacitor

Here  $h_c$  is the heat transfer coefficient produced by the fans which is determined through a computational fluid dynamics model and discussed in Section 7.8.7.  $L_2$  is the base length of aluminium heat sink,  $k_2$  is the thermal conductivity of aluminium.  $L_3$  is the characteristic length of PCM conduction, taken to be 1 mm as that is the maximum length it should travel,  $k_3$  is the thermal conductivity of paraffin wax. The values of these parameters are tabulated in Table 7.31.

$$R_1 = \frac{1}{h_c A_{airside}} \quad (7.20)$$

$$R_2 = \frac{L_2}{k_2 A_{base}} \quad (7.21)$$

$$R_3 = \frac{L_3}{k_3 A_{PCM}} \quad (7.22)$$

$$C_{PCM} = m_{PCM} * c_p \quad (7.23)$$

**Table 7.31:** Thermal circuit values

Parameter	Value	Unit
$h_c$	54	$\frac{W}{m^2 K}$
$A_{airside}$	0.739	$m^2$
$L_2$	3	mm
$k_2$	218	$\frac{W}{mK}$
$A_{base,shortheatfins}$	159	$mm^2$
$A_{base,longheatfins}$	176	$mm^2$
$A_{base,total}$	670	$mm^2$
$L_3$	1	mm
$k_3$	0.2	$\frac{W}{mK}$
$A_{PCM}$	1.64	$m^2$
$m_{PCM}$	8.8	kg
$c_{p,SHS}$	2000	$\frac{J}{kgK}$

The PCM in our system will experience both sensible heat storage and latent heat storage. To accurately model this behavior the thermal capacitance of the PCM is modeled temperature dependent. The used PCM does not have a melting/congealing point, but a melting/congealing area, which means there is a temperature range where the PCM will melt/congeal. During this period the required energy to melt the PCM will change based on the temperature. This behavior can be seen in the appendix, where the partial enthalpy for each PCM is given as a function of the temperature. The used  $c_p$  will thus be dependent on the temperature of the system. The value of  $c_p$  used in the calculation will therefore be the partial enthalpy for the PCM on the given temperature, as can be read in the appendix, plus  $c_{p,SHS}$ , the  $c_p$  associated with sensible heat storage.

The design parameters shall be to optimize the heat transfer coefficients of all the heat coefficients to obtain the most efficient heat transfer. The most important parameters dictating these coefficients are considered in Table 7.32.

## Convection from air to heatfins

To optimize the airflow from the air to the heat fins an air duct will be placed between the fans and the heat fins. To make an approximation of the heat transfer coefficient from the air to the heat fins, the flow will be assumed to be turbulent. This is also confirmed by the model by calculating the average Reynolds number. To find the relevant heat transfer coefficient the following equations are used:

$$h_c = (k/D_h) * Nu_D \quad (7.24)$$

To find the Nusselt number Gnielieski's formula is used [40]:

$$Nu_D = \frac{(f/8)(Re_D - 1000)Pr}{1 + 12.7(f/8)^{1/2}(Pr^{2/3} - 1)} \quad 3000 < Re_D < 10^6 \quad (7.25)$$

The air properties from air at 310 Kelvin and 1 atm is used for acquiring the viscosity, Prandtl number, and thermal conductivity. To calculate the Reynolds number, the Hydraulic Diameter is used, which is dependent upon the entrance surface area and its perimeter.

$$\text{Hydraulic Diameter } D_h = \frac{4A_c}{P} \quad (7.26)$$

$$Re_D = \frac{(\dot{m}/A_c)D_h}{\mu} \quad (7.27)$$

To calculate the friction factor, Petukhov's formula [41] is used:

$$f = (0.790 \ln(Re_D) - 1.64)^{-2} \quad 10^4 < Re_D < 10^6 \quad (7.28)$$

By using these in formula 7.25 the Nusselt number can be found. If a more accurate heat transfer coefficient is required, the entrance effects can also be considered. Using Mills [42] the effect of entrance configuration on the average heat transfer for turbulent pipe flow can be calculated. The ratio of average Nusselt number to the fully developed value for gas flow for a hydraulic diameter of 40 is 1.18 for an open end, 90° edge [42].

The estimated heat transfer coefficient from air to fins following from this calculation is  $50.39 \frac{W}{m^2 K}$ .

## Heat transfer to PCM

All the heat captured into the heat battery is modeled by a thermal analysis in Simcenter 3D. The heat transfer can be modeled through FEM analysis, as the primary mode of heat transfer in PCMs during initial charging is conduction. As the PCM start to enter the fluid phase, natural convection takes over as the main source of heat transfer [43]. Figure 7.34a shows the temperature gradient of a transient analysis of a slice of the heat battery after twenty seconds. The analysis showcases a temperature difference between the heat sink and the PCM as a result of the melting temperature of the PCM at 21 °C. After twenty seconds the quality of the elements closest to the base of the heat sink are 70% melted.

DH07\_mech\_heatbattery\_L\_varA\_1.stp; i1\_sim1 : Thermal Multiphysics Result  
Step - Thermal 1, 20, Increment 1, 20.00s  
Temperature - Elemental, Scalar  
Min : 20.534, Max : 24.410, Units = °C

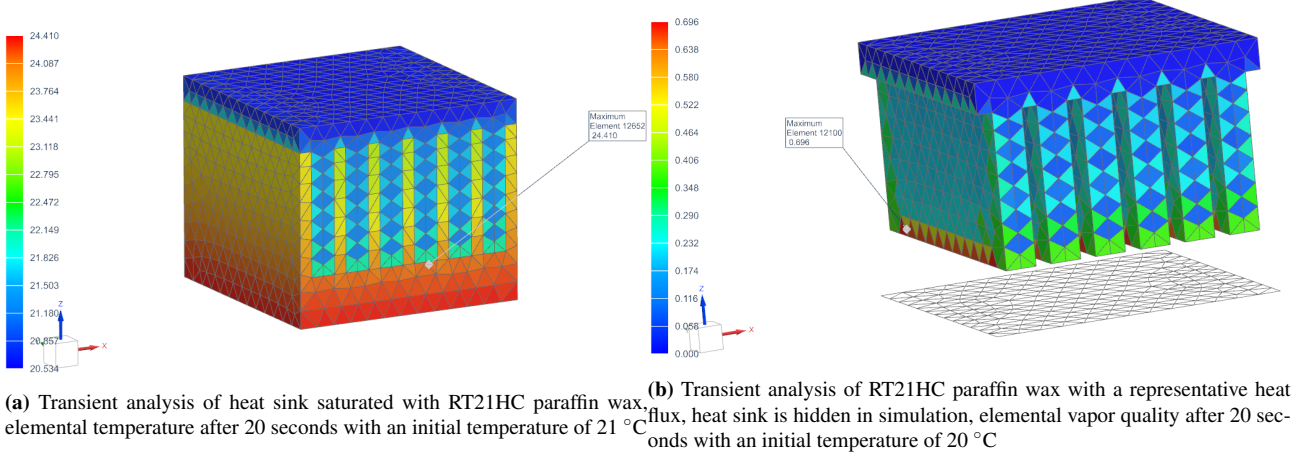


**Figure 7.34:** Thermal finite element analysis of RT21HC paraffin wax

### Cooling of PCM

Another relevant load case is the cooling of the PCM after the PCM has been subjected to a heat load for a long time it will be saturated and fully melted. The heat battery must then be discharged of its heat before it can be used again. A transient FEM analysis is done to determine the time it takes to return to its solid state. The initial temperature is 23 °C with an initial vapor quality of 1.0. Natural convection at a temperature of 15 °C cools the heat battery down from the bottom and top plane. After approximately one hour the PCM has reached a vapor quality ranging between 0.07 - 0.10, this is illustrated in Figure 7.35. It must be noted that this is an extreme case where more deliberate cooling is not available. In case the heat battery can be cooled using forced convection, or placed in a cooler environment which would significantly improve the cooling time.

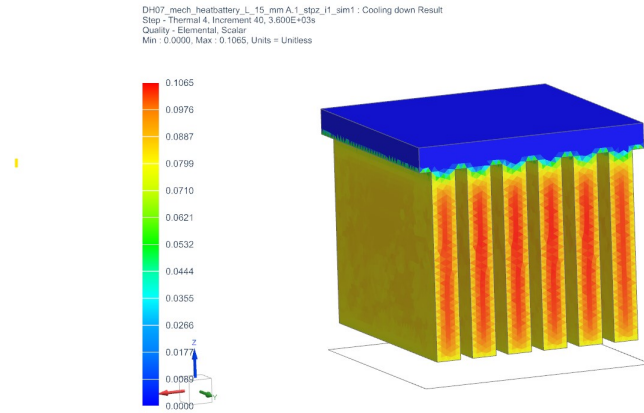


**Figure 7.35:** Transient analysis of cooling of RT21HC with an initial temperature of 23 °C, initial vapor quality of 1.0.

### 7.8.6 Final dimensioning

After optimization in the finite element modelling software, a final dimensioning for the heat sinks was determined with respect to thermal requirements, dimensional constraints and mass constraints. The values obtained from the calculations are depicted in Figure 7.36 and Table 7.32.

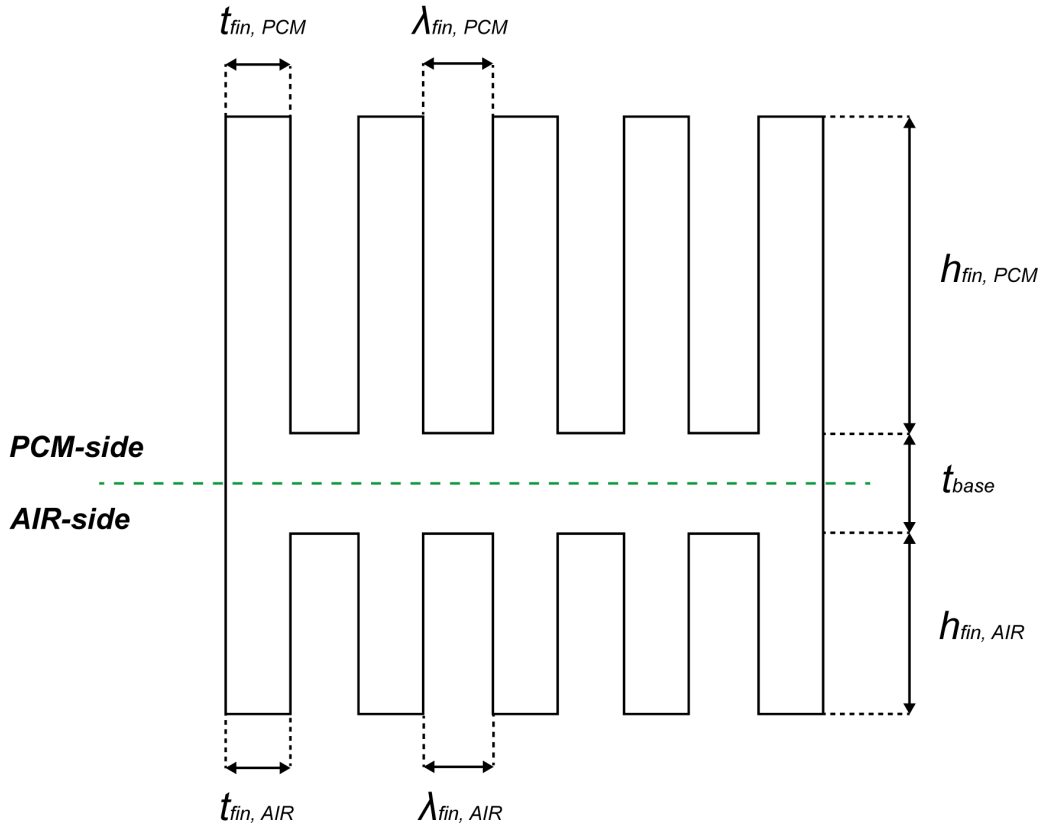
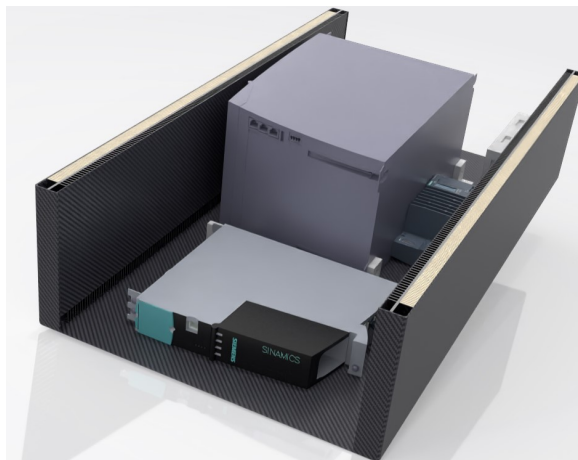


**Figure 7.36:** Dimensions of the heat sink

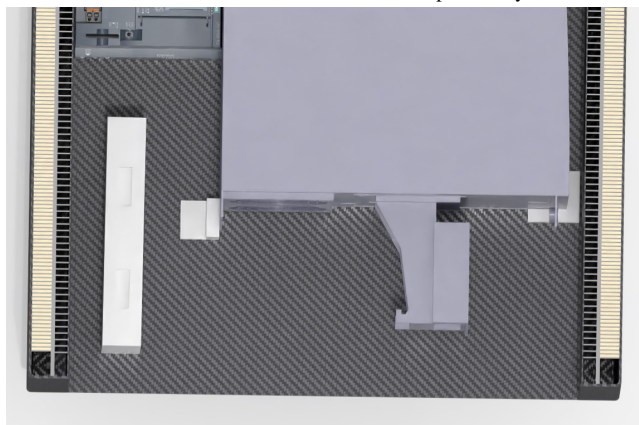
**Table 7.32:** Thermal System Parameters

Symbol	Parameter	Value	Unit
$t_{fin,PCM}$	Fin thickness PCM Side	1	mm
$\lambda_{fin,PCM}$	Fin distance PCM side	2	mm
$h_{fin,PCM}$	Fin height PCM side	10	mm
$t_{fin,AIR}$	Fin thickness Air side	1	mm
$\lambda_{fin,AIR}$	Fin distance Air side	4	mm
$h_{fin,AIR}$	Fin height Air side	10	mm
$t_{base}$	Base Thickness	3	mm
W	Width	195	mm
L	Length	924.6	mm
$n_{heatsinks}$	Number of heat sinks	4	
$n_{fans}$	Number of fans	12	
$v_{fan}$	Fan air speed	6	m/s
$m_{cooling}$	Total weight of the cooling system	24.9	kg

The heat sinks are situated on the flank side of the motor drive plate. Figure 7.37 shows the placement of the heat sinks with respect to the motor drives.



**(a)** Render depicting the thermal system with the Siemens motor drive. The outside of the heat fins are saturated with PCM, depicted in yellow



**(b)** Top view of the PCM - heat sink configuration

**Figure 7.37:** Placement of the heat battery with respect to the motor drives

### 7.8.7 CFD

To confirm the predicted heat transfer from the air to the PCM a CFD simulation has been created. The thermal model was set up as a slice of the vacuum box with two fans on each side. The motor drives were not modeled in this program to reduce complexity, rather the heat load is defined at the inlet of the fans. The goal of this simulation was to validate the results regarding heat transfer coefficient, as found in Section 7.8.5, to determine the correct fan choice with regards to volumetric airflow and pressure drop, and to validate the design.

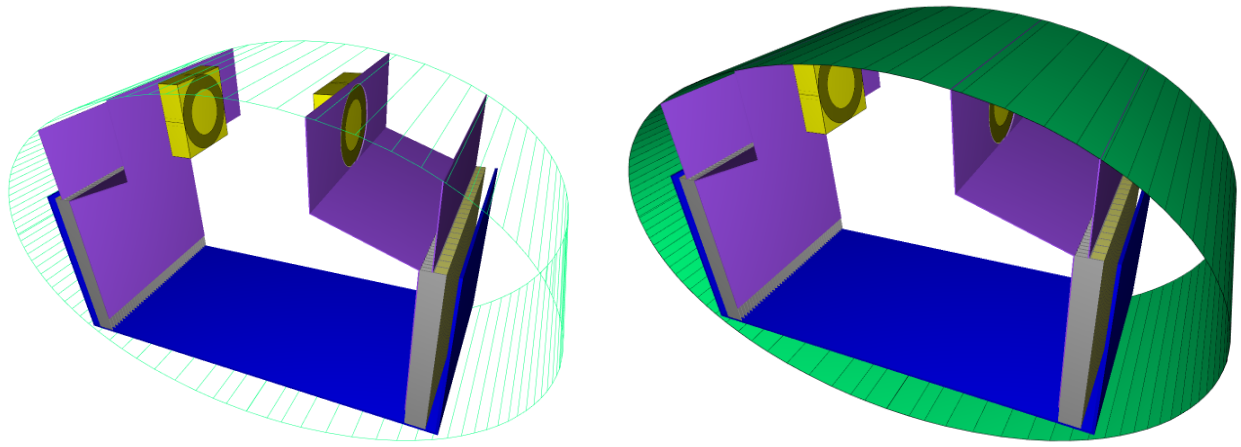


**Figure 7.38:** Model used for computational fluid dynamics calculation. The vacuum box is taken as a slice to reduce calculation times.

The model was solved with a heat load of 550 W per fan with twelve fans in the vacuum box. The initial temperature was set at 20 °C and the simulation was run until a steady state temperature is achieved. The heat transfer to the PCM was considered to be conductive heat transfer with a thermal conductivity of  $0.2 \frac{W}{mK}$ . To achieve this heat transfer, an air velocity of 6 m/s needs to be achieved at the top of the heat fin.

The results from Figure 7.39b and Figure 7.39c show that the proposed thermal storage design indeed works. Hot air entering the heat battery with a temperature of 47.2  $^circ$ C leave the heat battery with a lower temperature of 25.6 °C.

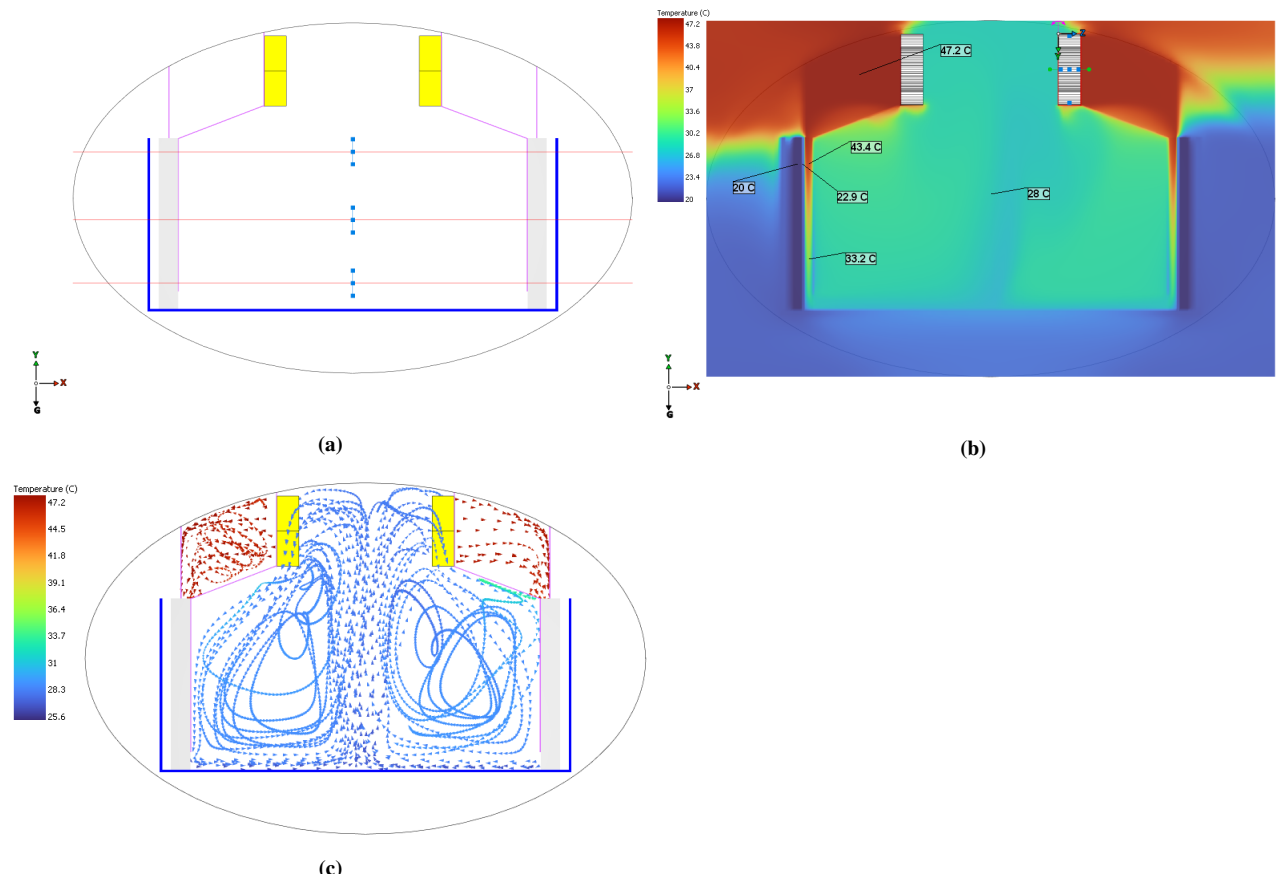
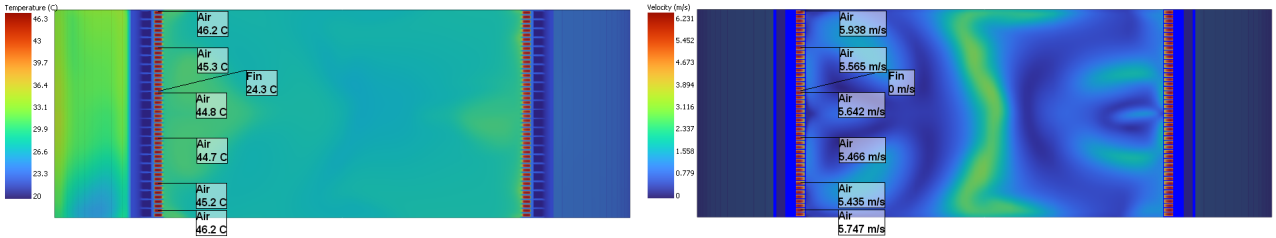


**Figure 7.39:** Front view of the vacuum box space with a schematic view and the steady state temperature distribution.

Figure 7.40, Figure 7.41 and Figure 7.42 show the temperature and velocity gradient of three horizontal planes in the

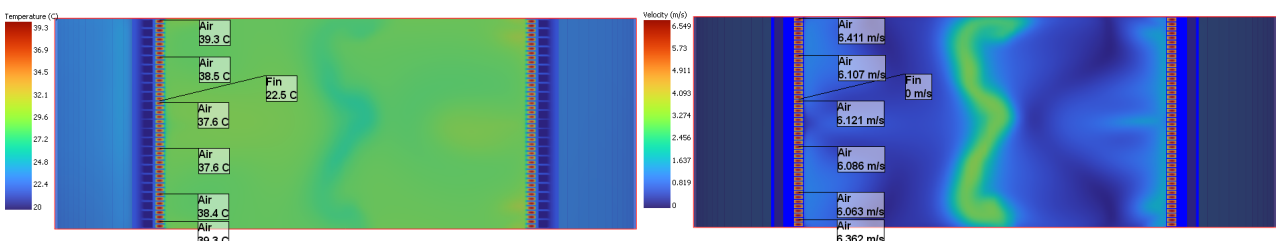
model. These planes are shown in Figure 7.39a with three red lines, the top, middle and bottom planes. These figures clearly show the reduction in air temperature within the fan ducts. Also, the air velocity in those planes generally lies within 5 - 6 m/s.



(a) Temperature in the top plane

(b) Air velocity in the top plane

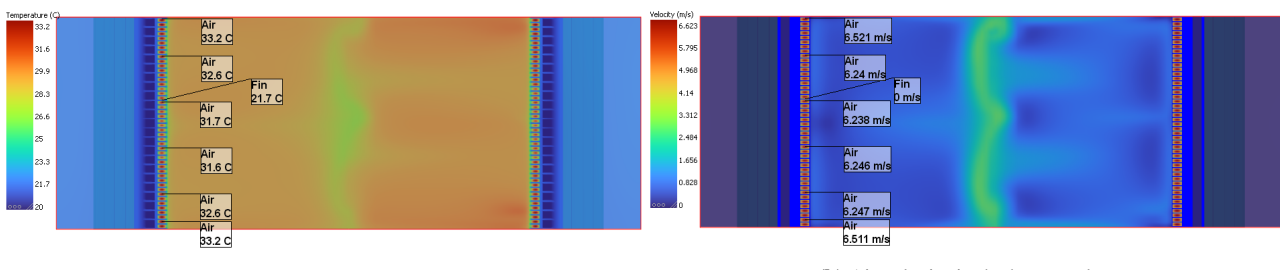
**Figure 7.40:** Top view of the vacuum box space with the steady state temperature and airflow distribution, top plane.



(a) Temperature in the middle plane

(b) Air velocity in the middle plane

**Figure 7.41:** Top view of the vacuum box space with the steady state temperature and airflow distribution, middle plane.



(a) Temperature in the bottom plane

(b) Air velocity in the bottom plane

**Figure 7.42:** Top view of the vacuum box space with the steady state temperature and airflow distribution, bottom plane.

As can be seen in Figure 7.40b, Figure 7.41b and Figure 7.42b, the air velocity in the ducts ranges between 5 - 6 m/s. The correct fan choice must be made to ensure optimal performance of the system. The most important parameters in this decision process are: the working point of the fan, the fan dimensions, and total power required. Figure 7.43 obtained from the CFD shows the required working point of the fan to be at  $32.2 \text{ m}^3/\text{h}$  and 60 Pa. Additionally, it is desirable that this working point is situated in the middle of the fan curve rather than towards the left or right as to ensure more efficient performance. Due to space limitations the fan dimensions may not be larger than 80x80x30mm. Power limitations requires the nominal current from the fans to be lower than 0.4A. Thus, the most suitable choice for these fans were the Adda AD0824VB-A7BGP, which meets all these requirements for which the datasheet can be found in the appendix.

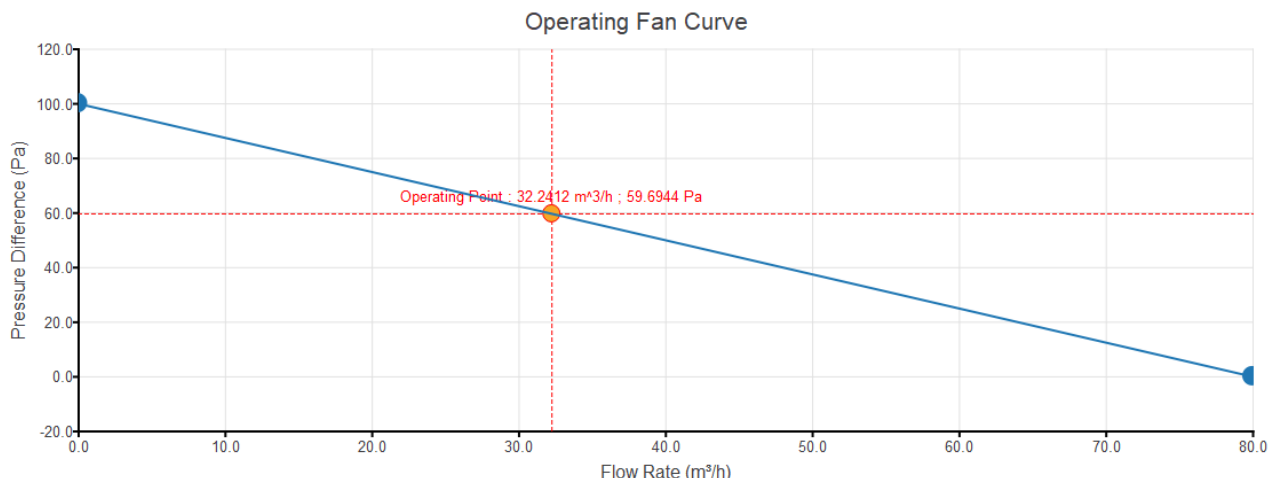


**Figure 7.43:** Operating curve and point of the fan, acquired from CFD model

In conclusion, the CFD analysis shows that the design choices made for the compact heat battery for Helios II result in satisfactory behaviour with regards to the design load and requirements.

## 7.9 Production

### 7.9.1 Printed circuit boards

All printed circuit boards and their corresponding electronic circuits are fully designed by Delft Hyperloop engineers. This includes the main controller, the braking circuit, the thermal controller and all localization boards. All boards are manufactured at Eurocircuits, after which the electronic components are soldered on by Delft Hyperloop engineers.

### 7.9.2 Sensors and localization

All sensors, except for the optical localization system, are bought off the shelf. The brackets used for these sensors are all designed and manufactured by Delft Hyperloop. All brackets are 3d printed with PLA plastic.

The optical localization system is completely custom made, with its board manufactured at Eurocircuits as described above.

### 7.9.3 Track Markers

The track markers for localization are manufactured in house by Delft Hyperloop engineers. This is done by laser cutting stainless steel sheet metal, and then bending the profile into an L shape. This method ensures accurate manufacturing while doing so at a low cost.

### 7.9.4 Thermal management

All constituent parts of the heat battery such as the heat sinks, paraffin wax and fans are outsourced. These are all then assembled in the Dream hall. The heat battery rests on a carbon fibre plate, which is made from SE-70 RC200T prepreg.

## 7.10 Design Adaptations for a Full-Scale Hyperloop System

The Hyperloop system described in this report is based on a prototype scale. Although the scope of the design is to be as close to a full-scale hyperloop system as possible, restrictions in time, available technological research, and resources lead to a few limitations. This section will explain what these limitations are and how they can be adapted in a full-scale hyperloop system.

### 7.10.1 Control

In a full-scale hyperloop system, an emergency brake at high speeds will take a lot of time, be very expensive due to shut down of operations, and will be possibly even dangerous. Therefore, the system should be as redundant as possible and be able to proceed when non-critical subsystems fail. As any subsystem in the Delft Hyperloop design is critical, any error or failure results in an immediate emergency brake to ensure safety at all times. In a full-scale system, the redundancy of subsystems should be maximized to optimize the robustness of the system. One step in this direction would be the use of a 'lockstep' configuration, which means the use of a double microcontroller to ensure that there is a fallback scenario in case one microcontroller fails. This is one of the requirements for complying with ISO 26262, which is the international standard for functional safety of electrical and/or electronic systems that are installed in serial production road vehicles. Setup by the International Organization for Standardization (ISO).[\[44\]](#) Complying with this kind of regulation will be one of the big steps that have to be taken to get the hyperloop to its full scale, both technically and legally.

### 7.10.2 Sensing

When the scale of the hyperloop system increases, more and more entities will have to be measured. On the pod these could be mechanical things like whether doors are open or closed or noncritical electronics like lights and air conditioning. Most of these sensing systems are relatively easy but will have to be added when the need for them arises. Moreover, when an actual vacuum tube is built, the corresponding sensors have to be implemented as well. These can include air pressure within and outside of the tube, but also noncritical electronics and mechanical things like doors. Moreover, when track-side infrastructure is implemented, like a line switch, this also requires the appropriate sensors. Lastly, to prevent dangerous situations in case of a connection loss between the pod and ground control, a localization system should be implemented on the track which is directly connected to ground control. Although variations are easily implemented, such a localization system is not essential in the scope of the current design and is therefore omitted.

### 7.10.3 Communication

The aim of the current design is to perform the most possible communication via the same protocol. Ethernet was chosen for its large bandwidth and its compatibility with most subsystems. Some subsystems, like the BMS, are however non compatible with ethernet and use CAN. In a full-scale system, all subsystems can and should be custom-made to be compatible with the same protocol, which allows for more uniformity in the system. Very likely, the best option for this protocol will be any form of industrial ethernet or CAN.[\[45\]](#)

### 7.10.4 Thermal Management

With an increase in the scale of the hyperloop system, alternative cooling solutions will open up. Full-scale hyperloop systems will require a cooling system that can operate at a steady state, accompanied by a thermal storage module to absorb excess heat production during acceleration and braking, or a module to dispel the heat to the outside.

At a larger scale, an increased surface area will open up the option for the use of radiation to dispel heat generated by all subsystems. It must be noted that the scaling of the surface area happens at a smaller rate than that of volume and weight (surface area scales quadratically with length and volume scales with the cube). Still, this mode of heat transfer is rather attractive due to the total heat transfer scaling with temperature to fourth ( $T^4$ ). This means that tiny changes in temperature result in significantly higher radiation. To achieve optimal radiative heat transfer, two key factors must be maximized: the surface area and the surface temperature, Equation 7.18. A possible solution for this are radiation panels [\[46\]](#), also applied in the International Space Station. Waste heat from high heat generators is removed through cold plates and heat exchangers and is directed toward the radiation panel. A hyperloop equipped with a fully scalable radiation panels with optimizations in surface area may be efficient enough to dissipate a large portion of the entire heat production of the pod, or even the total heat production of the pod. Another optimization consideration regarding radiation is the use of the entire pod as a radiation module. This greatly increases the available area through which heat can be radiated. Also, due to the round shape of the aeroshell, the view factors can be considered 1.0, causing no additional losses.

Thermal storage forms the second important aspect of thermal cooling systems for hyperloop. This can be achieved through different methods such as phase change materials and thermochemical storage. Both these different methods

are represent an immensely broad spectrum of different materials. Phase change materials are plentiful however when it comes to making the material choice one must make a choice between optimizing heat conductivity, heat capacity, weight and costs. Section 7.8 discusses the effectiveness of paraffin wax based PCMs. The biggest challenge concerning paraffin wax PCMs are its low heat conductivity. To tackle this problem in a full-scale hyperloop one can employ more complex pump and heat exchangers to aid in increasing the efficiency of the heat conductivity. For example gasketed plate heat exchangers are often used in the chemical industry due to their excellent effective area-to-volume ratio, resistance to fouling, and relatively cheap price compared to other heat exchangers [38].

Another novel method of cooling is a system that applies sublimation of ice [47], where the sublimation enthalpy of ice is used to cool down the pod. The sublimation enthalpy of ice is  $2838.4 \text{ kJ}\cdot\text{kg}^{-1}$  [48], which makes ice an extremely dense form of heat storage and puts it leagues above any phase change material. A cooling process based on sublimation would start with a cooling cycle with water as the working fluid. The heated water then arrives at the sublimation unit, where it subsequently freezes and sublimates into the tube. When working with such sublimation, one has to take into account the effect of water droplets forming in the vacuum pumps. Therefore additional condensers need to be placed at each vacuum pump to prevent any damage from occurring.

## **8 Mechanical**

**8.1 Introduction**

**8.2 Chassis**

**8.3 Track**

**8.4 Brakes**

**8.5 Vacuum Box**

**8.6 Aeroshell**

**8.7 Production**

**8.8 Design Adaptations for a Full-Scale Hyperloop System**

## **9 Demonstration**

### **9.1 Procedures**

### **9.2 Infrastructure**

## **10 Safety**

- 10.1 Hazardous Energy Storage**
- 10.2 Hazardous Materials**
- 10.3 Safety Features of the Pod**
- 10.4 Subsystem-Specific Safety Features**

## **11 Testing**

### **11.1 Testing Overview**

### **11.2 Test Setups**

## 12 Conclusion

## References

- K. Young, C. Wang, L. Y. Wang, and K. Strunz, “Electric vehicle battery technologies,” in *Electric vehicle integration into modern power networks*. Springer, 2013, pp. 15–56.
- C. Iclodean, B. Varga, N. Burnete, D. Cimerdean, and B. Jurchiș, “Comparison of different battery types for electric vehicles,” in *IOP conference series: materials science and engineering*, vol. 252, no. 1. IOP Publishing, 2017, p. 012058.
- G. Mulder, N. Omar, S. Pauwels, M. Meeus, F. Leemans, B. Verbrugge, W. De Nijs, P. Van den Bossche, D. Six, and J. Van Mierlo, “Comparison of commercial battery cells in relation to material properties,” *Electrochimica Acta*, vol. 87, pp. 473–488, 2013.
- S. M. A. S. Bukhari, J. Maqsood, M. Q. Baig, S. Ashraf, and T. A. Khan, “Comparison of characteristics—lead acid, nickel based, lead crystal and lithium based batteries,” in *2015 17th UKSim-AMSS International Conference on Modelling and Simulation (UKSim)*. IEEE, 2015, pp. 444–450.
- T. Kim, W. Song, D.-Y. Son, L. K. Ono, and Y. Qi, “Lithium-ion batteries: outlook on present, future, and hybridized technologies,” *Journal of materials chemistry A*, vol. 7, no. 7, pp. 2942–2964, 2019.
- R. Cook, “Lithium ion battery performance in low earth orbit satellite applications,” 2020.
- X. He, G. Zhang, X. Feng, L. Wang, G. Tian, and M. Ouyang, “A facile consistency screening approach to select cells with better performance consistency for commercial 18650 lithium ion cells,” *Int. J. Electrochem. Sci*, vol. 12, no. 11, pp. 10 239–10 258, 2017.
- Y. Nishi, K. Katayama, J. Shigetomi, and H. Horie, “The development of lithium-ion secondary battery systems for ev and hev,” in *Thirteenth Annual Battery Conference on Applications and Advances. Proceedings of the Conference*. IEEE, 1998, pp. 31–36.
- S.-i. Tobishima and J.-i. Yamaki, “A consideration of lithium cell safety,” *Journal of Power Sources*, vol. 81, pp. 882–886, 1999.
- J. B. Quinn, T. Waldmann, K. Richter, M. Kasper, and M. Wohlfahrt-Mehrens, “Energy density of cylindrical li-ion cells: a comparison of commercial 18650 to the 21700 cells,” *Journal of The Electrochemical Society*, vol. 165, no. 14, pp. A3284–A3291, 2018.
- R. Sheldon, Jr and D. Coates, “Safety and heat transfer optimization of lithium ion space flight satellite batteries,” in *16th International Communications Satellite Systems Conference*, 1996, p. 1025.
- L. Murata Manufacturing Co., “Cylindrical type lithium ion secondary battery us18650vtc5a.” [Online]. Available: <https://www.murata.com/-/media/webrenewal/products/batteries/cylindrical/datasheet/us18650vtc5a-product-datasheet.ashx?la=en&#amp;cvid=20220207015420000000>
- D. Li, D. Sutton, A. Burgess, D. Graham, and P. D. Calvert, “Conductive copper and nickel lines via reactive inkjet printing,” *Journal of Materials Chemistry*, vol. 19, no. 22, pp. 3719–3724, 2009.
- A. Kampker, S. Wessel, F. Fiedler, and F. Maltoni, “Battery pack remanufacturing process up to cell level with sorting and repurposing of battery cells,” *Journal of Remanufacturing*, vol. 11, no. 1, pp. 1–23, 2021.
- E. Sili, F. Koliatene, and J. Cambronne, “Pressure and temperature effects on the paschen curve,” in *2011 Annual Report Conference on Electrical Insulation and Dielectric Phenomena*. IEEE, 2011, pp. 464–467.
- E. Husain and R. Nema, “Analysis of paschen curves for air, n<sub>2</sub> and sf<sub>6</sub> using the townsend breakdown equation,” *IEEE transactions on electrical insulation*, no. 4, pp. 350–353, 1982.
- N. F. P. Association, N. B. of Fire Underwriters, and N. F. P. A. N. E. C. Committee, *National electrical code*. National Fire Protection Association., 1915, vol. 70.
- Pulse Width Modulation Control Circuit*, Texas Instruments, 1983.
- M. Lafoz, G. Navarro, J. Torres, Á. Santiago, J. Nájera, M. Santos-Herran, and M. Blanco, “Power supply solution for ultrahigh speed hyperloop trains,” *Smart Cities*, vol. 3, no. 3, pp. 642–656, 2020.
- S. Radovanovic, A.-J. Annema, and B. Nauta, *High-Speed Photodiodes in Standard CMOS Technology*. Springer, 2006.

- J. Smith, “Principles of lock-in detection and the state of the art,” Oct 2016. [Online]. Available: <https://www.zhinst.com/europe/en/resources/principles-of-lock-in-detection>
- B. R. Archambeault and J. Drewniak, *PCB Design for Real-World EMI Control*. Springer London, Limited, 2013.
- T. Instruments, “Snoa930c: Sensor design for inductive sensing applications using ldc,” May 2021.
- A. Girault, B. Lee, and E. A. Lee, “Hierarchical finite state machines with multiple concurrency models,” *IEEE Transactions on computer-aided design of integrated circuits and systems*, vol. 18, no. 6, pp. 742–760, 1999.
- S. Brunner, J. Roder, M. Kucera, and T. Waas, “Automotive e/e-architecture enhancements by usage of ethernet tsn,” in *2017 13th Workshop on Intelligent Solutions in Embedded Systems (WISER)*. IEEE, 2017, pp. 9–13.
- F. Bolger, “C++ language: Fit for purpose in embedded systems,” in *2nd Embedded Real Time Software Congress (ERTS'04)*, 2004.
- D. Herity, “C++ in embedded systems: Myth and reality,” *Embedded Systems Programming*, vol. 11, no. 2, pp. 48–71, 1998.
- E. Gamma, R. Helm, R. Johnson, J. Vlissides, and D. Patterns, “Elements of reusable object-oriented software,” *Design Patterns*, 1995.
- J. A. Ledin, “Hardware-in-the-loop simulation,” *Embedded Systems Programming*, vol. 12, pp. 42–62, 1999.
- N. Nikolov, “Research firmware update over the air from the cloud,” in *2018 IEEE XXVII International Scientific Conference Electronics-ET*. IEEE, 2018, pp. 1–4.
- S. Halder, A. Ghosal, and M. Conti, “Secure over-the-air software updates in connected vehicles: A survey,” *Computer Networks*, vol. 178, p. 107343, 2020.
- J. HART, V. HARTOVÁ, M. KOTEK, and V. ŠTEKEROVÁ, “Analysis of wireless transmission latency in the 2.4 ghz and 5 ghz ism under load of network with data stream.”
- D. Friesel and O. Spinczyk, “Data serialization formats for the internet of things,” *Electronic Communications of the EASST*, vol. 80, 2021.
- K. Ellsworth. [Online]. Available: <https://www.cirris.com/learning-center/general-testing/special-topics/177-temperature-coefficient-of-copper#:~:text=The%20Temperature%20Coefficient%20of%20Copper%20resistance%20will%20increase%200.39325>.
- J. He, R. Youssef, M. S. Hosen, M. Akbarzadeh, J. Van Mierlo, and M. Berecibar, “A novel methodology to determine the specific heat capacity of lithium-ion batteries,” *Journal of Power Sources*, vol. 520, p. 230869, 2022. [Online]. Available: <https://www.sciencedirect.com/science/article/pii/S0378775321013549>
- “Phase change materials handbook - nasa technical reports server (ntrs),” Sep 1971. [Online]. Available: <https://ntrs.nasa.gov/citations/19720012306>
- M. Usman, F. Siddiqui, A. Ehsan, R. A. Sadaqat, and A. Hussain, “Improvement of thermal conductivity of paraffin wax, a phase change material with graphite powder,” *2020 17th International Bhurban Conference on Applied Sciences and Technology (IBCAST)*, 2020.
- M. S. Peters, K. D. Timmerhaus, and R. E. West, *Plant Design and Economics for Chemical Engineers*. McGraw-Hill, 2006.
- R. Brogan, “Shell and tube heat exchangers.” [Online]. Available: <https://www.thermopedia.com/content/1121/#:~:text=Tube20diameter20layout20and20pitch,are20the20most20common20sizes>.
- V. Gnielinski, “New equations for heat and mass transfer in turbulent pipe and channel flow,” 1976.
- B. Petukhov, “Heat transfer and friction in turbulent pipe flow with variable physical properties,” in *Advances in Heat Transfer*. Elsevier, 1970, pp. 503–564. [Online]. Available: [https://doi.org/10.1016/s0065-2717\(08\)70153-9](https://doi.org/10.1016/s0065-2717(08)70153-9)
- A. F. Mills, “Experimental investigation of turbulent heat transfer in the entrance region of a circular conduit,” *Journal of Mechanical Engineering Science*, vol. 4, no. 1, pp. 63–77, Mar. 1962. [Online]. Available: [https://doi.org/10.1243/jmes\\_jour\\_1962\\_004\\_010\\_02](https://doi.org/10.1243/jmes_jour_1962_004_010_02)

R. Kothari, A. Ahmad, S. Kumar Chaurasia, O. Prakash, and O. Prakash, “Experimental analysis of the heat transfer rate of phase change material inside a horizontal cylindrical latent heat energy storage system,” *Materials Science for Energy Technologies*, vol. 5, p. 208–216, 2022.

“Iso 26262-1:2018,” Dec 2018. [Online]. Available: <https://www.iso.org/standard/68383.html>

D. Gao, Y. Zhang, and X. Li, “Information perception and intelligent management for electric vehicle charging-swap networks with the internet of things,” in *2012 IEEE 12th International Conference on Computer and Information Technology*. IEEE, 2012, pp. 311–315.

“Staying cool on the iss,” Mar 2001. [Online]. Available: [https://science.nasa.gov/science-news/science-at-nasa/2001/ast21mar\\_1](https://science.nasa.gov/science-news/science-at-nasa/2001/ast21mar_1)

B. J. Kooger and G. Spek, “Cooling system for a transportation vehicle arranged to be transported in a low-pressure environment,” Patent WO2022119439A1, 6 9, 2022.

M. J. Moran, H. N. Shapiro, D. D. Boettner, and M. B. Bailey, *Moran’s principles of engineering thermodynamics*. Wiley Global Education, 2020.

**A Propulsion**

**B Levitation**

**C Sense and Control**

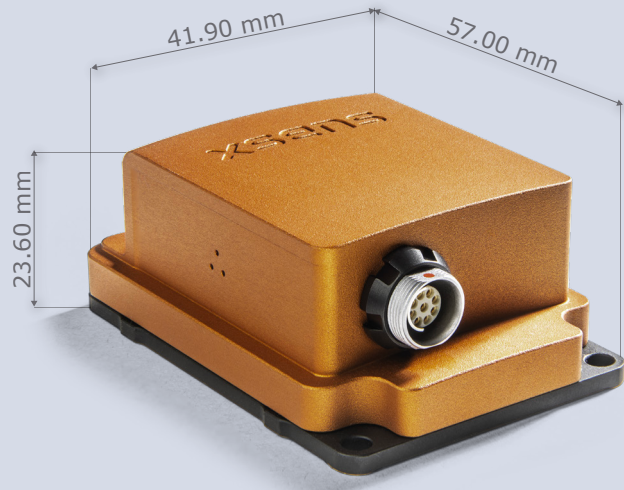
# MTi-300

- Xsens' high-performance product line
- 0.2 deg in roll/pitch, 1 deg in heading accuracy
- Complete SDK and development kits available

The MTi-200 features vibration-rejecting gyroscopes and offers high-quality inertial data, even in challenging environments.

The all-in-one sensor system supports optimized temperature calibration, high-frequency outputs, and has configurable output settings for synchronization with any third-party device.

The MTi-200 is supported by the MT Software Suite which includes MT Manager (GUI for Windows/Linux), SDK, example codes and drivers for many platforms.



- White label and OEM integration options available
- 3D models available on request
- Available online via Digi-Key, Mouser, Farnell and local distributors

## Sensor fusion performance

Roll, Pitch	0.2 deg RMS
Yaw/Heading	1 deg RMS
Strapdown Integration (SDI)	Yes

## Gyroscope

Standard full range	450 deg/s
In-run bias stability	10 deg/h
Bandwidth (-3dB)	415 Hz
Noise Density	0.01 °/s/√Hz
g-sensitivity (calibr.)	0.003 °/s/g

## Accelerometer

Standard full range	20 g
In-run bias stability	15 µg
Bandwidth (-3dB)	375 Hz
Noise Density	60 µg/√Hz

## Magnetometer

Standard full range	+/- 8 G
Total RMS noise	0.5 mG
Non-linearity	0.2%
Resolution	0.25 mG

## Barometer

Standard full range	300-1100 hPa
Total RMS noise	3.6 Pa
Resolution	~0.08m

Complete and detailed specifications are available at

[mtidocs.xsens.com](http://mtidocs.xsens.com)

## Mechanical

IP-rating	IP67
Operating Temperature	-40 to 85 °C
Casing material	Aluminum
Mounting orientation	No restriction, full 360° in all axes
Dimensions	57x41.90x23.60 mm
Connector	Fischer SV
Weight	55 g
Certifications	CE, FCC, RoHS, MIL-STD-202

## Electrical

Input voltage	3V3, 4.5V-34V
Power consumption (typ)	520 mW

## Interfaces / IO

Interfaces	USB, RS232, RS422, UART
Sync Options	SyncIn, SyncOut, ClockSync
Protocols	Xbus, ASCII (NMEA)
Clock drift	10 ppm (or external)
Output Frequency	Up to 2kHz
Built-in-self test	Gyr, Acc, Mag

## Software Suite

GUI (Windows/Linux)	MT Manager, Firmware updater, Magnetic Field Mapper
SDK (Example code)	C++, C#, Python, Matlab, Nucleo, public source code
Drivers	LabVIEW, ROS, GO
Support	BASE by XSENS: online manuals, community and knowledge base

# Data Sheet

## Temperature Sensor



Voltage: 5VDC

Current: 2mA

Resistance value: 10000Ω

Operating Temperature: -30°C to 105°C

**R---T TABLE**  
**R25°C=10KΩ±1%**      **B25°C/50°C=3950±1%**

T	Rmax	Rnor	Rmin	T	Rmax	Rnor	Rmin
-30	180.6235	173.7550	167.1313	10	20.4099	20.0690	19.7316
-29	170.1216	163.6524	157.4138	11	19.4330	19.1084	18.7872
-28	160.3086	154.2126	148.3339	12	18.5101	18.2009	17.8949
-27	151.1346	145.3874	139.8451	13	17.6370	17.3423	17.0508
-26	142.5535	137.1326	131.9050	14	16.8107	16.5299	16.2521
-25	134.1102	129.4075	124.8569	15	15.9907	15.7608	15.5326
-24	126.5855	122.1467	117.8514	16	15.2592	15.0398	14.8221
-23	119.5450	115.3531	111.2967	17	14.5665	14.3570	14.1492
-22	112.9476	108.9870	105.1545	18	13.9097	13.7097	13.5113
-21	106.7624	103.0187	99.3960	19	13.2867	13.0957	12.9061
-20	100.6616	97.4205	94.2737	20	12.6665	12.5131	12.3603
-19	94.9824	91.9241	88.9548	21	12.1035	11.9569	11.8110
-18	89.6693	86.7821	83.9790	22	11.5697	11.4296	11.2900
-17	84.6915	81.9646	79.3170	23	11.0478	10.9288	10.8099
-16	80.0256	77.4489	74.9472	24	10.5623	10.4531	10.3440
-15	75.4340	73.2141	71.0527	25	10.1000	10.0000	9.9000
-14	71.3828	69.2822	67.2368	26	9.6753	9.5753	9.4753
-13	67.5816	65.5929	63.6564	27	9.2665	9.1707	9.0749
-12	64.0097	62.1261	60.2920	28	8.8852	8.7857	8.6865
-11	60.6517	58.8669	57.1290	29	8.5146	8.4192	8.3242
-10	57.3344	55.8015	54.3044	30	8.1688	8.0703	7.9724
-9	54.3033	52.8515	51.4336	31	7.8289	7.7345	7.6406
-8	51.4562	50.0805	48.7369	32	7.5055	7.4150	7.3250
-7	48.7782	47.4741	46.2005	33	7.1974	7.1107	7.0244
-6	46.2580	45.0213	43.8135	34	6.9039	6.8207	6.7379
-5	43.7676	42.7122	41.6779	35	6.6380	6.5443	6.4512
-4	41.5325	40.5310	39.5495	36	6.3651	6.2752	6.1859
-3	39.4289	38.4781	37.5463	37	6.1053	6.0191	5.9334
-2	37.4461	36.5432	35.6583	38	5.8576	5.7750	5.6928
-1	35.5766	34.7187	33.8780	39	5.6216	5.5422	5.4633
0	33.7253	32.9977	32.2826	40	5.4075	5.3202	5.2338
1	32.0184	31.3276	30.6487	41	5.1918	5.1080	5.0250
2	30.4109	29.7548	29.1100	42	4.9862	4.9057	4.8260

## Data Sheet

T	Rmax	Rnor	Rmin	T	Rmax	Rnor	Rmin
3	28.8949	28.2716	27.6588	43	4.7899	4.7126	4.6360
4	27.4647	26.8721	26.2897	44	4.6025	4.5282	4.4547
5	26.0490	25.5513	25.0606	45	4.4324	4.3522	4.2730
6	24.8025	24.3286	23.8614	46	4.2613	4.1841	4.1080
7	23.6251	23.1737	22.7286	47	4.0979	4.0237	3.9505
8	22.5114	22.0813	21.6572	48	3.9417	3.8704	3.8000
9	21.4575	21.0475	20.6433	49	3.7925	3.7238	3.6561
50	3.6566	3.5835	3.5115	90	0.9497	0.9180	0.8873
51	3.5248	3.4543	3.3849	91	0.9215	0.8907	0.8609
52	3.3985	3.3305	3.2636	92	0.8944	0.8645	0.8356
53	3.2774	3.2119	3.1473	93	0.8681	0.8391	0.8110
54	3.1614	3.0981	3.0359	94	0.8428	0.8146	0.7873
55	3.0559	2.9891	2.9236	95	0.8196	0.7910	0.7633
56	2.9448	2.8805	2.8174	96	0.7955	0.7678	0.7409
57	2.8386	2.7766	2.7157	97	0.7724	0.7455	0.7194
58	2.7368	2.6770	2.6183	98	0.7501	0.7239	0.6986
59	2.6392	2.5816	2.5250	99	0.7285	0.7031	0.6785
60	2.5504	2.4901	2.4310	100	0.7087	0.6830	0.6581
61	2.4613	2.4031	2.3461	101	0.6903	0.6653	0.6411
62	2.3759	2.3197	2.2647	102	0.6726	0.6482	0.6246
63	2.2939	2.2396	2.1865	103	0.6554	0.6316	0.6086
64	2.2153	2.1628	2.1115	104	0.6386	0.6155	0.5931
65	2.1434	2.0891	2.0359	105	0.6235	0.6000	0.5774
66	2.0677	2.0153	1.9640	106	0.6059	0.5831	0.5612
67	1.9951	1.9445	1.8950	107	0.5890	0.5668	0.5455
68	1.9255	1.8767	1.8289	108	0.5726	0.5510	0.5303
69	1.8587	1.8116	1.7655	109	0.5567	0.5357	0.5155
70	1.7977	1.7491	1.7015	110	0.5421	0.5210	0.5006
71	1.7381	1.6911	1.6452	111	0.5282	0.5076	0.4877
72	1.6810	1.6355	1.5911	112	0.5147	0.4946	0.4752
73	1.6260	1.5820	1.5390	113	0.5015	0.4820	0.4631
74	1.5731	1.5305	1.4890	114	0.4889	0.4698	0.4514
75	1.5248	1.4810	1.4383	115	0.4772	0.4580	0.4395
76	1.4752	1.4329	1.3916	116	0.4643	0.4456	0.4276
77	1.4276	1.3867	1.3467	117	0.4518	0.4336	0.4161
78	1.3818	1.3421	1.3034	118	0.4397	0.4220	0.4050
79	1.3376	1.2993	1.2618	119	0.4280	0.4108	0.3942
80	1.2973	1.2580	1.2198	120	0.4173	0.4000	0.3833
81	1.2559	1.2180	1.1809				
82	1.2162	1.1794	1.1435				
83	1.1779	1.1423	1.1075				
84	1.1410	1.1065	1.0729				
85	1.1073	1.0720	1.0377				
86	1.0730	1.0389	1.0057				
87	1.0401	1.0070	0.9748				
88	1.0083	0.9762	0.9450				
89	0.9777	0.9466	0.9163				



## mm FDRF603 Series

Laser displacement sensors are used for non contact measurement of displacement, speed, acceleration, vibrations, deformation and profiles in static and dynamic applications in the research and industry to improve quality and save costs. The measurement ranges vary from 2mm up to 1250mm. And with blind ranges from 15mm up to 260mm you can mount the sensor at a safe distance from the moving target.

Due to the non contact measurement, you can avoid force on the target and wear of both target and sensor surfaces. Because the laser spot does not have mass, it will follow the target at target speed.



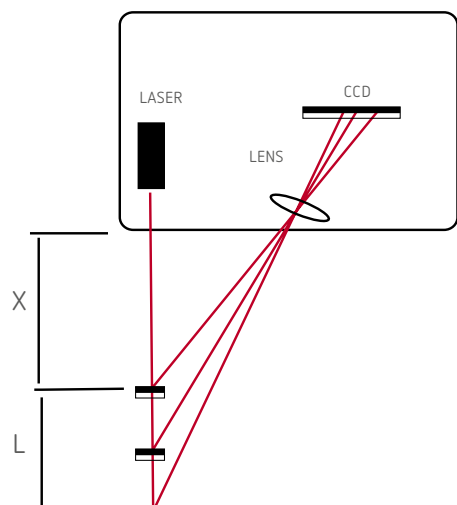
### Features

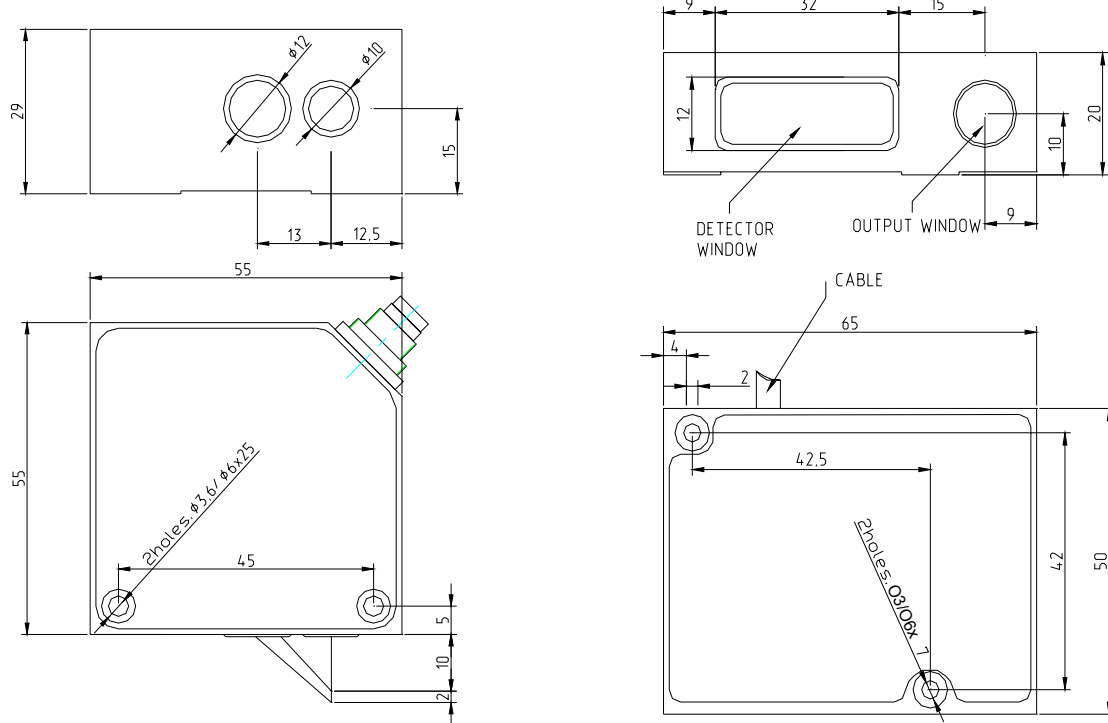
- Save distance to target
- Non contact
- Non wear
- Non force
- Fast, non mass laser spot

### Specifications

RF603-	R-X/4	X/2	X/5	X/10	X/15	X/25	X/30	X/50	X/100	X/250	X/500	X/750	X/1000	X/1250																
Base distance X, mm	39	15	15	15, 25, 60	15, 30, 65	25, 45, 80	35, 55, 95	45, 65, 105	60, 90, 140	80	125	145	245	260																
Measurement range, mm	4	2	5	10	15	25	30	50	100	250	500	750	1000	1250																
Linearity, %	±0.05 of the range											±0.1																		
Resolution, %	0.01 of the range (for the digital output only)											0.02																		
Temperature drift	0.02% of the range/°C																													
Max. measurement frequency	9.4 kHz																													
Light source	red semiconductor laser (660 nm wavelength) or UV semiconductor laser (450 nm or 405 nm wavelength, BLUE version)																													
Model	RF603																													
Output power	≤0,2	≤5 mW																												
Laser safety class	1	3R (IEC60825-1)																												
Model	RF603L																													
Output power	≤0,95 mW																													
Laser safety class	2 (IEC60825-1)																													
Model	RF603P																													
Output power	≤20 mW																													
Laser safety class	3B (IEC60825-1)																													
Output interface:																														
Digital №1	RS232 or RS485 (max. 921600 baud)																													
Digital №2 (optional)	Ethernet (max. 100 Mbit) or CAN V2.0B (max. 1 Mbit)																													
Analog	4...20 mA (load ≤ 500 Ohm) or 0...10 V																													
Synchronization input	2,4 – 24 V																													
Logic output	programmed functions, NPN: 100 mA max; 40 V max for output																													
Power supply	9...36 V																													
Power consumption	1,5...2 W																													
Environmental resistance:																														
Enclosure rating	IP67 (only for sensors with a connector on the housing)																													
Vibration	20 g /10...1000 Hz, 6 hours for each of XYZ axes																													
Shock	30 g / 6 ms																													
Operating ambient temperature	-10...+60°C, (-30...+60°C for the sensors with in-built heater), (-30...+120°C for the sensors with in-built heater and air cooling housing)																													
Permissible ambient light, lx	10000 – RF603L, 30000 – RF603, >30000 – RF603P																													
Relative humidity	5-95% (no condensation)																													
Storage temperature	-20...+70°C																													
Housing material	aluminum																													
Weight (without cable)	100 gram																													

Note: RF603-R-39/4 sensor is designed to use with mirror surfaces and glass.





### Ordering information

RF603(BLUE)(L/P).F-X/D(R)-SERIAL-ANALOG-IN-AL-CC(90X)(R)-M-H-P-B

Symbol	Description
(BLUE)	Blue (405/450 nm) laser option
L/P	Laser safety class: L - Class 2, P - Class 3B
F	Max. measurement frequency, kHz (2 or 10)
X	Base distance (beginning of the range), mm
D	Measurement range, mm
(R)	Round shape laser spot
SERIAL	The type of serial interface: 232 (RS232) or 485 (RS485); CAN or ET (Ethernet)
ANALOG	Attribute showing the presence of 4...20 mA (I) or 0...10 V (U)
IN	Trigger input (input of synchronization) presence
AL	User programmed input/output signal
CC(90X)(R)	Cable gland - CG, or cable connector - CC (Binder 712, IP67) Note 1: sensors with CAN or Ethernet interfaces have 2 connectors or two cable glands. Note 2: 90(X) option – angle cable connector Note 3: R option – robot cable
M	Cable length, m
H	Sensor with in-built heater
P	Sensor with protective air cooling housing
B	Sensor with spray guard

Example: RF603L.140/100R-232-I-IN-AL-24-CCR90A-3 – Class 2 laser, base distance – 140 mm, range – 100mm, round shape laser spot, RS232 serial port, 4...20 mA analog output, trigger input and AL input are available, cable connector, angle type, position "A", robot cable, 3 m cable length.

Page 2 / 2

The information provided herein is to the best of our knowledge true and accurate, it is provided for guidance only. All specifications are subject to change without prior notification.

Althen – Your expert partner in Sensors & Controls | [althensensors.com](http://althensensors.com)

Althen stands for pioneering measurement and custom sensor solutions. In addition we offer services such as calibration, design & engineering, training and renting of measurement equipment.

Germany/Austria/Switzerland  
[info@althen.de](mailto:info@althen.de)

Benelux  
[sales@althen.nl](mailto:sales@althen.nl)

France  
[info@althensensors.fr](mailto:info@althensensors.fr)

Sweden  
[info@althensensors.se](mailto:info@althensensors.se)

USA/Canada  
[info@althensensors.com](mailto:info@althensensors.com)

Other countries  
[info@althensensors.com](mailto:info@althensensors.com)

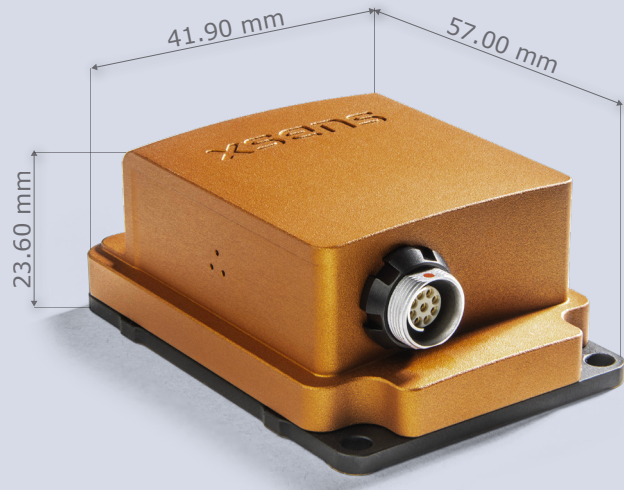
# MTi-300

- Xsens' high-performance product line
- 0.2 deg in roll/pitch, 1 deg in heading accuracy
- Complete SDK and development kits available

The MTi-200 features vibration-rejecting gyroscopes and offers high-quality inertial data, even in challenging environments.

The all-in-one sensor system supports optimized temperature calibration, high-frequency outputs, and has configurable output settings for synchronization with any third-party device.

The MTi-200 is supported by the MT Software Suite which includes MT Manager (GUI for Windows/Linux), SDK, example codes and drivers for many platforms.



- White label and OEM integration options available
- 3D models available on request
- Available online via Digi-Key, Mouser, Farnell and local distributors

## Sensor fusion performance

Roll, Pitch	0.2 deg RMS
Yaw/Heading	1 deg RMS
Strapdown Integration (SDI)	Yes

## Gyroscope

Standard full range	450 deg/s
In-run bias stability	10 deg/h
Bandwidth (-3dB)	415 Hz
Noise Density	0.01 °/s/√Hz
g-sensitivity (calibr.)	0.003 °/s/g

## Accelerometer

Standard full range	20 g
In-run bias stability	15 µg
Bandwidth (-3dB)	375 Hz
Noise Density	60 µg/√Hz

## Magnetometer

Standard full range	+/- 8 G
Total RMS noise	0.5 mG
Non-linearity	0.2%
Resolution	0.25 mG

## Barometer

Standard full range	300-1100 hPa
Total RMS noise	3.6 Pa
Resolution	~0.08m

Complete and detailed specifications are available at

[mtidocs.xsens.com](http://mtidocs.xsens.com)

## Mechanical

IP-rating	IP67
Operating Temperature	-40 to 85 °C
Casing material	Aluminum
Mounting orientation	No restriction, full 360° in all axes
Dimensions	57x41.90x23.60 mm
Connector	Fischer SV
Weight	55 g
Certifications	CE, FCC, RoHS, MIL-STD-202

## Electrical

Input voltage	3V3, 4.5V-34V
Power consumption (typ)	520 mW

## Interfaces / IO

Interfaces	USB, RS232, RS422, UART
Sync Options	SyncIn, SyncOut, ClockSync
Protocols	Xbus, ASCII (NMEA)
Clock drift	10 ppm (or external)
Output Frequency	Up to 2kHz
Built-in-self test	Gyr, Acc, Mag

## Software Suite

GUI (Windows/Linux)	MT Manager, Firmware updater, Magnetic Field Mapper
SDK (Example code)	C++, C#, Python, Matlab, Nucleo, public source code
Drivers	LabVIEW, ROS, GO
Support	BASE by XSENS: online manuals, community and knowledge base

# MEM1G series



## Ordering information

Example: **M EM1 G12 Z**

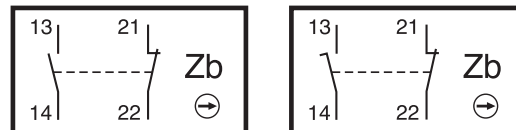
Casing:  
EM1 = metal casing  
30mm width

Actuators: codes G11 -  
G9999

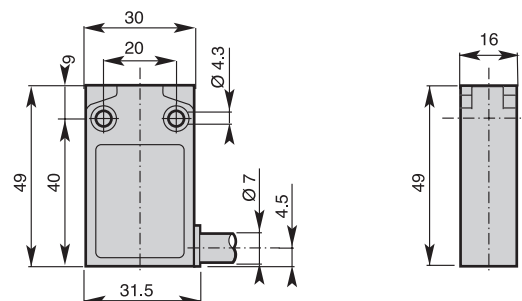
Contact block  
Z: Zb Snap action 1 N.O. + 1 N.C.  
X: Zb Slow action non-overlapping late make 1 N.O. + 1 N.C.

## Contacts

Z: Snap action 1 N.O. + 1 N.C. X: Slow action break before make 1 N.O. + 1 N.C.



## Dimensions (basic)





## Features

- Double Insulation
- 30mm width
- Casing made of metal
- Visible operation
- Able to switch strong currents (10A conventional thermal current)
- Electrically separated contacts
- Precise operating points (consistency)
- Immune to electromagnetic disturbances
- Degree of protection: IP67
- Standard cable length 1m\*..

## General technical data

	Metal casing		
Standards	Devices conform with international IEC 947-5-1 and European EN 60 947-5-1 standards		
Certifications - Approvals	UL (upon request)		
Ambient temperature – during operation – for storage	°C °C	– 25 ... + 70 – 40 ... + 70	
Mounting positions	All positions are authorised		
Protection against electrical shocks (acc. to IEC 536)	Class I		
Degree of protection (according to IEC 529 and EN 60 529)	IP67		
Degree of protection (according to UL50)	Type 4 - 4X - 6 enclosure ("outdoor use - raintight - water tight corrosion resistant")		
<b>Electrical Data</b>			
Rated insulation voltage $U_i$ - according to IEC 947-1 and EN 60 947-1 - according to UL 508 and CSA C22-2 n° 14	400V (pollution degree 3) (250V for M12 connector) B 300, R 300		
Rated impulse withstand voltage $U_{imp}$ (according to IEC 947-1 and EN 60 947-1)	kV	4	
Conventional free-air thermal current $I_{th}$ (according to IEC 947-5-1) $\sigma < 40^\circ\text{C}$	A	5 (4A for M12 connector)	
Short-circuit protection $U_e < 500\text{V a.c.} - \text{gG (gl) type fuses}$	A	6	
Rated operational current $I_e / \text{AC-15}$ (according to IEC 947-5-1)	24V - 50/60Hz 120V - 50/60Hz 240V - 50/60Hz	A A A	5.0 3.0 1.5
$I_e / \text{DC-13}$ (according to IEC 947-5-1)	24V DC 125V DC 250V DC	A A A	1.1 0.22 0.1
Switching frequency	Cycles/h	3600	
Load factor		0.5	
Resistance between contacts	mΩ	25	
Mechanical durability		10 millions of operations	

\* For other cable inlets and cable lengths, please contact your local sales office.

# MEM1G series

## Product number

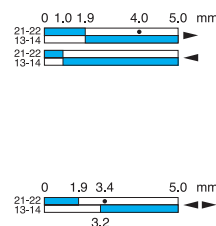
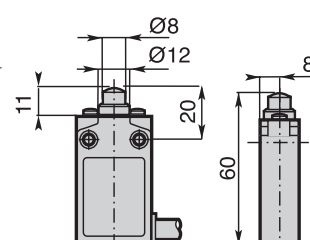
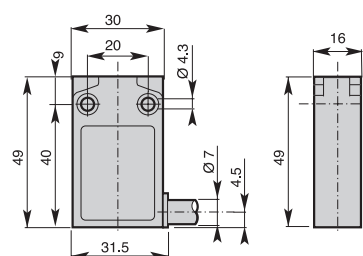
## Dimensions (basic)

## Dimensions (head)

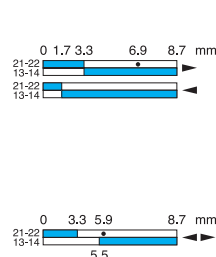
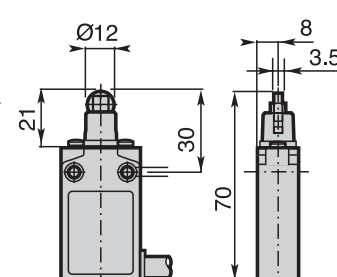
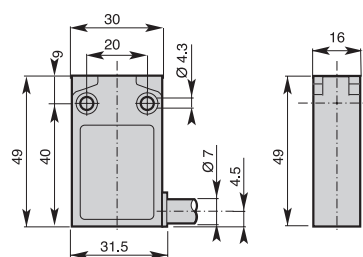
## Operation diagram



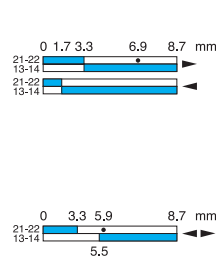
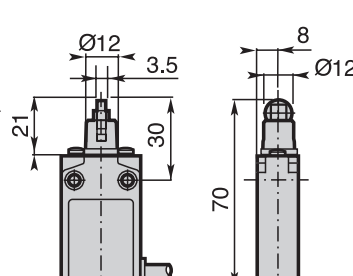
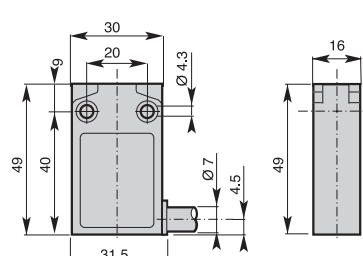
Plain plunger  
MEM1G11\*



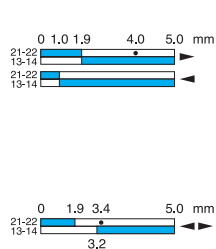
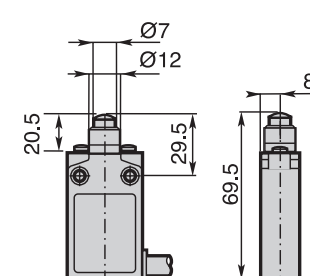
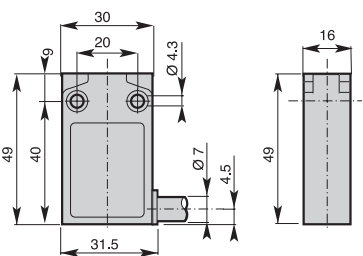
Roller plunger  
MEM1G12\*  
G12: metall roller  
G13: nylon roller



Cross roller plunger  
MEM1G14\*  
G14: metall roller  
G15: nylon roller



Plain plunger with  
dust protection cap  
MEM1G16\*\*



\* Snap action: Z or X  
\*\* Snap action: Z

**Product number**

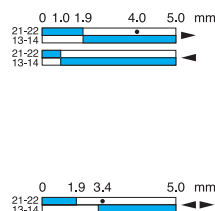
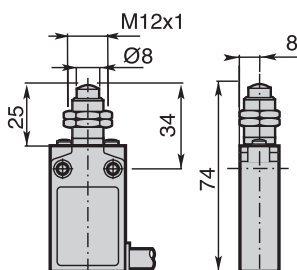
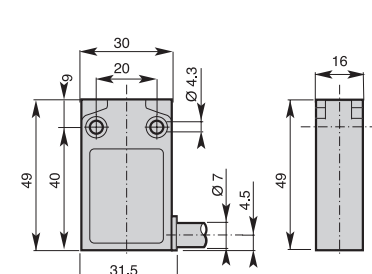
**Dimensions (basic)**

**Dimensions (head)**

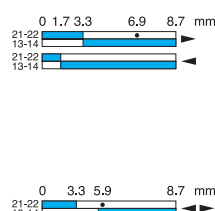
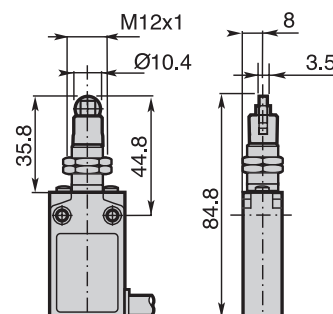
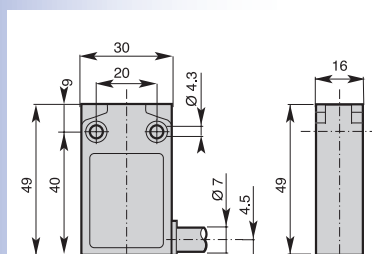
**Operation diagram**



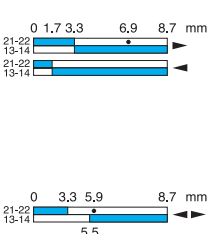
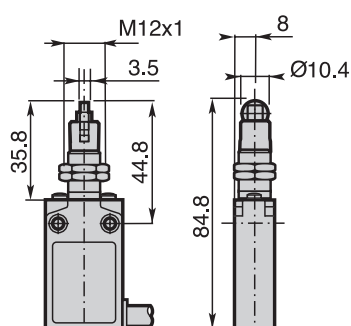
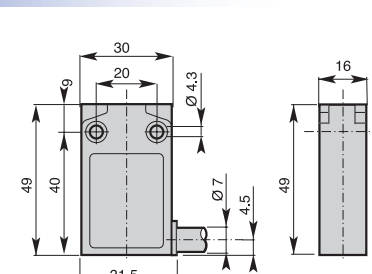
**Plain plunger with fixing nuts**  
MEM1G21\*



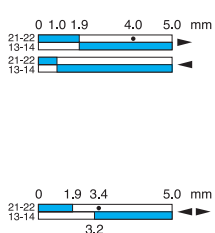
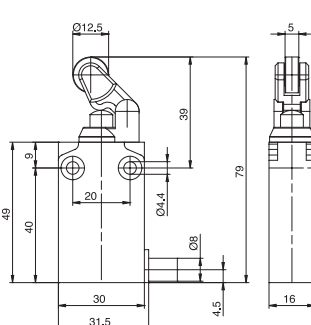
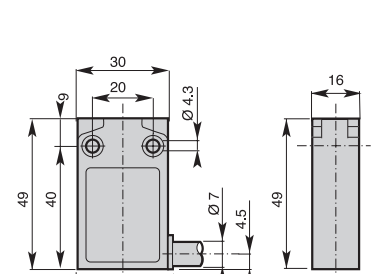
**Roller plunger with fixing nuts**  
MEM1G22\*  
G22: metall roller  
G23: nylon roller



**Cross roller plunger with fixing nuts**  
MEM1G24\*  
G24: metall roller  
G25: nylon roller



**Plain plunger with fixing nuts**  
MEM1G31\*



\* Snap action: Z or X  
\*\* Snap action: Z

## MEM1G series

### Product number

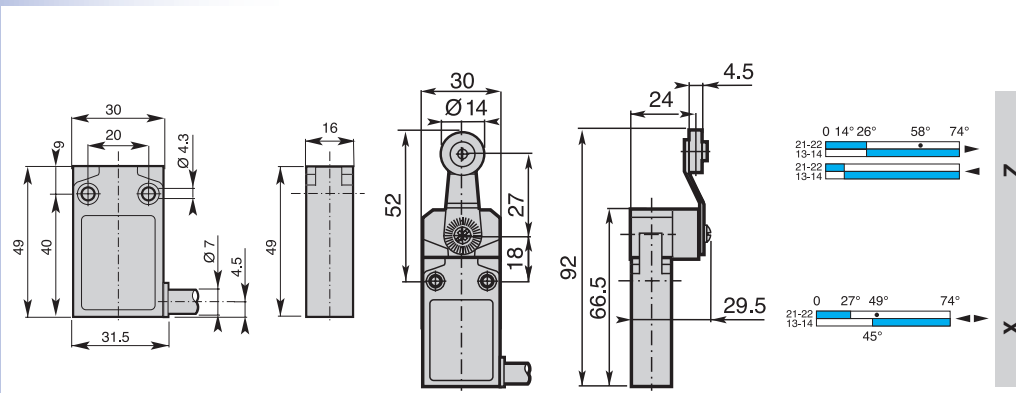
### Dimensions (basic)

### Dimensions (head)

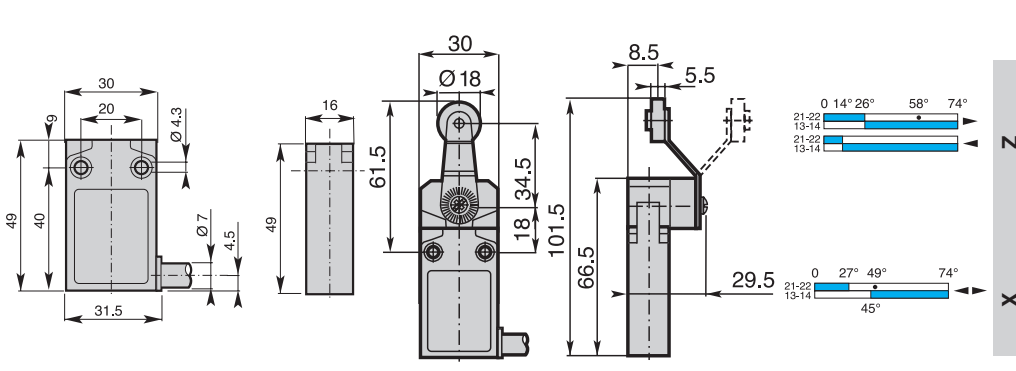
### Operation diagram



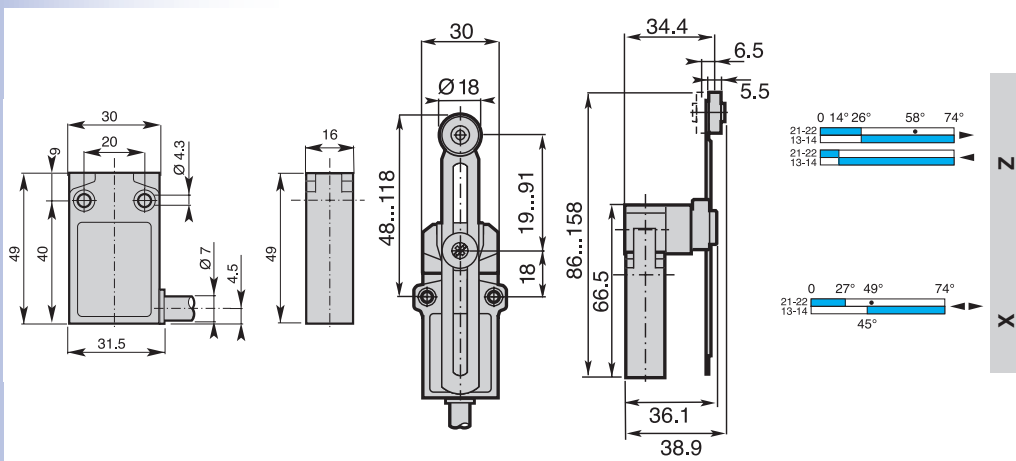
**Roller lever**  
MEM1G41\*  
G41: metal roller  
G42: nylon roller  
G43: ball bearing



**Roller lever**  
MEM1G45\*  
G45: nylon roller  
G46: metal roller



**Adjustable lever with roller**  
MEM1G51\*  
G51: nylon roller  
G53: metal roller



\* Snap action: Z or X

\*\* Snap action: Z

**Product number**

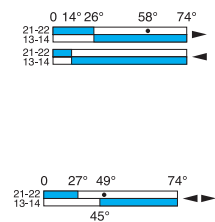
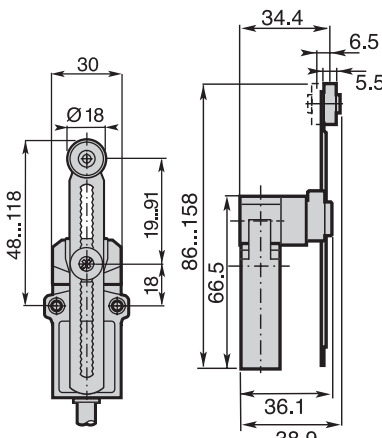
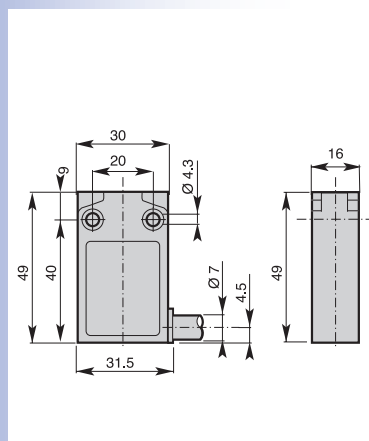
**Dimensions (basic)**

**Dimensions (head)**

**Operation diagram**



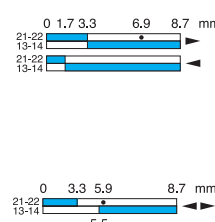
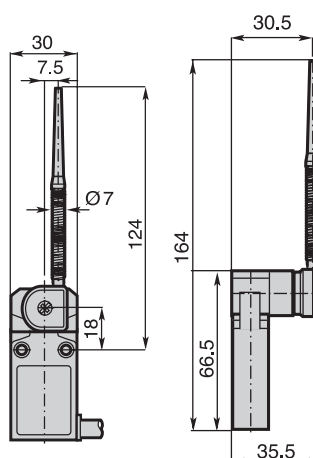
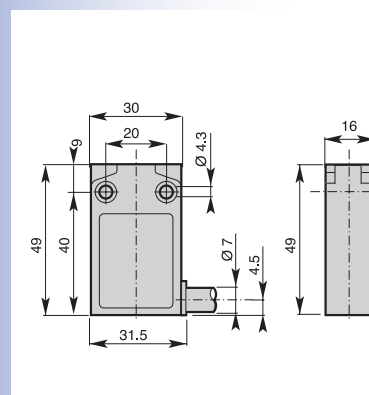
**Adjustable toothed lever (step 2mm)  
with nylon roller  
MEM1G5100\***



Z X



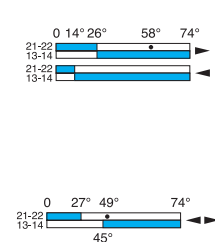
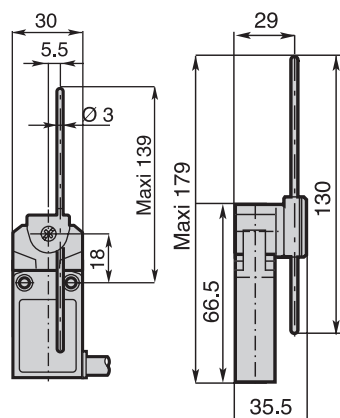
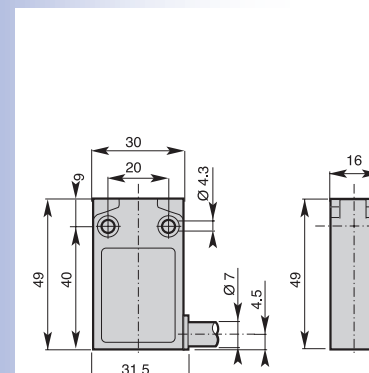
**Nylon actuator with  
stainless steel spring  
MEM1G61\***



Z X



**Adjustable rod lever  
MEM1G71\***  
G71: stainless steel rod  
G72: fiberglass rod  
G75: square steel rod



Z X

\* Snap action: Z or X  
\*\* Snap action: Z

## MEM1G series

### Product number

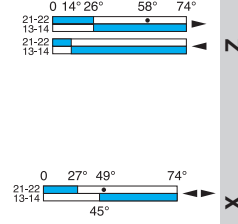
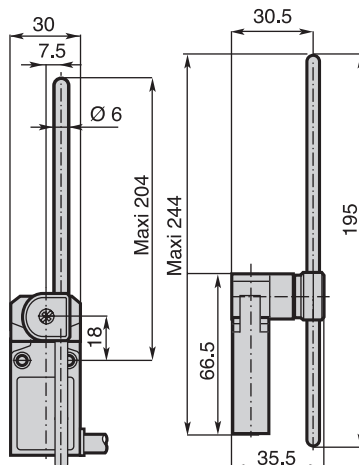
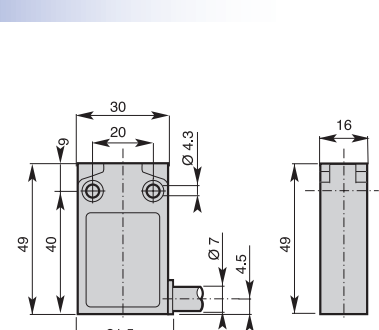
### Dimensions (basic)

### Dimensions (head)

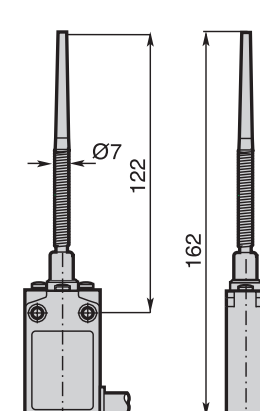
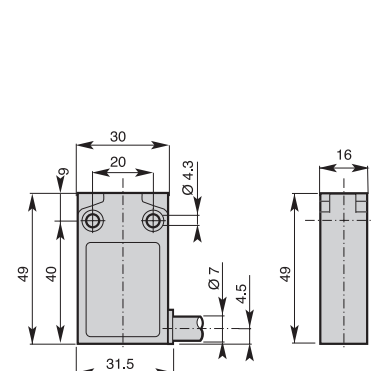
### Operation diagram



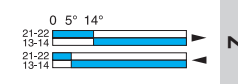
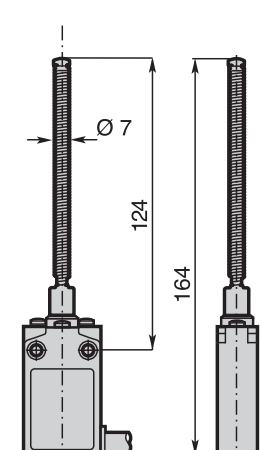
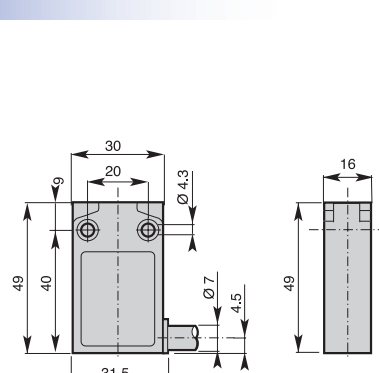
**Adjustable rod lever**  
MEM1G73\*  
G73: nylon rod  
G74: fiberglass rod



**Multidirectional nylon actuator with stainless steel spring**  
MEM1G92\*\*



**Multidirectional actuator with stainless steel spring**  
MEM1G93\*\*





## Laser diode modules

# Data Sheet

This data sheet covers the following items:

Device	RS stock no.	Device	RS stock no.
Beta TX series		Beta Cameo Series	
1mW modulating	564-504	0.8mW continuous wave	213-3590
3mW modulating	194-004	1mW continuous wave	213-3562
3mW modulating	111-368	3mW continuous wave	213-3584
Beta CW series		3mW continuous wave	213-3607
1mW continuous wave	194-010		
1.5mW continuous wave	111-346		
3mW continuous wave	111-352		
3mW continuous wave	194-026		
3mW line generator	194-032		
3mW Wide angle line generator	213-3613		
Single standard lens	194-048		
Line generator lens	194-054		
Line generator lens wide angle	213-3629		
Laser diode holder	213-3641		

### Introduction

These devices have been designed as complete laser diode systems for original equipment manufacturer (O.E.M.) use and although their output powers have been set in accordance with BS(EN)60825, they are not certified lasers as defined in the specification. When incorporated in a piece of equipment it may be necessary for additional safety features to be added before equipment complies fully with the standard. Read BS(EN)60825 before using any of these products.

### Description

These laser modules consist of a laser diode, lens and driver circuit housed in a metal case. The module body is electrically isolated. Electrical connections are made via flying leads. The lens is a single element of high refractive index glass which produces a high quality collimated beam over a long distance. Its position can be adjusted to bring the beam to a focused spot using the special key provided. The Beta CW and TX series standard collimating lens may be replaced by a line generating lens which produces a fan shaped beam that can be focused to a fine, straight line, (RS stock no. 194-032) is supplied with a line generator lens producing a beam angle of 16° fitted, (RS stock no. 213-3613) is supplied with a line generator lens producing a beam angle of 106° fitted. The lens on the Beta Cameo series cannot be replaced with a line generating lens.

### Continuous wave lasers Beta CW series

#### General characteristics

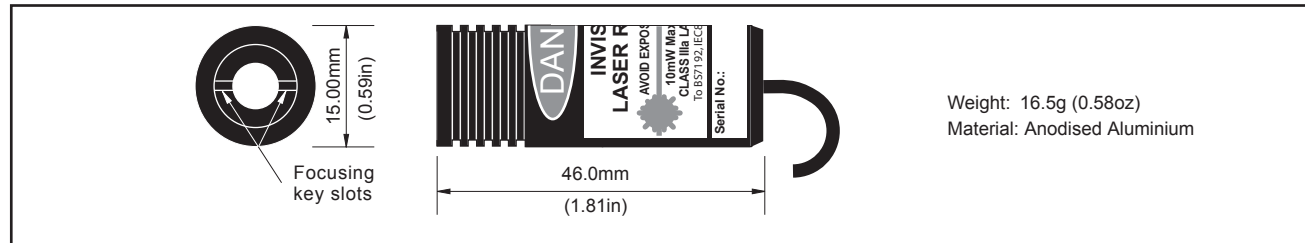
Parameter	RS stock no./Value					Units
	111-346	194-010	194-026	194-032	213-3613	
Nominal wavelength	635	670	670	670	785	nm
Maximum power output	1.5	1	3	3	3	mW
Typical power output stability (@ 20°C)			<1			%
Typical power output temperature dependence			15			µW/°C
Operating voltage	+3.5 to +5.5		-5 to -12			Volts
Typical operating current	30 - 75		25 - 50	50 - 85		mA
Power supply rejection ratio (50Hz-100kHz)	1.0		0.6			%/V
TTL disable voltage	-		>4			Volts
Maximum TTL pulse rate	-		10			Hz
Mean time to failure (MTTF) @ 30°C	>29000		>100000	>90000		Hours
Connections	250mm flying leads					
Red lead	+ve supply		-			
Black lead	-		-ve supply			
Green lead	0		0			Volts
Blue lead	-		TTL disable			

## Optical characteristics

Parameter	RS stock no./Value				Units
	111-346	194-010	194-026 213-3613 194-032	111-352	
Beam size	5 x 2	3.5 x 2	4.5 3 2.5 16° Fan 106° Fan	5 x 2	mm
Minimum focus (lens extended)		25	—	25	mm
Spot size at minimum focus		>50	—	>50	Micron
Polarisation ratio	90:1	80:1	100:1	60:1	
Pointing stability		<0.05			mRad
Output aperture	5.0	3.5	5.0		mm
Angular deviation of beam to case (front cell)			≤10		mRad

The spot size is determined by optical measurement. The relationship of the spot size to illumination is therefore the size to the human eye will appear bigger.  $(\frac{1}{EV})^2$

## Mechanical details



## Absolute maximum ratings

Parameter	RS stock no./Value			
	111-346	111-352	194-010	194-026 194-032 213-3613
Supply voltage	+6.0V		-12.7V	
TTL disable input voltage	—		-3 to +7V	
Operating Case temperature	-10 to +45°C -10 to +55°C		-10 to +55°C	
Storage temperature			-40 to +85°C	

## Power supplies and earthing

Laser modules which operate from a negative voltage can be run from an unregulated supply within the range of -5 to -12V. By operating at the lower (-5V) end of the power supply range, less heat will be dissipated within the device and hence the expected life will increase.

Laser modules which operate from a positive voltage may only be run from a supply which has been regulated to at least 5%, within the limits specified.

For all laser modules the case is isolated from the supply voltages.

It is advisable for any floating power supplies to have the '0' volts connection (and if used, the heatsink) taken to ground. If this is not done, then in electrically noisy environments, the power supply leads can act as aerials. Under these conditions any noise picked up can damage the laser module. If a heatsink is not used, then the barrel of the laser module should be grounded.

## TTL disable

This feature is only available on laser modules which operate from a negative supply voltage.

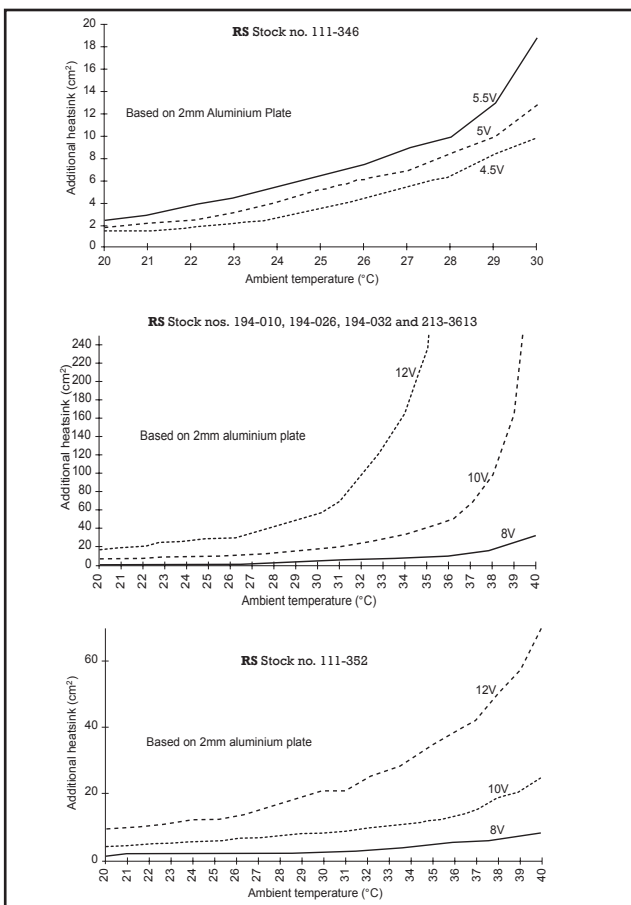
An input of between +4 and +7V applied to the TTL disable input will turn the laser 'off' and an input of 0V will turn it 'on'. If it is not in use it may be left floating. The laser may be pulsed 'on' and 'off' using this input to a frequency of at least 10Hz.

## Heat sink requirements

When operating above their minimum supply voltage and/or at elevated temperatures above 30°C ambient, an additional heat sink must be used. If the case temperature of the embedded laser diode should exceed its maximum specification, premature or even catastrophic failure may occur.

To help dissipate heat from the laser modules the following graphs have been provided which show the additional surface area of 2mm thick aluminium plate required by each model when operated from different supply voltages and in different ambient temperatures. It has been assumed that good contact exists between the module and the additional heat sink to ensure low thermal resistance.

For maximum effect position the heat sink so that it contacts the module just to the rear of the fluted front section (this may require peeling back the label) and use thermally conductive cream between surfaces.



When using a proprietary heat sink, the following equation may be used:

$$\varnothing h \sim \frac{T_c - T_a}{I_{op} \times V_{op}} - (\varnothing m + \varnothing c)$$

Where:

$\varnothing h$  = Thermal resistance of additional heat sink ( $^{\circ}\text{C}/\text{W}$ )

$\varnothing m$  = Thermal resistance of laser module ( $^{\circ}\text{C}/\text{W}$ )

$\varnothing c$  = Thermal resistance of contact, module to heat sink ( $^{\circ}\text{C}/\text{W}$ )

$T_c$  = Maximum operating case temperature for laser diode ( $^{\circ}\text{C}$ )

$T_a$  = Maximum expected ambient temperature ( $^{\circ}\text{C}$ )

$V_{op}$  = Operating voltage of laser module (V)

$I_{op}$  = Operating current @  $V_{op}$  (A)

$\varnothing m + \varnothing c$  for these laser modules is typically  $10^{\circ}\text{C}/\text{W}$  assuming a good thermal contact between module and heat sink.

$T_c$  is specified for each module as follows:

RS stock no.	$^{\circ}\text{C}$
111-352	55
111-346	45
194-026	55
194-010	55
194-032	55
213-3613	55

#### Example:

If:

$\varnothing m + \varnothing c = 10$ ,  $T_c = 50^{\circ}\text{C}$ ,  $T_a = 35^{\circ}\text{C}$ ,  $V_{op} = 10\text{V}$ ,  $I_{op} = 78\text{mA}$

$$\begin{aligned} \text{Then: } \varnothing h &\sim \frac{50 - 35}{0.078 \times 10} - 10 \\ &\sim 9.2^{\circ}\text{C}/\text{W} \end{aligned}$$

#### Expected life

The laser diode device contained within each module, while being a semiconductor, is a complex electro-optical material, the structure of which determines the wavelength of the light emitted. The mechanism which ultimately causes the laser diode to fail is the formation of dislocations or gaps in the material structure. Laser devices which operate in the visible region of the spectrum have a more brittle structure than those that operate in the infra-red and in consequence produce dislocations at a faster rate.

The rate at which dislocations form during normal use is related to the temperature at which the laser diode operates. Where possible every means should be used to minimise temperature, such as working at lower voltage levels, reducing operating ambients and providing adequate heat sinking, all of which will contribute to maximise the operating life. The figures quoted for 'mean time to failure' (MTTF) reflect the differences in device structure and operating power.

## Continuous wave lasers Beta Cameo series

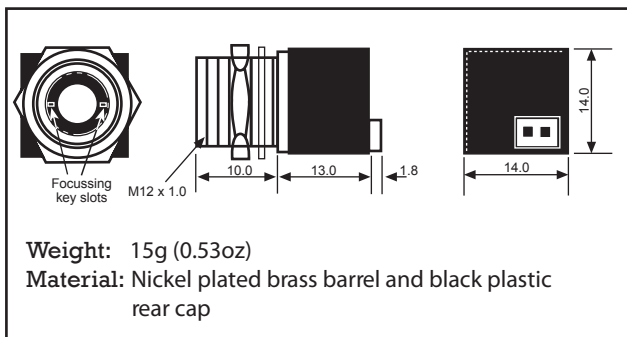
### General characteristics

Parameter	RS stock no./Value				Units
	213-3562	213-3590	213-3584	213-3607	
Nominal wavelength	635	670	635	670	nm
Maximum power output	1	0.8	3	3	mW
Typical power output stability (@20°C)			<1		%
Typical power output temperature dependence			15		$\mu\text{W}/^{\circ}\text{C}$
Operating voltage			+3.5 to 5.0		Volts
Typical operating current			65		mA
Power supply rejection ratio (50Hz-100kHz)			1		%/V
Mean time to failure (MTTF) @ 30°C	>29,000	>100,000	>29,000	>100,000	mm
Connections	2 pin socket (Pre wired plug supplied)				
Red lead	+ve supply				
Green lead	0				Volts

**Optical characteristics**

Parameter	RS stock no./Value				Units
	213-3562	213-3590	213-3584	213-3607	
Beam Size	2		5 x 2		mm
Minimum focus (lens extended)		25			mm
Spot size at minimum focus		>50			Micron
Polarisation ratio		10:1			
Pointing stability		<0.05			mRad
Output aperture	2.0		5.0		mm
Angular deviation of beam to case (front cell)		≤10			mRad

The spot size is determined by optical measurement. The relationship of the spot size to illumination is  $\left(\frac{1}{EV}\right)^2$  therefore the size to the human eye will appear bigger.

**Mechanical details****Absolute maximum ratings**

Parameter	RS stock no./Value		
	213-3562	213-3590	213-3607
Supply voltage	+8V		
Operating temperature	-10 to +45°C	-10 to +55°C	
Storage temperature	-40 to +85°C		

**Power supplies and earthing**

The Beta Cameo must be operated from a regulated, positive supply of 3.5 volts. The case, which may be connected externally to earth, is isolated from the supply.

Connections are made via the two pin latching connector, the mating half is supplied pre-wired, with 500mm of 7 3 0.2mm PVC insulated wire (red is positive and green is 0V).

**Heat sink requirements**

When operating above their minimum supply voltage and/or at elevated temperatures above 30°C ambient, an additional heat sink must be used. If the case temperature of the embedded laser diode should exceed its maximum specification, premature or even catastrophic failure may occur.

The module should be mounted into a metal bracket or bulkhead using the threaded barrel. Thermal transfer cream can be used to improve contact and heat dissipation.

When using a proprietary heat sink, the following equation may be used:

$$\emptyset h \sim \frac{T_c - T_a}{I_{op} \cdot V_{op}} - (\emptyset m + \emptyset c)$$

Where:

$\emptyset h$  = Thermal resistance of additional heat sink (°C/W)

$\emptyset m$  = Thermal resistance of laser module (°C/W)

$\emptyset c$  = Thermal resistance of contact, module to heat sink (°C/W)

$T_c$  = Maximum operating case temperature for laser diode (°C)

$T_a$  = Maximum expected ambient temperature (°C)

$V_{op}$  = Operating voltage of laser module (V)

$I_{op}$  = Operating current @  $V_{op}$  (A)

$\emptyset m + \emptyset c$  for these laser modules is typically 10°C/W assuming a good thermal contact between module and heat sink.

$T_c$  is specified for each module as follows:

RS stock no.	°C
213-3562	45
213-3590	55
213-3584	45
213-3607	55

Example:

If:

$\emptyset m + \emptyset c = 10$ ,  $T_c = 50^\circ\text{C}$ ,  $T_a = 35^\circ\text{C}$ ,  $V_{op} = 5\text{V}$ ,

$I_{op} = 68\text{mA}$

Then:

$$\emptyset h \sim \frac{50 - 35}{0.068 \cdot 3 \cdot 5} - 10$$

$$\sim 34.1 \text{ °C/W}$$

**Modulated lasers Beta TX series**  
**General characteristics**

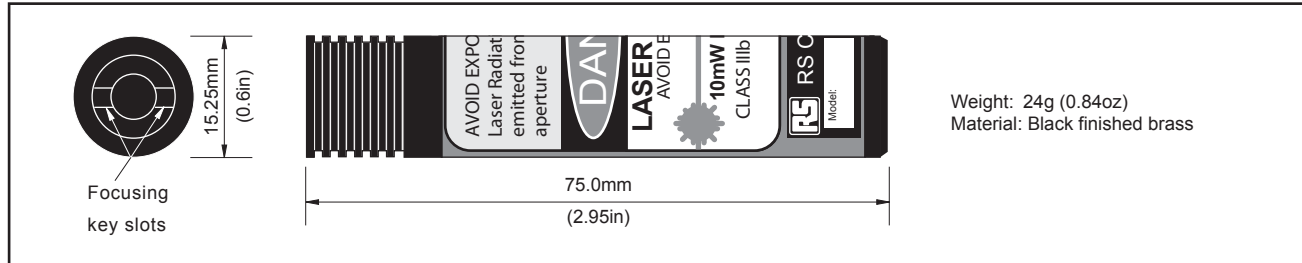
Parameter	RS stock no./Value			Units
	564-504	194-004	111-368	
Nominal wavelength	670	670	785	nm
Maximum power output	1	3	3	mW
Typical power output stability (@ 20°C)		2		%
Typical power output temperature dependence		15		µW/°C
Operating voltage		-5 to -12		Volts
Typical operating current at minimum voltage	75	40		mA
Power supply rejection ratio (50Hz-100kHz)		0.6		%/V
TTL disable voltage		>4		Volts
Maximum TTL pulse rate		0.2		Hz
Interlock 'enable'		-5 to +2.5		Volts
Modulation type	Analogue or digital			
Modulation signal levels into 50 Ω for linear response	500mV pk to pk			
Modulation frequency band width (-3dB points)	100Hz to 50MHz			
Frequency range	100Hz to 100MHz			
Modulation depth (Pulse)	90			%
Mean time to failure (MTTF) @ 25°C	>100,000	>90,000		Hours
Connections	250mm flying leads			
Black lead	-ve supply			
Green lead	0			Volts
Blue lead	TTL disable			
White lead	Interlock			
Yellow and green twisted pair	Modulation input			

**Optical characteristics**

Parameter	RS stock no./Value			Units
	564-504	194-004	111-368	
Beam size	3.5 × 2.0	5.0 × 2.0		mm
Minimum focus (lens extended)		25		mm
Spot size at minimum focus		>50		Micron
Polarisation ratio	80:1	100:1	60:1	
Pointing stability		<0.05		mRad
Output aperture diameter	3.5	5.0		mm
Angular deviation of beam to case (front cell)		≤10		mRad

The spot size is determined by optical measurement. The relationship of the spot size to illumination is  $(\frac{1}{EV})^2$   
therefore the size to the human eye will appear bigger.

## Mechanical details



## Absolute maximum ratings

Parameter	RS stock no./Value		
	564-504	194-004	111-368
Supply voltage	-	-12.7V	
TTL disable input voltage	-	-3 to +7V	
Modulation input voltage	-	-1 to +7V	
Interlock input voltage	-	-5 to +2.5V	
Operating temperature	-	-10 to +55°C	
Storage temperature	-	-40 to +85°C	

## Power supplies and earthing

These laser modules can be run from an unregulated supply within the range of -5 to -12V. By operating at the lower (-5V) end of the power supply range, less heat will be dissipated within the device and hence the expected life will increase. This may be particularly necessary for applications where they operate in a high ambient temperature.

For all laser modules the case is isolated from the supply voltages.

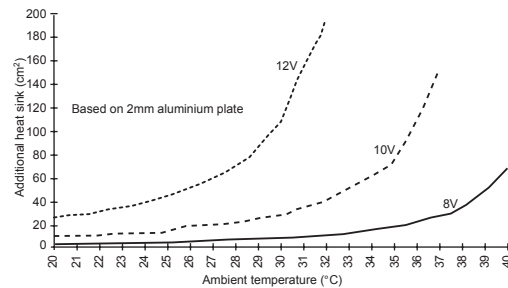
It is advisable for any floating power supplies to have the '0' volts connection (and if used, the heatsink) taken to ground. If this is not done, then in electrically noisy environments, the power supply leads can act as aerials. Under these conditions any noise picked up can damage the laser module. If a heatsink is not used, then the barrel of the laser module should be grounded.

## Heat sink requirements

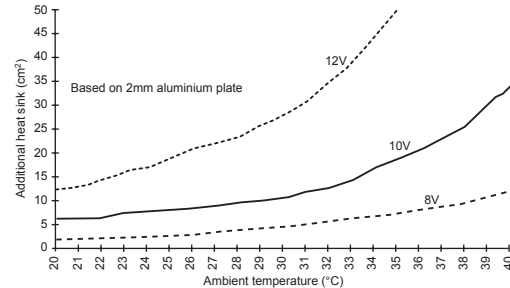
When operating above their minimum supply voltage and/or at elevated temperatures above 30°C ambient, an additional heat sink must be used. If the case temperature of the embedded laser diode should exceed its maximum specification, premature or even catastrophic failure may occur.

To help dissipate heat from the laser modules the following graphs have been provided which show the additional surface area of 2mm thick aluminium plate required by each model when operated from different supply voltages and in different ambient temperatures. It has been assumed that good contact exists between the module and the additional heat sink to ensure low thermal resistance.

Additional heat sink vs ambient temperature  
RS stock no. 194-004 and 564-504



Additional heat sink vs ambient temperature  
RS stock no. 111-368



For maximum effect position the heat sink so that it contacts the module just to the rear of the fluted front section (this may require peeling back the label) and use thermally conductive cream between surfaces.

When using a proprietary heat sink, the following equation may be used:

$$\text{Ø} h \sim \frac{T_c - T_a}{I_{op} \times V_{op}} = (\text{Ø} m + \text{Ø} c)$$

Where:

- $\emptyset h$  = Thermal resistance of additional heat sink ( $^{\circ}\text{C}/\text{W}$ )
- $\emptyset m$  = Thermal resistance of laser module ( $^{\circ}\text{C}/\text{W}$ )
- $\emptyset c$  = Thermal resistance of contact, module to heat sink ( $^{\circ}\text{C}/\text{W}$ )
- $T_c$  = Maximum operating case temperature for laser diode ( $^{\circ}\text{C}$ )
- $T_a$  = Maximum expected ambient temperature ( $^{\circ}\text{C}$ )
- $V_{op}$  = Operating voltage of laser module (V)
- $I_{op}$  = Operating current @  $V_{op}$  (A)
- $\emptyset m + \emptyset c$  for these laser modules is typically  $10^{\circ}\text{C}/\text{W}$  assuming a good thermal contact between module and heat sink.
- $T_c$  is specified for each module as follows:

RS stock no.	°C
564-504	55
194-004	55
111-368	55

#### Example:

If:

$$\emptyset m + \emptyset c = 10, T_c = 50^{\circ}\text{C}, T_a = 30^{\circ}\text{C}, V_{op} = 10\text{V}, I_{op} = 93\text{mA}$$

$$\begin{aligned} \text{Then: } \emptyset h &\sim \frac{50 - 30}{0.093 \times 10} - 10 \\ &\sim \underline{11.5^{\circ}\text{C}/\text{W}} \end{aligned}$$

#### Expected life

The laser diode device contained within each module, while being a semiconductor, is a complex electro-optical material, the structure of which determines the wavelength of the light emitted. The mechanism which ultimately causes the laser diode to fail is the formation of dislocations or gaps in the material structure. Laser devices which operate in the visible region of the spectrum have a more brittle structure than those that operate in the infra-red and in consequence produce dislocations at a faster rate.

The rate at which dislocations form during normal use is related to the temperature at which the laser diode operates. Where possible every means should be used to minimise temperature, such as working at lower voltage levels, reducing operating ambients and providing adequate heat sinking, all of which will contribute to maximise the operating life. The figures quoted for 'mean time to failure' (MTTF) reflect the differences in device structure and operating power.

#### Modulation

The modulation signal applied may be of any waveform, sinusoidal, digital or a mixture of both. It is essential, however, that its voltage does not exceed  $+7\text{V}$  or goes below  $-1\text{V}$  relative to the  $0\text{V}$  connection. If the  $500\text{mV}$  peak to peak signal is exceeded then premature failure could occur due to thermal effects.

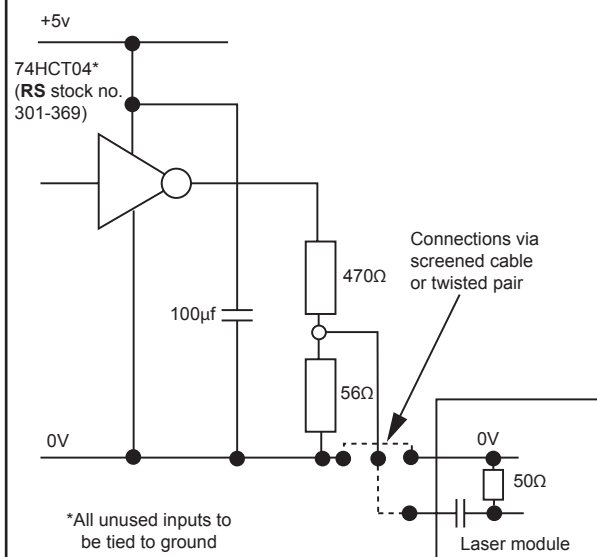
The modulation input is ac coupled.

The efficiency of modulation drops below  $100\text{Hz}$  and above  $50\text{MHz}$  due to the electronics circuit. These frequencies are approximately where the amplitude of the laser light modulation drops by  $3\text{dB}$  (0.7) of the mid-band amplitude for a constant modulation voltage. The total frequency range however extends beyond  $100\text{MHz}$ .

The impedance of the modulation input is  $50\ \Omega$ . Ideally at all frequencies a  $50\ \Omega$  co-axial cable should be used, driven from a signal source with a  $50\Omega$  output impedance. At frequencies below  $1\text{MHz}$  however, this is not always necessary.

Figure 1 shows a typical digital  $50\ \Omega$  modulation drive giving approximately  $250\text{mV}$  peak to peak input signal.

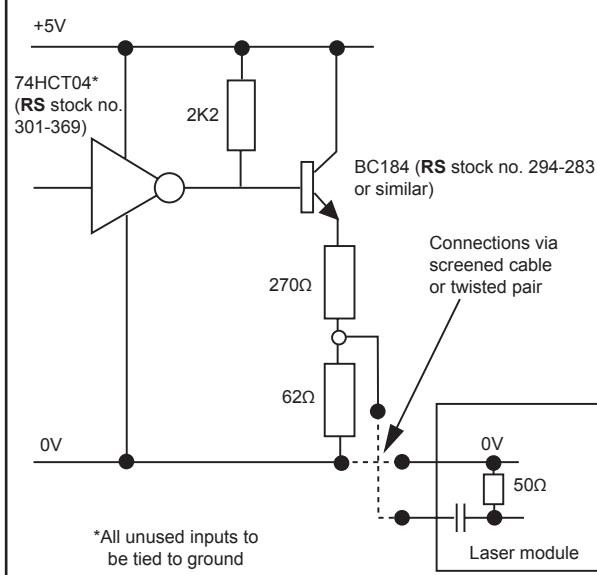
Figure 1



An alternative scheme using any TTL gate to obtain a modulation input of  $500\text{mV}$  peak to peak is shown in Figure 2.

When applying modulation to the laser module it is important to understand how the laser emission occurs.

Figure 2

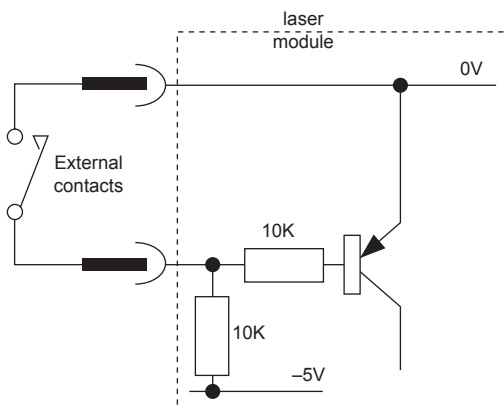


As current is applied light starts to be emitted, the intensity of which increases as the current increases. At a threshold level laser light starts to be emitted, the intensity of which increases with increasing current at a far greater rate. Modulation should be restricted to that part of the light due to laser emission (i.e. above the threshold). It is possible to modulate about 90% of the laser emission using a square wave signal and keeping within the specified input voltage limits. Within the range 0 to 500mV peak to peak, modulation is linear, above that there is a linearity error which varies from diode to diode. The modulation factor is typically  $-7.7\mu\text{W}/\text{mV}$  above the threshold. The minus sign indicates that a rise in modulation voltage produces a fall in laser intensity.

### Interlock

The interlock input is provided to allow a keyswitch or some other contacts to be used to turn the laser on or off. The 'enable' time is approximately 40mS. The interlock input must be connected to 0V to 'enable' the laser.

Figure 3 A typical schematic showing external contacts connected

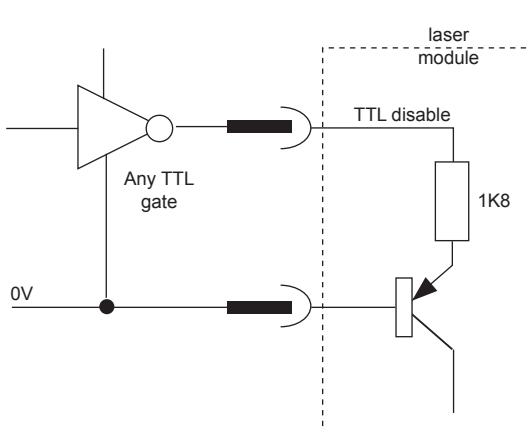


Any voltage applied to this input must not exceed +2.5V or be less than -5V.

### TTL disable

A TTL disable function is provided which can be used to turn the laser off and on. The 'enable' time for this input is the same as the interlock, approximately 40mS.

Figure 4



An input voltage above 4V will turn the laser off. When not in use, this input can be left floating or if preferred, connected to 0V.

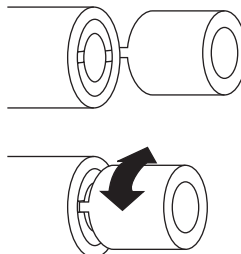
Any voltage applied to this input should not exceed +7V or be less than -3V.

### Operation data

When the laser module is switched on there is an 'enable' time of approximately 1S. This slow start limits the possibility of any spikes reaching the diode and causing catastrophic failure.

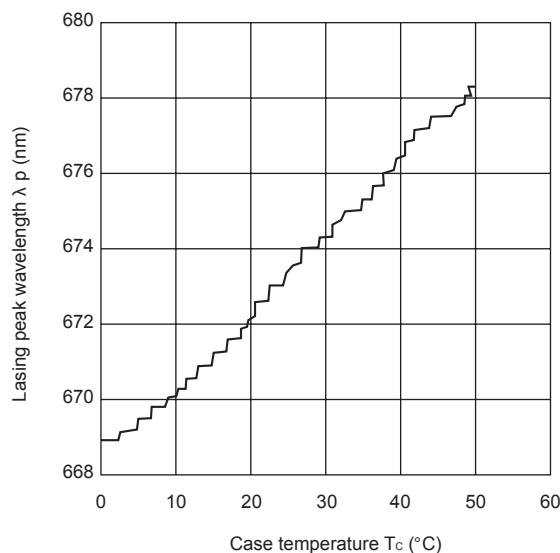
The lens will have been adjusted to give the optimum output beam. The standard collimator for instance will have been set to give a well collimated beam over a 10 metre range. If the lens needs to be adjusted, insert the tabs of the key in the lens slots so that the beam passes through the centre of the key uninterrupted. Rotate the lens with the key to produce the desired spot.

Figure 5



The wavelength of the laser output varies with temperature as shown in Figure 6.

Figure 6 Temperature dependence – Lasing spectrum



Temperature also affects the laser diode by altering the threshold current. An increase of 25°C increases the threshold current and therefore the supply current of the laser module by about 10mA. Operating at the higher current reduces the life of the diode and therefore every effort should be made to maintain the operating temperature of the laser module at the minimum practicable for the application.

### Controlling output power

The drive circuit used in these modules employs thick film surface mount technology to achieve its small size and high reliability. Incorporated within it are two potentiometers which control the intensity of the output beam. Neither of these should be adjusted as they may result in the power exceeding the limits stipulated for its safety classification, or even the failure of the laser diode.

The output power is set at the factory using a highly accurate laser power meter, the calibration of this instrument is traceable to international standards. The power set is the total light emitted through the lens. If the lens is removed, a higher power will be emitted but, due to the natural divergence of the laser diode, the power density will be lower.

Line generating optics may be fitted as an alternative lens system but these generally are less efficient than a standard collimator and have such a large divergence, that the power density when integrated over a circular aperture of 7mm diameter will be much less.

### Polarisation

The light emitted from a laser diode module is linearly polarised and has a polarisation ratio which varies with output power. The polarisation ratio also varies across the beam in relation to the intensity distribution. The table of optical characteristics shows the polarisation ratios for the different modules. For applications where a high polarisation ratio is required, a module with a higher power should be used together with an aperture placed co-axially which reduces the beam diameter.

### Beam position and pointing stability

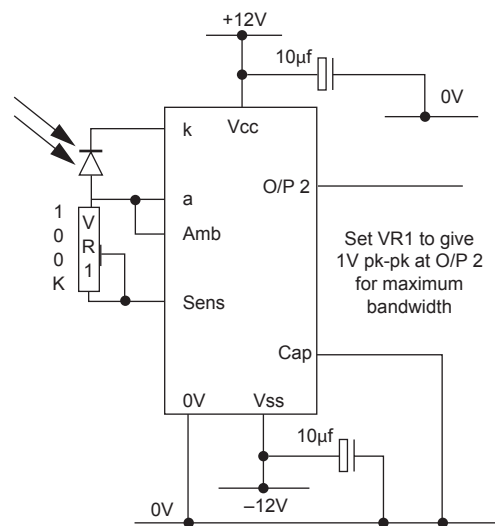
The position of the laser beam with respect to the laser housing depends on a number of factors including the position of the laser die within its mount, the concentricity of the mechanics of the housing and the eccentricity in the lens mount and focusing system. Change any one and the position of the laser spot is likely to move.

These modules have been designed to minimise such variations so that the emitted laser beam remains parallel to the case within 10m Radians.

However, variations in operating temperature can also cause mechanical movements which can alter the beam position during operation. Measurements carried out on these modules show that such movements (beam pointing stability) are less than 5μRadians per °C.

## Applications

Figure 7 RS stock no. 194-379 configured as an ambient light compensated modulated detector



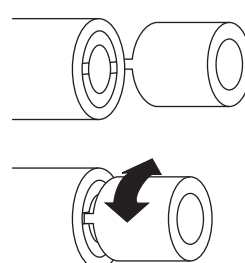
### Notes:

1. Resistor VR1 alters the sensitivity of the circuit, increasing the value increases the sensitivity.
2. RS stock no. 194-379 configured in this way rejects ambient and low frequency (50 and 100Hz) variations in light falling on the photodiode.
3. Other configurations are possible with this device including synchronous detection systems.
4. When using a small area PIN diode, light collection can be greatly improved by using a lens to focus the beam onto the surface. This lens need not be of any special quality and can even be a Fresnel lens made from moulded plastic.

### Densitometer

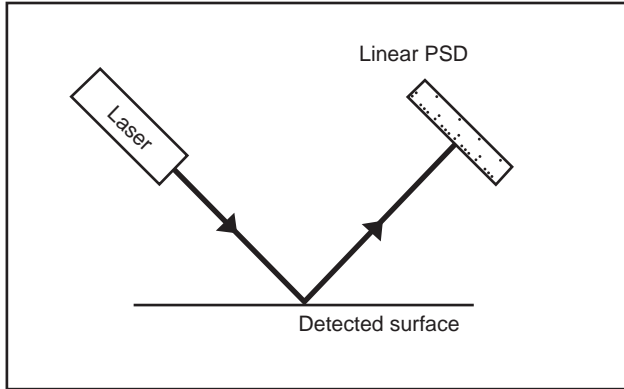
In the application shown in Figure 8, the output beam of a laser module is modulated by some frequency F MOD. This is also fed to the lock-in amplifier (or phase sensitive rectifier/demodulator) as the reference signal. The lock-in amplifier demodulates the detector output rejecting noise signals not in phase synchronism with the reference frequency. This system obviates the need for mechanical chopper wheels and their associated control electronics normally required with other types of laser. This type of system is capable of working with a beam attenuation of at least 1000.

Figure 8



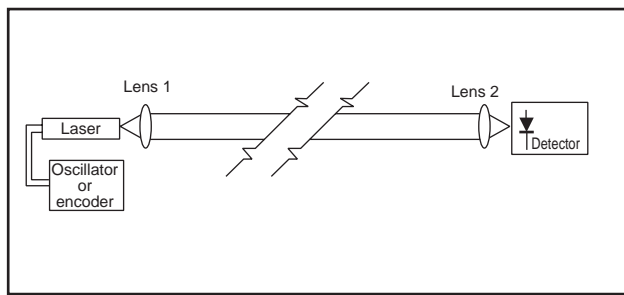
### Proximity measurement

In this application the laser projects a beam of light onto the surface or object being detected, the photometric centre of the return beam is detected by a linear position sensing detector. The laser and detector are configured so that they are effectively one unit. As the distance between laser and surface changes, the return beam travels across the linear PSD. The distance between laser and object can either be calculated by triangulation, or set specifically by varying the distance until the return beam is centred on the detector.



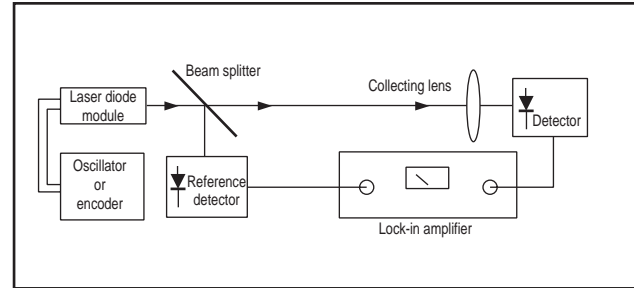
### Data transmission or beam break safety application for medium distances

In this system, Lens 1 increases the beam size so that even when air turbulence is present, some light will always fall onto the detector. Lens 2 improves capture of the beam onto the detector. A lens of 60mm focal length instead of the standard collimating lens would produce a beam of about 25mm diameter. If the beam is broken, transmission will be interrupted, it is therefore essential in data transmission applications that the equipment is sited where there is little chance of this happening. For safety and security applications beam break is used to detect the presence of people or objects passing through the beam, in this case the data being transmitted by the laser would be in the form of a coded 'word'.

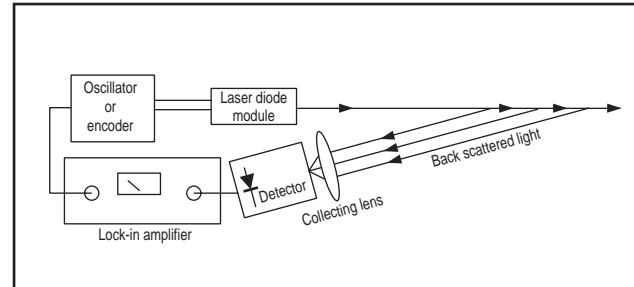


### Smoke or fog detector

This type of detector consists of a laser module which projects a beam of modulated light through the atmosphere and a detector which receives the signal. The presence of fog or smoke will attenuate the beam reducing the amplitude of the signal. The use of a reference beam eliminates any change in the output intensity of the laser.

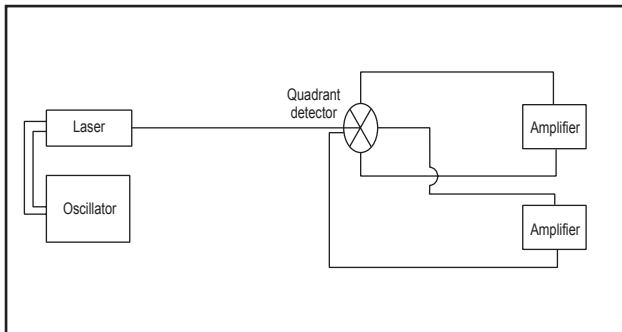


Alternatively the laser and detector can be mounted side by side so that the system responds to back scattered light. In this configuration the detector is looking for the laser signal and will only see it when there is sufficient fog or smoke present. As this system does not operate by changes in amplitude, the need for a reference beam is eliminated for most applications.

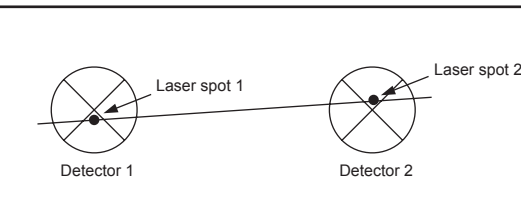


## Alignment

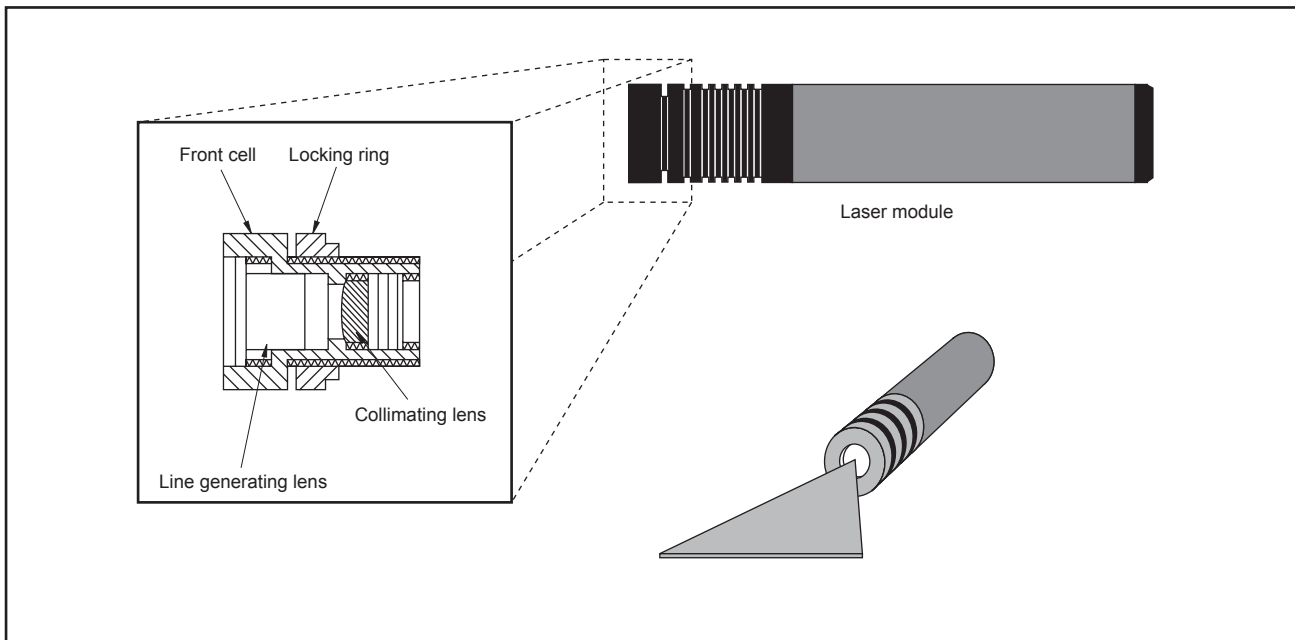
There are many applications for devices to align objects or position objects to a given point. The aligner described is ideal where there are changes in ambient light which could otherwise affect the accuracy of the result. By using the diametrically opposite quadrants of a quadrant detector, the position of a spot of light falling on the detector can be accurately identified. When the signal in each quadrant is equal, the spot is aligned with the centre of the detector. Any extraneous light falling on part of the diode would register as a shift in position but by using a modulated laser beam to produce the spot, it has no effect.



Two such systems used side by side on the item to be aligned not only give greater accuracy in the XY position, but also registers rotational errors. The spots of light from lasers 1 and 2 show not only vertical and horizontal position, but as the spot from laser 1 is below the centre of detector 1 and that from laser 2 is above the centre of detector 2, there is an element of rotation illustrated by the line joining the two spots.



## Line generating lens (RS stock no. 194-054 and 213-3629)



## Description

The line generator is a combination system consisting of a spherical lens to focus or collimate the light emitted from the laser diode and a cylindrical lens which generates the line. By rotating the front cell assembly the beam can be focussed or collimated, a locking ring is used to secure the final position. The line generator is rotated using the key supplied with the laser diode module in order to produce the best straight line.

The length of the line produced by the line generator is dependent on the focal length of the cylindrical lens while the thickness is dependent on the size of the focussed spot produced by the spherical lens. The greater the operating distance, the larger and thicker the line.

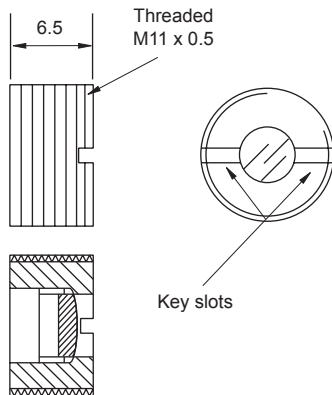
## Adjustment

Remove the line generator lens by unscrewing it from the front using the key provided. Focus the output beam to a spot at the distance required and tighten the locking ring against the main body. Replace the line generator lens so that it sits flush with the end of the front cell, then rotate it to achieve the best straight line.

## Specification

Length (extending beyond laser) \_\_\_\_\_ approx. 9mm  
 Diameter \_\_\_\_\_ 15.0mm  
 Angle of fan \_\_\_\_\_ 16° (RS stock no. 194-054)  
 106° (RS stock no. 213-3629)

## Collimating lens (RS stock no. 194-048)



The collimating lens consists of a single element of acrylic with a laser quality anti-reflection coating on both surfaces. This design is simple yet highly efficient, producing very low divergence coupled with well defined spots of light at short, medium and long range.

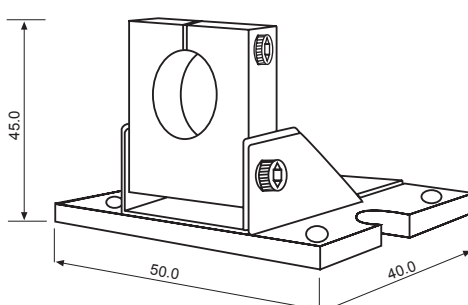
### Specification

Number of elements	-----
1	
Focal length	-----
7.9mm	
Numerical aperture	-----
0.3	
Working distance	-----
6.3mm	
Minimum clear aperture	-----
5.0mm	

### Replacing lenses

Lenses may be replaced by simply unscrewing one and screwing in another. It is necessary to use the 'key' supplied with the laser diode unit when removing or fitting the collimating lens.

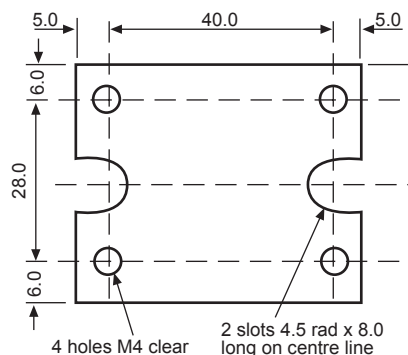
## Laser diode holder (RS stock no. 213-3641)



This laser diode holder has been designed for use with the Beta CW and TX series laser diodes combining a simple method of directing the laser beam with an additional heatsink. The laser diode unit is clamped into the holder by an M3 bolt while two M4 screws and an M4 bolt provide the means for pointing and locking the laser beam in the direction required. On the rear of the main block are two M3 threaded holes which enable heatsink fins to be attached. In the base plate there is a choice of mounting hole configurations by which the unit may be secured.

## Laser classification

### Mounting details



All laser devices produce beams of intense monochromatic light which can present potential biological hazards. These hazards depend on a number of factors including the wavelength, the power or energy of the beam and the emission duration. The eye is the most vulnerable organ as it will tend to focus light from the laser on to the retina, thereby increasing the energy density many times. If the irradiance of the laser is high enough, skin damage can also result from exposure to the beam.

RS stock nos. 111-368 and 111-352 produce infra-red radiation of a power and wavelength equivalent to a Class IIIb laser product which could cause retina burns, cataracts and even skin burns if the correct safety procedures are not followed.

Laser safety is covered by BS(EN)60825 which requires laser products to be classified according to their beam characteristics. This standard is essential reading for all laser users.

Depending on the version the laser diode modules produce continuous wave radiation with a nominal wavelength of between 635 and 785nm. While they are classified as O.E.M. devices, they conform to the wavelength and output power conditions of either Class II, Class IIIa or Class IIIb laser products.

For an O.E.M. laser diode module to comply with the full requirements of a certified laser product as described in BS(EN)60825, it may need the addition of a visible 'on' indicator, a beam shutter and a key switch. However, any product which incorporates a laser must be certified in its own right, irrespective of whether the incorporated laser is certified or not. The way in which the laser is used within the product may also alter its original classification. It is therefore the responsibility of the manufacturer of the product to ensure compliance with the relevant standards.

Class II laser products emit visible light and while they are not inherently safe, eye protection is normally afforded by the aversion responses, including the blink response. Accidental viewing is not hazardous even if optical aids\* are used, but the user should avoid staring into the beam. No skin damage will result from exposure to the beam. RS stock no. 194-010, 213-3562 and 213-3590 conforms to the wavelength and power limits of a Class II product.

**Class IIIa laser products** emit visible light and while they are not inherently safe, eye protection is normally afforded by the aversion responses, including the blink response. However, accidental viewing may be hazardous if optical aids\* are used. The user should not stare into the beam and a safety officer's approval should be obtained before using any form of optical instrument. No skin damage will result from exposure to the beam. RS stock nos. 111-346 and 194-032 conform to the wavelength and power limits of a Class IIIa product.

**Class IIIb laser products** may emit visible or invisible radiation, they are potentially hazardous if a direct beam or a specular reflection is viewed by an unprotected eye (intrabeam viewing). RS stock no. 111-352, 194-026, 194-004, 111-368, 213-3613, 213-3584 and 213-3607 conforms to the wavelength and power limits of a Class IIIb product.

The following precautions should be taken to avoid direct beam viewing and to control specular reflections:

1. The laser should only be operated in a controlled area.
2. Care should be taken to prevent unintentional specular reflections.
3. The laser beam should be terminated where possible at the end of its useful path by a material that is diffuse and of such a colour and reflectivity as to make beam positioning possible while still minimising reflection hazards.
4. Eye protection is required if there is any possibility of viewing the direct or specularly reflected beam, or of viewing a diffuse reflection not complying with the conditions of item (3).
5. The entrances to controlled areas should be posted with laser warning signs.

Any company or organisation which intends using Class IIIb lasers, or lasers which have comparable output powers and wavelengths, should appoint a safety officer whose duty is to ensure that the correct safety procedures are followed at all times.

## General

All laser diode modules are supplied with adjustable and removable optics for which the special key supplied with each unit is required. Focusing the beam to a small intense spot will not increase the risk of intrabeam viewing\*\*.

Removal of the entire optical assembly will subject the user to the full radiated power of the laser diode. However, the divergence of the laser beam from the diode surface is such that the energy density is low and will not subject the user to any hazard greater than that normally associated with its classification.

Any modification or alteration which may affect any aspect of the performance or intended function of these products will require to be examined and re-classified if necessary. The person or organisation performing any such modification or alteration is responsible for ensuring the re-classification and re-labelling of the product in accordance with BS(EN)60825 in total.

It is good practice to ensure that whenever possible, the laser beam from the laser diode module is terminated at the end of its useful path by diffusely reflecting material. It is also good practice to ensure that if the laser system is to be left switched on when not in use, the supplied plastic cap is used to terminate the beam at the laser aperture.

The laser diode modules, while being O.E.M. products, are supplied with labels showing their classification for wavelength and output power conforming to BS(EN)60825. Reproductions of these labels are shown opposite.

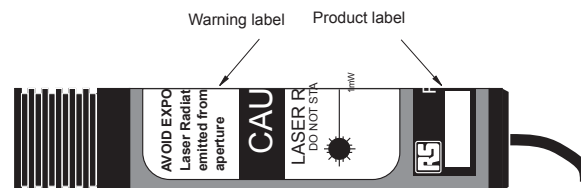
### Notes:

\* Optical aids are, spectacles, binoculars, telescopes, magnifiers and similar devices.

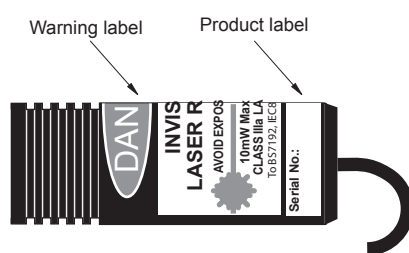
\*\*Intrabeam viewing means all viewing conditions whereby the eye is exposed to laser radiation, other than extended source viewing.

### Label positions

#### Modulated Beta TX lasers

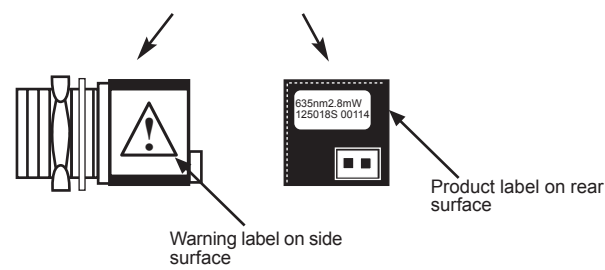


#### Continuous wave Beta CW lasers

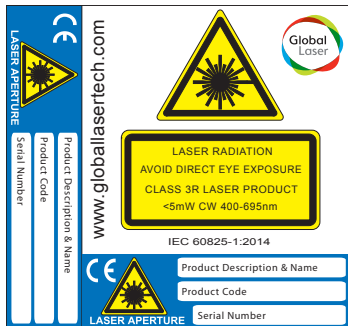


#### Continuous wave Beta Cameo lasers

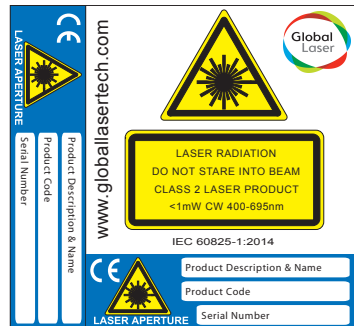
##### RS stock no. label on top surface



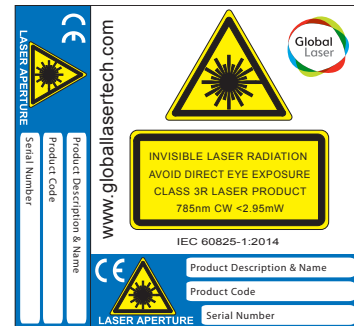
## Warning and product labels



Class 3R Label



Class 2 Label



Class 3R IR Label

The information provided in RS technical literature is believed to be accurate and reliable; however, RS Components assumes no responsibility for inaccuracies or omissions, or for the use of this information, and all use of such information shall be entirely at the user's own risk. No responsibility is assumed by RS Components for any infringements of patents or other rights of third parties which may result from its use. Specifications shown in RS Components technical literature are subject to change without notice.

# **OSRAM SFH 203 P**

## Datasheet

Published by ams-OSRAM AG  
Tobelbader Strasse 30, 8141 Premstaetten, Austria  
Phone +43 3136 500-0  
[ams-osram.com](http://ams-osram.com)  
© All rights reserved



Radial T1 3/4

# SFH 203 P

Silicon PIN Photodiode



## Applications

- Access Control & Security
- Appliances & Tools

## Features

- ESD: 2 kV acc. to ANSI/ESDA/JEDEC JS-001 (HBM, Class 2)
- Wavelength range ( $S_{10\%}$ ) 400 nm to 1100 nm
- Short switching time (typ. 5 ns)
- 5 mm LED plastic package

## Ordering Information

Type	Photocurrent <sup>1)</sup> $E_v = 1000 \text{ lx}; \text{Std. Light A}; V_R = 5 \text{ V}$ $I_P$	Photocurrent typ. $E_v = 1000 \text{ lx}; \text{Std. Light A}; V_R = 5 \text{ V}$ $I_P$	Ordering Code
SFH 203 P	$\geq 5.5 \mu\text{A}$	9.5 $\mu\text{A}$	Q62702P0942

## Maximum Ratings

$T_A = 25 \text{ }^\circ\text{C}$

Parameter	Symbol	Values
Operating Temperature	$T_{op}$	min. -40 °C
		max. 100 °C
Storage temperature	$T_{stg}$	min. -40 °C
		max. 100 °C
Reverse voltage	$V_R$	max. 20 V
Reverse voltage $t \leq 2 \text{ min}; T_A = 25 \text{ }^\circ\text{C}$	$V_R$	max. 50 V
Total power dissipation	$P_{tot}$	max. 150 mW
ESD withstand voltage acc. to ANSI/ESDA/JEDEC JS-001 (HBM, Class 2)	$V_{ESD}$	max. 2 kV

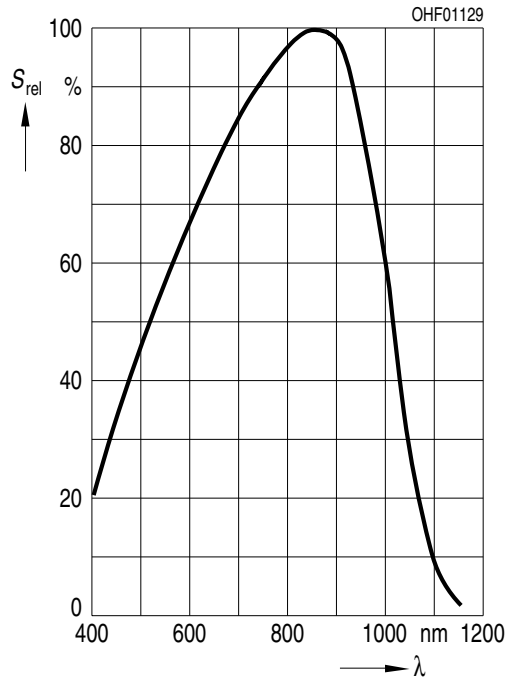
## Characteristics

$T_A = 25^\circ\text{C}$

Parameter	Symbol	Values
Wavelength of max sensitivity	$\lambda_{S\max}$	typ. 850 nm
Spectral range of sensitivity	$\lambda_{10\%}$	typ. 400 ... 1100 nm
Radiant sensitive area	A	typ. 1.00 mm <sup>2</sup>
Dimensions of active chip area	L x W	typ. 1 x 1 mm x mm
Half angle	$\varphi$	typ. 75 °
Dark current $V_R = 20\text{ V}$	$I_R$	typ. 1 nA max. 5 nA
Spectral sensitivity of the chip $\lambda = 850\text{ nm}$	$S_\lambda$	typ. 0.62 A / W
Quantum yield of the chip $\lambda = 850\text{ nm}$	$\eta$	typ. 0.90 Electrons / Photon
Open-circuit voltage $E_v = 1000\text{ lx}; \text{Std. Light A}; V_R = 0\text{ V}$	$V_o$	min. 300 mV typ. 350 mV
Short-circuit current $E_v = 1000\text{ lx}; \text{Std. Light A}; V_R = 0\text{ V}$	$I_{sc}$	typ. 9.3 $\mu\text{A}$
Rise time $V_R = 20\text{ V}; R_L = 50\text{ }\Omega; \lambda = 850\text{ nm}$	$t_r$	typ. 0.005 $\mu\text{s}$
Fall time $V_R = 20\text{ V}; R_L = 50\text{ }\Omega; \lambda = 850\text{ nm}$	$t_f$	typ. 0.005 $\mu\text{s}$
Forward voltage $I_F = 100\text{ mA}; E = 0$	$V_F$	typ. 1.3 V
Capacitance $V_R = 0\text{ V}; f = 1\text{ MHz}; E = 0$	$C_0$	typ. 11 pF
Temperature coefficient of voltage	$TC_V$	typ. -2.6 mV / K
Temperature coefficient of short-circuit current Std. Light A	$TC_I$	typ. 0.18 % / K
Noise equivalent power $V_R = 20\text{ V}; \lambda = 850\text{ nm}$	NEP	typ. 0.029 pW / Hz <sup>1/2</sup>
Detection limit $V_R = 20\text{ V}; \lambda = 850\text{ nm}$	$D^*$	typ. 3.5e12 cm x Hz <sup>1/2</sup> / W

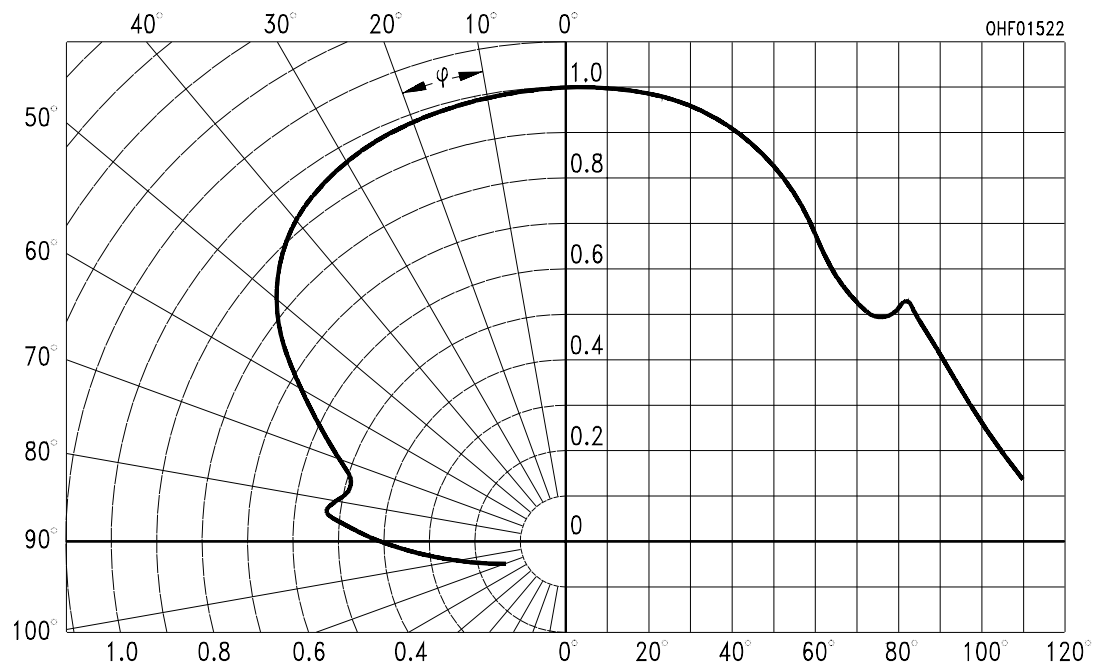
## Relative Spectral Sensitivity <sup>2), 3)</sup>

$$S_{\text{rel}} = f(\lambda)$$



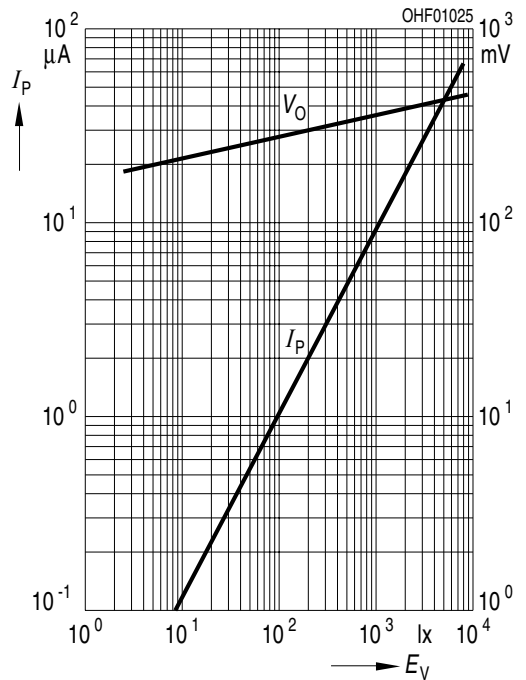
## Directional Characteristics <sup>2), 3)</sup>

$$S_{\text{rel}} = f(\phi)$$

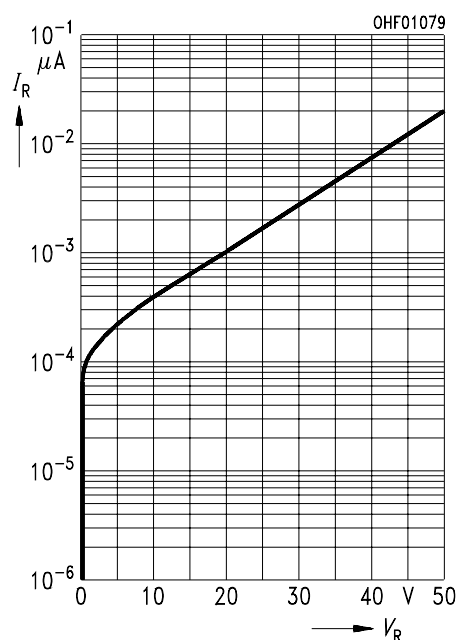


**Photocurrent/Open-Circuit Voltage** <sup>2), 3)</sup> **Dark Current** <sup>2), 3)</sup>

$$I_P (V_R = 5 \text{ V}) / V_O = f(E_v)$$

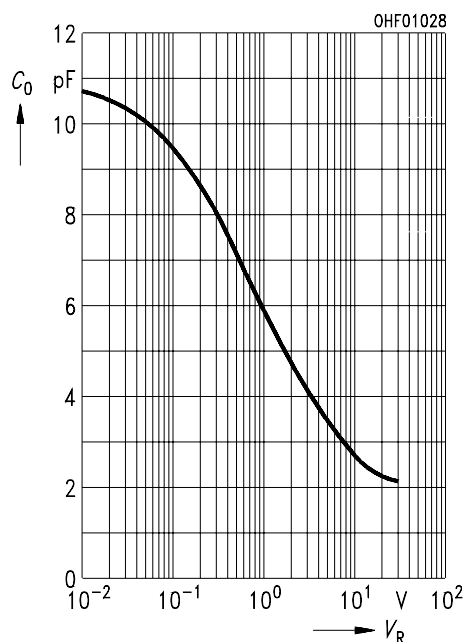


$$I_R = f(V_R); E = 0$$



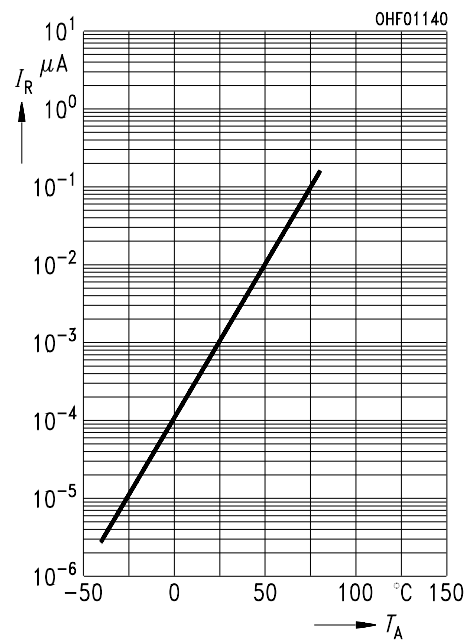
**Capacitance** <sup>2), 3)</sup>

$$C = f(V_R); f = 1\text{MHz}; E = 0; T_A = 25^\circ\text{C}$$

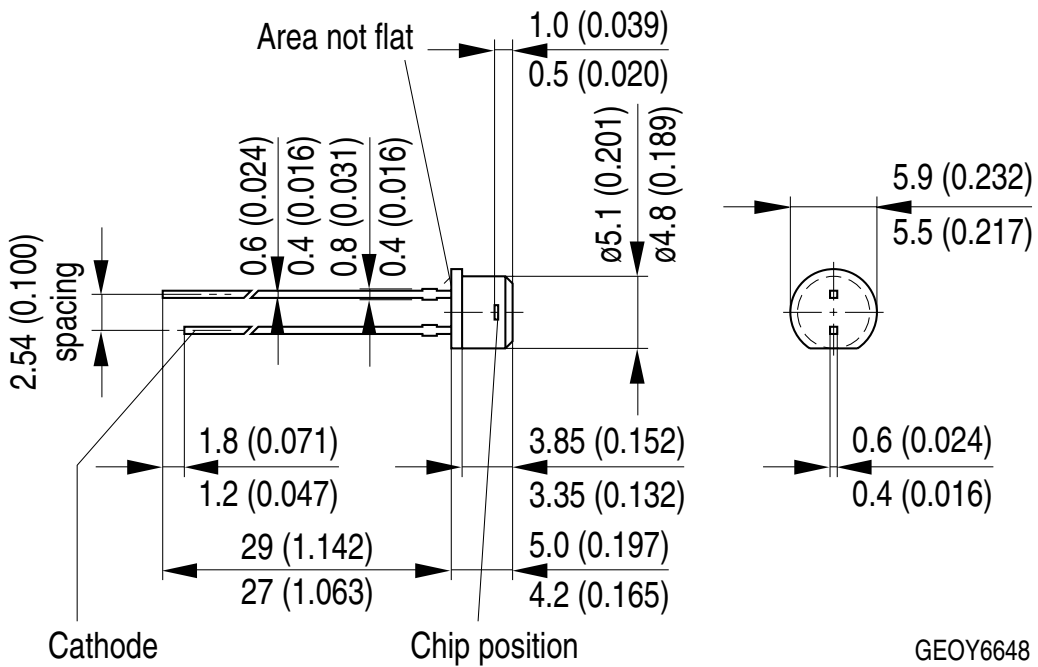


## Dark Current <sup>2)</sup>

$$I_R = f(T_A); E = 0; V_R = 20 \text{ V}$$



Dimensional Drawing <sup>4)</sup>



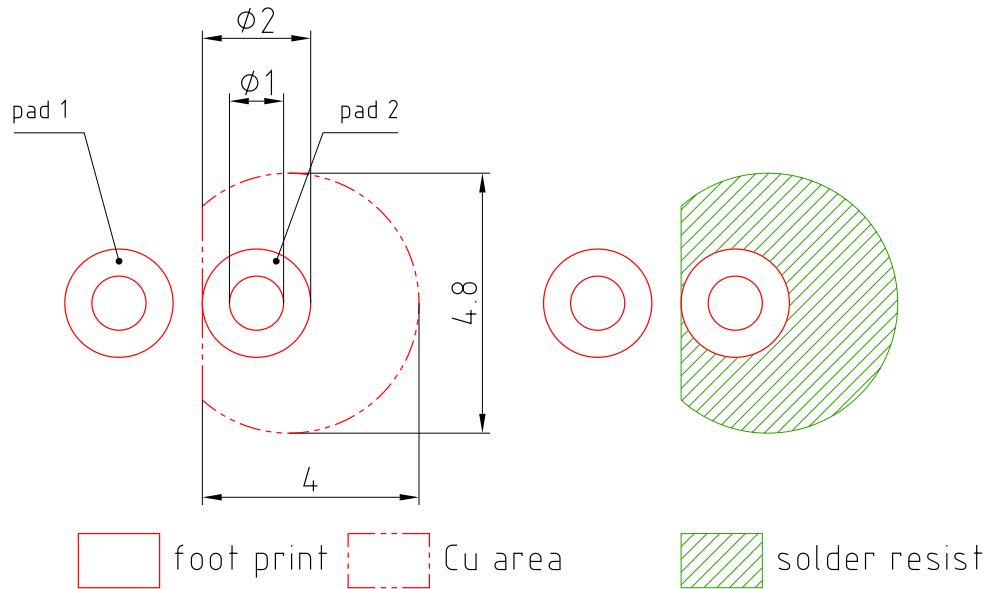
GEOY6648

Further Information:

Approximate Weight: 268.0 mg

Package marking: Cathode

**Recommended Solder Pad<sup>4)</sup>**

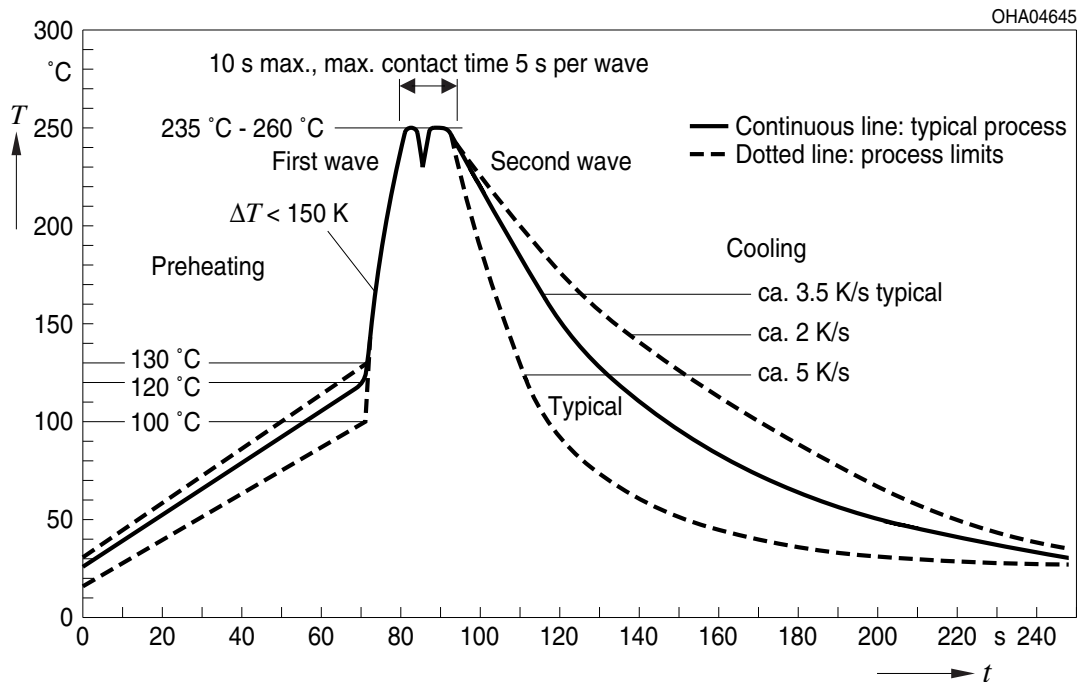


E062.3010.188-01

Pad 1: anode

## TTW Soldering

IEC-61760-1 TTW



## Notes

Subcomponents of this device contain, in addition to other substances, metal filled materials including silver. Metal filled materials can be affected by environments that contain traces of aggressive substances. Therefore, we recommend that customers minimize device exposure to aggressive substances during storage, production, and use. Devices that showed visible discoloration when tested using the described tests above did show no performance deviations within failure limits during the stated test duration. Respective failure limits are described in the IEC60810.

Packing information is available on the internet (online product catalog).

For further application related information please visit [www.osram-os.com/appnotes](http://www.osram-os.com/appnotes)

## Disclaimer

### Attention please!

The information describes the type of component and shall not be considered as assured characteristics. Terms of delivery and rights to change design reserved. Due to technical requirements components may contain dangerous substances.

For information on the types in question please contact our Sales Organization.  
If printed or downloaded, please find the latest version on our website.

### Packing

Please use the recycling operators known to you. We can also help you – get in touch with your nearest sales office. By agreement we will take packing material back, if it is sorted. You must bear the costs of transport. For packing material that is returned to us unsorted or which we are not obliged to accept, we shall have to invoice you for any costs incurred.

### Product and functional safety devices/applications or medical devices/applications

Our components are not developed, constructed or tested for the application as safety relevant component or for the application in medical devices.

Our products are not qualified at module and system level for such application.

In case buyer – or customer supplied by buyer – considers using our components in product safety devices/applications or medical devices/applications, buyer and/or customer has to inform our local sales partner immediately and we and buyer and /or customer will analyze and coordinate the customer-specific request between us and buyer and/or customer.

## Glossary

- 1) **Photocurrent:** The photocurrent values are measured (by irradiating the devices with a homogenous light source and applying a voltage to the device) with a tolerance of  $\pm 11\%$ .
- 2) **Typical Values:** Due to the special conditions of the manufacturing processes of semiconductor devices, the typical data or calculated correlations of technical parameters can only reflect statistical figures. These do not necessarily correspond to the actual parameters of each single product, which could differ from the typical data and calculated correlations or the typical characteristic line. If requested, e.g. because of technical improvements, these typ. data will be changed without any further notice.
- 3) **Testing temperature:** TA = 25°C (unless otherwise specified)
- 4) **Tolerance of Measure:** Unless otherwise noted in drawing, tolerances are specified with  $\pm 0.1$  and dimensions are specified in mm.

## Revision History

Version	Date	Change
1.4	2022-08-11	Applications New Layout



EU RoHS and China RoHS compliant product

此产品符合欧盟 RoHS 指令的要求；

按照中国的相关法规和标准，

不含有毒有害物质或元素。

**Published by ams-OSRAM AG**

Tobelbader Strasse 30, 8141 Premstaetten, Austria

Phone +43 3136 500-0

[ams-osram.com](http://ams-osram.com)

© All rights reserved

**am** **OSRAM**



# PJRC Teensy 4.1 Development Board

PRODUCT ID: 4622

## DESCRIPTION-

The Teensy 4.1, like the 4.0, also features an ARM Cortex-M7 processor at 600 MHz, with an NXP iMXRT1062 chip, the fastest microcontroller available today - ten times faster than the Teensy 3.2! The NXP iMXRT1062 is a 'cross-over' processor, which has the functionality of a microcontroller, at the speeds of a microcomputer. It's perfect for when you need tons of flash, RAM and, to crunch lots of data, or when you need two full-speed USB ports.

Teensy 4.1 comes with four times larger flash memory than the 4.0, and two new locations to optionally add *more* memory. The Teensy 4.1 has the same form factor as the Teensy 3.6 (2.4" by 0.7"), but provides a ton more I/O capability, including an 100MB Ethernet PHY, SD card socket (SDIO connected), and USB host port. Please check out the Teensy 4.0 page for common specifications and features.

### Memory

The bottom side of Teensy 4.1 has locations to solder 2 memory chips. The smaller location is meant for a PSRAM SOIC-8 chip. The larger location is intended for QSPI flash memory.

### USB Host

Teensy 4.1's USB Host port allows you to connect USB devices, like keyboards and MIDI musical instruments. A 5 pin header and a USB Host cable are needed to be able to plug in a USB device. You can also use one of these cables to connect to the USB pins

## Power Consumption & Management

When running at 600 MHz, the Teensy 4.1 consumes approximately 100mA current and provides support for dynamic clock scaling. Unlike traditional microcontrollers, where changing the clock speed causes wrong baud rates and other issues, Teensy 4.1 hardware and Teensyduino's software support for Arduino timing functions are designed to allow dynamically speed changes. Serial baud rates, audio streaming sample rates, and Arduino functions like `delay()` and `millis()`, and Teensyduino's extensions like `IntervalTimer` and `elapsedMillis`, continue to work properly while the CPU changes speed. Teensy 4.1 also provides a power shut off feature. By connecting a pushbutton to the On/Off pin, the 3.3V power supply can be completely disabled by holding the button for five seconds, and turned back on by a brief button press. If a coin cell is connected to VBAT, Teensy 4.1's RTC also continues to keep track of date & time while the power is off. Teensy 4.1 also can also be overclocked, well beyond 600MHz!

The ARM Cortex-M7 brings many powerful CPU features to a true real-time microcontroller platform. The Cortex-M7 is a dual-issue superscaler processor, meaning the M7 can execute two instructions per clock cycle, at 600MHz! Of course, executing two simultaneously depends upon the compiler ordering instructions and registers. Initial benchmarks have shown C++ code compiled by Arduino tends to achieve two instructions about 40% to 50% of the time while performing numerically intensive work using integers and pointers. The Cortex-M7 is the first ARM microcontroller to use branch prediction. On M4, loops and other code which much branch take three clock cycles. With M7, after a loop has executed a few times, the branch prediction removes that overhead, allowing the branch instruction to run in only a single clock cycle.

Tightly Coupled Memory is a special feature which allows Cortex-M7 fast single cycle access to memory using a pair of 64 bit wide buses. The ITCM bus provides a 64 bit path to fetch instructions. The DTCM bus is actually a pair of 32 bit paths, allowing M7 to perform up to two separate memory accesses in the same cycle. These extremely high speed buses are separate from M7's main AXI bus, which accesses other memory and peripherals. 512 of memory can be accessed as tightly coupled memory. Teensyduino automatically allocates your Arduino sketch code into ITCM and all non-malloc memory use to the fast DTCM, unless you add extra keywords to override the optimized default. Memory not accessed on the tightly coupled buses is optimized for DMA access by peripherals. Because the bulk of M7's memory access is done on the two tightly coupled buses, powerful DMA-based peripherals have excellent access to the non-TCM memory for highly efficient I/O.

Teensy 4.1's Cortex-M7 processor includes a floating point unit (FPU) which supports both 64 bit "double" and 32 bit "float". With M4's FPU on Teensy 3.5 & 3.6, and also Atmel SAMD51 chips, only 32 bit float is hardware accelerated. Any use of double, double functions like `log()`, `sin()`, `cos()` means slow software implemented math. Teensy 4.1 executes all of these with FPU hardware.

Information, documentation, and specs are on the Teensy site. Please check it out for more details!

Note: Teensy 4.1 does not include headers, a USB cable, or hub.

## TECHNICAL DETAILS–

### Technical Specifications

- ARM Cortex-M7 at 600 MHz
- 1024K RAM (512K is tightly coupled)
- 2048K Flash (64K reserved for recovery & EEPROM emulation)
- 2 USB ports, both 480 MBit/sec
- 3 CAN Bus (1 with CAN FD)
- 2 I2S Digital Audio
- 1 S/PDIF Digital Audio
- 1 SDIO (4 bit) native SD
- 3 SPI, all with 16 word FIFO
- 3 I2C, all with 4 byte FIFO
- 7 Serial, all with 4 byte FIFO
- 32 general purpose DMA channels
- 31 PWM pins
- 40 digital pins, all interrupt capable
- 14 analog pins, 2 ADCs on chip
- Cryptographic Acceleration
- Random Number Generator
- RTC for date/time
- Programmable FlexIO
- Pixel Processing Pipeline
- Peripheral cross triggering
- Power On/Off management

<https://www.adafruit.com/product/4622/5-27-20>

## FEATURES

- Unity-Gain Stable
- 45MHz Gain-Bandwidth
- 400V/ $\mu$ s Slew Rate
- 7V/mV DC Gain:  $R_L = 500\Omega$
- Maximum Input Offset Voltage: 2mV
- $\pm 12V$  Minimum Output Swing into  $500\Omega$
- Wide Supply Range:  $\pm 2.5V$  to  $\pm 15V$
- 7mA Supply Current
- 90ns Settling Time to 0.1%, 10V Step
- Drives All Capacitive Loads

## APPLICATIONS

- Wideband Amplifiers
- Buffers
- Active Filters
- Video and RF Amplification
- Cable Drivers
- Data Acquisition Systems

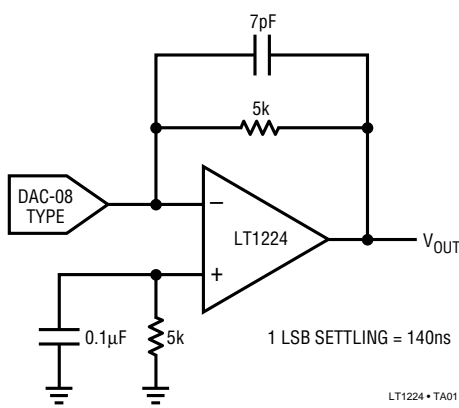
## DESCRIPTION

The LT1224 is a very high speed operational amplifier with excellent DC performance. The LT1224 features reduced input offset voltage and higher DC gain than devices with comparable bandwidth and slew rate. The circuit is a single gain stage with outstanding settling characteristics. The fast settling time makes the circuit an ideal choice for data acquisition systems. The output is capable of driving a  $500\Omega$  load to  $\pm 12V$  with  $\pm 15V$  supplies and a  $150\Omega$  load to  $\pm 3V$  on  $\pm 5V$  supplies. The circuit is also capable of driving large capacitive loads which makes it useful in buffer or cable driver applications.

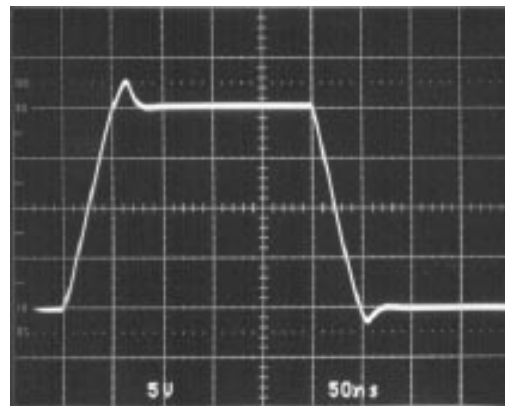
The LT1224 is a member of a family of fast, high performance amplifiers that employ Linear Technology Corporation's advanced bipolar complementary processing.

## TYPICAL APPLICATION

DAC Current-to-Voltage Converter



Inverter Pulse Response



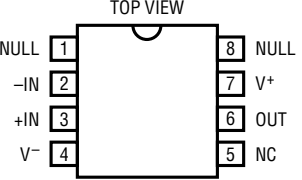
LT1224 • TA02

**ABSOLUTE MAXIMUM RATINGS**

Total Supply Voltage ( $V^+$ to $V^-$ ) .....	36V
Differential Input Voltage .....	$\pm 6V$
Input Voltage .....	$\pm V_S$
Output Short Circuit Duration (Note 1) .....	Indefinite
Operating Temperature Range	
LT1224C .....	0°C to 70°C
Maximum Junction Temperature	
Plastic Package .....	150°C
Storage Temperature Range .....	-65°C to 150°C
Lead Temperature (Soldering, 10 sec.) .....	300°C

**PACKAGE/ORDER INFORMATION**

ORDER PART NUMBER
LT1224CN8 LT1224CS8
S8 PART MARKING
1224

  
 TOP VIEW  
 N8 PACKAGE      S8 PACKAGE  
 8-LEAD PLASTIC DIP      8-LEAD PLASTIC SOIC  
LT1224 • PO101  
 $T_{JMAX} = 150^\circ\text{C}$ ,  $\theta_{JA} = 100^\circ\text{C/W}$  (N8)  
 $T_{JMAX} = 150^\circ\text{C}$ ,  $\theta_{JA} = 150^\circ\text{C/W}$  (S8)

**ELECTRICAL CHARACTERISTICS**  $V_S = \pm 15V$ ,  $T_A = 25^\circ\text{C}$ ,  $R_L = 1k$ ,  $V_{CM} = 0V$  unless otherwise noted.

SYMBOL	PARAMETER	CONDITIONS	MIN	TYP	MAX	UNITS
$V_{OS}$	Input Offset Voltage	(Note 2)		0.5	2.0	mV
$I_{OS}$	Input Offset Current			100	400	nA
$I_B$	Input Bias Current			4	8	$\mu\text{A}$
$e_n$	Input Noise Voltage	$f = 10\text{kHz}$		22		$\text{nV}/\sqrt{\text{Hz}}$
$i_n$	Input Noise Current	$f = 10\text{kHz}$		1.5		$\text{pA}/\sqrt{\text{Hz}}$
$R_{IN}$	Input Resistance	$V_{CM} = \pm 12V$ Differential	24	40	250	$\text{M}\Omega$ $\text{k}\Omega$
$C_{IN}$	Input Capacitance			2		pF
	Input Voltage Range +		12	14		V
	Input Voltage Range -			-13	-12	V
CMRR	Common-Mode Rejection Ratio	$V_{CM} = \pm 12V$	86	100		dB
PSRR	Power Supply Rejection Ratio	$V_S = \pm 5V$ to $\pm 15V$	75	84		dB
$A_{VOL}$	Large-Signal Voltage Gain	$V_{OUT} = \pm 10V$ , $R_L = 500\Omega$	3.3	7		V/mV
$V_{OUT}$	Output Swing	$R_L = 500\Omega$	$\pm 12.0$	$\pm 13.3$		V
$I_{OUT}$	Output Current	$V_{OUT} = \pm 12V$	24	40		mA
SR	Slew Rate	$A_{VCL} = -2$ , (Note 3)	250	400		$\text{V}/\mu\text{s}$
	Full Power Bandwidth	10V Peak, (Note 4)		6.4		MHz
GBW	Gain-Bandwidth	$f = 1\text{MHz}$		45		MHz
$t_r, t_f$	Rise Time, Fall Time	$A_{VCL} = 1$ , 10% to 90%, 0.1V		5		ns
	Overshoot	$A_{VCL} = 1$ , 0.1V		30		%
	Propagation Delay	50% $V_{IN}$ to 50% $V_{OUT}$		5		ns
$t_s$	Settling Time	10V Step, 0.1%		90		ns
	Differential Gain	$f = 3.58\text{MHz}$ , $R_L = 150\Omega$		1		%
	Differential Phase	$f = 3.58\text{MHz}$ , $R_L = 150\Omega$		2.4		Deg
$R_0$	Output Resistance	$A_{VCL} = 1$ , $f = 1\text{MHz}$		2.5		$\Omega$
$I_S$	Supply Current			7	9	mA

**ELECTRICAL CHARACTERISTICS**  $V_S = \pm 5V$ ,  $T_A = 25^\circ C$ ,  $R_L = 1k$ ,  $V_{CM} = 0V$  unless otherwise noted.

SYMBOL	PARAMETER	CONDITIONS	MIN	TYP	MAX	UNITS
$V_{OS}$	Input Offset Voltage	(Note 2)		1	4	mV
$I_{OS}$	Input Offset Current		100	400		nA
$I_B$	Input Bias Current		4	8		$\mu A$
	Input Voltage Range <sup>+</sup>		2.5	4		V
	Input Voltage Range <sup>-</sup>			-3	-2.5	V
CMRR	Common-Mode Rejection Ratio	$V_{CM} = \pm 2.5V$	86	98		dB
$A_{VOL}$	Large-Signal Voltage Gain	$V_{OUT} = \pm 2.5V$ , $R_L = 500\Omega$ $V_{OUT} = \pm 2.5V$ , $R_L = 150\Omega$	2.5	7		V/mV
$V_{OUT}$	Output Swing	$R_L = 500\Omega$ $R_L = 150\Omega$	$\pm 3.0$ $\pm 3.0$	$\pm 3.7$ $\pm 3.3$		V
$I_{OUT}$	Output Current	$V_{OUT} = \pm 3V$	20	40		mA
SR	Slew Rate	$A_{VCL} = -2$ , (Note 3)		250		V/ $\mu s$
	Full Power Bandwidth	3V Peak, (Note 4)		13.3		MHz
GBW	Gain-Bandwidth	$f = 1MHz$		34		MHz
$t_r$ , $t_f$	Rise Time, Fall Time	$A_{VCL} = 1$ , 10% to 90%, 0.1V	7			ns
	Overshoot	$A_{VCL} = 1$ , 0.1V		20		%
	Propagation Delay	50% $V_{IN}$ to 50% $V_{OUT}$		7		ns
$t_s$	Settling Time	-2.5V to 2.5V, 0.1%		90		ns
$I_S$	Supply Current			7	9	mA

**ELECTRICAL CHARACTERISTICS**  $0^\circ C \leq T_A \leq 70^\circ C$ ,  $R_L = 1k$ ,  $V_{CM} = 0V$  unless otherwise noted.

SYMBOL	PARAMETER	CONDITIONS	MIN	TYP	MAX	UNITS
$V_{OS}$	Input Offset Voltage	$V_S = \pm 15V$ , (Note 2) $V_S = \pm 5V$ , (Note 2)	1 2	4 5		mV
	Input $V_{OS}$ Drift			25		$\mu V/^\circ C$
$I_{OS}$	Input Offset Current	$V_S = \pm 15V$ and $V_S = \pm 5V$	100	600		nA
$I_B$	Input Bias Current	$V_S = \pm 15V$ and $V_S = \pm 5V$	4	9		$\mu A$
CMRR	Common-Mode Rejection Ratio	$V_S = \pm 15V$ , $V_{CM} = \pm 12V$ and $V_S = \pm 5V$ , $V_{CM} = \pm 2.5V$	83	98		dB
PSRR	Power Supply Rejection Ratio	$V_S = \pm 5V$ to $\pm 15V$	73	84		dB
$A_{VOL}$	Large-Signal Voltage Gain	$V_S = \pm 15V$ , $V_{OUT} = \pm 10V$ , $R_L = 500\Omega$ $V_S = \pm 5V$ , $V_{OUT} = \pm 2.5V$ , $R_L = 500\Omega$	2.5 2.0	7 7		V/mV V/mV
$V_{OUT}$	Output Swing	$V_S = \pm 15V$ , $R_L = 500\Omega$ $V_S = \pm 5V$ , $R_L = 500\Omega$ or $150\Omega$	$\pm 12.0$ $\pm 3.0$	$\pm 13.3$ $\pm 3.3$		V V
$I_{OUT}$	Output Current	$V_S = \pm 15V$ , $V_{OUT} = \pm 12V$ $V_S = \pm 5V$ , $V_{OUT} = \pm 3V$	24 20	40 40		mA mA
SR	Slew Rate	$V_S = \pm 15V$ , $A_{VCL} = -2$ , (Note 3)	250	400		V/ $\mu s$
$I_S$	Supply Current	$V_S = \pm 15V$ and $V_S = \pm 5V$		7	10.5	mA

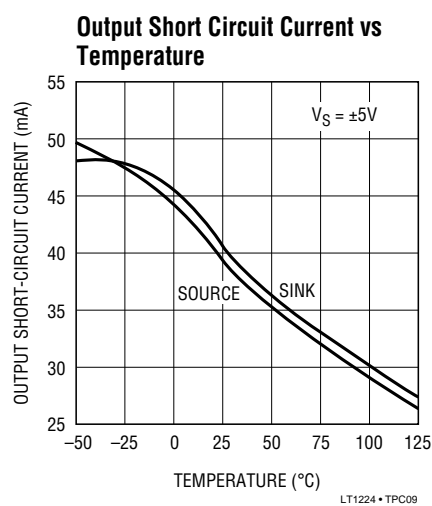
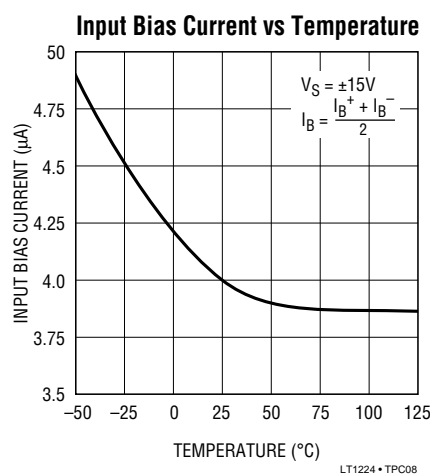
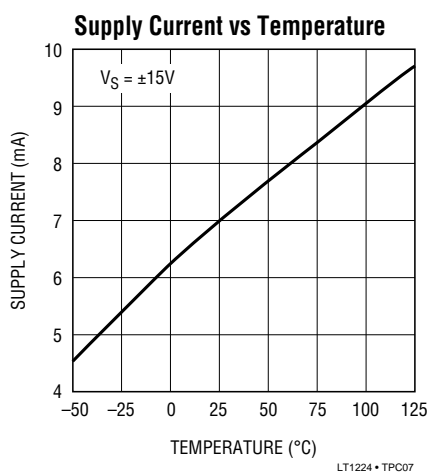
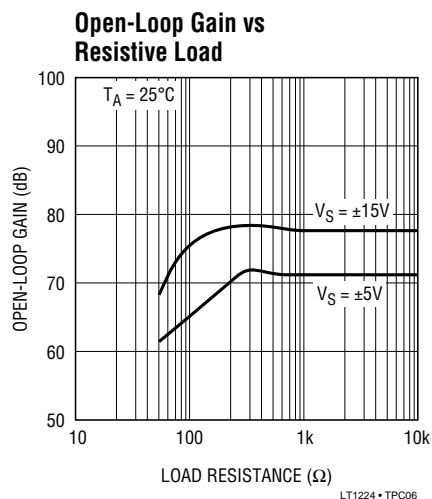
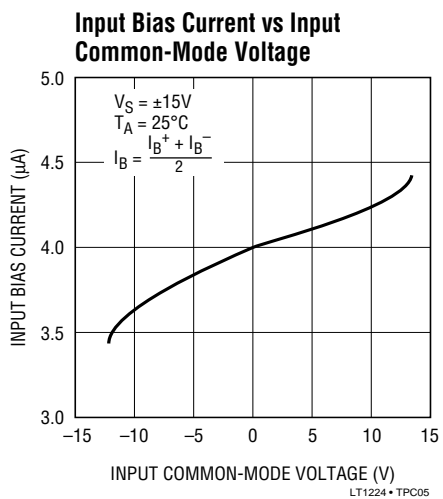
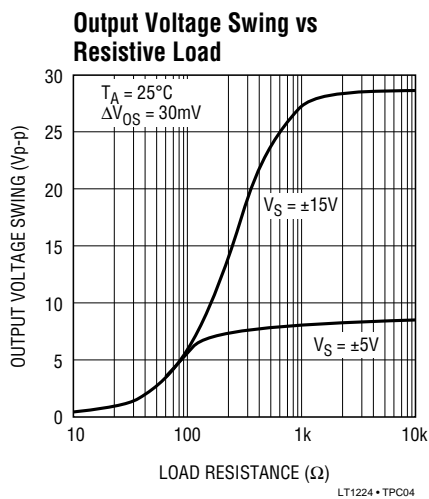
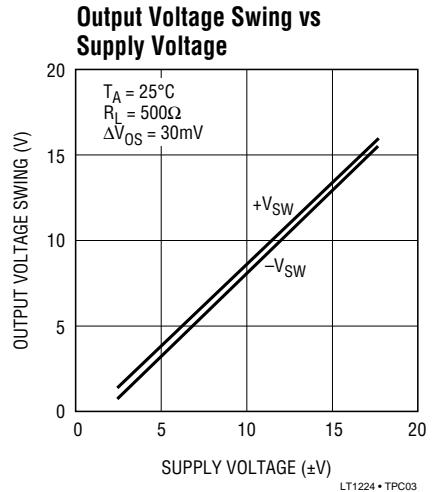
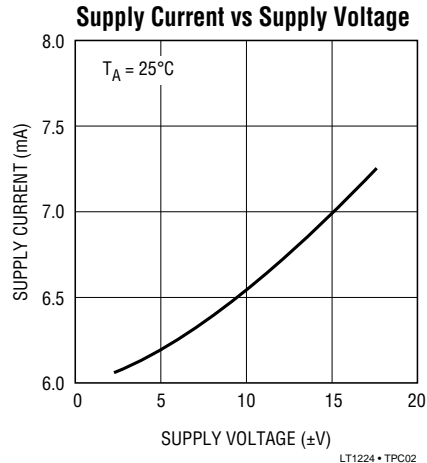
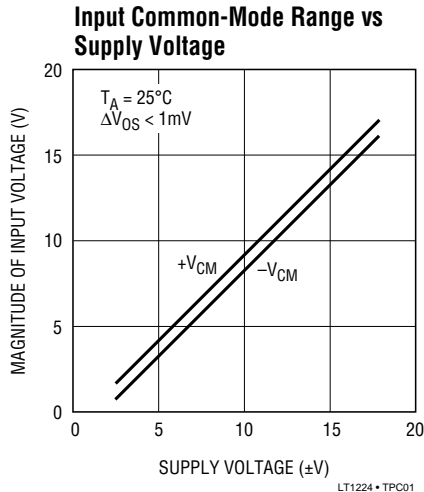
**Note 1:** A heat sink may be required to keep the junction temperature below absolute maximum when the output is shorted indefinitely.

**Note 2:** Input offset voltage is tested with automated test equipment in <1 second.

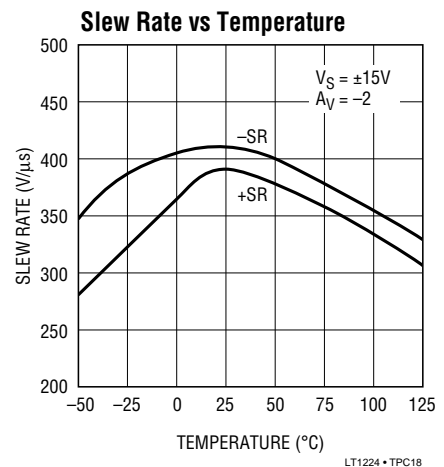
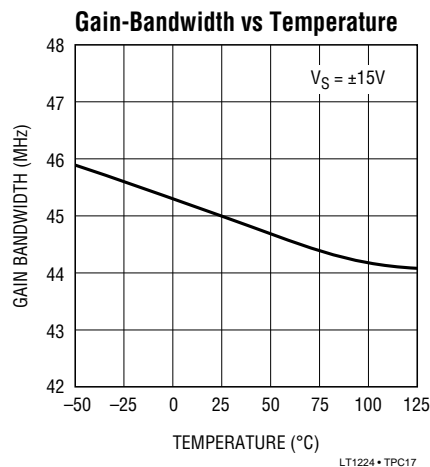
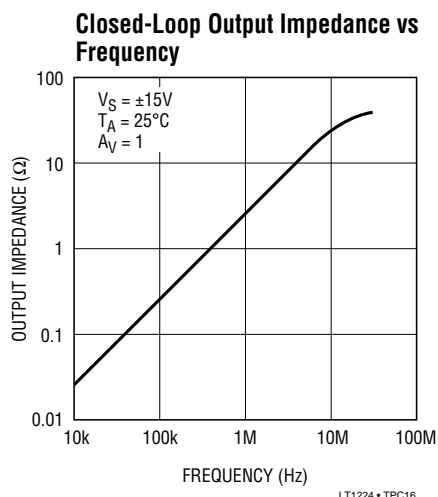
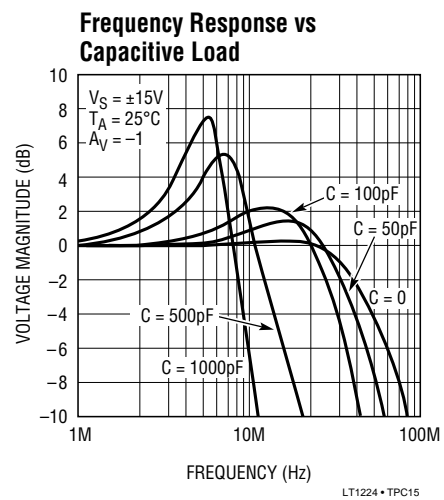
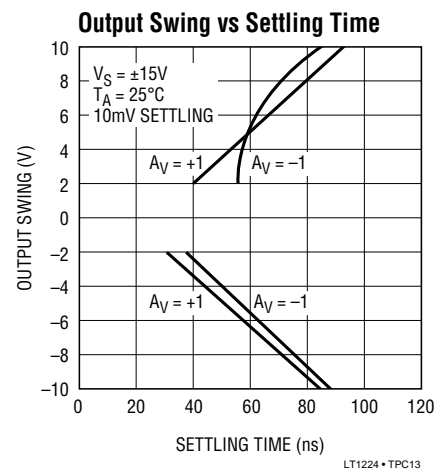
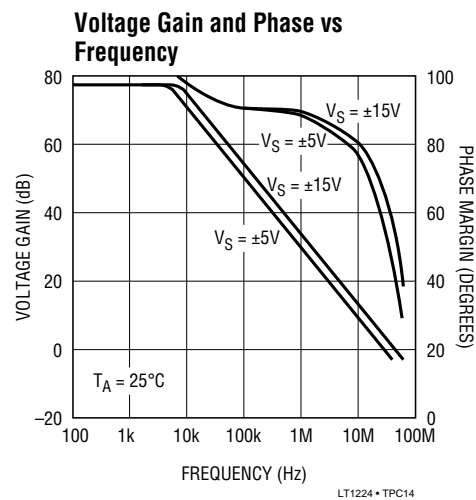
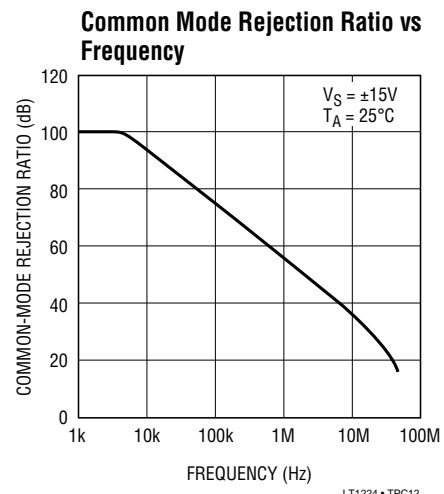
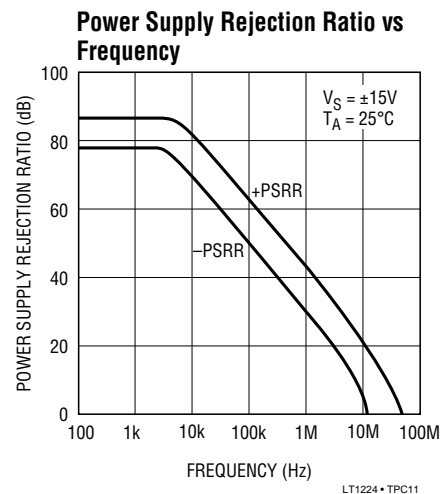
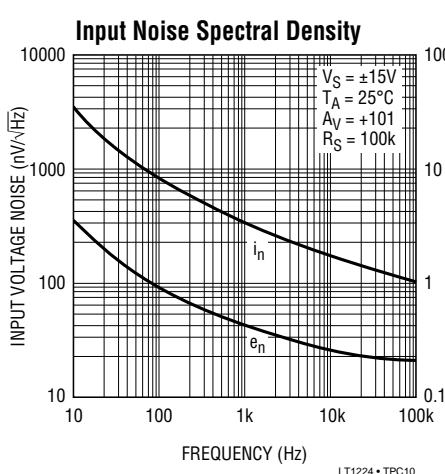
**Note 3:** Slew rate is measured in a gain of -2 between  $\pm 10V$  on the output with  $\pm 6V$  on the input for  $\pm 15V$  supplies and  $\pm 2V$  on the output with  $\pm 1.75V$  on the input for  $\pm 5V$  supplies.

**Note 4:** Full power bandwidth is calculated from the slew rate measurement:  $FPBW = SR/2\pi V_p$ .

## TYPICAL PERFORMANCE CHARACTERISTICS

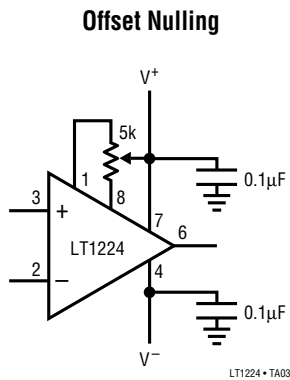


## TYPICAL PERFORMANCE CHARACTERISTICS



## APPLICATIONS INFORMATION

The LT1224 may be inserted directly into HA2541, HA2544, AD847, EL2020 and LM6361 applications, provided that the nulling circuitry is removed. The suggested nulling circuit for the LT1224 is shown below.



### Layout and Passive Components

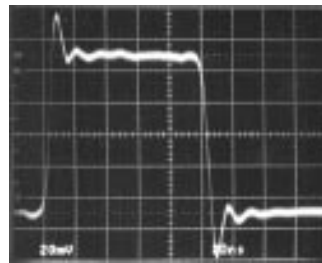
As with any high speed operational amplifier, care must be taken in board layout in order to obtain maximum performance. Key layout issues include: use of a ground plane, minimization of stray capacitance at the input pins, short lead lengths, RF-quality bypass capacitors located close to the device (typically  $0.01\mu F$  to  $0.1\mu F$ ), and use of low ESR bypass capacitors for high drive current applications (typically  $1\mu F$  to  $10\mu F$  tantalum). Sockets should be avoided when maximum frequency performance is required, although low profile sockets can provide reasonable performance up to 50MHz. For more details see Design Note 50. Feedback resistor values greater than 5k are not recommended because a pole is formed with the input capacitance which can cause peaking. If feedback resistors greater than 5k are used, a parallel capacitor of 5pF to 10pF should be used to cancel the input pole and optimize dynamic performance.

### Transient Response

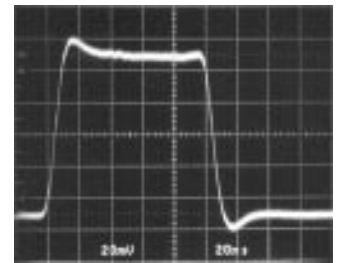
The LT1224 gain bandwidth is 45MHz when measured at  $f = 1\text{MHz}$ . The actual frequency response in unity-gain is considerably higher than 45MHz due to peaking caused by a second pole beyond the unity-gain crossover. This is reflected in the  $50^\circ$  phase margin and shows up as

overshoot in the unity-gain small-signal transient response. Higher noise gain configurations exhibit less overshoot as seen in the inverting gain of one response.

**Small Signal,  $A_V = 1$**



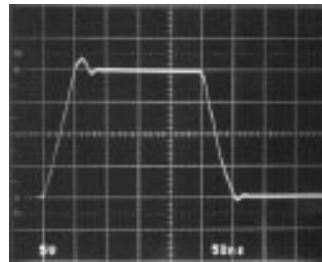
**Small Signal,  $A_V = -1$**



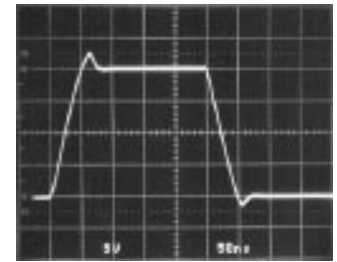
LT1224 + TA04

The large-signal responses in both inverting and non-inverting gain show symmetrical slewing characteristics. Normally the noninverting response has a much faster rising edge than falling edge due to the rapid change in input common-mode voltage which affects the tail current of the input differential pair. Slew enhancement circuitry has been added to the LT1224 so that the noninverting slew rate response is balanced.

**Large Signal,  $A_V = 1$**



**Large Signal,  $A_V = -1$**



LT1224 + TA06

### Input Considerations

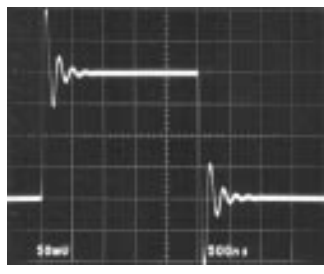
Resistors in series with the inputs are recommended for the LT1224 in applications where the differential input voltage exceeds  $\pm 6\text{V}$  continuously or on a transient basis. An example would be in noninverting configurations with high input slew rates or when driving heavy capacitive loads. The use of balanced source resistance at each input is recommended for applications where DC accuracy must be maximized.

## APPLICATIONS INFORMATION

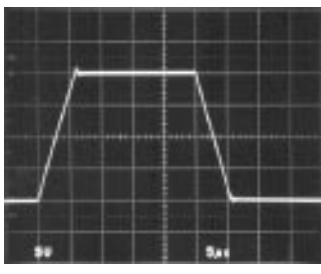
### Capacitive Loading

The LT1224 is stable with all capacitive loads. This is accomplished by sensing the load induced output pole and adding compensation at the amplifier gain node. As the capacitive load increases, both the bandwidth and phase margin decrease so there will be peaking in the frequency domain and in the transient response. The photo of the small-signal response with 1000pF load shows 50% peaking. The large-signal response with a 10,000pF load shows the output slew rate being limited by the short-circuit current.

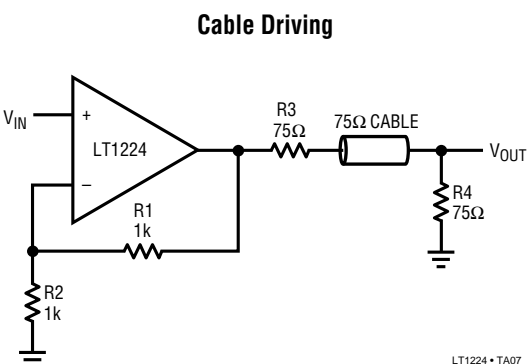
$A_V = -1, C_L = 1000\text{pF}$



$A_V = 1, C_L = 10,000\text{pF}$



The LT1224 can drive coaxial cable directly, but for best pulse fidelity the cable should be doubly terminated with a resistor in series with the output.



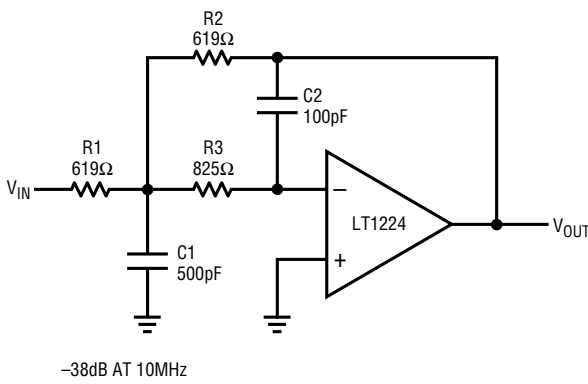
LT1224 • TA07

### DAC Current-to-Voltage Converter

The wide bandwidth, high slew rate and fast settling time of the LT1224 make it well-suited for current-to-voltage conversion after current output D/A converters. A typical application is shown on the first page of this data sheet with a DAC-08 type converter with a full-scale output of 2mA. A compensation capacitor is used across the feedback resistor to null the pole at the inverting input caused by the DAC output capacitance. The combination of the LT1224 and DAC settles to 40mV in 140ns for both a 0V to 10V step and for a 10V to 0V step.

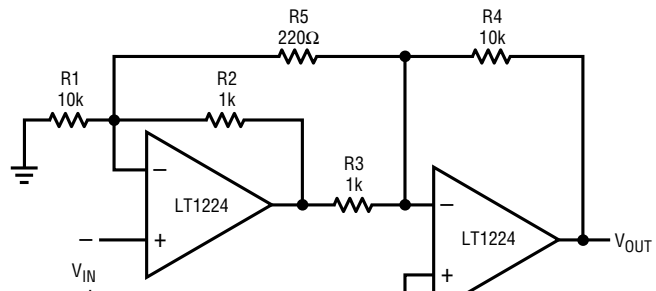
## TYPICAL APPLICATIONS

### 1MHz, 2nd Order Butterworth Filter



LT1224 • TA08

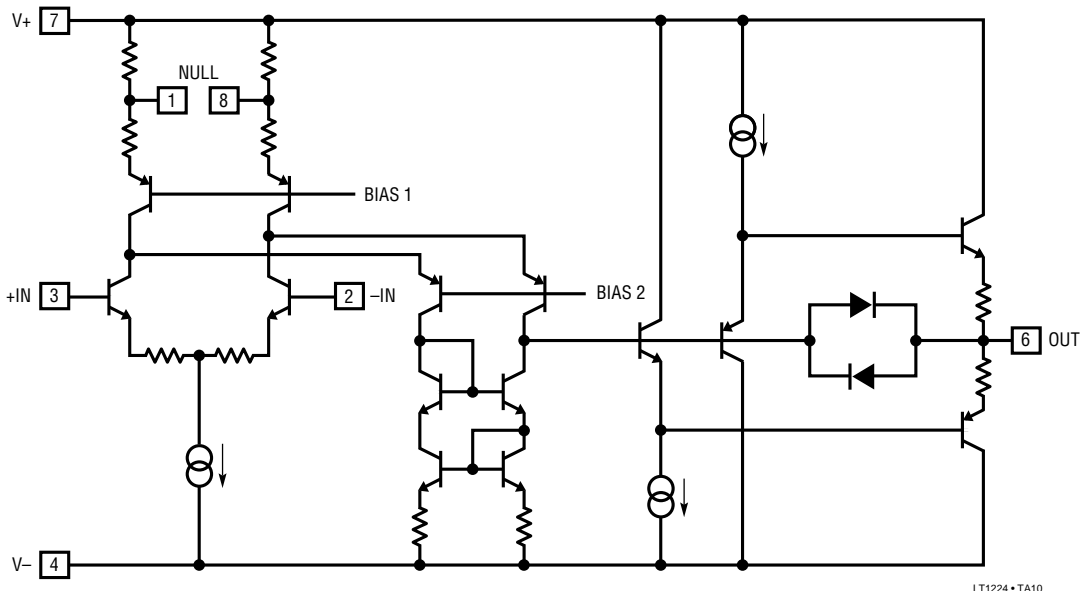
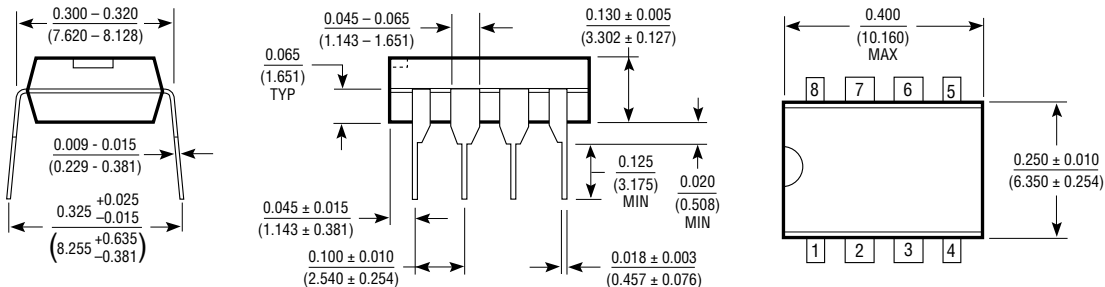
### Two Op Amp Instrumentation Amplifier



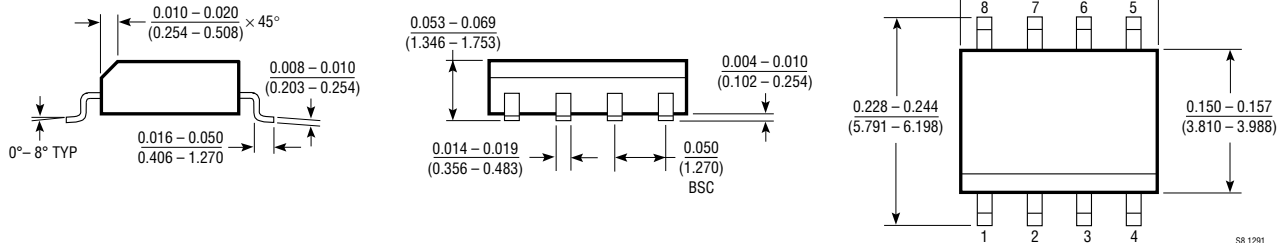
$$A_V = \frac{R_4}{R_3} \left[ 1 + \frac{1}{2} \left( \frac{R_2}{R_1} + \frac{R_3}{R_4} \right) + \frac{R_2 + R_3}{R_5} \right] = 102$$

TRIM R5 FOR GAIN  
TRIM R1 FOR COMMON-MODE REJECTION  
BW = 430kHz

LT1224 • TA09

**SIMPLIFIED SCHEMATIC****PACKAGE DESCRIPTION** Dimensions in inches (millimeters) unless otherwise noted.**N8 Package  
8-Lead Plastic DIP**

N8 1291

**S8 Package  
8-Lead Plastic SOIC**

S8 1291

# DATASHEET



## NanoStation® M NanoStation® locoM

Indoor/Outdoor airMAX® CPE

Models: NSM2, NSM3, NSM365, NSM5, locoM2, locoM5, locoM9

Cost-Effective, High-Performance

Compact and Versatile Design

Powerful Integrated Antenna



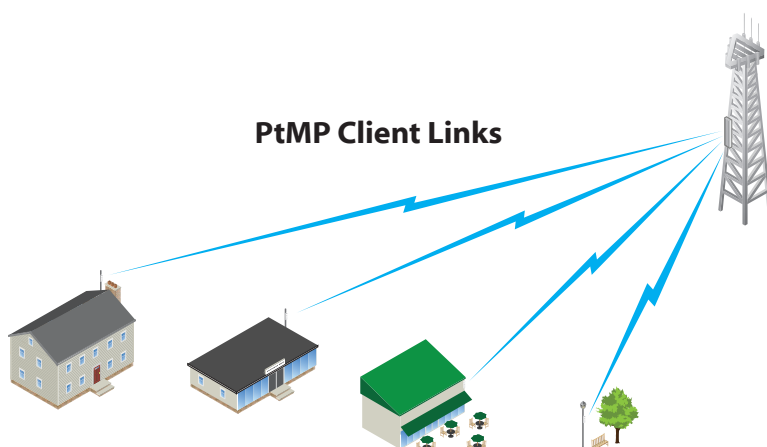
**UBIQUITI**  
N E T W O R K S

# Overview

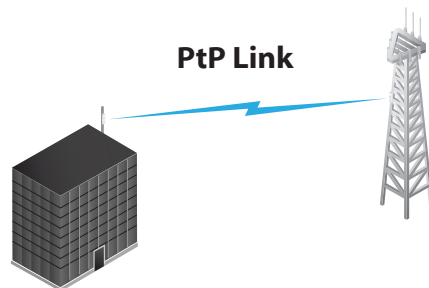
## Leading-Edge Industrial Design

Ubiquiti Networks sets the bar for the world's first low-cost and efficient broadband Customer Premises Equipment (CPE) with the original NanoStation®. The NanoStationM and NanoStationlocoM take the same concept to the future with sleek and elegant form factors, along with integrated airMAX® (MIMO TDMA protocol) technology.

The low cost, high performance, and small form factor of NanoStationM and NanoStationlocoM make them extremely versatile and economical to deploy.



NanoStationM used as powerful clients in an airMAX PtMP (Point-to-Multi-Point) network setup.



Use two NanoStationM devices to create a PtP link.

## Utilize airMAX Technology

Unlike standard Wi-Fi protocol, Ubiquiti's Time Division Multiple Access (TDMA) airMAX protocol allows each client to send and receive data using pre-designated time slots scheduled by an intelligent AP controller.

This "time slot" method eliminates hidden node collisions and maximizes airtime efficiency. It provides many magnitudes of performance improvements in latency, throughput, and scalability compared to all other outdoor systems in its class.

**Intelligent QoS** Priority is given to voice/video for seamless streaming.

**Scalability** High capacity and scalability.

**Long Distance** Capable of high-speed, carrier-class links.

**Latency** Multiple features dramatically reduce noise.

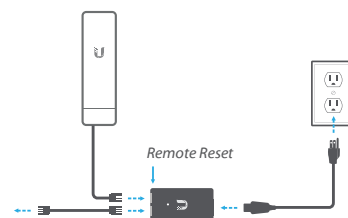
## Dual Ethernet Connectivity<sup>1</sup>

The NanoStationM provides a secondary Ethernet port with software-enabled PoE output for seamless IP video integration.



## Intelligent PoE<sup>2</sup>

The remote hardware reset circuitry of the NanoStationM allows the device to be remotely reset from the power supply location.



The NanoStationM may also be powered by the Ubiquiti Networks® EdgeSwitch™. In addition, any NanoStationM can easily become 48V, 802.3af compliant through use of the Ubiquiti® Instant 802.3af Adapter (sold separately).

<sup>1</sup> Only NanoStationM models

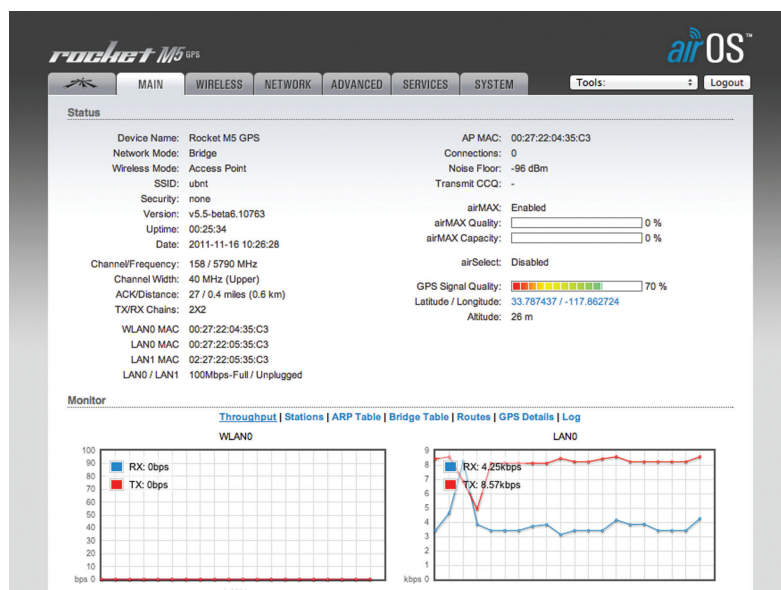
<sup>2</sup> Remote reset is an option that is sold separately as the POE-24. The NanoStationM includes a 24V PoE adapter without remote reset.

# Software



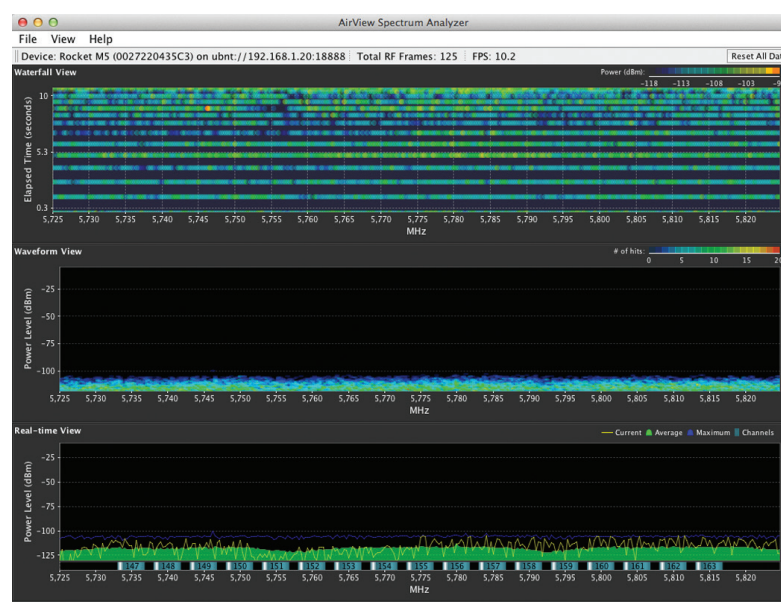
airOS® is an intuitive, versatile, highly developed Ubiquiti firmware technology. It is exceptionally intuitive and was designed to require no training to operate. Behind the user interface is a powerful firmware architecture, which enables high-performance, outdoor multi-point networking.

- Protocol Support
- Ubiquiti Channelization
- Spectral Width Adjustment
- ACK Auto-Timing
- AAP Technology
- Multi-Language Support



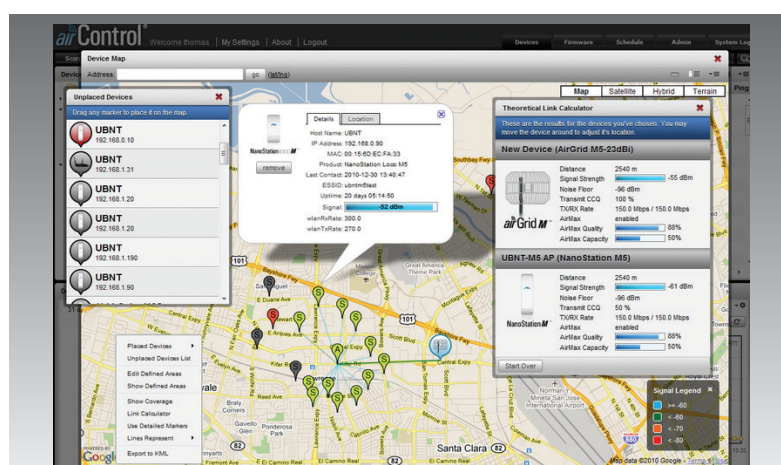
Integrated on all Ubiquiti M products, airView® provides advanced spectrum analyzer functionality: waterfall, waveform, and real-time spectral views allow operators to identify noise signatures and plan their networks to minimize noise interference.

- **Waterfall** Aggregate energy over time for each frequency.
- **Waveform** Aggregate energy collected.
- **Real-time** Energy is shown in real time as a function of frequency.
- **Recording** Automize AirView to record and report results.



airControl® is a powerful and intuitive, web-based server network management application, which allows operators to centrally manage entire networks of Ubiquiti devices.

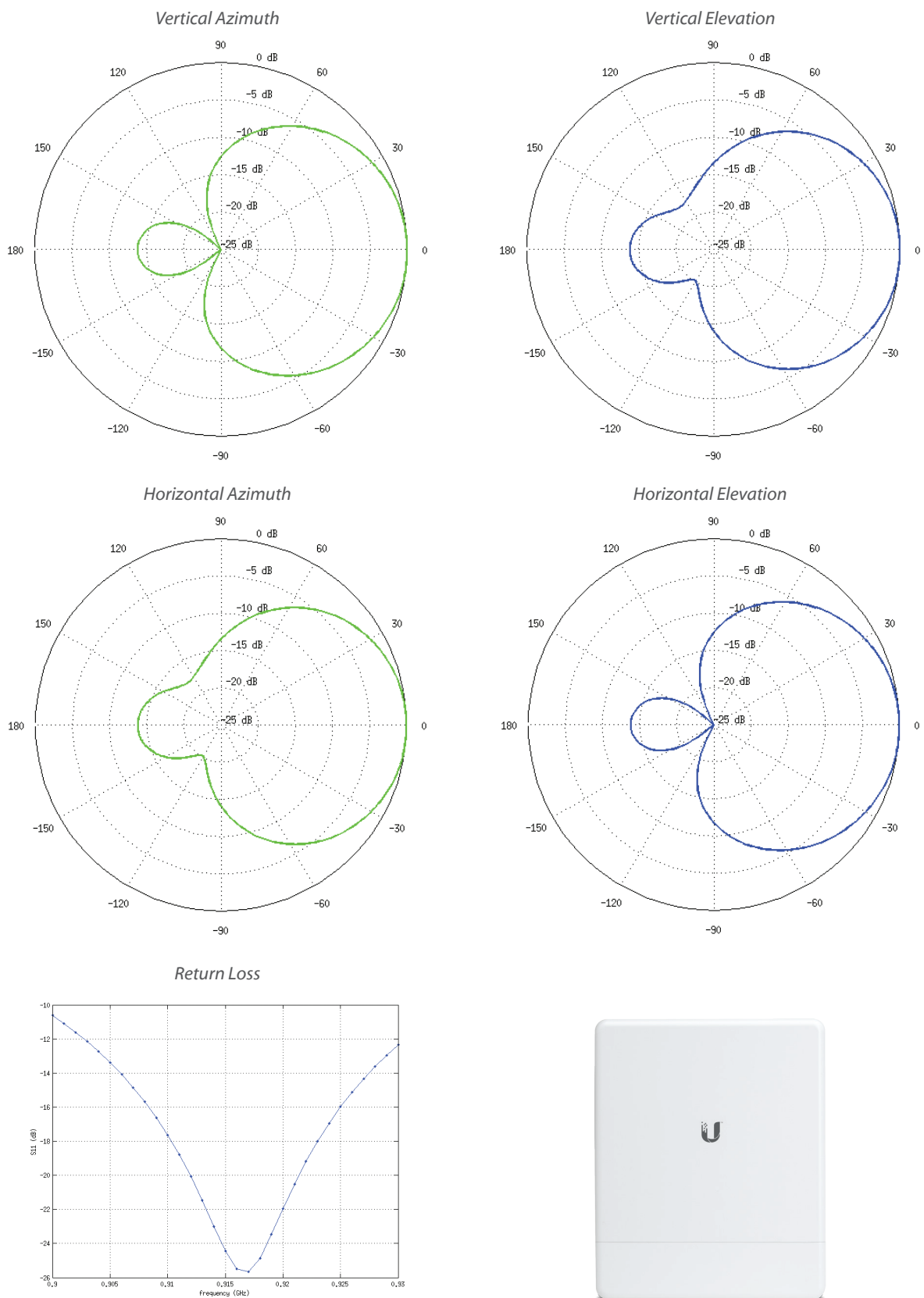
- Network Map
- Monitor Device Status
- Mass Firmware Upgrade
- Web UI Access
- Manage Groups of Devices
- Task Scheduling



# Specifications

locoM9	
Dimensions	164 x 72 x 199 mm (6.46 x 2.83 x 7.83")
Weight	900 g (1.98 lbs)
Power Supply (PoE)	24V, 0.5A
Max. Power Consumption	6.5W
Power Method	Passive PoE (Pairs 4, 5+; 7, 8 Return)
Operating Frequency	902-928 MHz
Gain	8 dBi
Networking Interface	(1) 10/100 Ethernet Port
Processor Specs	Atheros MIPS 24Kc, 400 MHz
Memory	64 MB SDRAM, 8 MB Flash
Frequency	900 MHz
Cross-pol Isolation	28 dB Minimum
Max. VSWR	1.3:1
Beamwidth	60° (H-pol) / 60° (V-pol) / 60° (Elevation)
Polarization	Dual Linear
Enclosure	Outdoor UV Stabilized Plastic
Mounting	Pole-Mount (Kit Included)
RF Connector	External RP-SMA
Operating Temperature	-30 to 75° C (-22 to 167° F)
Operating Humidity	5 to 95% Noncondensing
Wireless Approvals	FCC Part 15.247, IC RS210
RoHS Compliance	Yes
Shock & Vibration	ETSI300-019-1.4

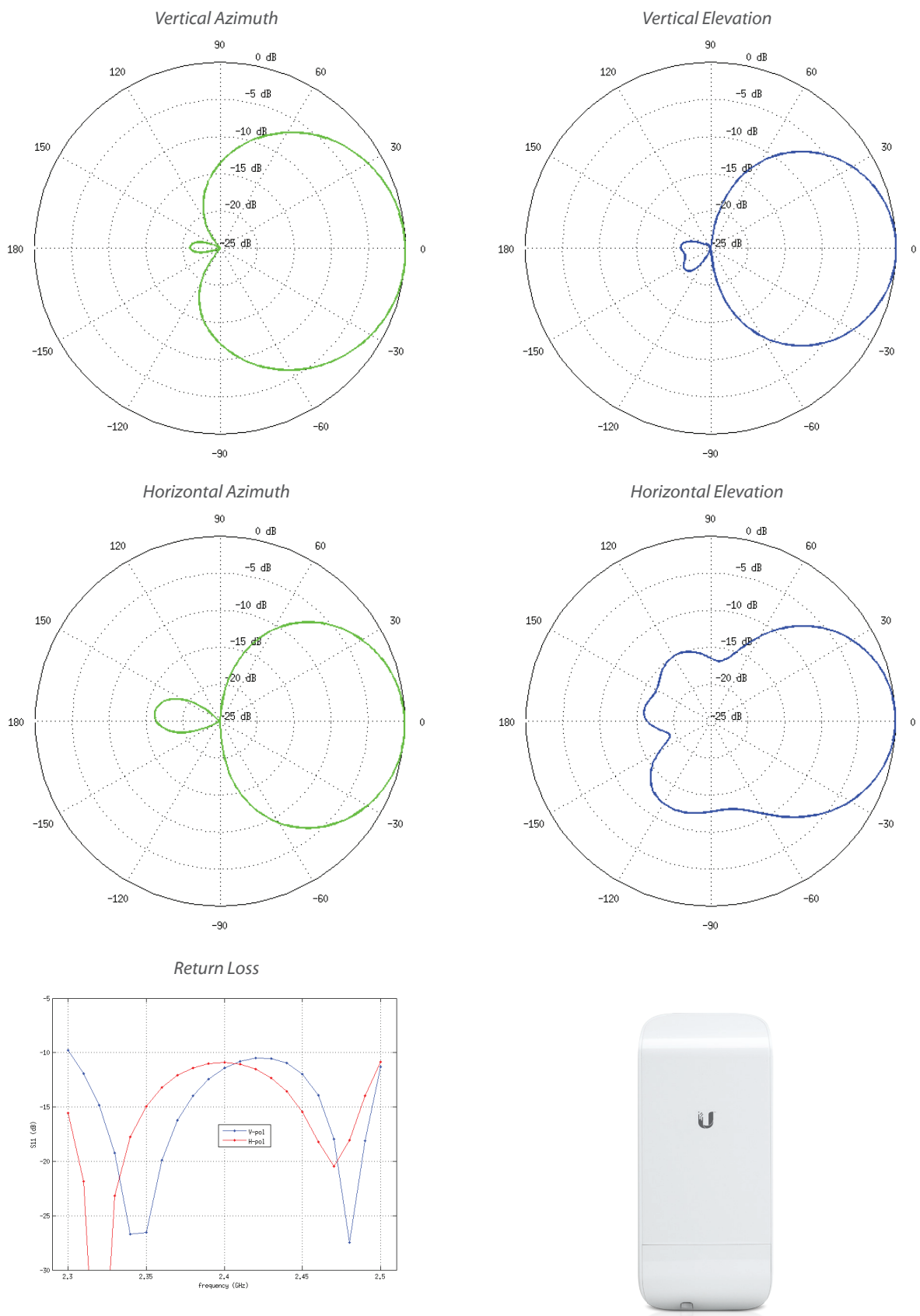
Output Power: 28 dBm							
900 MHz TX Power Specifications				900 MHz RX Power Specifications			
Modulation	MCS Index	Avg. TX	Tolerance	Modulation	MCS Index	Sensitivity	Tolerance
airMAX	MCS0	28 dBm	± 2 dB	airMAX	MCS0	-96 dBm	± 2 dB
	MCS1	28 dBm	± 2 dB		MCS1	-95 dBm	± 2 dB
	MCS2	28 dBm	± 2 dB		MCS2	-92 dBm	± 2 dB
	MCS3	28 dBm	± 2 dB		MCS3	-90 dBm	± 2 dB
	MCS4	28 dBm	± 2 dB		MCS4	-86 dBm	± 2 dB
	MCS5	24 dBm	± 2 dB		MCS5	-83 dBm	± 2 dB
	MCS6	22 dBm	± 2 dB		MCS6	-77 dBm	± 2 dB
	MCS7	21 dBm	± 2 dB		MCS7	-74 dBm	± 2 dB
	MCS8	28 dBm	± 2 dB		MCS8	-95 dBm	± 2 dB
	MCS9	28 dBm	± 2 dB		MCS9	-93 dBm	± 2 dB
	MCS10	28 dBm	± 2 dB		MCS10	-90 dBm	± 2 dB
	MCS11	28 dBm	± 2 dB		MCS11	-87 dBm	± 2 dB
	MCS12	28 dBm	± 2 dB		MCS12	-84 dBm	± 2 dB
	MCS13	24 dBm	± 2 dB		MCS13	-79 dBm	± 2 dB
	MCS14	22 dBm	± 2 dB		MCS14	-78 dBm	± 2 dB
	MCS15	21 dBm	± 2 dB		MCS15	-75 dBm	± 2 dB



# Specifications

locoM2	
Dimensions	161 x 31 x 80 mm (6.31 x 1.22 x 3.15")
Weight	180 g (6.35 oz)
Power Supply (PoE)	24V, 0.5A
Max. Power Consumption	5.5W
Power Method	Passive PoE (Pairs 4, 5+; 7, 8 Return)
Operating Frequency	2412-2462 MHz
Gain	8.5 dBi
Networking Interface	(1) 10/100 Ethernet Port
Processor Specs	Atheros MIPS 24Kc, 400 MHz
Memory	32 MB SDRAM, 8 MB Flash
Frequency	2.4 GHz
Cross-pol Isolation	20 dB Minimum
Max. VSWR	1.4:1
Beamwidth	60° (H-pol) / 60° (V-pol) / 60° (Elevation)
Polarization	Dual Linear
Enclosure	Outdoor UV Stabilized Plastic
Mounting	Pole-Mount (Kit Included)
Operating Temperature	-30 to 75° C (-22 to 167° F)
Operating Humidity	5 to 95% Noncondensing
Wireless Approvals	FCC Part 15.247, IC RS210, CE
RoHS Compliance	Yes
Shock & Vibration	ETSI300-019-1.4

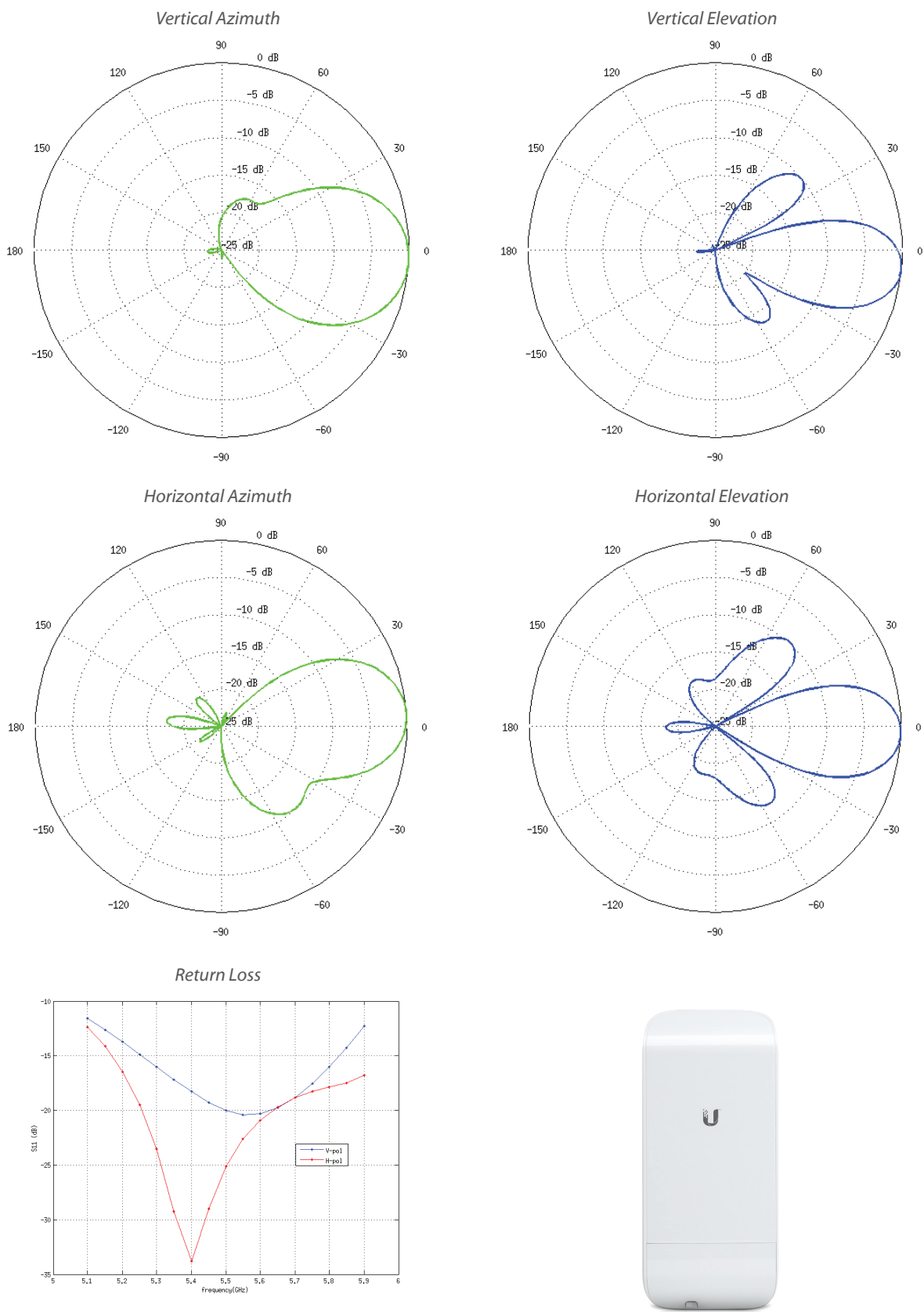
Output Power: 23 dBm							
2.4 GHz TX Power Specifications				2.4 GHz RX Power Specifications			
Modulation	Data Rate/MCS	Avg. TX	Tolerance	Modulation	Data Rate/MCS	Sensitivity	Tolerance
11b/g	1-24 Mbps	23 dBm	± 2 dB	11b/g	1-24 Mbps	-83 dBm	± 2 dB
	36 Mbps	21 dBm	± 2 dB		36 Mbps	-80 dBm	± 2 dB
	48 Mbps	19 dBm	± 2 dB		48 Mbps	-77 dBm	± 2 dB
	54 Mbps	18 dBm	± 2 dB		54 Mbps	-75 dBm	± 2 dB
airMAX	MCS0	23 dBm	± 2 dB	airMAX	MCS0	-96 dBm	± 2 dB
	MCS1	23 dBm	± 2 dB		MCS1	-95 dBm	± 2 dB
	MCS2	23 dBm	± 2 dB		MCS2	-92 dBm	± 2 dB
	MCS3	23 dBm	± 2 dB		MCS3	-90 dBm	± 2 dB
	MCS4	22 dBm	± 2 dB		MCS4	-86 dBm	± 2 dB
	MCS5	20 dBm	± 2 dB		MCS5	-83 dBm	± 2 dB
	MCS6	18 dBm	± 2 dB		MCS6	-77 dBm	± 2 dB
	MCS7	17 dBm	± 2 dB		MCS7	-74 dBm	± 2 dB
	MCS8	23 dBm	± 2 dB		MCS8	-95 dBm	± 2 dB
	MCS9	23 dBm	± 2 dB		MCS9	-93 dBm	± 2 dB
	MCS10	23 dBm	± 2 dB		MCS10	-90 dBm	± 2 dB
	MCS11	23 dBm	± 2 dB		MCS11	-87 dBm	± 2 dB
	MCS12	22 dBm	± 2 dB		MCS12	-84 dBm	± 2 dB
	MCS13	20 dBm	± 2 dB		MCS13	-79 dBm	± 2 dB
	MCS14	18 dBm	± 2 dB		MCS14	-78 dBm	± 2 dB
	MCS15	17 dBm	± 2 dB		MCS15	-75 dBm	± 2 dB



# Specifications

locoM5			
Dimensions	161 x 31 x 80 mm (6.31 x 1.22 x 3.15")		
Weight	180 g (6.35 oz)		
Power Supply (PoE)	24V, 0.5A		
Max. Power Consumption	5.5W		
Power Method	Passive PoE (Pairs 4, 5+; 7, 8 Return)		
Operating Frequency	Worldwide	USA	USA DFS
	5170-5875 MHz	5725-5850 MHz	5250-5850 MHz
Gain	13 dBi		
Networking Interface	(1) 10/100 Ethernet Port		
Processor Specs	Atheros MIPS 74Kc, 560 MHz		
Memory	64 MB DDR2, 8 MB Flash		
Frequency	5 GHz		
Cross-pol Isolation	20 dB Minimum		
Max. VSWR	1.4:1		
Beamwidth	45° (H-pol) / 45° (V-pol) / 45° (Elevation)		
Polarization	Dual Linear		
Enclosure	Outdoor UV Stabilized Plastic		
Mounting	Pole-Mount (Kit Included)		
Operating Temperature	-30 to 75° C (-22 to 167° F)		
Operating Humidity	5 to 95% Noncondensing		
Wireless Approvals	FCC Part 15.247, IC RS210, CE		
RoHS Compliance	Yes		
Shock & Vibration	ETSI300-019-1.4		

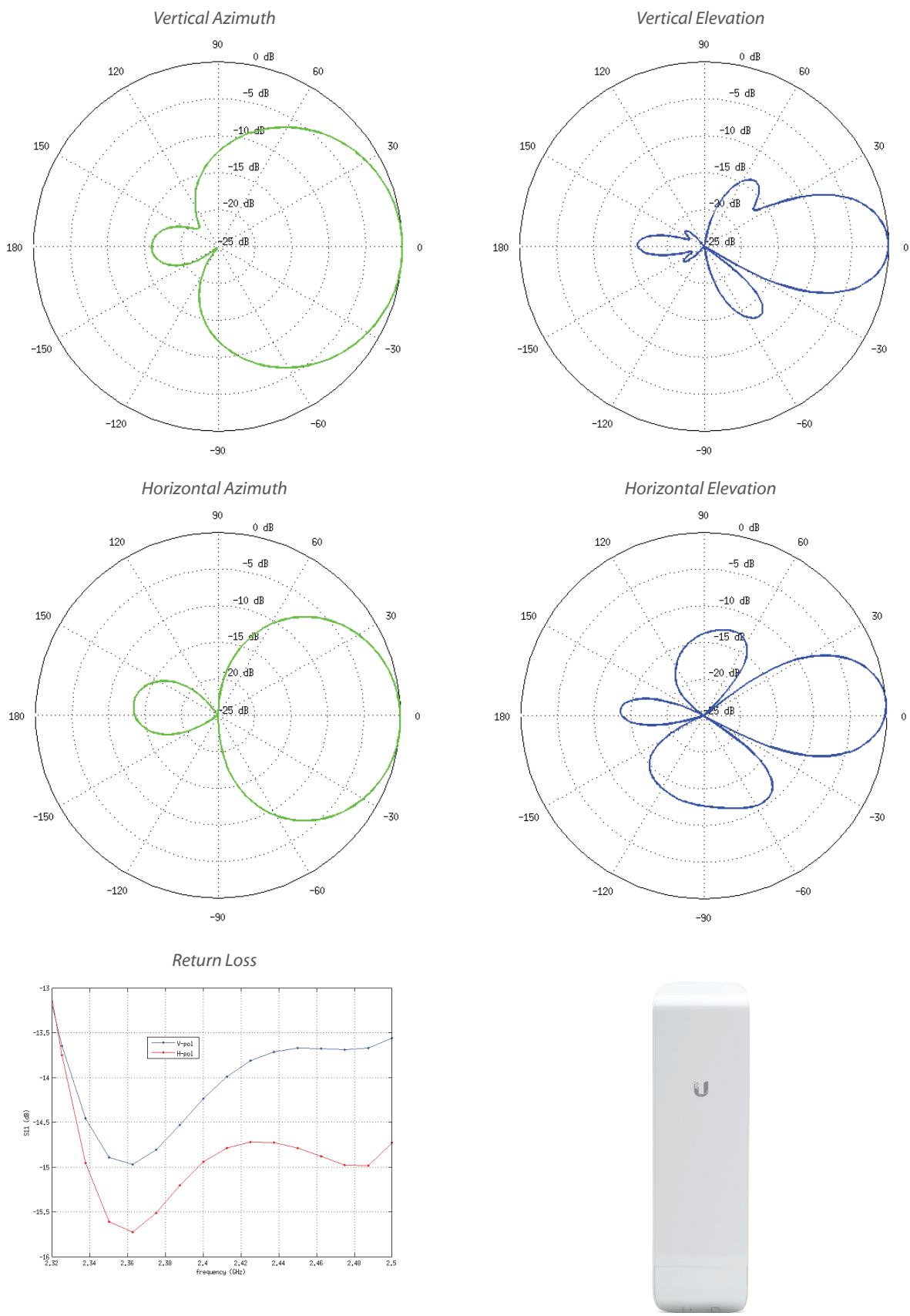
Output Power: 23 dBm							
5 GHz TX Power Specifications				5 GHz RX Power Specifications			
Modulation	Data Rate/MCS	Avg. TX	Tolerance	Modulation	Data Rate/MCS	Sensitivity	Tolerance
11a	6-24 Mbps	23 dBm	± 2 dB	11a	6-24 Mbps	-83 dBm	± 2 dB
	36 Mbps	21 dBm	± 2 dB		36 Mbps	-80 dBm	± 2 dB
	48 Mbps	19 dBm	± 2 dB		48 Mbps	-77 dBm	± 2 dB
	54 Mbps	18 dBm	± 2 dB		54 Mbps	-75 dBm	± 2 dB
11n/airMAX	MCS0	23 dBm	± 2 dB	11n/airMAX	MCS0	-96 dBm	± 2 dB
	MCS1	23 dBm	± 2 dB		MCS1	-95 dBm	± 2 dB
	MCS2	23 dBm	± 2 dB		MCS2	-92 dBm	± 2 dB
	MCS3	23 dBm	± 2 dB		MCS3	-90 dBm	± 2 dB
	MCS4	22 dBm	± 2 dB		MCS4	-86 dBm	± 2 dB
	MCS5	20 dBm	± 2 dB		MCS5	-83 dBm	± 2 dB
	MCS6	18 dBm	± 2 dB		MCS6	-77 dBm	± 2 dB
	MCS7	17 dBm	± 2 dB		MCS7	-74 dBm	± 2 dB
	MCS8	23 dBm	± 2 dB		MCS8	-95 dBm	± 2 dB
	MCS9	23 dBm	± 2 dB		MCS9	-93 dBm	± 2 dB
	MCS10	23 dBm	± 2 dB		MCS10	-90 dBm	± 2 dB
	MCS11	23 dBm	± 2 dB		MCS11	-87 dBm	± 2 dB
	MCS12	22 dBm	± 2 dB		MCS12	-84 dBm	± 2 dB
	MCS13	20 dBm	± 2 dB		MCS13	-79 dBm	± 2 dB
	MCS14	18 dBm	± 2 dB		MCS14	-78 dBm	± 2 dB
	MCS15	17 dBm	± 2 dB		MCS15	-75 dBm	± 2 dB



# Specifications

NSM2	
Dimensions	294 x 31 x 80 mm (11.57 x 1.22 x 3.15")
Weight	400 g (14.11 oz)
Power Supply (PoE)	24V, 0.5A
Max. Power Consumption	8W
Power Method	Passive PoE (Pairs 4, 5+; 7, 8 Return)
Operating Frequency	2412-2462 MHz
Gain	10.4-11.2 dBi
Networking Interface	(2) 10/100 Ethernet Ports
Processor Specs	Atheros MIPS 24Kc, 400 MHz
Memory	32 MB SDRAM, 8 MB Flash
Frequency	2.4 GHz
Cross-pol Isolation	23 dB Minimum
Max. VSWR	1.6:1
Beamwidth	55° (H-pol) / 53° (V-pol) / 27° (Elevation)
Polarization	Dual Linear
Enclosure	Outdoor UV Stabilized Plastic
Mounting	Pole-Mount (Kit Included)
Operating Temperature	-30 to 75° C (-22 to 167° F)
Operating Humidity	5 to 95% Noncondensing
Wireless Approvals	FCC Part 15.247, IC RS210, CE
RoHS Compliance	Yes
Shock & Vibration	ETSI300-019-1.4

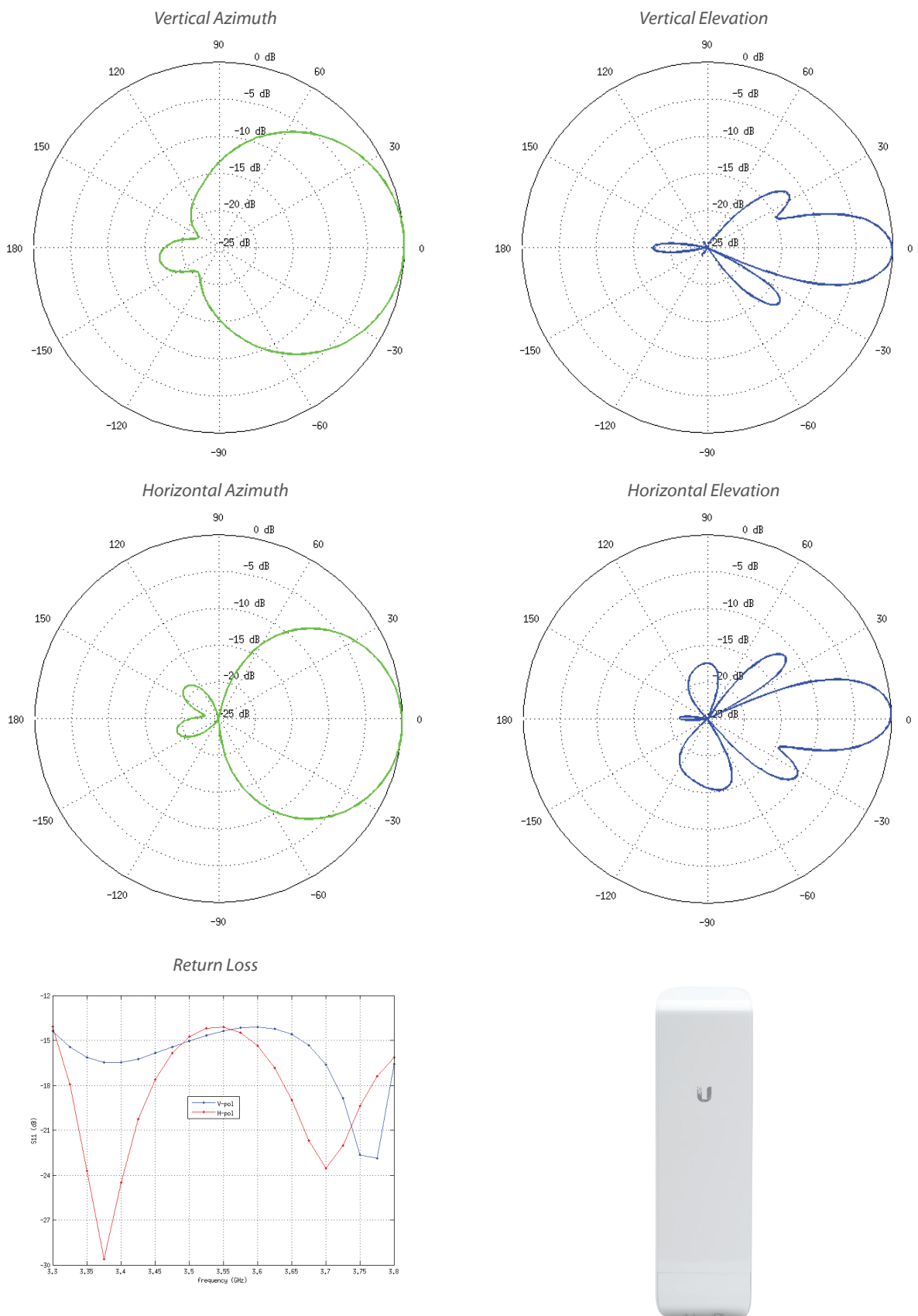
Output Power: 28 dBm							
2.4 GHz TX Power Specifications				2.4 GHz RX Power Specifications			
Modulation	Data Rate/MCS	Avg. TX	Tolerance	Modulation	Data Rate/MCS	Sensitivity	Tolerance
11b/g	1-24 Mbps	28 dBm	± 2 dB	11b/g	1-24 Mbps	-83 dBm	± 2 dB
	36 Mbps	26 dBm	± 2 dB		36 Mbps	-80 dBm	± 2 dB
	48 Mbps	25 dBm	± 2 dB		48 Mbps	-77 dBm	± 2 dB
	54 Mbps	24 dBm	± 2 dB		54 Mbps	-75 dBm	± 2 dB
airMAX	MCS0	28 dBm	± 2 dB	airMAX	MCS0	-96 dBm	± 2 dB
	MCS1	28 dBm	± 2 dB		MCS1	-95 dBm	± 2 dB
	MCS2	28 dBm	± 2 dB		MCS2	-92 dBm	± 2 dB
	MCS3	28 dBm	± 2 dB		MCS3	-90 dBm	± 2 dB
	MCS4	27 dBm	± 2 dB		MCS4	-86 dBm	± 2 dB
	MCS5	25 dBm	± 2 dB		MCS5	-83 dBm	± 2 dB
	MCS6	23 dBm	± 2 dB		MCS6	-77 dBm	± 2 dB
	MCS7	22 dBm	± 2 dB		MCS7	-74 dBm	± 2 dB
	MCS8	28 dBm	± 2 dB		MCS8	-95 dBm	± 2 dB
	MCS9	28 dBm	± 2 dB		MCS9	-93 dBm	± 2 dB
	MCS10	28 dBm	± 2 dB		MCS10	-90 dBm	± 2 dB
	MCS11	28 dBm	± 2 dB		MCS11	-87 dBm	± 2 dB
	MCS12	27 dBm	± 2 dB		MCS12	-84 dBm	± 2 dB
	MCS13	25 dBm	± 2 dB		MCS13	-79 dBm	± 2 dB
	MCS14	23 dBm	± 2 dB		MCS14	-78 dBm	± 2 dB
	MCS15	22 dBm	± 2 dB		MCS15	-75 dBm	± 2 dB



# Specifications

NSM3/M365		
Dimensions	294 x 31 x 80 mm (11.57 x 1.22 x 3.15")	
Weight	500 g (1.1 lbs)	
Power Supply (PoE)	24V, 0.5A	
Max. Power Consumption	8W	
Power Method	Passive PoE (Pairs 4, 5+; 7, 8 Return)	
Operating Frequency	NSM3	NSM365
	3400-3700 MHz	3650-3675 MHz
Gain	12.2-13.7 dBi	
Networking Interface	(2) 10/100 Ethernet Ports	
Processor Specs	Atheros MIPS 24Kc, 400 MHz	
Memory	32 MB SDRAM, 8 MB Flash	
Frequency	NSM3	NSM365
	3 GHz	3.65 GHz
Cross-pol Isolation	28 dB Minimum	
Max. VSWR	1.4:1	
Beamwidth	60° (H-pol) / 60° (V-pol) / 20° (Elevation)	
Polarization	Dual Linear	
Enclosure	Outdoor UV Stabilized Plastic	
Mounting	Pole-Mount (Kit Included)	
Operating Temperature	-30 to 75° C (-22 to 167° F)	
Operating Humidity	5 to 95% Noncondensing	
Wireless Approvals	NSM3	NSM365
	Not Applicable	FCC Part 90Z
RoHS Compliance	Yes	
Shock & Vibration	ETSI300-019-1.4	

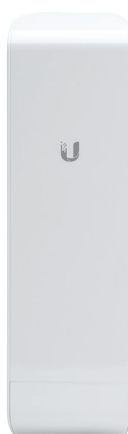
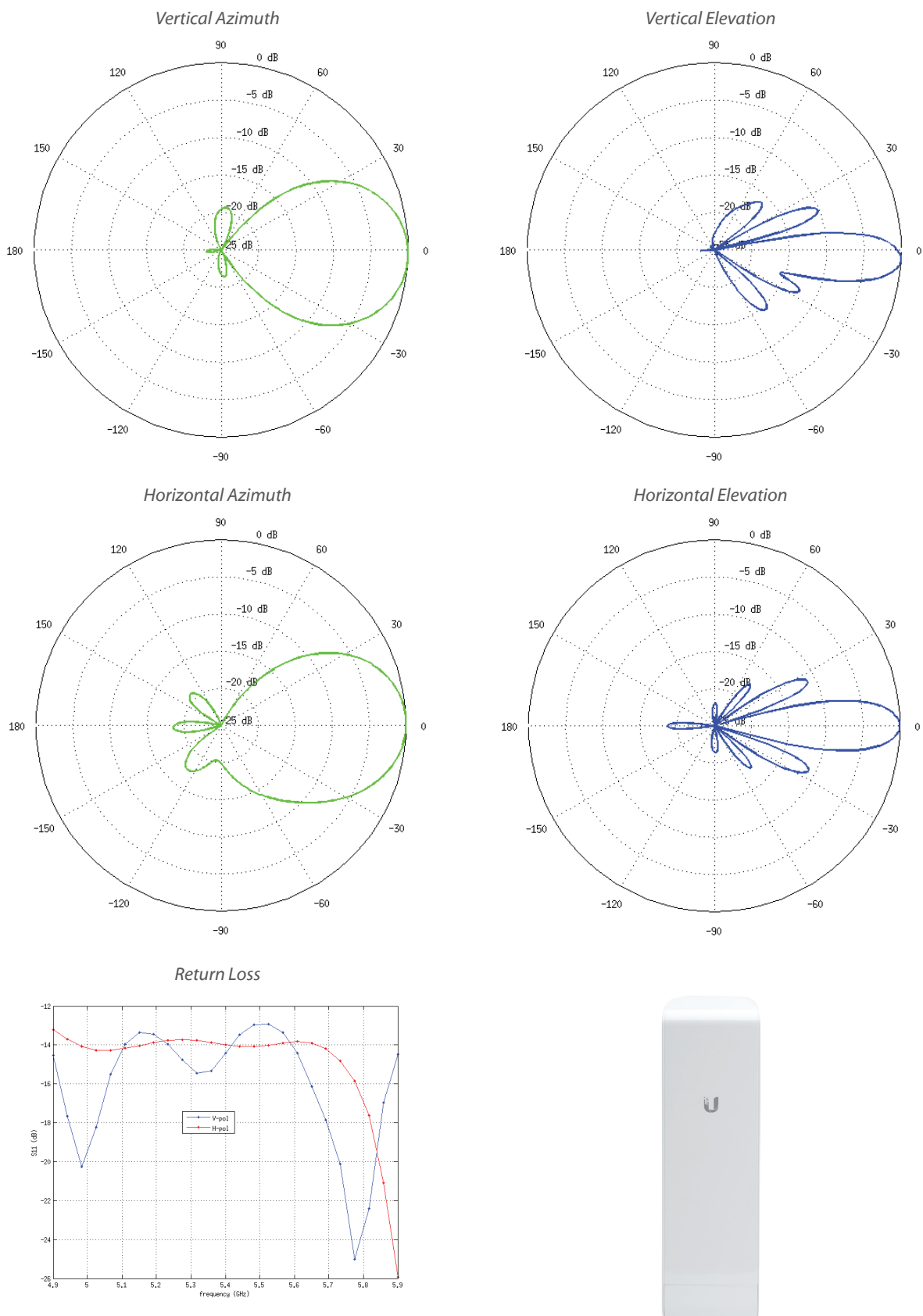
Output Power: 25 dBm							
TX Power Specifications				RX Power Specifications			
Modulation	MCS Index	Avg. TX	Tolerance	Modulation	MCS Index	Sensitivity	Tolerance
airMAX	MCS0	25 dBm	± 2 dB	airMAX	MCS0	-94 dBm	± 2 dB
	MCS1	25 dBm	± 2 dB		MCS1	-93 dBm	± 2 dB
	MCS2	25 dBm	± 2 dB		MCS2	-90 dBm	± 2 dB
	MCS3	25 dBm	± 2 dB		MCS3	-89 dBm	± 2 dB
	MCS4	24 dBm	± 2 dB		MCS4	-86 dBm	± 2 dB
	MCS5	23 dBm	± 2 dB		MCS5	-83 dBm	± 2 dB
	MCS6	22 dBm	± 2 dB		MCS6	-77 dBm	± 2 dB
	MCS7	20 dBm	± 2 dB		MCS7	-74 dBm	± 2 dB
	MCS8	25 dBm	± 2 dB		MCS8	-93 dBm	± 2 dB
	MCS9	25 dBm	± 2 dB		MCS9	-91 dBm	± 2 dB
	MCS10	25 dBm	± 2 dB		MCS10	-89 dBm	± 2 dB
	MCS11	25 dBm	± 2 dB		MCS11	-87 dBm	± 2 dB
	MCS12	24 dBm	± 2 dB		MCS12	-84 dBm	± 2 dB
	MCS13	23 dBm	± 2 dB		MCS13	-79 dBm	± 2 dB
	MCS14	22 dBm	± 2 dB		MCS14	-78 dBm	± 2 dB
	MCS15	20 dBm	± 2 dB		MCS15	-75 dBm	± 2 dB



# Specifications

NSM5			
Dimensions	294 x 31 x 80 mm (11.57 x 1.22 x 3.15")		
Weight	400 g (14.11 oz)		
Power Supply (PoE)	24V, 0.5A		
Max. Power Consumption	8W		
Power Method	Passive PoE (Pairs 4, 5+; 7, 8 Return)		
Operating Frequency	Worldwide	USA	USA DFS
	5170-5875 MHz	5725-5850 MHz	5250-5850 MHz
Gain	14.6-16.1 dBi		
Networking Interface	(2) 10/100 Ethernet Ports		
Processor Specs	Atheros MIPS 74Kc, 560 MHz		
Memory	64 MB DDR2, 8 MB Flash		
Frequency	5 GHz		
Cross-pol Isolation	22 dB Minimum		
Max. VSWR	1.6:1		
Beamwidth	43° (H-pol) / 41° (V-pol) / 15° (Elevation)		
Polarization	Dual Linear		
Enclosure	Outdoor UV Stabilized Plastic		
Mounting	Pole-Mount (Kit Included)		
Operating Temperature	-30 to 75° C (-22 to 167° F)		
Operating Humidity	5 to 95% Noncondensing		
Wireless Approvals	FCC Part 15.247, IC RS210, CE		
RoHS Compliance	Yes		
Shock & Vibration	ETSI300-019-1.4		

Output Power: 27 dBm							
5 GHz TX Power Specifications				5 GHz RX Power Specifications			
Modulation	Data Rate/MCS	Avg. TX	Tolerance	Modulation	Data Rate/MCS	Sensitivity	Tolerance
11a	6-24 Mbps	27 dBm	± 2 dB	11a	6-24 Mbps	-94 dBm	± 2 dB
	36 Mbps	25 dBm	± 2 dB		36 Mbps	-80 dBm	± 2 dB
	48 Mbps	23 dBm	± 2 dB		48 Mbps	-77 dBm	± 2 dB
	54 Mbps	22 dBm	± 2 dB		54 Mbps	-75 dBm	± 2 dB
11n/airMAX	MCS0	27 dBm	± 2 dB	11n/airMAX	MCS0	-96 dBm	± 2 dB
	MCS1	27 dBm	± 2 dB		MCS1	-95 dBm	± 2 dB
	MCS2	27 dBm	± 2 dB		MCS2	-92 dBm	± 2 dB
	MCS3	27 dBm	± 2 dB		MCS3	-90 dBm	± 2 dB
	MCS4	26 dBm	± 2 dB		MCS4	-86 dBm	± 2 dB
	MCS5	24 dBm	± 2 dB		MCS5	-83 dBm	± 2 dB
	MCS6	22 dBm	± 2 dB		MCS6	-77 dBm	± 2 dB
	MCS7	21 dBm	± 2 dB		MCS7	-74 dBm	± 2 dB
	MCS8	27 dBm	± 2 dB		MCS8	-95 dBm	± 2 dB
	MCS9	27 dBm	± 2 dB		MCS9	-93 dBm	± 2 dB
	MCS10	27 dBm	± 2 dB		MCS10	-90 dBm	± 2 dB
	MCS11	27 dBm	± 2 dB		MCS11	-87 dBm	± 2 dB
	MCS12	26 dBm	± 2 dB		MCS12	-84 dBm	± 2 dB
	MCS13	24 dBm	± 2 dB		MCS13	-79 dBm	± 2 dB
	MCS14	22 dBm	± 2 dB		MCS14	-78 dBm	± 2 dB
	MCS15	21 dBm	± 2 dB		MCS15	-75 dBm	± 2 dB



Specifications are subject to change. Ubiquiti products are sold with a limited warranty described at: [www.ubnt.com/support/warranty](http://www.ubnt.com/support/warranty)  
 ©2014-2018 Ubiquiti Networks, Inc. All rights reserved. Ubiquiti, Ubiquiti Networks, the Ubiquiti U logo, airFiber, airMAX, airOS, airView, NanoStationM, and NanoStationlocoM are trademarks or registered trademarks of Ubiquiti Networks, Inc. in the United States and in other countries. All other trademarks are the property of their respective owners.



[www.ubnt.com](http://www.ubnt.com)



## PFT-SRB250AG1SSAAMSSZ

PFT

DRUKSENSOREN

**SICK**  
Sensor Intelligence.



### Bestelinformatie

Type	Artikelnr.
PFT-SRB250AG1SSAAMSSZ	6041577

Meer apparaatuutvoeringen en accessoires → [www.sick.com/PFT](http://www.sick.com/PFT)

Afbeelding kan afwijken



### Gedetailleerde technische specificaties

#### Kenmerken

<b>Medium</b>	Vloeibaar, gasvormig
<b>Druktype</b>	Relatieve druk
<b>Drukeenheid</b>	bar
<b>Meetbereik</b>	0 bar ... 250 bar
<b>Procestemperatuur</b>	-30 °C ... +100 °C
<b>Outputsignaal</b>	4 mA ... 20 mA, 2-draads
<b>Bijzonderheid</b>	Zonder

#### Mechanisch/Elektrisch

<b>Procesaansluiting</b>	G 1/4 A volgens DIN 3852-E
<b>In aanraking komend met materialen</b>	Standaardmembraan: roestvast staal 1.4571, roestvast staal 1.4534 voor meetbereiken > 25 bar
<b>Interne overdrachtvloeibaarheid</b>	Synthetische olie (niet aanwezig bij niet vlak membraan voor meetbereiken > 25 bar)
<b>Kanaalboring</b>	, Standard
<b>Materiaal behuizing</b>	Roestvast staal 1.4571
<b>Aansluittype</b>	Ronde connector M12 x 1, 4-pins, IP67
<b>Voedingsspanning</b>	10 V DC ... 30 V DC 14 V DC ... 30 V DC bij uitgangssignaal 0 V ... 10 V
<b>Elektrische veiligheid</b>	Overspanningsbeveiliging: 36 V DC Kortsluitvastheid: Q <sub>A</sub> met M Ompoolbeveiliging: L <sup>+</sup> met M Isolatieklasse: III
<b>Spanningsvastheid</b>	500 V DC, NEC Class-02-voedingsspanning (laagspanning en lage stroom max. 100 VA ook bij storing)
<b>CE-conformiteit</b>	Richtlijn drukapparaten: 2014/68/EU, EMC-richtlijn: 2004/108/EC EN 61326-2-3
<b>Gewicht sensor</b>	Ca. 200 g
<b>Afdichting</b>	NBR
<b>Isolatieklasse</b>	IP67
<b>Beschermingsklasse III</b>	✓
<b>MTTF</b>	403 jaren

## Performance

<b>Niet-lineariteit</b>	$\leq \pm 0,2\%$ , van spanne (Best Fit Straight Line, BFSL) volgens IEC 61298-2
<b>Meetnauwkeurigheid</b>	$\leq \pm 0,25\%$ van spanne
<b>Niet-herhaalbaarheid</b>	$\leq \pm 0,1\%$ van spanne
<b>Insteltijd (10% ... 90%)</b>	$\leq 1\text{ ms} \leq 10\text{ ms}$ bij meetstoftemperatuur $< -30^\circ\text{C}$ voor meetbereiken tot 25 bar of bij vlak membraan
<b>Langetermijndrift / stabiliteit per jaar</b>	$\leq \pm 0,2\%$ van spanne (bij referentiecondities)
<b>Temperatuurcoëfficiënt in bereik meettemperatuur</b>	Gemiddeld TC van nulpunt: $\leq 0,2\%$ van spanne / 10 K ( $< 0,4\%$ voor meetbereiken $\leq 0,25$ bar), Gemiddeld TC van spanne: $\leq 0,2\%$ van spanne / 10 K
<b>Bereik meettemperatuur</b>	$0^\circ\text{C} \dots +80^\circ\text{C}$
<b>Levensduur</b>	Minimaal 100 mln. lastwissels

## Omgevingsgegevens

<b>Omgevingstemperatuur</b>	$-20^\circ\text{C} \dots +80^\circ\text{C}$
<b>Opslagtemperatuur</b>	$-40^\circ\text{C} \dots +100^\circ\text{C}$ , met vlak membraan en geïntegreerd koeltraject: $-20^\circ\text{C} \dots +100^\circ\text{C}$
<b>Schokbelasting</b>	1000 g volgens IEC 60068-2-27 (schok mechanisch) 400 g volgens IEC 60068-2-27 (schok mechanisch) voor variant met geïntegreerd koeltraject
<b>Trillingsbelasting</b>	20 g volgens IEC 60068-2-6 (trilling bij resonantie) 10 g volgens IEC 60068-2-6 (trilling bij resonantie) voor variant met geïntegreerd koeltraject

## Classificaties

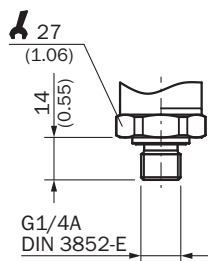
<b>eCl@ss 5.0</b>	27200614
<b>eCl@ss 5.1.4</b>	27200614
<b>eCl@ss 6.0</b>	27200614
<b>eCl@ss 6.2</b>	27200614
<b>eCl@ss 7.0</b>	27200614
<b>eCl@ss 8.0</b>	27200614
<b>eCl@ss 8.1</b>	27200614
<b>eCl@ss 9.0</b>	27200614
<b>eCl@ss 10.0</b>	27200614
<b>eCl@ss 11.0</b>	27200614
<b>eCl@ss 12.0</b>	27200614
<b>ETIM 5.0</b>	EC011478
<b>ETIM 6.0</b>	EC011478
<b>ETIM 7.0</b>	EC011478
<b>ETIM 8.0</b>	EC011478
<b>UNSPSC 16.0901</b>	41112410

# PFT-SRB250AG1SSAAMSSZ | PFT

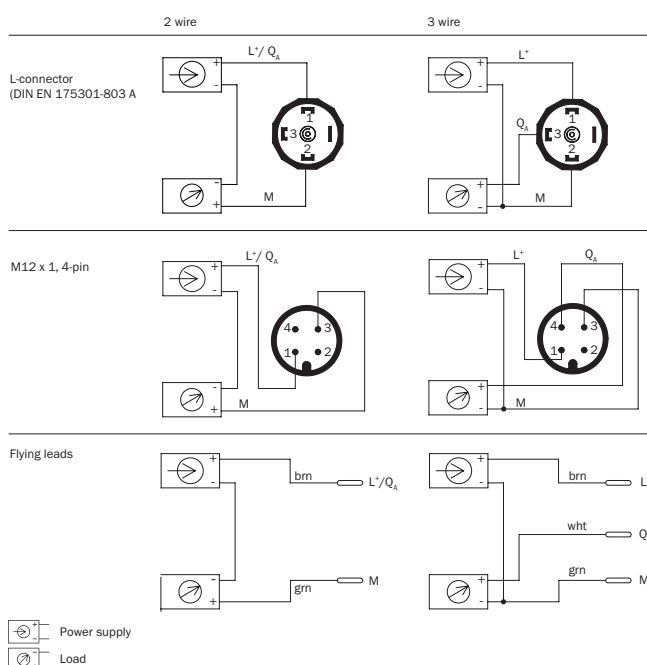
DRUKSENSOREN

**Maattekening** (Afmetingen in mm (inch))

G 1/4 A DIN 3852-E



## Aansluittype



## Aanbevolen accessoires

Meer apparaatuitvoeringen en accessoires → [www.sick.com/PFT](http://www.sick.com/PFT)

Korte beschrijving	Type	Artikelnr.
<b>Montagebeugels en -platen</b>		
 Bevestigingshoek voor de eenvoudig en stabiele wandmontage voor drucksensoren met zeskant 27 mm, Aluminium	BEF-FL-ALUPBS-HLDR	5322501
<b>Stekkers en kabels</b>		
 Kop A: Contactdoos, M12, 4-pins, haaks Kop B: open kabeluiteinde Kabel: Sensor-actuatorkabel, PVC, Niet geïsoleerd, 5 m	DOL-1204-W05MD	6020399

	Korte beschrijving	Type	Artikelnr.
	Kop A: Contactdoos, M12, 4-pins, recht, A-gecodeerd Kop B: open kabeluiteinde Kabel: Sensor-actuatkabel, PUR, halogeenvrij, Niet geïsoleerd, 2 m	YF2A14-020UB3XLEAX	2095607
	Kop A: Contactdoos, M12, 4-pins, recht, A-gecodeerd Kop B: open kabeluiteinde Kabel: Sensor-actuatkabel, PVC, Niet geïsoleerd, 2 m	YF2A14-020VB3XLEAX	2096234
	Kop A: Contactdoos, M12, 4-pins, recht, A-gecodeerd Kop B: open kabeluiteinde Kabel: Sensor-actuatkabel, PUR, halogeenvrij, Niet geïsoleerd, 5 m	YF2A14-050UB3XLEAX	2095608
	Kop A: Contactdoos, M12, 4-pins, recht, A-gecodeerd Kop B: open kabeluiteinde Kabel: Sensor-actuatkabel, PVC, Niet geïsoleerd, 5 m	YF2A14-050VB3XLEAX	2096235
	Kop A: Contactdoos, M12, 4-pins, recht, A-gecodeerd Kop B: open kabeluiteinde Kabel: Sensor-actuatkabel, PUR, halogeenvrij, Niet geïsoleerd, 10 m	YF2A14-100UB3XLEAX	2095609
	Kop A: Contactdoos, M12, 4-pins, recht, A-gecodeerd Kop B: open kabeluiteinde Kabel: Sensor-actuatkabel, PVC, Niet geïsoleerd, 10 m	YF2A14-100VB3XLEAX	2096236
	Kop A: Contactdoos, M12, 4-pins, recht, A-gecodeerd Kop B: open kabeluiteinde Kabel: Sensor-actuatkabel, PUR, halogeenvrij, Niet geïsoleerd, 15 m	YF2A14-150UB3XLEAX	2095610
	Kop A: Contactdoos, M12, 4-pins, recht, A-gecodeerd Kop B: open kabeluiteinde Kabel: Sensor-actuatkabel, PVC, Niet geïsoleerd, 15 m	YF2A14-150VB3XLEAX	2096237
	Kop A: Contactdoos, M12, 4-pins, recht, A-gecodeerd Kop B: open kabeluiteinde Kabel: Sensor-actuatkabel, PUR, halogeenvrij, Niet geïsoleerd, 20 m	YF2A14-200UB3XLEAX	2095611
	Kop A: Contactdoos, M12, 4-pins, recht, A-gecodeerd Kop B: open kabeluiteinde Kabel: Sensor-actuatkabel, PVC, Niet geïsoleerd, 20 m	YF2A14-200VB3XLEAX	2096238
	Kop A: Contactdoos, M12, 4-pins, recht, A-gecodeerd Kop B: open kabeluiteinde Kabel: Sensor-actuatkabel, PUR, halogeenvrij, Niet geïsoleerd, 25 m	YF2A14-250UB3XLEAX	2095615
	Kop A: Contactdoos, M12, 4-pins, haaks, A-gecodeerd Kop B: open kabeluiteinde Kabel: Sensor-actuatkabel, PUR, halogeenvrij, Niet geïsoleerd, 2 m	YG2A14-020UB3XLEAX	2095766
	Kop A: Contactdoos, M12, 4-pins, haaks, A-gecodeerd Kop B: open kabeluiteinde Kabel: Sensor-actuatkabel, PVC, Niet geïsoleerd, 2 m	YG2A14-020VB3XLEAX	2095895
	Kop A: Contactdoos, M12, 4-pins, haaks, A-gecodeerd Kop B: open kabeluiteinde Kabel: Sensor-actuatkabel, PUR, halogeenvrij, Niet geïsoleerd, 5 m	YG2A14-050UB3XLEAX	2095767
	Kop A: Contactdoos, M12, 4-pins, haaks, A-gecodeerd Kop B: open kabeluiteinde Kabel: Sensor-actuatkabel, PVC, Niet geïsoleerd, 5 m	YG2A14-050VB3XLEAX	2095897
	Kop A: Contactdoos, M12, 4-pins, haaks, A-gecodeerd Kop B: open kabeluiteinde Kabel: Sensor-actuatkabel, PUR, halogeenvrij, Niet geïsoleerd, 10 m	YG2A14-100UB3XLEAX	2095768
	Kop A: Contactdoos, M12, 4-pins, haaks, A-gecodeerd Kop B: open kabeluiteinde Kabel: Sensor-actuatkabel, PVC, Niet geïsoleerd, 10 m	YG2A14-100VB3XLEAX	2095898

# PFT-SRB250AG1SSAAMSSZ | PFT

DRUKSENSOREN

	Korte beschrijving	Type	Artikelnr.
	Kop A: Contactdoos, M12, 4-pins, haaks, A-gecodeerd Kop B: open kabeluiteinde Kabel: Sensor-actuatorkabel, PUR, halogeenvrij, Niet geïsoleerd, 15 m	YG2A14-150UB3XLEAX	2095769
	Kop A: Contactdoos, M12, 4-pins, haaks, A-gecodeerd Kop B: open kabeluiteinde Kabel: Sensor-actuatorkabel, PVC, Niet geïsoleerd, 15 m	YG2A14-150VB3XLEAX	2096213
	Kop A: Contactdoos, M12, 4-pins, haaks, A-gecodeerd Kop B: open kabeluiteinde Kabel: Sensor-actuatorkabel, PUR, halogeenvrij, Niet geïsoleerd, 20 m	YG2A14-200UB3XLEAX	2095770
	Kop A: Contactdoos, M12, 4-pins, haaks, A-gecodeerd Kop B: open kabeluiteinde Kabel: Sensor-actuatorkabel, PVC, Niet geïsoleerd, 20 m	YG2A14-200VB3XLEAX	2096214
	Kop A: Contactdoos, M12, 4-pins, haaks, A-gecodeerd Kop B: open kabeluiteinde Kabel: Sensor-actuatorkabel, PUR, halogeenvrij, Niet geïsoleerd, 25 m	YG2A14-250UB3XLEAX	2095771

## SICK IN ÉÉN OOGOPSLAG

SICK is één van de toonaangevende fabrikanten van intelligente sensoren en sensoroplossingen voor industriële toepassingen. Ons unieke aanbod van producten en services is de perfecte basis voor een veilige en efficiënte besturing van processen, voor de bescherming van mensen tegen ongevallen en het voorkomen van milieuverontreiniging.

Wij hebben uitgebreide ervaring in diverse uiteenlopende domeinen en kennen grondig de branchespecifieke processen en eisen. Zo kunnen wij met intelligente sensoren precies de oplossingen leveren die onze klanten nodig hebben. In onze testcentra in Europa, Azië en Noord-Amerika worden systeemoplossingen voor onze klanten getest en geoptimaliseerd. Dat alles maakt van ons een betrouwbare leverancier en R&D-partner.

Onze uitgebreide services vervolledigen ons aanbod. Met onze SICK LifeTime Services ondersteunen we u tijdens de gehele levenscyclus van de machine en zorgen we voor veiligheid en productiviteit.

**Dat is voor ons “Sensor Intelligence”.**

## WERELDWIJD BIJ U IN DE BUURT:

Contactpersonen en andere vestigingen → [www.sick.com](http://www.sick.com)



## PFT-SRB100AG1SSAAMSSZ

PFT

DRUKSENSOREN

**SICK**  
Sensor Intelligence.



### Bestelinformatie

Type	Artikelnr.
PFT-SRB100AG1SSAAMSSZ	6041576

Meer apparaatuutvoeringen en accessoires → [www.sick.com/PFT](http://www.sick.com/PFT)

Afbeelding kan afwijken



### Gedetailleerde technische specificaties

#### Kenmerken

<b>Medium</b>	Vloeibaar, gasvormig
<b>Druktype</b>	Relatieve druk
<b>Drukeenheid</b>	bar
<b>Meetbereik</b>	0 bar ... 100 bar
<b>Procestemperatuur</b>	-30 °C ... +100 °C
<b>Outputsignaal</b>	4 mA ... 20 mA, 2-draads
<b>Bijzonderheid</b>	Zonder

#### Mechanisch/Elektrisch

<b>Procesaansluiting</b>	G 1/4 A volgens DIN 3852-E
<b>In aanraking komend met materialen</b>	Standaardmembraan: roestvast staal 1.4571, roestvast staal 1.4534 voor meetbereiken > 25 bar
<b>Interne overdrachtvloeibaarheid</b>	Synthetische olie (niet aanwezig bij niet vlak membraan voor meetbereiken > 25 bar)
<b>Kanaalboring</b>	, Standard
<b>Materiaal behuizing</b>	Roestvast staal 1.4571
<b>Aansluittype</b>	Ronde connector M12 x 1, 4-pins, IP67
<b>Voedingsspanning</b>	10 V DC ... 30 V DC 14 V DC ... 30 V DC bij uitgangssignaal 0 V ... 10 V
<b>Elektrische veiligheid</b>	Overspanningsbeveiliging: 36 V DC Kortsluitvastheid: Q <sub>A</sub> met M Ompoolbeveiliging: L <sup>+</sup> met M Isolatieklasse: III
<b>Spanningsvastheid</b>	500 V DC, NEC Class-02-voedingsspanning (laagspanning en lage stroom max. 100 VA ook bij storing)
<b>CE-conformiteit</b>	Richtlijn drukapparaten: 2014/68/EU, EMC-richtlijn: 2004/108/EC EN 61326-2-3
<b>Gewicht sensor</b>	Ca. 200 g
<b>Afdichting</b>	NBR
<b>Isolatieklasse</b>	IP67
<b>Beschermingsklasse III</b>	✓
<b>MTTF</b>	403 jaren

## Performance

<b>Niet-lineariteit</b>	$\leq \pm 0,2\%$ , van spanne (Best Fit Straight Line, BFSL) volgens IEC 61298-2
<b>Meetnauwkeurigheid</b>	$\leq \pm 0,25\%$ van spanne
<b>Niet-herhaalbaarheid</b>	$\leq \pm 0,1\%$ van spanne
<b>Insteltijd (10% ... 90%)</b>	$\leq 1\text{ ms} \leq 10\text{ ms}$ bij meetstoftemperatuur $< -30^\circ\text{C}$ voor meetbereiken tot 25 bar of bij vlak membraan
<b>Langetermijndrift / stabiliteit per jaar</b>	$\leq \pm 0,2\%$ van spanne (bij referentiecondities)
<b>Temperatuurcoëfficiënt in bereik meettemperatuur</b>	Gemiddeld TC van nulpunt: $\leq 0,2\%$ van spanne / 10 K ( $< 0,4\%$ voor meetbereiken $\leq 0,25$ bar), Gemiddeld TC van spanne: $\leq 0,2\%$ van spanne / 10 K
<b>Bereik meettemperatuur</b>	$0^\circ\text{C} \dots +80^\circ\text{C}$
<b>Levensduur</b>	Minimaal 100 mln. lastwissels

## Omgevingsgegevens

<b>Omgevingstemperatuur</b>	$-20^\circ\text{C} \dots +80^\circ\text{C}$
<b>Opslagtemperatuur</b>	$-40^\circ\text{C} \dots +100^\circ\text{C}$ , met vlak membraan en geïntegreerd koeltraject: $-20^\circ\text{C} \dots +100^\circ\text{C}$
<b>Schokbelasting</b>	1000 g volgens IEC 60068-2-27 (schok mechanisch) 400 g volgens IEC 60068-2-27 (schok mechanisch) voor variant met geïntegreerd koeltraject
<b>Trillingsbelasting</b>	20 g volgens IEC 60068-2-6 (trilling bij resonantie) 10 g volgens IEC 60068-2-6 (trilling bij resonantie) voor variant met geïntegreerd koeltraject

## Classificaties

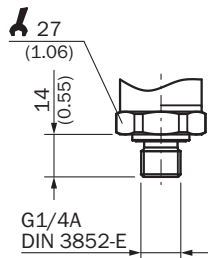
<b>eCl@ss 5.0</b>	27200614
<b>eCl@ss 5.1.4</b>	27200614
<b>eCl@ss 6.0</b>	27200614
<b>eCl@ss 6.2</b>	27200614
<b>eCl@ss 7.0</b>	27200614
<b>eCl@ss 8.0</b>	27200614
<b>eCl@ss 8.1</b>	27200614
<b>eCl@ss 9.0</b>	27200614
<b>eCl@ss 10.0</b>	27200614
<b>eCl@ss 11.0</b>	27200614
<b>eCl@ss 12.0</b>	27200614
<b>ETIM 5.0</b>	EC011478
<b>ETIM 6.0</b>	EC011478
<b>ETIM 7.0</b>	EC011478
<b>ETIM 8.0</b>	EC011478
<b>UNSPSC 16.0901</b>	41112410

# PFT-SRB100AG1SSAAMSSZ | PFT

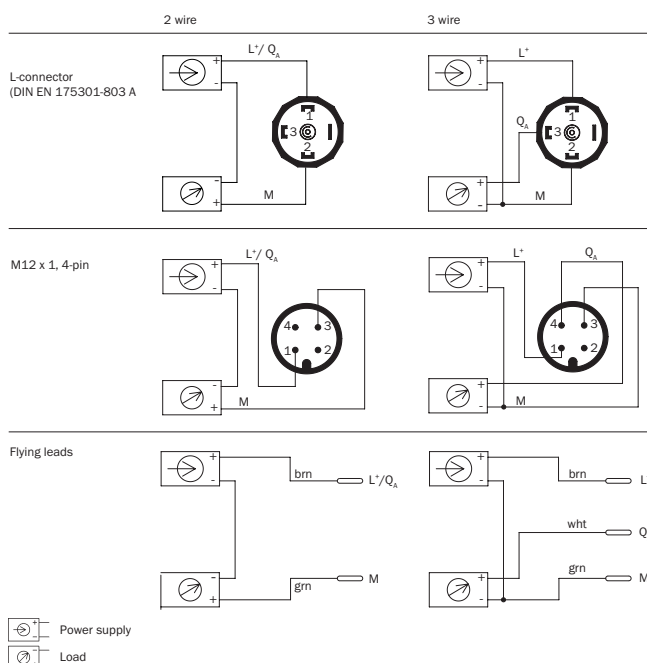
DRUKSENSOREN

**Maattekening** (Afmetingen in mm (inch))

G 1/4 A DIN 3852-E



## Aansluittype



## Aanbevolen accessoires

Meer apparaatuitvoeringen en accessoires → [www.sick.com/PFT](http://www.sick.com/PFT)

Korte beschrijving	Type	Artikelnr.
<b>Montagebeugels en -platen</b>		
Bevestigingshoek voor de eenvoudig en stabiele wandmontage voor drucksensoren met zeskant 27 mm, Aluminium	BEF-FL-ALUPBS-HLDR	5322501
<b>Stekkers en kabels</b>		
Kop A: Contactdoos, M12, 4-pins, haaks Kop B: open kabeluiteinde Kabel: Sensor-actuatorkabel, PVC, Niet geïsoleerd, 5 m	DOL-1204-W05MD	6020399

	Korte beschrijving	Type	Artikelnr.
	Kop A: Contactdoos, M12, 4-pins, recht, A-gecodeerd Kop B: open kabeluiteinde Kabel: Sensor-actuatkabel, PUR, halogeenvrij, Niet geïsoleerd, 2 m	YF2A14-020UB3XLEAX	2095607
	Kop A: Contactdoos, M12, 4-pins, recht, A-gecodeerd Kop B: open kabeluiteinde Kabel: Sensor-actuatkabel, PVC, Niet geïsoleerd, 2 m	YF2A14-020VB3XLEAX	2096234
	Kop A: Contactdoos, M12, 4-pins, recht, A-gecodeerd Kop B: open kabeluiteinde Kabel: Sensor-actuatkabel, PUR, halogeenvrij, Niet geïsoleerd, 5 m	YF2A14-050UB3XLEAX	2095608
	Kop A: Contactdoos, M12, 4-pins, recht, A-gecodeerd Kop B: open kabeluiteinde Kabel: Sensor-actuatkabel, PVC, Niet geïsoleerd, 5 m	YF2A14-050VB3XLEAX	2096235
	Kop A: Contactdoos, M12, 4-pins, recht, A-gecodeerd Kop B: open kabeluiteinde Kabel: Sensor-actuatkabel, PUR, halogeenvrij, Niet geïsoleerd, 10 m	YF2A14-100UB3XLEAX	2095609
	Kop A: Contactdoos, M12, 4-pins, recht, A-gecodeerd Kop B: open kabeluiteinde Kabel: Sensor-actuatkabel, PVC, Niet geïsoleerd, 10 m	YF2A14-100VB3XLEAX	2096236
	Kop A: Contactdoos, M12, 4-pins, recht, A-gecodeerd Kop B: open kabeluiteinde Kabel: Sensor-actuatkabel, PUR, halogeenvrij, Niet geïsoleerd, 15 m	YF2A14-150UB3XLEAX	2095610
	Kop A: Contactdoos, M12, 4-pins, recht, A-gecodeerd Kop B: open kabeluiteinde Kabel: Sensor-actuatkabel, PVC, Niet geïsoleerd, 15 m	YF2A14-150VB3XLEAX	2096237
	Kop A: Contactdoos, M12, 4-pins, recht, A-gecodeerd Kop B: open kabeluiteinde Kabel: Sensor-actuatkabel, PUR, halogeenvrij, Niet geïsoleerd, 20 m	YF2A14-200UB3XLEAX	2095611
	Kop A: Contactdoos, M12, 4-pins, recht, A-gecodeerd Kop B: open kabeluiteinde Kabel: Sensor-actuatkabel, PVC, Niet geïsoleerd, 20 m	YF2A14-200VB3XLEAX	2096238
	Kop A: Contactdoos, M12, 4-pins, recht, A-gecodeerd Kop B: open kabeluiteinde Kabel: Sensor-actuatkabel, PUR, halogeenvrij, Niet geïsoleerd, 25 m	YF2A14-250UB3XLEAX	2095615
	Kop A: Contactdoos, M12, 4-pins, haaks, A-gecodeerd Kop B: open kabeluiteinde Kabel: Sensor-actuatkabel, PUR, halogeenvrij, Niet geïsoleerd, 2 m	YG2A14-020UB3XLEAX	2095766
	Kop A: Contactdoos, M12, 4-pins, haaks, A-gecodeerd Kop B: open kabeluiteinde Kabel: Sensor-actuatkabel, PVC, Niet geïsoleerd, 2 m	YG2A14-020VB3XLEAX	2095895
	Kop A: Contactdoos, M12, 4-pins, haaks, A-gecodeerd Kop B: open kabeluiteinde Kabel: Sensor-actuatkabel, PUR, halogeenvrij, Niet geïsoleerd, 5 m	YG2A14-050UB3XLEAX	2095767
	Kop A: Contactdoos, M12, 4-pins, haaks, A-gecodeerd Kop B: open kabeluiteinde Kabel: Sensor-actuatkabel, PVC, Niet geïsoleerd, 5 m	YG2A14-050VB3XLEAX	2095897
	Kop A: Contactdoos, M12, 4-pins, haaks, A-gecodeerd Kop B: open kabeluiteinde Kabel: Sensor-actuatkabel, PUR, halogeenvrij, Niet geïsoleerd, 10 m	YG2A14-100UB3XLEAX	2095768
	Kop A: Contactdoos, M12, 4-pins, haaks, A-gecodeerd Kop B: open kabeluiteinde Kabel: Sensor-actuatkabel, PVC, Niet geïsoleerd, 10 m	YG2A14-100VB3XLEAX	2095898

# PFT-SRB100AG1SSAAMSSZ | PFT

DRUKSENSOREN

	Korte beschrijving	Type	Artikelnr.
	Kop A: Contactdoos, M12, 4-pins, haaks, A-gecodeerd Kop B: open kabeluiteinde Kabel: Sensor-actuatorkabel, PUR, halogeenvrij, Niet geïsoleerd, 15 m	YG2A14-150UB3XLEAX	2095769
	Kop A: Contactdoos, M12, 4-pins, haaks, A-gecodeerd Kop B: open kabeluiteinde Kabel: Sensor-actuatorkabel, PVC, Niet geïsoleerd, 15 m	YG2A14-150VB3XLEAX	2096213
	Kop A: Contactdoos, M12, 4-pins, haaks, A-gecodeerd Kop B: open kabeluiteinde Kabel: Sensor-actuatorkabel, PUR, halogeenvrij, Niet geïsoleerd, 20 m	YG2A14-200UB3XLEAX	2095770
	Kop A: Contactdoos, M12, 4-pins, haaks, A-gecodeerd Kop B: open kabeluiteinde Kabel: Sensor-actuatorkabel, PVC, Niet geïsoleerd, 20 m	YG2A14-200VB3XLEAX	2096214
	Kop A: Contactdoos, M12, 4-pins, haaks, A-gecodeerd Kop B: open kabeluiteinde Kabel: Sensor-actuatorkabel, PUR, halogeenvrij, Niet geïsoleerd, 25 m	YG2A14-250UB3XLEAX	2095771

## SICK IN ÉÉN OOGOPSLAG

SICK is één van de toonaangevende fabrikanten van intelligente sensoren en sensoroplossingen voor industriële toepassingen. Ons unieke aanbod van producten en services is de perfecte basis voor een veilige en efficiënte besturing van processen, voor de bescherming van mensen tegen ongevallen en het voorkomen van milieuverontreiniging.

Wij hebben uitgebreide ervaring in diverse uiteenlopende domeinen en kennen grondig de branchespecifieke processen en eisen. Zo kunnen wij met intelligente sensoren precies de oplossingen leveren die onze klanten nodig hebben. In onze testcentra in Europa, Azië en Noord-Amerika worden systeemoplossingen voor onze klanten getest en geoptimaliseerd. Dat alles maakt van ons een betrouwbare leverancier en R&D-partner.

Onze uitgebreide services vervolledigen ons aanbod. Met onze SICK LifeTime Services ondersteunen we u tijdens de gehele levenscyclus van de machine en zorgen we voor veiligheid en productiviteit.

**Dat is voor ons “Sensor Intelligence”.**

## WERELDWIJD BIJ U IN DE BUURT:

Contactpersonen en andere vestigingen → [www.sick.com](http://www.sick.com)

creation date: 22.12.2012

revised: 30.06.2022

**SECTION 1: IDENTIFICATION OF THE SUBSTANCE/MIXTURE AND OF THE COMPANY****1.1 Product identifier:****Product name:** RT28HC**1.2 Relevant identified uses of the substance or mixture**

Application area: latent heat accumulators

**1.3 Details of the supplier of the safety data sheet****Company:** Rubitherm Technologies GmbH**Address:** Imhoffweg 6,

DE - 12307 Berlin

**Phone/Fax/E-Mail:** +49 (30) 7109622-0 / msds@rubitherm.com**Internet:** www.rubitherm.com**1.4 Emergency call number**

+49 (30) 7109622-0 ; Mo-Fr; 8:00-16:00,

**SECTION 2: HAZARDS IDENTIFICATION****2.1 Classification of the substance or mixture****Regulation (EC) No 1272/2008**

Aspiration hazard, category 1

**2.2 Label elements****Regulation (EC) Nr.1272/2008****Hazard statements**

H304 May be fatal if swallowed and enters airways.

**Precautionary statements:**

P301 + P310 IF SWALLOWED: Immediately call a POISON CENTER or doctor/physician.

P331 Do NOT induce vomiting.

P405 Store locked up.

**2.3 Other hazards**

EUH066: Repeated exposure may cause skin dryness or cracking.

creation date: 22.12.2012

revised: 30.06.2022

**SECTION 3: COMPOSITION/INFORMATION ON INGREDIENTS****3.1 Substances**

This product is a substance.

<b>Substance</b>	Paraffins, normal C>10
CAS.No.	64771-71-7
EG-No.	
Index-No.	
REACH reg.-No.	
EINEC-No.	265-233-4
<b>hazard</b>	
1272/2008/EG	Asp.1; H304

For the wording of the listed risk phrases refer to section 16

**SECTION4: FIRST AID MEASURES****4.1 Description of first aid measures**

**General advice:** Due spilled liquids surfaces can become slippery. Take off contaminated clothing immediately. If you feel unwell, seek medical advice (show safety data sheet where possible).

**If inhaled:** In case of inhalation the liquid product, call a physician immediately (H304). In the case of inhalation of aerosol/mist move the person concerned to fresh air. If breathing is irregular or stopped, administer artificial respiration and call a physician. If breathing difficulty persists, consult a physician. If necessary supply them with oxygen. At normal ambient temperatures this product will be unlikely to present an inhalation hazard because of its low volatility. At high temperature aerosol/mist can cause an irritation of the respiratory tract.

**In case of skin contact:** Take off all contaminated clothing. Wash off with soap and plenty of water. If skin irritation persists, call a physician.

**In case of eye contact:** Rinse thoroughly with plenty of water for at least 15 minutes and consult a physician. If eye irritation persists, consult a specialist.

**If swallowed:** Do NOT induce vomiting. Keep respiratory tract clear. Call a physician immediately( H304).

**4.2 Most important symptoms and effects, both acute and delayed**

No known symptoms to date.

**4.3 Indication of any immediate medical attention and special treatment needed**

Symptomatic treatment.

creation date: 22.12.2012

revised: 30.06.2022

**SECTION 5: FIREFIGHTING MEASURES****5.1 Extinguishing media****Suitable extinguishing media:**Water spray, carbon dioxide (CO<sub>2</sub>), foam (qualified personnel only), dry (extinguishing) powder**Unsuitable extinguishing media:**

Do not focus the water jet directly to the burning product; could induce spray and spread the fire.  
Avoid simultaneous use of foam and water, water destroys the foam.

**5.2 Special hazards arising from the substance or mixture specific hazards during firefighting**

Exposition to high temperatures may produce hazardous decomposition products such as: carbon dioxide, carbon monoxide, smoke and hot particles. Adapt extinguishing measures to suit the environment.

**5.3 Advice for firefighters special protective equipment for firefighters**

Wear self-contained breathing apparatus and chemical protective suit. Adapt extinguishing measures to the environment.

**SECTION 6: ACCIDENTAL RELEASE MEASURES****6.1 Personal precautions, protective equipment and emergency procedures**

Use personal protective equipment.

Small spilled quantities: normal antistatic working clothes are appropriate.

Large spilled quantities: Use a bodysuit made of chemical resistant and heat resistant material.

**6.2 Environmental precautions**

If the product contaminates rivers and lakes or sewers inform respective authorities. Avoid water ingress underground. Do not flush into surface water or sanitary sewer system.

**6.3 Methods and materials for containment and cleaning up**

Contain escaping material with a non flammable, absorbent substance (e.g. sand), and disposal container in accordance with the legal requirements (see Section 13).

**6.4 Reference to other sections**

Information for safe handling see section 7.

Information about personal protection equipment see section 8.

Information about disposal see section 13.

**SECTION 7: HANDLING AND STORAGE****7.1 Precautions for safe handling****Advice on safe handling:**

Use personal protective equipment. Avoid dust formation and do not breathe in dust. Avoid contact with eyes and skin.

Do not smoke, drink or eat in the working area.

**Advice on protection against fire and explosion**

creation date: 22.12.2012

revised: 30.06.2022

---

Usual measures of preventive fire protection. Keep away from flammable material. Take precautionary measures against static discharges. No smoking.

## **7.2 Conditions for safe storage, including any incompatibilities**

### **Requirements for storage areas and containers:**

**Storage class (TRGS 510):** VCI-storage category (LGK): 10-13 Miscellaneous combustible and non-combustible substances

Store in a cool, dry and well ventilated place, away from foodstuffs in closed containers.

Protect against frost, heat and solar irradiation. Storage of product only in original package. Do not store in passages.

## **SECTION 8: Exposure Control/Personal Protection**

### **8.1 Control Parameters**

**National Occupational Exposure Limits**      No data available.

**European Occupational Exposure Limits**      No data available.

#### **DNEL-value:**

**Paraffins , normal C>10**      No data available.

#### **PNEC-value:**

**Paraffins , normal C>10**      No data available.

## **8.2 Exposure Controls**

### **Personal Protective Equipment:**

Please follow the usual instructions when dealing with chemicals.

Avoid contact with eyes and skin.

Wear suitable protective clothing, gloves and safety glasses.

Do not smoke, drink or eat in the working area.

### **Technological protection:**

Ensure good ventilation at the workplace especially while working with liquid product. Keep storage and handling temperature as low as possible.

### **Material of gloves:**

Fluorinated rubber (FKM), nitrile rubber(NBR), Polychloroprene (CR), (observe the instructions of the manufacturer)

### **Hand protection:**

Wear protective gloves. Consider the data of the manufacturers at the permeability and break-through times. Time of duration can be shortened by environmental and use conditions. Inspect for damages after and before use, replace them if necessary. Use skincare after work.

### **unsuitable gloves:**

creation date: 22.12.2012

revised: 30.06.2022

**Eye protection:**

Safety glasses with side guard. In case of high danger of splashing use additional face shield.

**SECTION 9: PHYSICAL AND CHEMICAL PROPERTIES****9.1 Information on basic physical and chemical properties****Appearance:**

**Physical state:** solid; 20°C; 1013hPa

**Form:** solid

**Colour:** white

**Odour:** almost odourless

**Odour Threshold:** unapplicable

**Safety related data:**

**Explosive properties:** not explosive

**Steam pressure:** No data available.

**Density:** No data available.

**Water solubility:** insoluble

**pH-value:** unapplicable

**Melting point:** 27-28°C

**Boiling point:** >250°C

**Flash point:** 165°C

**Ignition temperature:** >200°C

**9.2 Other data****SECTION 10: STABILITY AND REACTIVITY****10.1 Reactivity**

Stable at room temperature and atmospheric pressure.

**10.2 Chemical stability**

At appropriate storage and handling, the product is stable.

**10.3 Possibility of hazardous reactions**

In case of fire or heating above the recommended maximum temperature the formation of hazardous decomposition products and / or irritating gases may occur.

**10.4 Conditions to avoid**

Direct heating, contamination, direct sunlight, UV or ionizing radiation. Contact with strong oxidizing agents can lead to the risk of fire.

**10.5 Incompatible materials to avoid**

Strong oxidizing agents.

creation date: 22.12.2012

revised: 30.06.2022

**10.6 Hazardous decomposition products** No hazardous decomposition if used and stored according to specifications.

## SECTION 11: TOXICOLOGICAL INFORMATION

### 11.1 Information on toxicological effects

The mixture was not examined in its entirety on toxicological effects. The data refer to the respective component.

#### Paraffins, normal C>10

<b>Acute toxicity:</b>	Oral: LD50 Rat: > 2.000 mg/kg; OECD-Method 401 (literature value) Dermal: LD50 Rabbit: > 2.000 mg/kg; OECD-Methode 402 (literature value)
<b>Skin corrosion/irritation:</b>	Skin: Rabbit: slight irritating; OECD- Method 404 (literature value) Eye: Rabbit: slight irritating; OECD- Method 405 (literature value)
<b>Sensitisation:</b>	Maximization test: Guinea-Pig: not sensitizing; OECD-Method 406 (literatur value)
<b>Carcinogenicity:</b>	No carcinogenic potential expected.
<b>Mutagenicity:</b>	Ames-test: not mutagenic; OECD TG 471; (literature value)
<b>Reproductive toxicity:</b>	No data available.
<b>Additional information:</b>	May be fatal if swallowed and enters airways.

## SECTION 12: ECOLOGICAL INFORMATION

### 12.1 Toxicity

substance	toxicity to fish	toxicity to daphnia	toxicity to algae
Paraffins, normal C5-20	No data available.	Alkanes, C12-26-branched and linear: In range of water solubility not toxic under test conditions.	Alkanes, C12-26-branched and linear: In range of water solubility not toxic under test conditions.

### 12.2 Persistence and degradability

Alkane, C12-26-: easily biodegradable; > 60 %; 28 d; aerob; OECD TG 301 F (conclusion by analogy)

### 12.3 Bioaccumulation potential

No data available.

### 12.4 Mobility in soil

No data available.

### 12.5 Results of PBT and vPvB assessment

No data available.

### 12.6 Other adverse effects

No data available.

## SECTION 13: DISPOSAL CONSIDERATIONS

### 13.1 Waste treatment methods

**Recommendation:** Disposal must be made according to official regulations. The product can be incinerated in accordance with local regulations.

creation date: 22.12.2012

revised: 30.06.2022

**Waste code:** A waste code in accordance with the European Waste Catalogue (EWC) may not be assigned to this product since it admits of a classification only when the consumer uses it for some purpose. The waste code must be determined in agreement with the regional waste disposal authority or company. Disposal should be in accordance with applicable regional, national, and local laws and regulations. EU Waste Disposal Code (EWC): 13 08 99 oil waste not otherwise specified. Classification of waste is always the responsibility of the end user.

**Contaminated packaging:** Contaminated packaging must be handled in the same way as the product.

**Cleaned packaging:** Offer rinsed packaging material to local recycling facilities.

## SECTION 14: TRANSPORT INFORMATION

### 14.1 UN number

#### International Carriage of Dangerous Goods by Road

ADR : No dangerous goods

#### International Carriage of Dangerous Goods by Rail

RID: No dangerous goods

#### International Carriage of Dangerous Goods by Inland Waterways

ADN: No dangerous goods

#### International Maritime Dangerous Goods

IMDG: No dangerous goods

#### Technical Instructions for the Safe Transport of Dangerous Goods by Air

ICAO/IATA: No dangerous goods

### 14.2 Proper shipping name

ADR: No dangerous goods

RID: No dangerous goods

ADN: No dangerous goods

IMDG: No dangerous goods

ICAO/IATA: No dangerous goods

### 14.3 Transport hazard class

ADR: No dangerous goods

RID: No dangerous goods

ADN: No dangerous goods

IMDG: No dangerous goods

ICAO/IATA: No dangerous goods

### 14.4 Packaging group

ADR: No dangerous goods

RID: No dangerous goods

ADN: No dangerous goods

IMDG: No dangerous goods

ICAO/IATA: No dangerous goods

### 14.5 Environmental hazards

creation date: 22.12.2012

revised: 30.06.2022

**ADR:** Not Environmentally Hazardous.**RID:** Not Environmentally Hazardous.**ADN:** Not Environmentally Hazardous.**IMDG:** Not marine pollutant.**ICAO/IATA:** Not Environmentally Hazardous.**14.6 Transport in bulk according to Annex II of MARPOL 73/78 and the IBC Code**

The product is not covered by international regulation on the transport of dangerous goods.

**14.7 Transport in bulk according to Annex II of MARPOL 73/78 and the IBC Code**

not relevant

**SECTION 15: REGULATORY INFORMATION****15.1 Safety, health and environmental regulations/legislation specific for the substance or mixture****Directive 96/82/EC** Directive 96/82/EC does not apply.**Occupational restrictions:** Employment restrictions for children and young workers in accordance with Directive 94/33/EC and the respective national provisions are to be observed.**water hazard class:** WGK 1: water hazard class 1; slightly hazardous to water; classification into Annex 3 of VwVwS;**15.2 Chemical Safety Assessment**

A Chemical Safety Assessment has not been carried out.

**SECTION 16: OTHER INFORMATION****Changes made since the last version:**

This information is based on our present knowledge. However, this shall not constitute a guarantee for any specific product features and shall not establish a legally valid contractual relationship.

**literature references and sources for data:**

<http://gestis.itrust.de/>  
<http://echa.europa.eu/>  
<http://www.reach-clp-helpdesk.de/>

**Rules:**

Substance directive (67/548/EEC).

REACH Regulation 1907/2006/EC.

CLP Regulation (EC) No 1272/2008.

**Full text of H-Statements referred to under sections 2 and 3.**

H304 May be fatal if swallowed and enters airways.

**Safety note:**

P301 + P310 IF SWALLOWED: Immediately call a POISON CENTER or doctor/physician.

P331 Do NOT induce vomiting.

P405 Store locked up.

**safety data sheet****RT28HC**

according to: 1907/2006/EG



creation date: 22.12.2012

revised: 30.06.2022

---

All information in this material safety data sheet (MSDS) is correct to the best of our knowledge, information and belief at the date of its publication. The data given is designed only as guidance for safe handling, use, processing, storage, transportation, disposal and release and is not to be considered a warranty or quality specification. Each customer shall make his own evaluation of appropriate use, shipping and storage for each specific material. Rubitherm makes no warranty either express or implied, including any warranties of fitness for a specific purpose. This safety datasheet does not replace any product information or specification.

# SPECIFICATION FOR APPROVAL

MODEL NO. : AD0824VB-A7BGP P.S. (21)

DESCRIPTION : \_\_\_\_\_

SPEC NO. : SA-0120181016003

ISSUE DATE : 2019.10.24

REVISION : A01

THIS OFFER IS MADE ACCORDING TO YOUR CURRENT INQUIRY.  
UNLESS OTHERWISE REVISED, THIS SPECIFICATION WILL BE FINAL FOR  
ALL FUTURE PRODUCTION OF ORDERS FROM YOUR RESPECTED COMPANY

KINDLY STUDY IN DETAILS AND RETURN TO US THE DUPLICATE DULY  
SIGNED AS YOUR CONFIRMATION OF SAME.



**ADDA CORPORATION**



## DATA-SHEET

Engineering

Printed On: 19/10/24

## BRUSHLESS AXIAL COOLING FANS

Customer	:	Ref: (RoHS)
Adda Model No	: AD0824VB-A7BGP	P.S: (21)
Samples attached	: Piece(s),	
Safety Approval	: UL,CUL,TUV,CE	TUV:EN 60950-1:2006+A11+A1+A12+A2 UL:UL507 CE:EN 61000-6-1:2007 EN 61000-6-3:2007+A1

## Specifications

ITEM	SPECIFICATION / CONDITION				
DIMENSIONS	:	80x80x25	mm		
BEARING TYPE	:	TWO BALL			
RATED VOLTAGE	:	24	VDC		
OPERATING VOLTAGE RANGE	:	22.8	VDC	—	25.2 VDC
OPERATING DUTY CYCLE RANGE	:	30% ~ 100%			
START-UP DUTY CYCLE	:	30% Max	(AT RATED VOLTAGE)		
REAL CURRENT	:	0.24	Amp		
REAL POWER	:	5.76	Watt		
RATED CURRENT	:	0.38	Amp	+ 10	%MAX (Duty cycle 100%)
RATED POWER	:	9.12	Watt		(Duty cycle 100%)
RATED SPEED	:	5000	RPM	± 10	% (Duty cycle 100%)
		(IN FREE AIR AT RATED VOLTAGE)			
AIR FLOW	:	68.858	CFM	(min.: 61.972	CFM)
AIR FLOW	:	1.948	CMM	(min.: 1.753	CMM)
		(IN FREE AIR AT RATED VOLTAGE)			
STATIC AIR PRESSURE	:	0.388	Inch H <sub>2</sub> O	(min.: 0.314	Inch H <sub>2</sub> O)
STATIC AIR PRESSURE	:	9.855	mm H <sub>2</sub> O	(min.: 7.982	mm H <sub>2</sub> O)
		(IN FREE AIR AT RATED VOLTAGE)			
NOISE LEVEL	:	48.9	dB (A)	(max.: 52.9	dB(A))
MOTOR PROTECTION	:	BY	IC		
POLARITY PROTECTION	:	YES			
CONNECTION LEAD TYPE	:	WIRE, AWG#	26		
LIFE EXPECTANCY	:	70000	Hours at	40°C / 65% RH	
NET WEIGHT	:	95	Gram.		
PACKING	:	200	pcs. Per Export Carton.		

\* If no PWM signal is present (no connection to the PWM drive signal),

the fan should be run at rated speed RPM.

\* The fan should be run,at Max of start -up duty cycle.

Unless otherwise stated, the relative humidity is 65%, and the temperature is 25°C for the standard testing.

Should you have any doubt, please refer to the environmental conditions specified in the acknowledgement document.



ADDA CORPORATION	Model No.: AD0824VB-A7BGP	P.S: (21)	Page 1/6
------------------	---------------------------	-----------	----------

# SPECIFICATION

## 1 · 0 SCOPE

- 1.1 If the information or other related document is inconsistent with this acknowledgement document, please refer to the acknowledge document.
- 1.2 This documentation defines the mechanical & electrical characteristics of DC brushless fans.
- 1.3 The specification of this product is described in details in the acknowledgement document. No guarantee is given to our product under the use of over specifications.
- 1.4 For any change or amendment to the specifications, such change will be noticed in writing beforehand.
- 1.5 If the product is used on the MIS system, please specify the specification in the purchase order.

## 2 · 0 MATERIAL

- |                 |   |  |
|-----------------|---|--|
| 2 · 1 Frame     | : | UL94V-0 Glass Filled polyester (P.B.T) |
| 2 · 2 Fan Blade | : | UL94V-0 Glass Filled polyester (P.B.T) |
| 2 · 3 RoHS      | : | (V) YES                                |
| HF              | : | ( ) YES                                |

## 3 · 0 DIMENSIONS & CONSTRUCTION

All dimensions, Direction of rotation and air flow were specified as per drawing attached.

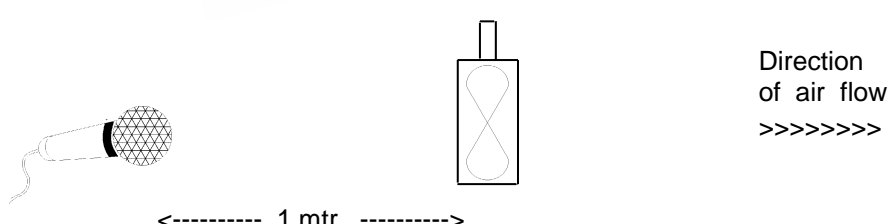
## 4 · 0 CHARACTERISTICS & DEFINITION

- 4 · 1 All rated characteristics were specified as per data sheet enclosed.
- 4 · 2 Rated Current : Rated Current shall be measured after 3 minutes of continuous rotation at rated voltage.
- 4 · 3 Rated Speed : Rated Speed shall be measured after 3 minutes of continuous rotation at rated voltage.
- 4 · 4 Start Voltage : The voltage which is able to start the fan to operate by suddenly switching 'ON'.
- 4 · 5 Input Power : Input Power shall be measured after 3 minutes of continuous rotation at rated voltage.
- 4 · 6 Locked Rotor Current : Locked current shall be measured within one minute of rotor locked, after 3 minutes of continuous rotation at rated voltage in clean air.
- 4 · 7 Air Flow & Static Pressure : The air flow data and static pressures should be determined in accordance with AMCA-210 standard in a doublechamber testing with intake – side measurement.
- 4 · 8 Noise Level : The measurement of noise level is carried out with reference to ISO7779 in a semi-anechoic chamber with the microphone positioned 1 meter from the air intake. Testing fan shall be hung in clean air .

### NOISE LEVEL MEASUREMENT

Mic.

Fan



# SPECIFICATION

## 5.0 MECHANICAL INSPECTION

### 5.1 Rotation Direction

Counterclockwise when look into impeller side.

### 5.2 Protection

All fans have integrated protection against locked rotor condition so that there will be no damage to winding or any electronic component.

Restarting is automatic as soon as any constraint to rotation has been released.

As fan placed at dead angle position, and the switch was changed from off to on. Restarting was automatic normal as soon as and proved that this fan is good fan.

### 5.3 Locked Rotor Protection

No damage shall be found after 72 hours continuously at condition of rotation locked.

Restarting is automatic as soon as constraint to running has been released.

### 5.4 Avoid the damage, check the correct voltage and proper polarity before connecting with power.

### 5.5 Free Drop Shock

In minimum package condition, the fan should withstand drops on any three faces from a height of 30cm onto a wood board of 10mm thick.

### 5.6 Please do not stick a grease and/or an oil to the fan housing or blade which may have a harmful influence by a chemical reaction at high humidity.

### 5.7 If the fan is reinstalled, please pay special attention to the noise due to the vibration (or resonance).

### 5.8 During the testing of the fan, please make sure the finger guard is used for safety.

## 6.0 ELECTRICAL INSPECTION

### 6.1 Insulation Resistance

Not less than 10M ohm between housing and positive end of lead wire (red) at 500V DC.

### 6.2 Dielectric Strength

No damage should be found at 500 VAC for 60 seconds, measured with 1mA trip current between housing and positive end of lead wire.

### 6.3 Life Expectancy

The continuous duty life at given temperature after which, 90% of testing units shall still be running.

### 6.4 While the fan is running, do not intentionally lock the fan for a long time since the overheating of the motor produced by the long-time locking will damage the fan.

## 7.0 ENVIRONMENTAL

### 7.1 Improper use such as disassembling the fan, being covered with dust, or dipping the fan in water that results in defects is not covered in the warranty. Do not use the fan in the environment with corrosive air or liquid.

### 7.2 Operating Temperature / Humidity

-10°C to +70°C at humidity 65%+/-20% RH.

### 7.3 Storage Temperature

All function shall be normal after 500 hours storage at -40°C to +70 °C with a 24 hour recovery period at room temperature.

### 7.4 Humidity

After 96 hours, 95% RH, 40+/-2°C per MIL-STD-202F, method 103B humidity test, the measured data on insulation resistance and dielectric strength shall meet the specification.

### 7.5 Do not place or store the fan in the environment with high/low temperature/humidity. If the fan is stored for more than 6 months, functional test is highly recommended before using.



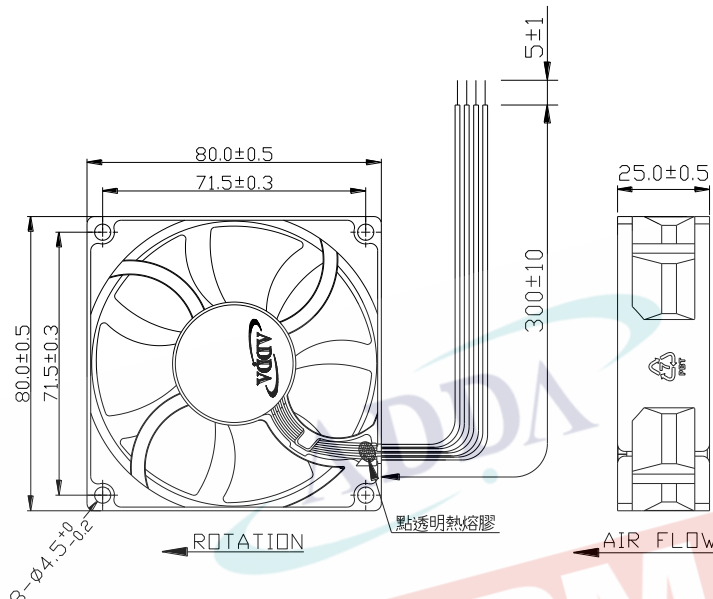
# SPECIFICATION

## 8.0 REMARKS

- 8.1 Material and construction are subject to change without advance notice. The changes should be within specification.  
8.2 All fans shall meet the quality inspection under sampling plan MIL-STD-105E as follow:

Critical	0.25%
Major	1.00%
Minor	2.50%

## 9.0 OUTLINE STYLING & DIMENSIONS



LEAD WIRES : UL 1061, AWG26, L =  $300\pm 10$  mm  
Red = positive ; Black = negative.  
White = FG ; Blue = PWM

## 10.0 Notes:

- 10.1 Please do not touch and push Fan Blade with fingers or others, fan blade and ball bearings may be damaged and it causes noise defect.
- 10.2 Do not carry the fan by its lead wires.
- 10.3 If the fan does not have the polarity protection function, the connection of the colored wires should be red + red, and black + black, or else the fan will be damaged in no time.
- 10.4 For the models without reverse connection of polarity protection, please do not connect the lead wire in reverse
- 10.5 Please don't install this fan in series with 2x voltage inputs. For example, if a single fan rated at 12V, then don't install two of them in series with 24V input.
- 10.6 Every specific fan is designed for its certain application (project). Therefore, if you want to use this fan in other application (project), please inform ADDA first so that we can confirm whether there is any issue which might be incurred from the reason of this different application (project) or not.
- 10.7 The "Life Expectancy" of this fan has not been evaluated for use in combination with any end application. Therefore, the Life Expectancy in the Test Reports(L10 and MTTF Report) that relate to this fan is for reference only and shall not construe any kind of warranty of ADDA to the life of any specific fan, either expressed or implied.
- 10.8 The period of product warranty, unless otherwise agreed by ADDA in written, shall be 12 months starting from the date of production.
- 10.9 In Lead Wire, there is a possibility to come off from frame.
- 10.10 In order to avoid abnormal bumping or interference caused by deformed impeller when fan is fastened, suggested distance of at least 0.5mm is strongly reserved in front of the frame (the sight from the impeller face).
- 10.11 Hot swapping or Hot plugging is not allowed to cause damage to fans. Notice in advance is strongly requested if design for Hot swapping or Hot plugging is needed.



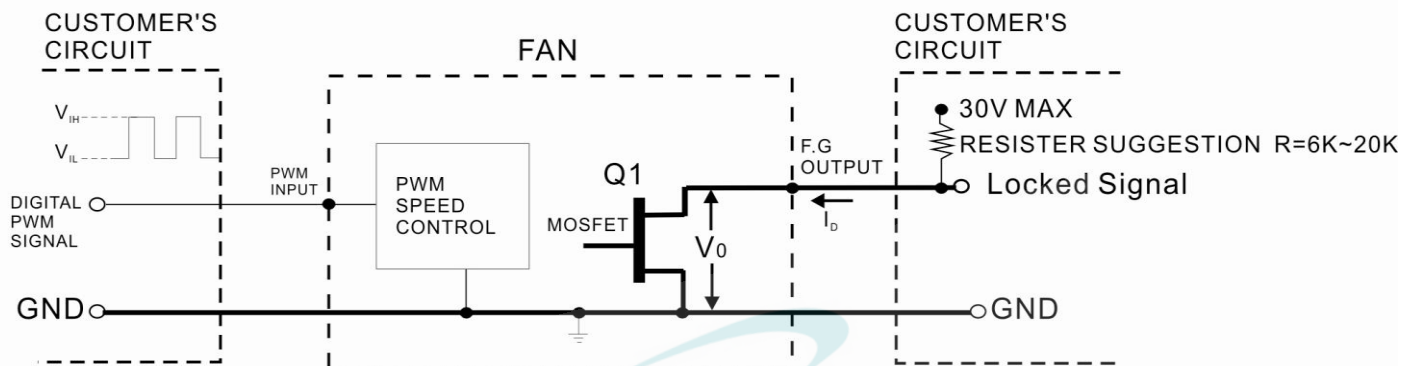


## PROVISION OF DIGITAL PWM SPEED CONTROL &amp; LOCKED SIGNAL(F.G)

• OUTPUT OF LOCKED SIGNAL -----OPEN DRAIN TYPE

\*Electrical design suggestion: R=3K~10K

(External signal function design is decided by customer)



\*MOSFET Q1 AT "ON" POSITION

DRAIN CURRENT----- $I_D = 5\text{mA MAX}$

SATURATION VOLTAGE----- $V_{OL} = 1.0\text{V MAX}$

\*MOSFET Q1 AT "OFF" POSITION

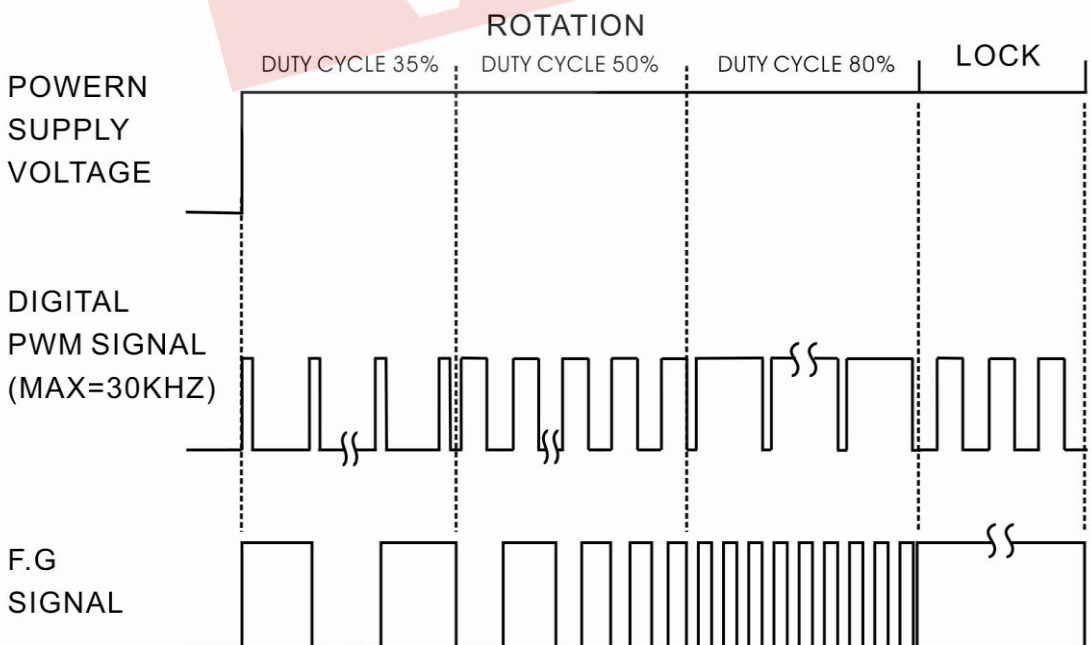
RELEASE VOLTAGE----- $V_{OH} = 30\text{V MAX}$

\*DIGITAL PWM SPEED CONTROL POSITION

PWM INPUT VOLTAGE HIGH----- $V_{IH} = 3.0\text{V} \sim 5.5\text{V}$

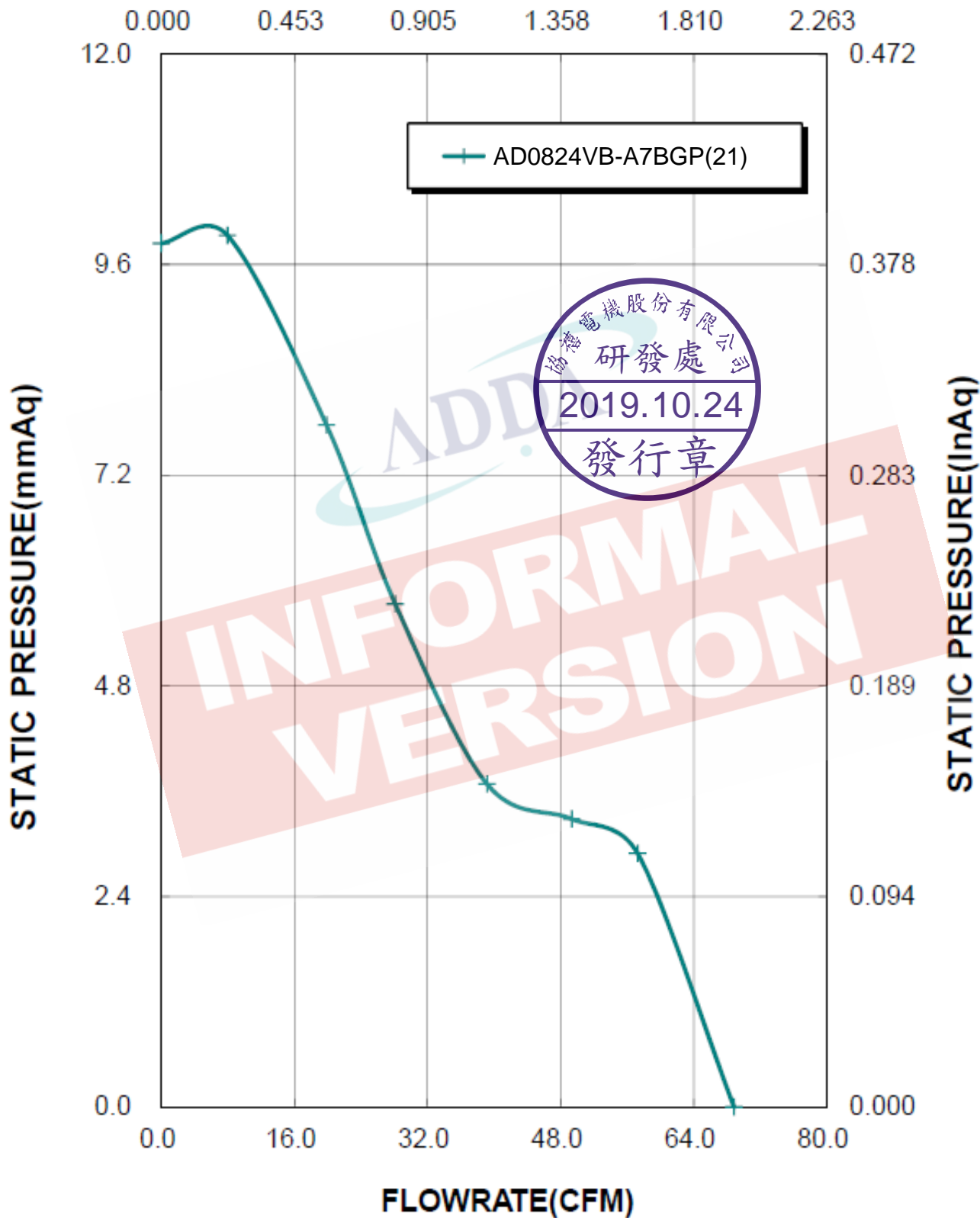
PWM INPUT VOLTAGE LOW----- $V_{IL} = 0\text{V} \sim 0.5\text{V}$

\*PWM INPUT FREQUENCY----- FPWM:18~30KHZ



## Fan Performance Curve

FLOWRATE(CMM)



# MEM1G series



## Ordering information

Example:

M EM1 G12 Z

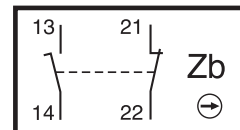
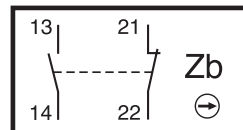
Casing:  
EM1 = metal casing  
30mm width

Actuators: codes G11 -  
G9999

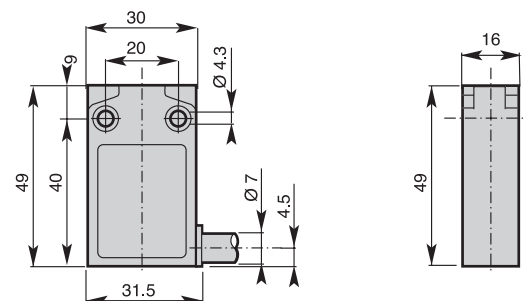
Contact block  
Z: Zb Snap action 1 N.O. + 1 N.C.  
X: Zb Slow action non-overlapping late make 1 N.O. + 1 N.C.

## Contacts

Z: Snap action 1 N.O. + 1 N.C. X: Slow action break before make 1 N.O. + 1 N.C.



## Dimensions (basic)





## Features

- Double Insulation
- 30mm width
- Casing made of metal
- Visible operation
- Able to switch strong currents (10A conventional thermal current)
- Electrically separated contacts
- Precise operating points (consistency)
- Immune to electromagnetic disturbances
- Degree of protection: IP67
- Standard cable length 1m\*..

## General technical data

	Metal casing		
Standards	Devices conform with international IEC 947-5-1 and European EN 60 947-5-1 standards		
Certifications - Approvals	UL (upon request)		
Ambient temperature – during operation – for storage	°C °C	– 25 ... + 70 – 40 ... + 70	
Mounting positions	All positions are authorised		
Protection against electrical shocks (acc. to IEC 536)	Class I		
Degree of protection (according to IEC 529 and EN 60 529)	IP67		
Degree of protection (according to UL50)	Type 4 - 4X - 6 enclosure ("outdoor use - raintight - water tight corrosion resistant")		
<b>Electrical Data</b>			
Rated insulation voltage $U_i$ - according to IEC 947-1 and EN 60 947-1 - according to UL 508 and CSA C22-2 n° 14	400V (pollution degree 3) (250V for M12 connector) B 300, R 300		
Rated impulse withstand voltage $U_{imp}$ (according to IEC 947-1 and EN 60 947-1)	kV	4	
Conventional free-air thermal current $I_{th}$ (according to IEC 947-5-1) $\sigma < 40^\circ\text{C}$	A	5 (4A for M12 connector)	
Short-circuit protection $U_e < 500\text{V a.c.} - \text{gG (gl) type fuses}$	A	6	
Rated operational current $I_e / \text{AC-15}$ (according to IEC 947-5-1)	24V - 50/60Hz 120V - 50/60Hz 240V - 50/60Hz	A A A	5.0 3.0 1.5
$I_e / \text{DC-13}$ (according to IEC 947-5-1)	24V DC 125V DC 250V DC	A A A	1.1 0.22 0.1
Switching frequency	Cycles/h	3600	
Load factor		0.5	
Resistance between contacts	mΩ	25	
Mechanical durability		10 millions of operations	

\* For other cable inlets and cable lengths, please contact your local sales office.

# MEM1G series

## Product number

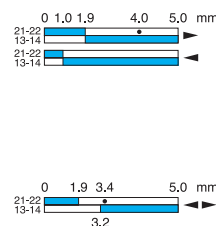
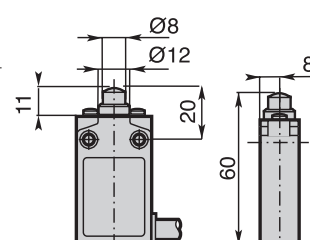
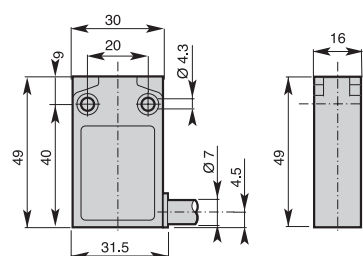
## Dimensions (basic)

## Dimensions (head)

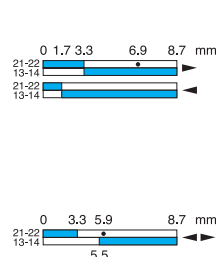
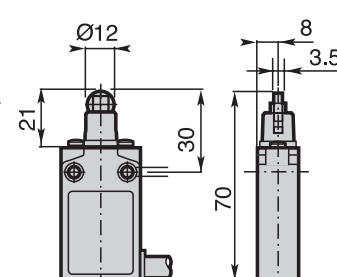
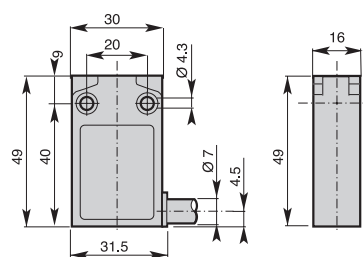
## Operation diagram



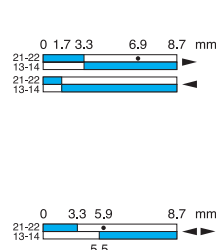
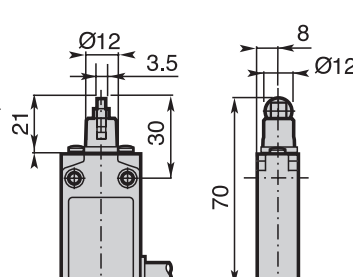
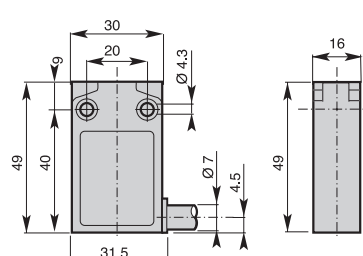
Plain plunger  
MEM1G11\*



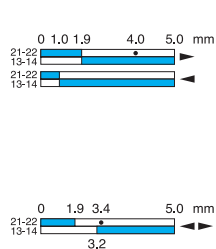
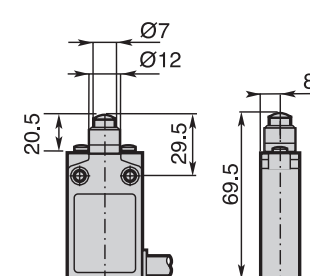
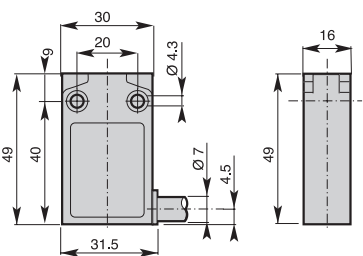
Roller plunger  
MEM1G12\*  
G12: metall roller  
G13: nylon roller



Cross roller plunger  
MEM1G14\*  
G14: metall roller  
G15: nylon roller



Plain plunger with  
dust protection cap  
MEM1G16\*\*



\* Snap action: Z or X  
\*\* Snap action: Z

**Product number**

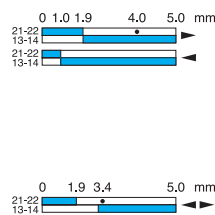
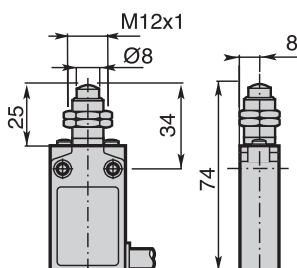
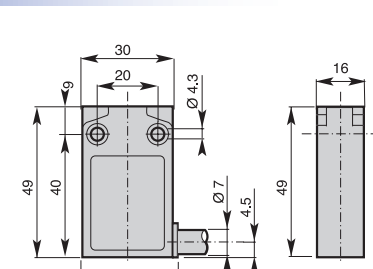
**Dimensions (basic)**

**Dimensions (head)**

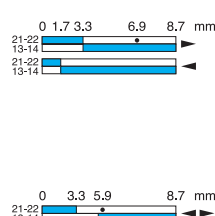
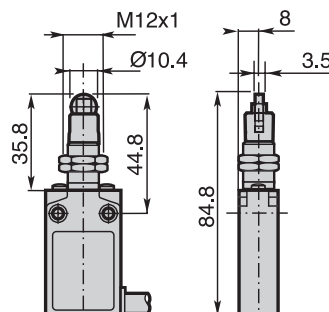
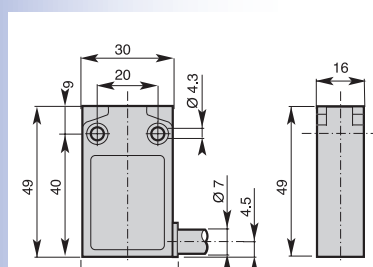
**Operation diagram**



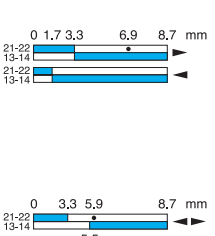
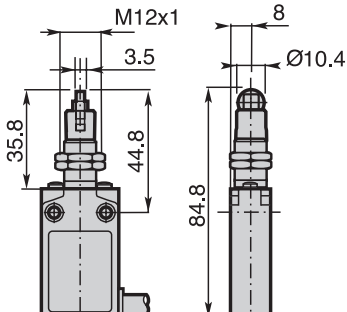
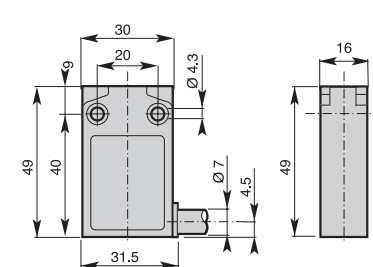
**Plain plunger with fixing nuts**  
MEM1G21\*



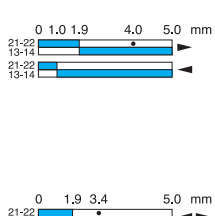
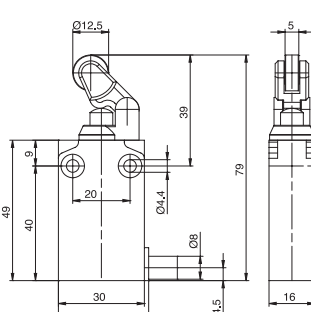
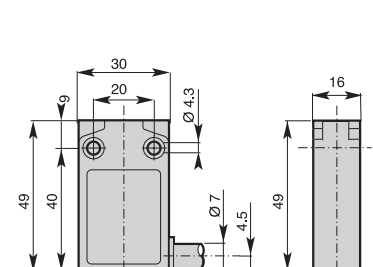
**Roller plunger with fixing nuts**  
MEM1G22\*  
G22: metall roller  
G23: nylon roller



**Cross roller plunger with fixing nuts**  
MEM1G24\*  
G24: metall roller  
G25: nylon roller



**Plain plunger with fixing nuts**  
MEM1G31\*



\* Snap action: Z or X  
\*\* Snap action: Z

## MEM1G series

### Product number

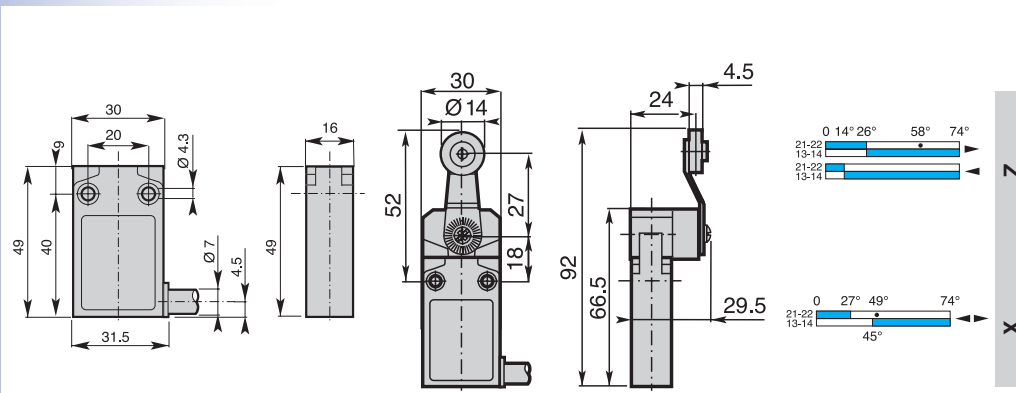
### Dimensions (basic)

### Dimensions (head)

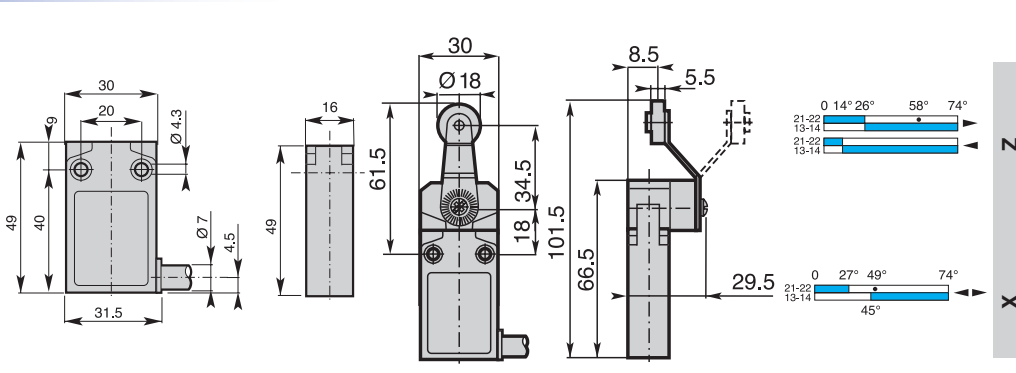
### Operation diagram



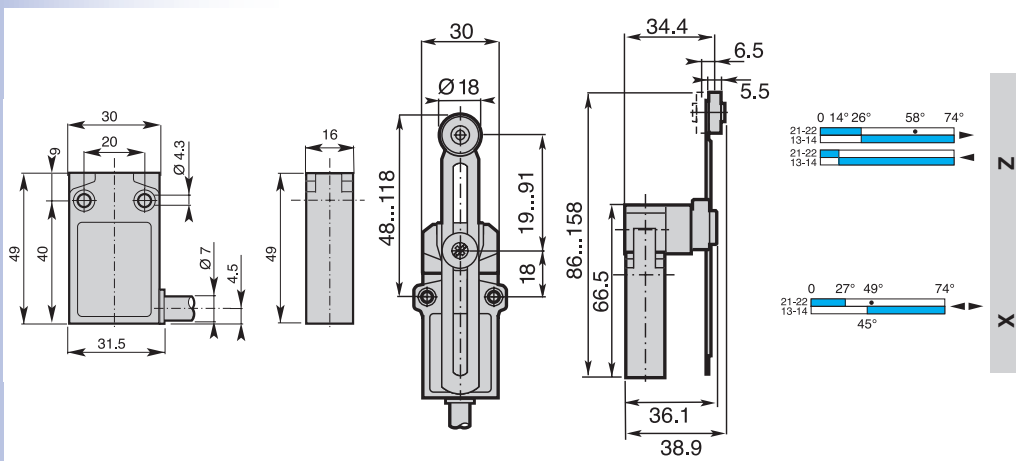
**Roller lever**  
MEM1G41\*  
G41: metal roller  
G42: nylon roller  
G43: ball bearing



**Roller lever**  
MEM1G45\*  
G45: nylon roller  
G46: metal roller



**Adjustable lever with roller**  
MEM1G51\*  
G51: nylon roller  
G53: metal roller



\* Snap action: Z or X

\*\* Snap action: Z

**Product number**

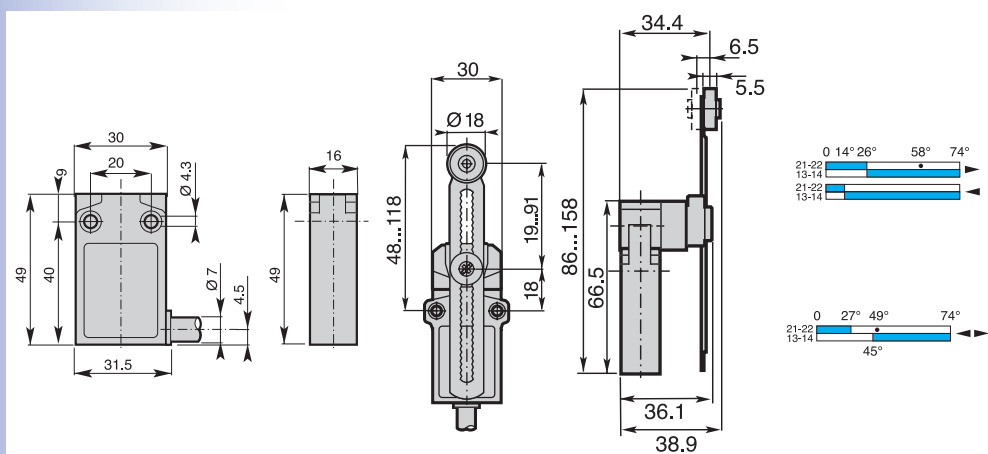
**Dimensions (basic)**

**Dimensions (head)**

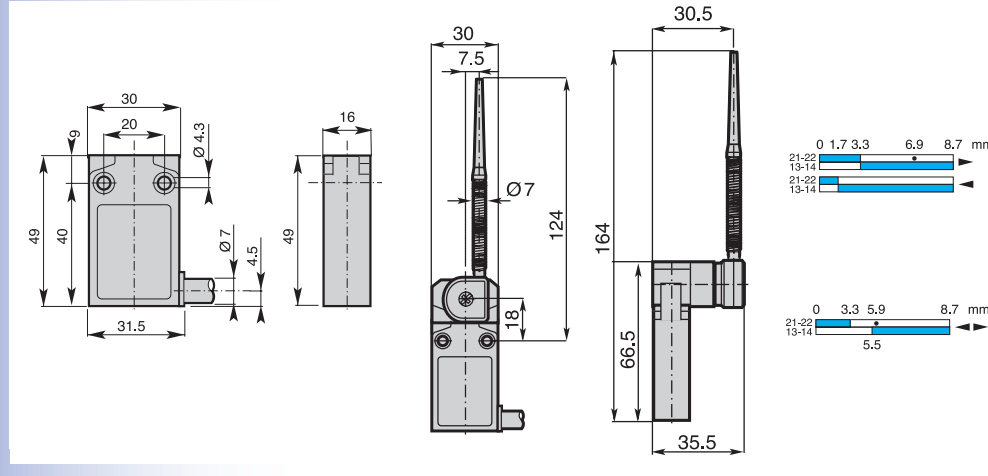
**Operation diagram**



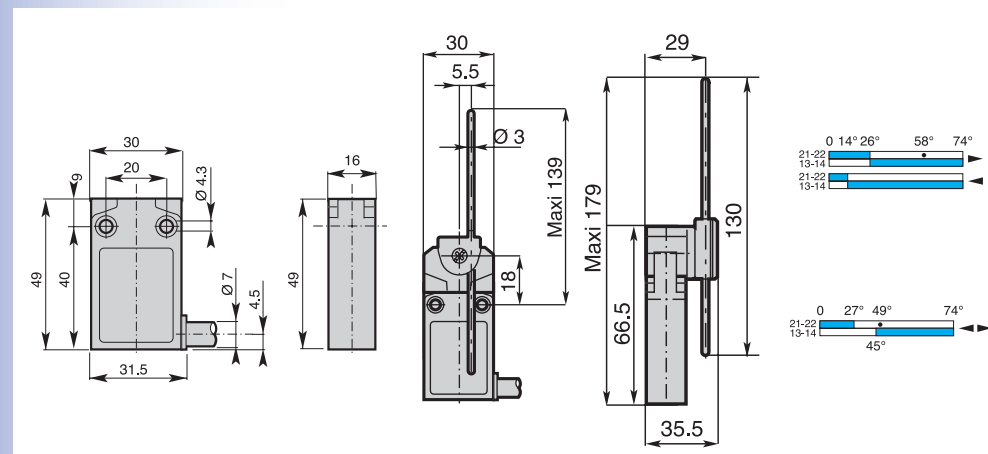
Adjustable toothed lever (step 2mm)  
with nylon roller  
MEM1G5100\*



Nylon actuator with  
stainless steel spring  
MEM1G61\*



Adjustable rod lever  
MEM1G71\*  
G71: stainless steel rod  
G72: fiberglass rod  
G75: square steel rod



\* Snap action: Z or X

\*\* Snap action: Z

## MEM1G series

### Product number

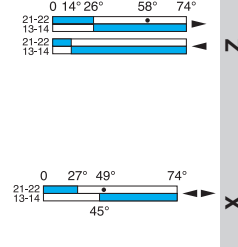
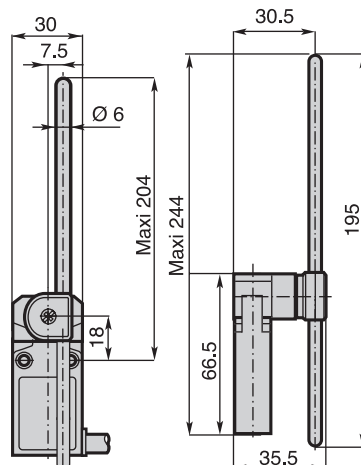
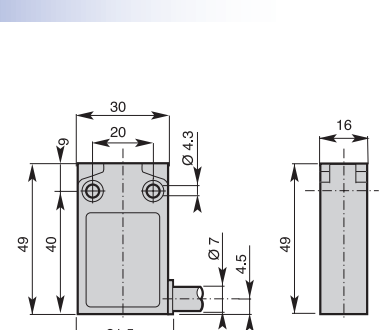
### Dimensions (basic)

### Dimensions (head)

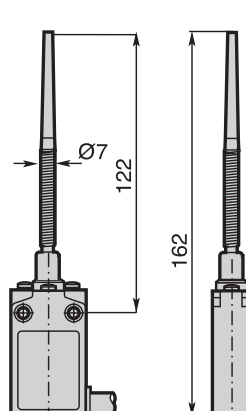
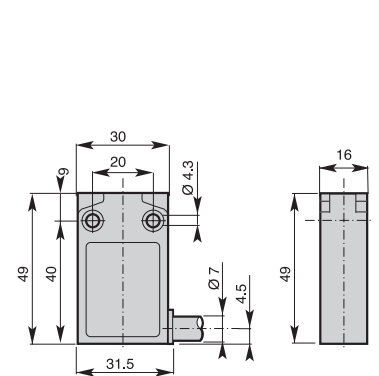
### Operation diagram



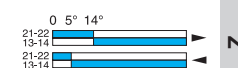
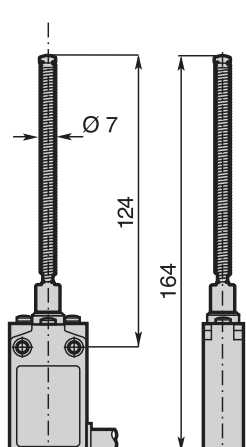
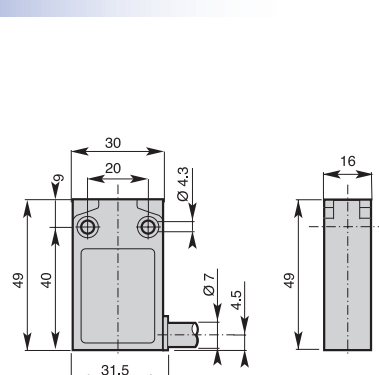
**Adjustable rod lever**  
MEM1G73\*  
G73: nylon rod  
G74: fiberglass rod



**Multidirectional nylon actuator with stainless steel spring**  
MEM1G92\*\*



**Multidirectional actuator with stainless steel spring**  
MEM1G93\*\*



# Data sheet

**RUBITHERM**  
PHASE CHANGE MATERIAL

## RT28HC



RUBITHERM® RT is a pure PCM, this heat storage material utilising the processes of phase change between solid and liquid (melting and congealing) to store and release large quantities of thermal energy at nearly constant temperature. The RUBITHERM® phase change materials (PCM's) provide a very effective means for storing heat and cold, even when limited volumes and low differences in operating temperature are applicable.

### Properties for RT-line:

- high thermal energy storage capacity
- heat storage and release take place at relatively constant temperatures
- no supercooling effect, chemically inert
- long life product, with stable performance through the phase change cycles
- melting temperature range between -9 °C and 100 °C available

### The most important data:

**Melting area**

#### Typical Values

**27-29** [°C]

main peak: 28

**Congealing area**

**29-27** [°C]

main peak: 27

**Heat storage capacity ± 7,5%**

**250** [kJ/kg]\*

Combination of latent and sensible heat in a temperatur range of 21°C to 36 °C.

**70** [Wh/kg]\*

**Specific heat capacity**

**2** [kJ/kg·K]

**Density solid**  
at 15°C

**0,88** [kg/l]

**Density liquid**  
at 40°C

**0,77** [kg/l]

**Heat conductivity (both phases)**

**0,2** [W/(m·K)]

**Volume expansion**

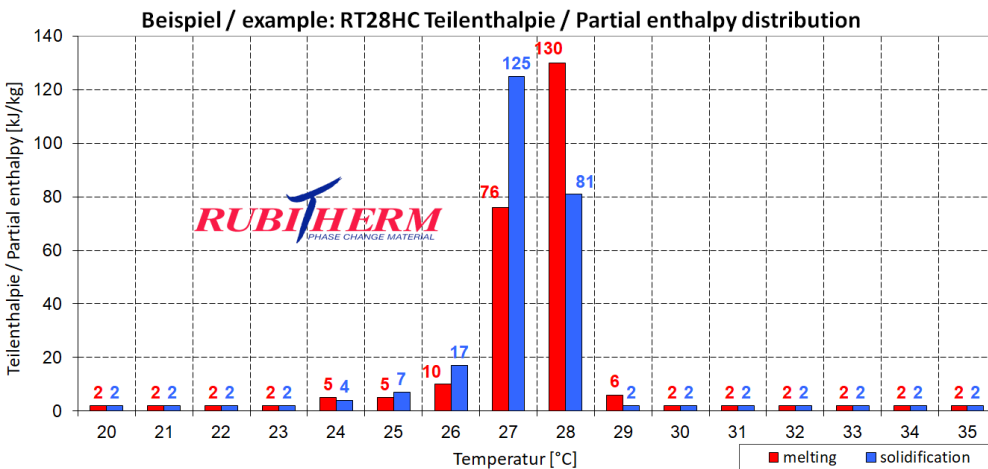
**12,5** [%]

**Flash point**

**165** [°C]

**Max. operation temperature**

**50** [°C]



\*Measured with 3-layer-calorimeter.

# Data sheet

## RT24HC



RUBITHERM® RT is a pure PCM, this heat storage material utilising the processes of phase change between solid and liquid (melting and congealing) to store and release large quantities of thermal energy at nearly constant temperature. The RUBITHERM® phase change materials (PCM's) provide a very effective means for storing heat and cold, even when limited volumes and low differences in operating temperature are applicable.

### Properties for RT-line:

- high thermal energy storage capacity
- heat storage and release take place at relatively constant temperatures
- no supercooling effect, chemically inert
- long life product, with stable performance through the phase change cycles
- melting temperature range between -9 °C and 100 °C available

### The most important data:

**Melting area**

#### Typical Values

**23-26** [°C]

main peak: 24

**Congealing area**

**24-22** [°C]

main peak: 24

**Heat storage capacity ± 7,5%**

**200** [kJ/kg]\*

Combination of latent and sensible heat in a temperatur range of 16°C to 31 °C.

**56** [Wh/kg]\*

**Specific heat capacity**

**2** [kJ/kg·K]

**Density solid**  
at 20°C

**0,8** [kg/l]

**Density liquid**  
at 28°C

**0,7** [kg/l]

**Heat conductivity (both phases)**

**0,2** [W/(m·K)]

**Volume expansion**

**12** [%]

**Flash point**

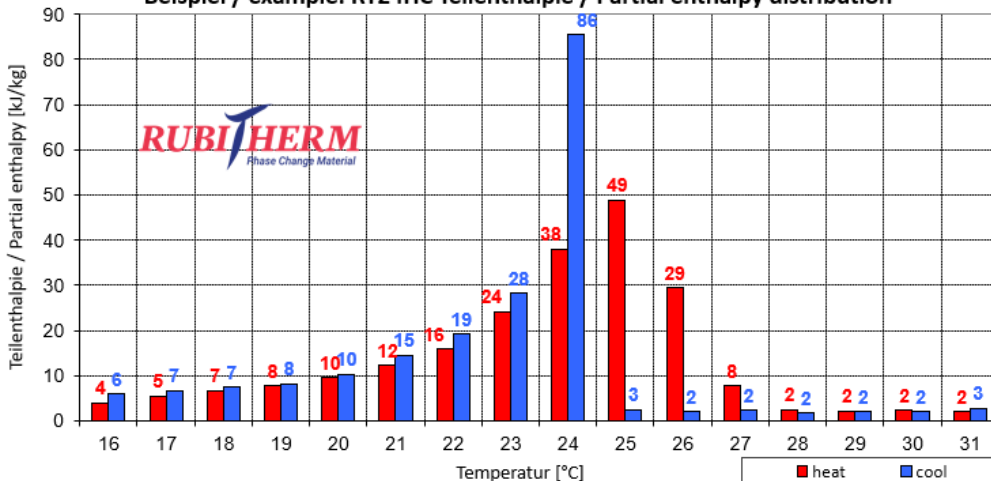
**150** [°C]

**Max. operation temperature**

**56** [°C]



Beispiel / example: RT24HC Teilenthalpie / Partial enthalpy distribution\*



Rubitherm Technologies GmbH  
Imhoffweg 6  
D-12307 Berlin  
phone: +49 (30) 7109622-0  
E-Mail: info@rubitherm.com  
Web: www.rubitherm.com

The product information given is a non-binding planning aid, subject to technical changes without notice.  
Version: 18.11.2022

\*Measured with 3-layer-calorimeter.

# Data sheet

**RUBITHERM**  
PHASE CHANGE MATERIAL

## RT21HC



RUBITHERM® RT is a pure PCM, this heat storage material utilising the processes of phase change between solid and liquid (melting and congealing) to store and release large quantities of thermal energy at nearly constant temperature. The RUBITHERM® phase change materials (PCM's) provide a very effective means for storing heat and cold, even when limited volumes and low differences in operating temperature are applicable.

### Properties for RT-line:

- high thermal energy storage capacity
- heat storage and release take place at relatively constant temperatures
- no supercooling effect, chemically inert
- long life product, with stable performance through the phase change cycles
- melting temperature range between -9 °C and 100 °C available

### The most important data:

**Melting area**

#### Typical Values

**20-23** [°C]

main peak: 21

**Congealing area**

**21-19** [°C]

main peak: 21

**Heat storage capacity ± 7,5%**

**190** [kJ/kg]\*

Combination of latent and sensible heat in a temperatur range of 13°C to 28 °C.

**53** [Wh/kg]\*

**Specific heat capacity**

**2** [kJ/kg·K]

**Density solid**  
at 15°C

**0,88** [kg/l]

**Density liquid**  
at 25°C

**0,77** [kg/l]

**Heat conductivity (both phases)**

**0,2** [W/(m·K)]

**Volume expansion**

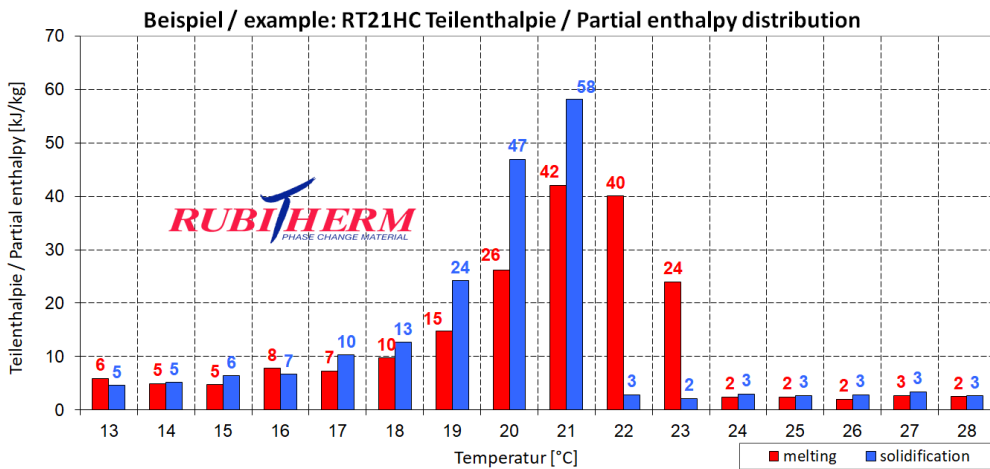
**14** [%]

**Flash point**

**140** [°C]

**Max. operation temperature**

**45** [°C]



\*Measured with 3-layer-calorimeter.

# Data sheet

**RUBITHERM**  
PHASE CHANGE MATERIAL

## RT18HC



RUBITHERM® RT is a pure PCM, this heat storage material utilising the processes of phase change between solid and liquid (melting and congealing) to store and release large quantities of thermal energy at nearly constant temperature. The RUBITHERM® phase change materials (PCM's) provide a very effective means for storing heat and cold, even when limited volumes and low differences in operating temperature are applicable.

### Properties for RT-line:

- high thermal energy storage capacity
- heat storage and release take place at relatively constant temperatures
- no supercooling effect, chemically inert
- long life product, with stable performance through the phase change cycles
- melting temperature range between -9 °C and 100 °C available

### The most important data:

**Melting area**

#### Typical Values

**17-19** [°C]

main peak: 18

**Congealing area**

**19-17** [°C]

main peak: 17

**Heat storage capacity ± 7,5%**

**260** [kJ/kg]\*

Combination of latent and sensible heat in a temperatur range of 11°C to 26 °C.

**72** [Wh/kg]\*

**Specific heat capacity**

**2** [kJ/kg·K]

**Density solid**  
at 15°C

**0,88** [kg/l]

**Density liquid**  
at 25°C

**0,77** [kg/l]

**Heat conductivity (both phases)**

**0,2** [W/(m·K)]

**Volume expansion**

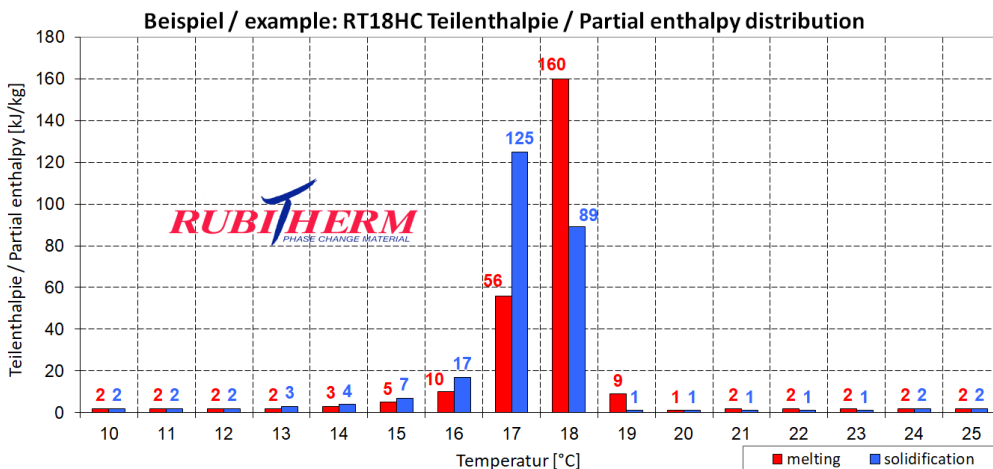
**12,5** [%]

**Flash point**

**135** [°C]

**Max. operation temperature**

**50** [°C]

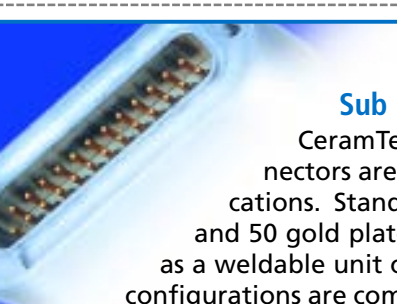


Rubitherm Technologies GmbH  
Imhoffweg 6  
D-12307 Berlin  
phone: +49 (30) 7109622-0  
E-Mail: info@rubitherm.com  
Web: www.rubitherm.com

The product information given is a non-binding planning aid, subject to technical changes without notice.  
Version: 09.10.2020

\*Measured with 3-layer-calorimeter.

### **C.0.1 Vacuum feedthrough connectors**



### Sub D Type (MIL-C-24308) Connectors

CeramTec's hermetic Subminiature D type connectors are designed to meet MIL-C-24308 specifications. Standard configurations include 9, 15, 25, and 50 gold plated pin connectors, which are available as a weldable unit or in a ConFlat® or ISO flange. Custom configurations are commonplace and available upon request. CeramTec is able to achieve a very high pin/lead density (standard - up to 50 pins) using glass-ceramic sealing technology. The rugged stainless steel shell design is built to withstand severe environments and reduces seal failure due to overheating while welding. These connectors are used primarily to provide instrumentation signals, voltage and/or current into a high-vacuum or ultra-high vacuum environment, with an in-line connection to outside instrumentation.

### In-Vacuum Ribbon Cable

CeramTec's in-vacuum ribbon cable is designed to complement our Sub D Type (MIL-C-24308) hermetic multipin connector product line and therefore cable configurations include 9, 15, or 25 conductor cable. Note that 50 conductor cables are created by using two 25 conductor cables. Each of the Kapton® wrapped (19 x 0.0063) 22 AWG silver plated copper conductors are woven with a PEEK (polyether ether ketone) monofilament in order to achieve the ribbon cable form. The multistranded wrapped cable offers the most flexible solution and has a temperature range up to 200° C. All ribbon cable assembly materials are ultra-high vacuum (UHV) compatible. The ribbon cables are vacuum baked out prior to shipping. Additional vacuum bake out prior to use is also recommended. All cable assembly components are sold separately.

### Specifications

#### Materials

Shell: 304 Stainless steel

Pins: 300 Series Stainless steel (Gold Plated)

Insulation: Glass-ceramic

Magnetic Materials: No

**Voltage Rating** 500 V DC

**Current Rating** 5 Amps per pin

**Temperature Range** -269°C to 450°C, ISO KF -25°C to 205°C

**Pressure @ 20°C** ISO KF 0 PSIG

9 Pin - 1350 PSIG (93.1 Bar)	25 Pin - 1200 PSIG (82.7 Bar)
15 Pin - 1250 PSIG (86.2 Bar)	50 Pin - 900 PSIG (62.1 Bar)

### Vacuum Side Plug Specifications

#### Materials

Shell/Insulation: PEEK (polyether ether ketone)

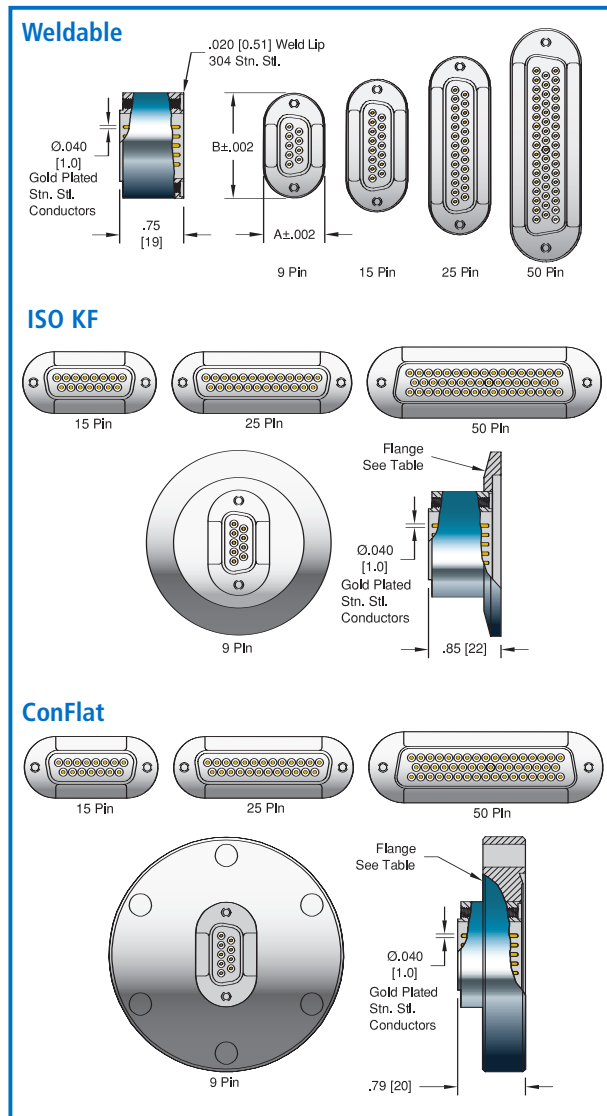
Crimp Contacts: Copper alloy (Gold Plated)

Magnetic Materials: No

**Voltage Rating** 500 V DC

**Current Rating** 15 Amps

**Temperature Range** -269°C to 200°C



### Ribbon Cable Specifications

#### Materials

Insulation: Kapton® Type FN

Weave: PEEK (polyether ether ketone) monofilament

**Number of Conductors** 9, 15, 25

#### Conductor

22 AWG 19 / 0.0063" stranded silver plated copper

**Voltage Rating** 600 V AC, 850 V DC

**Current Rating** 5 Amps per conductor

**Temperature Range** -55°C to 200°C

**Resistance @ 20°C** 119Ω/km



NO. PINS	INSTALLATION	DIMENSIONS		PART NUMBER
		A	B	
9	Weld	0.720 [18.29]	1.234 [31.34]	16800-01-W
15	Weld	0.720 [18.29]	1.562 [39.67]	16801-01-W
25	Weld	0.720 [18.29]	2.102 [53.39]	16802-01-W
50	Weld	0.832 [21.13]	2.738 [69.54]	16804-01-W



ISO FLANGE				
9	NW40KF	-	-	18605-01-KF
15	NW50KF	-	-	18606-01-KF
25	NW63LF	-	-	20306-01-CLF
50	NW100LF	-	-	20307-01-CLF



CONFLAT FLANGE				
9	2 3/4" (NW35CF)	-	-	18607-01-CF
15	3 3/8" (NW50CF)	-	-	18608-01-CF
15	4 1/2" (NW63CF)	-	-	21108-01-CF
25	4 1/2" (NW63CF)	-	-	18609-01-CF
50 (2x25)	4 1/2" (NW63CF)	-	-	21109-01-CF
50	6" (NW100CF)	-	-	18610-01-CF
100 (2x50)	6" (NW100CF)	-	-	21641-01-CF



TYPE	VOLTAGE DC	QTY	CONTACTS AMPS	MATERIAL	D	DIMENSIONS W	H	TEMPERATURE °C MIN MAX	MAGNETIC MATERIALS	PART NUMBER
Air Side	500 V	9	5	Copper Alloy	1.7 [43]	1.2 [31]	0.6 [15]	-55 105	Yes	18076-01-A
Air Side	500 V	15	5	Copper Alloy	1.6 [41]	1.6 [41]	0.6 [15]	-55 105	Yes	18076-02-A
Air Side	500 V	25	5	Copper Alloy	1.9 [48]	2.2 [56]	0.6 [15]	-55 105	Yes	18076-03-A†
Air Side	500 V	50	5	Copper Alloy	2.0 [51]	2.6 [66]	0.7 [18]	-55 105	Yes	18076-04-A
Vacuum Side-Female	500 V	9	5	Copper Alloy	1.3 [33]	0.4 [11]	0.63 [16]	-200 200	No	16810-01-A
Vacuum Side-Female	500 V	15	5	Copper Alloy	1.6 [40]	0.4 [11]	0.63 [16]	-200 200	No	16811-01-A
Vacuum Side-Female	500 V	25	5	Copper Alloy	2.2 [55]	0.4 [11]	0.63 [16]	-200 200	No	16812-01-A†
Vacuum Side-Female	500 V	50	5	Copper Alloy	2.7 [69]	0.5 [14]	0.63 [16]	-200 200	No	16814-01-A
Vacuum Side-Male	500 V	9	5	Copper Alloy	1.3 [33]	0.4 [11]	0.63 [16]	-200 200	No	19827-01-A
Vacuum Side-Male	500 V	15	5	Copper Alloy	1.6 [40]	0.4 [11]	0.63 [16]	-200 200	No	19828-01-A
Vacuum Side-Male	500 V	25	5	Copper Alloy	2.2 [55]	0.4 [11]	0.63 [16]	-200 200	No	17411-01-A
Vacuum Side-Male	500 V	50	5	Copper Alloy	2.7 [69]	0.5 [14]	0.63 [16]	-200 200	No	19829-01-A

Note that contacts are included with all plugs.



CONDUCTOR QUANTITY*	CABLE LENGTH	CABLE WIDTH	INSULATION DIAMETER	WIRE DIAMETER	PART NUMBER
9	19"	0.4	Ø .035	19 X 0.0063	20370-19-WW
9	39"	0.4	Ø .035	19 X 0.0063	20370-39-WW
15	19"	0.7	Ø .035	19 X 0.0063	20371-19-WW
15	39"	0.7	Ø .035	19 X 0.0063	20371-39-WW
25	19"	1.2	Ø .035	19 X 0.0063	20372-19-WW
25	39"	1.2	Ø .035	19 X 0.0063	20372-39-WW

Adjustable Wire Stripper For 20 - 30 AWG (0.25 - 0.80 mm)Cable

21128-01

\*The 50 conductor cables are created by using two 25 conductor cables. Contact CeramTec for custom lengths.



TYPE	MATERIAL	DESCRIPTION	PART NUMBER
0.040 Female Crimp Contacts	Copper Alloy	Female accepts wire up to 0.040 [1.0]	16757-02-A
0.040 Male/Pin Crimp Contacts	Copper Alloy	Male/Pin contact - 0.040 [1.0] Pin	17412-02-A
Crimp Tool		For 0.025" – 0.075" Crimp Diameters	2840-05

\*\*Contacts priced and sold in packages of 5. See the Accessories section for more information on all accessories.

**Specifications****Materials**

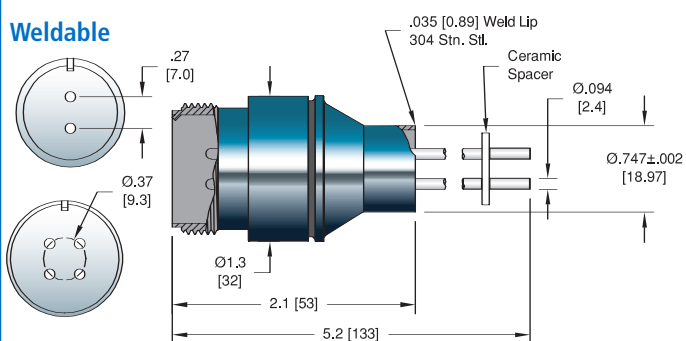
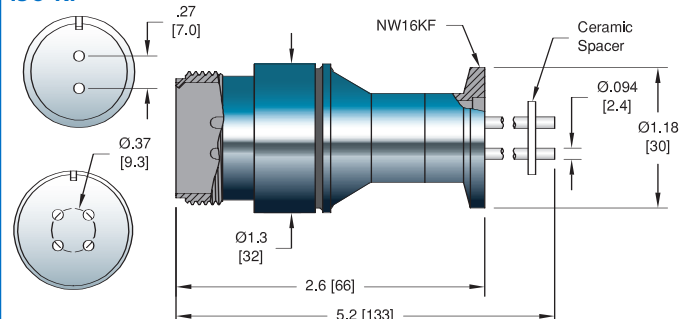
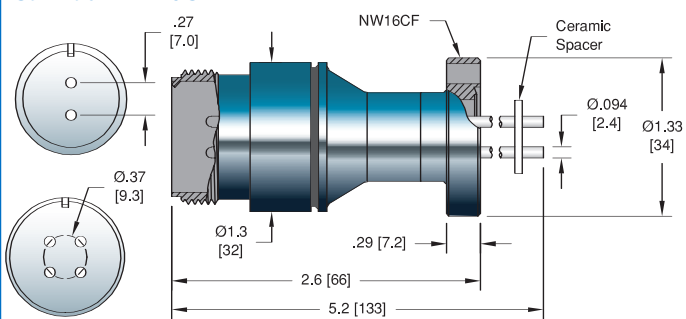
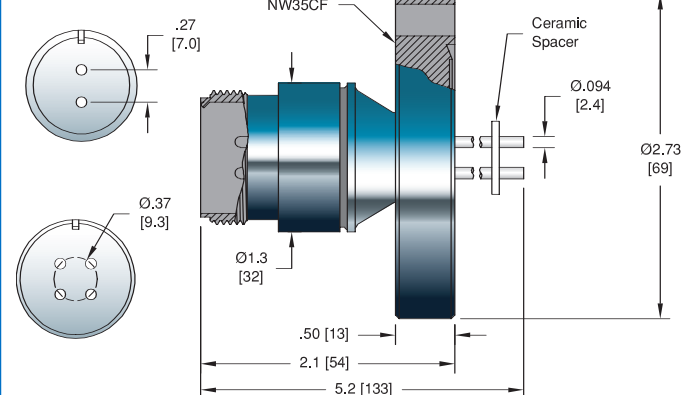
Shell: 304 Stainless steel  
 Pins: Nickel or Molybdenum  
 Insulation: Alumina ceramic  
 Magnetic Materials: See table

**Voltage Rating** 700 V DC

**Current Rating** See table

**Temperature Range** -269°C to 450°C, ISO KF -25°C to 205°C

**Pressure @ 20°C** 475 PSIG (33 Bar), ISO KF 0 PSIG

**Ø .094 Conductor****Weldable****ISO KF****ConFlat - NW16CF****ConFlat - NW35CF**

# Multipin Connector

Circular: Single Ended  
Power: MIL-C-5015

B.5



NO. PINS	AMPS	CONDUCTORS MATERIAL	INSTALLATION	MAGNETIC MATERIALS	PART NUMBER
2	16	Nickel	Weld	Yes	18093-02-W
2	28	Molybdenum	Weld	No	18093-04-W
4	16	Nickel	Weld	Yes	18093-06-W
4	28	Molybdenum	Weld	No	18093-08-W



ISO FLANGE				
2	16	Nickel	NW16KF	Yes
2	28	Molybdenum	NW16KF	No
4	16	Nickel	NW16KF	Yes
4	28	Molybdenum	NW40KF	No



CONFLAT FLANGE				
2	16	Nickel	1 1/3" (NW16CF)	Yes
2	28	Molybdenum	1 1/3" (NW16CF)	No
2	16	Nickel	2 3/4" (NW35CF)	Yes
2	28	Molybdenum	2 3/4" (NW35CF)	No
4	16	Nickel	1 1/3" (NW16CF)	Yes
4	28	Molybdenum	1 1/3" (NW16CF)	No
4	16	Nickel	2 3/4" (NW35CF)	Yes
4	28	Molybdenum	2 3/4" (NW35CF)	No

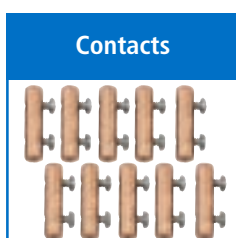


TYPE	VOLTAGE DC	CONDUCTOR AMPS	NO. CONTACTS	DIMENSIONS H	L	PART NUMBER
Air Side	700 V	23	2	2.5 [63]	1.2 [32]	18600-01-A
Air Side	700 V	23	4	2.6 [65]	1.4 [36]	18600-02-A

Note that contacts are included with all plugs.



VOLTAGE DC	CONDUCTOR AMPS	TYPE	WIRE LENGTH	DIAMETER	INSULATION DIAMETER	PART NUMBER
850 V	20	12 AWG Stranded	15'	37 x 0.013	Ø .101	21702-02-A



TYPE	MATERIAL	DESCRIPTION	PART NUMBER
0.094 Barrel Type	Beryllium Copper	Accepts .094 [2.4] Pin	7332-04-A <sup>†</sup>
0.094 Set Screw Type	Beryllium Copper	Accepts .094 [2.4] Pin	7429-01-A

\*Contacts priced and sold in packages of 10. <sup>†</sup>Shown in photo. See the Accessories section for more information on all accessories.



## Specifications

### Materials

Shell: 304 Stainless steel  
Pins: Nickel or molybdenum  
Insulation: Alumina ceramic  
Magnetic Materials: See table

**Voltage Rating** 700 V DC

**Current Rating** See table

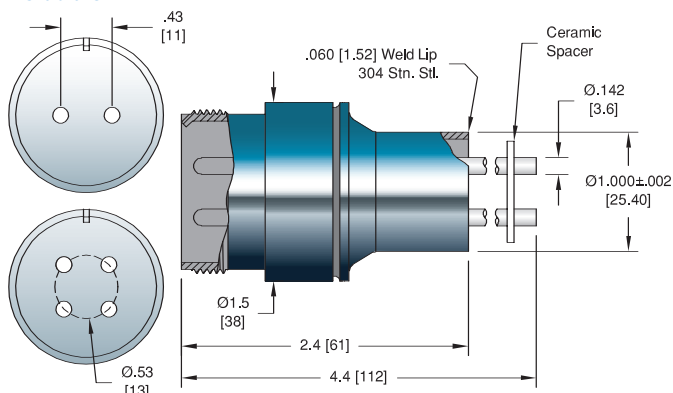
**Temperature Range** -269°C to 450°C, ISO KF -25°C to 205°C

**Pressure @ 20°C** ISO KF 0 PSIG

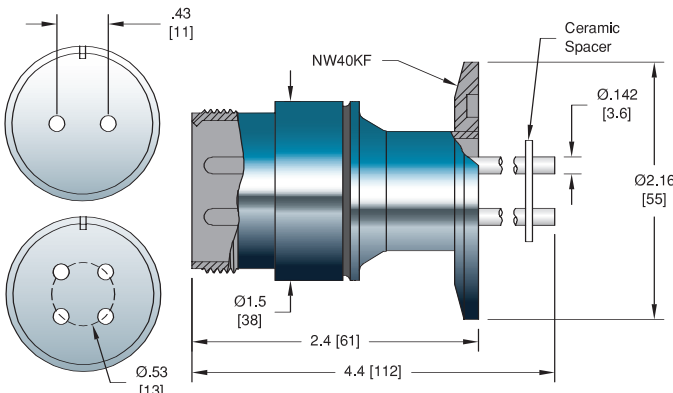
2 Pin - 600 PSIG (41 Bar)  
4 Pin - 500 PSIG (34 Bar)

### Ø .142 Conductor

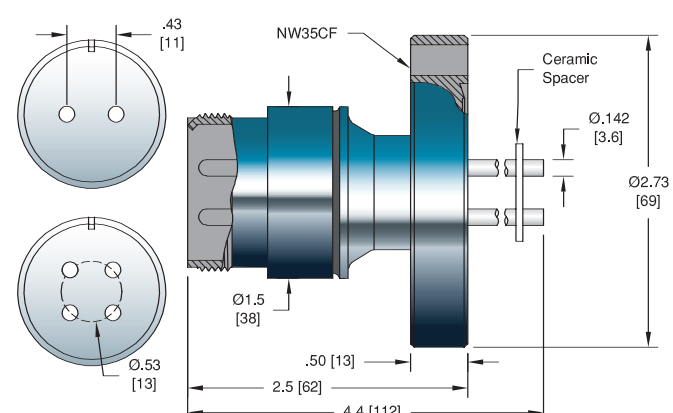
#### Weldable



### ISO KF



### ConFlat



# Multipin Connector

Circular: Single Ended  
Power: MIL-C-5015

B.5



NO. PINS	CONDUCTORS AMPS	INSTALLATION	MAGNETIC MATERIALS	PART NUMBER
2	25	Nickel	Weld	Yes
2	46	Molybdenum	Weld	No
4	25	Nickel	Weld	Yes
4	46	Molybdenum	Weld	No



ISO FLANGE				
2	25	Nickel	NW40KF	Yes
2	46	Molybdenum	NW40KF	No
4	25	Nickel	NW40KF	Yes
4	46	Molybdenum	NW40KF	No

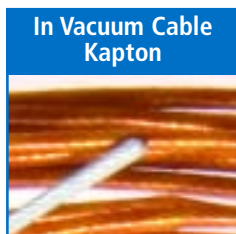


CONFLAT FLANGE				
2	25	Nickel	2 3/4" (NW35CF)	Yes
2	46	Molybdenum	2 3/4" (NW35CF)	No
4	25	Nickel	2 3/4" (NW35CF)	Yes
4	46	Molybdenum	2 3/4" (NW35CF)	No

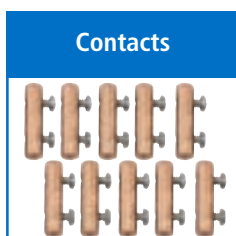


TYPE	VOLTAGE DC	CONDUCTOR AMPS	NO. CONTACTS	DIMENSIONS H	DIMENSIONS L	PART NUMBER
Air Side	700 V	46	2	2.5 [63]	1.2 [32]	18601-01-A
Air Side	700 V	46	4	2.6 [65]	1.4 [36]	18601-02-A

Note that contacts are included with all plugs.



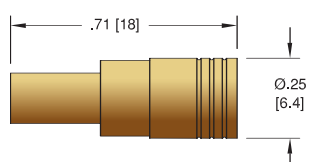
VOLTAGE DC	CONDUCTOR AMPS	TYPE	WIRE LENGTH	DIAMETER	INSULATION DIAMETER	PART NUMBER
850 V	20	12 AWG Stranded	15'	37 x 0.013	Ø .101	21702-02-A



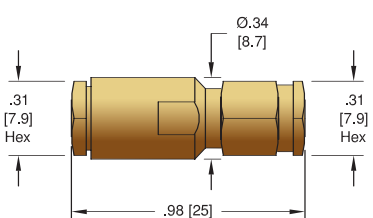
TYPE	MATERIAL	DESCRIPTION	PART NUMBER
0.154 Barrel Type	Beryllium Copper	Accepts 0.154 [3.9] Pin	7332-07-A

\*Contacts priced and sold in packages of 10. See the Accessories section for more information on all accessories.

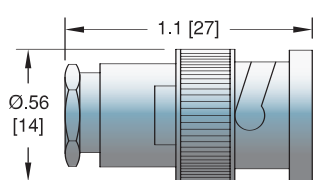
SMB



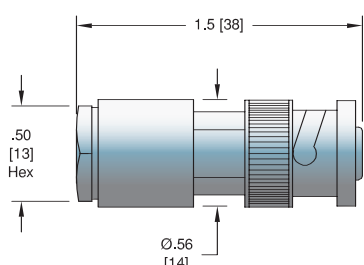
SMA



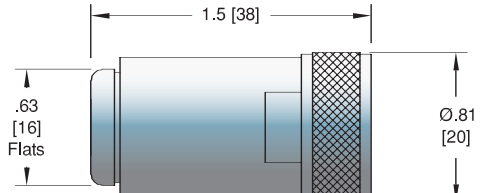
BNC



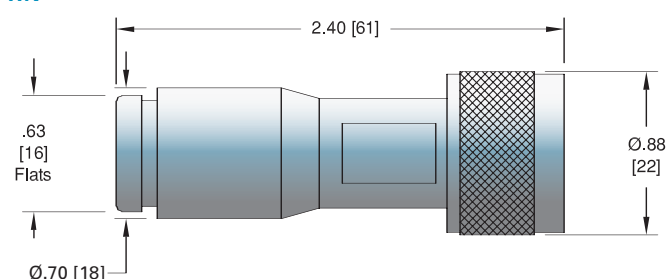
MHV



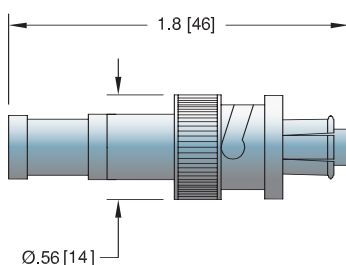
Type N



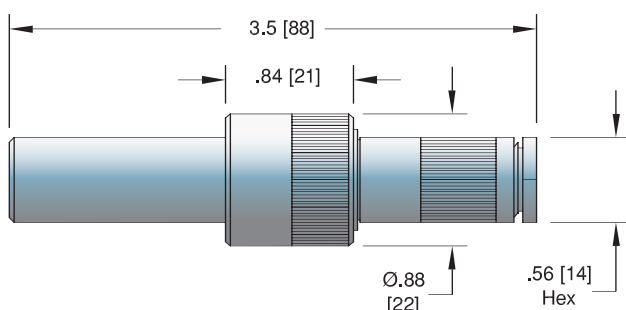
HN



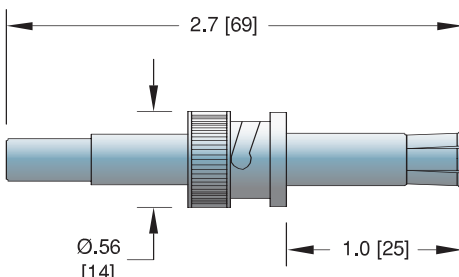
SHV - 5 KV



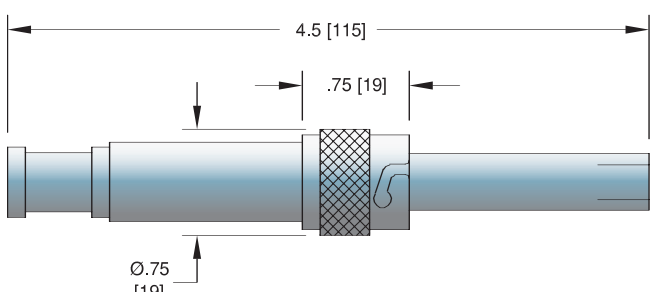
BSHV - 7.5 KV



SHV - 10 KV



SHV - 20 KV





TYPE	VOLTAGE DC	CONDUCTOR AMPS	TEMPERATURE °C MIN	TEMPERATURE °C MAX	MAGNETIC MATERIALS	PART NUMBER
SMB Plug: Air Side	375 V	5	-65	165	No	3095-12



SMA	SMA Plug: Air Side	500 V	5	-65	165	No	6524-02
-----	--------------------	-------	---	-----	-----	----	---------



BNC & MHV	BNC Plug: Air Side	500 V	5	-65	165	No	7116-02†
	MHV Plug: Air Side	5 kV	10	-65	165	No	7116-01



Type N	Type N Plug: Air Side	1.5 kV	5	-65	165	No	7707-01
--------	-----------------------	--------	---	-----	-----	----	---------



HN	HN Plug: Air Side	7 kV	10	-55	165	No	6524-05
----	-------------------	------	----	-----	-----	----	---------



BSHV - 7.5 KV	BSHV Plug: Air Side	7.5 kV	8	-65	400	Yes	7604-01-A
---------------	---------------------	--------	---	-----	-----	-----	-----------



SHV	SHV - 5 kV Plug: Air Side	5 kV	10	-65	165	No	8058-01†
	SHV - 10 kV Plug: Air Side	10 kV	10	-65	165	No	8058-02
	SHV - 20 kV Plug: Air Side	20 kV	20	-20	125	No	8208-02

†Shown in photo.

**MIL-DTL-83513 – Micro D Type  
Air Side Plug**

The drawing shows a cross-section of the plug assembly. Key dimensions include:  
 - Total length: A = 6.0 [152]  
 - Pin pitch: .42 [11]  
 - Pin contact types: Gold Plated Pin Contact (9 Pin, 15 Pin, 25 Pin, 51 Pin)

**MIL-C-26482 Type  
Air Side Plug**

The drawing shows various pin configurations:  
 - 3 Pin, 6 Pin, 10 Pin, 19 Pin, 32 Pin  
 - 41 Pin (detailed view of the contacts)

**Vacuum Side Plug – PEEK**

The drawing shows various pin configurations:  
 - 51 PIN, 25 PIN, 15 PIN, 9 PIN  
 - Gold Plated Crimp Contacts (Accepts .020 [.05] Pin)

**MIL-C-24308 – Sub D Type  
Air Side Plug**

The drawing shows a cross-section of the plug assembly. Key dimensions include:  
 - Total length: C = 6.0 [152]  
 - Pin pitch: B = .42 [11]  
 - Pin contact types: Gold Plated Solder Cup Contacts (9 Pin, 15 Pin, 25 Pin, 50 Pin)

**Vacuum Side Plug – PEEK**

The drawing shows various pin configurations:  
 - 50 Pin, 25 Pin, 15 Pin, 9 Pin  
 - Gold Plated Solder / Crimp Contacts (Accepts .040 [1.0] Pin)

**MIL-C-5015 Type  
Air Side Plug**

The drawing shows various pin configurations:  
 - 4 Pin, 6 Pin, 10 Pin, 20 Pin  
 - Solder Cup Contacts (35 Pin)

**Power-MIL-C-5015 Type**

The drawing shows a detailed view of the contacts:  
 - 2 Pin, 4 Pin  
 - Solder Cup Contacts



Micro D Type

Type	Voltage DC	Qty	Conductor Amps	Material	Dimensions A	B	Temperature °C Min	Max	Magnetic Materials	Part Number
Air Side	500 V	9	3	Copper Alloy	0.775 [20]	0.298 [8]	-55	125	No	21585-01-A
Air Side	500 V	15	3	Copper Alloy	0.925 [23]	0.298 [8]	-55	125	No	21586-01-A
Air Side	500 V	25	3	Copper Alloy	1.175 [30]	0.298 [8]	-55	125	No	21587-01-A <sup>†</sup>
Air Side	500 V	51	3	Copper Alloy	1.425 [36]	0.341 [9]	-55	125	No	21589-01-A
Vacuum Side	500 V	9	2	Beryllium Copper	0.790 [20]	0.390 [10]	-269	200	No	21573-01-A
Vacuum Side	500 V	15	2	Beryllium Copper	0.935 [24]	0.390 [10]	-269	200	No	21574-01-A
Vacuum Side	500 V	25	2	Beryllium Copper	1.185 [30]	0.390 [10]	-269	200	No	21575-01-A
Vacuum Side	500 V	51	2	Beryllium Copper	1.135 [36]	0.390 [10]	-269	200	No	21577-01-A



Sub D Type

Type	Voltage DC	Qty	Contacts Amps	Material	Dimensions A	B	C	Temperature °C Min	Max	Magnetic Materials	Part Number
Air Side	500 V	9	5	Copper Alloy	1.7 [43]	1.2 [31]	0.6 [15]	-55	105	Yes	18076-01-A
Air Side	500 V	15	5	Copper Alloy	1.6 [41]	1.6 [41]	0.6 [15]	-55	105	Yes	18076-02-A
Air Side	500 V	25	5	Copper Alloy	1.9 [48]	2.2 [56]	0.6 [15]	-55	105	Yes	18076-03-A <sup>†</sup>
Air Side	500 V	50	5	Copper Alloy	2.0 [51]	2.6 [66]	0.7 [18]	-55	105	Yes	18076-04-A
Vacuum Side-Female	500 V	9	5	Copper Alloy	1.3 [33]	0.4 [11]	-	-200	200	No	16810-01-A
Vacuum Side-Female	500 V	15	5	Copper Alloy	1.6 [40]	0.4 [11]	-	-200	200	No	16811-01-A
Vacuum Side-Female	500 V	25	5	Copper Alloy	2.2 [55]	0.4 [11]	-	-200	200	No	16812-01-A <sup>†</sup>
Vacuum Side-Female	500 V	50	5	Copper Alloy	2.7 [69]	0.5 [14]	-	-200	200	No	16814-01-A
Vacuum Side-Male	500 V	9	5	Copper Alloy	1.3 [33]	0.4 [11]	-	-200	200	No	19827-01-A
Vacuum Side-Male	500 V	15	5	Copper Alloy	1.6 [40]	0.4 [11]	-	-200	200	No	19828-01-A
Vacuum Side-Male	500 V	25	5	Copper Alloy	2.2 [55]	0.4 [11]	-	-200	200	No	17411-01-A
Vacuum Side-Male	500 V	50	5	Copper Alloy	2.7 [69]	0.5 [14]	-	-200	200	No	19829-01-A



MIL-C-26482 Type

Type	Voltage DC	Qty	Contacts Amps	Material	Dimensions A	B	Temperature °C Min	Max	Magnetic Materials	Part Number
Air Side	1 kV	3	1	Copper Alloy	0.8 [20]	1.9 [48]	-55	200	No	16060-01-A <sup>†</sup>
Air Side	1 kV	6	1	Copper Alloy	1.0 [25]	1.9 [48]	-55	200	No	16060-02-A
Air Side	1 kV	10	1	Copper Alloy	1.0 [25]	1.9 [48]	-55	200	No	16060-03-A
Air Side	1 kV	19	1	Copper Alloy	1.2 [31]	1.9 [48]	-55	200	No	16060-04-A
Air Side	1 kV	32	1	Copper Alloy	1.4 [36]	2.1 [53]	-55	200	No	16060-05-A
Air Side	1 kV	41	1	Copper Alloy	1.5 [38]	2.3 [58]	-55	200	No	16060-06-A
Vacuum Side	1 kV	3	5	Copper Alloy	0.8 [20]	-	-200	200	No	16026-02-A <sup>†</sup>
Vacuum Side	1 kV	6	5	Copper Alloy	0.9 [22]	-	-200	200	No	16027-02-A
Vacuum Side	1 kV	10	5	Copper Alloy	1.0 [25]	-	-200	200	No	16028-02-A
Vacuum Side	1 kV	19	5	Copper Alloy	1.1 [28]	-	-200	200	No	16029-02-A
Vacuum Side	1 kV	32	5	Copper Alloy	1.4 [34]	-	-200	200	No	16030-02-A
Vacuum Side	1 kV	41	5	Copper Alloy	1.5 [37]	-	-200	200	No	16031-02-A



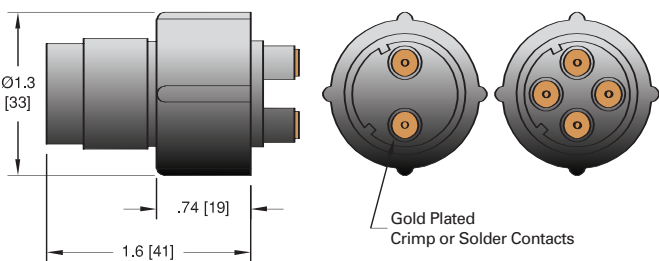
MIL-C-5015 Type

Type	Voltage DC	Qty	Contacts Amps	Material	Dimensions A	B	C	Temperature °C Min	Max	Magnetic Materials	Part Number
Air Side	700 V	4	13	Copper Alloy	2.6 [65]	1.4 [36]	1.8 [44]	-55	125	No	15910-01-A
Air Side	700 V	6	13	Copper Alloy	2.6 [65]	1.4 [36]	1.8 [44]	-55	125	No	15911-01-A
Air Side	700 V	10	13	Copper Alloy	2.6 [65]	1.4 [36]	1.8 [44]	-55	125	No	15912-01-A
Air Side	700 V	20	13	Copper Alloy	2.9 [74]	1.9 [49]	1.4 [36]	-55	125	No	15913-01-A <sup>†</sup>
Air Side	700 V	35	13	Copper Alloy	3.0 [77]	2.5 [62]	1.2 [30]	-55	125	No	15914-01-A
Air Side: Hi-Temp PEEK	700 V	4	4.8	Alumel	2.6 [65]	1.4 [36]	1.8 [44]	-55	260	Yes	15910-32-A
Air Side: Hi-Temp PEEK	700 V	6	4.8	Alumel	2.6 [65]	1.4 [36]	1.8 [44]	-55	260	Yes	15911-32-A
Air Side: Hi-Temp PEEK	700 V	10	4.8	Alumel	2.6 [65]	1.4 [36]	1.8 [44]	-55	260	Yes	15912-32-A
Power: .094 Contacts	700 V	2	23	Copper Alloy	2.5 [63]	1.2 [32]	-	-55	125	No	18600-01-A
Power: .094 Contacts	700 V	4	23	Copper Alloy	2.5 [63]	1.4 [36]	-	-55	125	No	18600-02-A
Power: .142 Contacts	700 V	2	46	Copper Alloy	2.6 [65]	1.6 [40]	-	-55	125	No	18601-01-A
Power: .142 Contacts	700 V	4	46	Copper Alloy	2.6 [65]	1.6 [40]	-	-55	125	No	18601-02-A

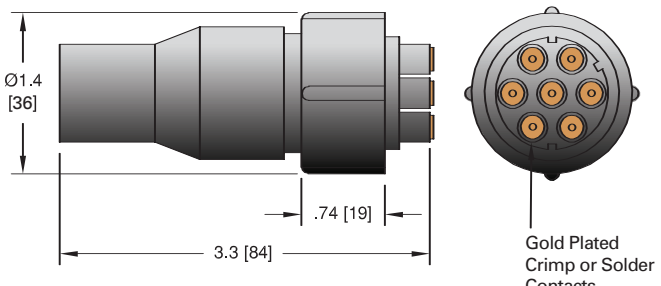
Note that contacts are included with all plugs. <sup>†</sup>Shown in photo.



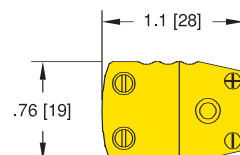
### High Voltage 2 & 4 Contacts



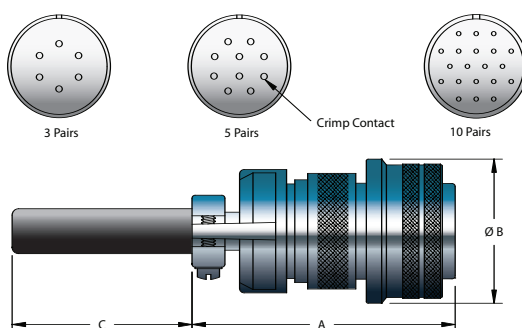
### 7 Contacts



### Thermocouple Spade Type



### Thermocouple MIL-C-5015 Type





TYPE	VOLTAGE DC	QTY	CONTACTS AMPS	MATERIAL	TEMPERATURE °C MIN	MAX	MAGNETIC MATERIALS	PART NUMBER
Air Side	12 kV	2	13	Copper Alloy	-15	85	No	2871-02-A†
Air Side	12 kV	4	13	Copper Alloy	-15	85	No	2871-03-A
Air Side	12 kV	7	13	Copper Alloy	-15	85	No	2871-01-A



ANSI TYPE	THERMOCOUPLE MATERIALS	TYPE	PLUG MATERIALS	TEMPERATURE °C MIN	MAX	COLOR CODE	MAGNETIC MATERIALS	PART NUMBER
K	Chromel/Alumel	Standard	Glass Filled Nylon	-29	218	Yellow	Yes	08151-01†
K	Chromel/Alumel	High Temp	Ceramic	-73	650	Yellow	Yes	08151-09
C	Tungsten - Rhenium	Standard	Glass Filled Nylon	-29	218	Red	Yes	08151-04
C	Tungsten - Rhenium	High Temp	Ceramic	-73	250	Red	Yes	08151-07



ANSI TYPE	T/C PAIRS	THERMOCOUPLE MATERIALS	A	DIMENSIONS B	C	TEMPERATURE °C MIN	MAX	MAGNETIC MATERIALS	PART NUMBER
K	3	Chromel/Alumel	2.6 [65]	1.4 [36]	1.8 [44]	-55	125	Yes	15911-02-A
K	5	Chromel/Alumel	2.6 [65]	1.4 [36]	1.8 [44]	-55	125	Yes	15912-02-A
K	10	Chromel/Alumel	2.9 [74]	1.9 [49]	1.4 [36]	-55	125	Yes	15913-02-A†

Note that contacts are included with all plugs. †Shown in photo.

**D Mechanical**

**E Power**

# CCGM – Centralized CAN Cell Group Module (CCGM023A)

## INTRODUCTION

EMUS Centralized Cell Group Module (CCGM) is a battery cells communication adapter (or "Slave unit") equipped with two CAN connectors for easy BMS system assembly and integrated proprietary EMUS software that allows data transfer within 100ms frequency. CCGM performs all cell data measuring by itself, so the product allows saving space by reducing the need of having cell modules and three-way connectors. CCGM increases the speed of the cell data broadcasting and provides for each connected battery cell balancing functionality.



## APPLICATIONS

- Any lithium chemistry, series-connected battery pack, or a pack of multiple parallel strings, of up to 512 cells total if using 32 EMUS Centralized CAN Cell Group Modules with connected 16 cells on each. (centralized cell monitoring)

## FEATURES

- 2x CAN connectors. Enables communication with CAN equipped EMUS G1 Control Unit and EMUS Centralized Cell Group Modules.
- Supports from 6 up to 16 lithium cells.
- 5x external temperature sensors.
- Using Temperature Breakout (or Extender) board (TBB010A) possible to extend up to 16 temperature sensors.
- Balancing of cells, 400mA per each cell.
- Supports 50, 125, 250, 500, 800 kbit/s and 1 Mbit/s CAN baud rates.

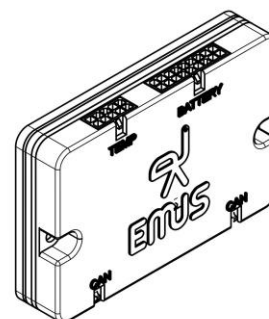
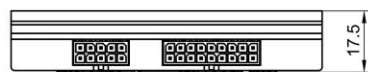
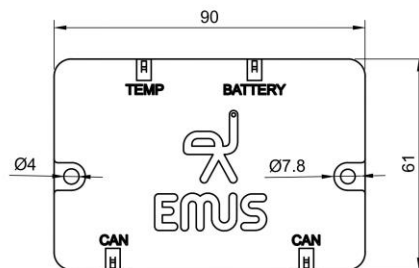
## MECHANICAL INFORMATION



Battery Management Systems

battery made simple

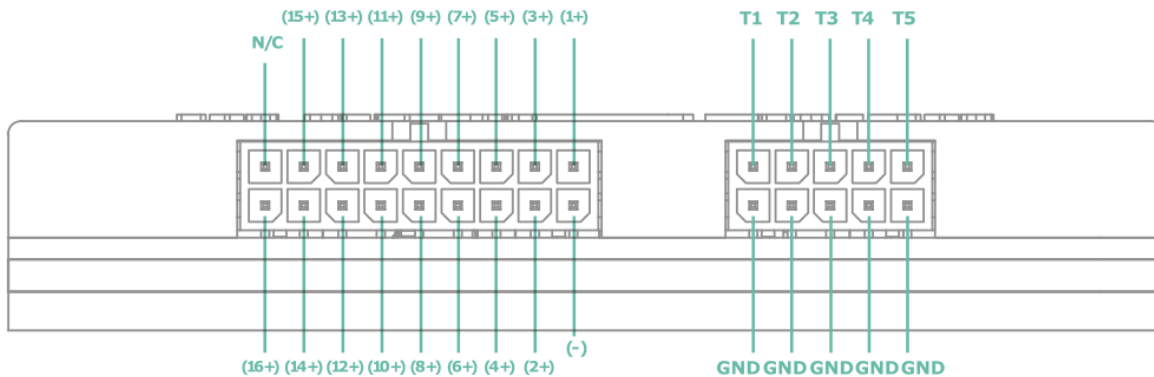
[www.emusbms.com](http://www.emusbms.com)



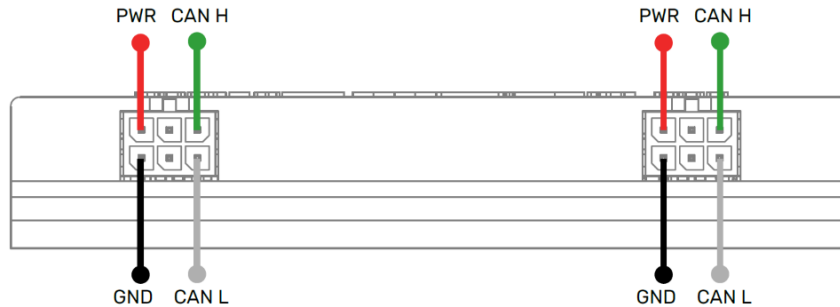
## CONNECTION LAYOUT

Cells Layout:

Ext. Temperature Sensors Layout:



Assignment	Mating Housing	Terminal
(-)		
1+		
2+		
3+		
4+		
5+		
6+		
7+		
8+		
9+		
10+		
11+		
12+		
13+		
14+		
15+		
16+		
N/C		
5XGND	Microfit 43025-1800 cell connector	43030-0003Molex Micro-latch crimps (recommended crimp tool Molex Hand Crimp Tool P/N: 638190000)
T1		
T2		
T3		
T4		
T5		

CAN Connection Layout:


Assignment	Mating Housing	Terminal
PWR		
GND		
CAN_H	2x microfit 43025-0600	43030-0003 (recommended crimp tool Molex Hand Crimp Tool P/N: 638190000)
CAN_L		

## ELECTRICAL CHARACTERISTICS

Item	Value
Supply voltage	12-95V
Supply voltage battery	12.0 VDC to 79.2 VDC (firmware limited by 72.8VDC)
Power supply reverse protection	yes
Current consumption	5.6 mA @ 68V - 8.7 mA @ 15V
Isolation voltage	1000V
Transient/overvoltage protection between CAN H/CAN L and GND (and vice versa)	24V
Cell voltage limits	0-4.95V

## OTHER SPECIFICATIONS

Item	Conditions	Value
Cell Count	Other Li chemistries	6-16
	LTO cell chemistry	8-16*
CAN Speed		50kbps, 125kbps, 250kbps, 500kbps, 800kbps, 1Mbps (by default 250kbps)
Reserved CAN IDs		0x1FFFFEE5, 0x1FFFFEE6, 0x1FFF5E5, and 0x1FFF5E6
Operating Temperature		-40 to +85 °C
IP rating		IP40
Weight	Without Quick Start Kit	105g
	With Quick Start Kit	145g
Cell communication wire length	In our Quick Start Kit	45cm
Temperature sensors wire length	In our Quick Start Kit	45cm
Cell Voltage	General Firmware	2.01 – 4.54V
	LTO Firmware	1.01 – 3.54V

## INSTALLATION



\* Minimum cell count depends on the cell chemistry used. The lowest supported battery pack voltage by internal CCGM parts is 12V, therefore if LTO cells are used then the minimum cell count should be calculated accordingly.

E.g. if LTO cell's expected lowest voltage is 1.5V then the minimum number of cells required would be 8 [12V / 1.5V = 8 cells].

$$V_{BatTotal} \div V_{CellMin} = \text{MinimumNumOfCells}$$

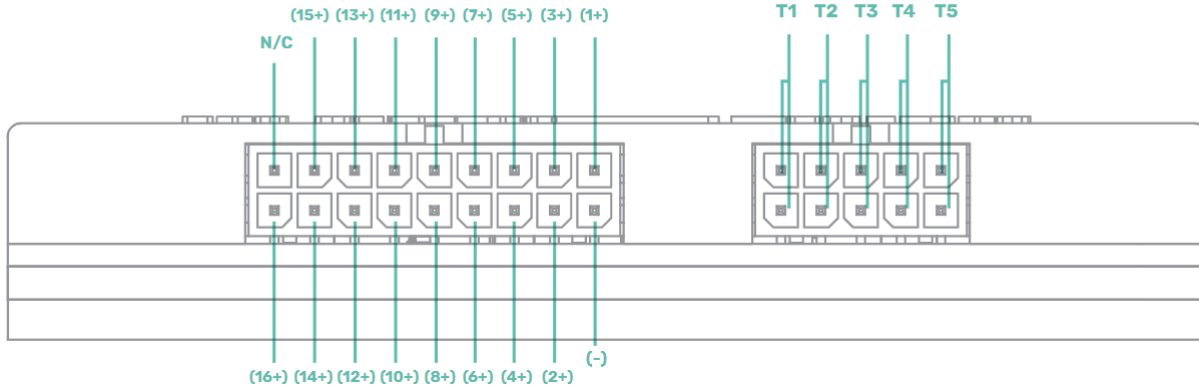
**NOTE:** the absolute minimum total battery pack voltage is 9V, however it is not guaranteed that the device will sense cell voltages correctly.



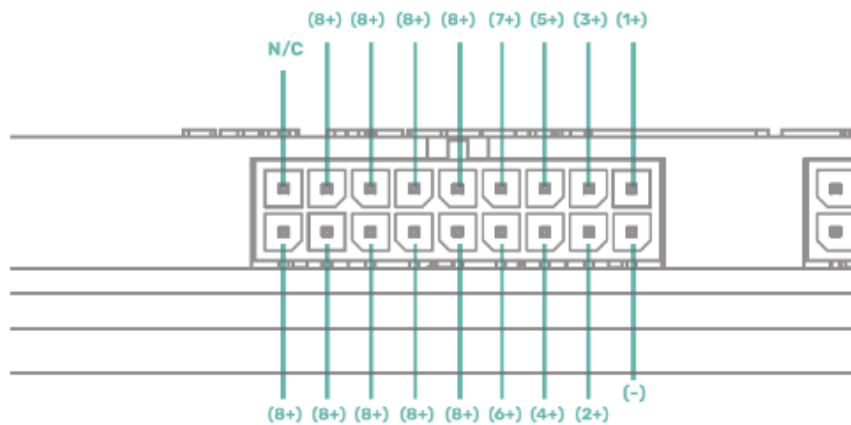
**NOTE:** Connection must start from the most negative cell to the most positive. In cases when cells number is less than 16, e.g. 8 cells, then free cells connection wires (dedicated for 9th-16th cells) must ALL be connected to the last 8<sup>th</sup> (most positive cell).

To setup the 16 cells and 5 external temperature sensors please refer to figure below.

Cells Layout:



Cells Layout: (using other amount of cells)



# Control Unit – G1 Control Unit (CU021A)

## INTRODUCTION

EMUS G1 Control Unit (or simply Control Unit) is the main controller that autonomously executes all core and utility functions of battery management. It interacts with all other first party and third-party components in the system using various inputs, outputs, and interfaces that are populated on its main 22 pin and secondary 8 pin connectors. The device also is flexible and allows by using EMUS Control Panel, to monitor and configure more than 300 battery management system parameters



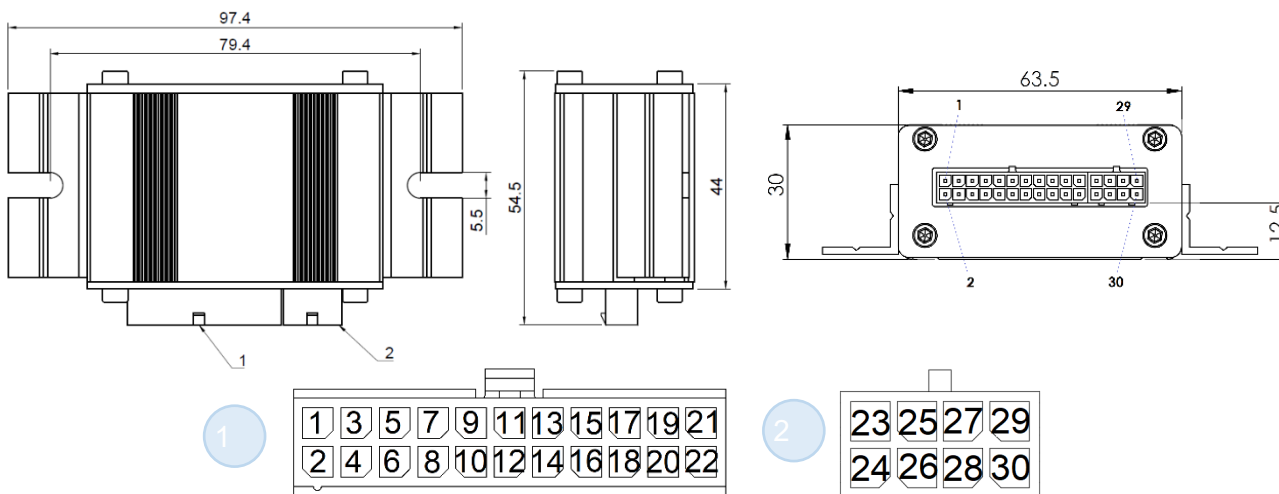
## APPLICATIONS

- Any lithium chemistry, series connected battery pack of up to 100 cells if using serial cell communication. (distributed regular)
- Any lithium chemistry, series connected battery pack, or pack of multiple parallel strings, of up to 3200 cells total, if using EMUS CAN Cell Group Modules. (distributed grouped)
- Any lithium chemistry, series connected battery pack, or multiple parallel string, of up to 512 cells total, if using EMUS Centralized CAN Cell Group Modules. (centralized CCGM)

## FEATURES

- USB data interface for quick connection to a host device when configuration, diagnostics, or maintenance is needed.
- RS232 data interface for continuous BMS activity monitoring by using third party or first party EMUS G1 BMS devices.
- Serial interface for cell communication.
- Non isolated CAN 2.0 A/B data interface. Enables to communicate with CAN equipped EMUS G1 BMS components, control third party charging devices
- State of Charge (SOC), State of Health (SOH) calculations.

## MECHANICAL INFORMATION





Pin No.	Assignment	Mating Housing	Terminal
1	PWR	43025-2200 Microfit 22 Pin Header or equivalent	
2	GROUND		
3	CELL RX+		
4	CELL RX-		
5	CELL TX+		
6	CELL TX-		
7	USB PWR		
8	GROUND		
9	USB D+		
10	USB D-		
11	DISP.TX		
12	DISP.RX		
13	HEATER		
14	BAT.LOW		
15	BUZZER		
16	CHG.IND.		
17	CHARGER		
18	FAST CHG.		
19	IGN.IN		
20	AC SENSE		
21	CAN+	43025-0800 Microfit 8pin Connector or equivalent	
22	CAN-		
23	SPEED IN		
24	SOC OUT		
25	+5V OUT		
26	GROUND		
27	INPUT 4		
28	INPUT 3		
29	INPUT 2		
30	INPUT 1		

## ELECTRICAL CHARACTERISTICS

Item	Conditions	Value	
Operating voltage		9 to 32 VDC	
Power supply reverse polarity protection		Yes	
Current consumption	At typical supply voltage, with nothing else connected	12 VDC typical 54 mA	24 VDC typical 20 mA
	At typical supply voltage, with Current Sensor connected	12 VDC typical 72 mA	24 VDC typical 25.5 mA



General purpose output max sinking current (resettable fuse trip current)		0.5 A
General purpose output max voltage		32 VDC
General purpose input ON voltage		5 to 32 VDC
General purpose input OFF voltage		0 VDC
Current sensor input ON voltage	Applies when pin is mapped with function other than PF14 Current	5 VDC
Current sensor input OFF voltage		0 VDC
SOC OUT output voltage range	Sensor Input	0 to 5 VDC
SOC OUT output resistance		1 kOhm
SOC OUT output PWM signal frequency	Applies when pin is mapped with function PF11 State of Charge Output or function PF18 Analog Charger Control Output	7.8125 kHz
SPEED IN input signal frequency range	Applies when SPEED IN input is mapped with function PF1 Speed Sensor Input	7kHz
SPEED IN input ON voltage		5 to 32 VDC
SPEED IN input OFF voltage		0 VDC
USB interface controller		FT232R
USB power supply data line transient/overvoltage protection		5 VDC
USB/RS232 interface galvanic isolation		None
USB interface duplexity		Full duplex (send and receive)
RS232 interface duplexity	USB not connected	Full duplex (send and receive)
	USB connected	Half duplex (send only)
USB/RS232 interface baud rate		57.6kbps
USB/RS232 interface data bits		8 bits
USB/RS232 interface parity		None
USB/RS232 interface stop bits		1 bit

## OTHER SPECIFICATIONS

Item	Condition	Value
Max number of Cell Modules in cell communication daisy chain when using Top and Bottom Isolators		100
Max number of CAN Cell Group Modules on CAN bus		32
Max number of Centralized CAN Cell Group Modules on CAN bus		32
Operating temperature		-40 to +85°C
IP rating		IP54
Weight	With quick start kit	114 g
	Without quick start kit	92 g

## COMPATIBLE CHARGERS AND INVERTERS

Charger Name	Communication Protocol
TC	CAN J1939
Elcon	CAN J1939
HF/PFC	CAN J1939
IEB	CAN J1939
Eltek Valere EV Power	CAN
Zivan NG and SG series	CAN
Powerfinn Robust and PAP3200	CAN
Delta-Q	CANOpen
EDN	CAN
G-Power EV33	CAN
Sunny Island inverter	CAN
TSM	CAN
Shinry	CAN
Micropower Group Lion	CAN
Brusa NLG644	CAN
ZVU	I/O Controlled
Victron Inverter	CAN
ATIB Electronica HTC	CAN
Analog Controlled Charger	I/O Controlled
Non-CAN	I/O Controlled



**NOTE:** For all chargers recently supported please refer to <https://emusbms.com>.



**NOTE:** For more information on each charger communication protocol, contact the charger manufacturer.

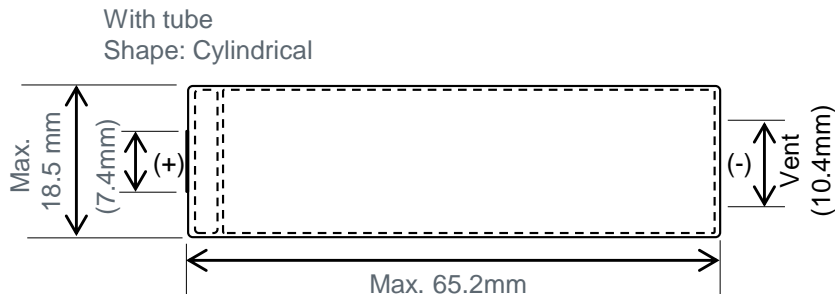
# Cylindrical Type Lithium Ion Secondary Battery US18650VTC5A

## Specifications

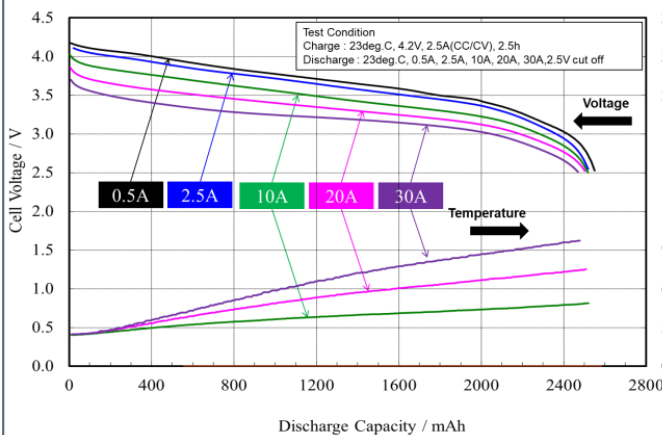
Nominal Capacity*	2600 mAh
Rated (minimum) Capacity*	2500 mAh
Nominal Voltage	3.6 V
Weight (typical)	44.9 g

\* Charge: CCCV, 2.5 A, 4.2 V, 2.5 h, at 23deg.C  
Discharge: 0.2 lta (500 mA), 2.0 V cutoff at 23deg.C

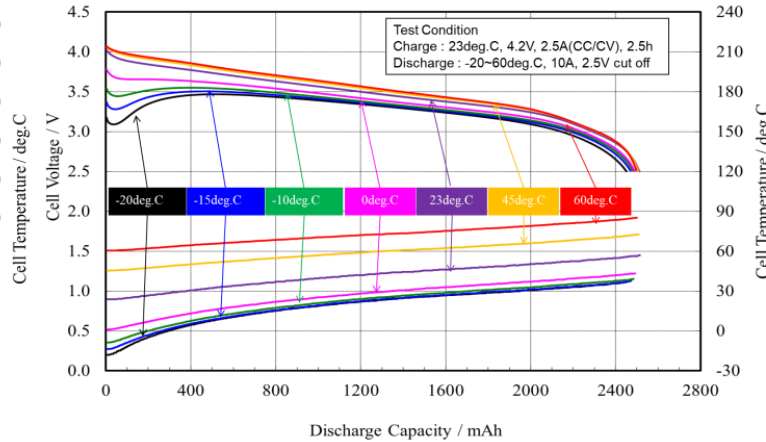
## Dimensions



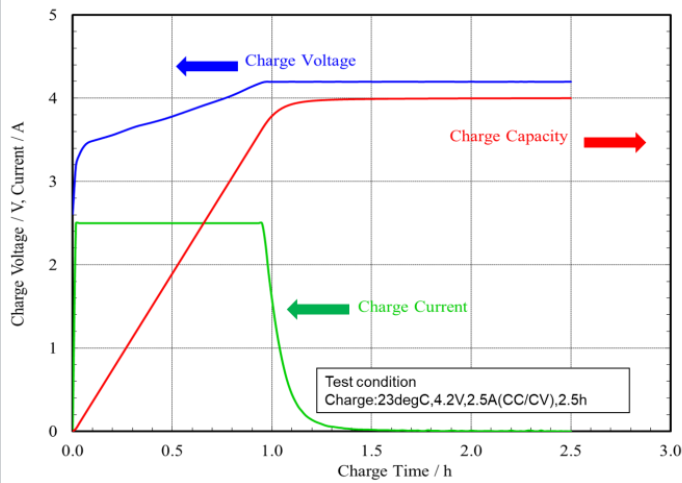
## Discharge characteristics by discharge rate



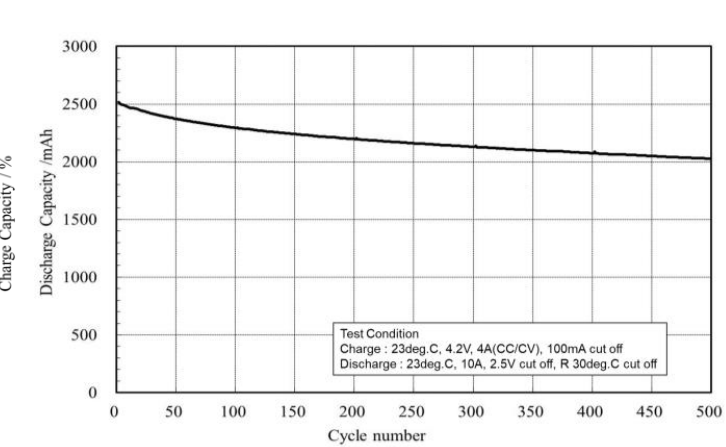
## Discharge characteristics by temperature



## Charge characteristics



## Cycle life



### Attention

- This datasheet is downloaded from the website of Murata Manufacturing Co., Ltd. Therefore, its specifications are subject to change or our products in it may be discontinued without advance notice. Please check with our sales representatives or product engineers before ordering.
- This datasheet has only typical specifications because there is no space for detailed specifications. Therefore, please review our product specifications or consult the approval sheet for product specifications before ordering.
- Lithium-ion secondary batteries have a high energy density, Murata only sells lithium-ion secondary batteries to corporate customers to be embedded and sold in end products (finished products) in a form which provides the appropriate safety measures (protection circuits, etc. to prevent overcurrents and overcharging) according to the usage environment.

# BMS Mini 3

## INTRODUCTION

EMUS BMS Mini 3 is a compact, all-in-one BMS device, that autonomously executes all core and utility functions of battery management. It interacts with all other components in the system, monitors cell voltage levels, and controls charging and balancing functions, using various inputs, outputs, and interfaces.

It is designed to use for battery packs consisting of 6 up to 16 cells connected in series.



## APPLICATIONS

Any lithium chemistry, series-connected battery pack, or a pack of multiple parallel strings, from minimum 6 of up to 16 cells:

- AGV, UGV
- Scooters
- Bikes
- 2-wheelers, 3-wheelers
- Motorcycles.
- Mobile energy storages.

## FEATURES

- USB interface that is intended for quick and straightforward connection to a host device (e.g. computer, tablet, smartphone) when configuration, diagnostics, or maintenance is needed.
- CAN data interface. Enables to communicate with CAN equipped EMUS devices and third-party devices.
- Supports 50, 125, 250, 500, 800 kbit/s and 1 Mbit/s CAN baud rates (default 250kbit/s).
- RS232, a single-ended transmission mode protocol, allows continuously monitor BMS activity using first-party or third-party devices (feature to be active in future product revisions).
- RS485 is a differential transmission mode protocol, which allows to continuously monitor BMS activity and control chargers (feature to be active in future product revisions).
- SD card enables to store all sent messages from the EMUS BMS Mini 3 and recover all unexpected situations which occurred in the past (feature to be active in future product revisions).
- Each BMS Mini 3 monitor from 6 up to 16 battery cells.
- State of Charge (SOC) and State of Health (SOH) (gen1 algorithm) allows to monitor cell's degradation factors. SOC calculations depend on real cell capacity and internal cell parameters.

## MECHANICAL INFORMATION

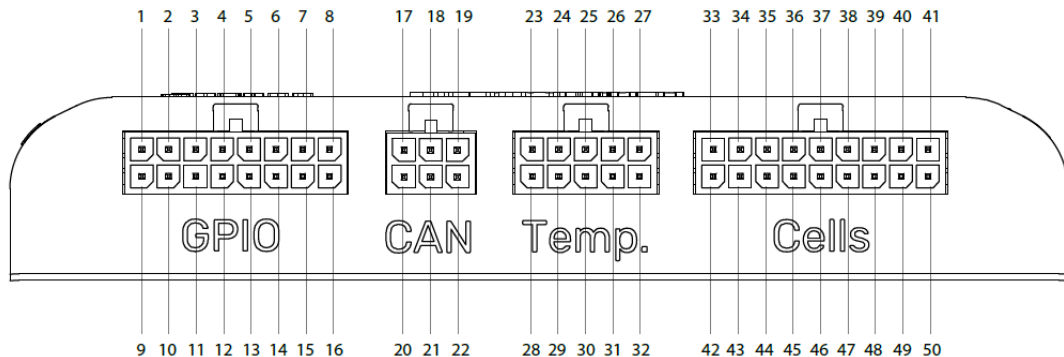


Figure 1 BMS MINI 3 (MNC310) pinout

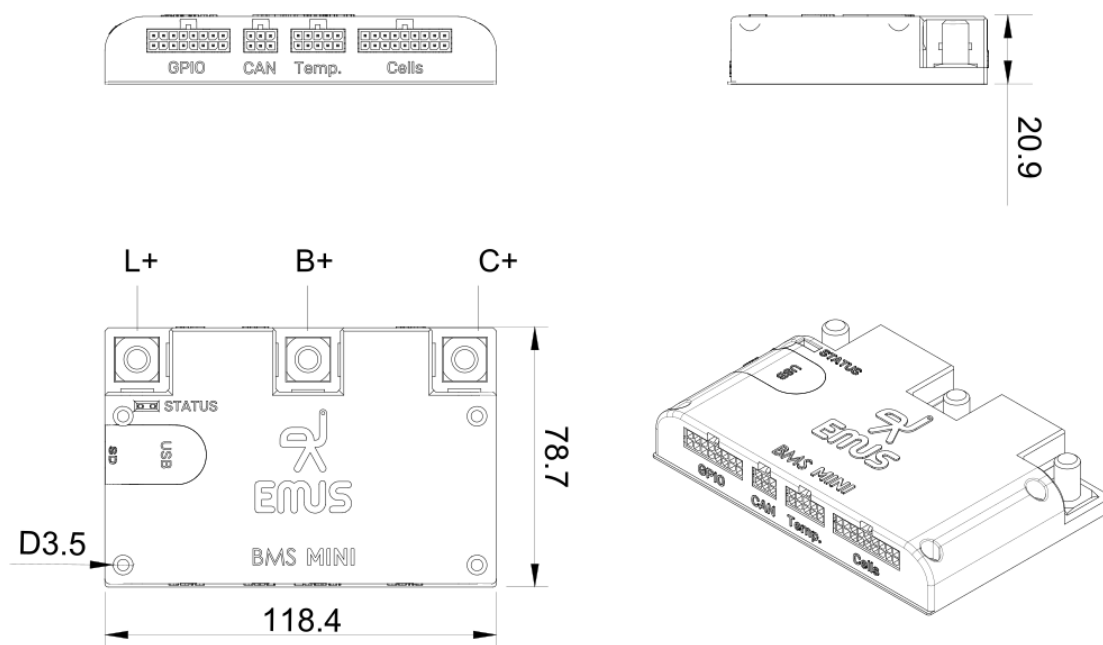


Figure 2 EMUS Mini 3 (MNC310) dimension



Pin No.	Assignment	Mating Housing	Terminal		
1	5V/12V/BAT_SENS	Micro-Fit 3.0 Receptacle Housing 43025-1600	Molex MicroFit 43045-1600 (recommended crimp tool Molex Hand Crimp Tool P/N: 638190000)		
2	GPAI2				
3	GPO1				
4	GPO2				
5	GPO3				
6	GPO4				
7	RS232_TX				
8	RS485_A				
9	GND				
10	GPAI1				
11	GPI1				
12	GPI2				
13	GPI3				
14	GPI4				
15	RS232_RX				
16	RS485_B				
17	5V/12V/BAT_SENS	Micro-Fit 3.0 Receptacle Housing 43025-0600	Molex MicroFit 43045-0600 (recommended crimp tool Molex Hand Crimp Tool P/N: 638190000)		
18	GPO5				
19	CAN_H				
20	GND				
21	GPI5				
22	CAN_L				
23	TEMP1	Micro-Fit 3.0 Receptacle Housing 43025-1000	Molex MicroFit 43045-1000 (recommended crimp tool Molex Hand Crimp Tool P/N: 638190000)		
24	TEMP2				
25	TEMP3				
26	TEMP4				
27	TEMP5				
28	GND				
29					
30					
31					
32	-	Micro-Fit 3.0 Receptacle Housing 43025-1800	Molex MicroFit 43045-1800 (recommended crimp tool Molex Hand Crimp Tool P/N: 638190000)		
33	-				
34	CELL15+				
35	CELL13+				
36	CELL11+				
37	CELL9+				
38	CELL7+				
39	CELL5+				
40	CELL3+				

41	CELL1+		
42	CELL16+		
43	CELL14+		
44	CELL12+		
45	CELL10+		
46	CELL8+		
47	CELL6+		
48	CELL4+		
49	CELL2+		
50	CELL1-		

## ELECTRICAL CHARACTERISTICS

Item	Conditions	Value	
Operating voltage		12 to 72.8 VDC	
Current consumption	At typical supply voltage, with nothing else connected	12 VDC typical 28 mA	72.8 VDC typical 10 mA
General purpose output GP01-GP05 max sinking current (resettable fuse trip current)		1.25A	
General purpose output max voltage		32 VDC	
General purpose input ON voltage		5 to 72.8 VDC	
General purpose input OFF voltage		0 VDC	
USB interface controller		F232R	
USB power supply data line transient/overvoltage protection	VS protection (Pd - 85W)	6V	
RS232 interface voltage	TVS protection (Pd - 200W)	-15V to 15V	
USB/RS232 interface galvanic isolation		None	
CAN interface	TVS protection (Pd - 350W)	-24V to 24V	
RS485 interface voltage	TVS protection (Pd - 600W)	-7V to 12V	
USB interface duplexity	USB not connected	Full duplex (send and receive)	
RS232 interface duplexity	USB connected	Full duplex (send and receive)	
		Half duplex (send only)	
USB/RS232 interface baud rate		57.6kbps	
USB/RS232 interface data bits		8 bits	

USB/RS232 interface parity		None	
USB/RS232 interface stop bits		1 bit	
External temp sensors		5	
Individual cell voltage limits	Firmware v2.x	2V to 4.55V	
	Firmware v3.x and above	1V to 4.95V <sup>1</sup>	
Individual cell voltage measurement accuracy	Firmware v2.x	12mV	
	Firmware v3.x and above	2mV	
Individual cell voltage measurement resolution	Firmware v2.x	10mV	
	Firmware v3.x and above	1mV	
CAN speeds		50, 125, 250, 500, 800 kbit/s and 1 Mbit/s	
Load current	Continuous	without heatsink	100A
		with heatsink <sup>2</sup>	200A
	Peak	without heatsink, 10s	250A
		with heatsink, 60s	300A
Charge current	Continuous	without heatsink	50A
		with heatsink	100A
	Peak	without heatsink, 10s	100A
		with heatsink, 60s	150A
Balancing	Resistor	8.2 Ohm	
	Current @4.2V	500mA	
Pre-Charge Resistor		250 Ohm	
5V/12V	Hold current	1A	

## ■ OTHER SPECIFICATIONS

Item	Condition	Value
Number of cells limits		6 to 16 cells <sup>3</sup>
Operating temperature		-40°C to +85°C
Maximum number of external temperature sensors		5
External temperature sensor measurement accuracy		±5°C
External temperature sensors measurement resolution		1°C
IP rating		IP40
Weight		0.154kg
Terminal tightening torque on M8 L+, C+, B+ terminals	Maximum	15Nm
	Destruction	18Nm

<sup>1</sup> Maximum voltage per cell is limited by full pack voltage depending on number of cells used.

<sup>2</sup> Used Heatsink with at least 0.7 K/W thermal resistance.

<sup>3</sup> Minimum cells count depends on full battery pack voltage. Minimum full battery pack voltage must be above 12V.

## COMPATIBLE CHARGERS AND INVERTERS

Charger Name	Communication Protocol
Elcon	CAN J1939-based
Zivan RE	CAN Zivan proprietary
Powerfinn	CAN
Delta-Q	CANOpen - Profiles: CiA 418/419 [default] DeltaQ standard [supported]
Non-CAN	I/O Controlled

 **NOTE:** More chargers, inverters integrations are planned for the next product revision.

 **NOTE:** For all chargers recently supported please refer to <https://emusbms.com>.

 **NOTE:** For more information on each charger's communication protocol, please contact the charger manufacturer.

# Specifications for NCR18650BD

1

## Specifications

Rated capacity <sup>(1)</sup>	2980mAh	2910mAh
Capacity <sup>(2)</sup>	Minimum Typical	3030mAh 3180mAh
Nominal voltage		3.6V
Charging	Method Voltage Current	CC-CV 4.20V 4.15V Std. 0.3CA
Weight (max.) Without tube		49.5g
Temperature	Charge Discharge Storage	10 to +45° C -20 to +60° C -20 to +50° C
Energy density <sup>(3)</sup>	Volumetric Gravimetric	630 Wh/l 217 Wh/kg
		615 Wh/l 212 Wh/kg

<sup>(1)</sup> At 20° C   <sup>(2)</sup> At 25° C

<sup>(3)</sup> Energy density is calculated using bare cell dimensions (without tube).

## Dimensions

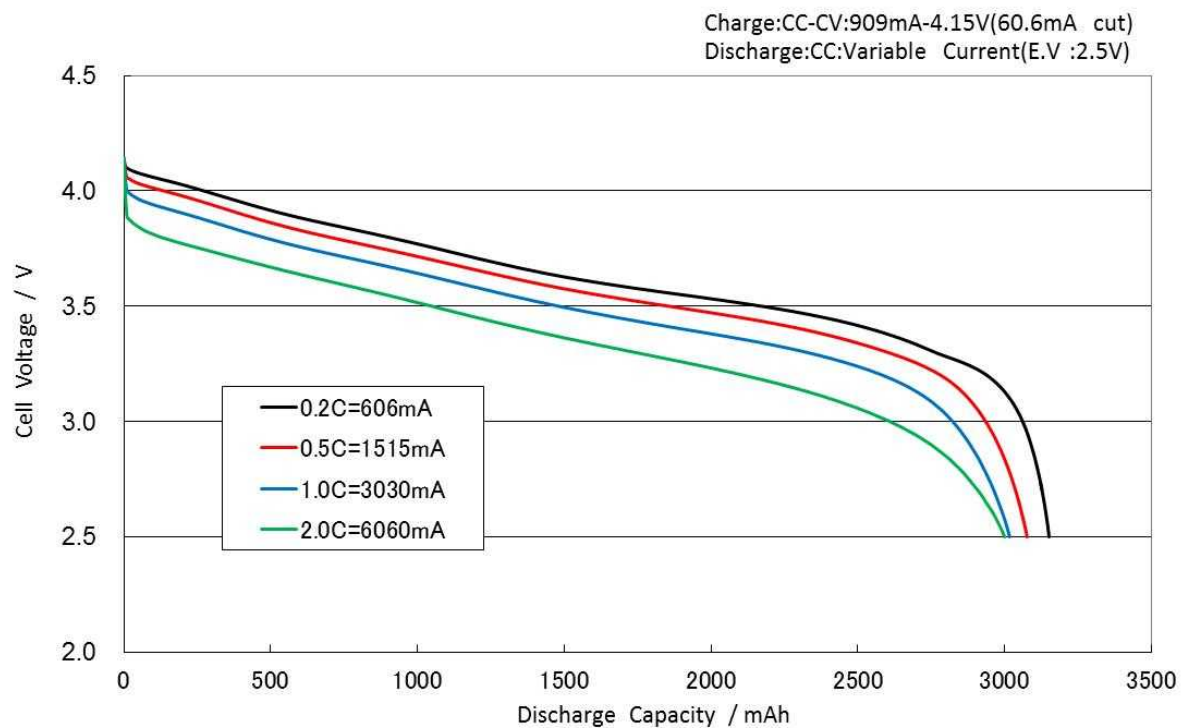
Without tube	D	d
	(+)	(-)
	H	Max. 65.10mm
	D	Max. 18.25mm
	d	Max. 6.6mm

When designing a pack, refer to the cell's mechanical drawing for precise dimensions.

**Panasonic**

## Discharge Rate Characteristics for NCR18650BD

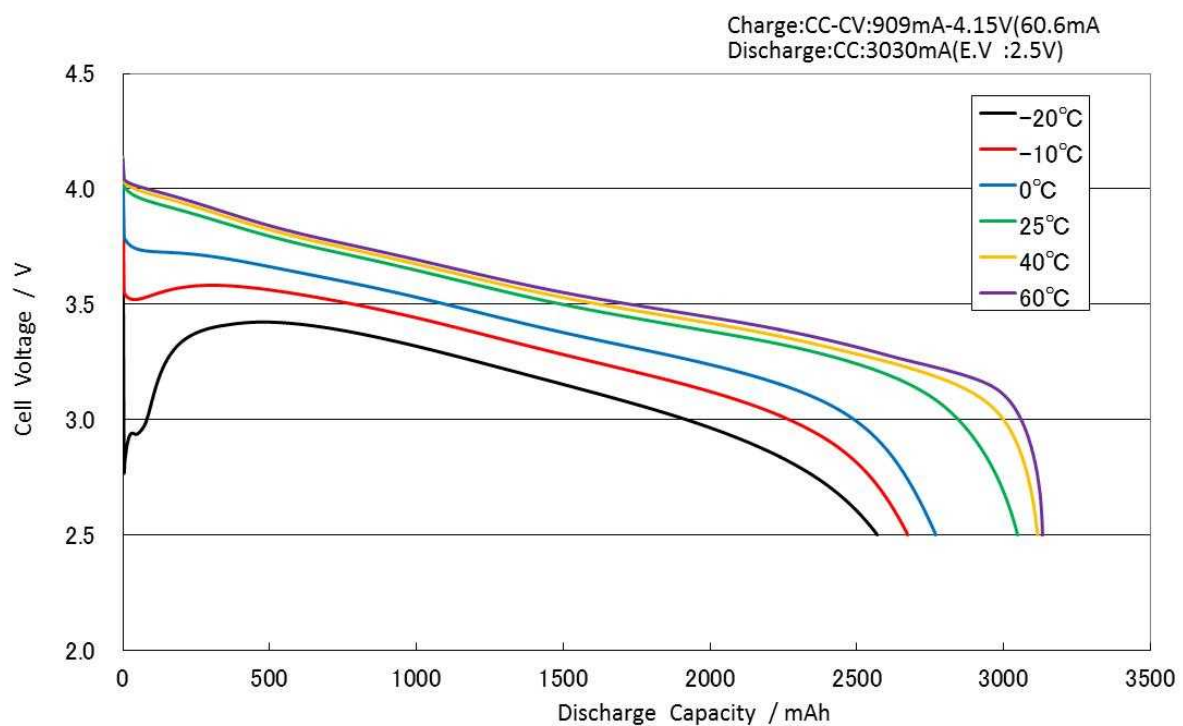
2



Panasonic

## Discharge Temperature Characteristics for NCR18650BD

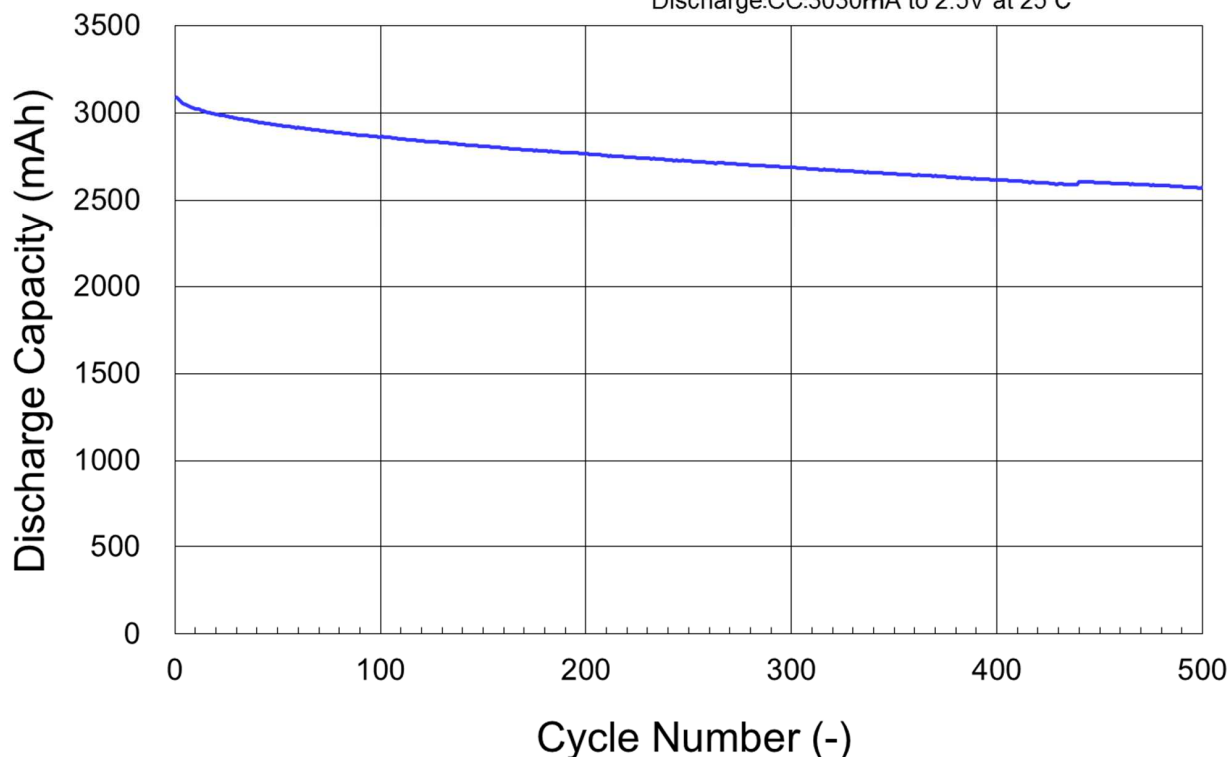
3



Panasonic

## Cycle Characteristics for NCR18650BD

Charge :CC-CV:909mA-4.15V(61mA cut) at 25°C  
Discharge:CC:3030mA to 2.5V at 25°C



Panasonic

# ISOMETER® IR155-3203/IR155-3204

Insulation monitoring device (IMD) for unearthed DC drive systems  
(IT systems) in electric vehicles

**Version V004**



# ISOMETER® IR155-3203/IR155-3204

**Insulation monitoring device (IMD) for unearthed DC drive systems (IT systems) in electric vehicles**



**ISOMETER® IR155-3204**

## Product description

The ISOMETER® IR155-3203/-3204 monitors the insulation resistance between the insulated and active HV-conductors of an electrical drive system ( $U_h = \text{DC } 0 \text{ V} \dots 1000 \text{ V}$ ) and the reference earth (chassis ground ▶ KI.31). The patented measurement technology is used to monitor the condition of the insulation on the DC side as well as on the AC motor side of the electrical drive system. Existing insulation faults will be signalled reliably, even under high system interferences, which can be caused by motor control processes, accelerating, energy recovering etc.

Due to its space-saving design and optimised measurement technology, the device is optimised for use in hybrid or fully electric vehicles. The device meets the increased automotive requirements with regard to the environmental conditions (e.g. temperatures and vibration, EMC...).

The fault messages (insulation fault at the HV-system, connection or device error of the IMD) will be provided at the integrated and galvanic isolated interface (high- or low-side driver). The interface consists of a status output ( $OK_{HS}$  output) and a measurement output ( $M_{HS}/M_{LS}$  output). The status output signalises errors or that the system is error free, i.e. the "good" condition as shown by the "Operating principle PWM driver" diagram on page 5. The measurement output signalises the actual insulation resistance. Furthermore, it is possible to distinguish between different fault messages and device conditions, which are base frequency encoded.

## Function

The ISOMETER® iso-F1 IR155-3203/-3204 generates a pulsed measuring voltage, which is superimposed on the IT system via terminals L+/L- and E/KE. The latest measured insulation condition is available as a pulse-width-modulated (PWM) signal at terminals  $M_{HS}$  (for IR155-3204) or  $M_{LS}$  (for IR155-3203). The connection between the terminals E/KE and the chassis ground (▶ KI.31) is continuously monitored. Therefore it is necessary to install two separated conductors from the terminals E or KE to chassis ground.



*Connection monitoring of the earth terminals E/KE is specified for  $R_F \leq 4 \text{ M}\Omega$  if the ISOMETER® is connected as shown in the application diagram on page 3.*

Once power is switched on, the device performs an initialisation and starts the system state (SST) measurement. The ISOMETER® provides the first estimated insulation resistance during a maximum time of 2 seconds. The DCP measurement (▶ continuous measurement method) starts subsequently. Faults in the connecting wires or functional faults will be automatically recognised and signalled.

During operation, a self test is carried out automatically every five minutes. The interfaces will not be influenced by these self tests.



*Connection monitoring of the earth terminals E/KE may not work as intended when  $R_F > 4 \text{ M}\Omega$  if the supply terminals (KI.15/KI.31) are not galvanically isolated from the chassis earth (KI.31).*

## Standards

### Corresponding standards and regulations\* \* Normative exclusion

IEC 61557-8	2014-12
IEC 61010-1	2010-06
IEC 60664-1	2004-04
ISO 6469-3	2011-12
ISO 23273-3	2006-11
ISO 16750-1	2006-08
ISO 16750-2	2010-03
ISO 16750-4	2010-04
E1 (ECE regulation No. 10 revision 5)	
acc. 72/245/EWG/EEC	2009/19/EG/EC
DIN EN 60068-2-38	Z/AD:2010
DIN EN 60068-2-30	Db:2006
DIN EN 60068-2-14	Nb:2010
DIN EN 60068-2-64	Fh:2009
DIN EN 60068-2-27	Ea:2010

The device went through an automotive test procedure in combination with multi customer requirements reg. ISO16750-x.

The standard IEC61557-8 will be fulfilled by creating the function for LED warning and test button at the customer site if necessary.

The device includes no surge and load dump protection above 50 V. An additional central protection is necessary.

## Approvals



### ATTENTION



Observe precautions for handling electrostatic sensitive devices.

Handle only at safe work stations.

### ATTENTION



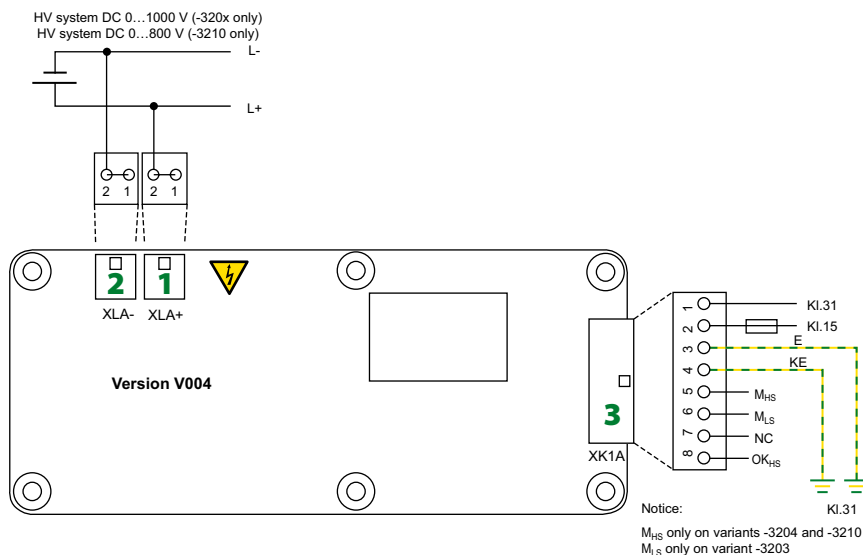
The device is monitoring HIGH VOLTAGE.

Be aware of HIGH VOLTAGE near to the device.

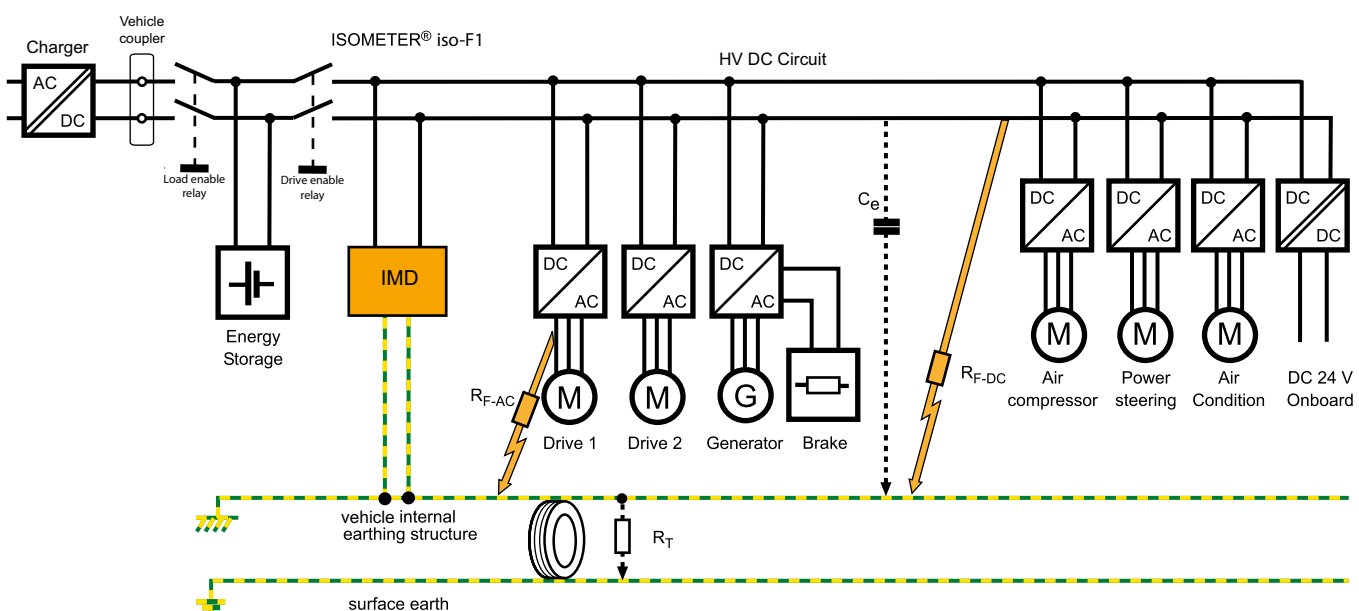
## Abbreviations

DCP	Direct Current Pulse
SST	Speed Start Measuring

## Wiring diagrams



## Typical application



## Technical data

### Insulation coordination acc. to IEC 60664-1

Protective separation (reinforced insulation)  
between (L+/L-) – (Kl. 31, Kl. 15, E, KE,  $M_{HS}$ ,  $M_{LS}$ ,  $OK_{HS}$ )

Voltage test AC 3500 V/1 min

### Supply/IT system being monitored

Supply voltage  $U_S$  DC 10...36 V

Max. operating current  $I_S$  150 mA

Max. current  $I_k$  2 A

6 A/2 ms inrush current

HV voltage range (L+/L-)  $U_n$  AC 0...1000 V (peak value)

0...660 V r.m.s. (10 Hz...1 kHz)

DC 0...1000 V

Power consumption < 2 W

### Response values

Response value hysteresis (DCP) 25 %

Response value  $R_{an}$  100 kΩ...1 MΩ

Undervoltage detection 0...500 V

### Measuring range

Measuring range 0...10 MΩ

Undervoltage detection 0...500 V default setting: 0 V (inactive)

Relative uncertainty

SST (≤ 2 s) good > 2\*  $R_{an}$ ; bad < 0.5\*  $R_{an}$

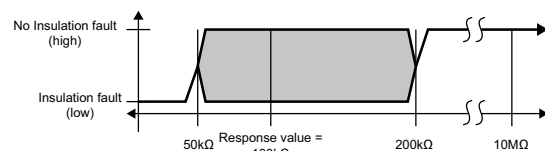
Relative uncertainty DCP 0...85 kΩ ▶ ±20 kΩ

(default setting 100 kΩ) 100 kΩ...10 MΩ ▶ ±15 %

Relative uncertainty output M (fundamental frequency) ±5 % at each frequency  
(10 Hz; 20 Hz; 30 Hz; 40 Hz; 50 Hz)

Relative uncertainty under voltage detection  $U_n \geq 100$  V ▶ ±10 %; at  $U_n \geq 300$  V ▶ ±5 %

Relative uncertainty (SST) "Good condition" ≥ 2\*  $R_{an}$   
"Bad condition" ≤ 0.5\*  $R_{an}$



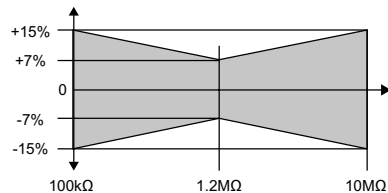
Relative uncertainty DCP 100 kΩ...10 MΩ ±15 %

100 kΩ...1.2 MΩ ▶ ±15 % to ±7 %

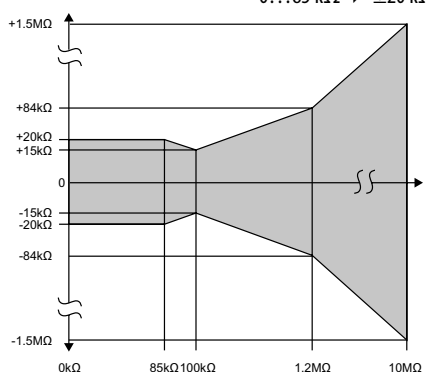
1.2 MΩ ▶ ±7 %

1.2...10 MΩ ▶ ±7 % to ±15 %

10 MΩ ▶ ±15 %



Absolute uncertainty 0...85 kΩ ▶ ±20 kΩ



### Time response

Response time  $t_{an}$  ( $OK_{HS}$ ; SST)  $t_{an} \leq 2$  s (typ. < 1 s at  $U_n > 100$  V)

Response time  $t_{an}$  ( $OK_{HS}$ ; DCP)

(when changing over from  $R_F = 10$  MΩ to  $R_{an}/2$ ; at  $C_e = 1$  μF;  $U_n = DC 1000$  V)

$t_{an} \leq 20$  s (at  $F_{ave} = 10^*$ )

$t_{an} \leq 17.5$  s (at  $F_{ave} = 9$ )

$t_{an} \leq 17.5$  s (at  $F_{ave} = 8$ )

$t_{an} \leq 15$  s (at  $F_{ave} = 7$ )

$t_{an} \leq 12.5$  s (at  $F_{ave} = 6$ )

$t_{an} \leq 12.5$  s (at  $F_{ave} = 5$ )

$t_{an} \leq 10$  s (at  $F_{ave} = 4$ )

$t_{an} \leq 7.5$  s (at  $F_{ave} = 3$ )

$t_{an} \leq 7.5$  s (at  $F_{ave} = 2$ )

$t_{an} \leq 5$  s (at  $F_{ave} = 1$ )

during the self test  $t_{an} + 10$  s

Switch-off time  $t_{ab}$  ( $OK_{HS}$ ; DCP)

(when changing over from  $R_{an}/2$  to  $R_F = 10$  MΩ; at  $C_e = 1$  μF;  $U_n = DC 1000$  V)

$t_{ab} \leq 40$  s (at  $F_{ave} = 10$ )

$t_{ab} \leq 40$  s (at  $F_{ave} = 9$ )

$t_{ab} \leq 33$  s (at  $F_{ave} = 8$ )

$t_{ab} \leq 33$  s (at  $F_{ave} = 7$ )

$t_{ab} \leq 33$  s (at  $F_{ave} = 6$ )

$t_{ab} \leq 26$  s (at  $F_{ave} = 5$ )

$t_{ab} \leq 26$  s (at  $F_{ave} = 4$ )

$t_{ab} \leq 26$  s (at  $F_{ave} = 3$ )

$t_{ab} \leq 20$  s (at  $F_{ave} = 2$ )

$t_{ab} \leq 20$  s (at  $F_{ave} = 1$ )

during a self test  $t_{ab} + 10$  s

Duration of the self test 10 s

(every five minutes; should be added to  $t_{an}/t_{ab}$ )

### Measuring circuit

System leakage capacitance  $C_e$  ≤ 1 μF

Smaller measurement range and increased measuring time at  $C_e$  > 1 μF

(e.g. max. range 1 MΩ at 3 μF,

$t_{an} = 68$  s when changing over from  $R_F = 1$  MΩ to  $R_{an}/2$ )

Measuring voltage  $U_M$  ±40 V

Measuring current  $I_M$  at  $R_F = 0$  ±33 μA

Impedance  $Z_i$  at 50 Hz ≥ 1.2 MΩ

Internal DC resistance  $R_i$  ≥ 1.2 MΩ

\*  $F_{ave} = 10$  is recommended for electric and hybrid vehicles

**Output****Measurement output (M)** **$M_{HS}$  switches to  $U_S - 2\text{ V}$  (3204)**(external pull-down resistor to Kl. 31 necessary  $2.2\text{ k}\Omega$ ) **$M_{LS}$  switches to Kl. 31 + 2 V (3203)**(external pull-up resistor to Kl. 15 required  $2.2\text{ k}\Omega$ )

**0 Hz** ▶ Hi > short-circuit to  $U_b +$  (Kl. 15); Low > IMD off or short-circuit to Kl. 31

**10 Hz** ▶ Normal condition  
Insulation measurement DCP;  
starts two seconds after power on;  
First successful insulation measurement at  $\leq 17.5\text{ s}$   
PWM active 5...95 %

**20 Hz** ▶ undervoltage condition  
Insulation measurement DCP (continuous measurement);  
starts two seconds after power on;  
First successful insulation measurement at  $\leq 17.5\text{ s}$   
Undervoltage detection 0...500 V

(Bender configurable)

**30 Hz** ▶ Speed start measurement  
Insulation measurement (only good/bad evaluation)  
starts directly after power on  $\leq 2\text{ s}$ ;  
PWM 5...10 % (good) and 90...95 % (bad)

**40 Hz** ▶ Device error  
Device error detected; PWM 47.5...52.5 %

**50 Hz** ▶ Connection fault earth  
Fault detected on the earth connection (Kl. 31)  
PWM 47.5...52.5 %

**Status output ( $OK_{HS}$ )** **$OK_{HS}$  switches to  $U_S - 2\text{ V}$** (external pull-down resistor to Kl. 31 required  $2.2\text{ k}\Omega$ )

High ▶ No fault;  $R_F >$  response value  
Low ▶ Insulation resistance  $\leq$  response value detected;  
Device error; Fault in the earth connection  
Undervoltage detected or device switched off

**Operating principle PWM driver**

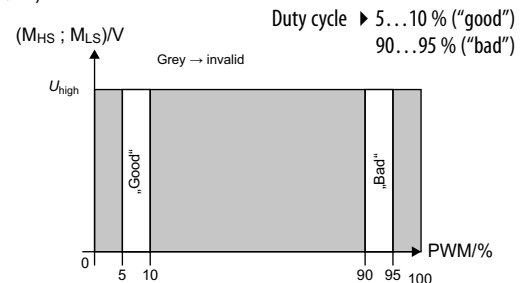
- Condition "Normal" and "Undervoltage detected" (10 Hz; 20 Hz)

Duty cycle 5 % =  $> 50\text{ M}\Omega (\infty)$ Duty cycle 50 % =  $1200\text{ k}\Omega$ Duty cycle 95 % =  $0\text{ k}\Omega$ 

$$R_F = \frac{90\% \times 1200\text{ k}\Omega}{dc_{meas} - 5\%} - 1200\text{ k}\Omega$$

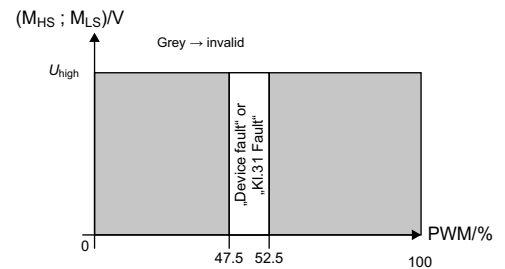
 $dc_{meas}$  = measured duty cycle (5 %...95 %)**Operating principle PWM driver**

- Condition "SST" (30 Hz)

**Operating principle PWM driver**

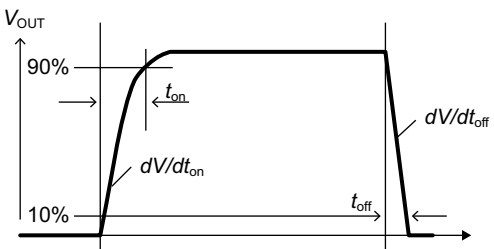
- Condition "Device error" and "Kl.31 fault" (40 Hz; 50 Hz;)

Duty cycle ▶ 47.5...52.5 %



Load current $I_L$	80 mA
Turn-on time ▶ to 90 % $V_{out}$	max. 125 $\mu\text{s}$
Turn-off time ▶ to 10 % $V_{out}$	max. 175 $\mu\text{s}$
Slew rate on ▶ 10...30 % $V_{out}$	max. 6 V/ $\mu\text{s}$
Slew rate off ▶ 70...40 % $V_{out}$	max. 8 V/ $\mu\text{s}$

Timing 3204 (inverse to 3203)

**EMC**Load dump protection  $< 50\text{ V}$ 

Measurement method Bender-DCP technology

Factor averaging  $F_{ave}$  (output M) 1...10 (factory set: 10)**ESD protection**Contact discharge – directly to terminals  $\leq 10\text{ kV}$ Contact discharge – indirectly to environment  $\leq 25\text{ kV}$ Air discharge – handling of the PCB  $\leq 6\text{ kV}$ **Connection**On-board connectors TYCO-MICRO MATE-N-LOK  
1 x 2-1445088-8  
(Kl. 31, Kl.15, E, KE,  $M_{HS}$ ,  $M_{LS}$ ,  $OK_{HS}$ )

2 x 2-1445088-2 (L+, L-); The connection between the respective connecting pins at L+ or L- may only be used as redundancy. Cannot be used for looping through!

Crimp contacts TYCO-MICRO MATE-N-LOK Gold  
14 x 1-794606-1  
Conductor cross section: AWG 20...24Enclosure for crimp contacts TYCO-MICRO MATE-N-LOK receptor HSG single R -1445022-8  
TYCO-MICRO MATE-N-LOK receptor HSG single R -1445022-2

## General data

Necessary crimp tongs (TYCO)	91501-1
Operating mode/mounting	continuous operation/any position
Temperature range	-40...+105 °C
Voltage failure	≤ 2 ms
Flammability class acc. to	UL 94 V-0

## Mounting

M4 metal screws with locking washers between screw head and PCB. Torx, T20 with a maximum tightening torque of 4 Nm for the screws. Furthermore, a maximum of 10 Nm tightening torque to the PCB at the mounting points.

**Mounting and connector kits are not included in delivery, but are available as accessories.** The maximum diameter of the mounting points is 10 mm.

Before mounting the device, ensure sufficient insulation between the device and the vehicle or the mounting points (min. 11.4 mm to other parts). If the device is mounted on a metal or conductive subsurface, this subsurface has to be at earth potential (Kl.31; vehicle mass).

Deflection max. 1 % of the length or width of the PCB

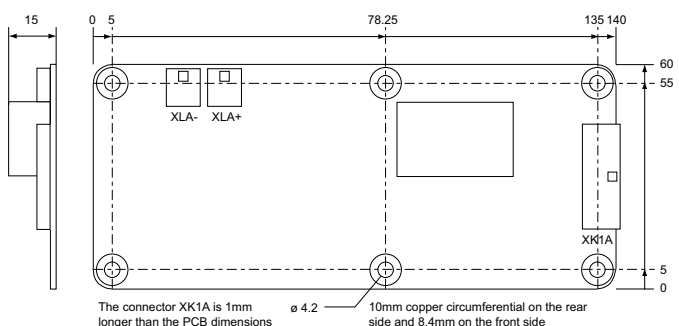
Coating thick-film lacquer

Weight 52 g ±2 g

## Dimension diagram

Dimensions in mm

PCB dimensions (L x W x H) 140 mm x 60 mm x 15 mm



## Ordering information

Parameters	Response value $R_{an}$	$f_{ave}$	Undervoltage detection	Measured value output	Type	Art. No.
Continuously set value	100 kΩ	10	300 V	Low side	IR155-3203	B91068138V4
			0 V (inactive)	High side	IR155-3204	B91068139V4
Customer-specific setting	100 kΩ...1 MΩ	1...10	0 V...500 V	Low side	IR155-3203	B91068138CV4
				High side	IR155-3204	B91068139CV4

## Accessories

Type designation	Art. No.
Fastening set	B91068500
Connector set IR155-32xx	B91068501

## Example for ordering

IR155-3204-100kΩ-0V + B 9106 8139V4

IR155-3204-200kΩ-100V + B 9106 8139CV4

The parameters, i.e. the response value and undervoltage protection value must be included in the order.



## Bender GmbH & Co. KG

Londorfer Straße 65 • 35305 Grünberg • Germany

Tel.: +49 6401 807-0 • info@bender.de • www.bender.de



BENDER Group

# High Current & Voltage Cartridge Fuses

Lead-free > 10x32mm Fuse > 607 Series



## Description

The 607 series fuses are specifically designed and tested to cater to the circuit protection needs of compact applications, which is 500Vdc/Vac rated with remarkable interrupting rating.

## Features

- RoHS compliant and Lead-free
- High Interrupt Rating
- Rated voltage 500 Vdc/Vac

## Benefits

- |  |  |
|--|--|
| <ul style="list-style-type: none"> <li>■ Small size</li> <li>■ High current</li> </ul> | <ul style="list-style-type: none"> <li>■ High voltage</li> <li>■ High breaking capacity</li> </ul> |
|--|--|

## Applications

- Data Center Power Supplies
- Uninterruptible Power Supply (UPS)
- Power conversion equipment like inverters and rectifiers

## Additional Information



Resources



Accessories



Samples

## Agency Approvals

Agency	Agency File Number	Ampere Range
cULus	E71611	40 A to 63 A
△	J 50514752	40 A to 63 A

## Electrical Characteristics

% of Ampere Rating	Ampere Rating	Opening Time at 25°C
100%	40 A to 63 A	4hrs, Min.
200%	40 A to 63 A	120 seconds, Max.

## Electrical Specifications

Ampere Rating (A)	Amp Code	Max Voltage Rating (V)	Interrupting Rating (AC/DC)	Nominal Code Resistance (Ohm)	Nominal Melting I <sup>2</sup> t (A <sup>2</sup> sec)	Agency Approvals	
						cULus	△
40	040.	500VDC 500VAC	10KA@500VDC 10KA@500VAC	0.00187	2570	x	x
50	050.			0.00145	4230	x	x
63	063.	500VDC 500VAC 300VAC	10KA@500VDC 5KA@500VAC 10KA@300VAC	0.00102	7060	x	x

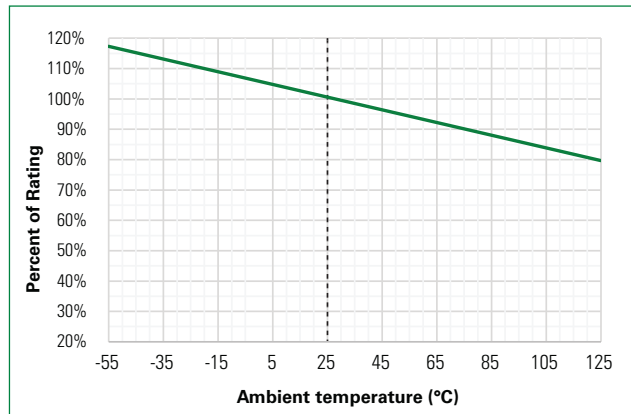
Note

Unless otherwise stated, all specifications are referenced at room ambient temperature.

# High Current & Voltage Cartridge Fuses

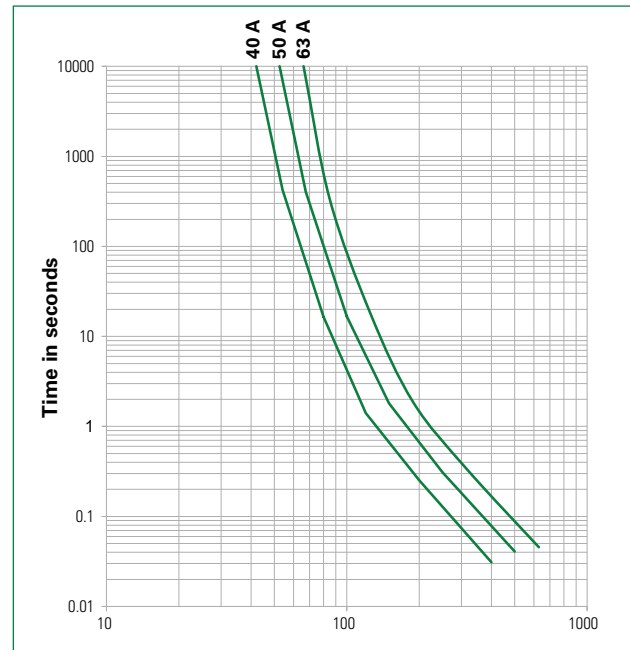
Lead-free > 10x32mm Fuse > 607 Series

## Temperature Re-rating Curve



**Note:**  
Derating depicted in this curve is in addition to the standard derating of 25% for continuous operation.

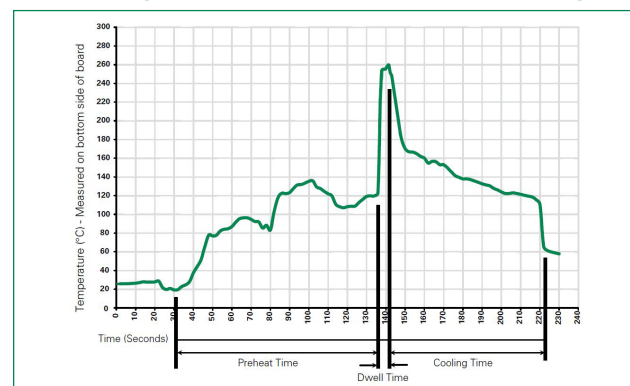
## Average Time Current Curves



## Product Characteristics

<b>Materials</b>	<b>Body:</b> Glass fiber <b>Cap:</b> Ni plated copper alloy <b>Terminal:</b> Tin plated copper alloy
<b>Mechanical Shock</b>	MIL-STD-202, Method 213, Test Condition I (100 G's peak for 6 milliseconds)
<b>Solderability</b>	Reference MIL-STD-202 method 208
<b>Product Marking</b>	Cap 1: Brand logo, current and voltage ratings Cap 2: Agency approval marks
<b>Resistance to Solder Heat</b>	MIL-Std 202 Method 210 Test Condition B (10sec at 260 °C)
<b>Operating Temperature</b>	-55 °C to +125 °C
<b>Thermal Shock</b>	MIL-STD-202G, Method 107G, Test condition B
<b>Vibration</b>	MIL-STD-202G, Method 201A
<b>Moisture Resistance</b>	MIL-STD-202G, Method 103B, Test condition A
<b>Salt Spray</b>	MIL-STD-202G, Method 101E, Test condition B

## Soldering Parameters—Wave Soldering

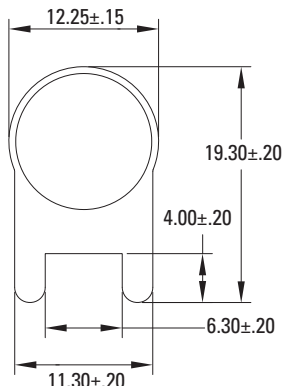
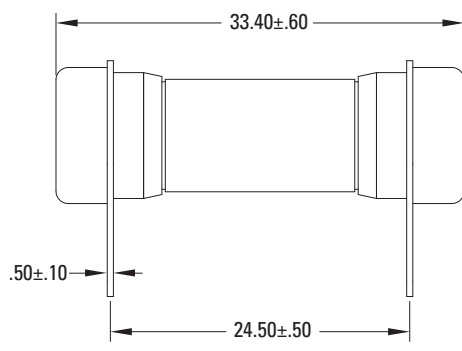


Wave Parameter	Lead-Free Recommendation
<b>Preheat:</b> (Depends on Flex Activation Temperature)	(Typical Industry Recommendation)
Temperature Minimum	100 °C
Temperature Maximum	150 °C
Preheat Time	60–180 seconds
<b>Solder Pot Temperature</b>	260 °C Maximum
<b>Solder Dwell Time</b>	2–5 seconds
<b>Recommended Hand-Solder Parameters:</b> Solder Iron Temperature: 350 °C +/- 5 °C Heating Time: 5 seconds max.	
<b>Note:</b> These devices are not recommended for IR or Convection Reflow process.	

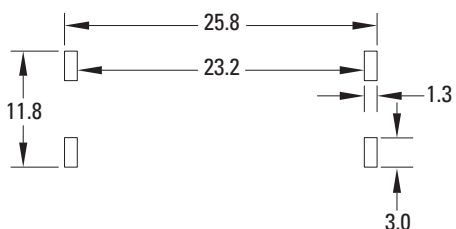
# High Current & Voltage Cartridge Fuses

Lead-free > 10x32mm Fuse > 607 Series

## Dimensions

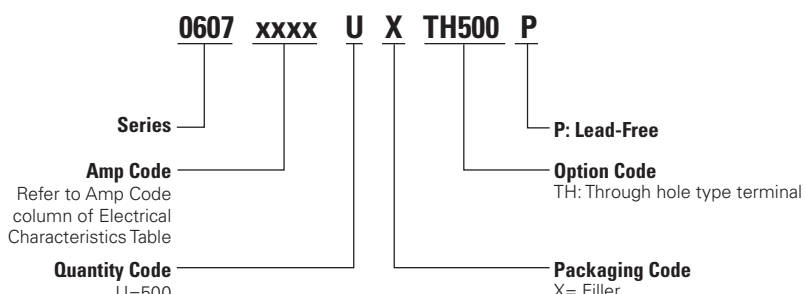


## Recommended PCB Layout



All dimensions in mm

## Part Numbering System



## Packaging

Packaging Option	Packaging Specification	Quantity	Quantity & Packaging Code	Reel Size
<b>607 Series</b>				
Tray	NA	500	NA	NA

**Disclaimer Notice** - Information furnished is believed to be accurate and reliable. However, users should independently evaluate the suitability of and test each product selected for their own applications. Littelfuse products are not designed for, and may not be used in, all applications. Read complete Disclaimer Notice at <http://www.littelfuse.com/disclaimer-electronics>.

# 461 Series TeleLink® Fuse

## Surge Resistant



### Additional Information



Resources



Accessories



Samples

### Agency Approvals

Agency	Agency File Number	Ampere Range
	E10480	0.5A - 2A
	29862	0.5A - 2A
	J50502555	0.5A - 2A

### Electrical Characteristics for Series

% of Ampere Rating	Opening Time
100%	4 hours, Minimum
250%	1 sec., Minimum; 120 secs., Maximum

### Maximum Temperature Rise

Telecom Nano® Fuse	Temperature Reading
04611.25	< 82°C (180°F)
0461002.	< 50°C (122°F)

Higher Currents and PCB layout designs can affect this parameter.  
Readings are measured at rated current after temperature stabilizes.

### Description

The Littelfuse 461 Series TeleLink® Surface Mount, Surge Resistant Fuse, offers over-current protection for a wide range of telecom applications without requiring a series resistor. When used in conjunction with a Littelfuse SIDACtor® Transient Voltage Suppressor (TVS) or a GreentubeTM Gas Plasma Arrestor, this combination provides a compliant solution for standards and recommendations such as GR-1089-Core, TIA-968-A, UL/EN/IEC 60950, and ITU K.20 and K.21. The coordination requirement contained in GR-1089-Core, and ITU K.20/21 may require a series of impedance devices.

### Features & Benefits

- Surface mount surge resistant Slo-Blo® fuse
- Meet UL 60950 3rd Edition power cross requirements standard alone
- Designed to allow compliance with Telcordia GR-1089-CORE and TIA-968-A (formerly FCC Part 68) Surge Specifications
- Provide coordinated protection with Littelfuse SIDACtor® Transient Voltage Suppressor (TVS) or a GreentubeTM Gas Plasma Arrestor, without series resistors
- Designed to serve the requirements of a wide range of telecommunication and networking equipment
- 2A rating has improved temperature rise performance under 2.2A surge current testing when compared with 1.25A rating
- Product is Halogen Free and RoHS compliant and compatible with lead-free solder and higher temperature profiles when ordered with Standard Silver Plated Brass Caps
- UL Recognized to UL/CSA/NMX 248-1 and UL/CSA/NMX 248-14
- Conforms to IEC/EN 60127-1 and IEC/EN 60127-7

### Applications

- T1/E1/J1 and HDSL2/4
- SLIC interface portion of Fiber to the Curb (FTTC) and Fiber to the Premises (FTTP)
- Non-Fiber SLIC interface for Central Office (CO) locations and Remote Terminals (RT)
- xDSL applications such as ADSL, ADSL2+, VDSL, and VDSL2+
- Ethernet 10/100/1000BaseT
- POTS applications such as modems, answering machines, telephones, fax machines, and security systems
- ISDN "U" interface
- Baystation T1/E1/J1, T3 (DS3) trunk cards

# 461 Series TeleLink® Fuse

## Surge Resistant

### Electrical Specifications by Item

Ampere Rating (A)	Amp Code	Max Voltage Rating (V)	Interrupting Rating <sup>2</sup>	Nominal Cold Resistance (Ohms)	Nominal Melting I <sup>2</sup> t (A <sup>2</sup> sec)	Agency Approvals		
0.500	.500	600	50A @ 250 VAC	0.560	0.840 <sup>1</sup>	x	x	x
1.25	1.25	600	60 A @ 600 VAC	.1040	16.5 <sup>1</sup>	x	x	x
2.00	002.	600	100 A @ 80 VDC	.0450	17.5 <sup>1</sup>	x	x	x

<sup>1</sup> I<sup>2</sup>t is calculated at 10 msec. or less. I<sup>2</sup>t at 10 times rated current has a typical value of: 24 A<sup>2</sup>sec (2.0A), 22 A<sup>2</sup>sec (1.25A), 1.3 A<sup>2</sup>sec (0.5A).

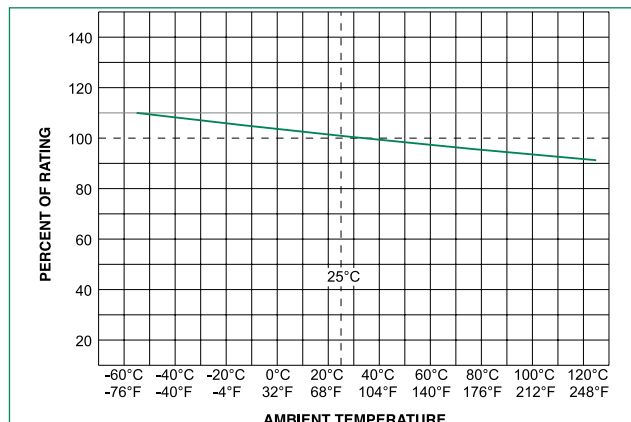
■ Typical inductance <40nH up to 500 MHz.

■ Resistance changes 0.5% for every °C.

■ Resistance is measured at 10% rated current.

<sup>2</sup> Interrupting Rating may differ based on Agency Approval. See Agency Approval certificate for more details.

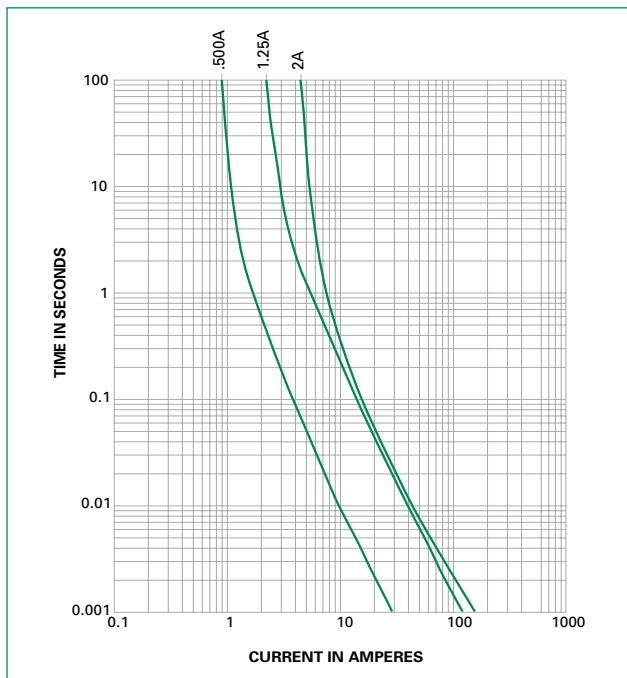
### Temperature Re-rating Curve



#### Note:

1. Re-rating depicted in this curve is in addition to the standard re-rating of 25% for continuous operation.

### Average Time Current Curves



### GR 1089 Inter-building requirements

**GR 1089 1st level lighting surge inter-building**  
(Equipment under test can not be damaged and must continue to operate properly)

Surge	Minimum Peak Voltage (V)	Minimum Peak Current (A)	Max. Rise/Min. Decay (μs)	Repetitions Each Polarity	Fuse Choices
1	600	100	10/1000	25	1.25, 2.0
2	1000	100	10/360	25	1.25, 2.0
3	1000	100	10/1000	25	1.25, 2.0
4	2500	500	2/10	10	1.25, 2.0
5	1000	25	10/360	5	0.5, 1.25, 2.0

If sufficient series resistance is used, then the 0.5 fuse may be used in test conditions 1-4.

**GR 1089 2nd level lightning surge telecom port**  
(Equipment under test shall not become a fire or electrical safety hazard)

Surge	Minimum Peak Voltage (V)	Minimum Peak Current (A)	Max. Rise/Min. Decay (μs)	Repetitions Each Polarity	Fuse Choices
1	5000	500	2/10	1	0.5, 1.25, 2.0
Alter-native	5000	500/8=625	8/10	1	0.5, 1.25, 2.0

The 0.5 fuse will open during these test conditions. The 1.25 & 2.0 will not open thus providing operational compliance.

# 461 Series TeleLink® Fuse

## Surge Resistant

### GR 1089 AC power fault 1st level inter-building (fuse not allowed to open)

Test	Vrms	Short Circuit Current (A)	Hits	Duration	Primary Protector	Fuse Choices
1	50	0.33	1	15 min.	removed	1.25, 2.0
2	100	0.17	1	15 min.	removed	1.25, 2.0
3	200,400, 600	1	60	1 sec.	removed	1.25, 2.0
4	1000	1	60	1 sec.	operative	1.25, 2.0
5	Diagram	Diagram	60	5 secs.	removed	1.25, 2.0
6	600	0.5	1	30 secs.	removed	1.25, 2.0
7	440	2.2	5	2 secs.	removed	1.25, 2.0
8	600	3	1	1.1 secs.	removed	1.25, 2.0
9	1000	5	1	0.4 sec.	in place	1.25, 2.0

### GR 1089 AC power fault 2nd level (fuse can open but must open in a safe and controlled manner)

Test Circuit	Vrms	Short Circuit Current(A)	Duration	Fuse
1	120,277	25	15 min.	0.5, 1.25, 2.0
2	600	60	5 secs.	0.5, 1.25, 2.0
3	600	7	5 secs.	0.5, 1.25, 2.0
4	100-600	2.2	15 min..	0.5, 1.25, 2.0
5	Diagram	Diagram	15 min.	0.5, 1.25, 2.0

Fuse must open before wiring simulator fuse (MDL 2.0).

### TIA –968-A (formerly FCC Part 68) Surge Waveforms (fuse can not open during type B events)

Surge	Voltage (V)	Waveform (μs)	Current (A)	Repetitions	Recommended Fuse
Metallic A	800	10×560	100	1 ea. polarity	1.25
Longitudinal A	1500	10×160	200	1 ea. polarity	1.25
Metallic B	1000	9×720	25	1 ea. polarity	1.25
Longitudinal B	1500	9×720	375	1 ea. polarity	1.25

For the type A events the 0.5 fuse will open, providing non-operational compliance. The 1.25 & 2.0 will not open, providing for operational compliance with TIA-968-A type A surge events.

## UL 60950 requirements

### UL60950 (EN 60950) (formerly UL 1950) Power Cross (L = longitudinal, M = metallic)

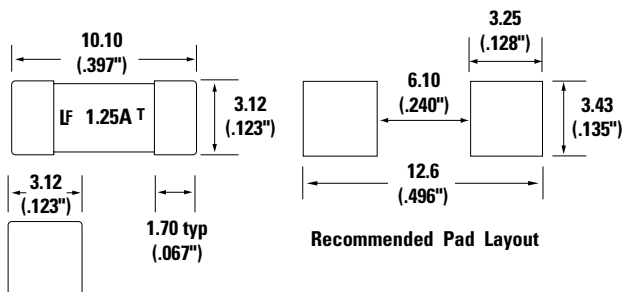
Test Number	Voltage (V)	Current (A)	Time	Fuse Choices
L1	600	40	1.5 secs.	0.5, 1.25, 2.0
L2	600	7	5 secs.	0.5, 1.25, 2.0
L3	600	2.2	30 min.	0.5, 1.25, 2.0
L4	200	2.2	30 min.	0.5, 1.25, 2.0
L5	120	25	30 min.	0.5, 1.25, 2.0
M1	600	40	1.5 secs.	0.5, 1.25, 2.0
M2	600	7	5 secs.	0.5, 1.25, 2.0
M3	600	2.2	30 min.	0.5, 1.25, 2.0
M4	600	2.2	30 min.	0.5, 1.25, 2.0

Selection of test number depends on current limiting F fire enclosure/spacing of end product

- 26 AWG line cord removes L1/M1 test requirement
- L5 conducted only if product does not pass section 6.1.2
- L2,M2,L3,M3,L4,M4 conducted if not in a fire enclosure

Fuse must open before the wiring simulator fuse (MDL 2.0).

### Dimensions



### UL60950 (EN 60950) (formerly UL 1950) Impulse Test and Steady-State Electric Strength Test

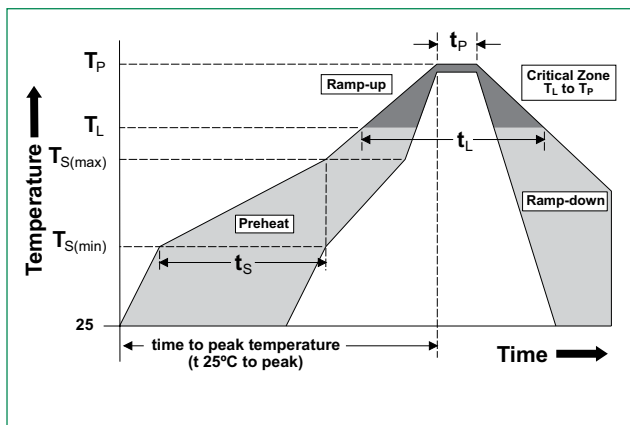
Test	Voltage (V)	Current (A)	Waveform	Repetitions	Fuse Choices
<b>Impulse</b>					
For handheld units	2500	62.5	10×700ms	+/- 10 w/60 secs. rest	0.5, 1.25, 2.0
Non handheld	1500	37.5	10×700ms	+/- 10 w/60 secs. rest	0.5, 1.25, 2.0
<b>Steady-State</b>					
For handheld units	1500		60Hz		0.5, 1.25, 2.0
Non handheld	1000		60Hz		0.5, 1.25, 2.0

# 461 Series TeleLink® Fuse

## Surge Resistant

### Soldering Parameters

Reflow Condition		Pb – free assembly
Pre Heat	- Temperature Min ( $T_{s(min)}$ )	150°C
	- Temperature Max ( $T_{s(max)}$ )	200°C
	- Time (Min to Max) ( $t_s$ )	60 – 180 seconds
Average Ramp-up Rate (Liquidus Temp ( $T_L$ ) to peak)		5°C/second max.
$T_{s(max)}$ to $T_L$ - Ramp-up Rate		5°C/second max.
Reflow	- Temperature ( $T_L$ ) (Liquidus)	217°C
	- Temperature ( $t_L$ )	60 – 150 seconds
Peak Temperature ( $T_p$ )		260 <sup>+0/-5</sup> °C
Time within 5°C of actual peak Temperature ( $t_p$ )		20 – 40 seconds
Ramp-down Rate		6°C/second max.
Time 25°C to peak Temperature ( $T_p$ )		8 minutes max.
Do not exceed		260°C



### Product Characteristics

Materials	Body: Ceramic Terminations: Silver-plated Caps
Product Marking	Brand Logo, Ampere Rating, T
Operating Temperature	-55°C to 125°C
Moisture Sensitivity Level	Level 1, J-STD-020
Solderability	IEC 60127-4 (215°C immersion, 3 seconds)
Resistance to Dissolution of Metallization	IPC / EIA J-STD-002-Test D 260°C for 120 seconds
Thermal Shock	MIL-STD-202, Method 107, Test Condition B, -55°C to +125°C, 30 minutes @ each extreme
Mechanical Shock	MIL-STD-202, Method 213, Test Condition A - Half Sine, 50 G's, 11 msec. duration
High Frequency Vibration	MIL-STD-202, Method 204, Test Condition D
Moisture Resistance	MIL-STD-202, Method 106, 50 cycles
Terminal Strength	Board deflection per EIA / IS-722, 1mm deflection for 1 minute
Terminal Attachment	MIL-STD-202, Method 211, Test Condition A, 5 lbs applied to end caps

### Part Numbering System

0461 1.25 E R

Series \_\_\_\_\_

Amp Code\* \_\_\_\_\_

Refer to Electrical Characteristics table

Quantity code \_\_\_\_\_

E = 2500 pcs

Packaging code \_\_\_\_\_

R = Tape and Reel

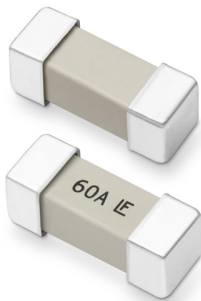
\*Example:  
2 amp product is 0461002\_ER  
(1.25 amp product shown above)

### Packaging

Packaging Option	Packaging Specification	Quantity	Quantity & Packaging Code
24mm Tape and Reel	EIA RS-481-2 (IEC 60286-3)	2500	ER

**Disclaimer Notice** - Information furnished is believed to be accurate and reliable. However, users should independently evaluate the suitability of and test each product selected for their own applications. Littelfuse products are not designed for, and may not be used in, all applications. Read complete Disclaimer Notice at: [www.littelfuse.com/disclaimer-electronics](http://www.littelfuse.com/disclaimer-electronics).

### 456SDE Series Fuse



#### Description

The High Current NANO<sup>2®</sup> Fuse is a small square surface mount fuse that is designed to support higher current requirements of various applications.

#### Features

- Available in ratings of 40 A to 60 A
- Surface mountable high current fuse
- High interrupting rating of 600 A @ 80 VDC
- Very low cold resistance, temperature rise, and voltage drop
- UL Recognized UL/CSA/NMX 248-1 and UL/CSA/NMX 248-14

#### Benefits

- Single fuse solution for high current application
- Avoids nuisance opening due to high inrush and surge current inherent in the system
- Suitable for a wide variety of voltage requirements and applications
- Compatible with high volume assembly requirements
- Enhances power efficiency

#### Applications

- Voltage regulator Module for PC Server
- Storage System Power
- Basestation Power Supply
- Cooling Fan System for PC Server
- Power Tools

#### Agency Approvals

Agency	Agency File Number	Ampere Rating
	E10480	40 A -60 A

#### Electrical Characteristics

% of Ampere Rating	Opening Time
100%	4 hours, Minimum
200%	60 seconds, Maximum

#### Additional Information


[Datasheet](#)

[Resources](#)

[Samples](#)

#### Electrical Specifications

Ampere Rating (A)	Amp Code	Max Voltage Rating (V)	Interrupting Rating	Nominal Cold Resistance (Ohms) <sup>1</sup>	Nominal Melting I <sup>2</sup> t (A <sup>2</sup> Sec.) <sup>3</sup>	Nominal Voltage Drop (mV)	Agency Approvals <sup>2</sup>
40	040.	250	150A @ 250VAC 600A @ 80VDC	0.00130	1700	110	x
50	050.	250	150A @ 250VAC 600A @ 80VDC	0.00105	2700	115	x
60	060.	250	150A @ 250VAC 600A @ 80VDC	0.00085	4260	106	x

##### Notes:

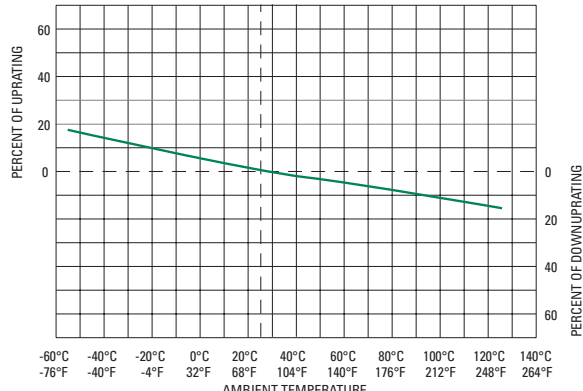
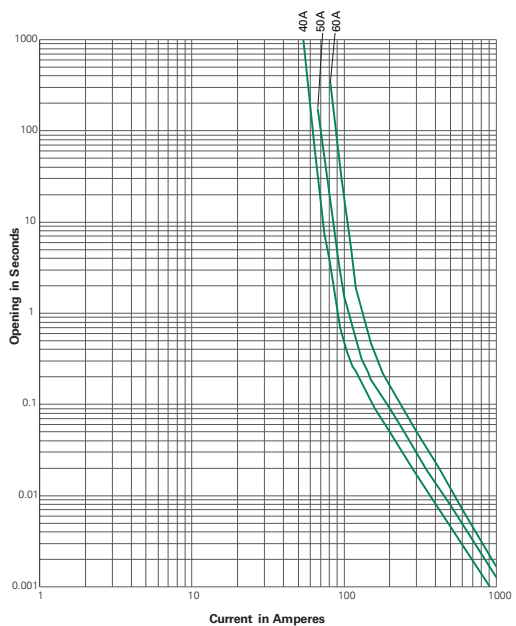
1. Cold resistance measured at less than 10% of rated current at 23° C.

2. Agency Approval Table Key: X = Approved or Certified, P = Pending.

3. I<sup>2</sup>t values stated for 8msec opening time.

# Surface Mount Fuses

## NANO<sup>2</sup>® > Fast Acting Fuse > 456SDE Series

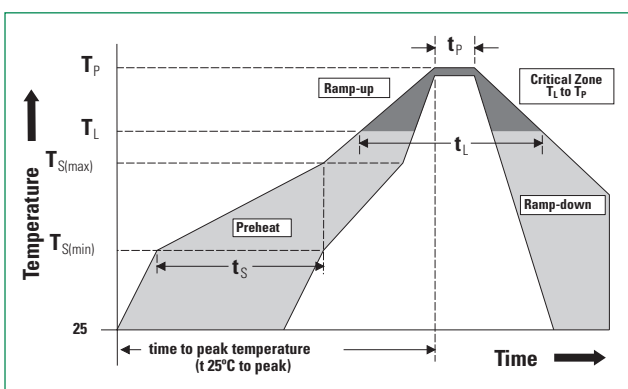
**Temperature Re-rating Curve**

**Average Time Current Curves**


Note:

1. Re-rating depicted in this curve is in addition to the standard derating of 25% for continuous operation.

**Soldering Parameters – Reflow Soldering**

Reflow Condition		Pb – Free assembly
Pre Heat	- Temperature Min ( $T_{s(min)}$ )	150°C
	- Temperature Max ( $T_{s(max)}$ )	200°C
	- Time (Min to Max) ( $t_s$ )	60 – 180 secs
Average ramp up rate (Liquidus Temp ( $T_L$ ) to peak		5°C/second max.
$T_{s(max)}$ to $T_L$ - Ramp-up Rate		5°C/second max.
Reflow	- Temperature ( $T_L$ ) (Liquidus)	217°C
	- Temperature ( $t_L$ )	60 – 150 seconds
Peak Temperature ( $T_p$ )		260 <sup>+0/-5</sup> °C
Time within 5°C of actual peak Temperature ( $t_p$ )		20 – 40 seconds
Ramp-down Rate		5°C/second max.
Time 25°C to peak Temperature ( $T_p$ )		8 minutes max.
Do not exceed		260°C



# Surface Mount Fuses

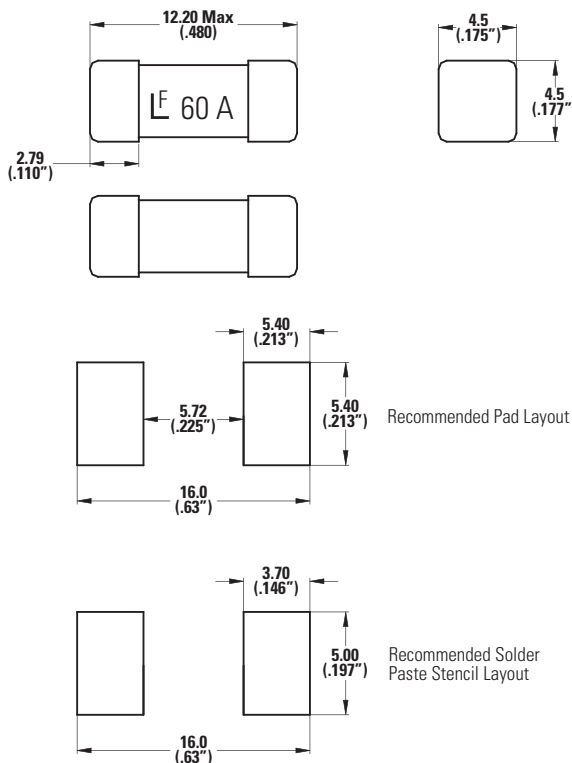
## NANO<sup>2</sup>® > Fast Acting Fuse > 456SDE Series

### Product Characteristics

<b>Materials</b>	Body: Ceramic Cap: Silver Plated Brass
<b>Product Marking</b>	Body: Brand Logo, Current Rating
<b>Insulation Resistance</b>	MIL-STD-202, Method 302, Test Condition A (10,000 ohms, Minimum)
<b>Solderability</b>	MIL-STD-202, Method 208
<b>Resistance to Soldering Heat</b>	MIL-STD-202, Method 210, Test Condition B (10 sec at 260°C)
<b>PCB Recommendation for Thermal Management</b>	<p>Minimum copper trace width = 15 mm (40 A)/25 mm (50 A/60 A)            Recommended copper trace weight = 3oz (40A) / 6oz (50 A/60 A)</p> <p>For PSE requirements:            Minimum Copper trace width = 35mm Recommended Copper trace weight = 6oz</p> <p>Alternate methods of thermal management may be used. In such cases, under normal operations, the maximum temperature of the fuse body should not exceed 90°C in a 25°C environment.</p>

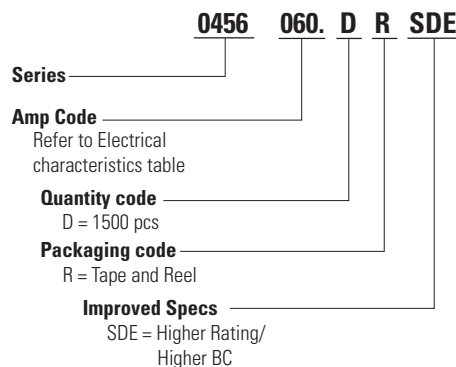
<b>Operating Temperature</b>	-55°C to 125°C with proper derating
<b>Thermal Shock</b>	MIL-STD-202, Method 107, Test Condition B (5 cycles -65°C to 125°C)
<b>Vibration</b>	MIL-STD-202, Method 201 (10-55 Hz)
<b>Moisture Sensitivity Level</b>	J-STD-020, Level 1
<b>Moisture Resistance</b>	MIL-STD-202 Method 106, High Humidity (90-98% RH), Heat (65°C)
<b>Salt Spray</b>	MIL-STD-202, Method 101, Test Condition B
<b>Mechanical Shock</b>	MIL-STD-202, Method 213, Test Condition I (100 G's peak for 6 milliseconds)

### Dimensions



Note: Recommended Stencil Thickness: 0.152 mm  
 Dimensions are in millimeters (inches)

### Part Numbering System



### Packaging

Rating	Packaging Option	Packaging Specification	Quantity	Quantity & Packaging Code
40 A-60 A	24 mm Tape and Reel	EIA RS-481-2 (IEC 286, Part 3)	1500	DR

**Disclaimer Notice** - Information furnished is believed to be accurate and reliable. However, users should independently evaluate the suitability of and test each product selected for their own applications. Littelfuse products are not designed for, and may not be used in, all applications. Read complete Disclaimer Notice at <https://www.littelfuse.com/legal/disclaimers/product-disclaimer.aspx>.

# High Current & Voltage Cartridge Fuses

Lead-free > 10x32mm Fuse > 607 Series



## Description

The 607 series fuses are specifically designed and tested to cater to the circuit protection needs of compact applications, which is 500Vdc/Vac rated with remarkable interrupting rating.

## Features

- RoHS compliant and Lead-free
- High Interrupt Rating
- Rated voltage 500 Vdc/Vac

## Benefits

- |  |  |
|--|--|
| <ul style="list-style-type: none"> <li>■ Small size</li> <li>■ High current</li> </ul> | <ul style="list-style-type: none"> <li>■ High voltage</li> <li>■ High breaking capacity</li> </ul> |
|--|--|

## Applications

- Data Center Power Supplies
- Uninterruptible Power Supply (UPS)
- Power conversion equipment like inverters and rectifiers

## Additional Information



Resources



Accessories



Samples

## Agency Approvals

Agency	Agency File Number	Ampere Range
cULus	E71611	40 A to 63 A
△	J 50514752	40 A to 63 A

## Electrical Characteristics

% of Ampere Rating	Ampere Rating	Opening Time at 25°C
100%	40 A to 63 A	4hrs, Min.
200%	40 A to 63 A	120 seconds, Max.

## Electrical Specifications

Ampere Rating (A)	Amp Code	Max Voltage Rating (V)	Interrupting Rating (AC/DC)	Nominal Code Resistance (Ohm)	Nominal Melting I <sup>2</sup> t (A <sup>2</sup> sec)	Agency Approvals	
						cULus	△
40	040.	500VDC 500VAC	10KA@500VDC 10KA@500VAC	0.00187	2570	x	x
50	050.			0.00145	4230	x	x
63	063.	500VDC 500VAC 300VAC	10KA@500VDC 5KA@500VAC 10KA@300VAC	0.00102	7060	x	x

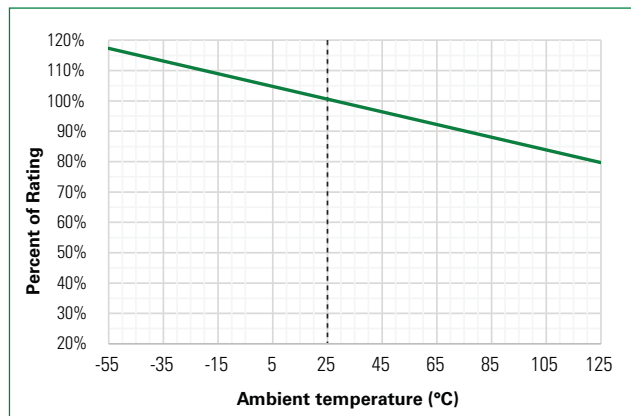
Note

Unless otherwise stated, all specifications are referenced at room ambient temperature.

# High Current & Voltage Cartridge Fuses

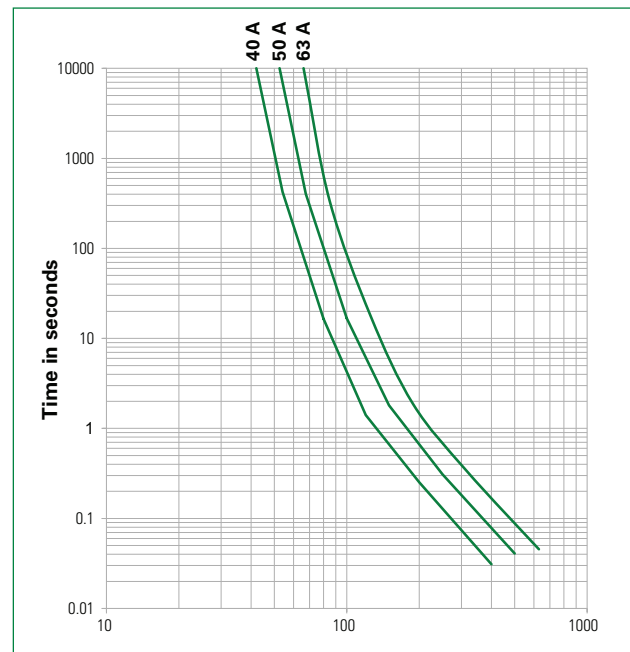
Lead-free > 10x32mm Fuse > 607 Series

## Temperature Re-rating Curve



**Note:**  
Derating depicted in this curve is in addition to the standard derating of 25% for continuous operation.

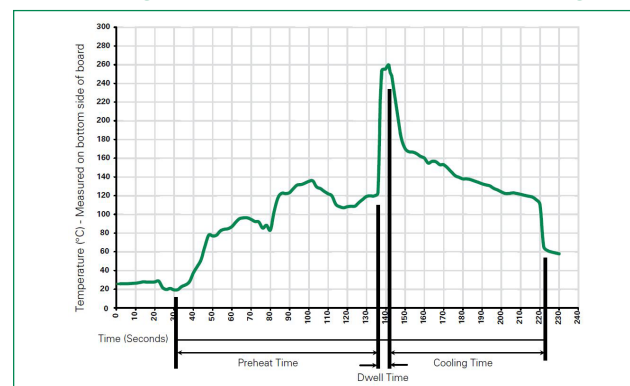
## Average Time Current Curves



## Product Characteristics

<b>Materials</b>	<b>Body:</b> Glass fiber <b>Cap:</b> Ni plated copper alloy <b>Terminal:</b> Tin plated copper alloy
<b>Mechanical Shock</b>	MIL-STD-202, Method 213, Test Condition I (100 G's peak for 6 milliseconds)
<b>Solderability</b>	Reference MIL-STD-202 method 208
<b>Product Marking</b>	Cap 1: Brand logo, current and voltage ratings Cap 2: Agency approval marks
<b>Resistance to Solder Heat</b>	MIL-Std 202 Method 210 Test Condition B (10sec at 260 °C)
<b>Operating Temperature</b>	-55 °C to +125 °C
<b>Thermal Shock</b>	MIL-STD-202G, Method 107G, Test condition B
<b>Vibration</b>	MIL-STD-202G, Method 201A
<b>Moisture Resistance</b>	MIL-STD-202G, Method 103B, Test condition A
<b>Salt Spray</b>	MIL-STD-202G, Method 101E, Test condition B

## Soldering Parameters—Wave Soldering

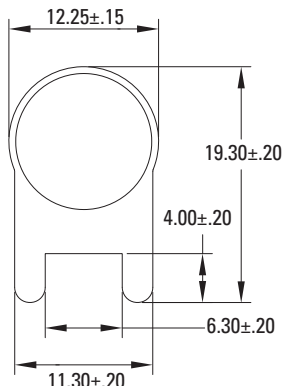
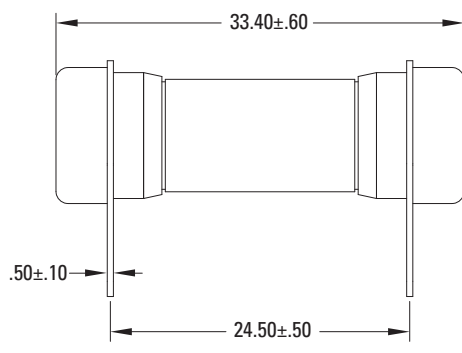


Wave Parameter	Lead-Free Recommendation
<b>Preheat:</b> (Depends on Flex Activation Temperature)	(Typical Industry Recommendation)
Temperature Minimum	100 °C
Temperature Maximum	150 °C
Preheat Time	60–180 seconds
<b>Solder Pot Temperature</b>	260 °C Maximum
<b>Solder Dwell Time</b>	2–5 seconds
<b>Recommended Hand-Solder Parameters:</b> Solder Iron Temperature: 350 °C +/- 5 °C Heating Time: 5 seconds max.	
<b>Note:</b> These devices are not recommended for IR or Convection Reflow process.	

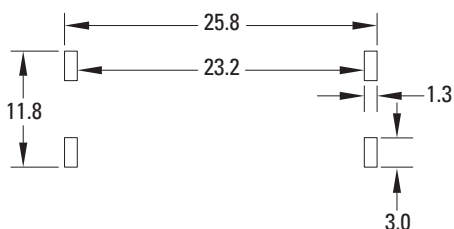
# High Current & Voltage Cartridge Fuses

Lead-free > 10x32mm Fuse > 607 Series

## Dimensions

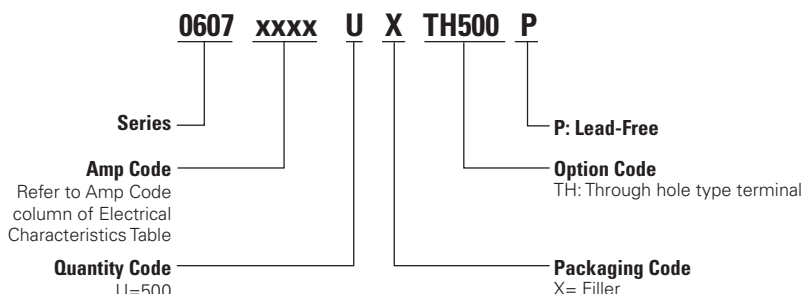


### Recommended PCB Layout



All dimensions in mm

## Part Numbering System



## Packaging

Packaging Option	Packaging Specification	Quantity	Quantity & Packaging Code	Reel Size
<b>607 Series</b>				
Tray	NA	500	NA	NA

**Disclaimer Notice** - Information furnished is believed to be accurate and reliable. However, users should independently evaluate the suitability of and test each product selected for their own applications. Littelfuse products are not designed for, and may not be used in, all applications. Read complete Disclaimer Notice at <http://www.littelfuse.com/disclaimer-electronics>.